Appendix 12

Computational modelling of sediment transport in the Southern North Sea by tide, wave and surge

Southern North Sea Sediment Transport Study, Phase 2

Appendix 12 Computational modelling of sediment transport in the Southern North Sea by tide, wave and surge

1 INTRODUCTION

1.1 Background

In this Southern North Sea sediment transport study Phase 2, a range of methods and approaches were applied as a means of gaining as much information as possible for incorporation into the study, including data collected as part of the consultation exercise, interpretation of new field data and seabed maps and the application of various numerical computational models.

The numerical model studies were aimed at providing complementary information to the project, and have the advantage of allowing the various processes to be represented as required, and the sensitivity of the sediment transport patterns to these processes to be determined. Both area and profile models were applied in this study. Area models are able to simulate the transport processes in two horizontal dimensions, for a range of typical conditions, whereas profile models are suitable for analysing the sediment transport on the coast due to the complete spectrum of wave conditions as well as tidal characteristics. By this means the modelling studies represent a powerful tool and were an intrinsic part of the overall study.

The study area is shown in Figure 1. Numerical modelling was undertaken at both the regional scale and also at the local scale for selected areas where detailed attention was required, following the consultation exercise.

This report comprises output arising from the application of the area models used in this study to provide information on the sediment transport pathways throughout the study area. The profile modelling studies of longshore drift are described in Appendix 11 to the main Sediment Transport Report.

1.2 Aim

The aim of this element of the study was to apply calibrated numerical models to simulate a range of conditions as a means of gaining an overall assessment of the sediment transport patterns throughout the study area. Given the variety of hydrodynamic and sediment characteristics, the models were required to simulate a range of tidal and wave conditions, and also the transport of a range of sediment types.

This report constitutes an atlas of sediment transport results which, in conjunction with the additional analysis provided in the main report, is aimed at informing the reader about the general dynamics of sediment transport throughout the study area. Results have been presented at the scale of the entire study area and also at a larger scale for specific coastal areas indicated on Figure 2.

In addition, further numerical modelling was also undertaken at a local level, in order to simulate the sediment transport processes in detail at specific regions within the study area where the present understanding of the sediment transport was either sparse or not well understood. Following the consultation exercise, two areas were selected for further study: the coastal region around Winterton Ness on the east coast of East Anglia, and the region between the Clacton frontage and Gunfleet Sands sandbank in Essex. Results of the model applications in these areas is also provided in this report.

2 REGIONAL MODELLING

2.1 Model setup

The regional modelling was based on the HR Wallingford Southern North Sea area model which extends from north of Flamborough Head in the North Sea to Plymouth in the English Channel (see insert to Figure 1). This is a 2D depth average flow model with the capability to simulate tidal and wind driven flows, wave action and sediment transport. Siting the southern boundary this far away from the study area enabled good resolution of the tidal propagation through the Straits of Dover, and also simplified the boundary specification by using harmonic data from Primary ports and other published literature (the national BODC database).

The bathymetry for the regional model is presented in Figure 1, which was obtained by digitising UK Admiralty Charts that cover the area and interpolating the information onto the model mesh which is shown in Figure 3. Clearly, for these regional model studies, the full detail of the bathymetry is not resolved as reproduction of the seabed at scales below the grid size is not possible. This means that narrow channels or banks may not be represented to such a degree that the fine detailed transport processes are reproduced. However, the representation of the seabed is sufficient to determine the overall propagation of the tidal currents within the entire study area, and thereby to simulate the sediment transport regime over this area.

The regional flow model used was the TELEMAC finite element model developed by LNH-EDF of France and used at HR Wallingford for a number of years and in many comparable applications. TELEMAC has the significant benefit of allowing fine model resolution in specified areas, which allows a large area to be simulated as well as sufficient representation of the flow field in complex areas (within the bounds of accuracy required for this regional modelling exercise). This capability has the added advantage of optimising the computational effort in the area of local interest, e.g. in the area to the south of Felixstowe shown in Figure 3.

The regional flow model was run by supplying a time history of water levels along the two open boundaries – north and east in the North Sea and in the South-West approaches of the English Channel - and imposing a surface wind stress when required. The water levels were determined either from a harmonic analysis using published information from the national BODC database or, in the case of the surge tide simulation, from a synthesised time history of water levels at strategic points along each boundary (provided by POL from their Coastal Shelf model).

The transport of very fine material that remains in suspension was assessed by analysing the tidal currents in detail, and calculating the residual velocity over a tidal cycle. This procedure in effect removes the transport pathways that water "packets" (containing the sediment) undergo within a tidal cycle, leaving the net drift over the tidal cycle. This is comparable to placing a drogue or float track into the water column and following its motion over the tidal cycle.

Sand transport was simulated using the HR Wallingford SANDFLOW model, which is a non-equilibrium finite element sediment transport that simulates the total load (suspended and bedload), with input flows from TELEMAC, and the specified wave conditions. For the coarser gravels simulated, SANDFLOW was modified to represent the bedload fraction only. Although SANDFLOW has the capability of masking discrete areas of the seabed with deposits of the grain size for simulation (with other areas devoid of sediment) all model simulations were performed assuming an abundant supply of material over the entire domain. This approach is preferred because it results in model predictions that are not dependent on this initial starting condition, but this does require careful interpretation of the model results.

Output from SANDFLOW comprises the suspended sediment concentration and sediment flux patterns throughout the period simulated (typically an individual tidal cycle), and the net residual transport over this period. This net residual is the field that has been analysed in detail in this report, in order to focus on the longer-term transport pathways rather than intra-tidal detail.

2.2 Flow model calibration

The aim of the calibration exercise was to tune the parameters available for adjustment, which for the flow model comprise the bed friction term and the co-efficient for eddy diffusivity of momentum (e.g. turbulent mixing).

The flow model was calibrated against synthesised tide curves based on published tidal harmonics for stations down the coast, and against current measurements and information presented on tidal charts (tidal diamonds).

Calibration was carried out by comparing tidal levels and currents for the spring tide of 22 April 2001. Tests were carried out using a seabed roughness length, k_s of 0.1m (which is appropriate for sand) and of 0.01m (which is appropriate for finer material on the bed), and also for a synthesised distribution of k_s with a corresponding variable roughness over the domain.

An assessment of the model tidal level predictions was carried out for locations on the coast over the entire study area by comparing with predicted tidal levels generated with the TIDECALC package. TIDECALC is a propriety package produced by the Admiralty that generates tidal levels from supplied tidal harmonics. In our experience the package is generally accurate on the open coast around the UK, but does not reproduce the tidal response well in complex estuaries where non-linear processes give rise to complex response of the tidal levels. Consequently, the prediction from TIDECALC at locations close to estuaries or large shallow bays may not be accurate. In addition, for these simulations, the TELEMAC model was driven with a tide curve at each boundary derived from 10-12 tidal constituents whereas the TIDECALC predictions were based on many more constituents which represent the main harmonic contributions.

Spring tide model levels for the simulation using a k_s of 0.1m and those predicted with TIDECALC are presented in Figures 4a to 4c. In general the model reproduces the form of the tidal profile well, with large tide range in the north and south of the study area (Figures 4a and 4c), and smaller tides in the region of East Anglia (Figure 4b). In some instances the predicted range differs between the two sets of data (modelled and reconstituted by TIDECALC) and this is likely to be due to a combination of the difference in the number of harmonics used in the two approaches, and the response of the model in areas that do not resolve the complex bathymetry in sufficient detail.

Figures 5a to 5g show the corresponding model currents for the same simulation with k_s of 0.1m, compared to reconstituted currents based on CEFAS harmonic data (Figures 4a to 4g) derived from their archive of field measurements (as discussed in HR Wallingford, 2001) and also against tidal diamonds. It was noted that for the comparison against the CEFAS data there was a consistent phase lag between the two data sets for many locations which was unexplained, although the agreement in the magnitudes and directions of the current was generally good. (It is interesting to note that the CEFAS data for almost identical locations at sites 232 and 230 in the Thames, Figure 5a, show markedly different reconstituted currents, which may be due to bathymetric changes that had taken place between the two measurement periods). The model correctly simulates the change in sense of rotation of the tidal current at site 255 (Figure 5d). Conversely, the comparison against the tidal diamonds is poor in places, with a tendency for the model to underpredict the strength of these currents.

The model results using a k_s of 0.01m showed that the tidal levels are only marginally affected at most locations, but the tidal currents are significantly affected. Agreement with the tidal diamonds is better, but the model tends to consistently overpredict against the CEFAS data.

Overall, the model simulations using a k_s of 0.1m are preferred, the agreement against the CEFAS data is better, and this level of bed roughness is more appropriate for the range of sediment sizes and bedforms present in the North Sea. A value of k_s of 0.01m is only justifiable for smooth fine-sediment seabeds.

2.3 Flow model validation

Validation of the flow model was carried out by running the neap tide conditions of the 13 April 2001 without further model tuning (using k_s of 0.1m), and comparing tidal levels and currents as for the calibration exercise.

Model tidal levels are compared with predictions using TIDECALC in Figure 6a to 6c. Again, the tidal propagation throughout the study area is well reproduced, and the model generally agrees well with the predictions at most locations. As for the spring tide simulation, the reproduction of the tidal levels in the southern area around Southend differs from the TIDECALC predictions, perhaps due to non-linear tidal processes in the Thames estuary.

The validation against neap tide currents are presented in Figures 7a to 7g and the magnitudes and directions generally agree well with the CEFAS data (Figures 7a to 7d).

2.4 Sensitivity test to bed roughness

Given the sensitivity to bed roughness highlighted in Section 2.2, a further sensitivity test was carried out with a specified variable seabed roughness based on a schematisation of the BGS seabed map (Cameron et al, 1992), as shown in Figure 8. The associated values of seabed roughness were based on typical values derived from field measurements over different seabed substrates by Soulsby (1997). Despite the complexity of this distribution, and the large areas of the model with low roughness values, the resulting tidal levels and currents shown in Figure 9a to 9c and 10a to 10g are generally comparable to the case with a k_s of 0.1m.

2.5 Sediment transport validation

For the case of local area models, development and validation of a site-specific sediment transport model is possible if there is adequate data (hydrodynamic and sedimentological) to define the transport mechanisms. More frequently, predictions are performed using an established transport formula, and this is also the case for regional modelling predictions where there is unlikely to be sufficient information to derive an appropriate transport law that is representative of the whole area.

For these regional studies the sediment transport model, SANDFLOW utilised a total load transport formula according to Van Rijn, modified by Soulsby to include the effect of waves (Soulsby, 1997), which has been subject to various cases of favourable comparison with sediment transport data (e.g. Williams and Rose, 2001), and other model predictions. This approach is valid because the principal aim of the study is to provide information on the sediment transport pathways and variability in these pathways due to the various physical processes. Absolute quantities of the sediment drift rates, whilst informative, were not the main focus of the study.

2.6 Model simulations

Sediment transport simulations were aimed at defining the transport pathways under a variety of hydrodynamic conditions including tides, winds, surges and waves. Most applications comprised running the TELEMAC flow model for the required scenario and passing the model output to the SANDFLOW model. To maintain a consistent approach a value of k_s = 0.1m was used throughout these simulations.

In order to assess the sensitivity of the sediment transport patterns to wave effects, a wave height and period was specified for the whole regional model area (with depth-limiting of the wave height if necessary), from which the main wave contribution of the stirring effect due to the wave orbital velocity at the seabed was calculated. The effects of wave breaking were not represented in the regional modelling.

All the results are mapped with the coastline shown and the axes are plotted with metres East and metres North. The depth contours of bathymetry are also shown colour coded. Depths are with respect to Ordnance Datum Newlyn.

2.6.1 Transport of fine material

The transport pathways of fine material carried in suspension was assessed by calculating the residual currents over the entire model domain (see inset of Figure 1). These currents are due to tidal effects, modified by the surface stress of the wind, and also by surge conditions. It is assumed that the fine material carried in suspension remains in the water column and does not exchange with the seabed over the short term. This approach serves to identify the transport pathways, and sources and sinks of this grade of sediment material.

Figures 11 and 12 show the tidal residual currents for spring and neap tides. For the purposes of presentation all results in vector form are represented on a regular mesh that is coarser than the mesh used to define the currents.

The most striking feature of these plots is the indication of a net northerly drift that flows adjacent to the eastern portion of the study area. Note that the limits of this plot area are not the model boundaries.

This drift does not correspond very well with the well-known drift across the North Sea identified from a number of sources (including satellite imagery on front cover and Figure 29 of the main report) and referred to as the "English River". However, there is some agreement with the sub-surface currents predicted with a fully 3D model of the North Sea (which also included temperature and salinity fields) (Odd and Cooper (1992)). This 3D model was able to reproduce the "English River", which is most apparent in the surface layers, and in particular when a winter wind field is applied. Accordingly, reproduction of the detail of this flow structure with a depth-averaged model should not be anticipated. The correspondence of the results from the 2D model with the sub-surface flow patters is, however, encouraging and demonstrates that the model is capable of reproducing the general flow patterns.

On neap tides there is a general northerly drift over most of the southern part of the Southern North Sea.

Spring tide patterns show a significant net drift south through the Straits of Dover, that does not feature on the neap tides. The outer Thames area is generally not well organised, probably as a consequence of the banks in this area, whereas further north around the East Anglian coast the net drift is weak, and to the east on springs but other than at the coast shows a more northerly drift on neaps. There is an identifiable coastal drift to the east around the NE Norfolk coast, that reverses between neaps and springs, whereas the drift within the Wash is consistent for both tides, with an apparently weak drift in through the centre and stronger outwards flow around both coasts. The Lincolnshire and Northumberland coasts both exhibit southerly drift which is quite strong across the Humber, and tends to flow due east further offshore (especially on spring tides). Similarly, net flows off Flamborough Head are eastwards.

From this analysis the indication is that, other than the Outer Thames region and the Wash, there will be an easterly and northerly drift of fine material. Clearly, there will also be small areas not resolved by this model where fine sediment accumulates, including the estuaries.

Figures 13 to 23 show the spring tide residual velocity patterns presented in Figure 11 at a larger scale, for the various sections of the coast throughout the study area.

A winter wind condition was simulated by applying a 10m/s wind from the west over the entire domain for spring tide conditions, and the results are presented in Figure 24. The effect of this wind is to drive flows through the Straits of Dover and generally northwards. Also the pattern of flows towards the eastern extent of the study area northeast of Great Yarmouth show the beginnings of the drift pattern across the North Sea.

Conversely, Figure 25 shows the net tidal current residual for the case of a specific surge event, and the tidal residual is dominated by a general southerly drift in the southern half of the North Sea, which is very high through the Straits of Dover.

2.6.2 Sand and gravel transport

The SANDFLOW model was used to simulate the transport of sand (bedload and suspension load) and gravel (bedload only) over the model domain.

Figure 26 shows the seabed mobility under spring tide conditions, in terms of the maximum grain size that is capable of being mobilised by the tidal current. This figure indicates that the greatest mobility occurs off the coasts of East Kent, Northeast Norfolk, the Outer Wash and offshore of the Humber entrance and Flamborough Head. Over the majority of the domain the maximum grain size capable of being moved on a spring tide is typically coarse sand (0.5 to 2.0mm). In the Outer Thames the currents in some areas are weaker and only medium sand is moved (0.25 to 0.50mm), whereas off the coast of east Kent the energy is sufficient to move even pebbles (sizes larger than 2mm).

Sediment transport was simulated for a variety of conditions summarised in the table below.

Sediment grain size (mm)	Hydrodynamic condition						
	Neaps	Springs					Surge
	calm	calm	1m, 5s waves	3m, 6s waves	3m, 10s waves	5m, 10s waves	5m, 10s waves
0.1	✓	✓	✓	✓	✓	✓	✓
0.4		✓					
2.0		✓					✓

The net tidal sediment transport patterns are presented in the remaining figures of this report using the vector style shown in Figure 27. The arrowhead shows the direction in which sediment is moving. The rate of increase in the magnitude of sediment transport with current velocity is extremely non-linear, with areas of high current transporting material at a rate some orders of magnitude higher than the calmer areas. Accordingly, a non-linear vector scale is used on these plots with colour coding. The magnitude of the transport rate (kg/m/tide net dry mass of sediment moved per metre width of seabed at that location during one complete tidal cycle) is colour coded using logarithmic banding to allow the smallest and largest values to be represented on one plot. Although the lowest band has a lower limit of zero values of zero flux are not plotted because of the logarithmic scale. In addition, the larger transport vectors have a vector "tail" where the length of the tail increases in linear proportion to the flux as indicated in the following diagram.

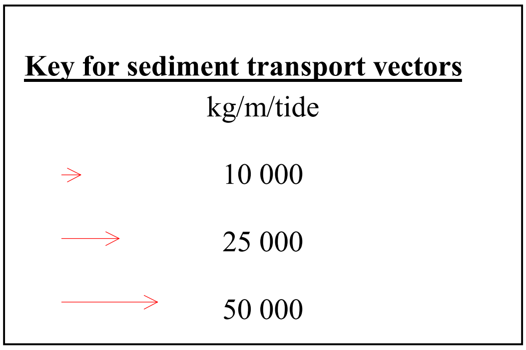

Figure 27 shows the net spring tidal residual sediment flux for 0.1mm sand. There is a strong southerly flux of sand past Flamborough Head and along the Holderness coast, and the transport across the seabed offshore the mouth of the Humber is relatively strong and southerly. This trend continues down the Lincolnshire coast and there is a significant influx into the Wash through the main deep water channel. Transport along the north Norfolk coast is eastwards round as far as Great Yarmouth. From Great Yarmouth to the Outer Thames there is a general northerly flux within the main coastal strip (i.e. 20km from the shore). The Outer Thames region is relatively disorganised, with complex flux circulation patterns around the linear banks. The drift on the North Kent coast is relatively weak and immediately adjacent to the East Kent coast there is a net northerly flux. Figures 28 to 38 show the same information at larger scale.

Figures 39 to 49 show the sediment transport patterns for 0.1mm sand for the spring tide currents calculated with the variable seabed roughness. Comparison with Figures 27 to 38 indicates a number of important features of this test. Although the flux in the deeper areas of the eastern part of the study area is not significantly modified, the transport around the English coast shows particular differences to that predicted with a constant roughness. The sediment flux in the Holderness to Wash region is not substantially modified (other than the transport rate magnitude). However, the net flux direction off Holderness has reversed well offshore and the drift offshore (>10km) past the North Norfolk coast is reversed to a northwest direction. Along the East Anglian reach the drift is stronger and reversed northerly, and whereas the Outer Thames region is not substantially modified there is now a strong southerly drift offshore (>10km) East Kent into the English Channel. This sensitivity test highlights those areas where the drift direction as well as magnitude may be variable.

Figure 50 to 61 show the peak sediment transport rates for 0.1mm sand during a spring tidal cycle, which may correspond more directly with the orientation of bed features mapped during this study. It is interesting to note that the pattern is comparable with the net transport (Figure 27), and that the pattern of flux around the North Norfolk banks off Great Yarmouth is complex. This ties in with the information resulting from the seabed features analysis.

Figure 62 to 73 show the sediment transport rates for coarser 0.4mm sand. The overall pattern of transport is predominantly similar to those for the fine 0.1mm sand, the magnitudes are generally lower and some detailed circulation patterns are slightly different.

The transport of gravel is limited to the higher energy areas of the model domain (Figures 74 to 85). There is the potential for southerly transport to the north of the Humber entrance and also outside the Wash. Off the North Norfolk coast the transport is generally northwesterly and off Orford Ness also northerly. In the south the transport is generally south through the Straits of Dover. Increasing levels of wave action would increase the transport rate and expand the potential area for gravel sized materials to be transported.

Figures 86 to 97 show the sediment flux patterns for 0.1mm sand under neap tides. The most striking feature is the lower transport rates over most of the study area, but that the direction of transport is generally similar to that under springs within 5km of the coastline. Further offshore (e.g. off Holderness) the direction of the net transport becomes reversed.

Figures 98 to 145 present the simulation of 0.1mm sand transport under spring tides but with wave enhancement (for the four wave conditions given in the table above). The general effect of the wave enhancement is to increase the magnitude of the transport rate, although the net direction can also be modified (by changing the proportions of the gross transport in each direction). The figures show that the transport rate increases with wave height and also with wave period, which is to be expected. Under the 5m storm wave conditions the transport rate is increased over much of the study area by an order of magnitude or more. It should be remembered that wave breaking effects are not included in the simulation.

A test of the influence of storm surge on transport rate was undertaken, with both 0.1mm sand (net and peak) and gravel simulations, and the resulting patterns of transport are presented in Figures 146 to 181. Interpretation of the surge condition simulated is given in the Appendix 13 to the main Sediment Transport Report. For these tests SANDFLOW was run using tidal currents which included the wind stress during the time of the surge, and 5m 10s waves were assumed to occur over the study area. In both cases the sediment transport under this surge condition is dominated by southerly drift (as also for the fine sediment transport approximated as the net tidal residual velocity). The flux magnitude of the 0.1mm sand fraction is an order of magnitude higher, and greatest over the southern part of the Southern North Sea from North Norfolk through to the English Channel. The transport of gravel is also significantly enhanced, where the conditions mobilise the gravel over a much larger area than due to spring tide current action alone. Areas of specific interest for the enhanced flux are off the mouth of the Humber (Figure 148), east of the Wash and along the North Norfolk coast (Figures 149 and 150), down through the banks off Great Yarmouth (Figure 151), off Suffolk and Essex (Figures 152 and 153) and around East Kent (Figure 156).

The interpretation of the conditions simulated are presented in Appendix 13 of the main Sediment Transport Report.

2.6.3 Integration of sediment fluxes through model boundaries

The calculated sediment fluxes (sand and gravel) for the various scenarios were integrated across strategic boundaries shown in Figure 182. The resulting quantities are presented in Figures 183a to c, where the convention is that a positive flux is eastwards or northwards, and a negative flux is westwards or southwards. As can be seen from Figure 182 the transects were of considerably varying lengths:

North	185.2km
South	68.7km
East	304.6km
Thames	21.9km
Humber	20.0km
Wash	32.1km

This means that the total magnitude of the fluxes will vary between transects and it is the relative behaviour of the sediment flux at each transect line for the different sediment grades and levels of forcing that is of primary interest. The integrated net tidal flux in kg/tide is plotted as a histogram for all the scenarios run for the standard bed roughness of 0.1m, with the results from the spatially varying bed roughness condition (Section 2.4) presented for comparison.

The Wash is subject to net influx for all conditions, and wave activity is significant in increasing this flux (Figure 183c). The surge condition increases the flux into this basin still further. Conversely, the Thames (Figure 183b) and Humber (Figure 183c) are net exporting sediment, except for during surge events. For the tide plus wave conditions the increasing wave action gives rise to higher sediment concentrations which can be exported by the tidal flow. Full wave effects are not included in these simulations. The surge event includes modifications to the tidal dynamics by atmospheric pressure fields and wind stress and hence is expected to be more realistic of the high energy events. Through the northern model boundary the flux is southwards, for all cases simulated, although the surge event gives rise to lower flux than "normal" conditions due to a northerly flux offshore. Through the southern boundary the flux direction varies from being northerly under tidal and low wave conditions switching to southerly under increased wave action. The surge event gives rise to a strong southerly flux through this boundary. Finally, through the eastern boundary (which is not demarked by any specific physical criterion) the flux is low in magnitude and variable in direction (east or west). Under surge conditions the flux is strong westerly due to the influx of sediment across this line at an acute angle in the southern part of the study area (Figure 146).

The results of these integrations indicate the level of variability that might be expected in the sediment flux across a particular transect. For the North boundary sediment flux is always to the south, including the predictions from spatially varying bed roughness, but the magnitude varies. For the South boundary the flux is to the north for all sediment grades modelled, switching to the south under increasing wave height and with the surge condition; it also switches to the south for the variable bed roughness case under tidal conditions alone. The East boundary has a net easterly movement of sediment except for the case with the variable bed roughness and the simulated surge. The Thames and Humber are both net exporters of sediment, except under surge conditions. The detailed estuary processes are not reproduced in this model and hence the results may not be reliable as it is considered likely that both estuaries are accreting material even if not at a very fast rate. What is significant however is the influence of the surge storm tide in reversing the flux so that it is directed into these estuaries. The results for the Wash are always for a flux into the embayment which is in general accord with recent historic experience of sediment accretion.

3 LOCAL AREA SIMULATIONS

3.1 Introduction

Model simulations were undertaken at two local areas within the study limits: the regions around Winterton Ness and around Gunfleet Sands. These were two regions identified in the consultation exercise as locations where additional knowledge on the sediment transport pathways was desired.

The sediment transport processes around Winterton Ness are dependent on both wave action and tidal currents. Of particular interest at this location was the evidence for any linkage between the coastal zone and the banks that extend south from this region. Given the range of processes operating at this location, fully integrated wave transformation, wave breaking and tidal current modelling was undertaken.

At Gunfleet Sands, the aim of the study was to inform on the sediment transport pathways, with particular focus on the confirmation or otherwise of a linkage between the coast on the Clacton-Jaywick frontage and Gunfleet Sands. This linkage had been postulated in the Phase 1 studies as a means of "closing" the sediment budget following an appraisal of littoral drift on this stretch of coastline. In this case, although littoral processes and sediment transport over the bank are likely to be dependent on wave activity, the deep area between (known as the Wallet) is dominated by tidal action. Accordingly, in order to assess the sediment transport pathways in this region the regional flow model was refined in this area and tidal sediment transport processes were simulated.

3.2 Winterton Ness sediment transport assessment

3.2.1 Introduction

Combined wave and tidal sediment transport pathways were required to be simulated. This was undertaken using the HR Wallingford model PISCES. PISCES is a state-of-the-art, fully-interactive coastal area modelling framework, capable of simulating the various processes of wave propagation, current distribution, and the resulting sediment transport in complex coastal areas.

For this study PISCES comprised the wave propagation model, COWADIS in combination with the finite element flow model TELEMAC and the SANDFLOW sand transport model. The application of PISCES comprised setting up a bathymetric database, selection of specific input wave conditions for simulation, calculating the corresponding currents and sand transport pathways and analysing the results. A consequence of detailed model resolution and sophistication of the models means that it is not usually possible to model all wave conditions in a particular climate, and in any event this would not be a practical option since the sequence of wave conditions is not known. Accordingly, PISCES is used to model representative patterns of drift for a selection of waves and the results are integrated to yield the gross and net longshore drift. The considerable experience of HR Wallingford was applied in the selection of wave conditions to be representative of this total littoral drift.

During the field survey a fluorescent tracer study was undertaken off Winterton Ness (Appendix 6 to the main Sediment Transport Report), to provide more detailed information on the sediment transport pathways. This findings of this study were that, of the tracer recovered, more was found to the north of the source than to the south.

3.2.2 Model Setup

A local model was set up centred on Winterton Ness, and extending approximately 5km along the coast to the north and south (Figure 184), and including the northern-most part of Cockle Shoal/Scroby Sands. Bathymetry for the model was extracted from the bathymetric database used in the regional modelling, as derived from Admiralty Charts.

The tidal boundary conditions chosen to run this model were extracted from the regional model, in the form of elevations at the north shore normal boundary and along the offshore boundary, and velocities along the southern shore normal boundary.

Wave conditions throughout the model area were modelled with the COWADIS model, which simulates the propagation of waves specified along the offshore boundary. Wave conditions were taken from an offshore wave climate derived in a previous study, for the period 1988-1994, which is listed in Tables 1 and 2. The objective in this study was to simulate the effects of wave-generated currents in combination with the tidal currents on the sediment transport pathways. Representative wave conditions were derived using a technique developed by HR Wallingford that filters the average annual climate into single wave conditions for each directional band. This technique is described in Annex 1, and the resulting conditions are presented in Table 3.

3.2.3 Model calibration

Field data collected during the course of this project is summarised in Appendix 6 to the main Sediment Transport Report. Using this data the parameters that are able to be tuned as part of the calibration process comprising the friction and eddy viscosity co-efficients were selected (values of k_s=0.01m and D=1m^2/s respectively).

Figure 185 shows a comparison of model currents with the ADCP measurements at five locations on13/14 April 2001. This figure indicates that the magnitude and direction of the model currents agrees well with the field measurements, although there appears to be a phase error of order 1 hour which is not explained. However, for the purposes of assessing the patterns of sediment transport it is concluded that the flow model was able to accurately reproduce the tidal current field.

3.2.4 Model simulations and analysis

Model simulations of the sediment transport patterns were performed for spring tide currents alone, and including the effects of the wave conditions described in Table 3. Figures 186 and 187 show peak flood and ebb spring tide currents, and Figures 188 and 189 show the same spring tide conditions in combination with waves from the north. Figures 190 and 191 show the same spring tide conditions with waves from the southwest quadrant 120N. Figures 188 to 191 show strong wave-generated currents along the coast where the waves break, whereas the offshore currents are dominated by the tidal conditions.

SANDFLOW was run for spring tide conditions and for spring tides with each of the wave conditions shown in Table 3. The median grain diameter was 0.2mm, based on information from a previous study (HR Wallingford, May 1999). The resulting patterns of sediment transport were integrated using the frequencies shown in Table 1 to yield a net pattern of sediment transport, scaled up to represent a whole year, as shown in Figure 192.

Figure 192 highlights a number of important aspects. The net direction of transport on the coast is southerly, and this is consistent with other information for this area (Hamer et al, 1998). In addition the transport rate north of Winterton Ness is greater than that to the south of the Ness, and this pattern is consistent with the fact that the Ness is an accretional feature. Further offshore the sediment transport rate is highest over the banks, with net northerly transport over Winterton Overfalls and net southerly transport on Cockle Shoal/Scroby Sands.

The magnitude of the littoral drift (net tidal flux) was analysed at three cross-shore profiles shown in Figure 193. These profiles highlight the narrow zone near the coast where the wave-induced transport dominates (500m to 1000m) under all wave conditions (waves from 0, 30, 60, 90, 120, 330°N). The magnitude of the longshore drift over the width of coastal zone where wave-driven transport dominates (indicated by the nearshore peak on the plots in Figure 193) was calculated and is shown in the table below.

Sand flux (Tonnes/year)	Northern profile (Nearshore 500m)	Central profile (Nearshore 1000m)	Southern profile (Nearshore 500m)
Gross North	440	2450	890
Gross South	9830	11740	3040
Net	9390	9290	2150

When considering these figures, it should be borne in mind that the sediment transport law used is generic according to Soulsby (1997) and has not been specifically calibrated for this site. Soulsby highlights the typical errors involved in sediment transport, and it is noted that a difference in the predicted and measured sediment transport of up to a factor 5 is not unreasonable. In addition, it should be borne in mind that the calculated sediment transport rates above represent the movement of sand over the nearshore and not only that which is transported on the intertidal area.

In order to assess the net annual sediment transport pathways sediment flux streamlines were calculated from the field presented in Figure 192. These streamlines are tracks that connect up the net sediment flux vectors and highlight the net movement of sediment (but not necessarily the movement of individual sand grains). Streamlines were calculated along a line extending offshore from Winterton Ness, and are shown in Figure 194. These indicate that the nearshore sediment transport pathways are southerly (consistent with Figure 192), whereas further offshore the tidally dominated transport is northerly. Significantly, there does not appear to be any evidence of direct exchange of sediment between the coast and the banks. This conclusion raises the question of the source of sediment for Scroby Sands, and an inspection of the transport patterns in Figure 192 suggests that there is a feed of sand from Winterton Shoal into Scroby Bank, and highlights the potential for northerly transport on the outermost banks supplying the nearshore Scroby Bank system.

3.3 Gunfleet Sands sediment transport assessment

3.3.1 Introduction

In order to investigate the sediment transport pathways between Gunfleet Sands and the coast at Clacton tidal sediment transport studies were undertaken. These consisted of repeat simulations of the regional model but with increased model resolution in the area around Gunfleet Sands and the coast between Jaywick and Clacton.

The principal aim of these studies was to examine the hypothesis of a direct sediment transport pathway between Gunfleet Sands and the coast.

3.3.2 Model validation

Field studies undertaken in this area are presented in Appendix 6 of the Sediment Transport Report EX4526, and provided current measurements from both Minipod and ADCP devices.

A comparison of measured spring tide currents from the Minipod and the TELEMAC flow model is provided in Figure 195, for a period spanning four tidal cycles. It can be seen that the magnitude of the currents is well reproduced, in particular the bias in the currents with stronger northerly (ebb) current than the southerly flow. Whilst the southerly current direction is well reproduced there is a discrepancy between the model and observations for the northerly current, which may be due to local seabed features not resolved by the flow model.

A comparison of measured spring tide currents from the ADCP and the flow model is presented in Figure 196. This also demonstrates good reproduction of the currents by the TELEMAC flow model, with generally good agreement between the currents speeds and directions. The value of seabed roughness used in this local modelling was smaller than the value with the regional model (0.01m as opposed to 0.1m). Validity of the use of this value of roughness is justified because the model mesh is smaller so that greater bathymetric detail is represented and also the seabed in the Wallet comprises London Clay which has a smoother surface than sand ripples.

3.3.3. Model simulations

Figures 197 and 198 show the spring tide peak flood and ebb current vectors, and highlight the general south-west/north-east tidal currents in the area of Gunfleet Sands, with currents generally running parallel to the coast. The tidal streams are stronger in the deep channels, and weaker over the top of the banks where friction is higher.

The spring tide net sediment transport patterns are presented in Figure 34, and indicate that through The Wallet (between Gunfleet Sands and Clacton) the net transport is to the north-east. Over Gunfleet Sands the transport rate is weaker, but is also generally to the north east over much of its length. In the south-western half of the bank there is a suggestion of movement across the main axis, but there is no evidence to suggest a transport pathway between Gunfleet Sands and the coastline between Jaywick and Clacton under tidal conditions nor directly under large storm waves (e.g. Figure 141) although, as would be expected, there is evidence of cross bank transport.

References

Cameron, T D J, Crosby, A, Balson, P, Jeffrey, D H, Lott, G K, Bulat, J and Harrison, D J (1992). United Kingdom offshore regional geology report: the geology of the southern North Sea. London, HMSO for the British Geological Survey.

Hamer, BA, SJ Hayman, PA Elsdon, and CA Fleming (1998). Happisburgh to Winterton Sea Defences: Stage two. Coastlines, Structures and Breakwaters. Allsop (Ed). Thomas Telford.

HR Wallingford (1999). Simulation of the sediment budget for the Happisburgh to Winterton Reefs, PISCES application study, HR Wallingford report TR83, May 1999

HR Wallingford (2001). Southern North Sea Sediment Transport Study, Phase 2. Inception Report. HR Wallingford report EX4341, March.

Odd NVM and Cooper AJ (1992). Calibration of a 20km gridded 3D model simulating representative winter and summer M2 tidal and residual currents. HR Wallingford Report SR287.

Williams JJ and Rose CP (2001). Measured and predicted rates of sediment transport in storm conditions. Marine Geology, Vol. 179 (1-2) (2001) pp. 121-133

Annex 1: Input filtering of wave climate information

A wave climate consists of many different components in terms of wave height, wave period and direction. Although a wave spectrum can be described in terms of representative parameters, such as significant wave height and mean period, all the components need to be taken into account, when the sediment transport is determined. This results in a large number of simulations and large amounts of computer time. In this annex a procedure for wave climate filtering is presented.

Firstly the incoming waves are grouped in discrete direction intervals. The size of the angle of incidence intervals depend on the information available, but typically 10 to 15 degree bands are appropriate. For each direction interval the approximate functional relationship between the littoral drift, Q, and the wave climate, H and T, is established. From these functional relationships it is possible to derive the factors 'n' and 'm' in

$Q \sim H^n$ for $H > H_{cr}$
$Q \sim T^m$

Where Q = Longshore sediment transport rate [m^3/s] and H_{cr} and T_{cr} are the critical values below which no sediment transport takes place.

On the basis of earlier studies, the following parameter values were determined:

$n = 4.3$
$m = 1.0$
$H_{cr} = 0.5m$

These values are applied as global default values in the absence of a site specific parameter study.

Given the parameter values above a representative wave height and period is derived using the following nonlinear averaging formulae;

$H_{repr} = [\sum f(H)H^n]^{1/n}$ for $H > H_{cr}$
$T_{repr} = [\sum f(T)T^m]^{1/m}$

The normalised frequencies of occurrence, f(H) and f(T), are obtained from the joint probability distribution of H and T.

Once H_{repr} and T_{repr} are found for the various discrete direction intervals, simulations are performed with only one set of parameters, namely H_{repr} and T_{repr}, rather than with the whole wave climate.

In effect the application of H_{repr} and T_{repr} for a given directional sector, will yield the same result, in terms of littoral drift, as the application of the entire joint probability distribution of H and T for that particular directional sector.

Although the method is based on a littoral drift situation, the techniques have been applied to other sediment process applications, including harbour entrance sedimentation, crescentic bay sediment transport, and port breakwater bypassing.

Table 1 Wave climate for offshore Winterton Ness based on HINDWAVE predictions for January 1988 – December 1994

H1	H2	P(H>H1)	Wave direction in degrees North											
			-15	15	45	75	105	135	165	195	225	255	285	315
			15	45	75	105	135	165	195	225	255	285	315	345
0	0.5	0.96066	1480	1351	1100	1305	5518	8087	2470	1462	2003	2267	6075	5007
0.5	1	0.57942	3484	1893	943	1235	3732	8602	401	192	678	710	3886	5651
1	1.5	0.26533	3530	2562	1234	999	2237	1395	5	2	24	20	647	3885
1.5	2	0.09995	1545	1496	724	482	539	41	0	0	0	0	46	1504
2	2.5	0.03619	270	396	228	173	103	2	0	0	0	0	2	455
2.5	3	0.01991	383	473	160	46	16	0	0	0	0	0	0	212
3	3.5	0.00702	254	168	2	0	11	0	0	0	0	0	0	86
3.5	4	0.00181	34	23	0	0	0	0	0	0	0	0	0	46
4	4.5	0.00078	16	0	0	0	0	0	0	0	0	0	0	0
4.5	5	0.00062	0	0	0	0	0	0	0	0	0	0	0	24
5	5.5	0.00037	0	0	0	0	0	0	0	0	0	0	0	33
5.5	6	0.00005	2	0	0	0	0	0	0	0	0	0	0	3
Parts per thousand for each direction			110	84	44	42	122	181	29	17	27	30	107	169

Table 2 Total number of hours = 61368 based on HINDWAVE predictions for January 1988 – December 1994

H1	H2	P(H>H1)	Peak wave period in seconds (Tp)															
			0	1	2	3	4	5	6	7	8	9	10	11	12	13	14	15
			1	2	3	4	5	6	7	8	9	10	11	12	13	14	15	16
0	0.5	0.96066	523	16166	4442	14159	1018	1815	0	0	0	0	0	0	0	0	0	0
0.5	1	0.57942	0	2058	924	10993	6580	7158	3696	0	0	0	0	0	0	0	0	0
1	1.5	0.26533	0	0	36	51	896	4786	8957	1625	187	0	0	0	0	0	0	0
1.5	2	0.09995	0	0	0	0	80	253	1889	3961	194	0	0	0	0	0	0	0
2	2.5	0.03619	0	0	0	0	2	18	104	636	869	0	0	0	0	0	0	0
2.5	3	0.01991	0	0	0	0	0	0	7	70	1212	0	0	0	0	0	0	0
3	3.5	0.00702	0	0	0	0	0	0	0	10	512	0	0	0	0	0	0	0
3.5	4	0.00181	0	0	0	0	0	0	0	0	103	0	0	0	0	0	0	0
4	4.5	0.00078	0	0	0	0	0	0	0	0	16	0	0	0	0	0	0	0
4.5	5	0.00062	0	0	0	0	0	0	0	0	24	0	0	0	0	0	0	0
5	5.5	0.00037	0	0	0	0	0	0	0	0	33	0	0	0	0	0	0	0
5.5	6	0.00005	0	0	0	0	0	0	0	0	5	0	0	0	0	0	0	0
Parts per thousand for each wave period			5	182	54	252	86	140	147	63	32	0	0	0	0	0	0	0

Table 3 Representative waves for Winterton Ness modelling

	Direction (N)											
	-15	15	45	75	105	135	165	195	225	255	285	315
	15	45	75	105	135	165	195	225	255	285	315	345
H rep (m)	1.83	1.88	1.69	1.52	1.28	0.91	0.77	0.76	0.79	0.79	0.93	1.81
T rep (s)	7.12	7.12	7.12	7.12	6.21	4.36	4.36	4.36	4.36	4.36	4.36	7.12

Figures

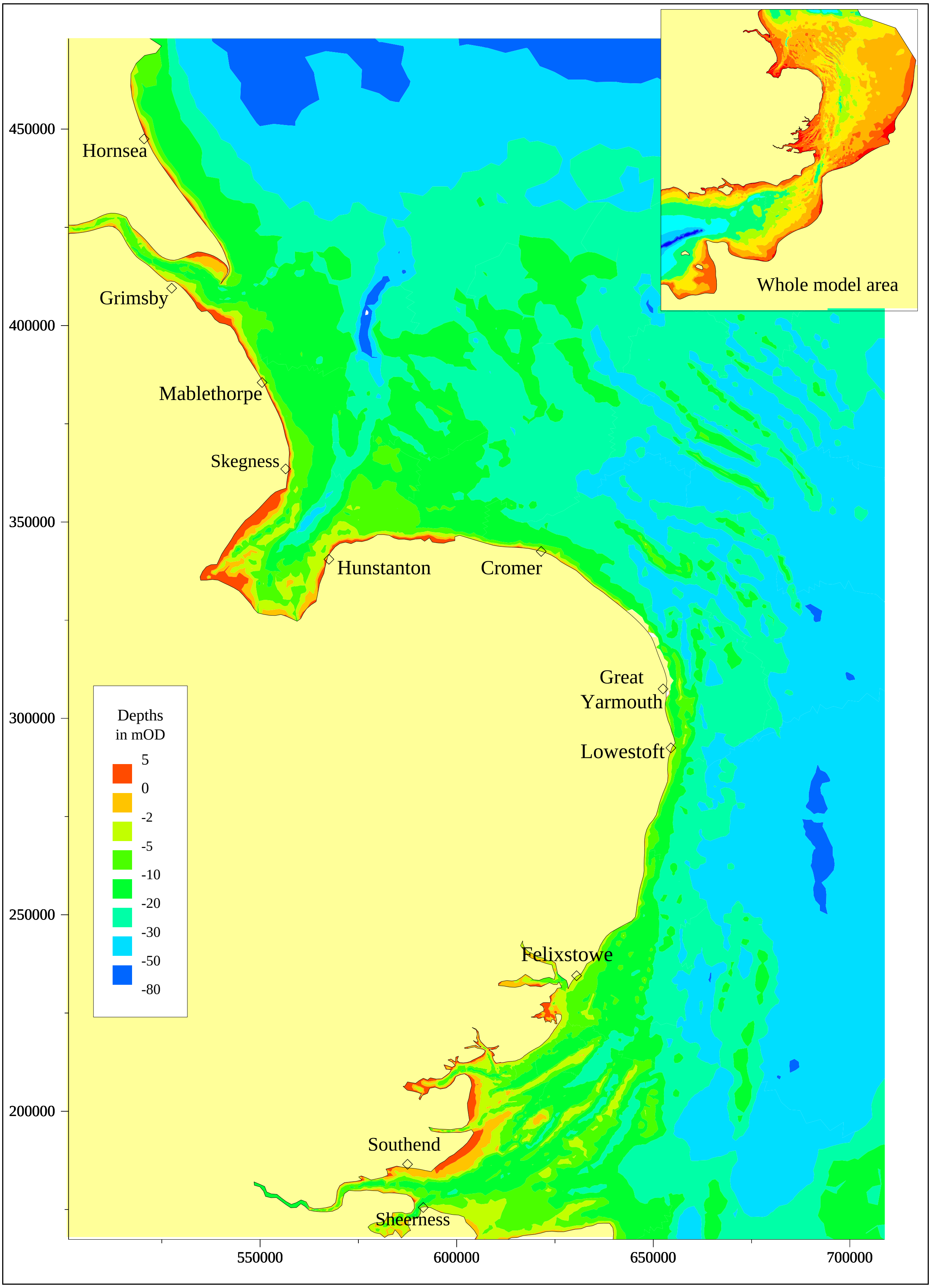

Figure 1 **Study area, showing model bathymetry, and insert showing whole model area**

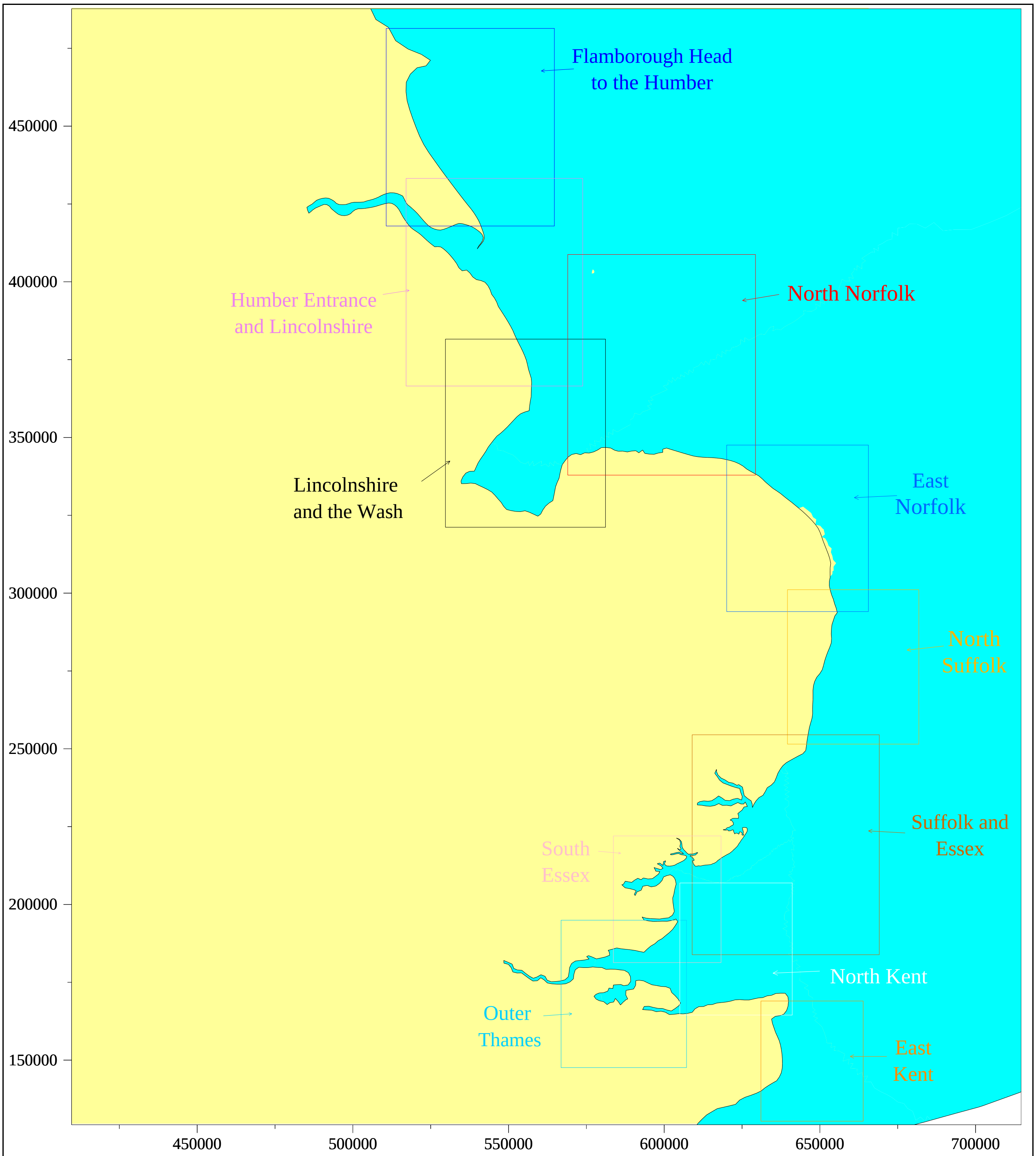

Figure 2 **Location map showing coastal areas for which results are presented in this report**

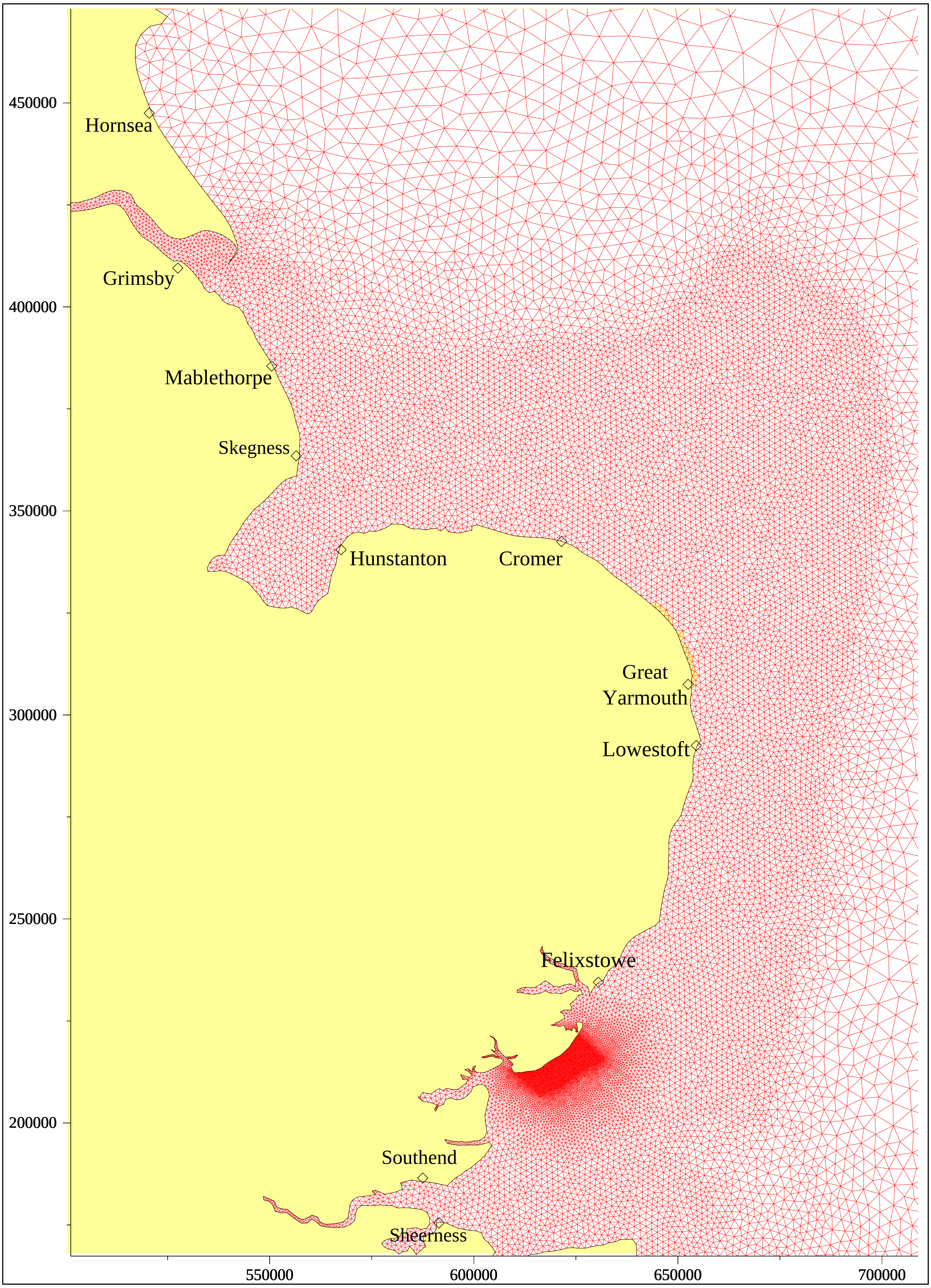

Figure 3 TELEMAC Regional model mesh

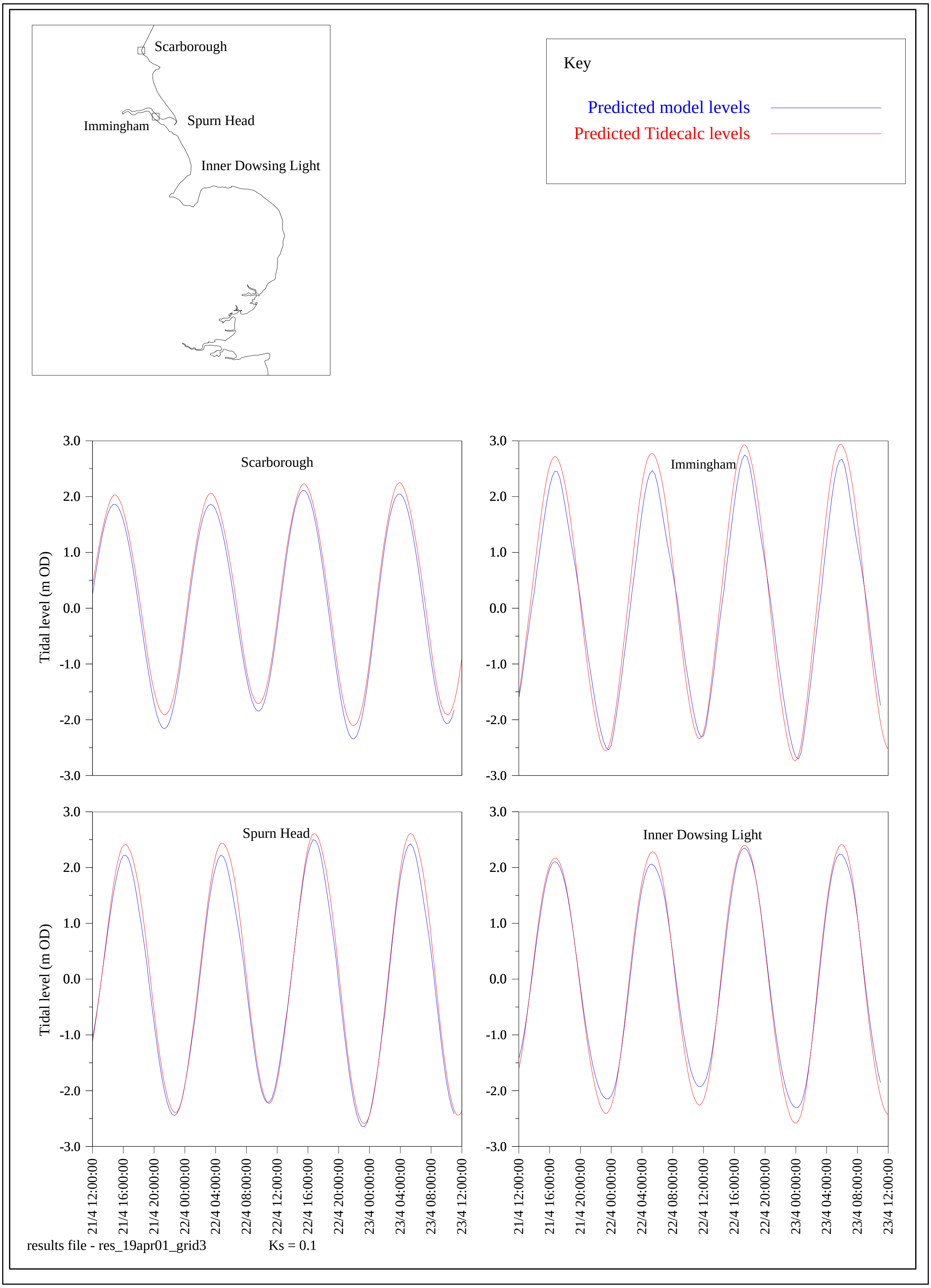

Figure 4a **Comparison with spring tide water levels from TIDECALC**

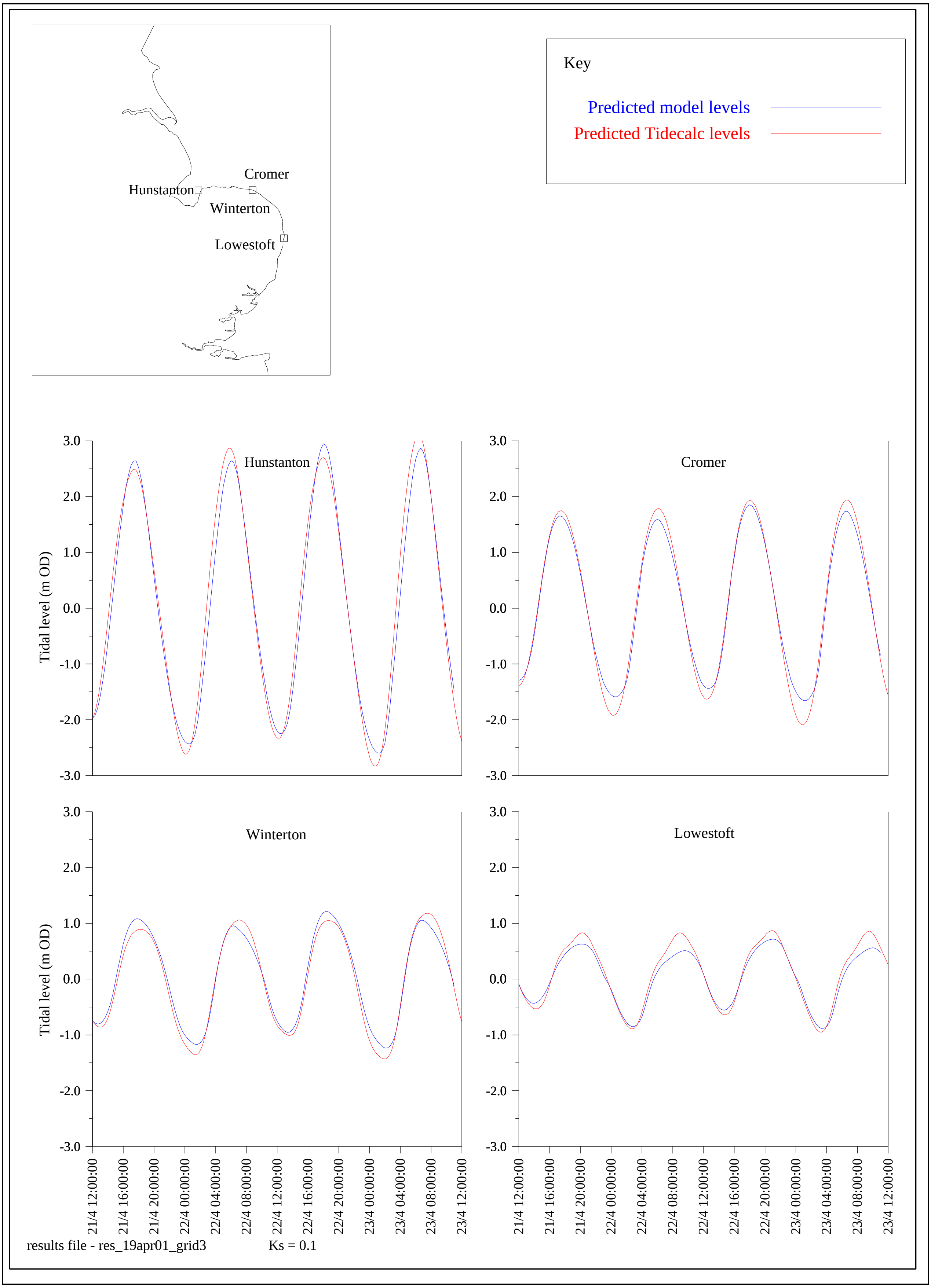

Figure 4b **Comparison with spring tide water levels from TIDECALC**

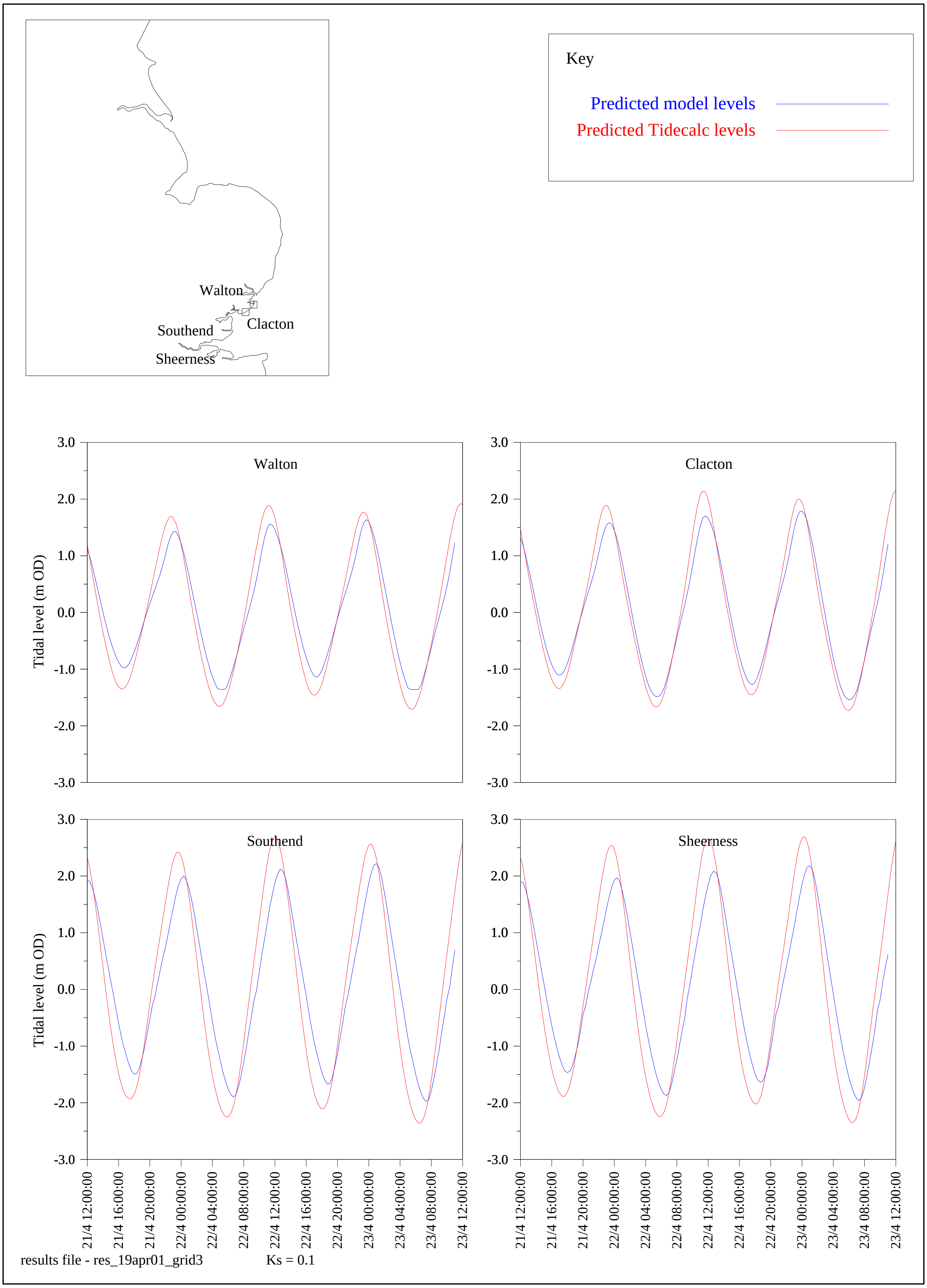

Figure 4c Comparison with spring tide water levels from TIDECALC

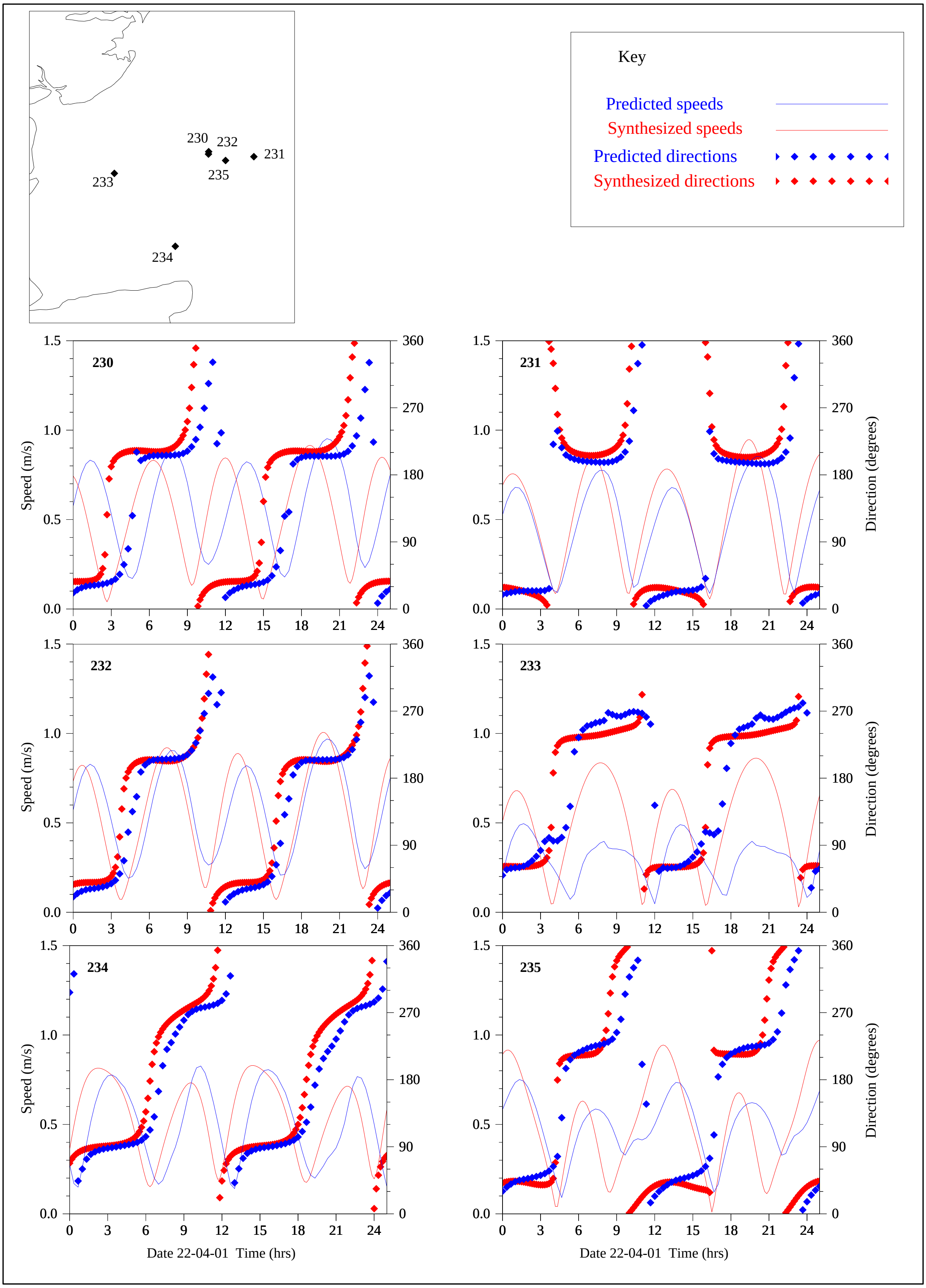

Results file - res_19apr01_grid3

Figure 5a Comparison with spring tide currents, derived from CEFAS field data archive

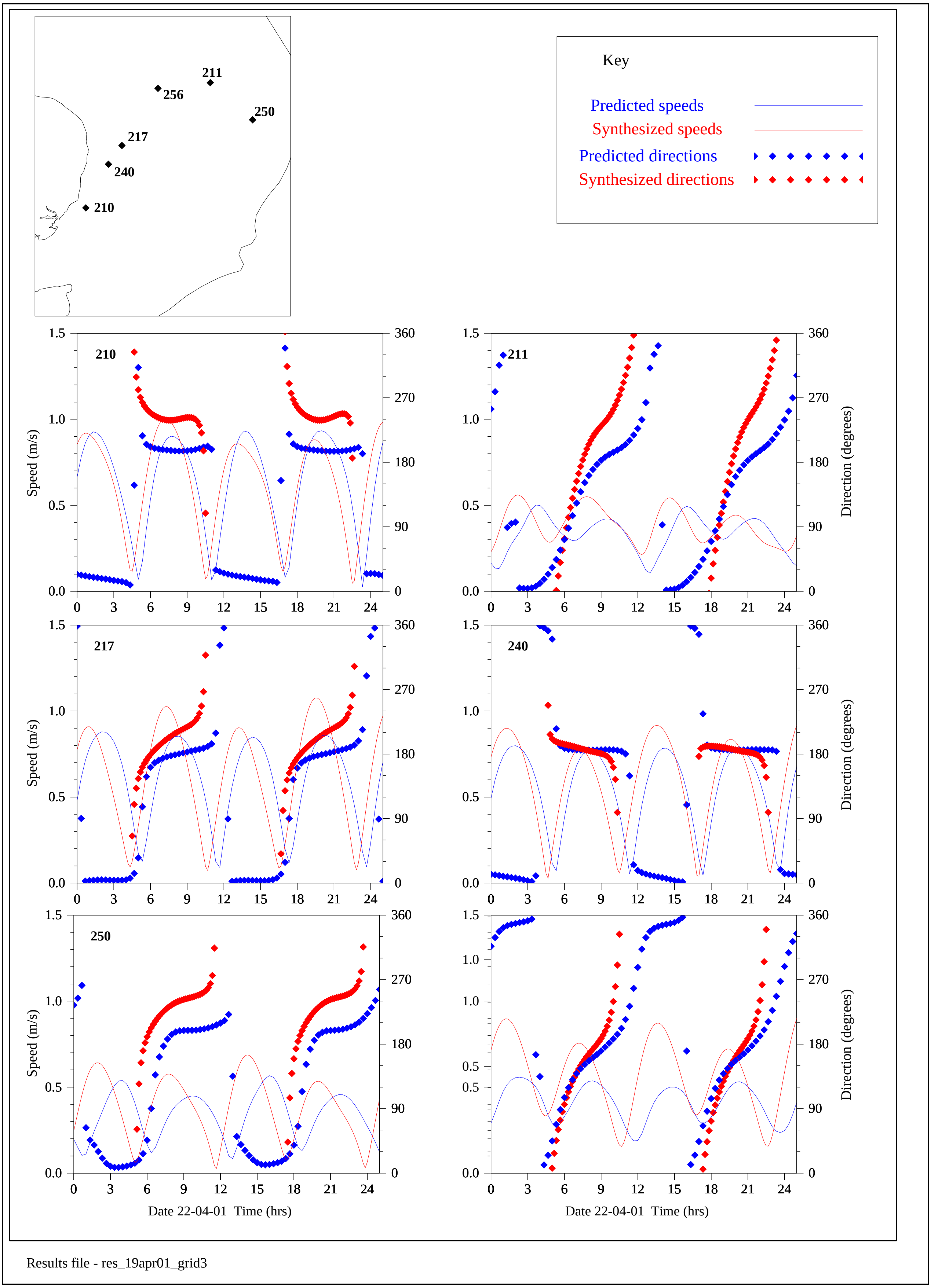

Figure 5b **Comparison with spring tide currents, derived from CEFAS field data archive**

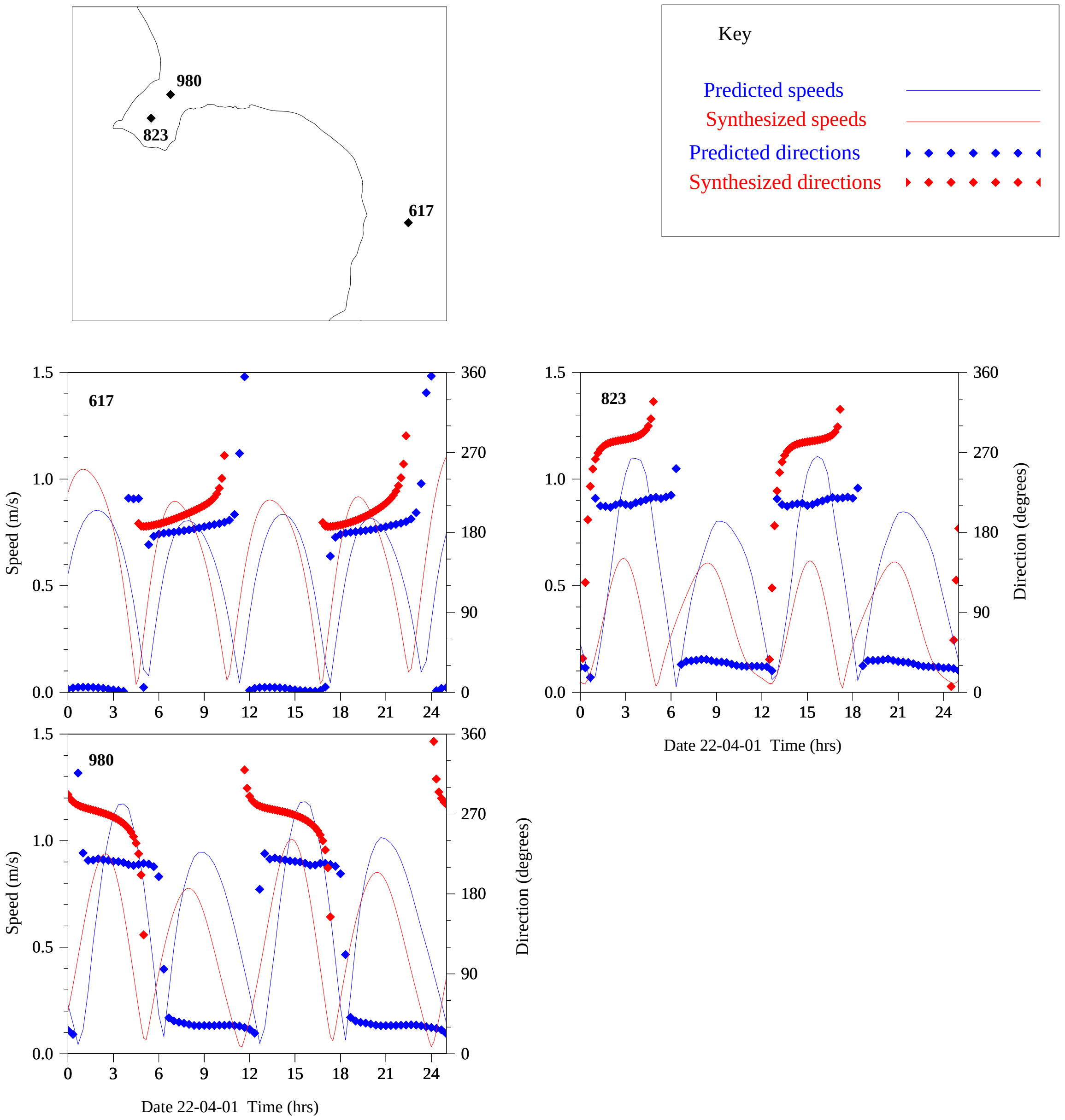

Results file - res_19apr01_grid3

Figure 5c Comparison with spring tide currents, derived from CEFAS field data archive

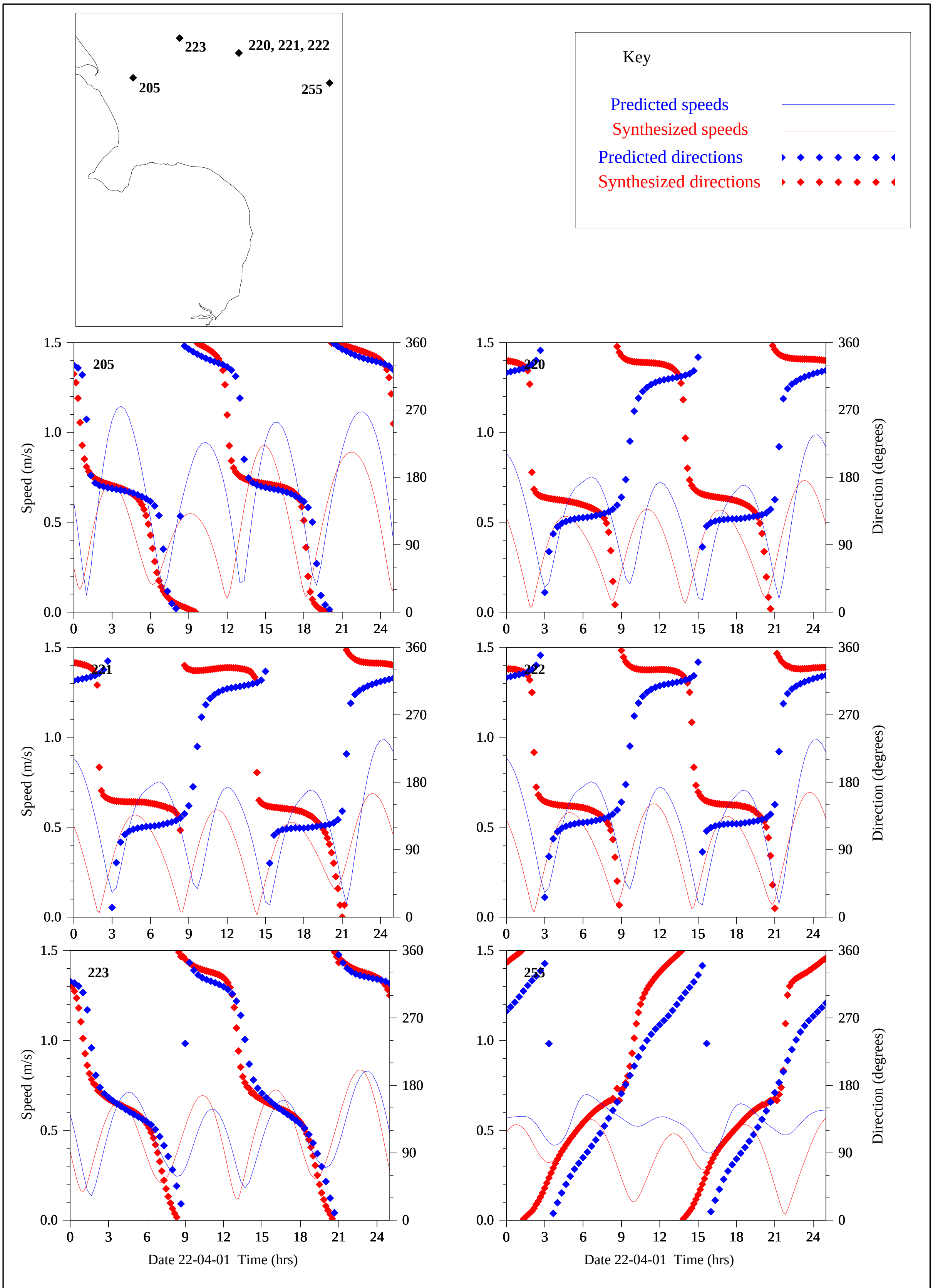

Results file - res_19apr01_grid3_s1

Figure 5d **Comparison with spring tide currents, derived from CEFAS field data archive**

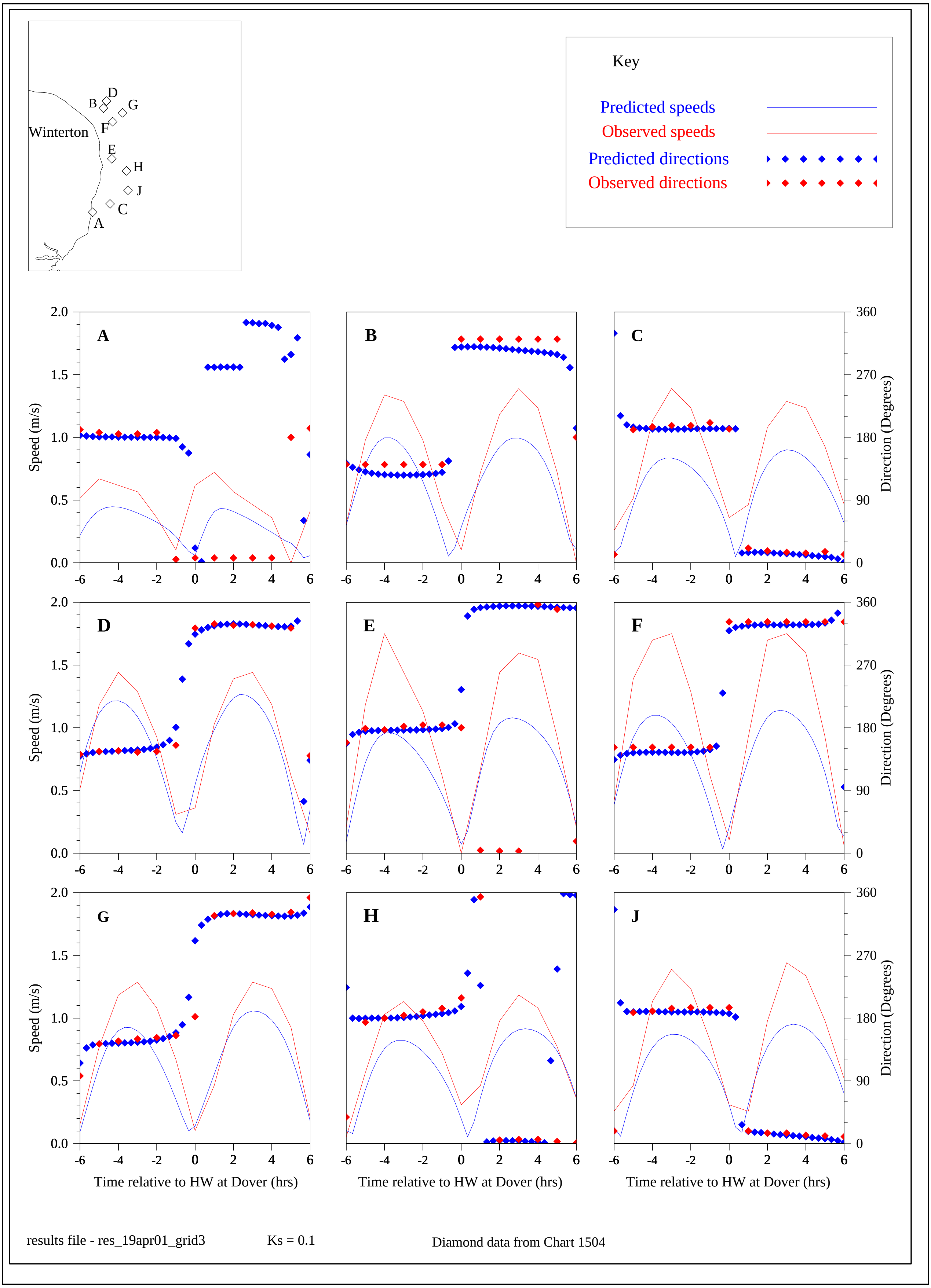

Figure 5e Comparison with spring tide currents, from Admiralty diamonds

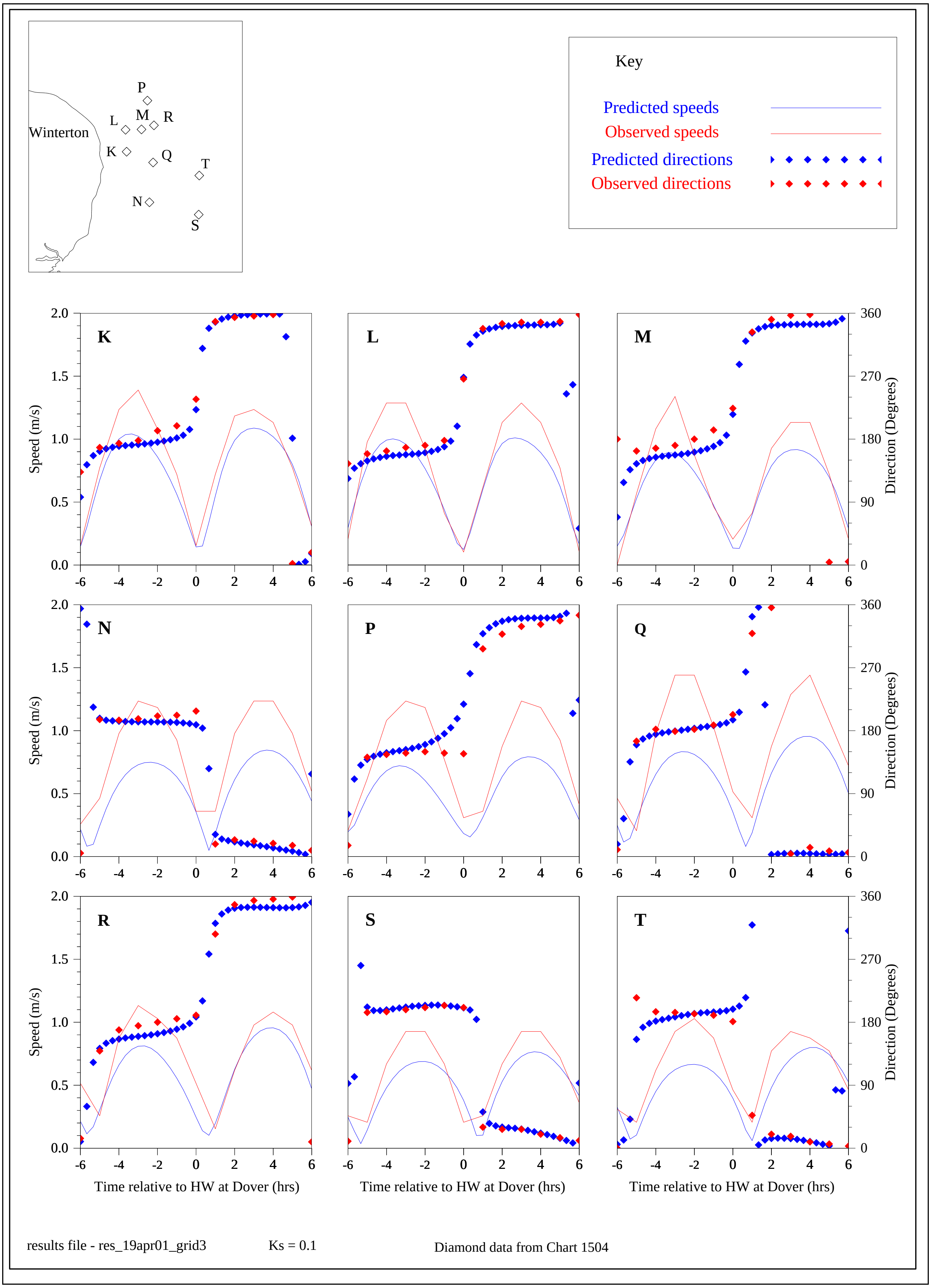

Figure 5f Comparison with spring tide currents, from Admiralty diamonds

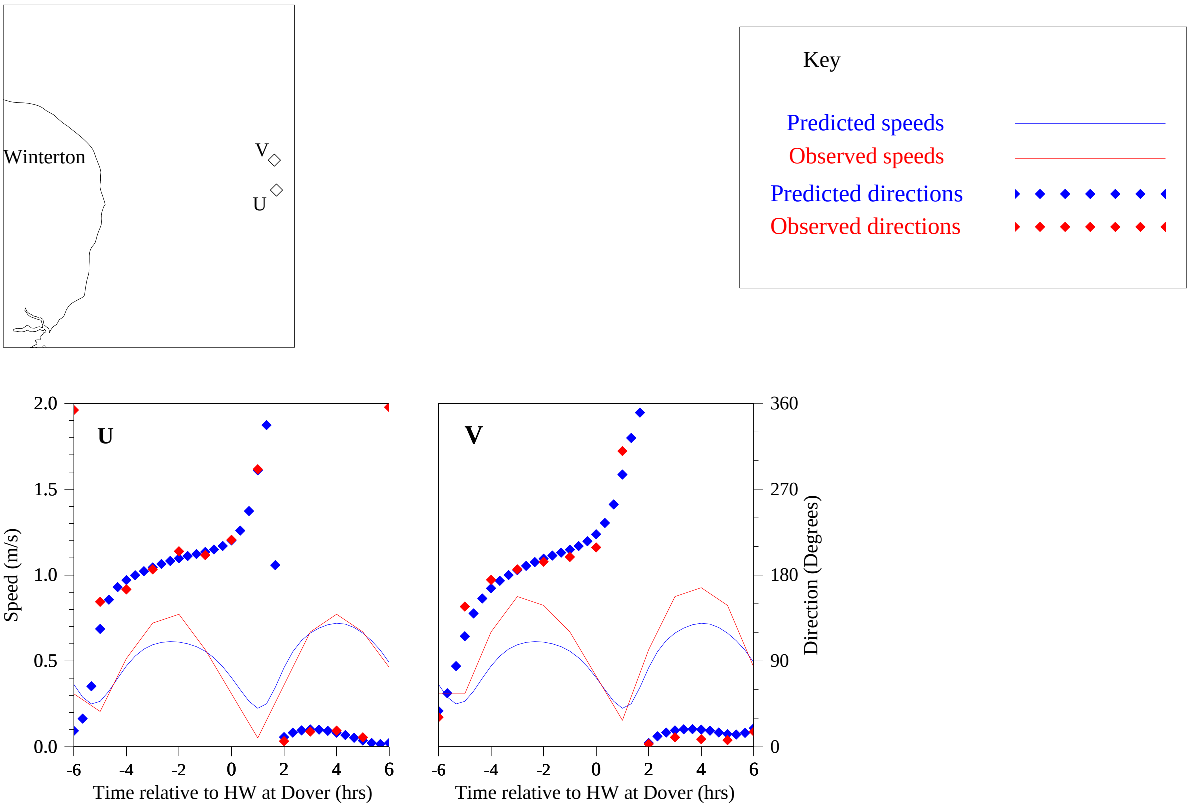

results file - res_19apr01_grid3 Ks = 0.1 Diamond data from Chart 1504

Figure 5g Comparison with spring tide currents, from Admiralty diamonds

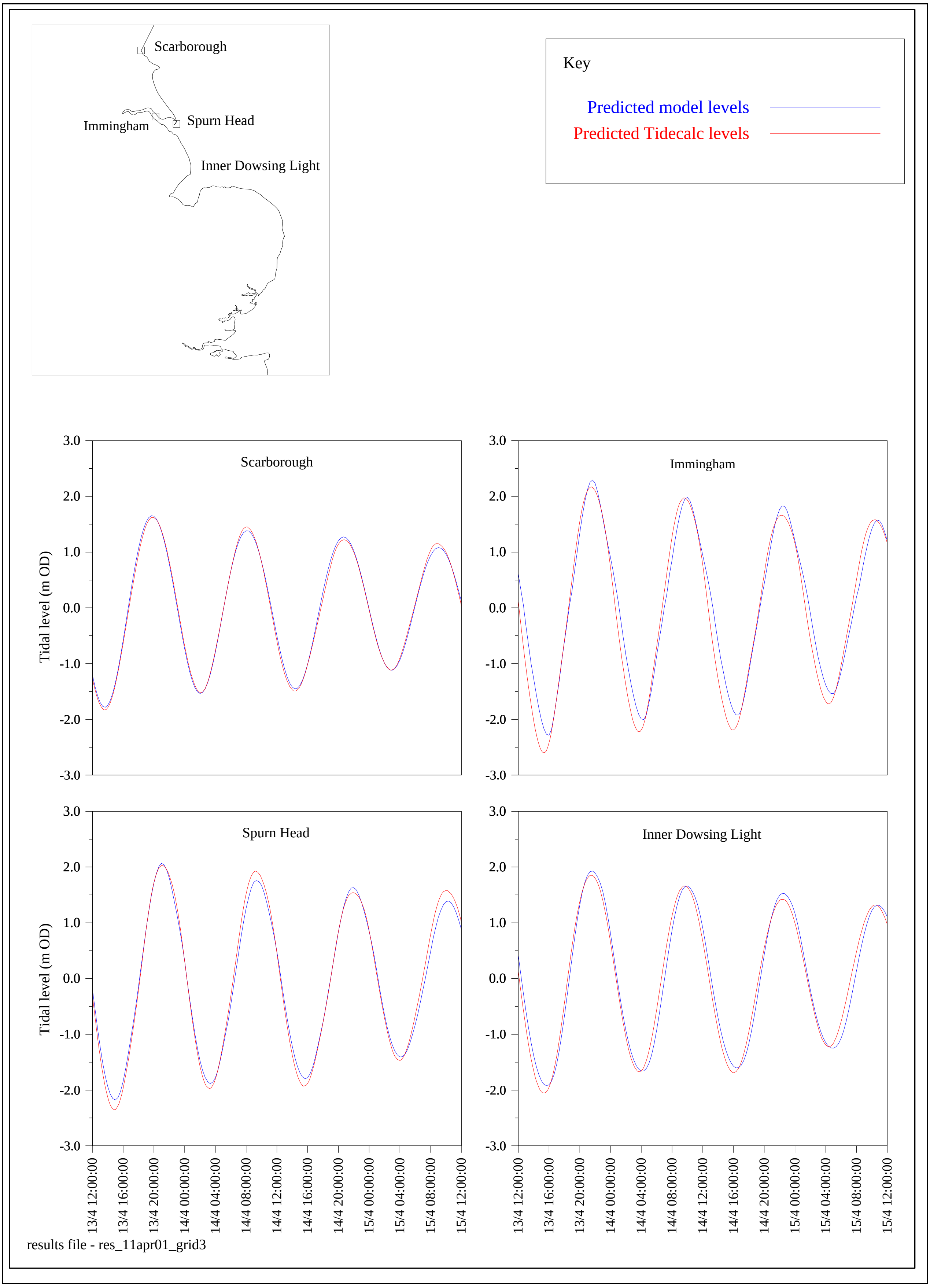

Figure 6a Validation with neap tide water levels from TIDECALC

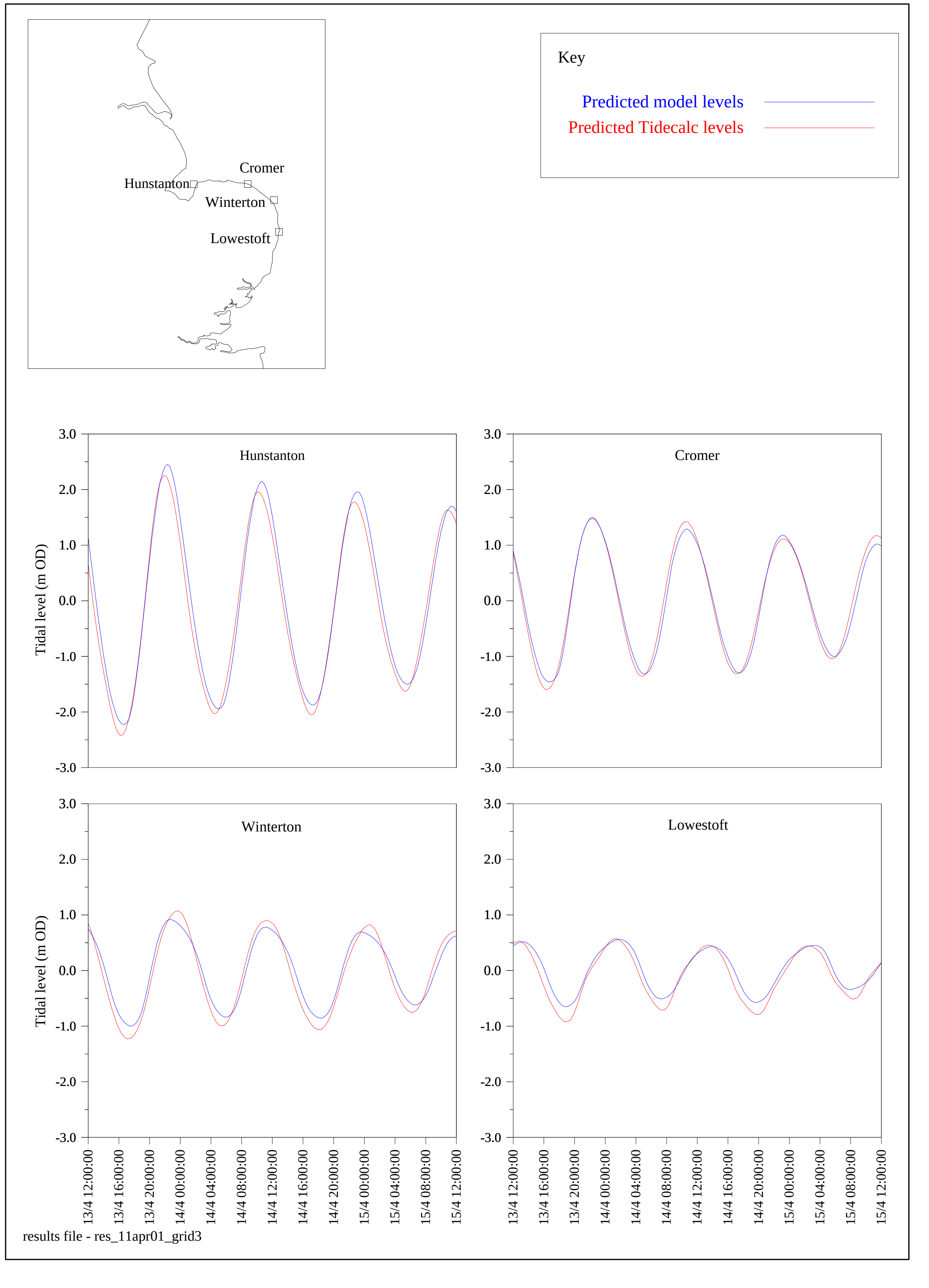

Figure 6b Validation with neap tide water levels from TIDECALC

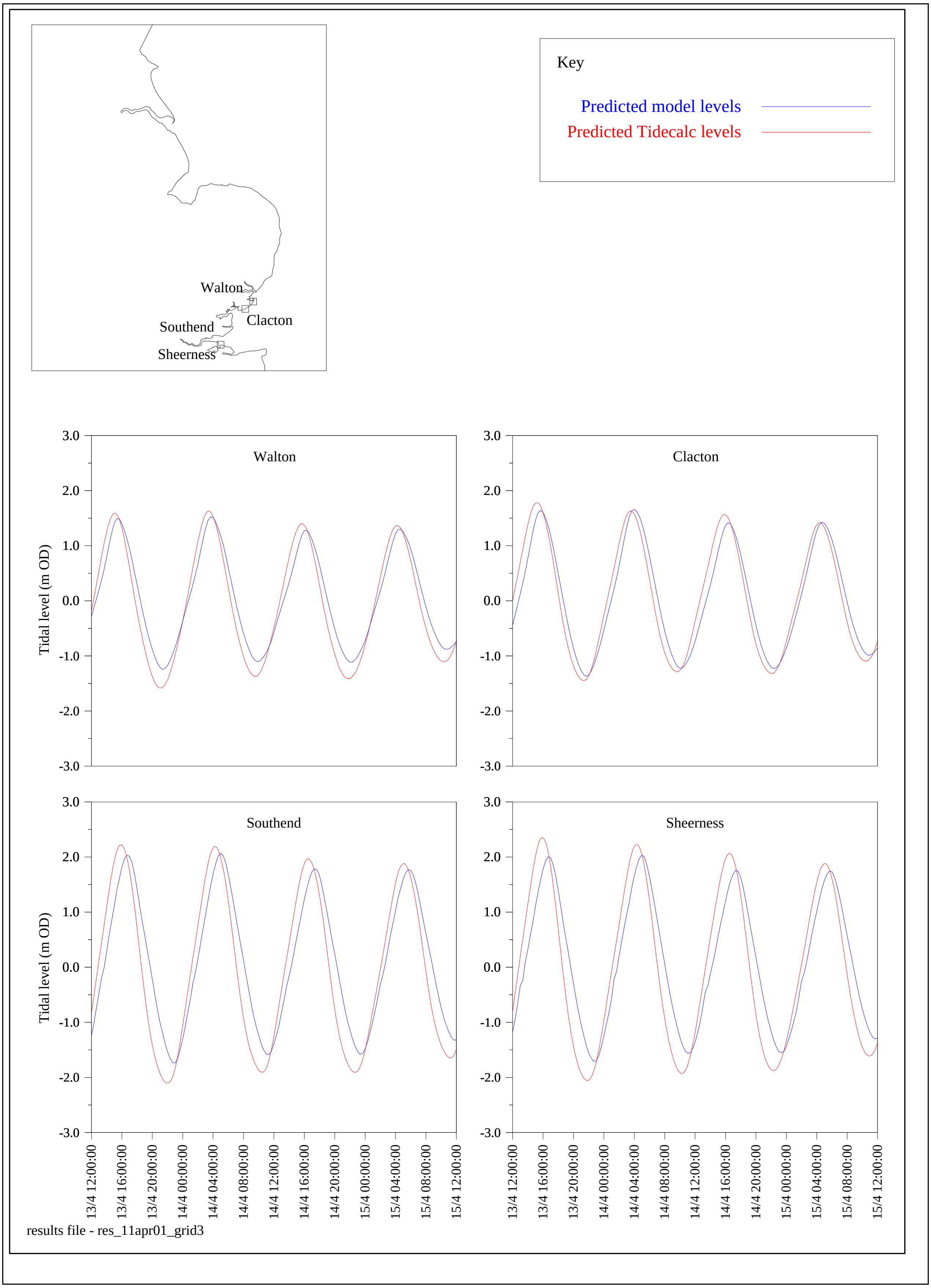

Figure 6c **Validation with neap tide water levels from TIDECALC**

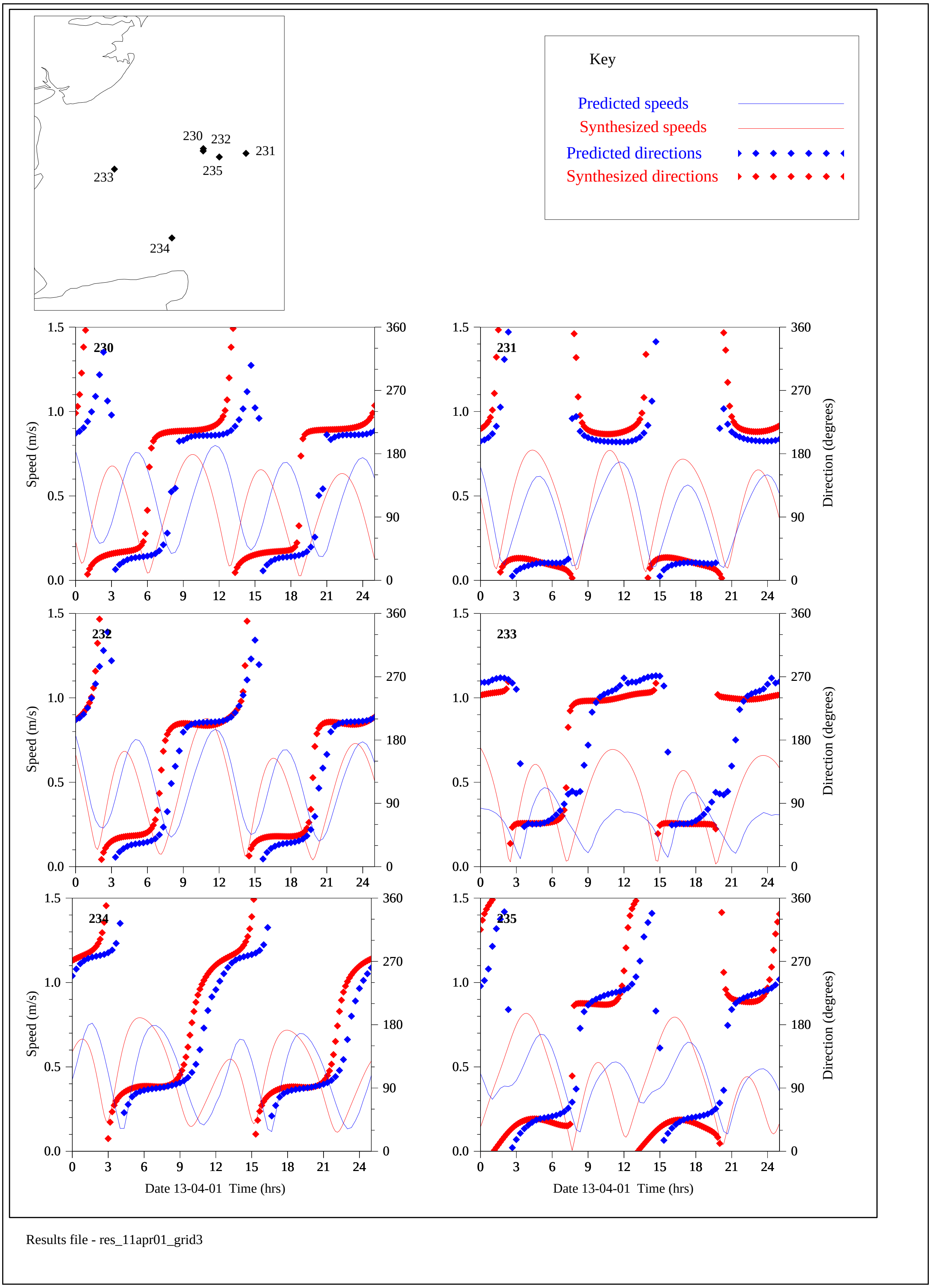

Figure 7a Validation with neap tide currents derived from CEFAS data archive

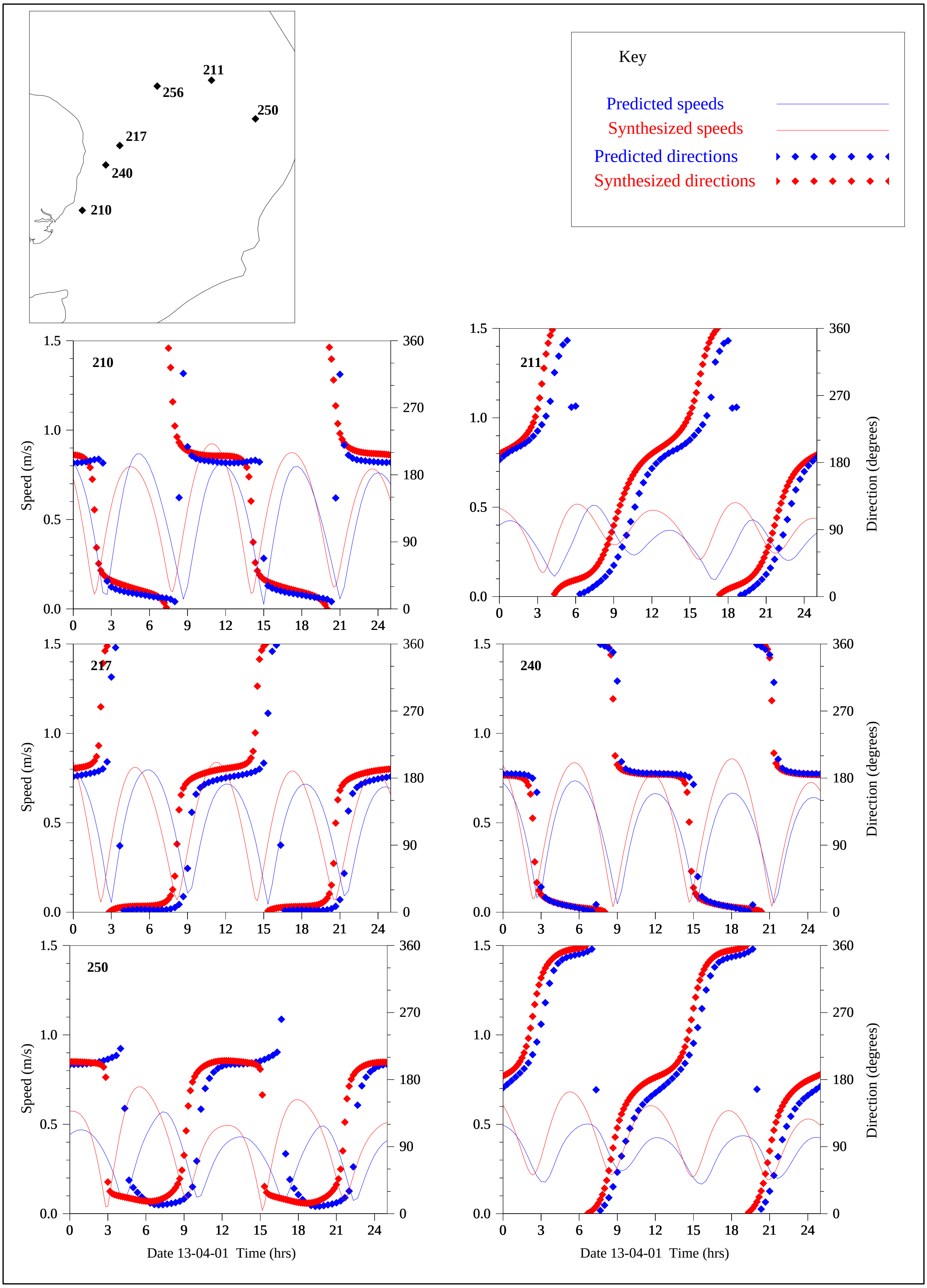

Figure 7b Validation with neap tide currents derived from CEFAS data archive

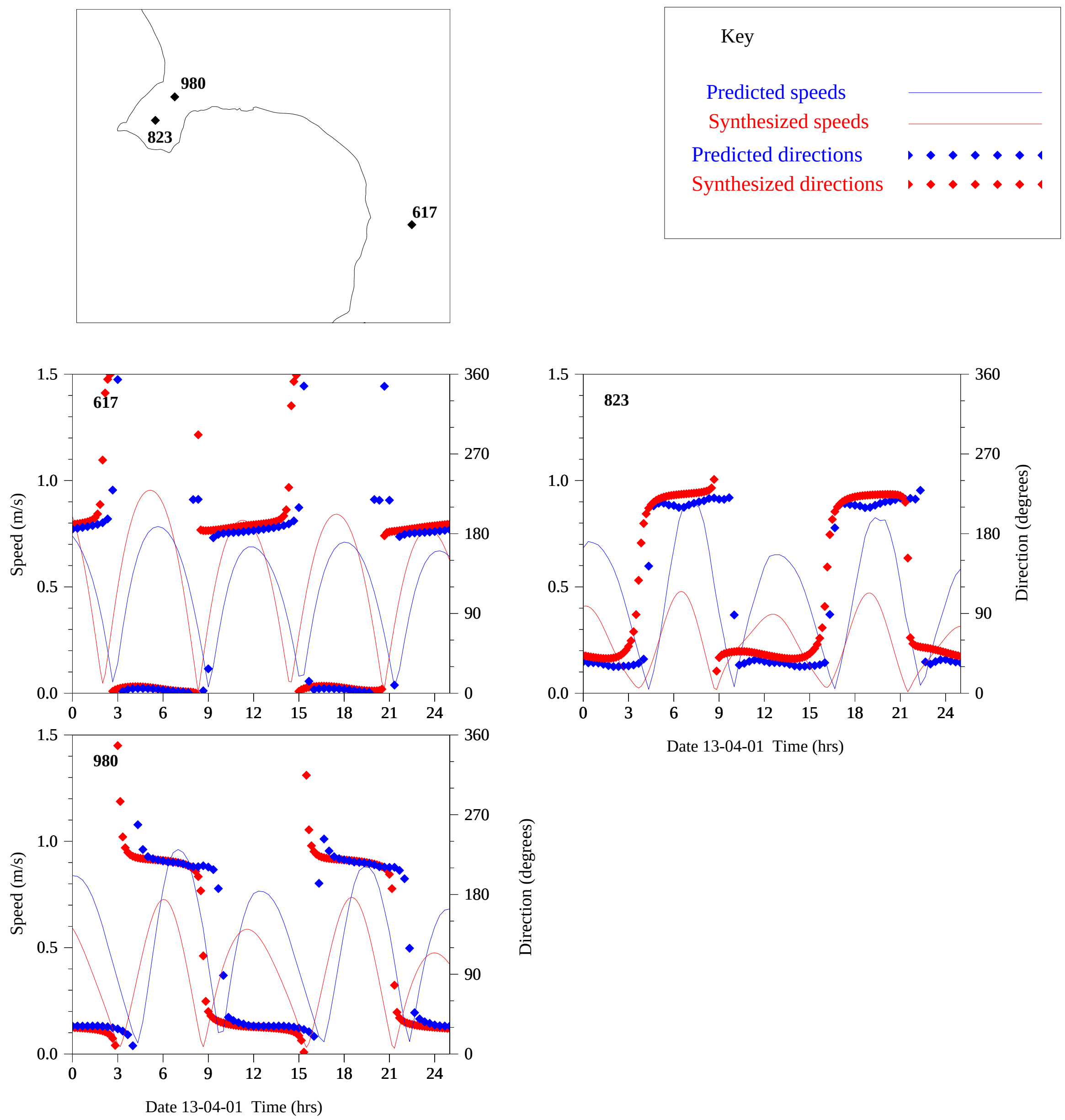

Results file - res_11apr01_grid3

Figure 7c Validation with neap tide currents derived from CEFAS data archive

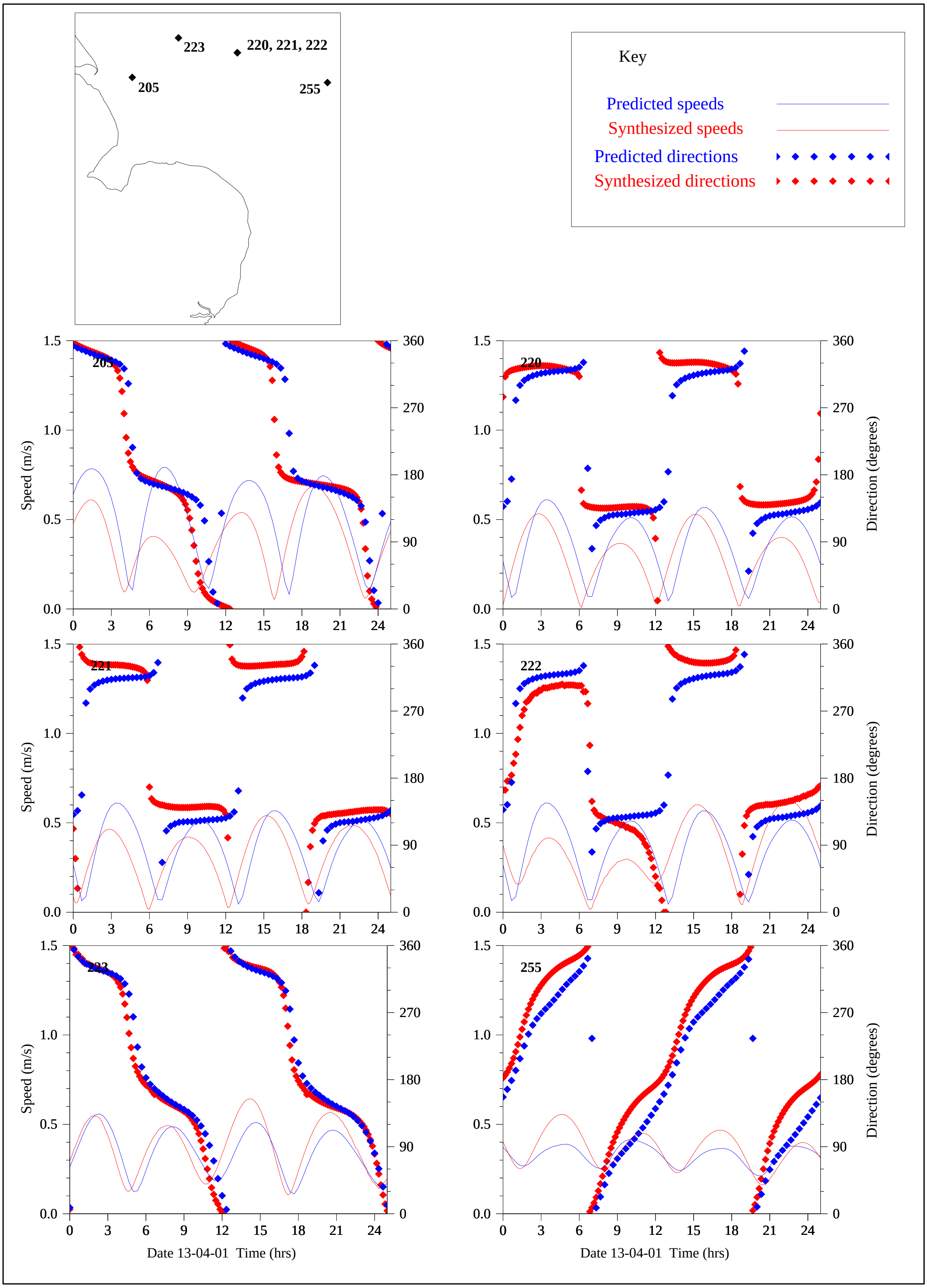

Figure 7d **Validation with neap tide currents derived from CEFAS data archive**

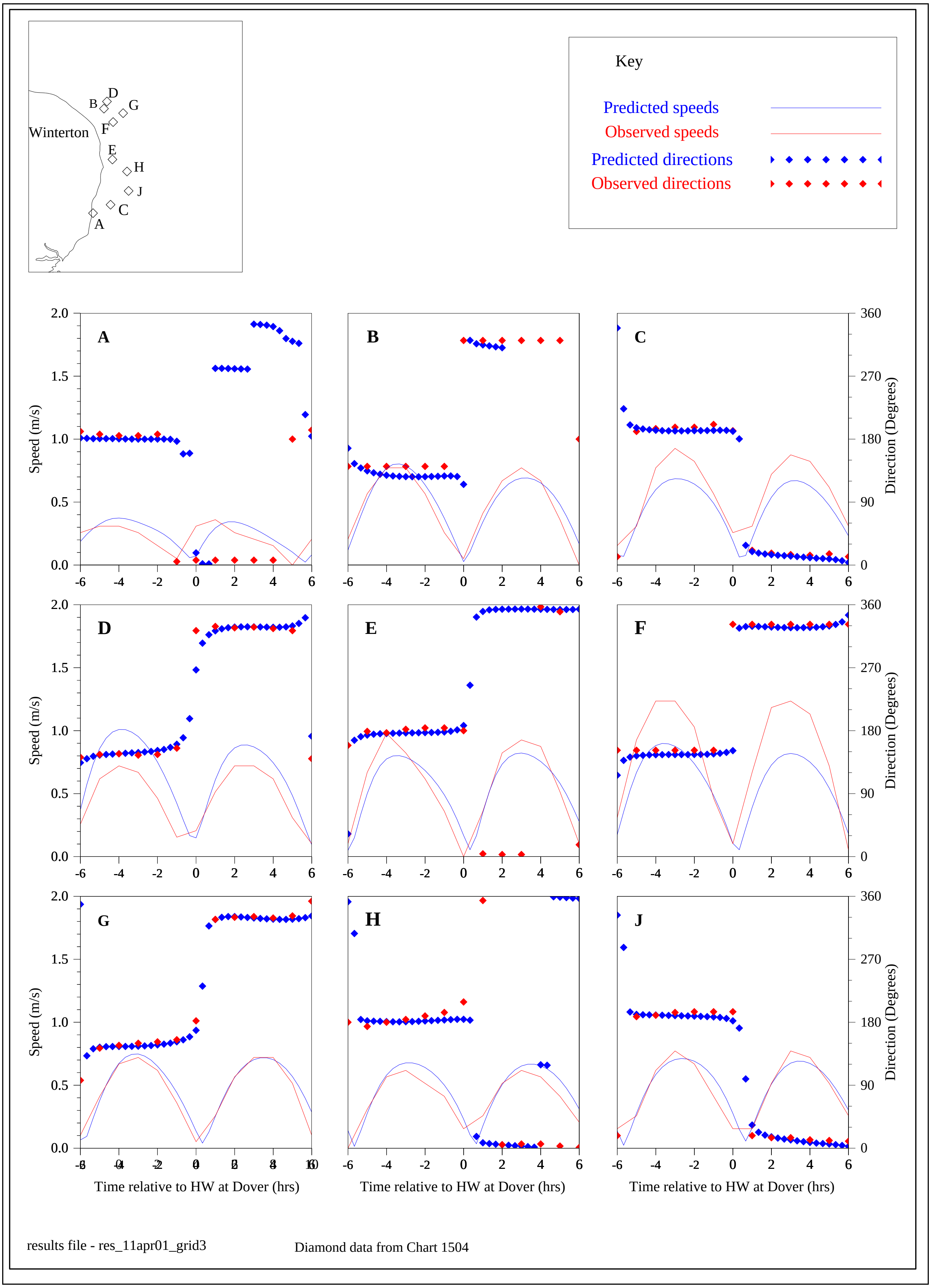

Figure 7e Validation with neap tide currents from Admiralty diamonds

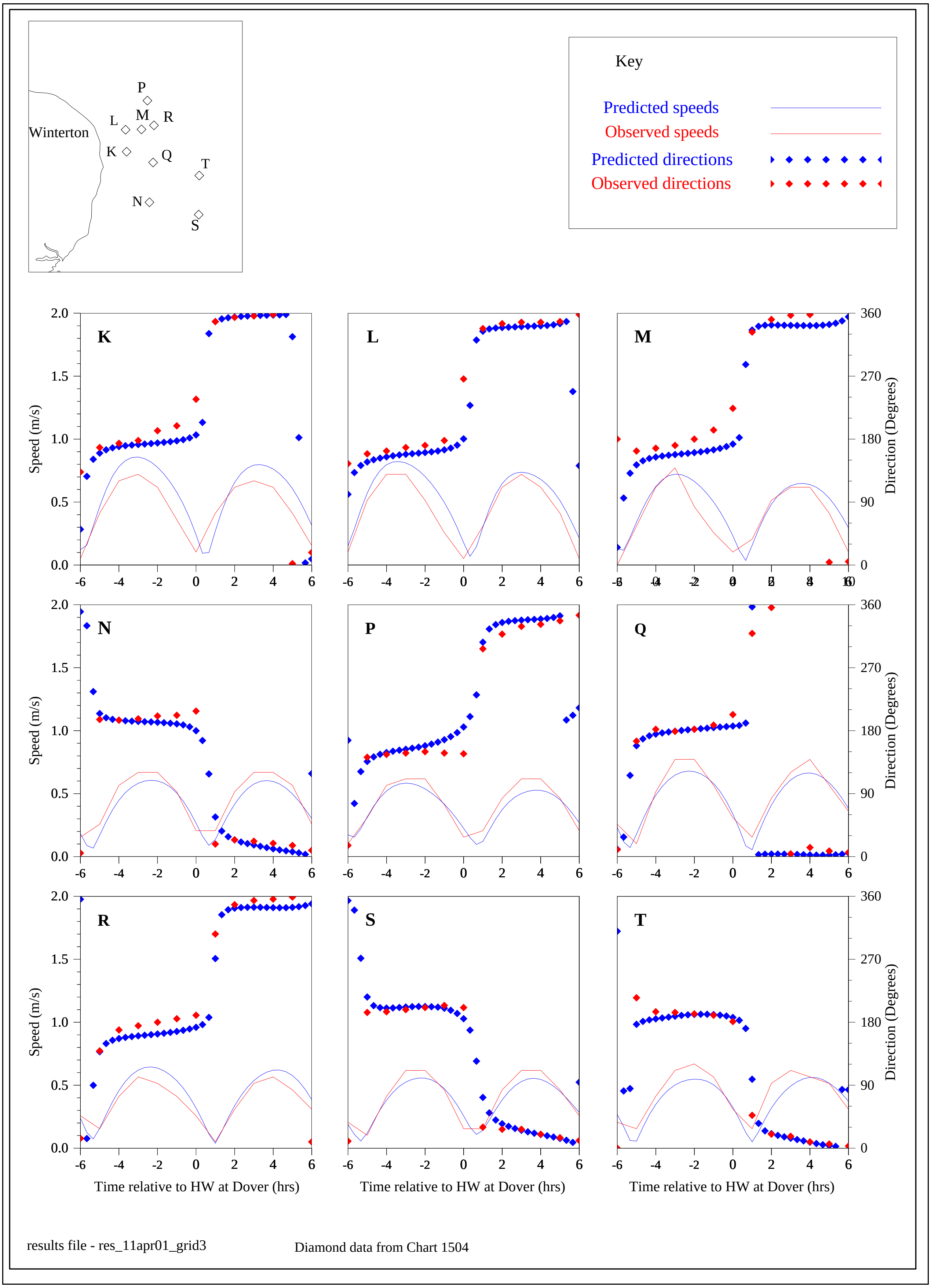

Figure 7f Validation with neap tide currents from Admiralty diamonds

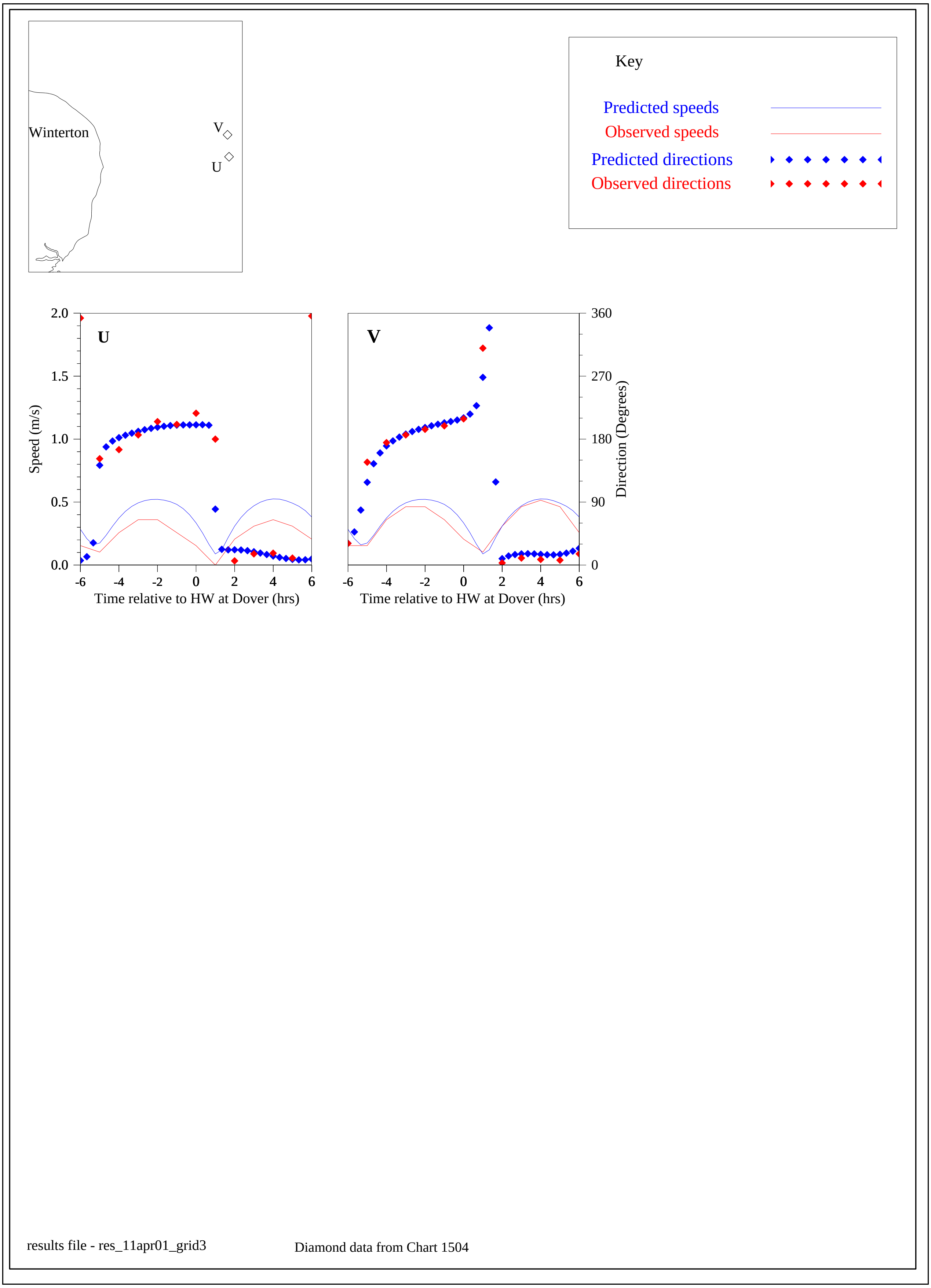

Figure 7g Validation with neap tide currents from Admiralty diamonds

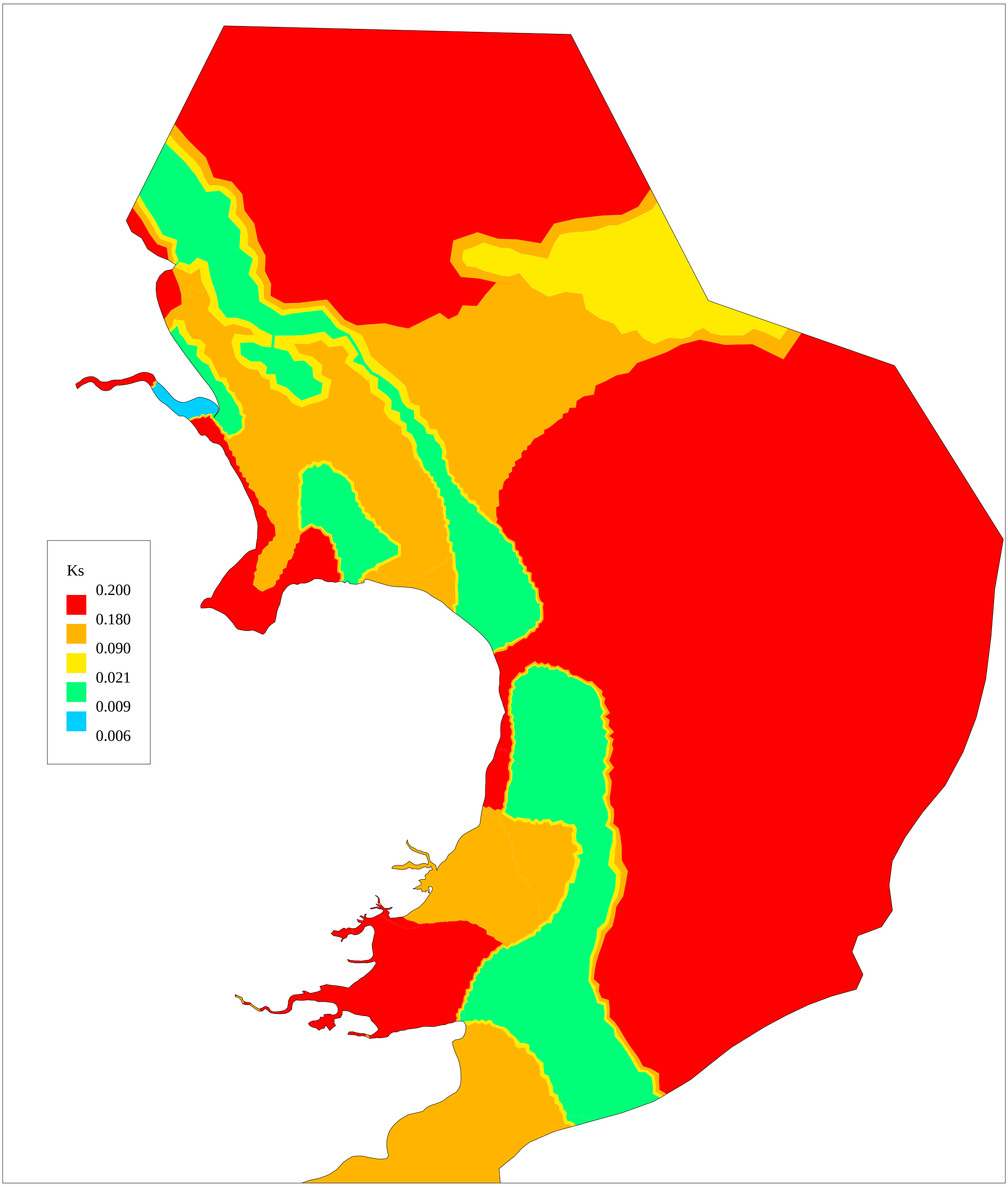

Figure 8 **Spatial distribution of seabed roughness length used in sensitivity test. Distribution based on BGS seabed sediment map (Cameron *et al*, 19XX) using standard values from Soulsby (1997)**

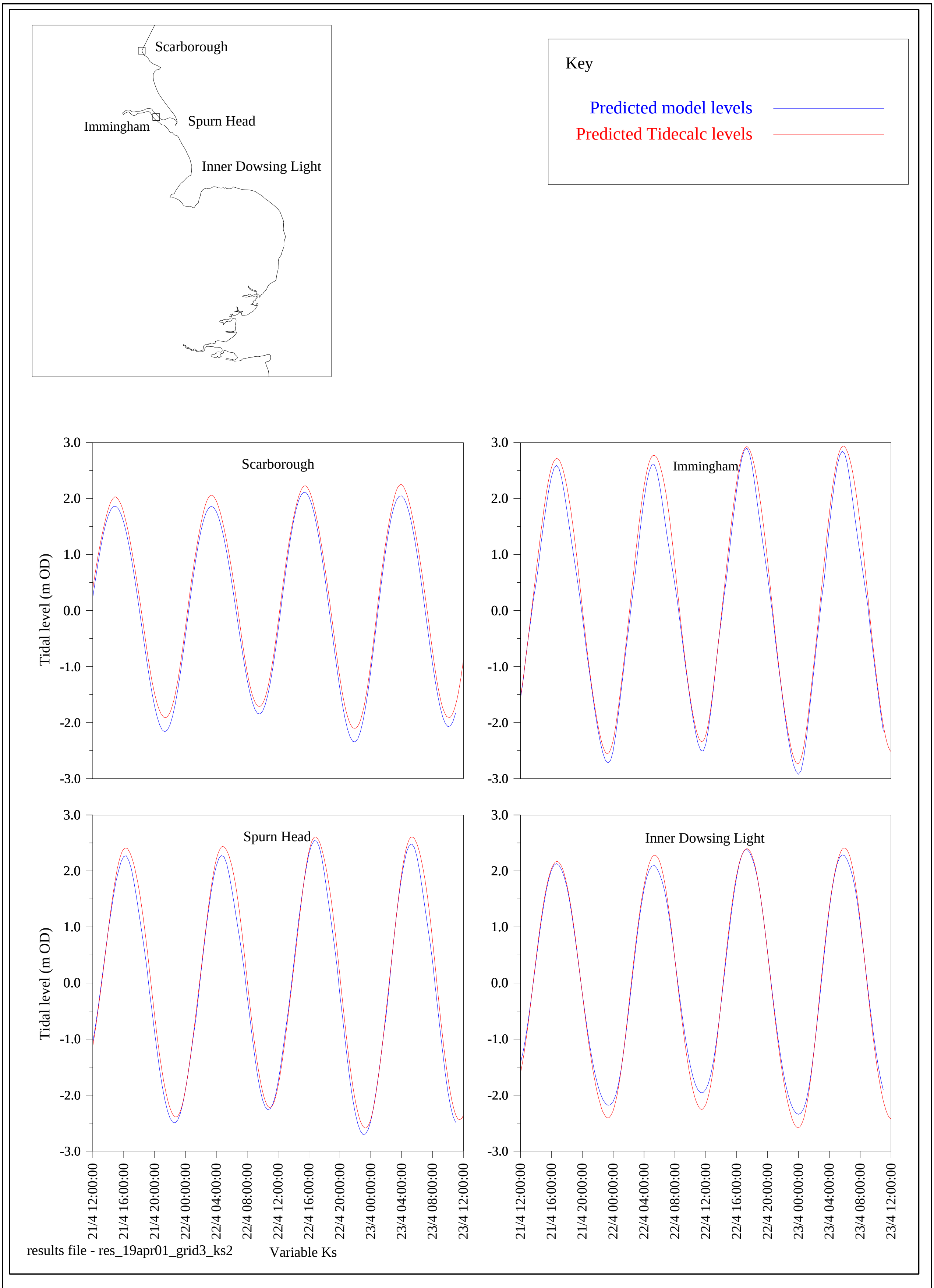

Figure 9a **Sensitivity test to water levels (variable roughness)**

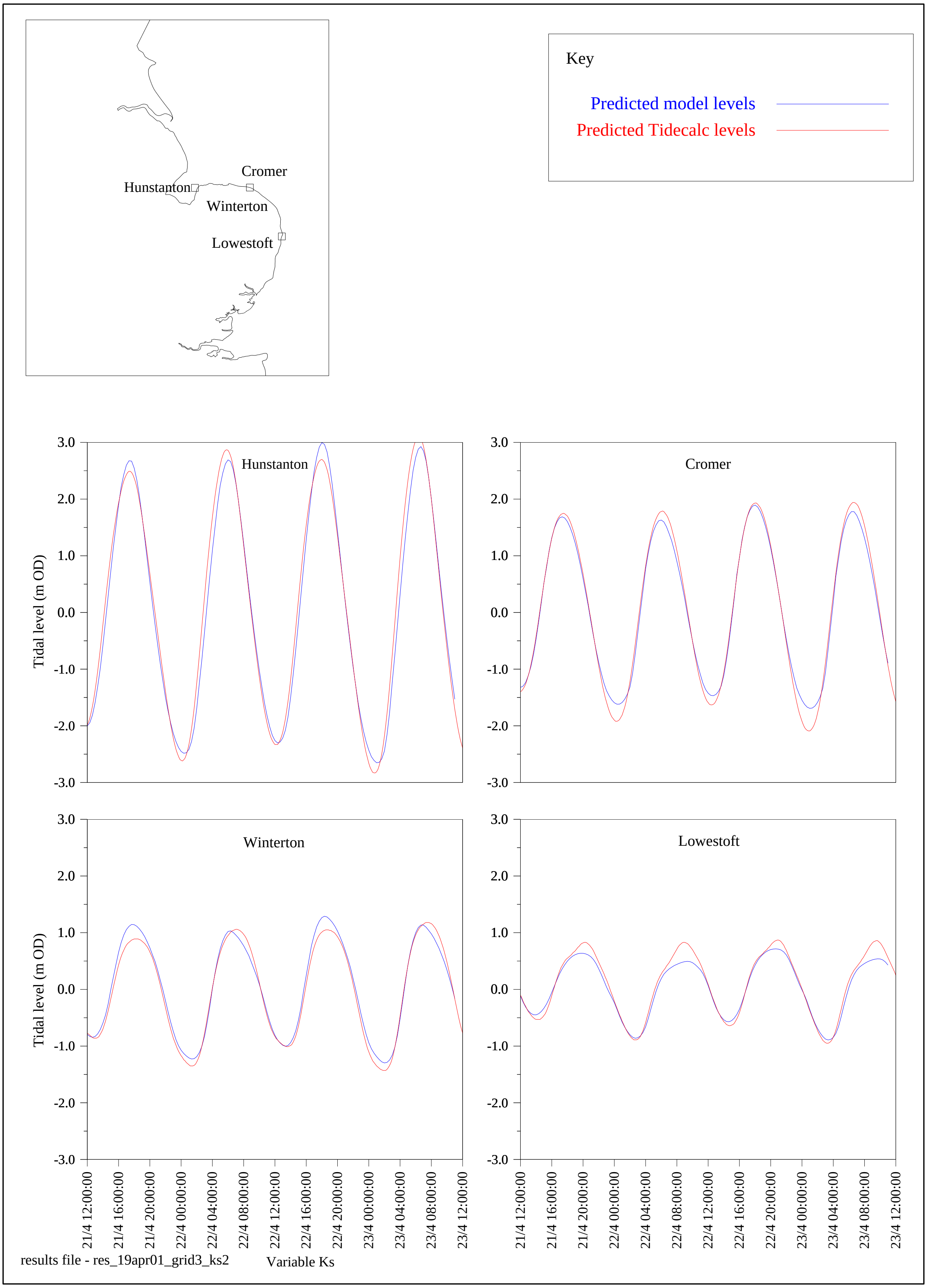

Figure 9b **Sensitivity test to water levels (variable roughness)**

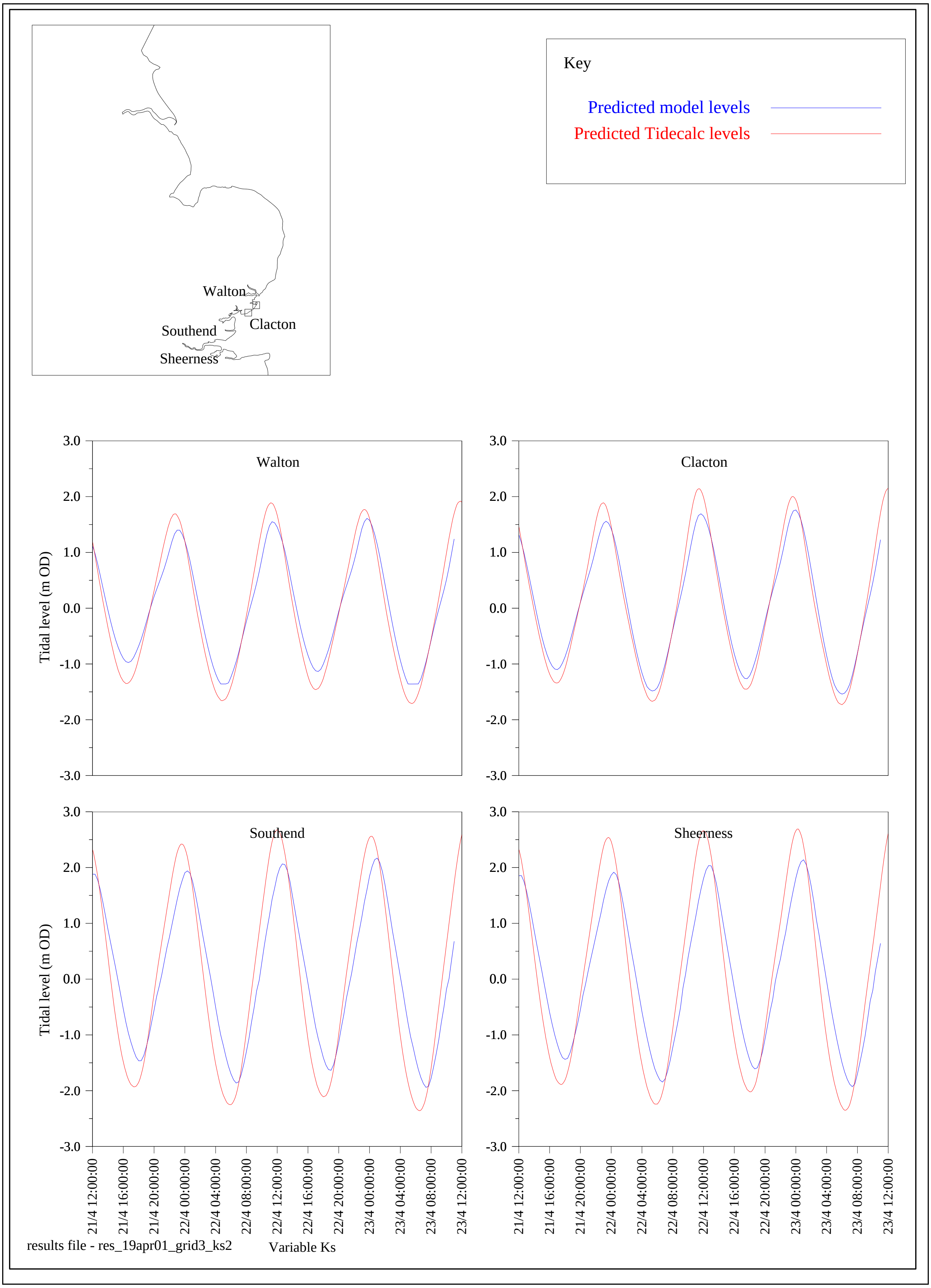

Figure 9c **Sensitivity test to water levels (variable roughness)**

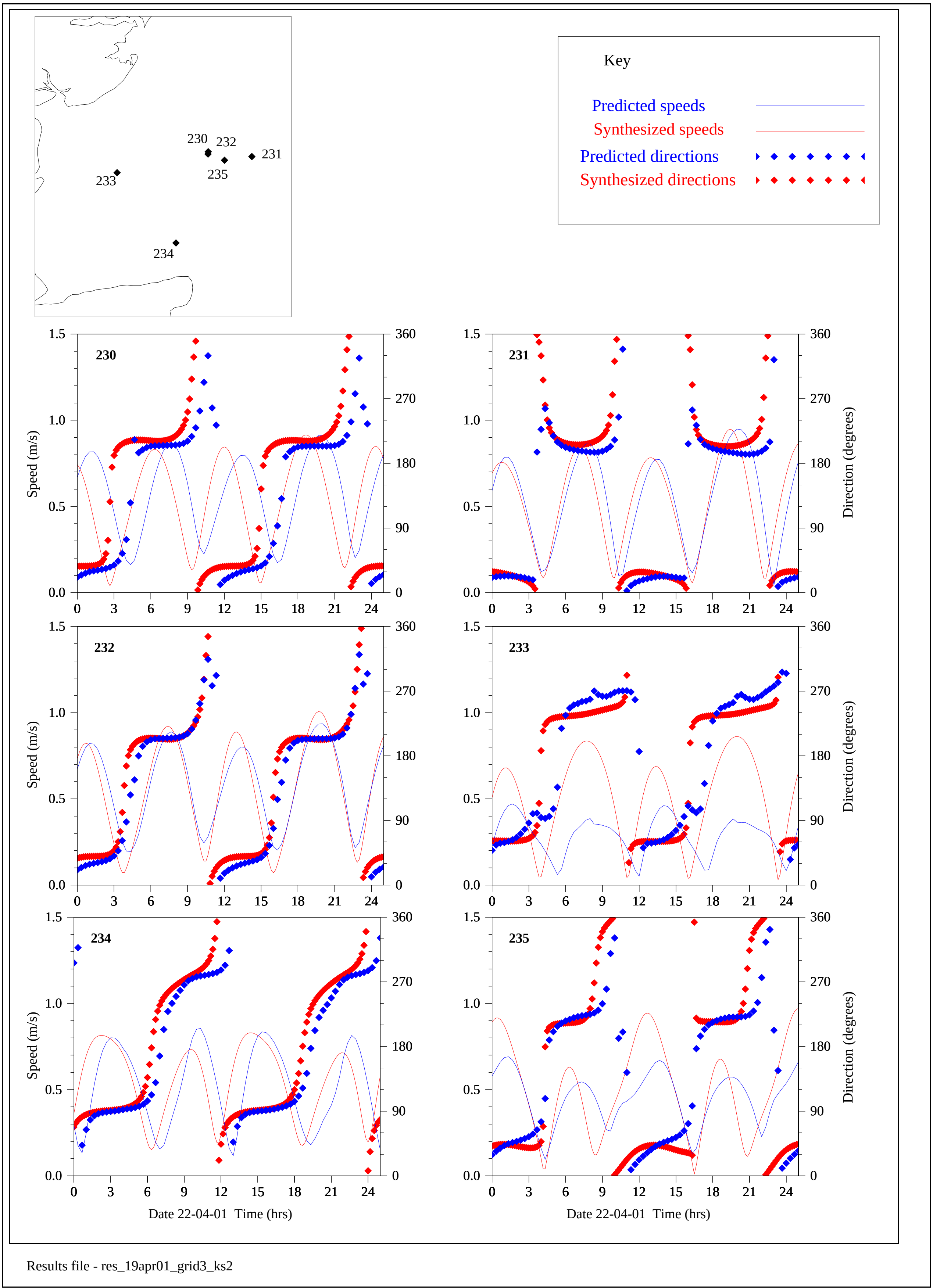

Figure 10a Sensitivity test to currents (variable roughness) derived from CEFAS data archive

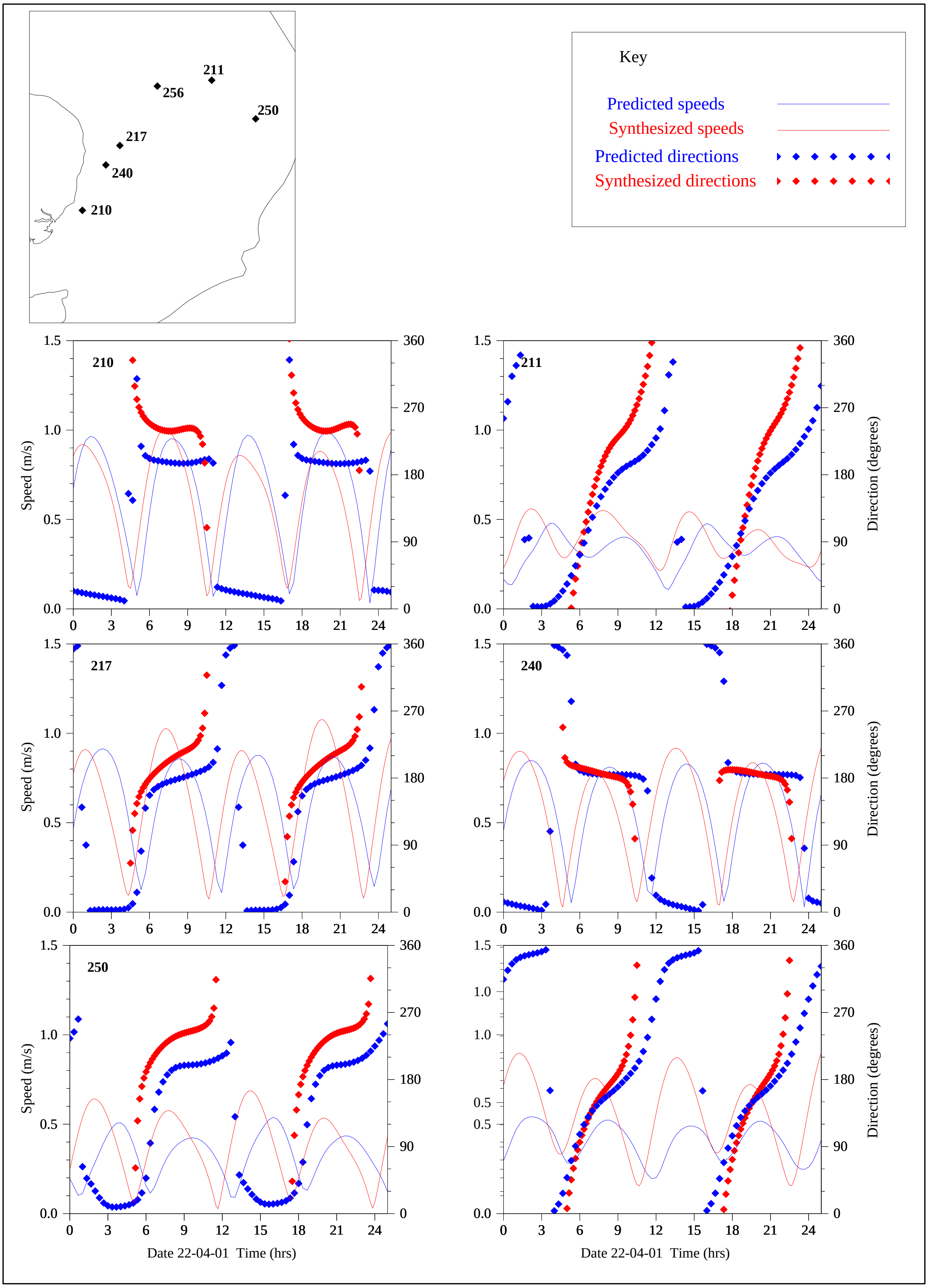

Results file - res_19apr01_grid3_ks2

Figure 10b Sensitivity test to currents (variable roughness) derived from CEFAS data archive

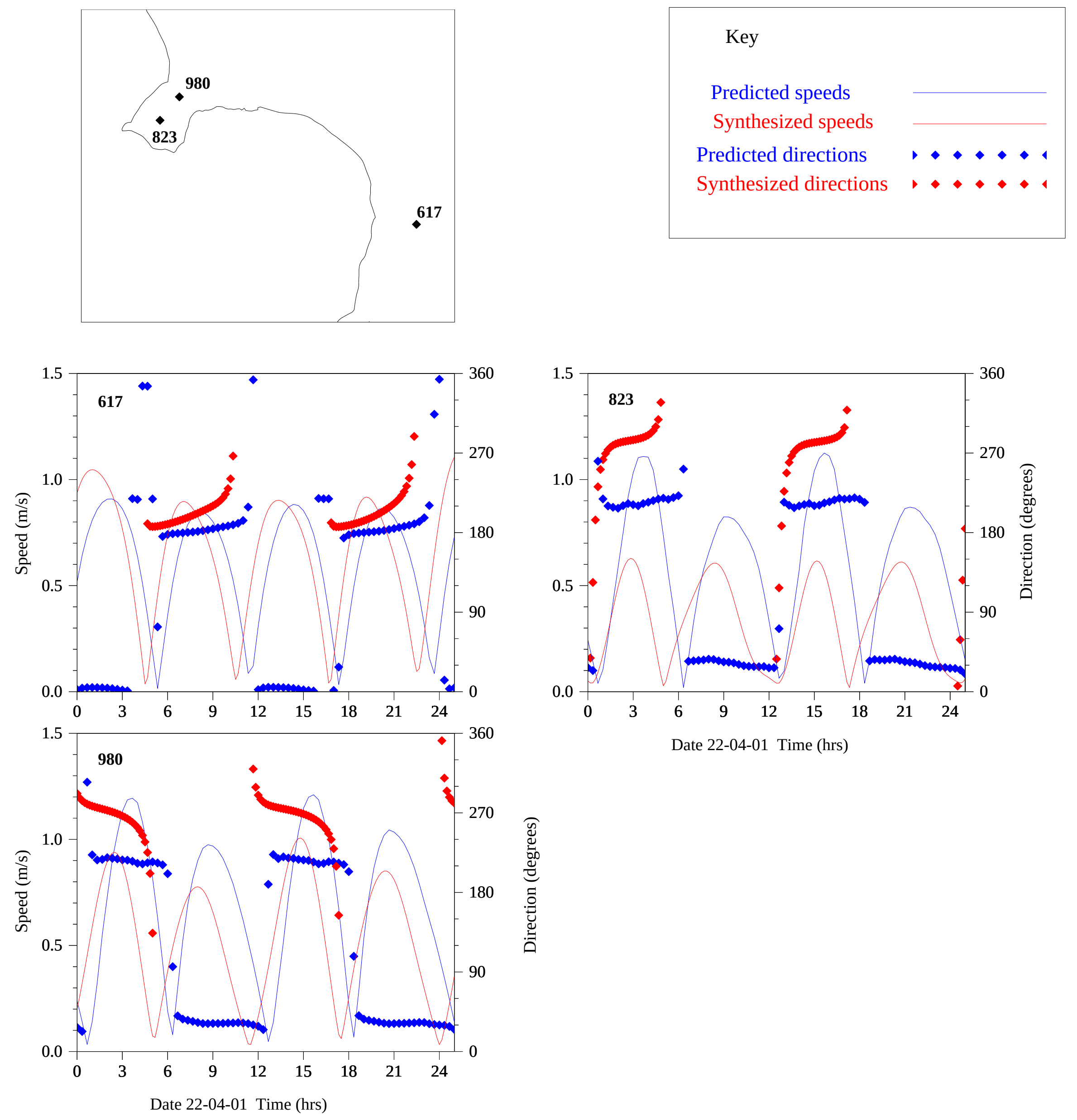

Results file - res_19apr01_grid3_ks2

Figure 10c Sensitivity test to currents (variable roughness) derived from CEFAS data archive

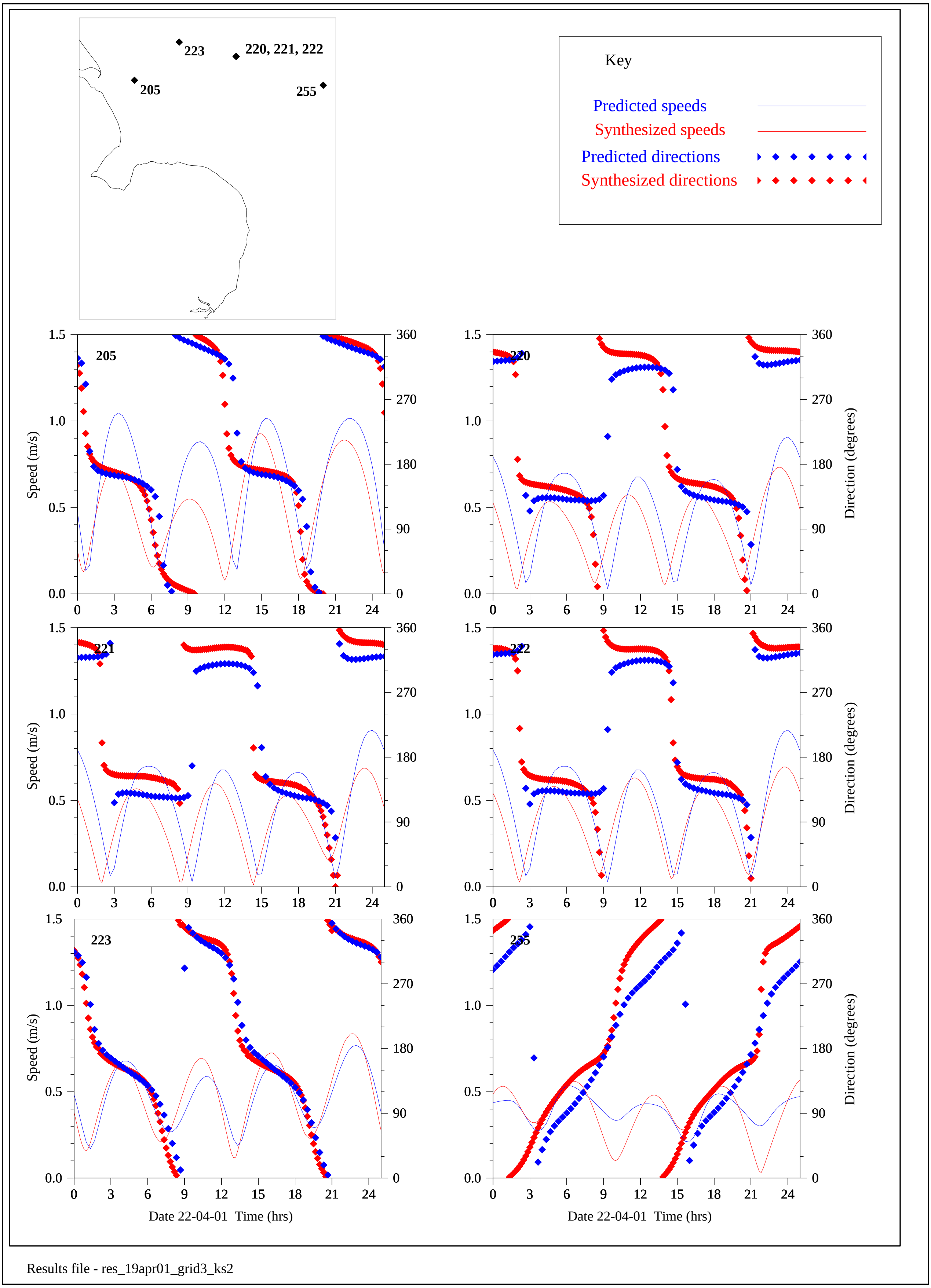

Figure 10d Sensitivity test to currents (variable roughness) derived from CEFAS data archive

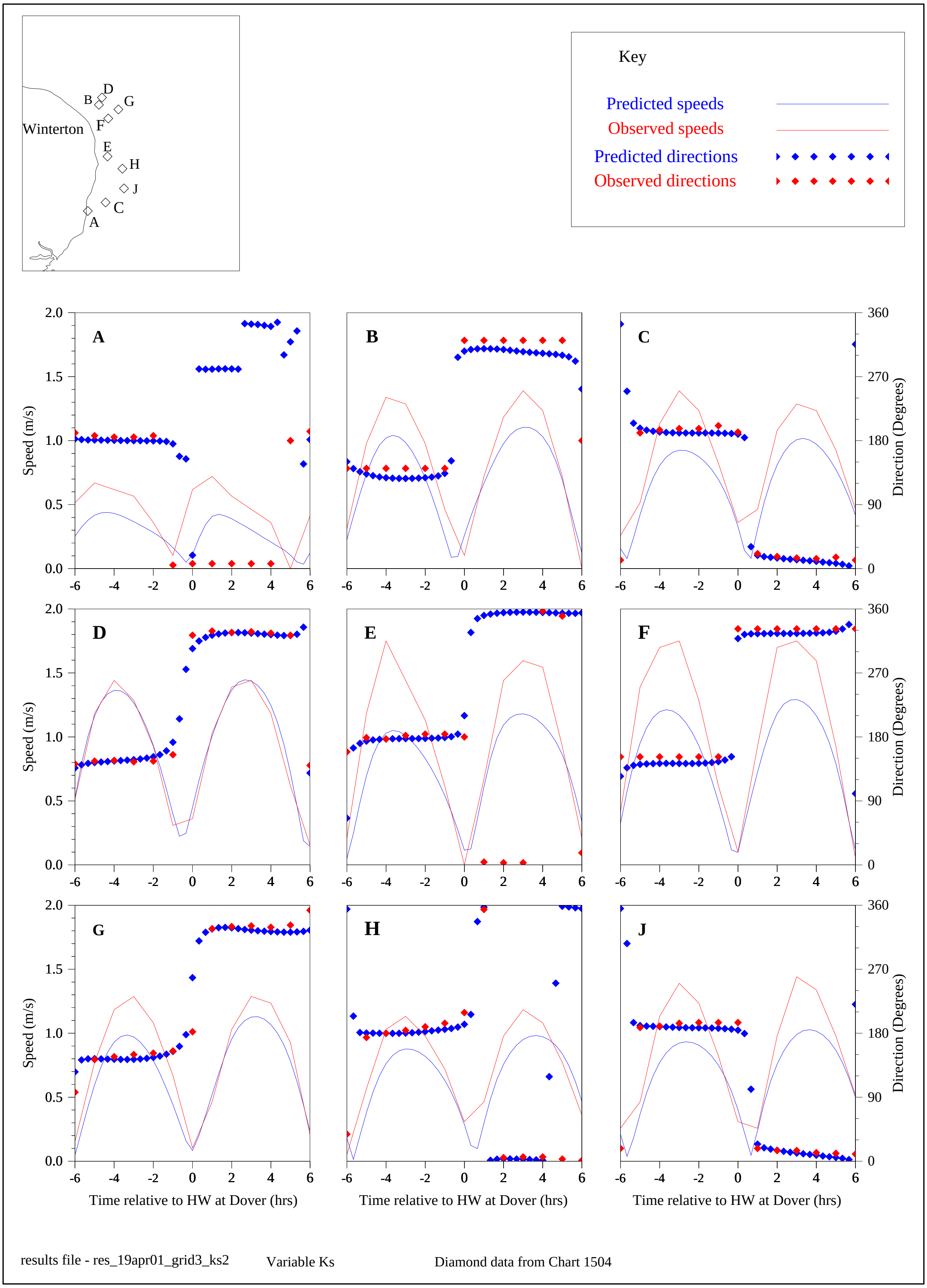

Figure 10e Sensitivity test to currents (variable roughness) from Admiralty diamonds

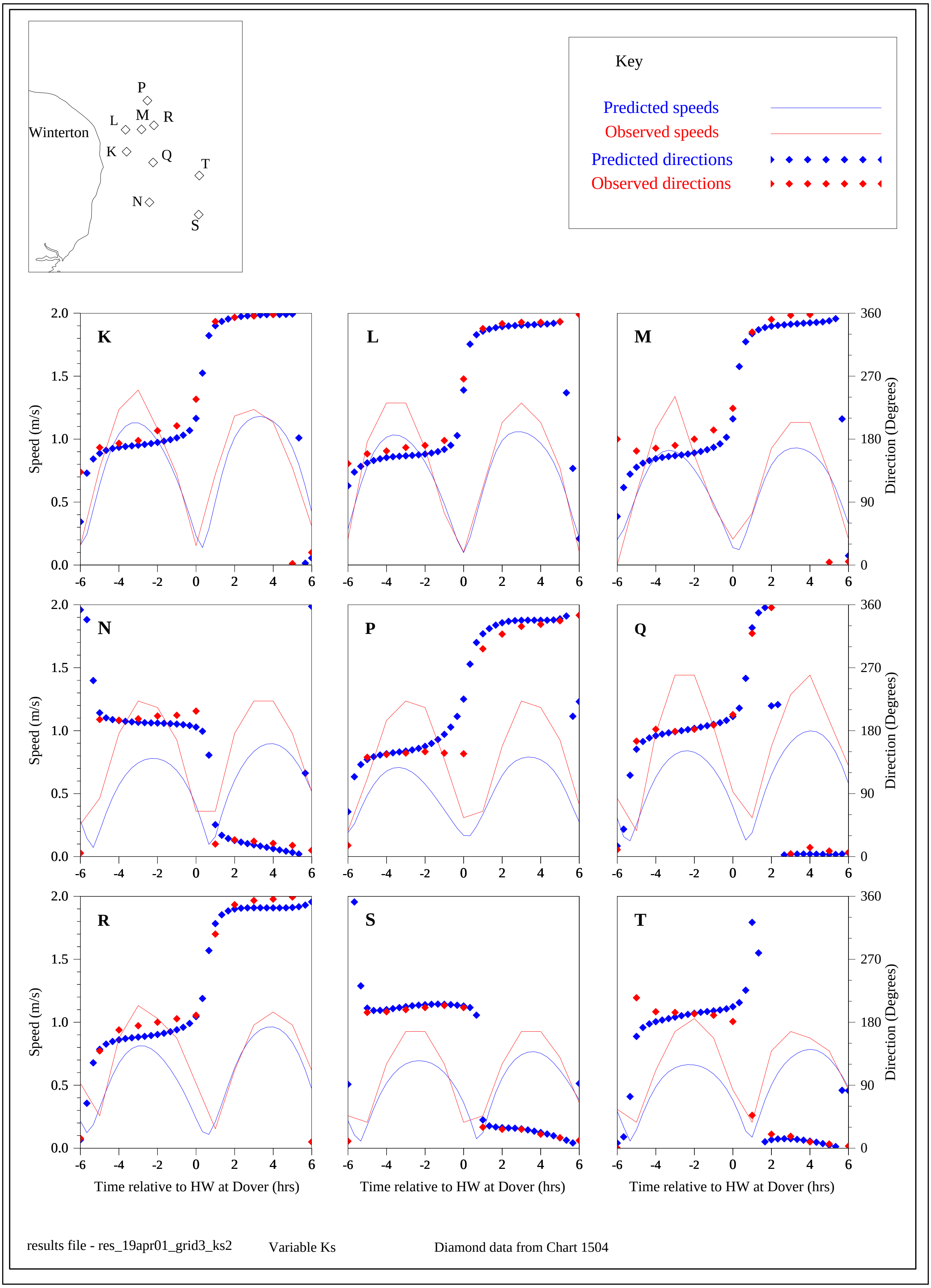

Figure 10f Sensitivity test to currents (variable roughness) from Admiralty diamonds

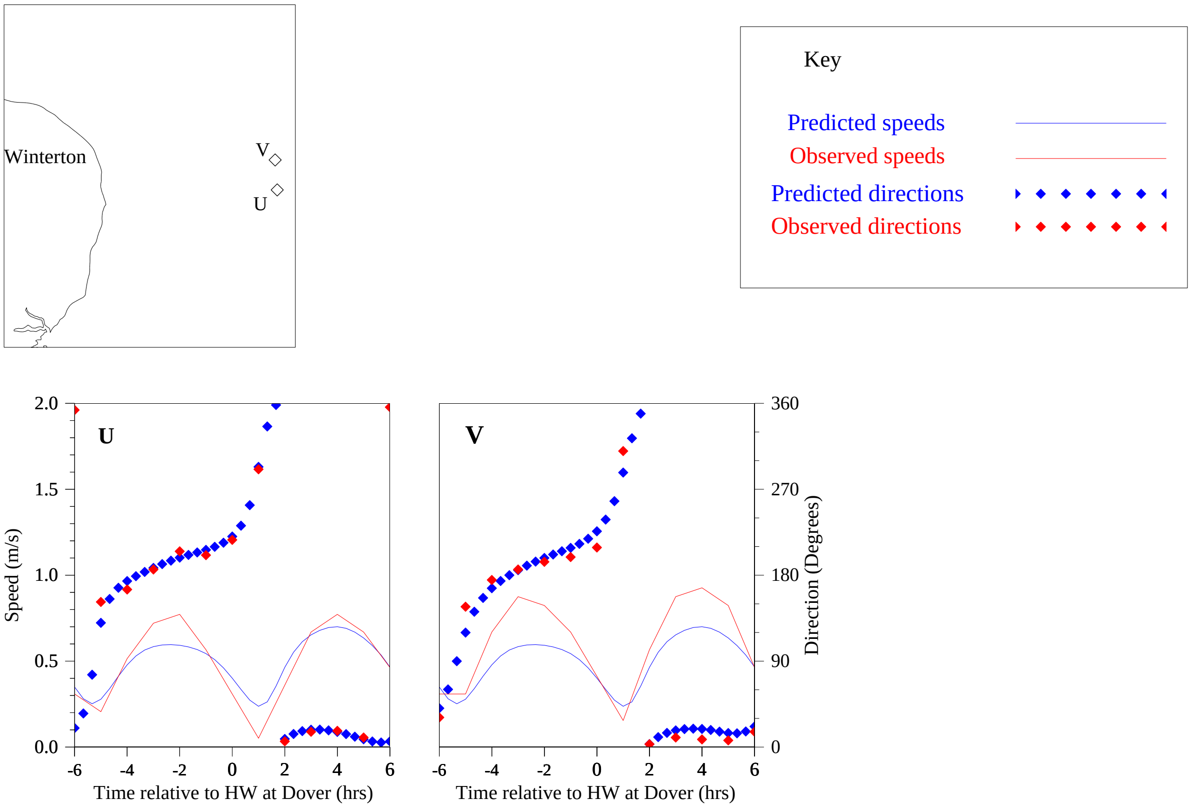

results file - res_19apr01_grid3_ks2 Variable Ks Diamond data from Chart 1504

Figure 10g Sensitivity test to currents (variable roughness) from Admiralty diamonds

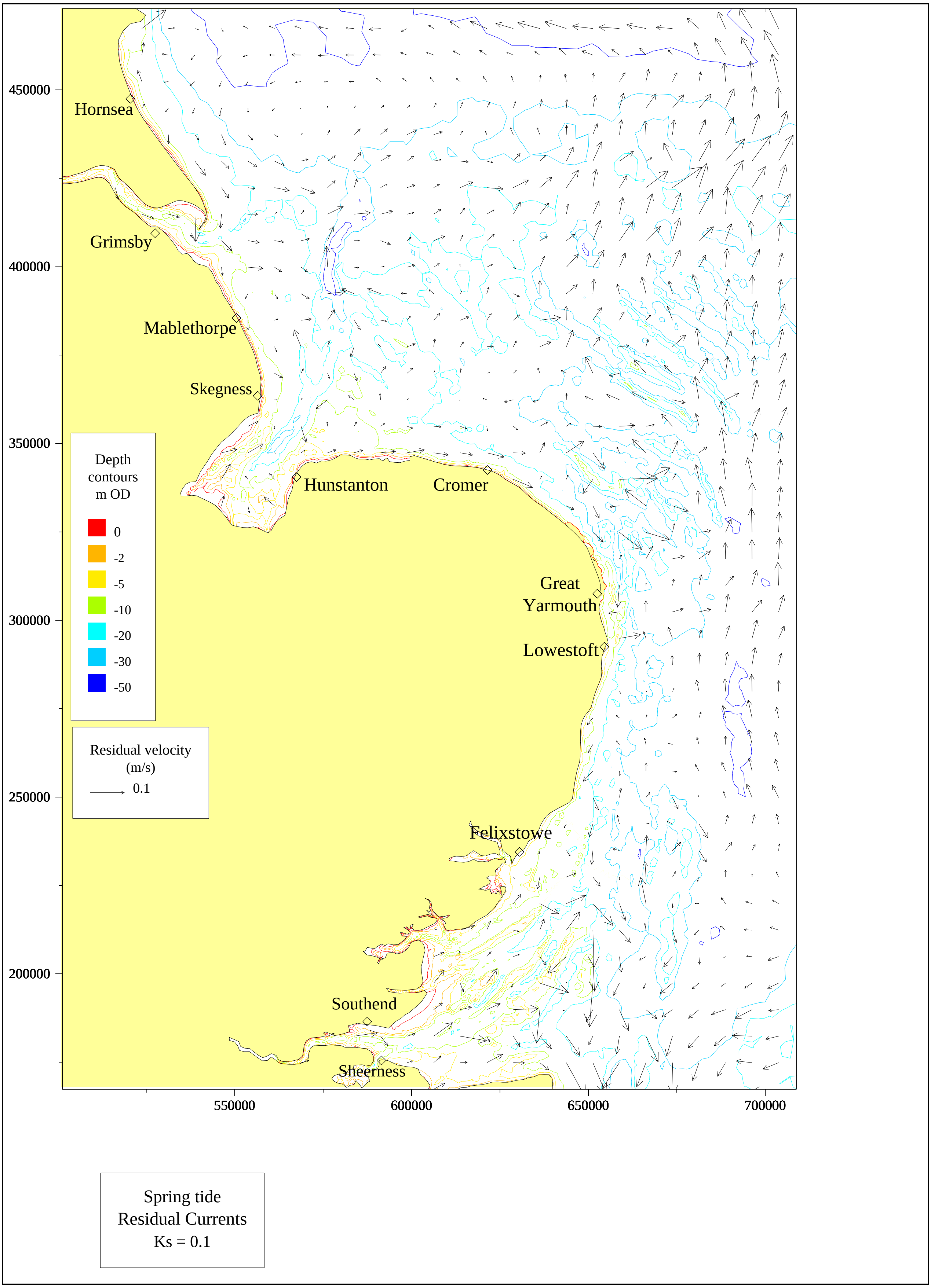

Figure 11 **Spring tide residual velocity**

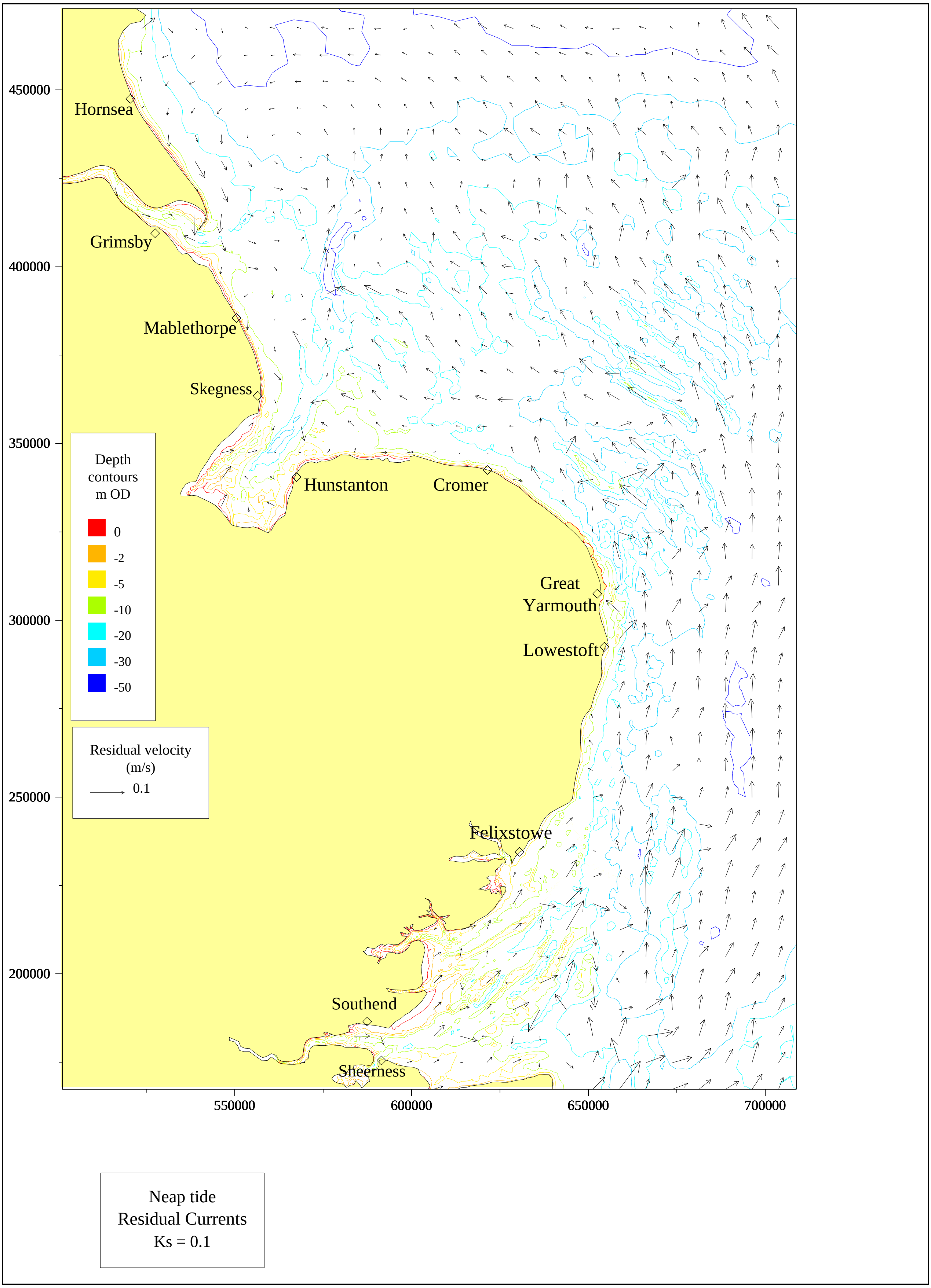

Figure 12 **Neap tide residual velocity**

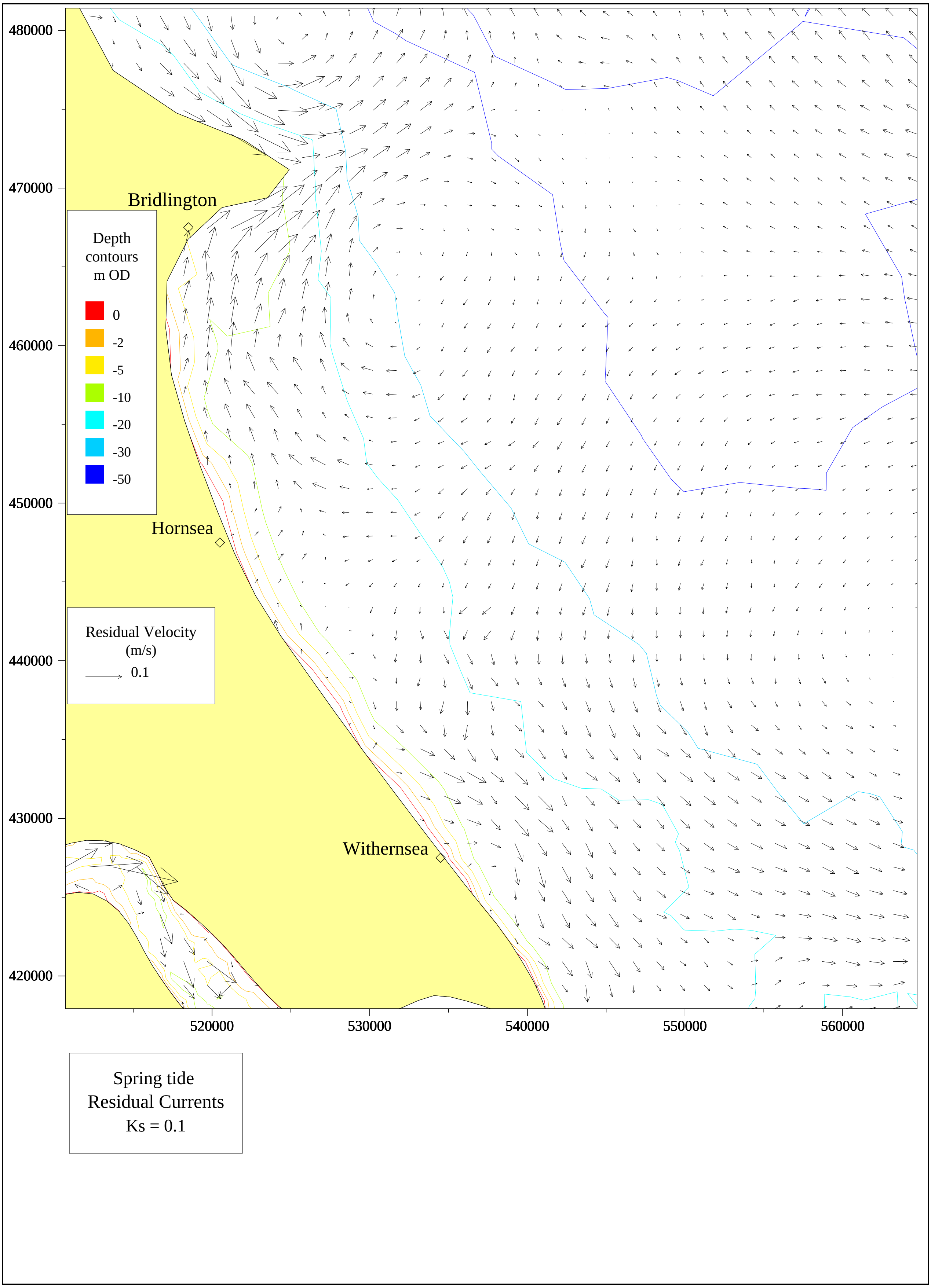

Figure 13 Spring tide residual velocity detail: Flamborough Head to the Humber

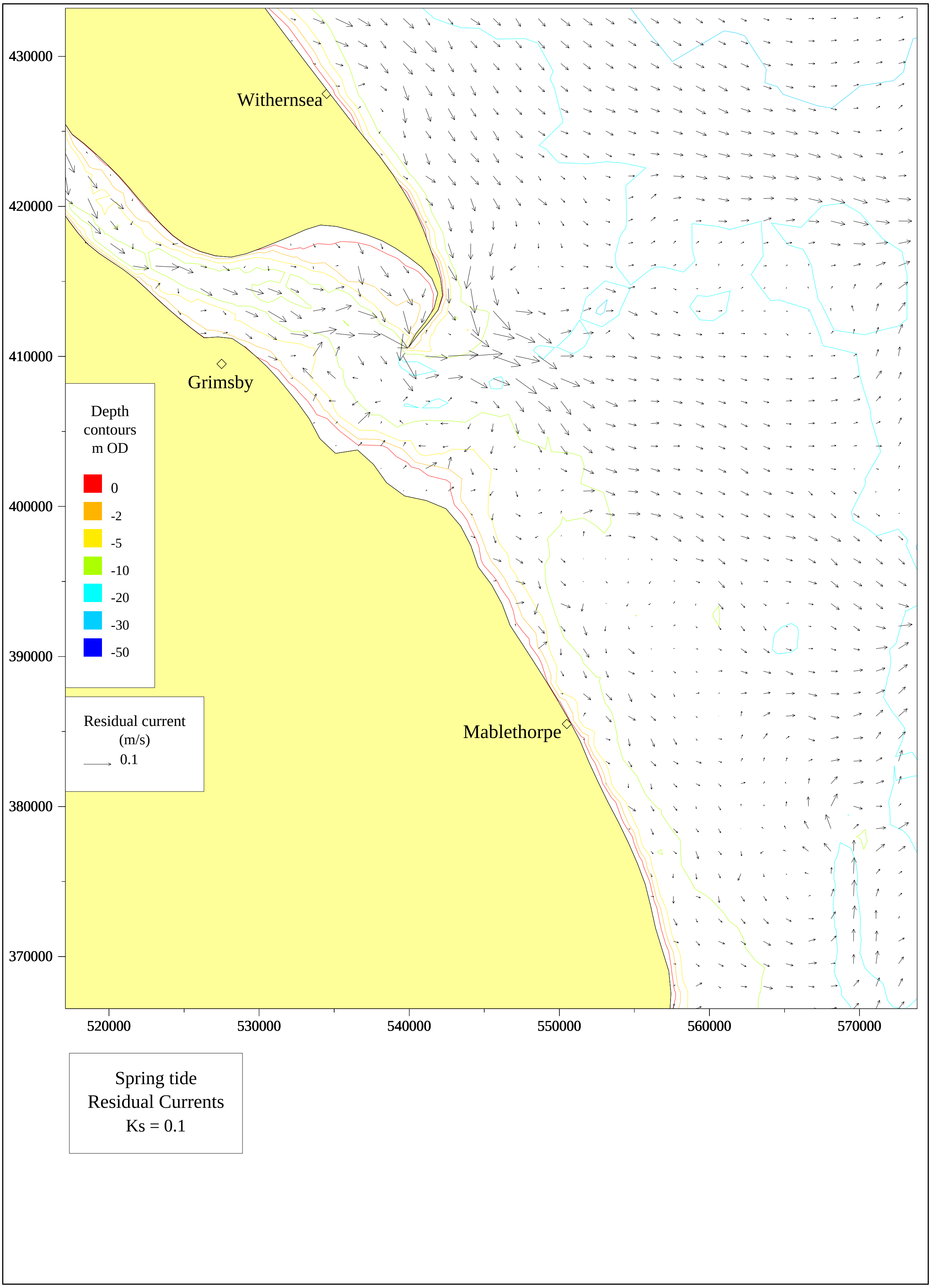

Figure 14 **Spring tide residual velocity detail: Humber Entrance and Lincolnshire**

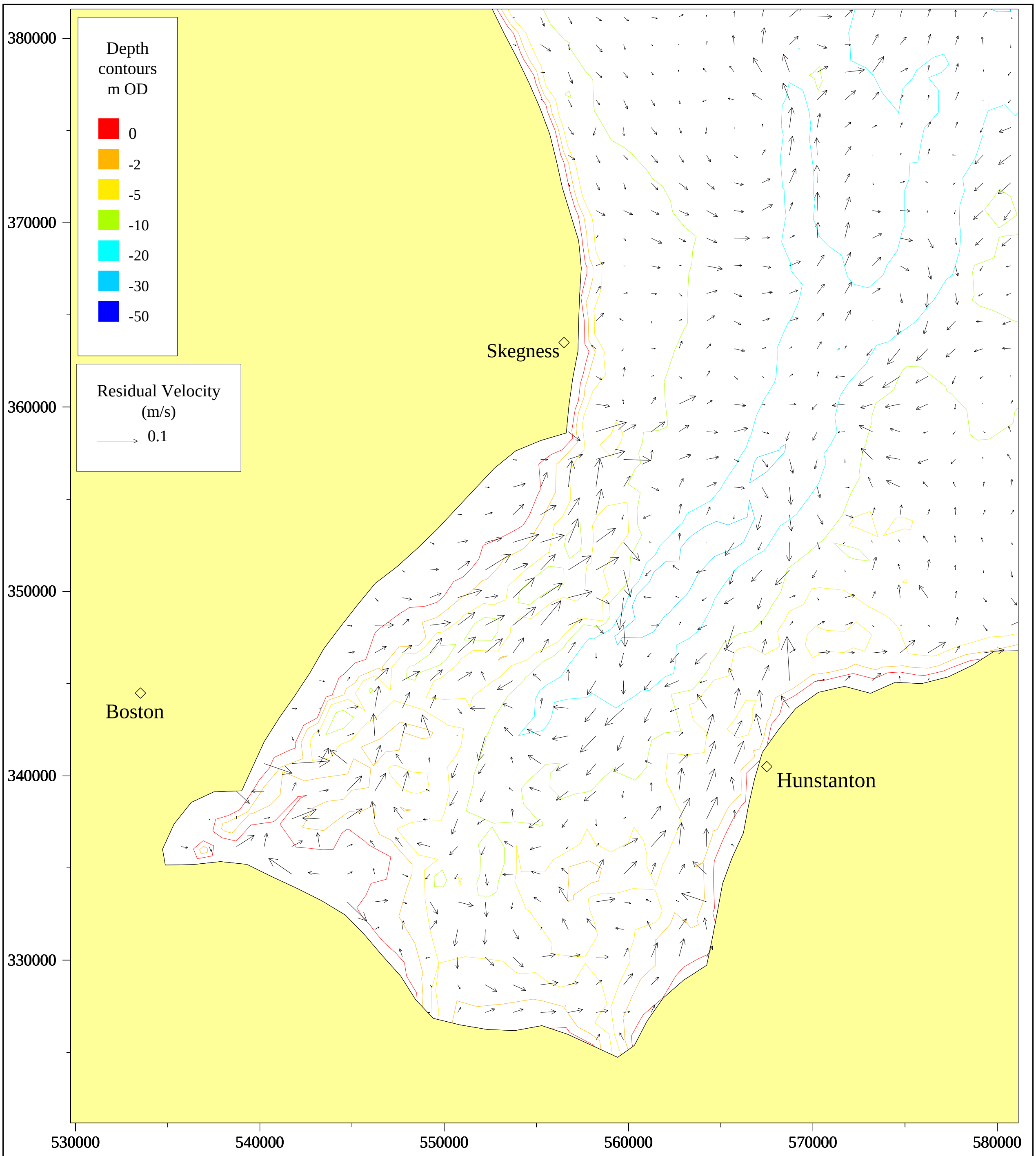

Spring tide
Residual Currents
Ks = 0.1

Figure 15 Spring tide residual velocity detail: Lincolnshire and the Wash

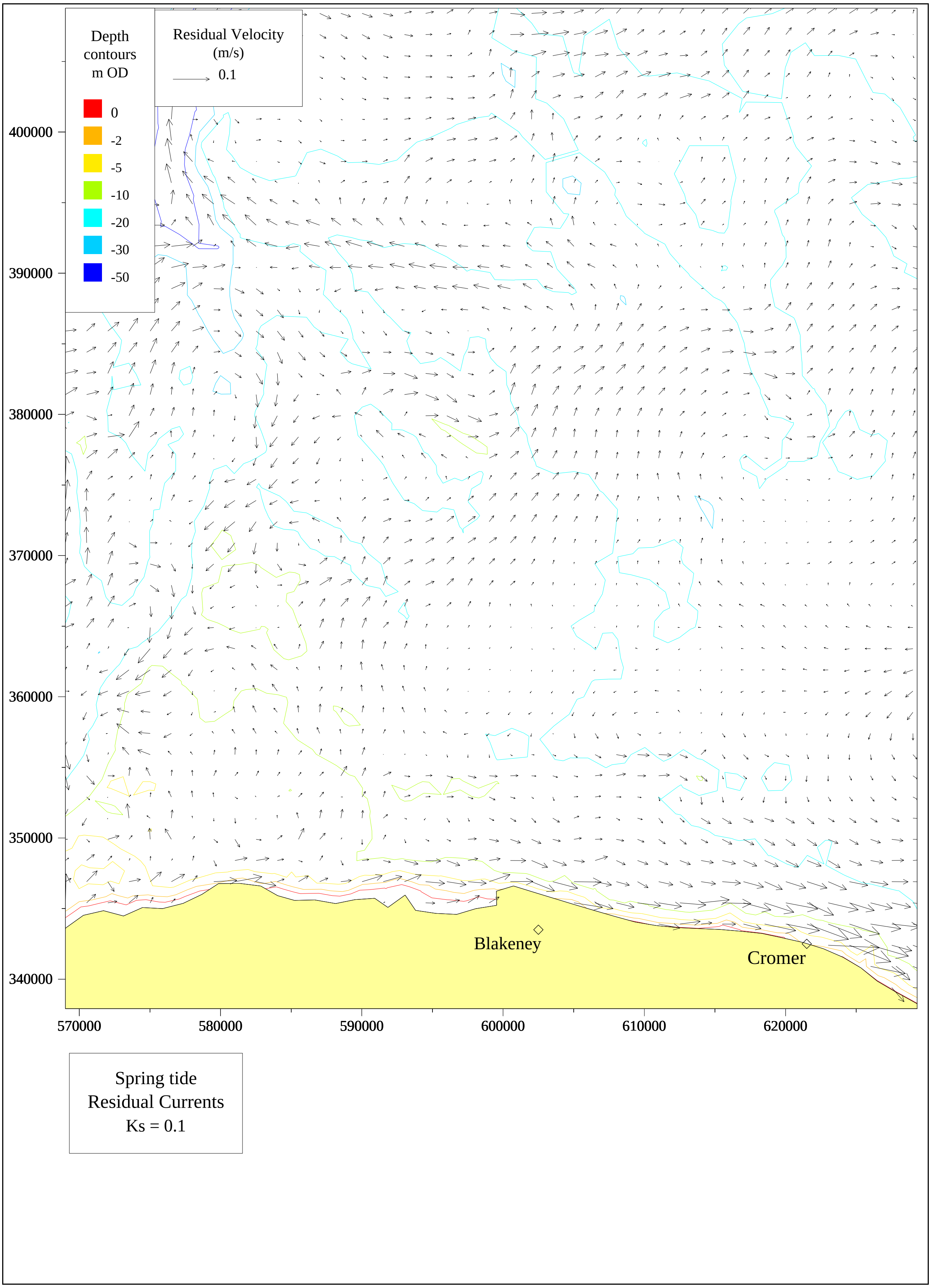

Figure 16 Spring tide residual velocity detail: North Norfolk

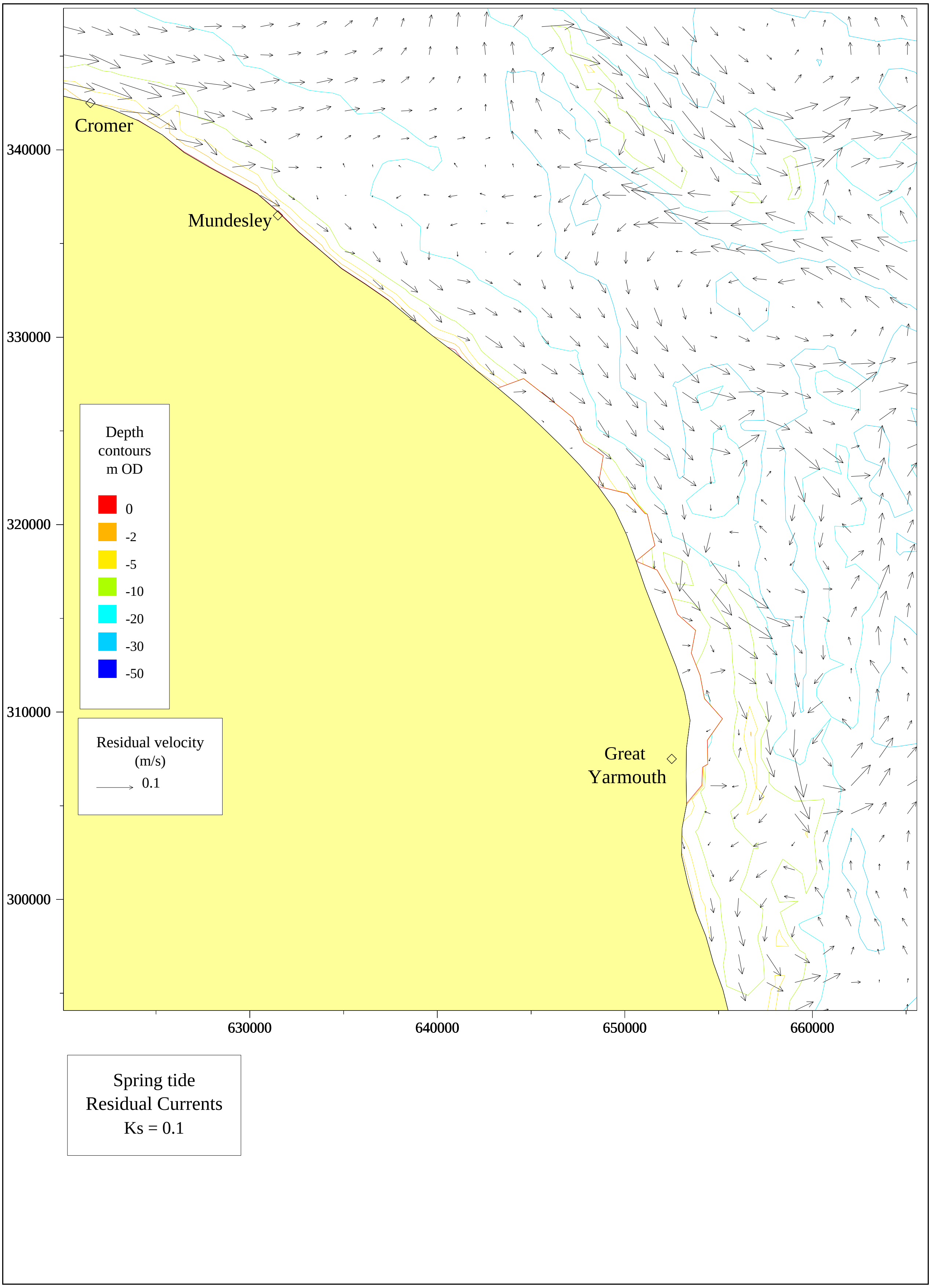

Figure 17 **Spring tide residual velocity detail: East Norfolk**

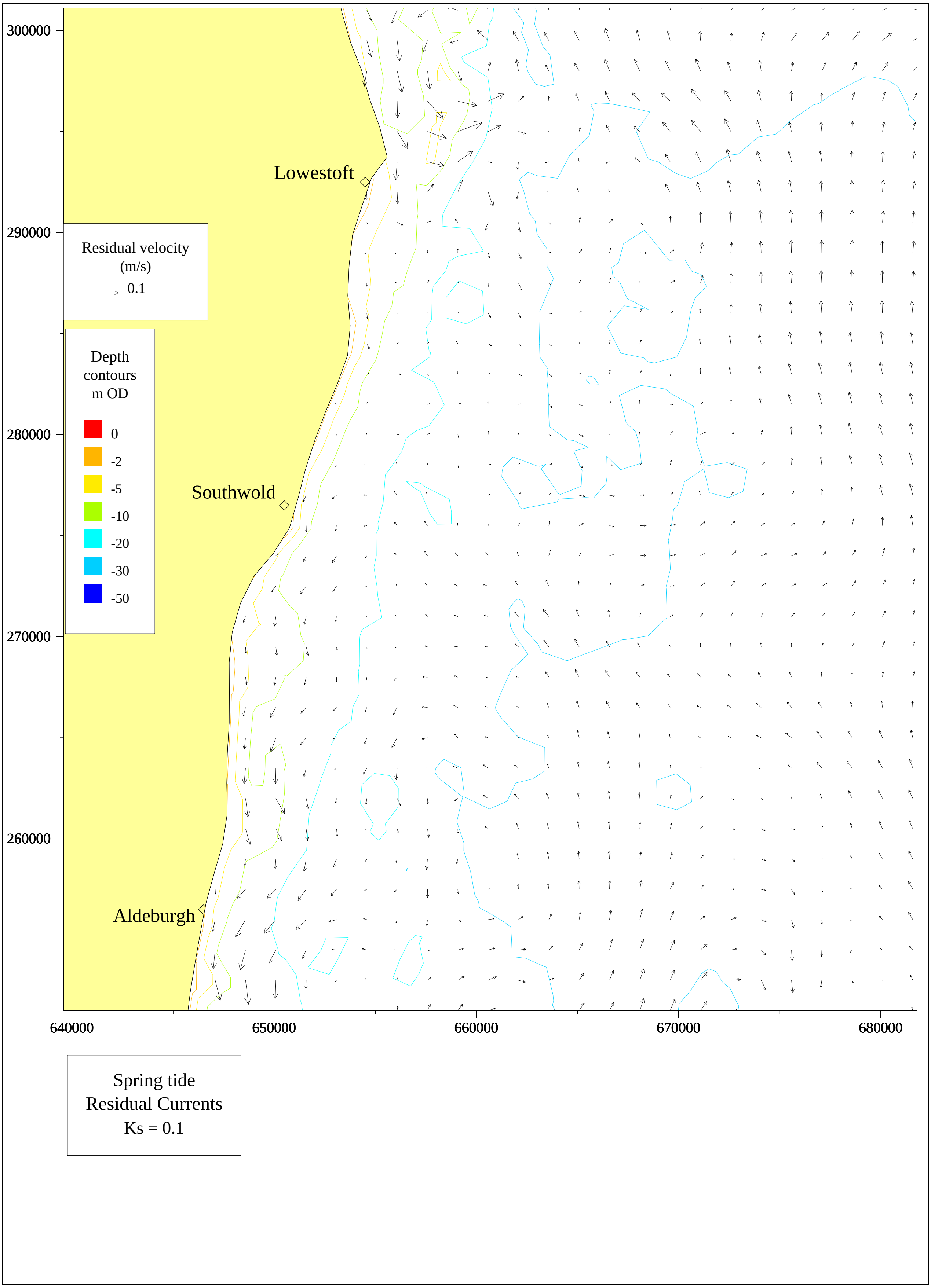

Figure 18 Spring tide residual velocity detail: North Suffolk

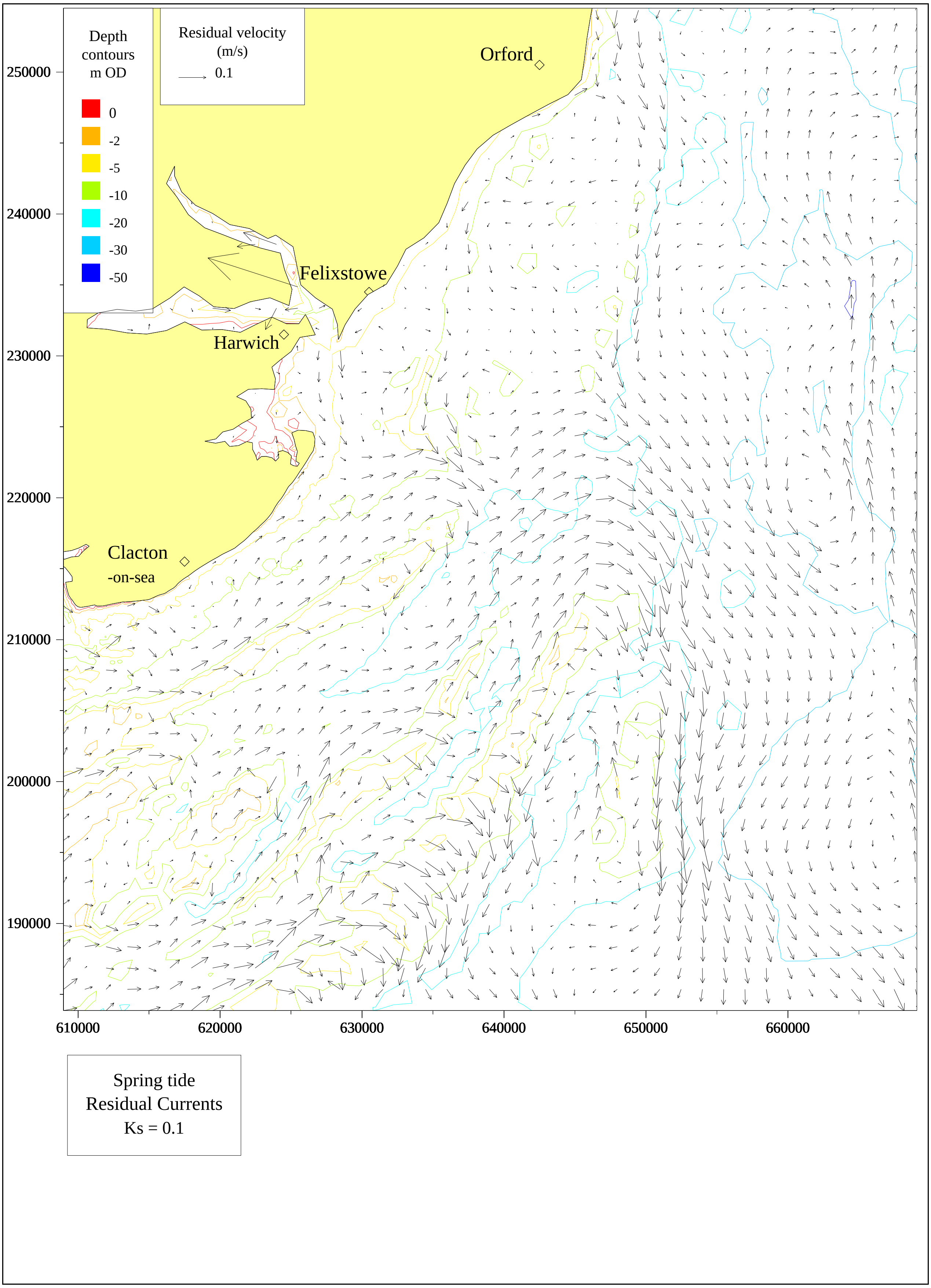

Figure 19 Spring tide residual velocity detail: Suffolk and Essex

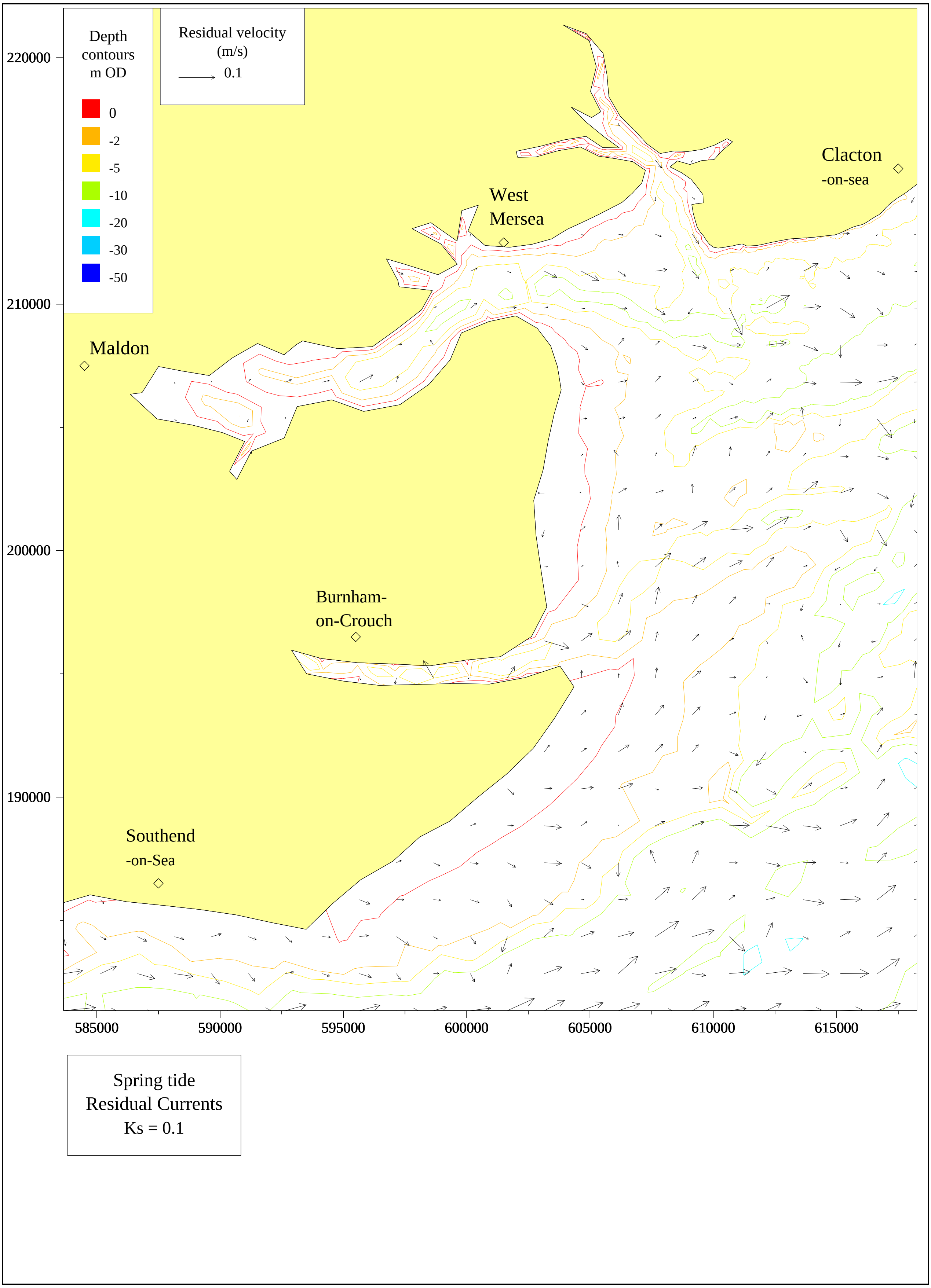

Figure 20 **Spring tide residual velocity detail: South Essex**

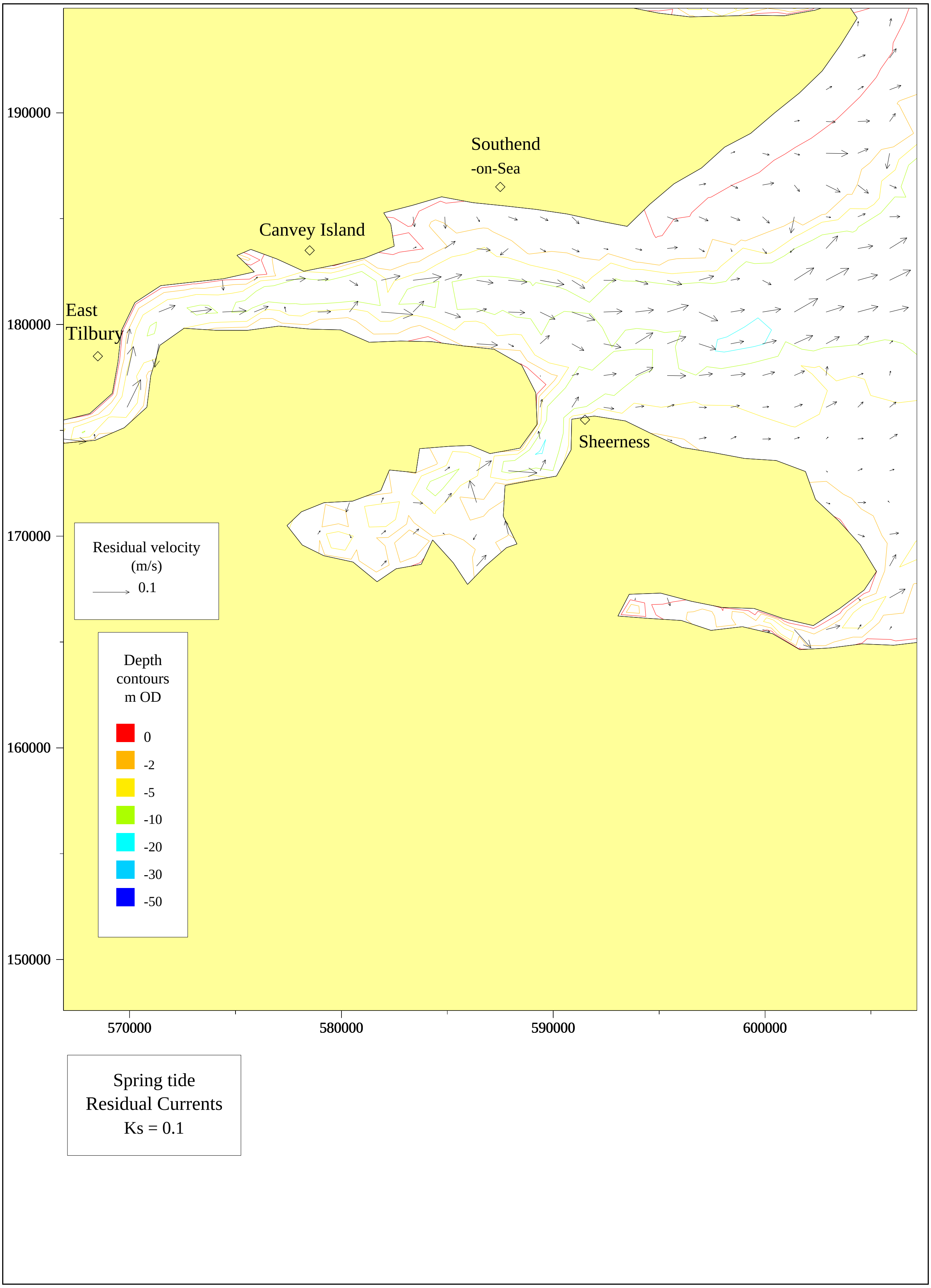

Figure 21 **Spring tide residual velocity detail: Outer Thames**

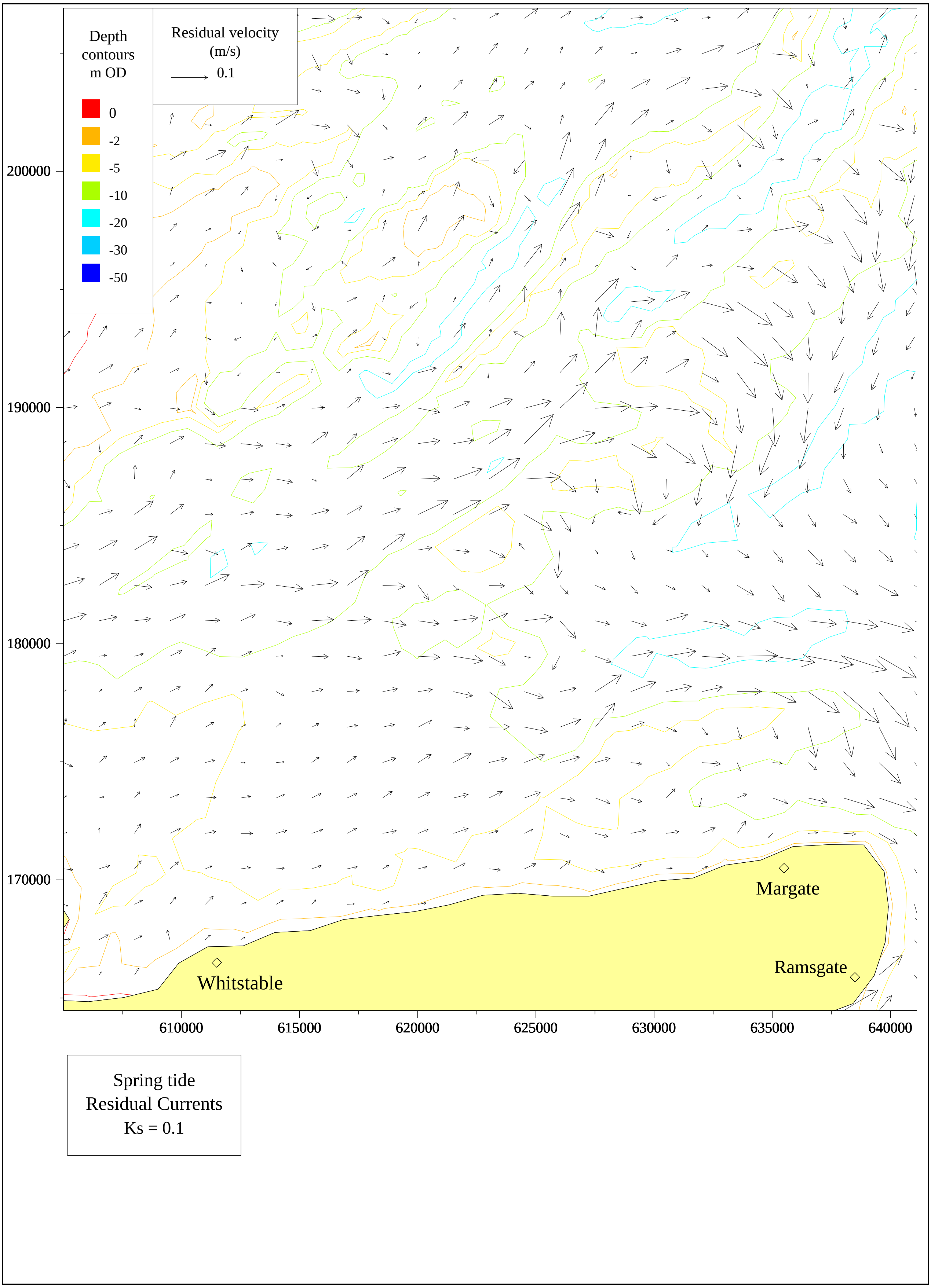

Figure 22 Spring tide residual velocity detail: North Kent

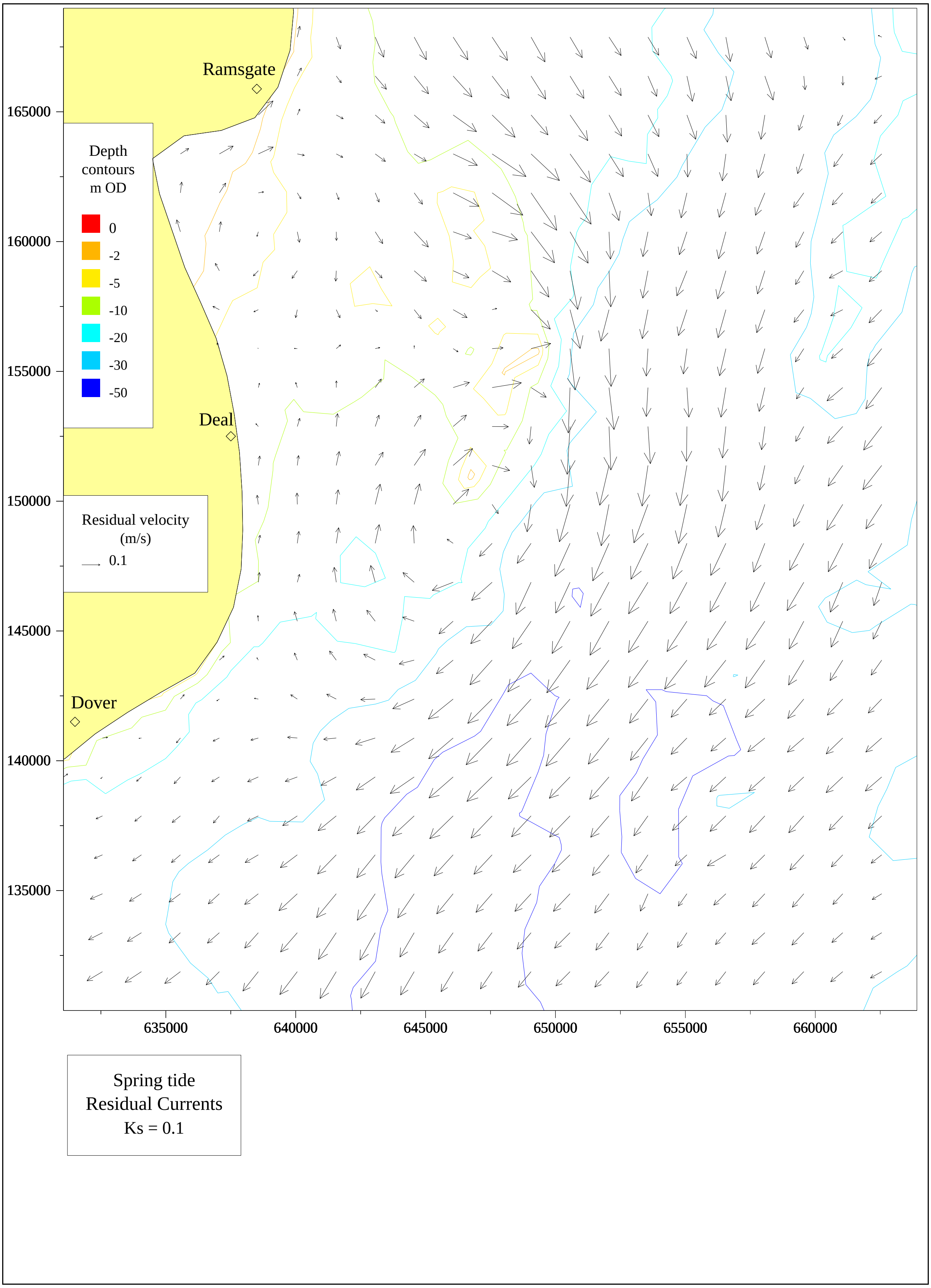

Figure 23 Spring tide residual velocity detail: East Kent

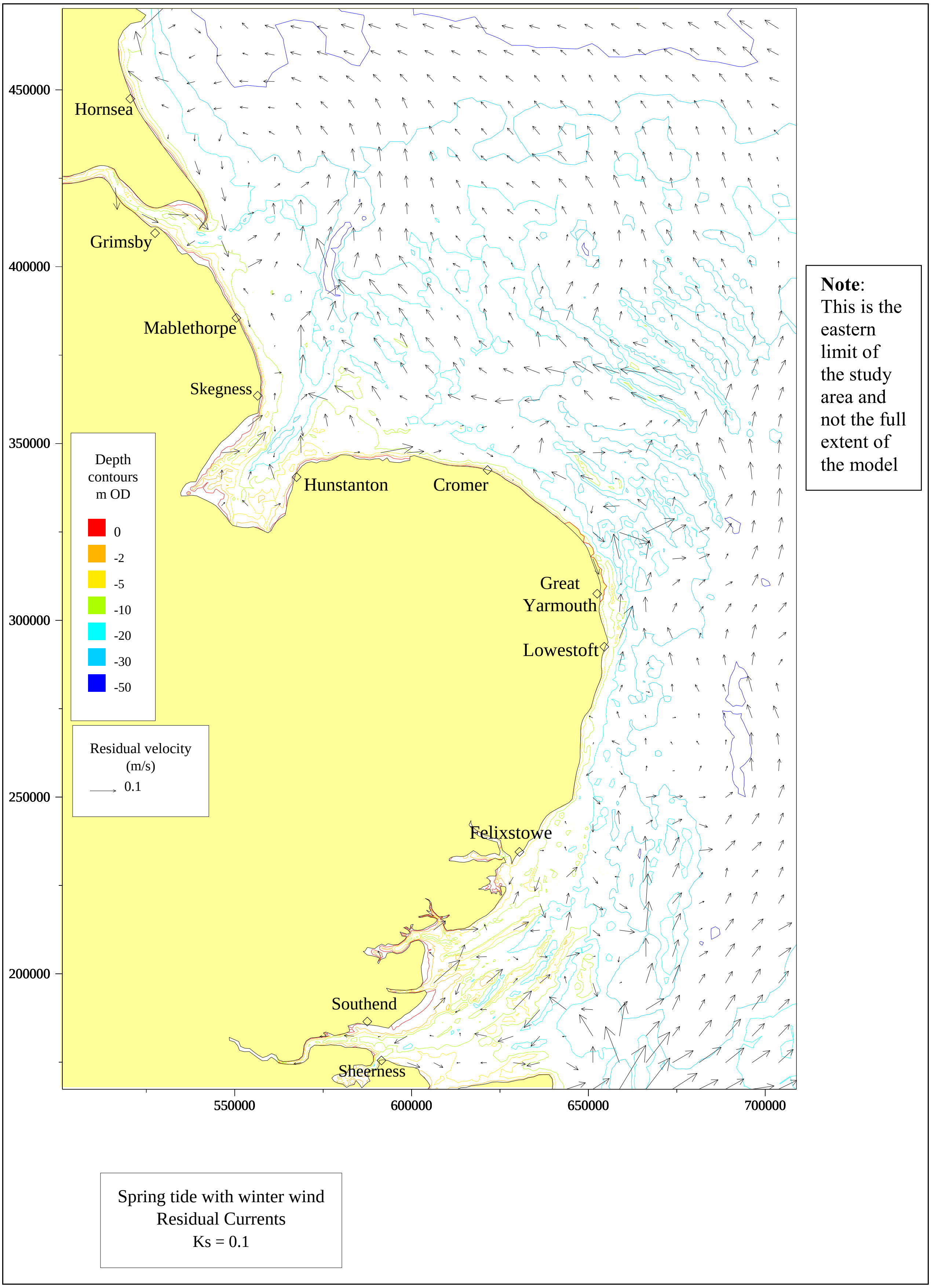

Figure 24 **Net spring tide residual velocity with winter wind**

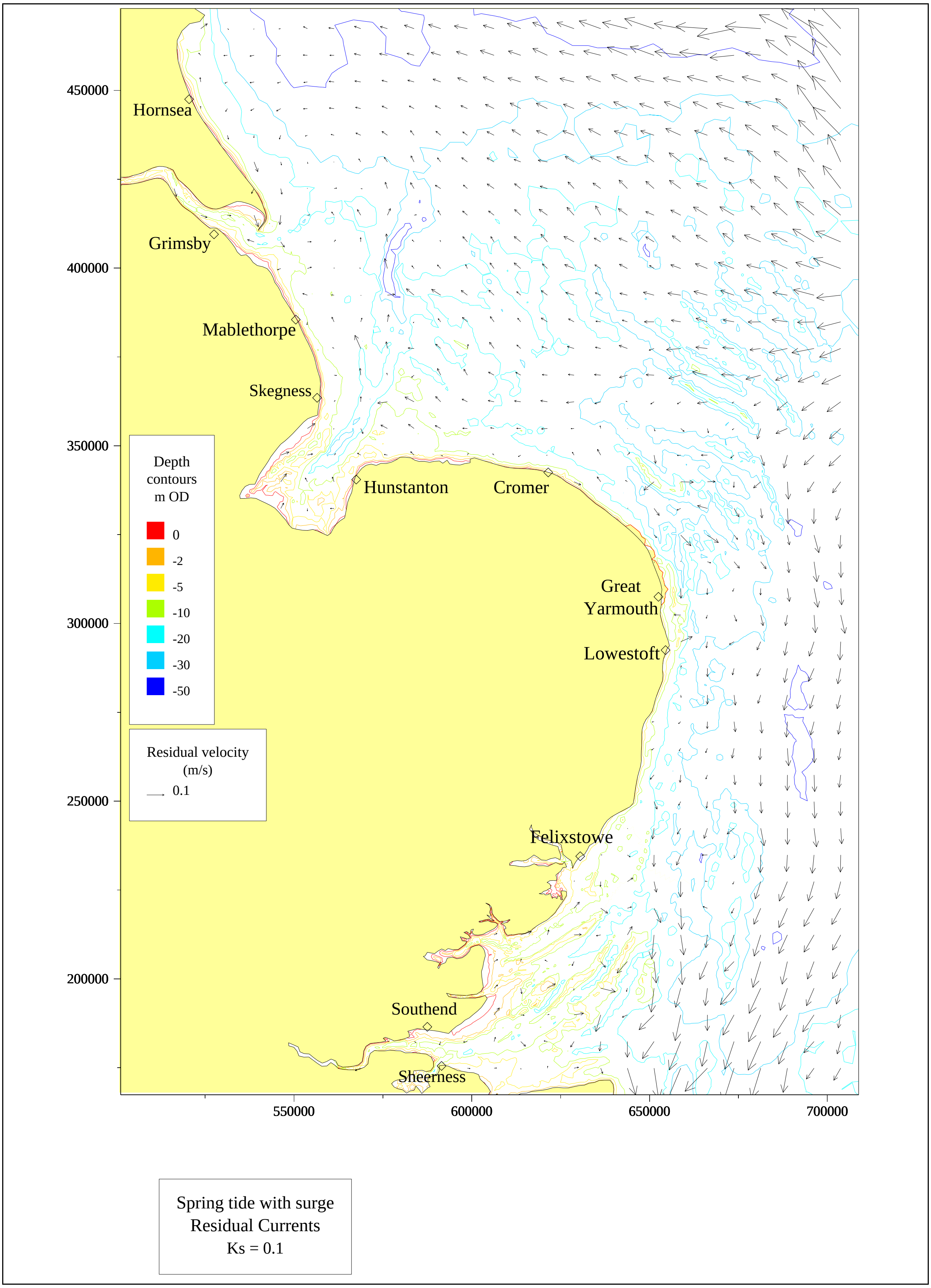

Figure 25 **Net spring tide residual velocity with surge and wind**

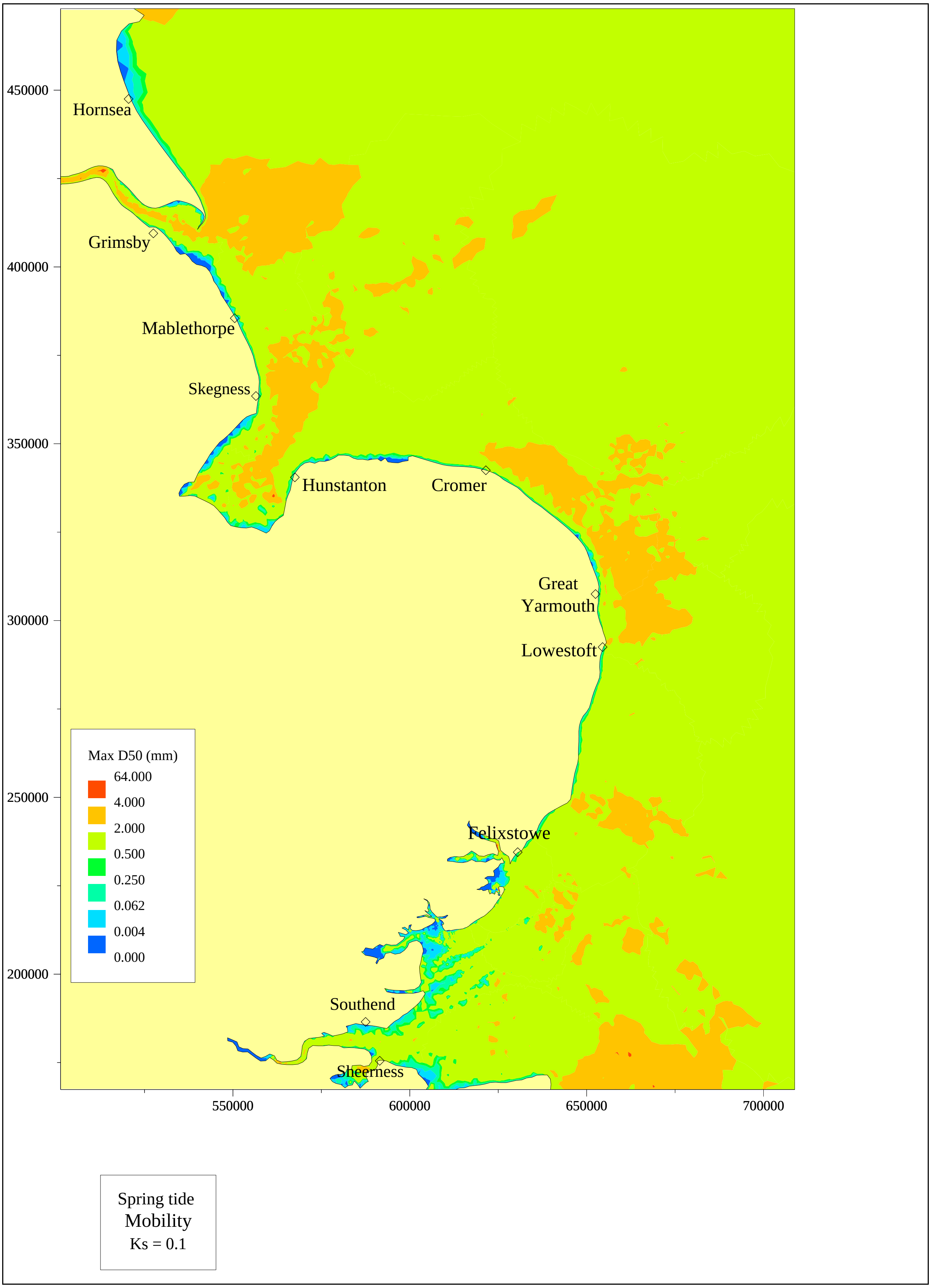

Figure 26 Seabed mobility: maximum mobile grain size under spring tides

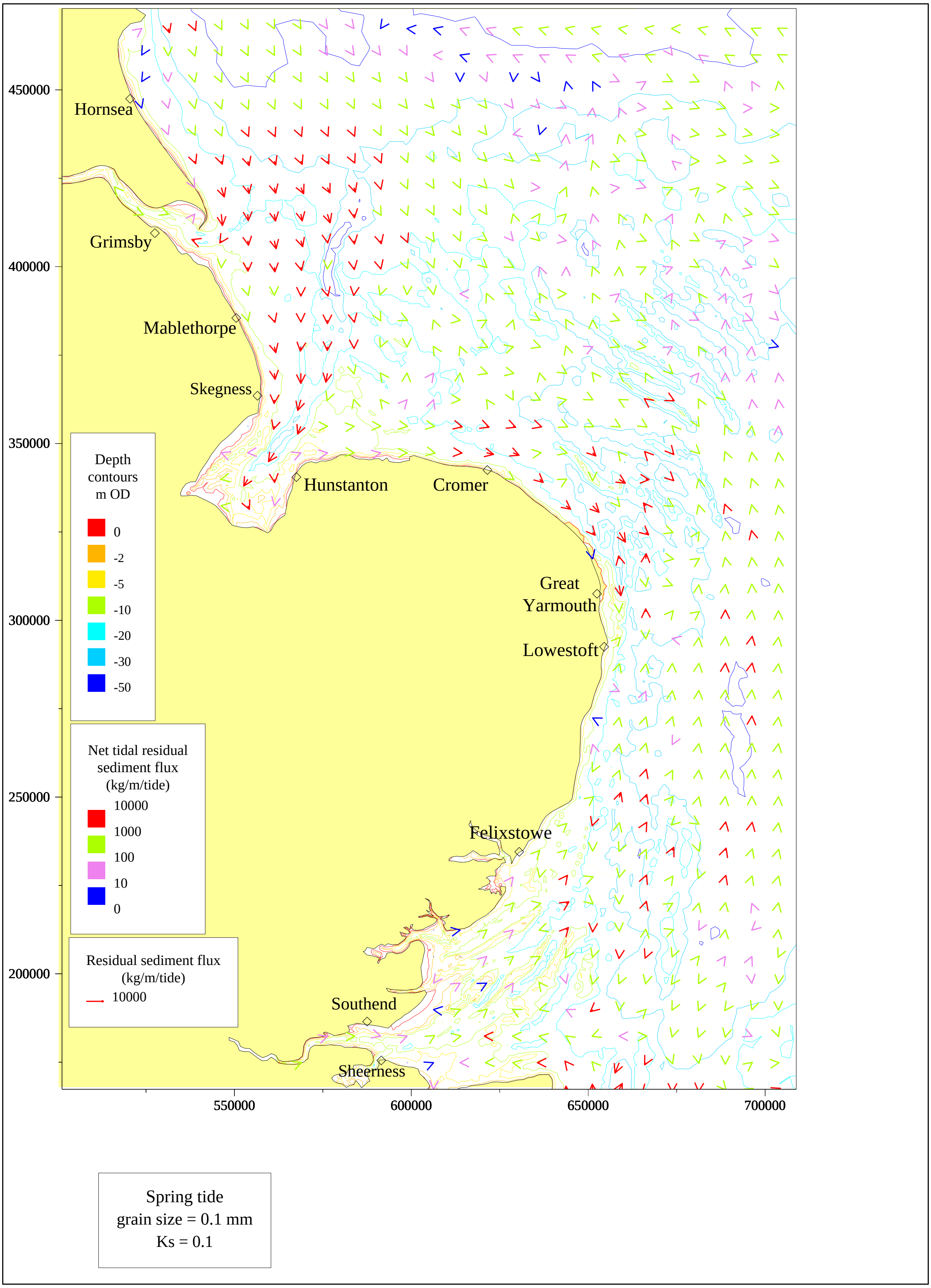

Figure 27 Spring tide net sediment flux patterns (0.1mm sand)

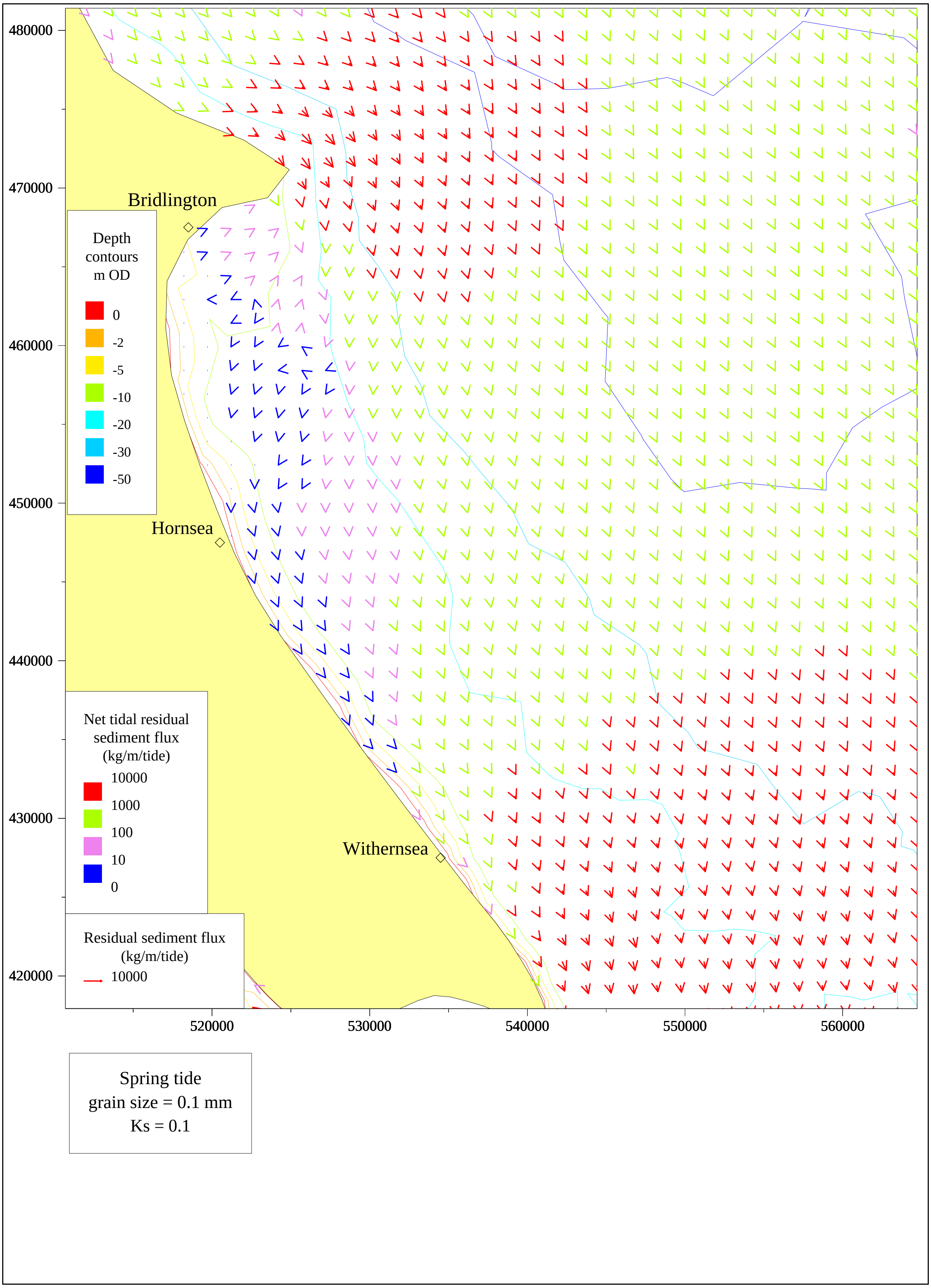

Figure 28 Spring tide net sediment flux patterns (0.1mm sand) detail: Flamborough Head to the Humber

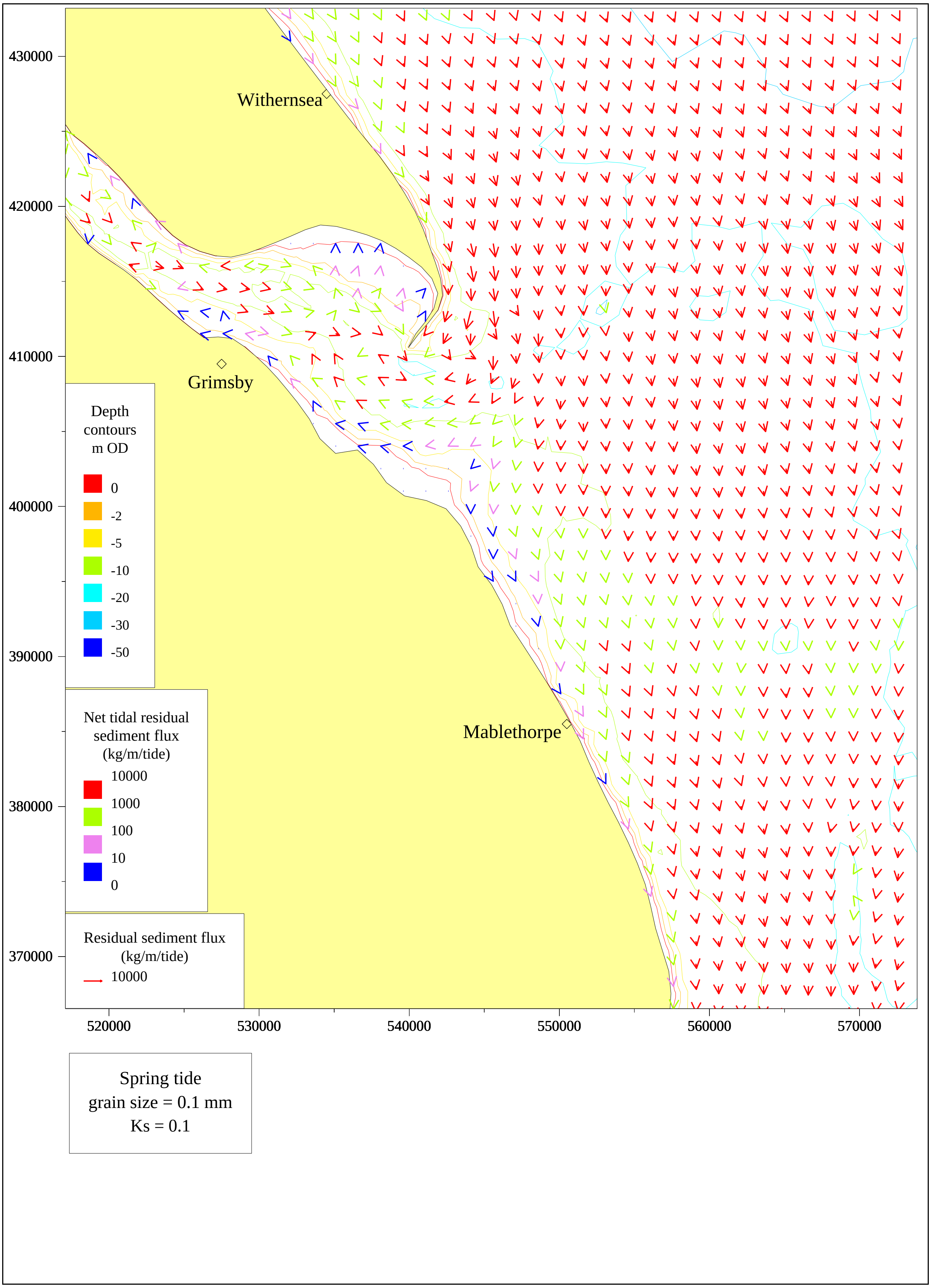

Figure 29 **Spring tide net sediment flux patterns (0.1mm sand) detail: Humber Entrance and Lincolnshire**

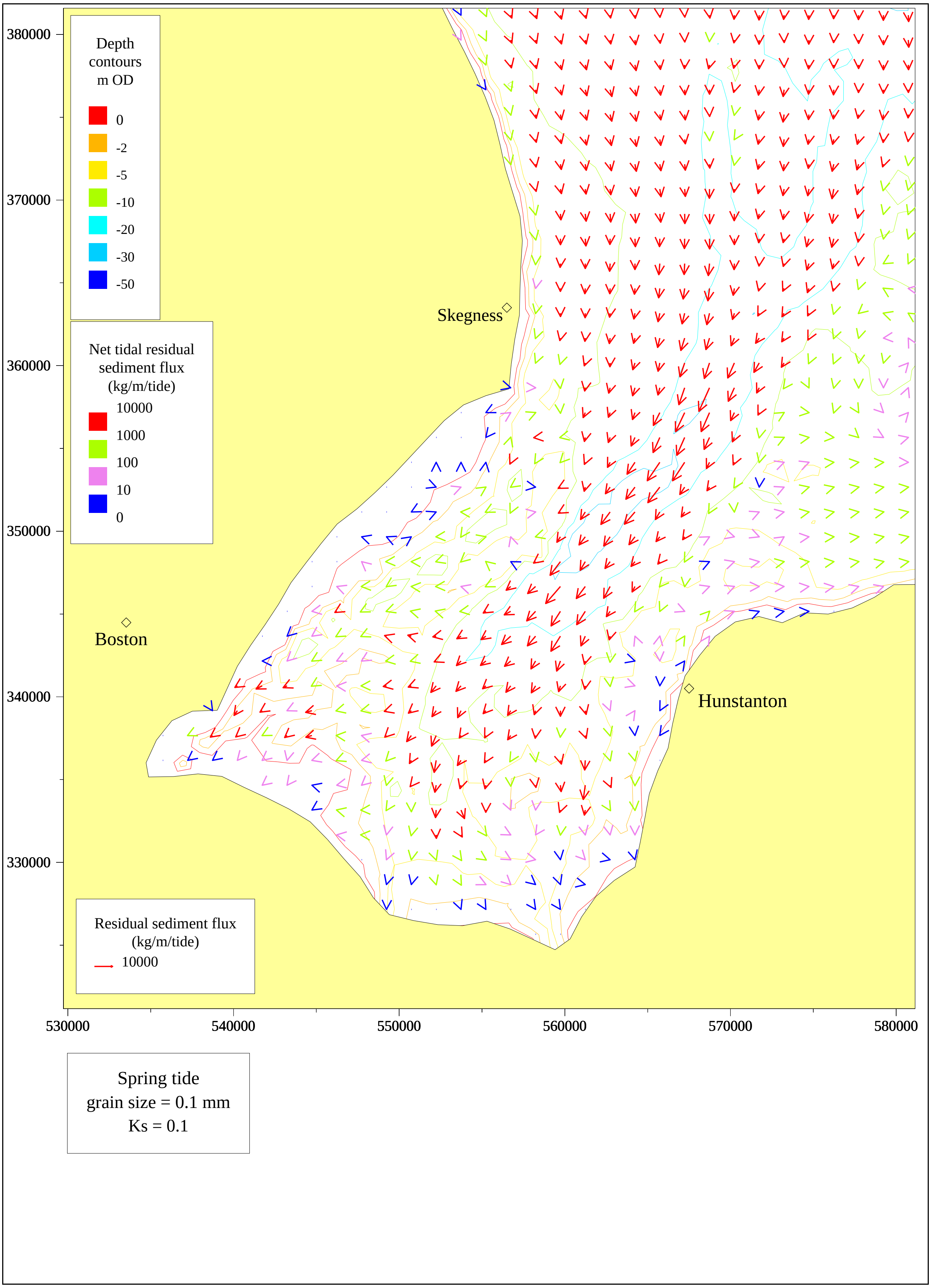

Figure 30 **Spring tide net sediment flux patterns (0.1mm sand) detail: Lincolnshire and the Wash**

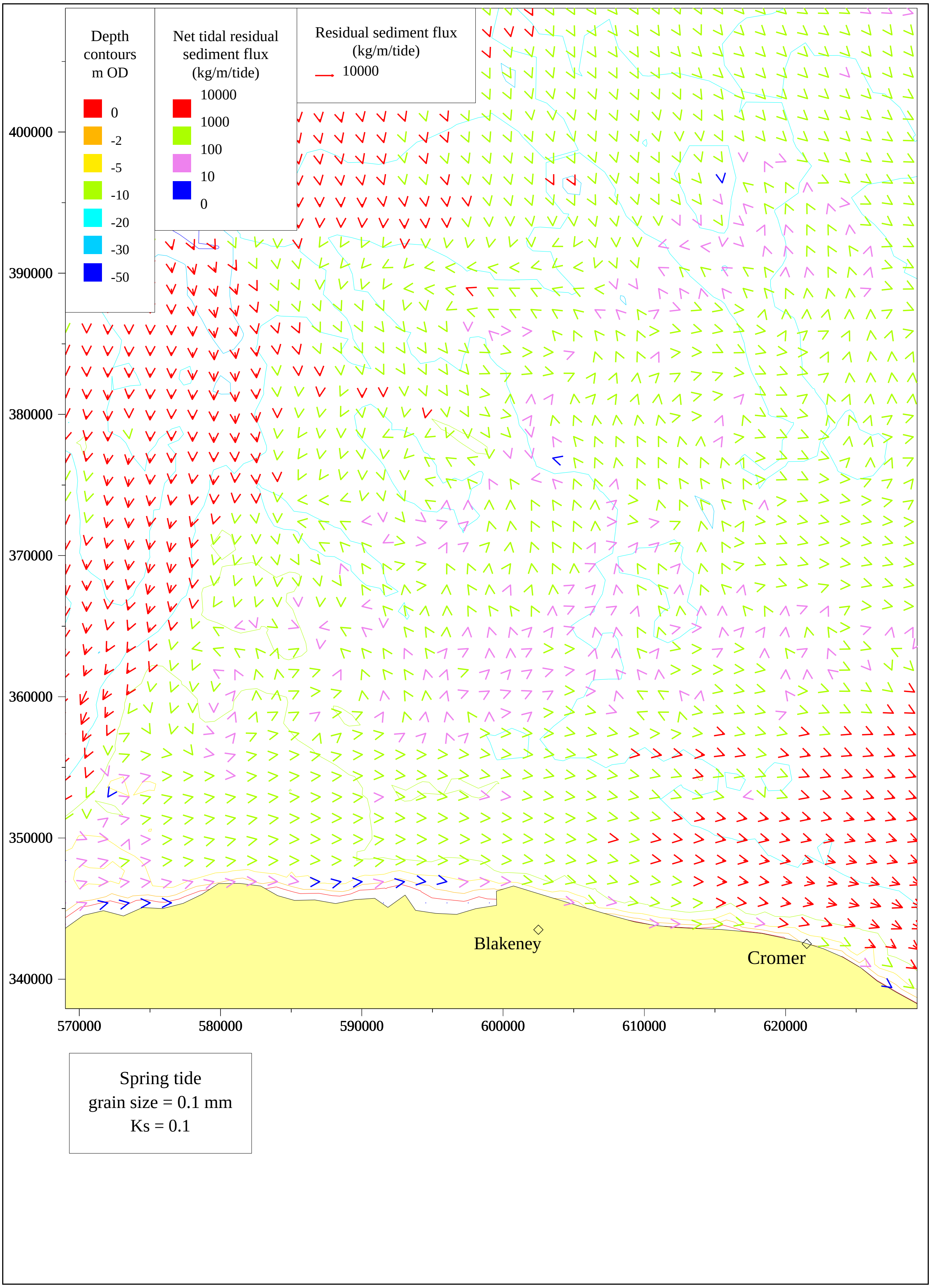

Figure 31 Spring tide net sediment flux patterns (0.1mm sand) detail: North Norfolk

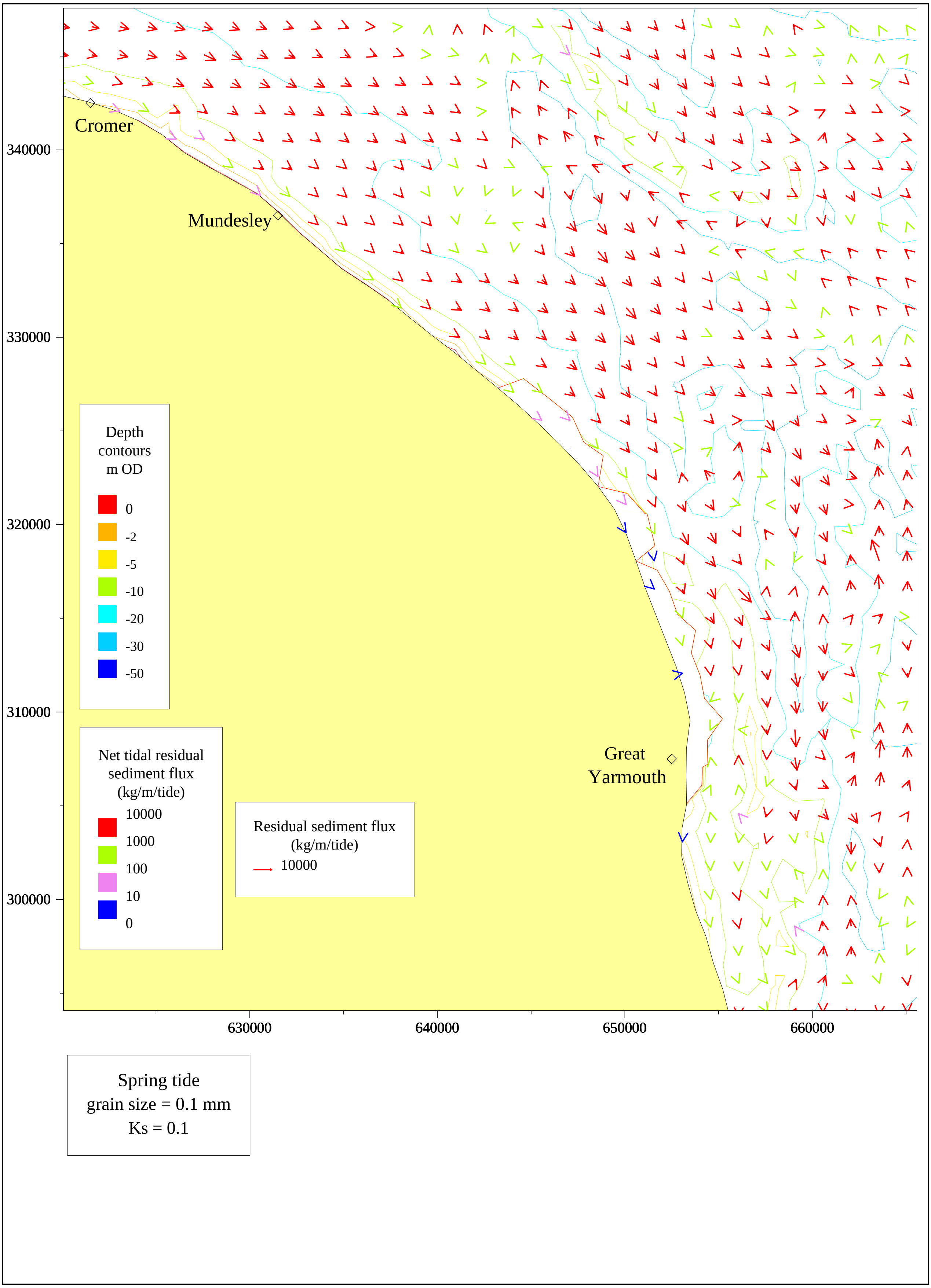

Figure 32 **Spring tide net sediment flux patterns (0.1mm sand) detail: East Norfolk**

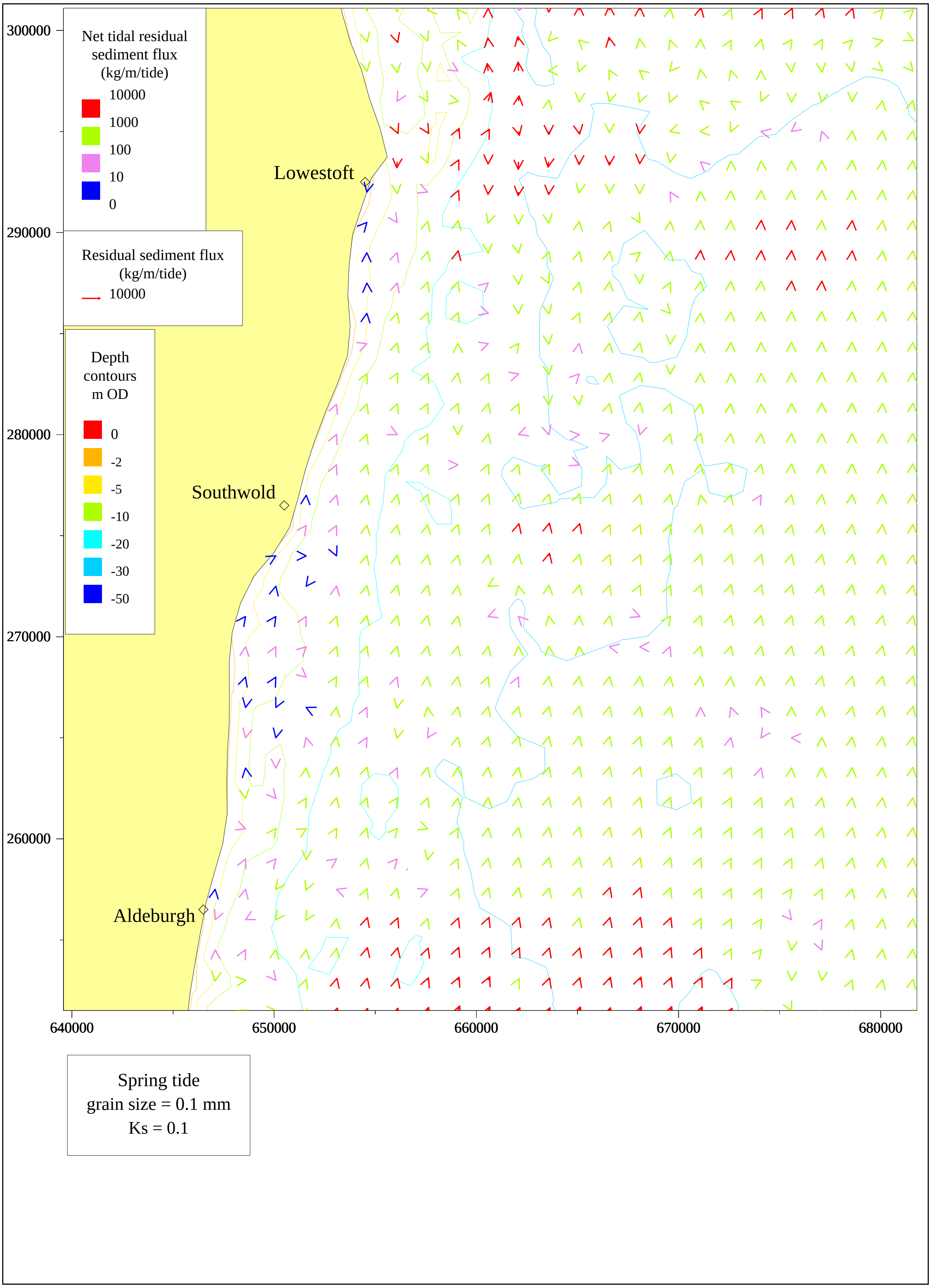

Figure 33 **Spring tide net sediment flux patterns (0.1mm sand) detail: North Suffolk**

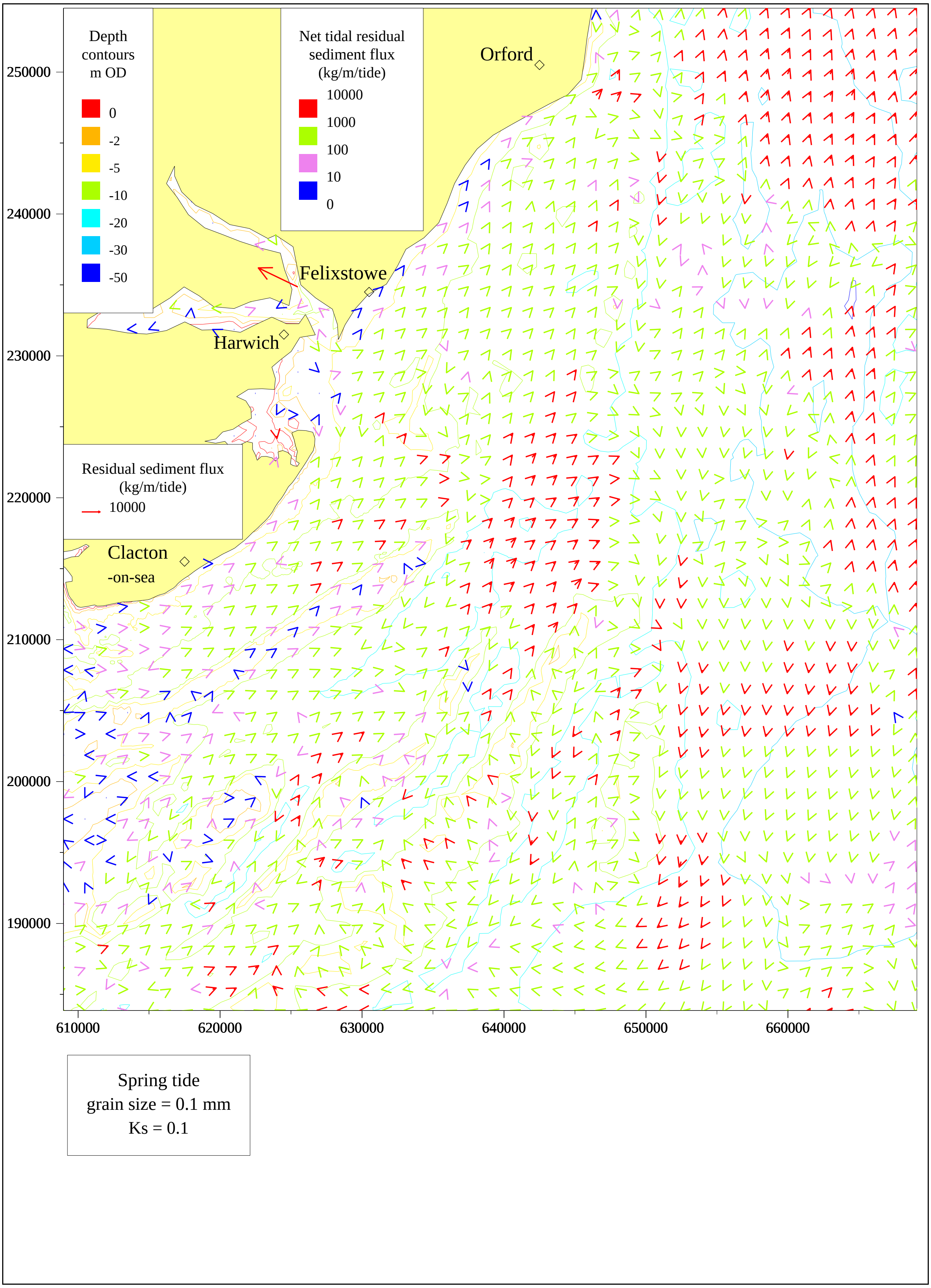

Figure 34 Spring tide net sediment flux patterns (0.1mm sand) detail: Suffolk and Essex

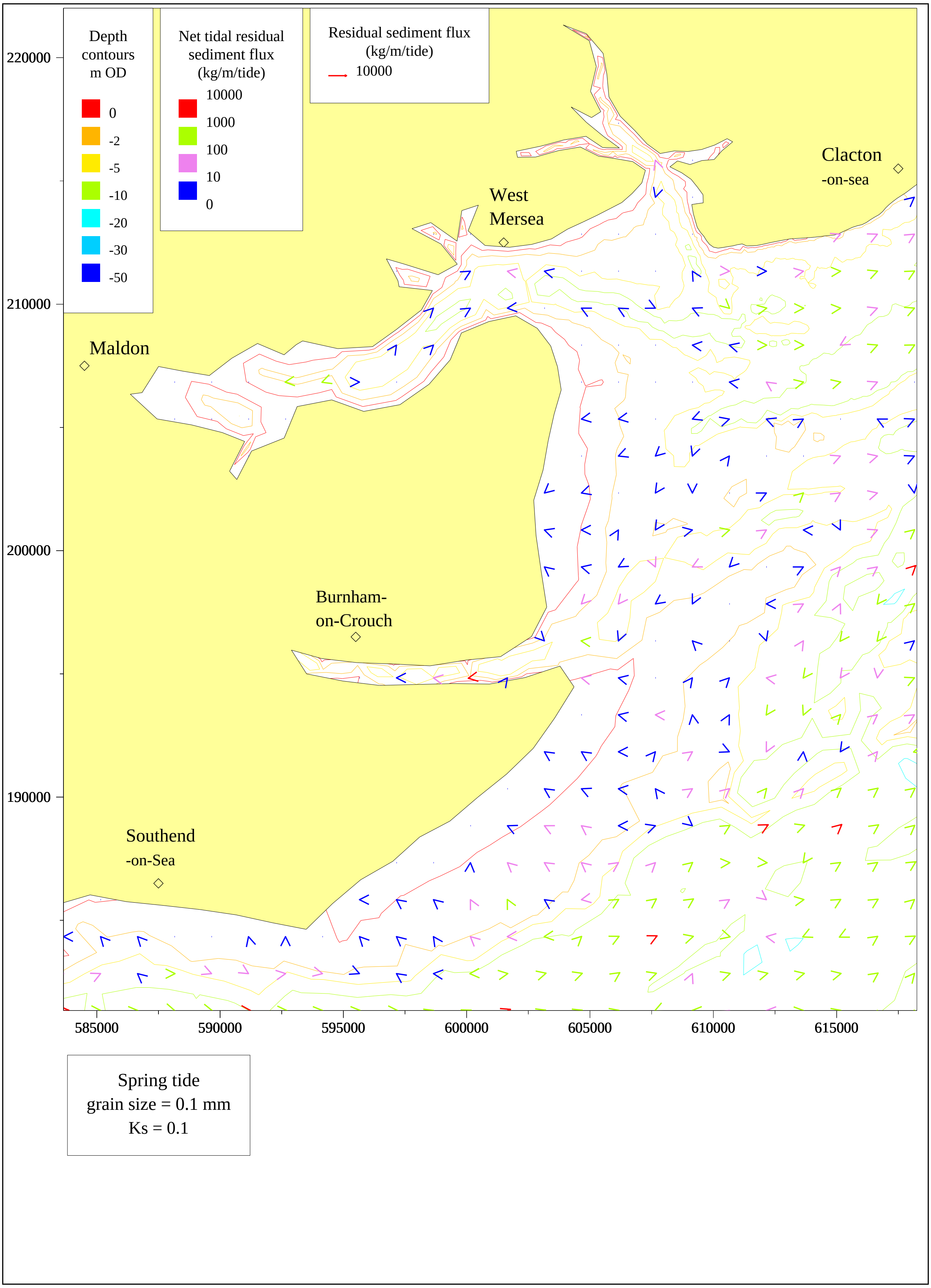

Figure 35 Spring tide net sediment flux patterns (0.1mm sand) detail: South Essex

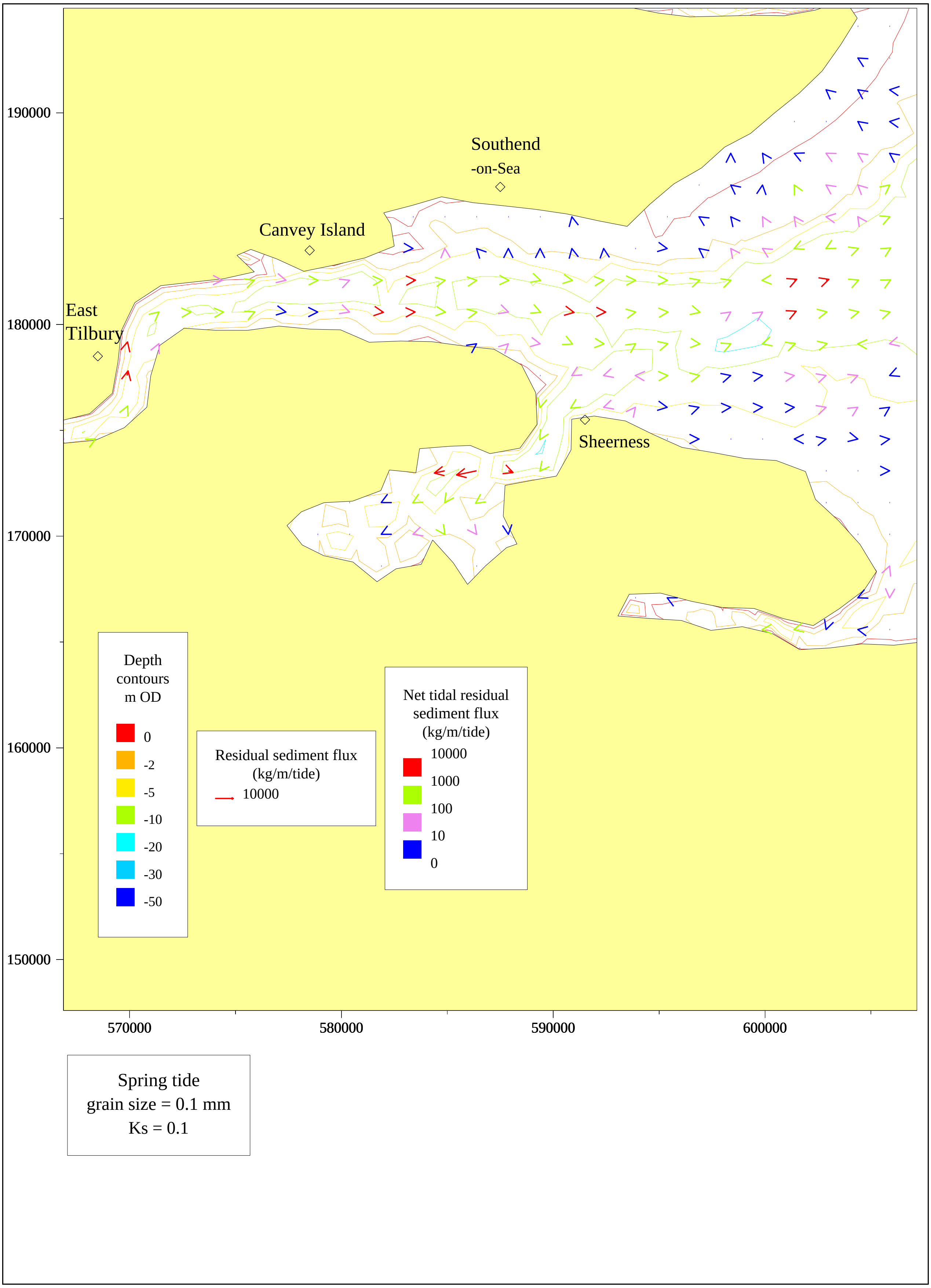

Figure 36 Spring tide net sediment flux patterns (0.1mm sand) detail: Outer Thames

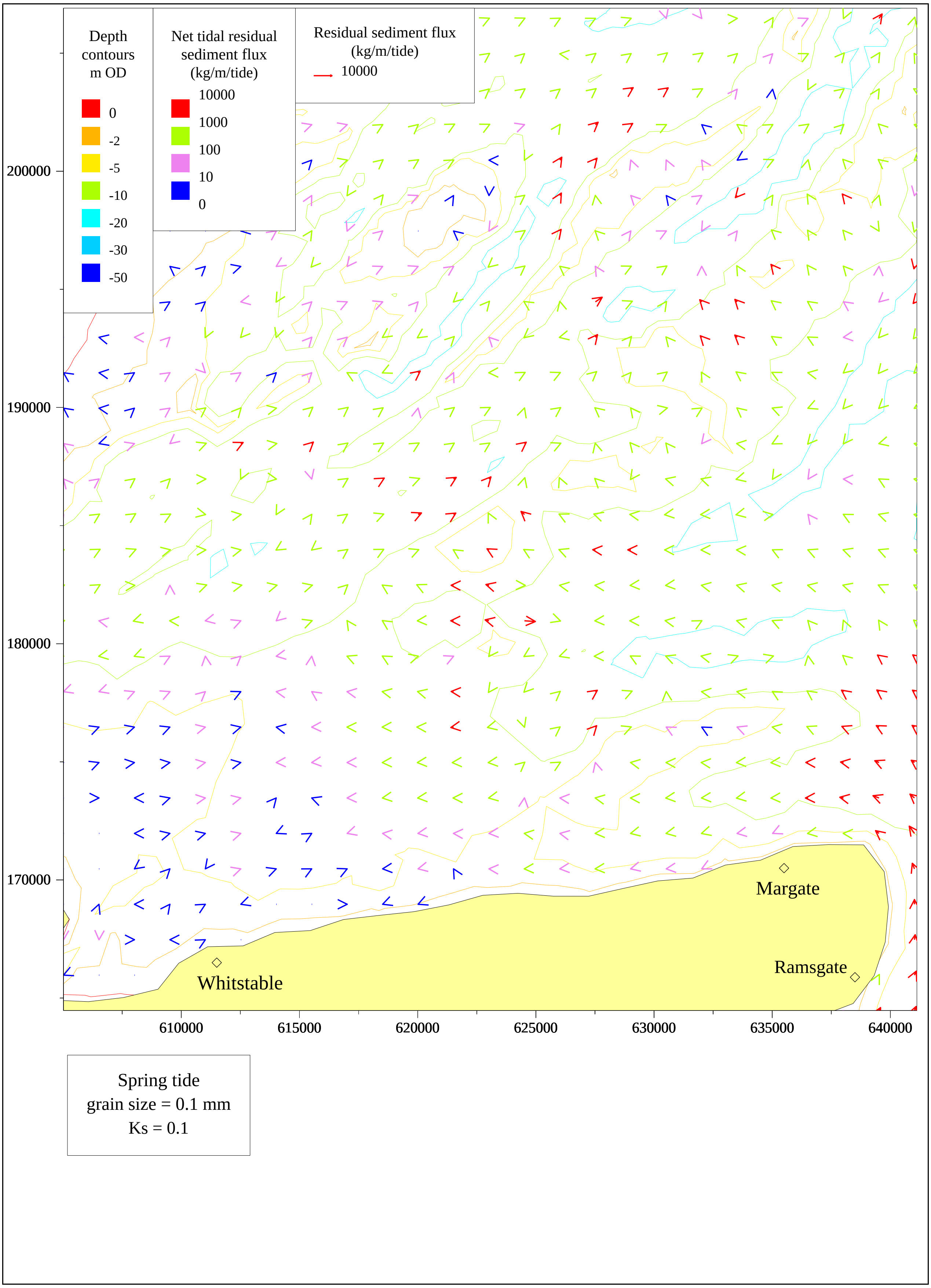

Figure 37 **Spring tide net sediment flux patterns (0.1mm sand) detail: North Kent**

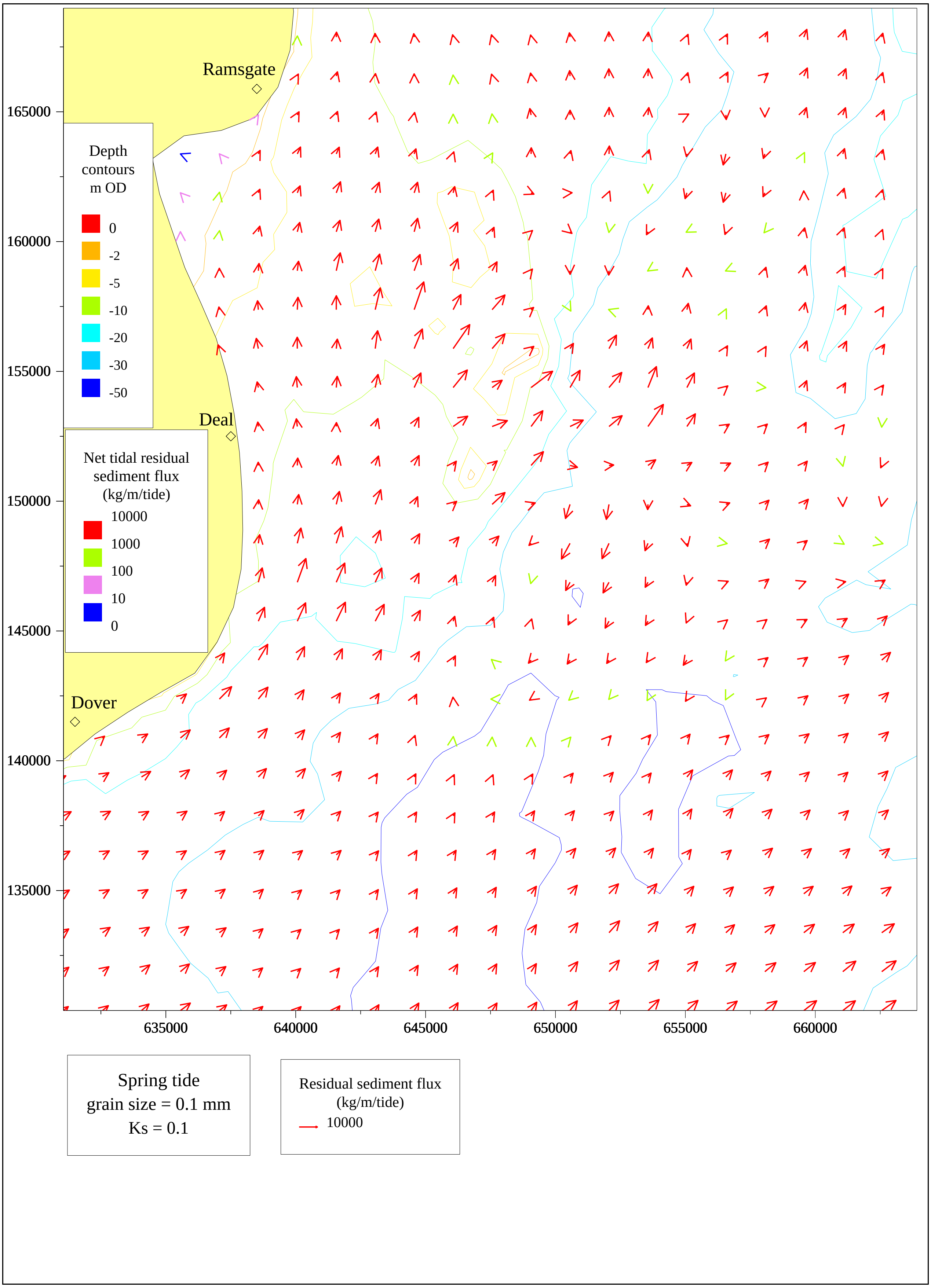

Figure 38 **Spring tide net sediment flux patterns (0.1mm sand) detail: East Kent**

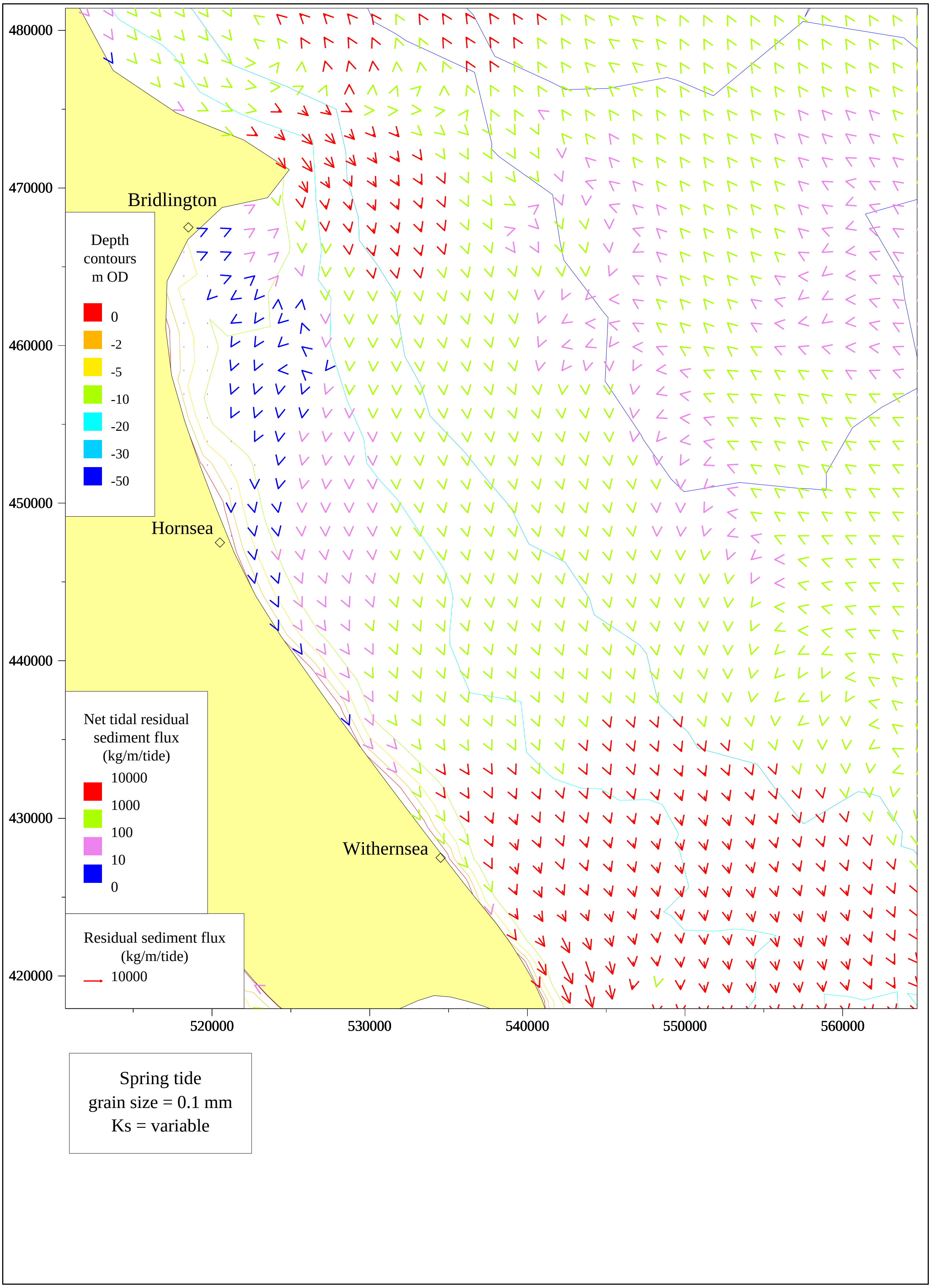

Figure 39 **Spring tide net sediment flux patterns (0.1mm sand), variable roughness, detail: Flamborough Head to the Humber**

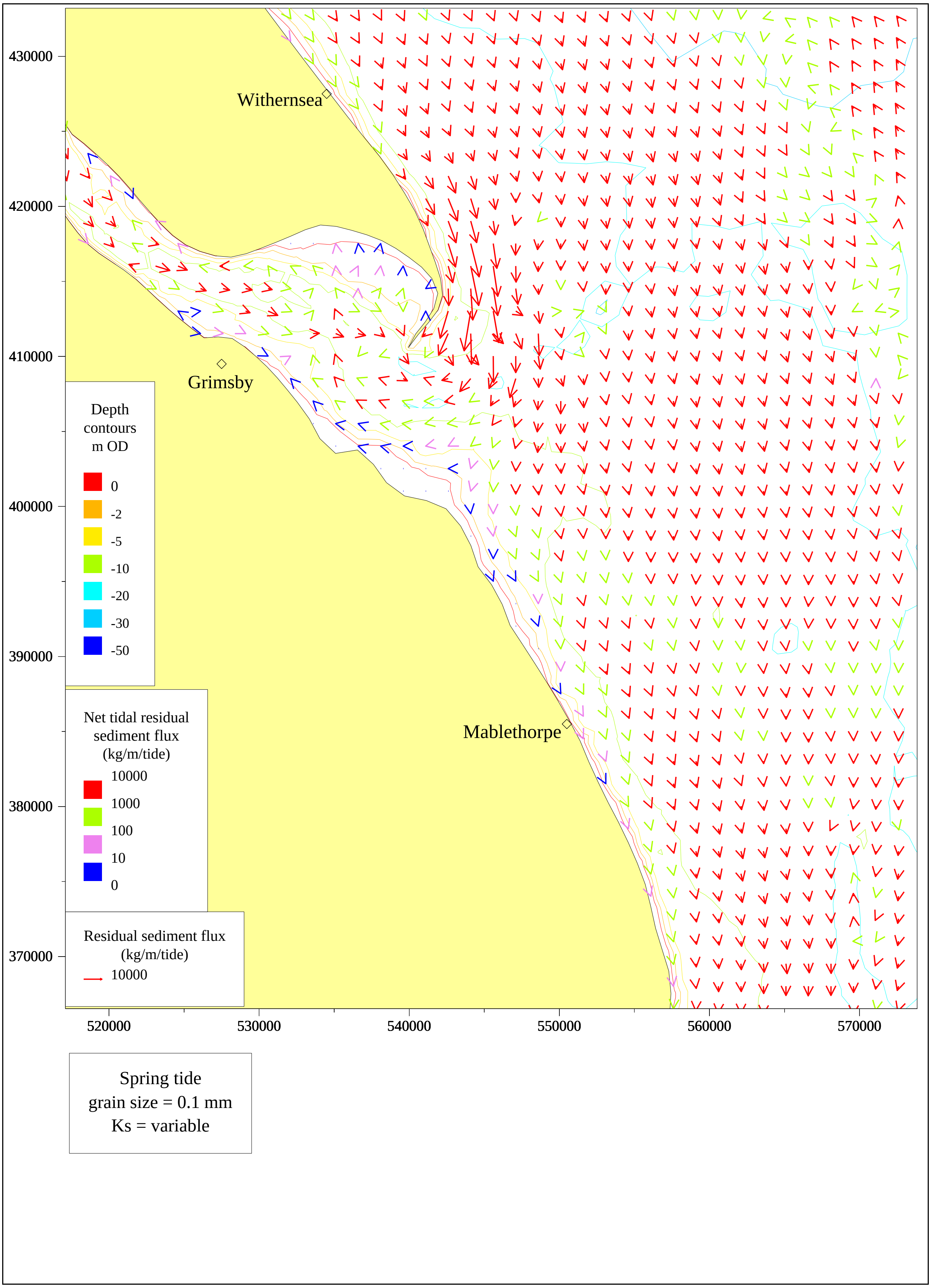

Figure 40 **Spring tide net sediment flux patterns (0.1mm sand), variable roughness, detail: Humber Entrance and Lincolnshire**

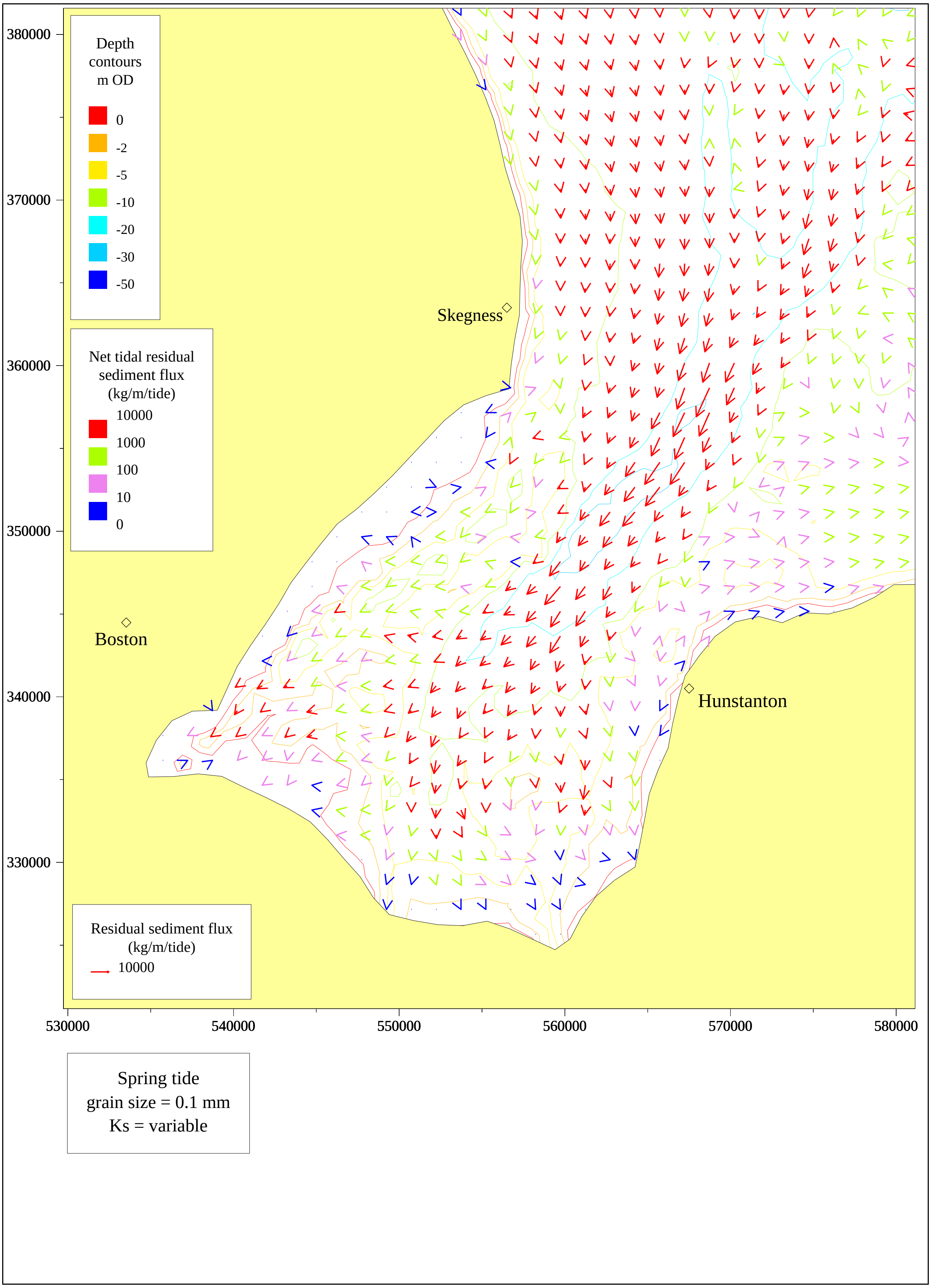

Figure 41 **Spring tide net sediment flux patterns (0.1mm sand), variable roughness, detail: Lincolnshire and the Wash**

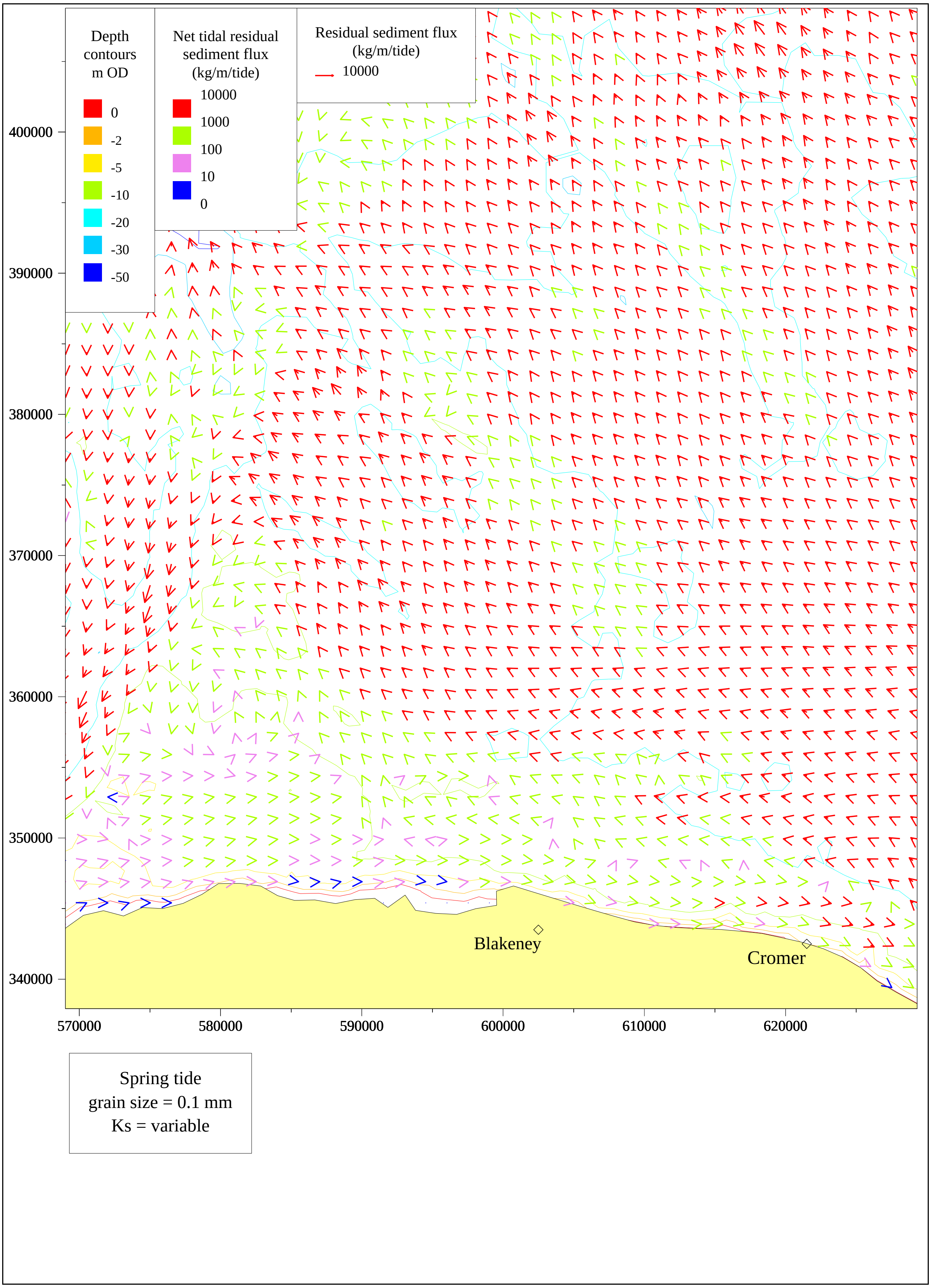

Figure 42 **Spring tide net sediment flux patterns (0.1mm sand), variable roughness, detail: North Norfolk**

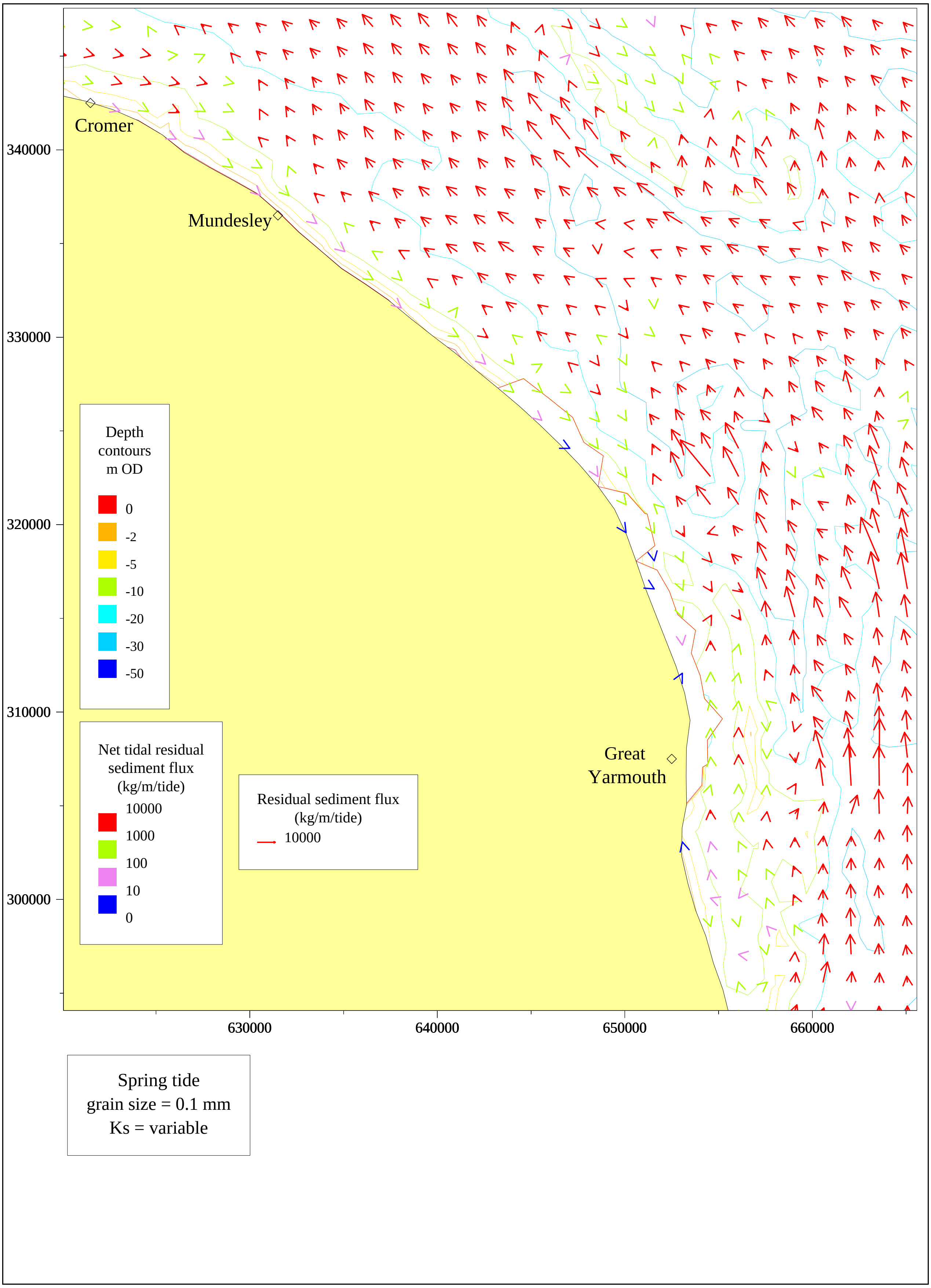

Figure 43 **Spring tide net sediment flux patterns (0.1mm sand), variable roughness, detail: East Norfolk**

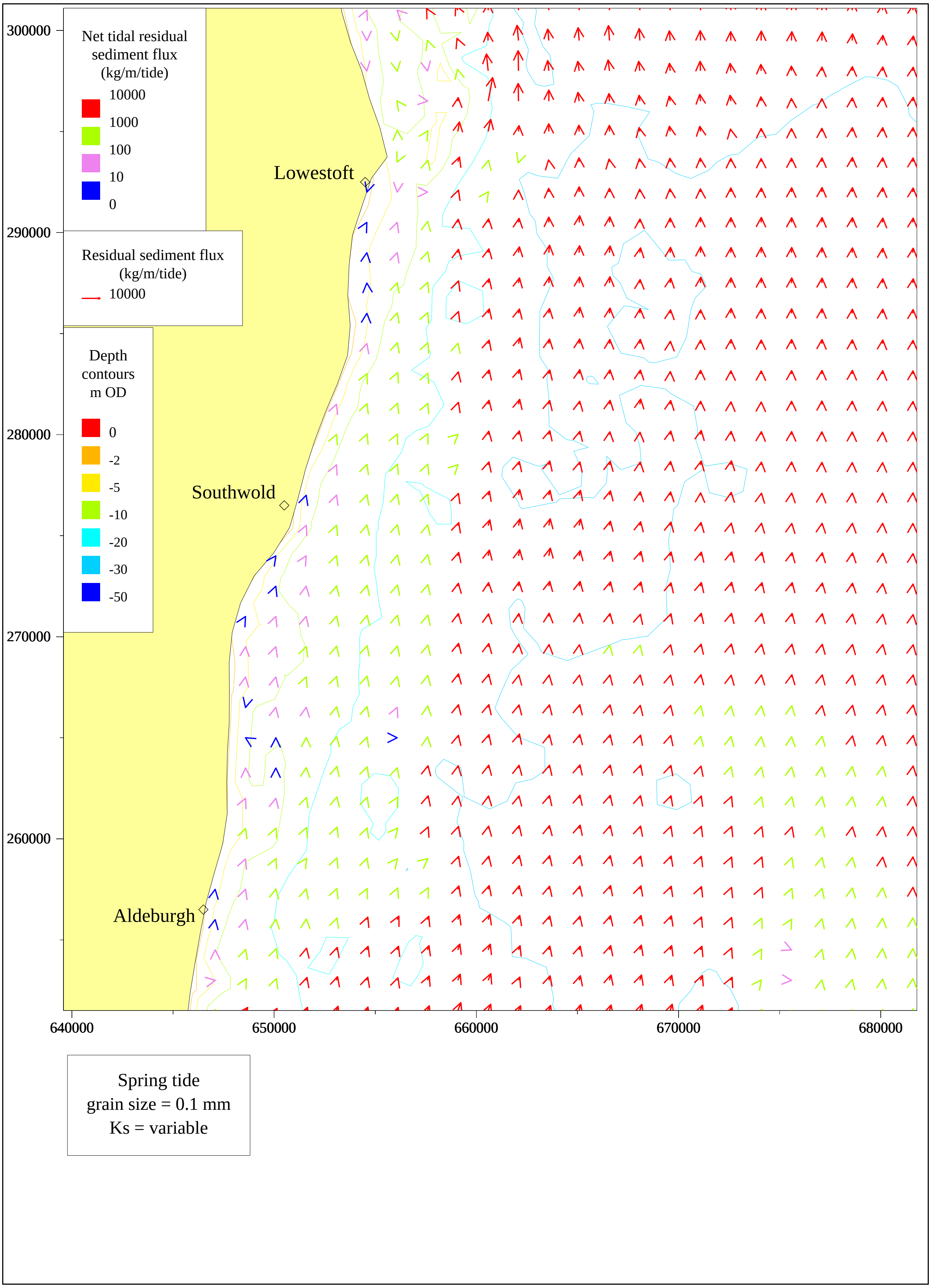

Figure 44 **Spring tide net sediment flux patterns (0.1mm sand), variable roughness, detail: North Suffolk**

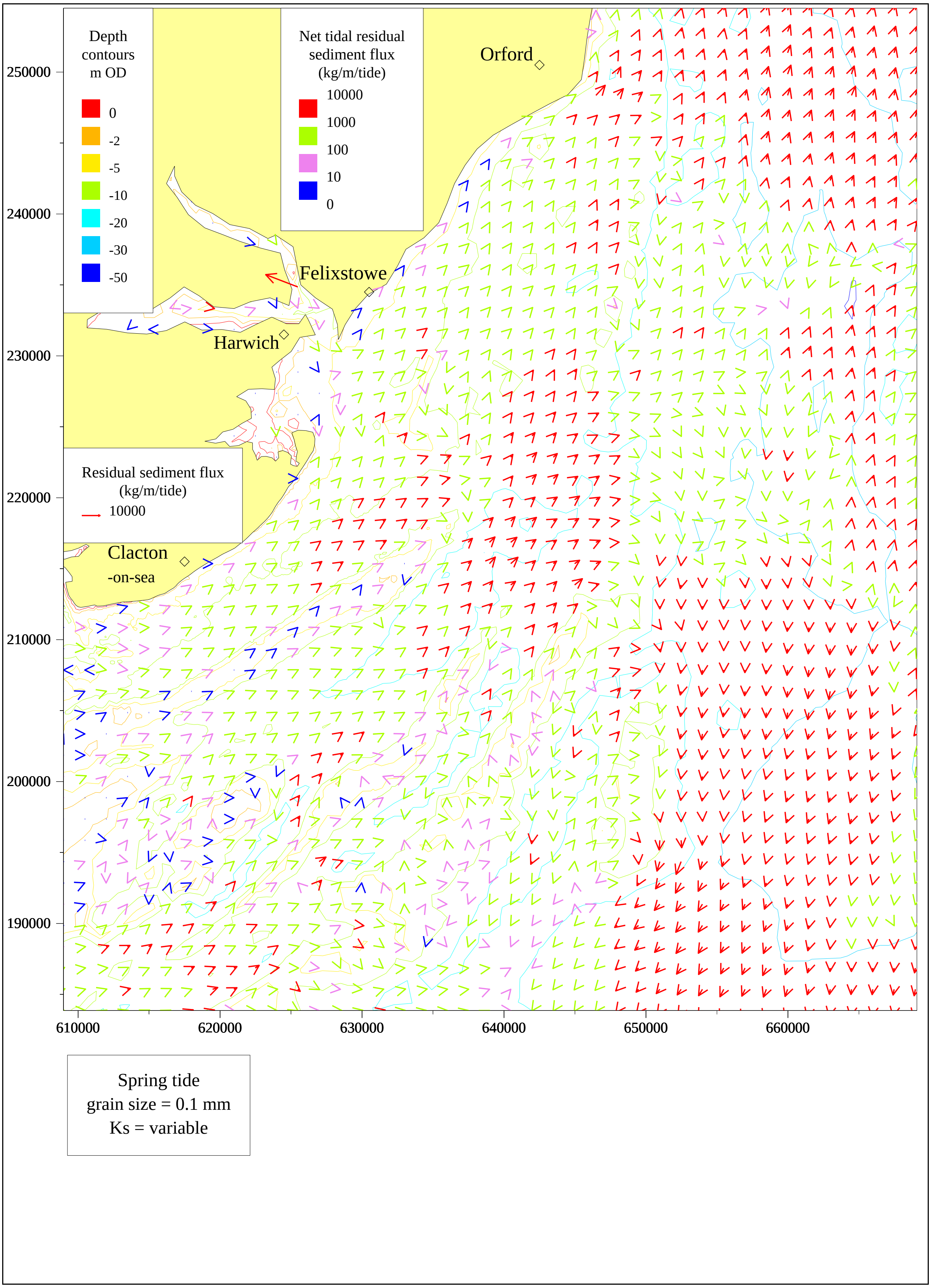

Figure 45 **Spring tide net sediment flux patterns (0.1mm sand), variable roughness, detail: Suffolk and Essex**

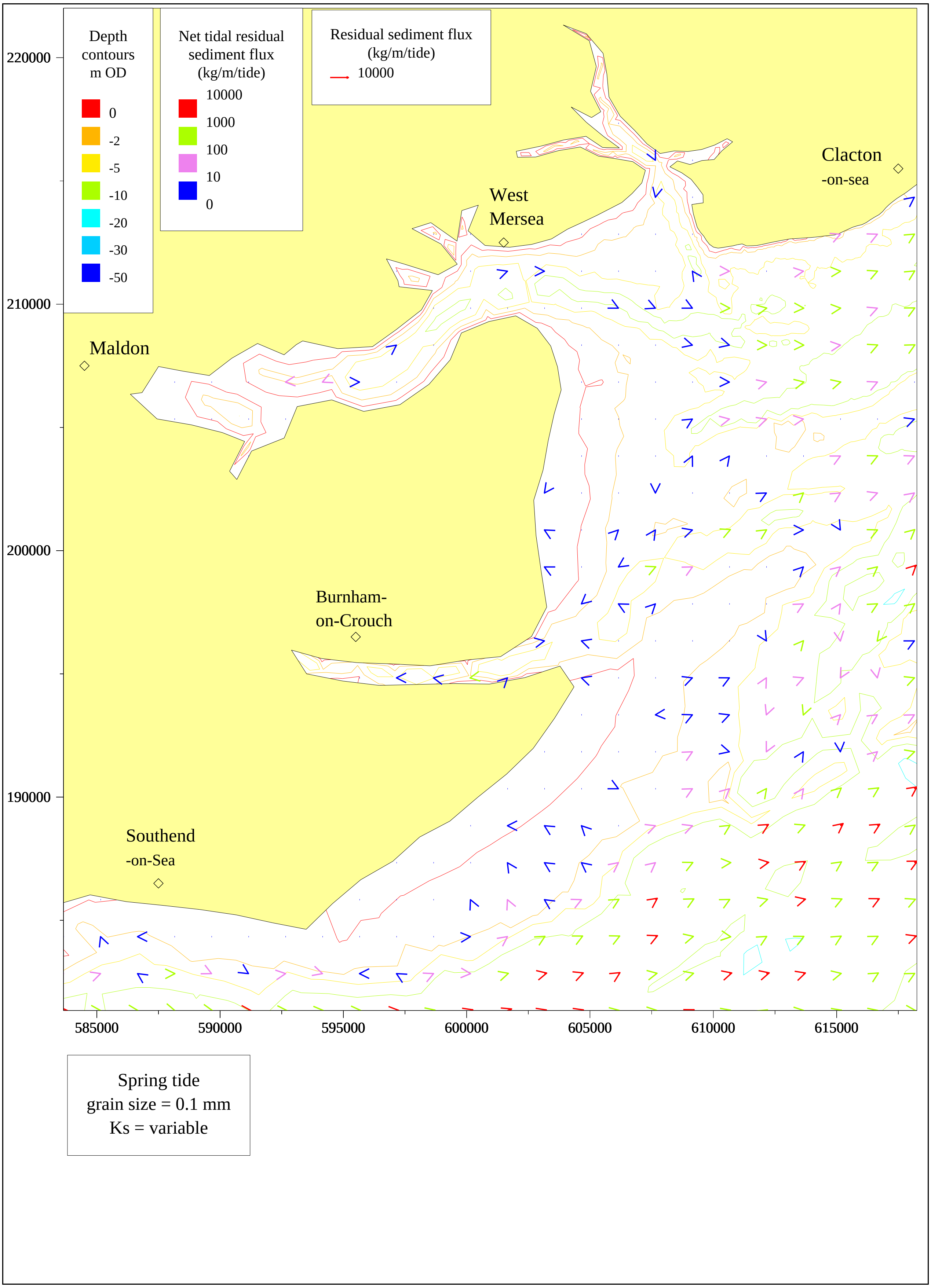

Figure 46 **Spring tide net sediment flux patterns (0.1mm sand), variable roughness, detail: South Essex**

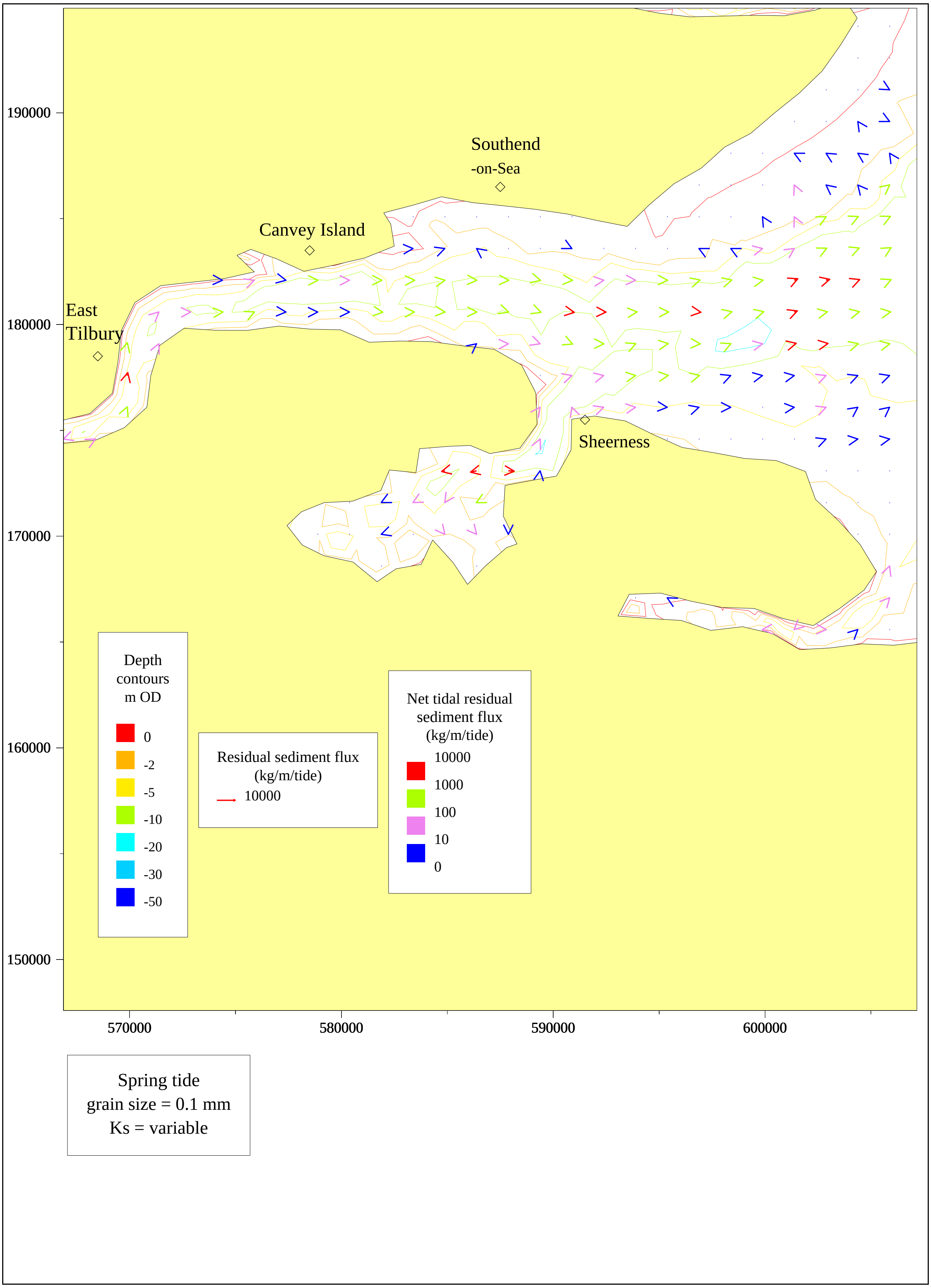

Figure 47 **Spring tide net sediment flux patterns (0.1mm sand), variable roughness, detail: Outer Thames**

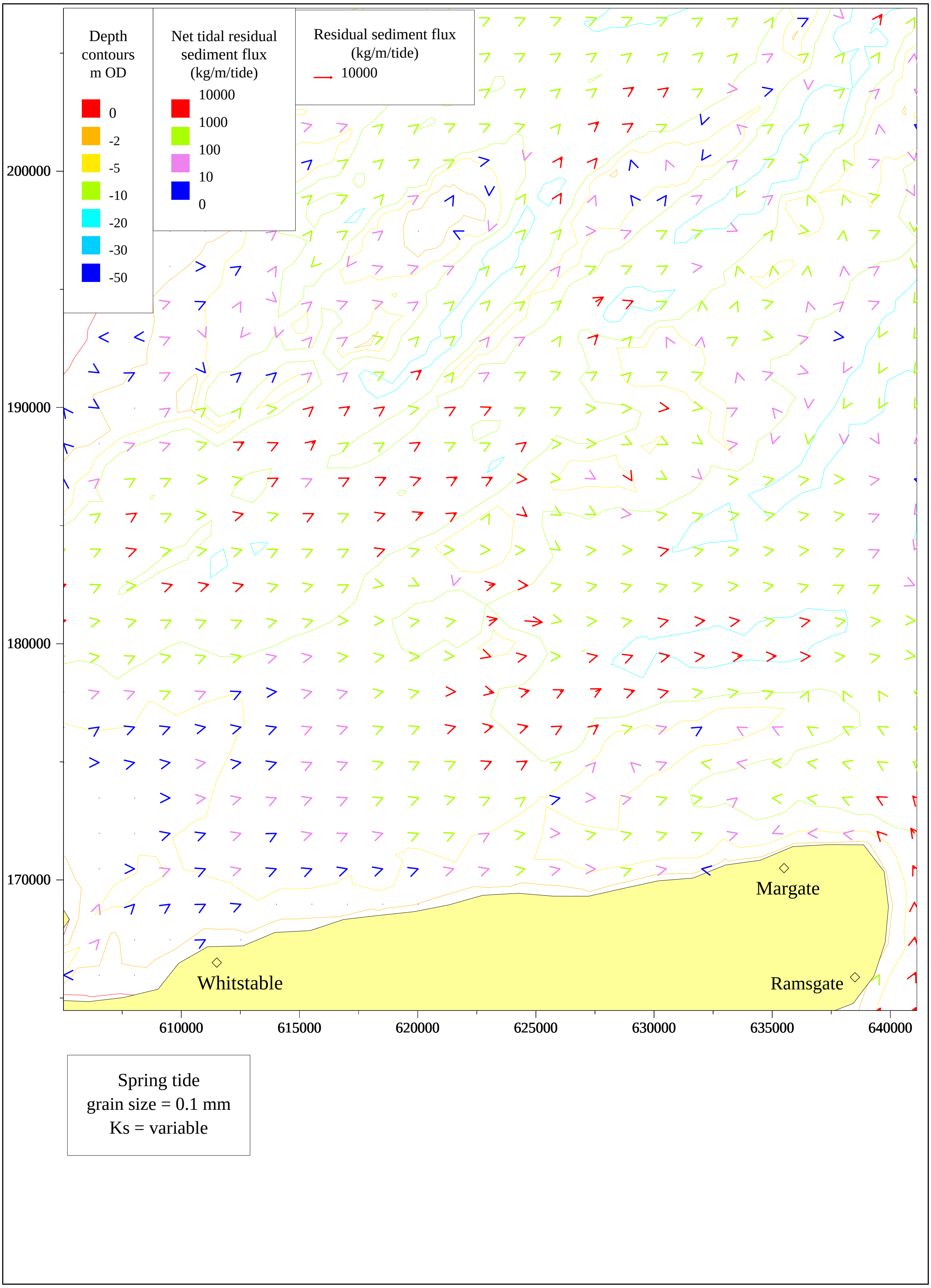

Figure 48 **Spring tide net sediment flux patterns (0.1mm sand), variable roughness, detail: North Kent**

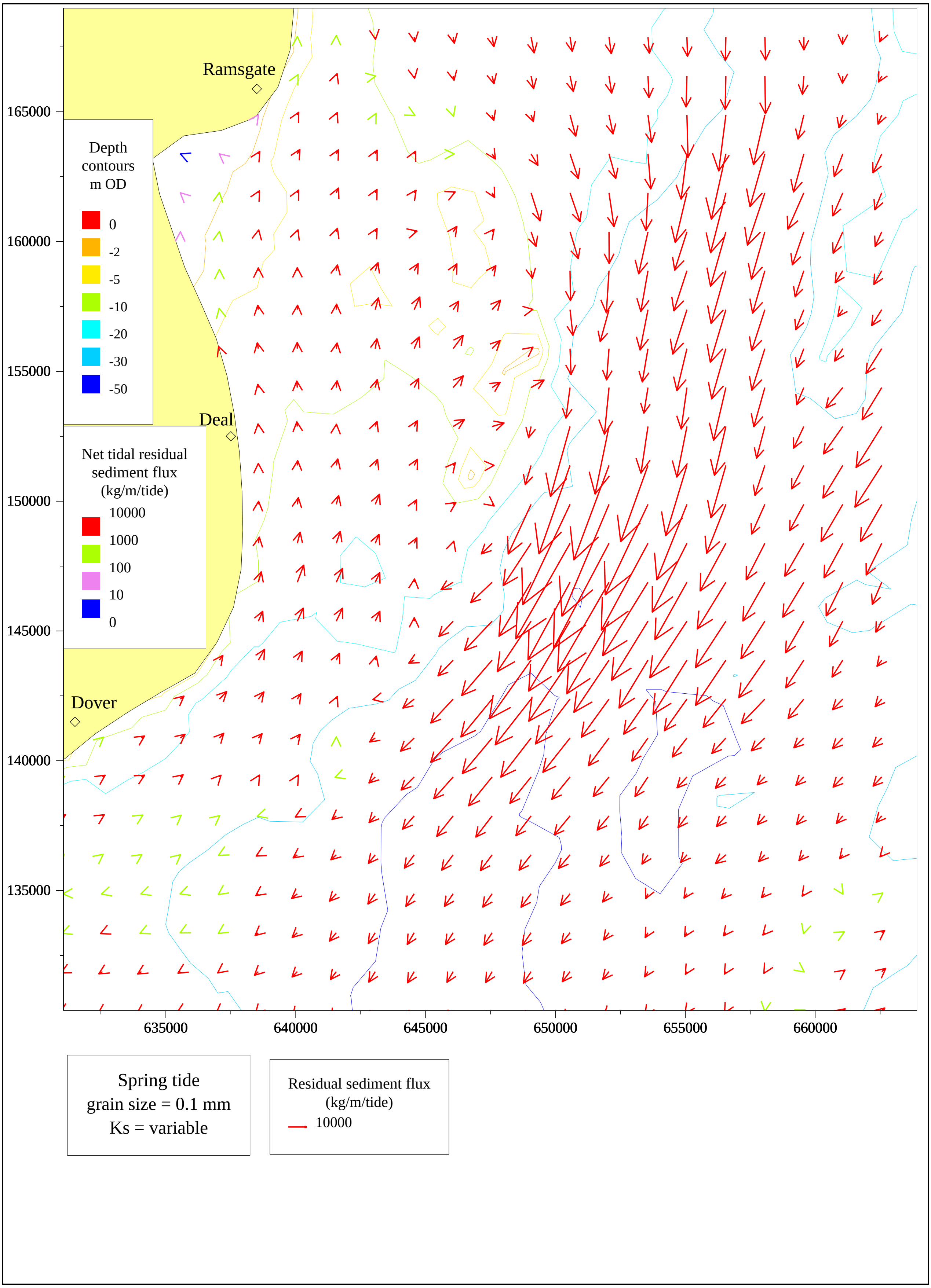

Figure 49 **Spring tide net sediment flux patterns (0.1mm sand), variable roughness, detail: East Kent**

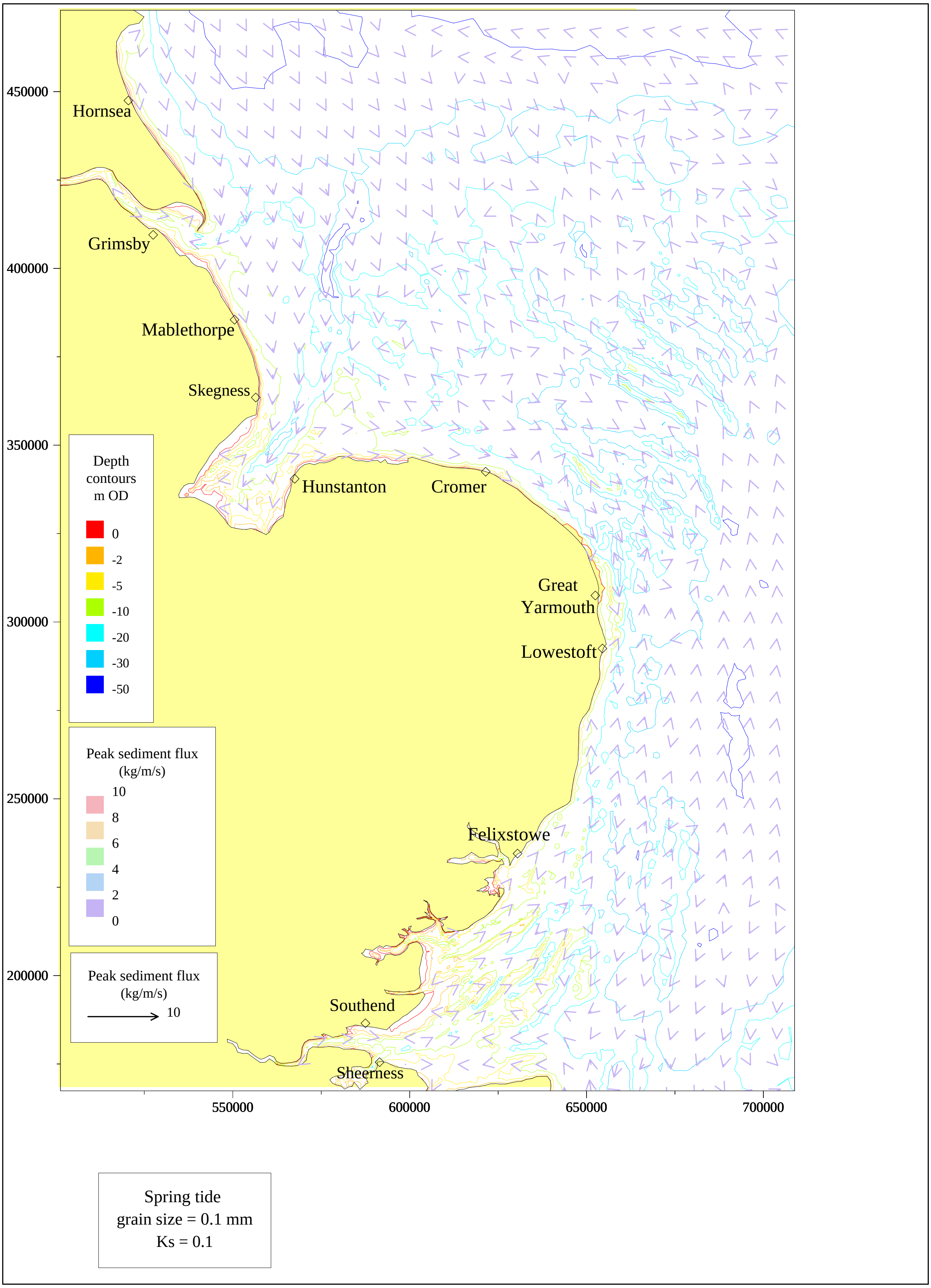

Figure 50 **Peak sediment flux during spring tide (0.1mm sand)**

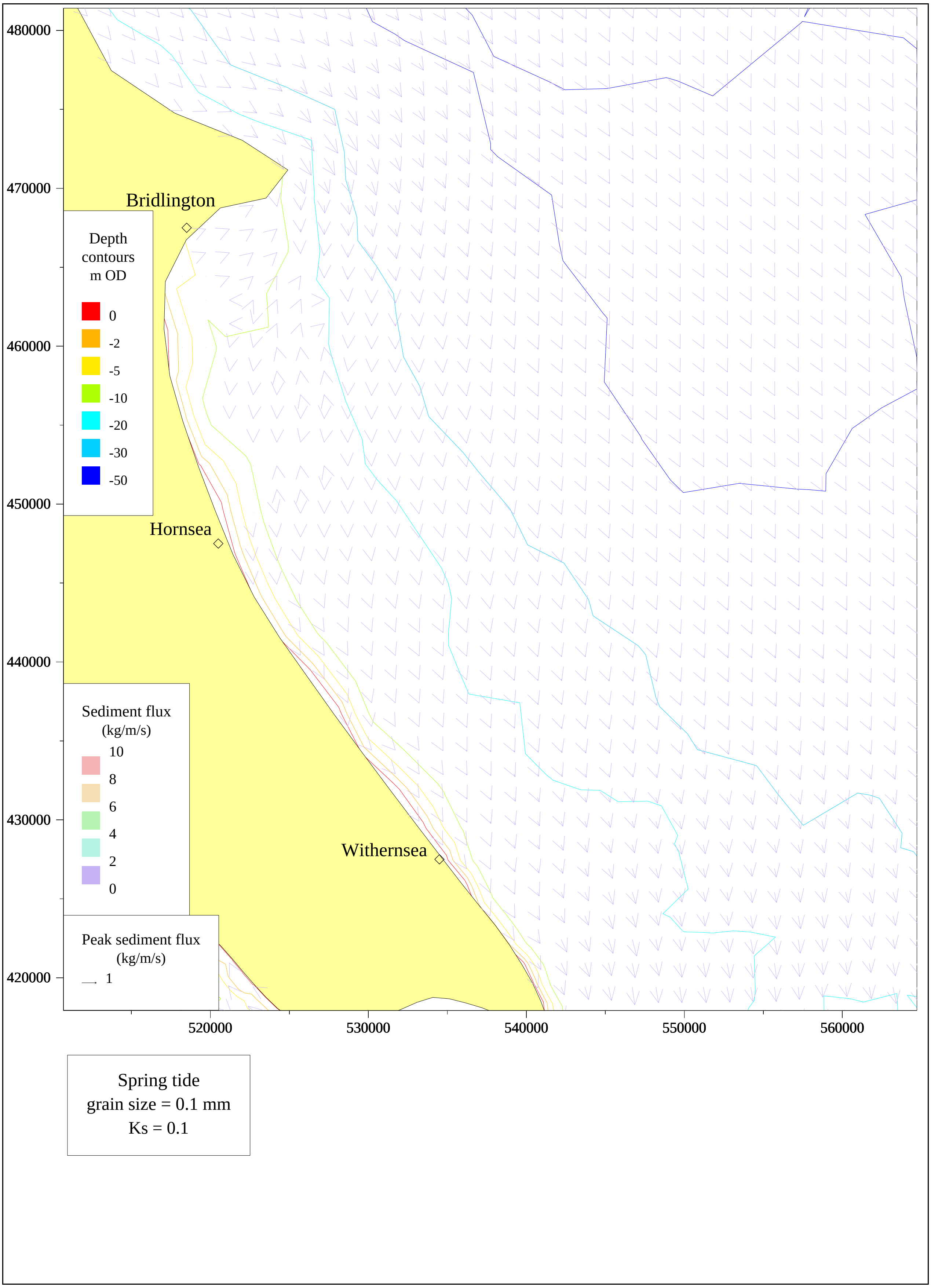

Figure 51 **Peak sediment flux during spring tide (0.1mm sand) detail: Flamborough Head to the Humber**

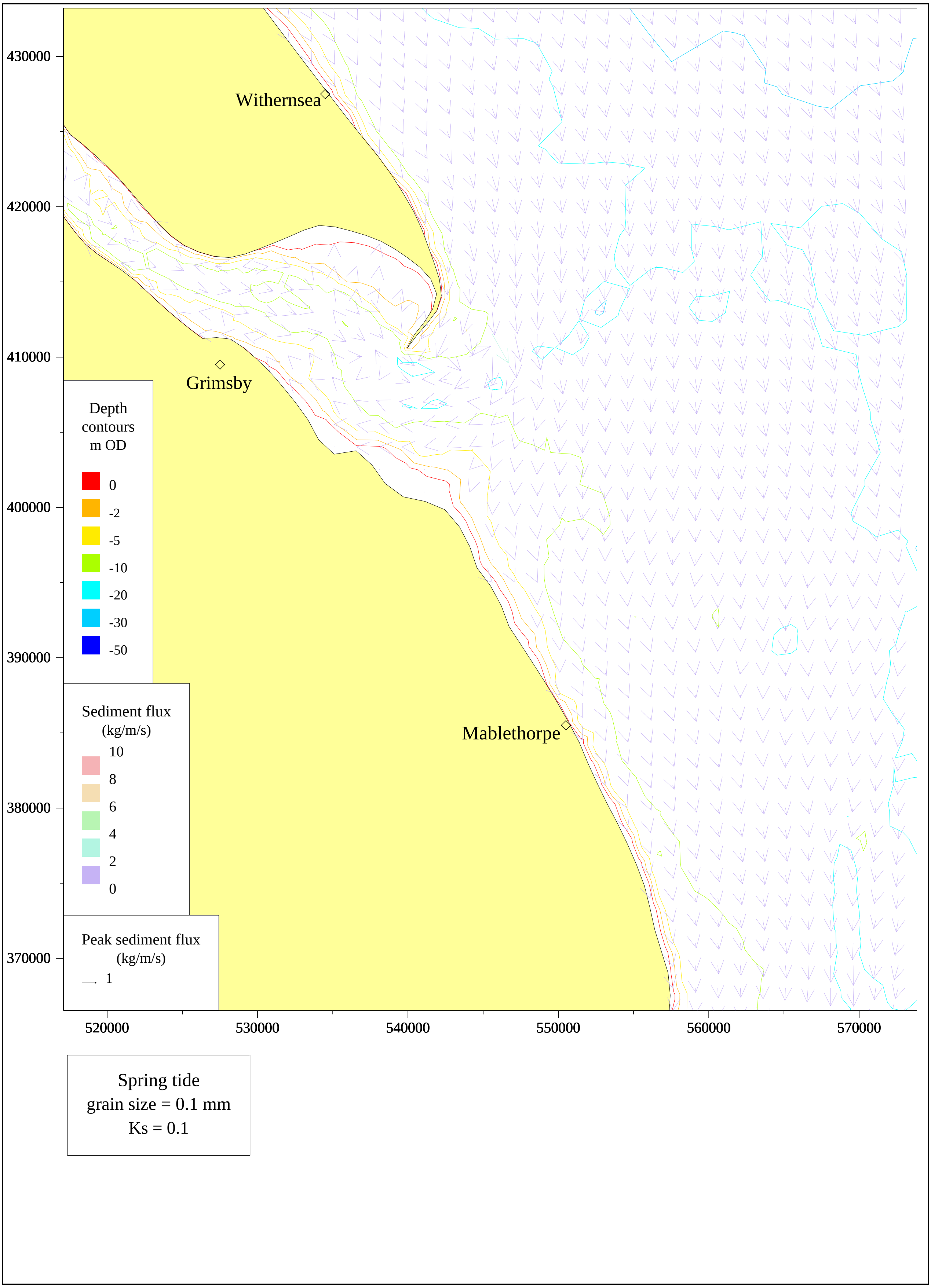

Figure 52 **Peak sediment flux during spring tide (0.1mm sand) detail: Humber Entrance and Lincolnshire**

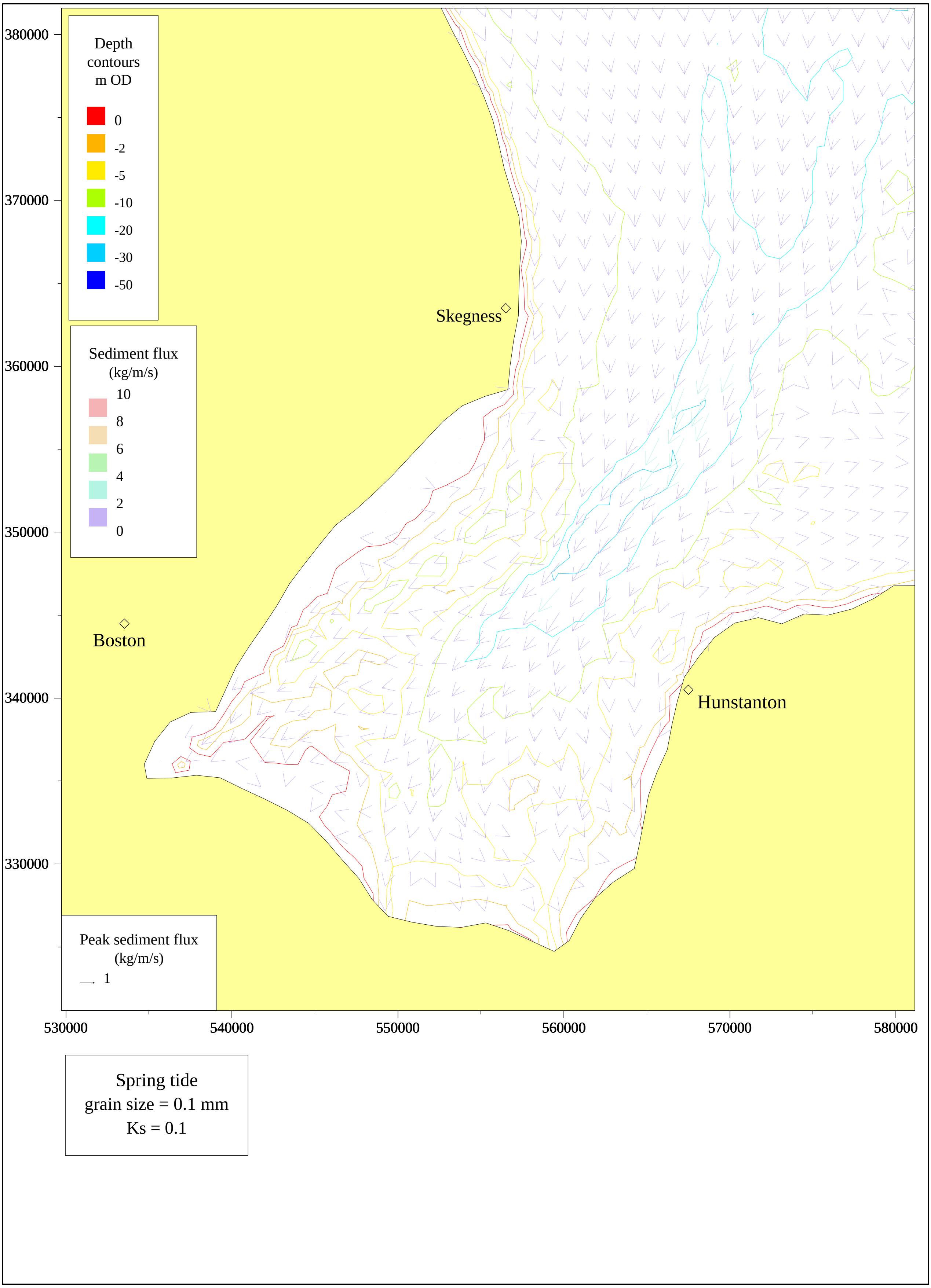

Figure 53 **Peak sediment flux during spring tide (0.1mm sand) detail: Lincolnshire and the Wash**

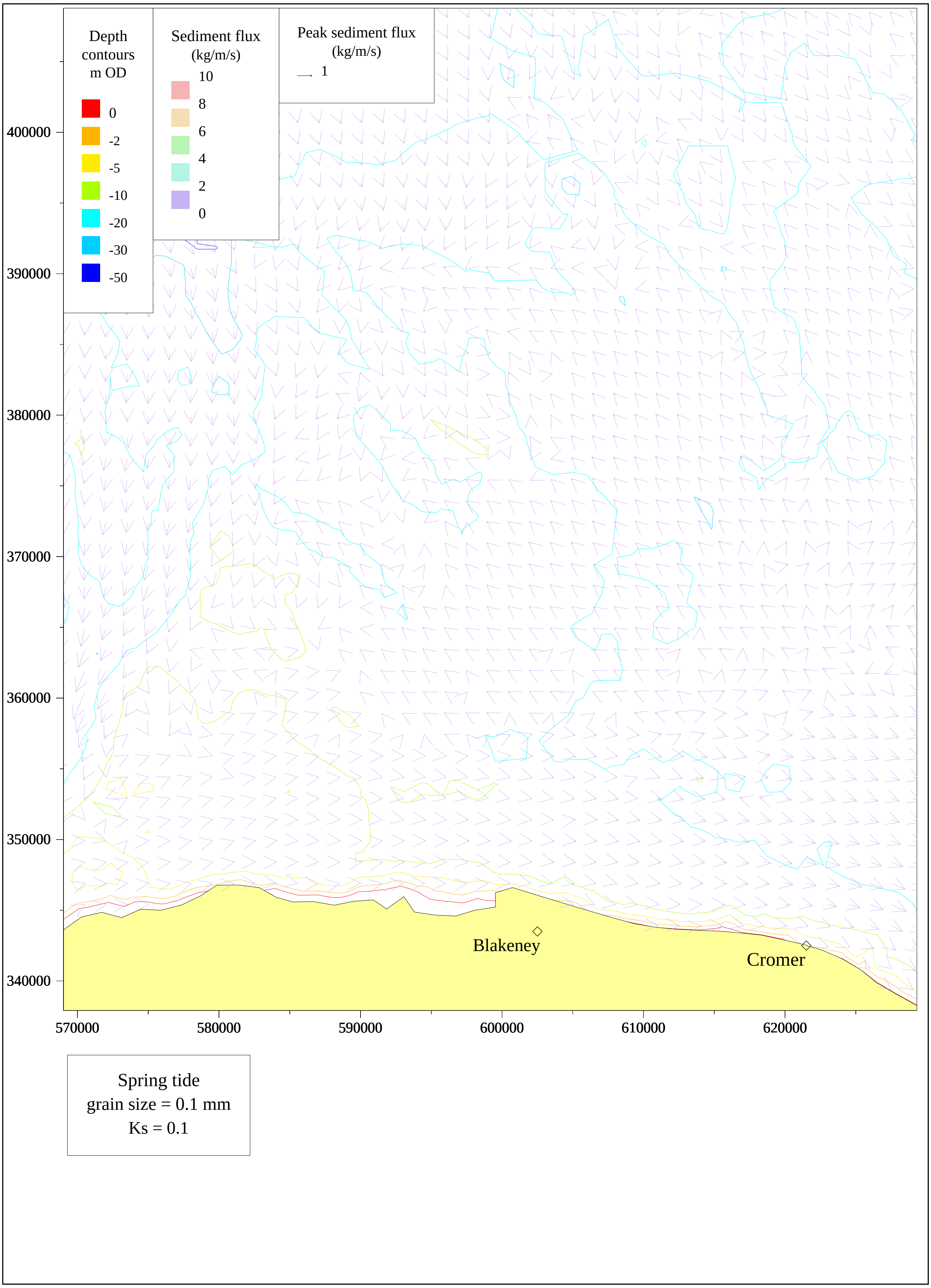

Figure 54 **Peak sediment flux during spring tide (0.1mm sand) detail: North Norfolk**

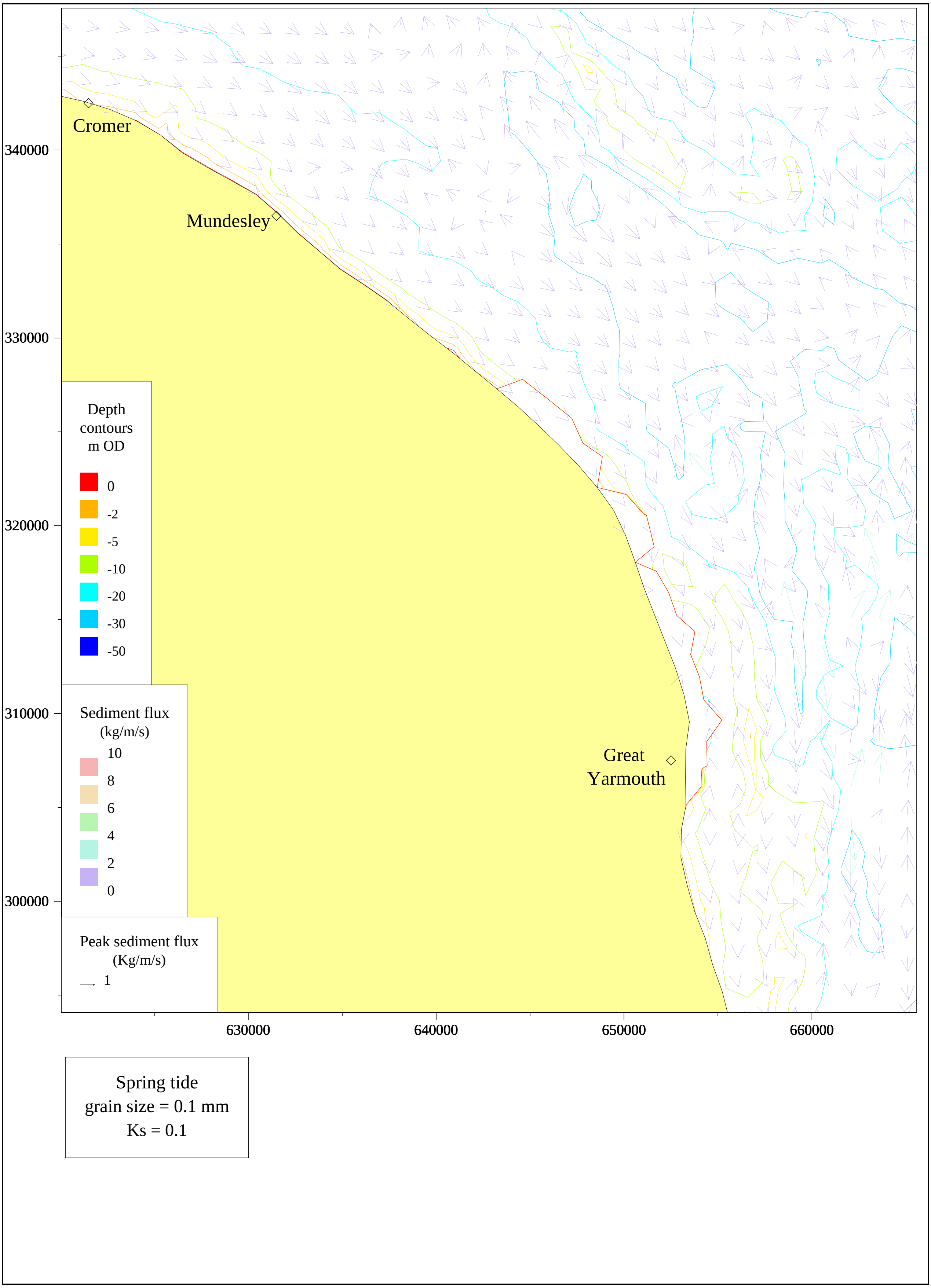

Figure 55 **Peak sediment flux during spring tide (0.1mm sand) detail: East Norfolk**

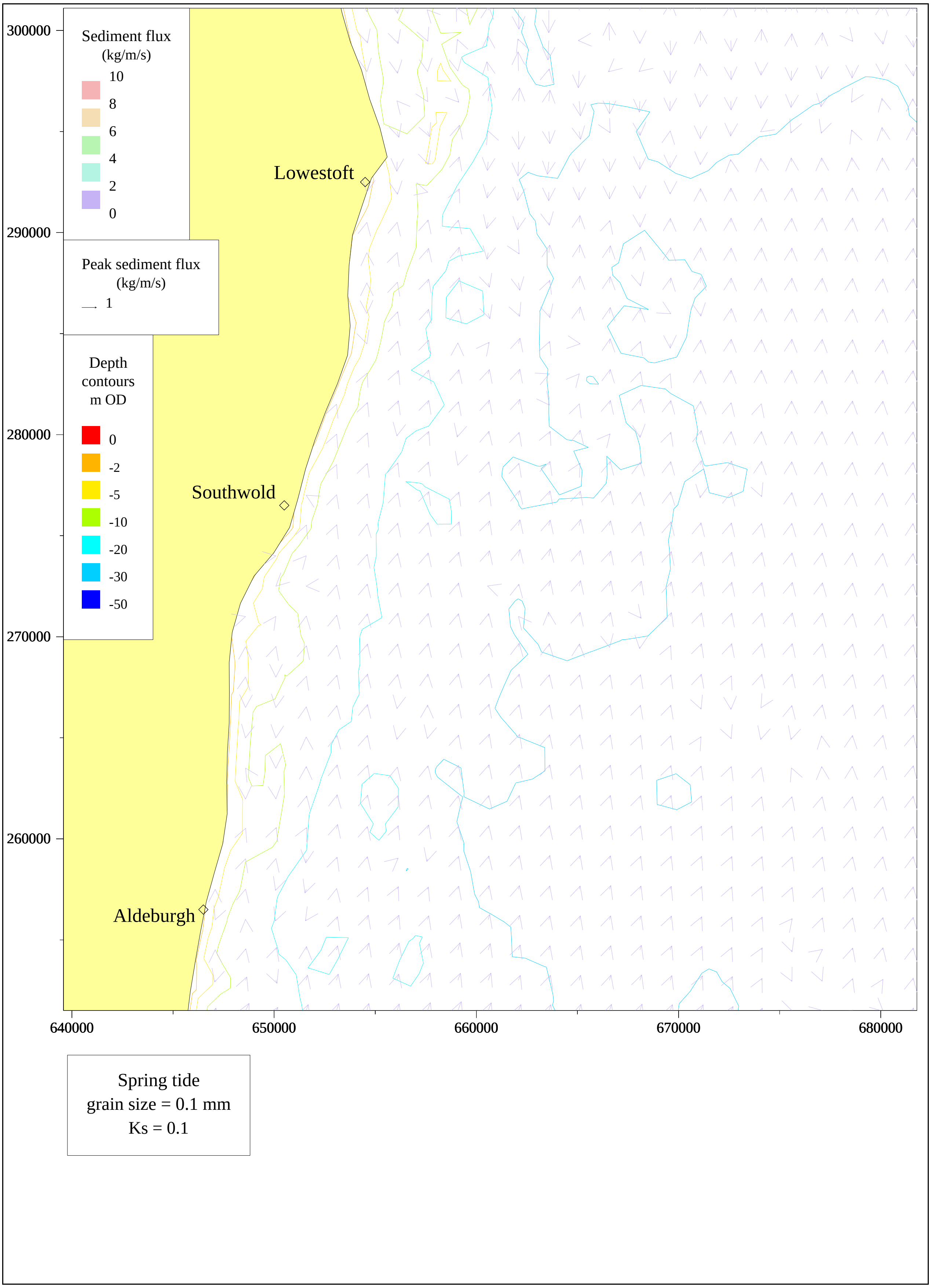

Figure 56 **Peak sediment flux during spring tide (0.1mm sand) detail: North Suffolk**

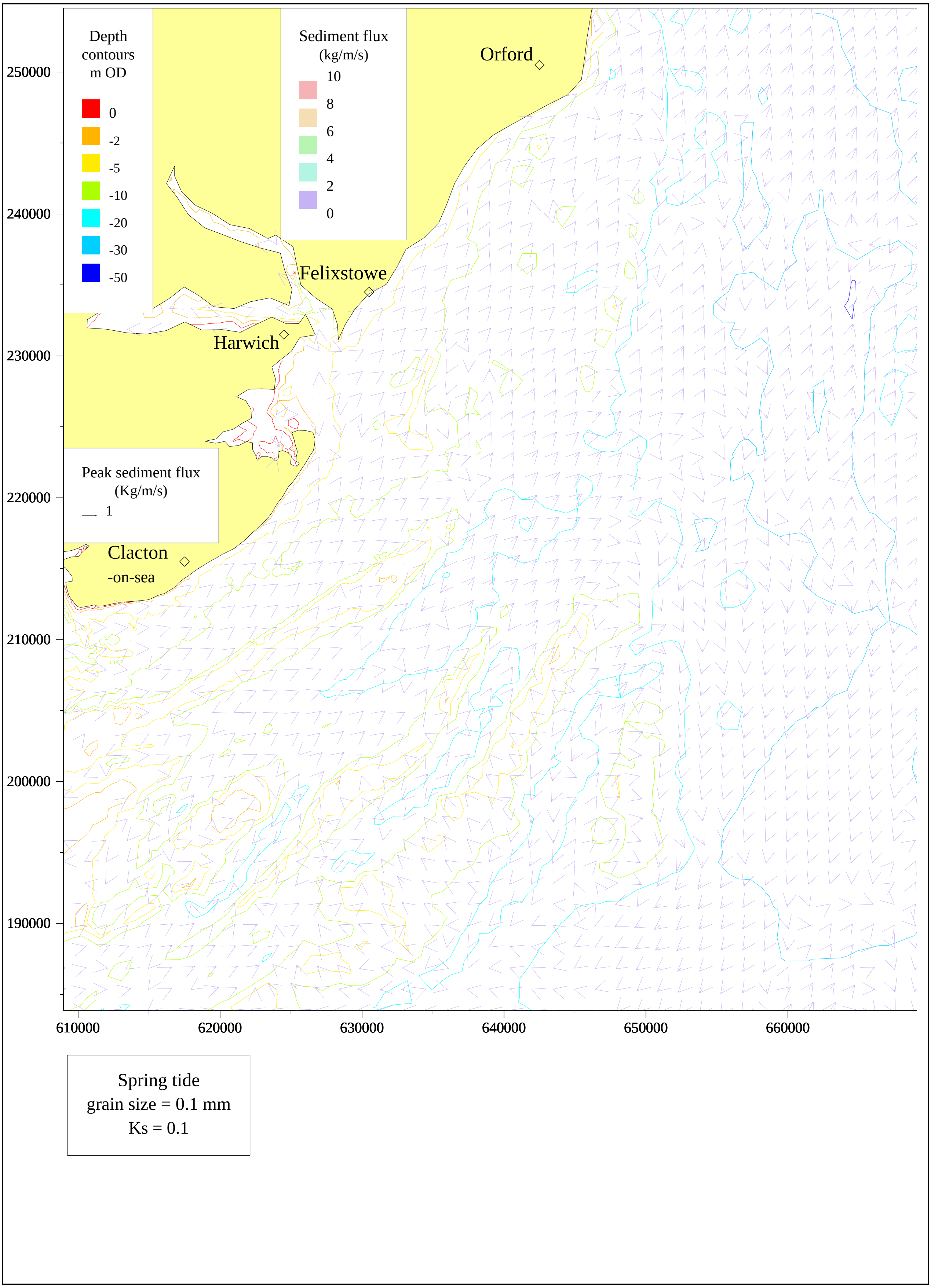

Figure 57 **Peak sediment flux during spring tide (0.1mm sand) detail: Suffolk and Essex**

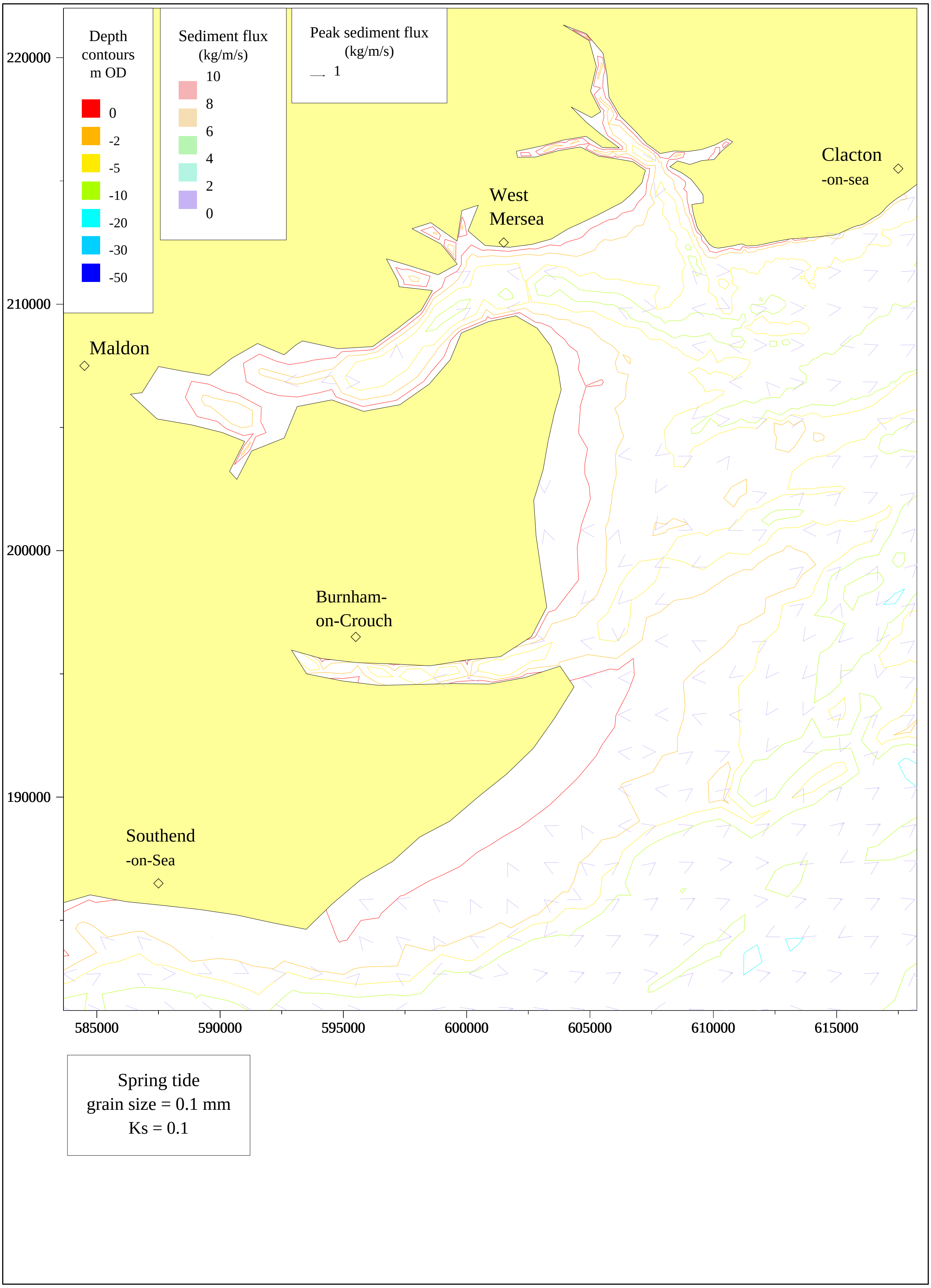

Figure 58 **Peak sediment flux during spring tide (0.1mm sand) detail: South Essex**

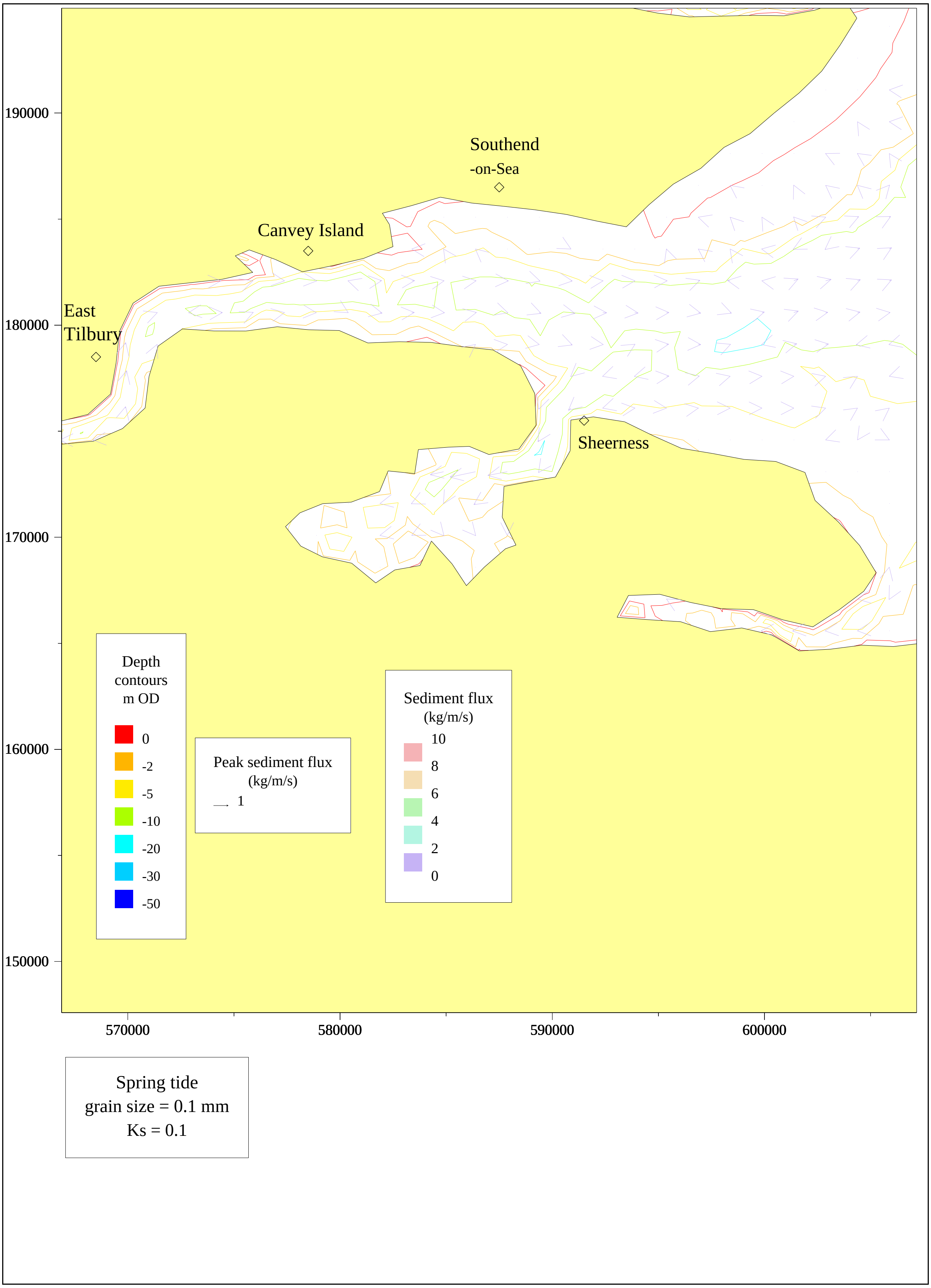

Figure 59 **Peak sediment flux during spring tide (0.1mm sand) detail: Outer Thames**

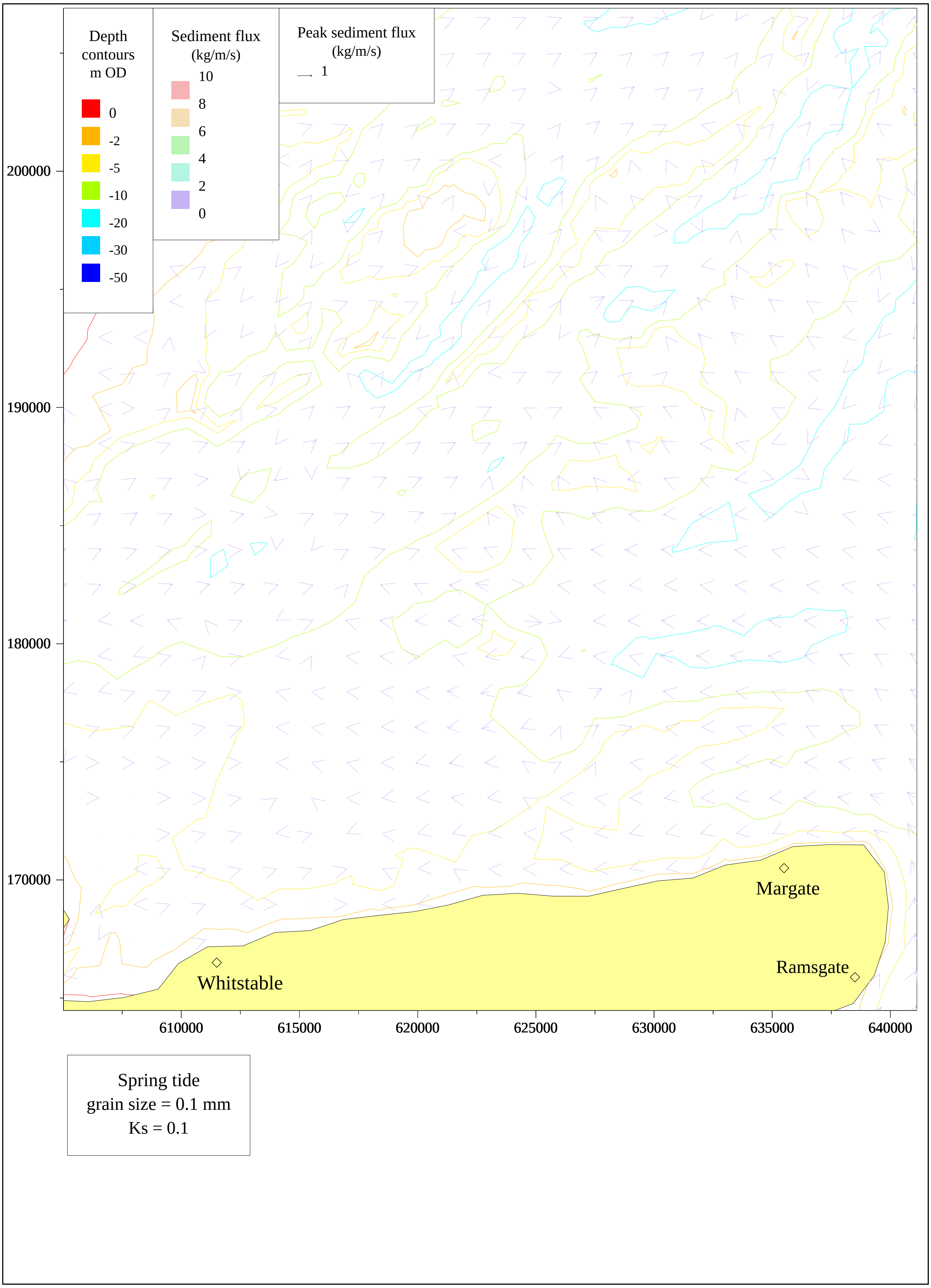

Figure 60 Peak sediment flux during spring tide (0.1mm sand) detail: North Kent

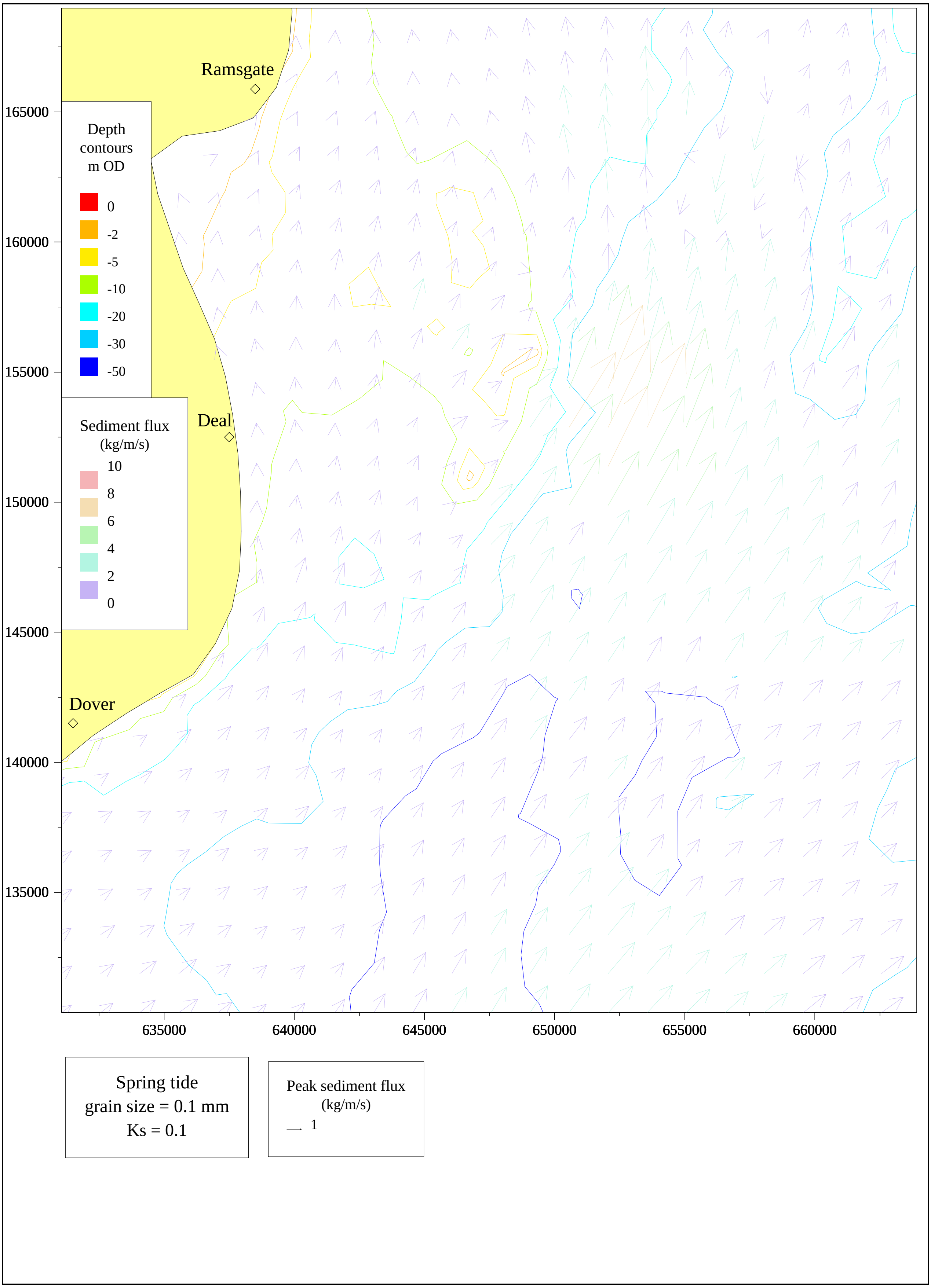

Figure 61 Peak sediment flux during spring tide (0.1mm sand) detail: East Kent

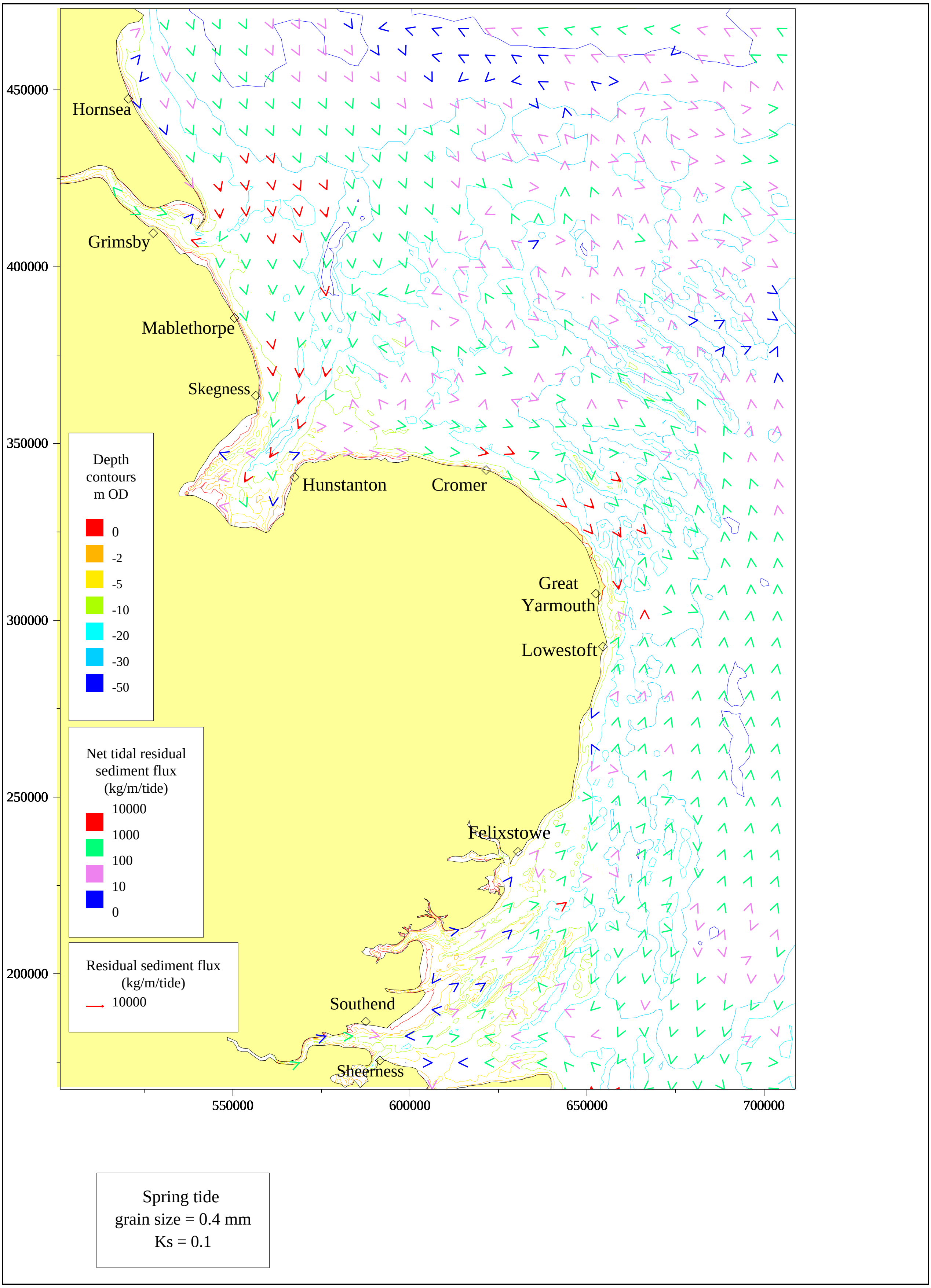

Figure 62 Spring tide net sediment flux patterns (0.4mm sand)

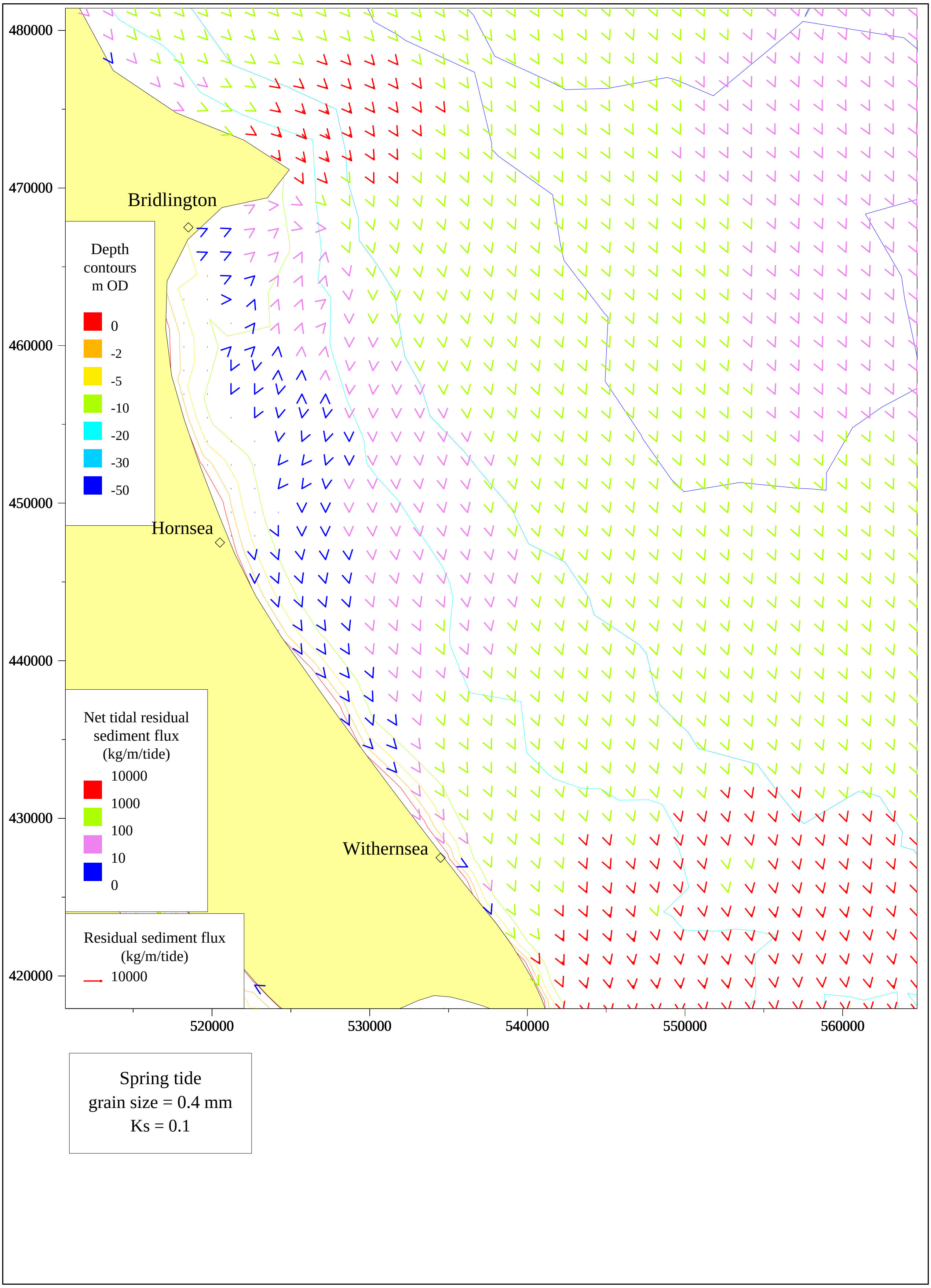

Figure 63 **Spring tide net sediment flux patterns (0.4mm sand) detail: Flamborough Head to the Humber**

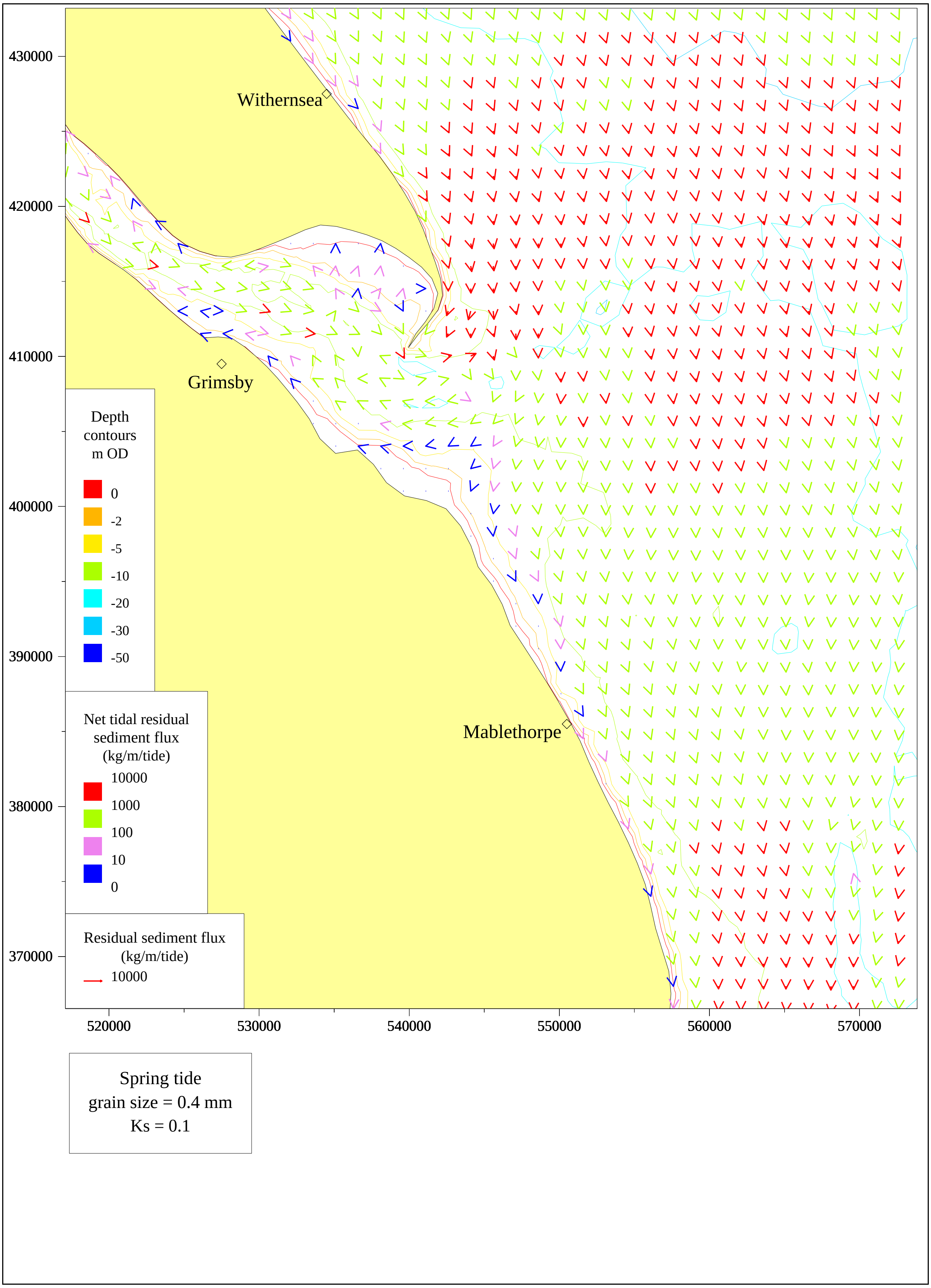

Figure 64 **Spring tide net sediment flux patterns (0.4mm sand) detail: Humber Entrance and Lincolnshire**

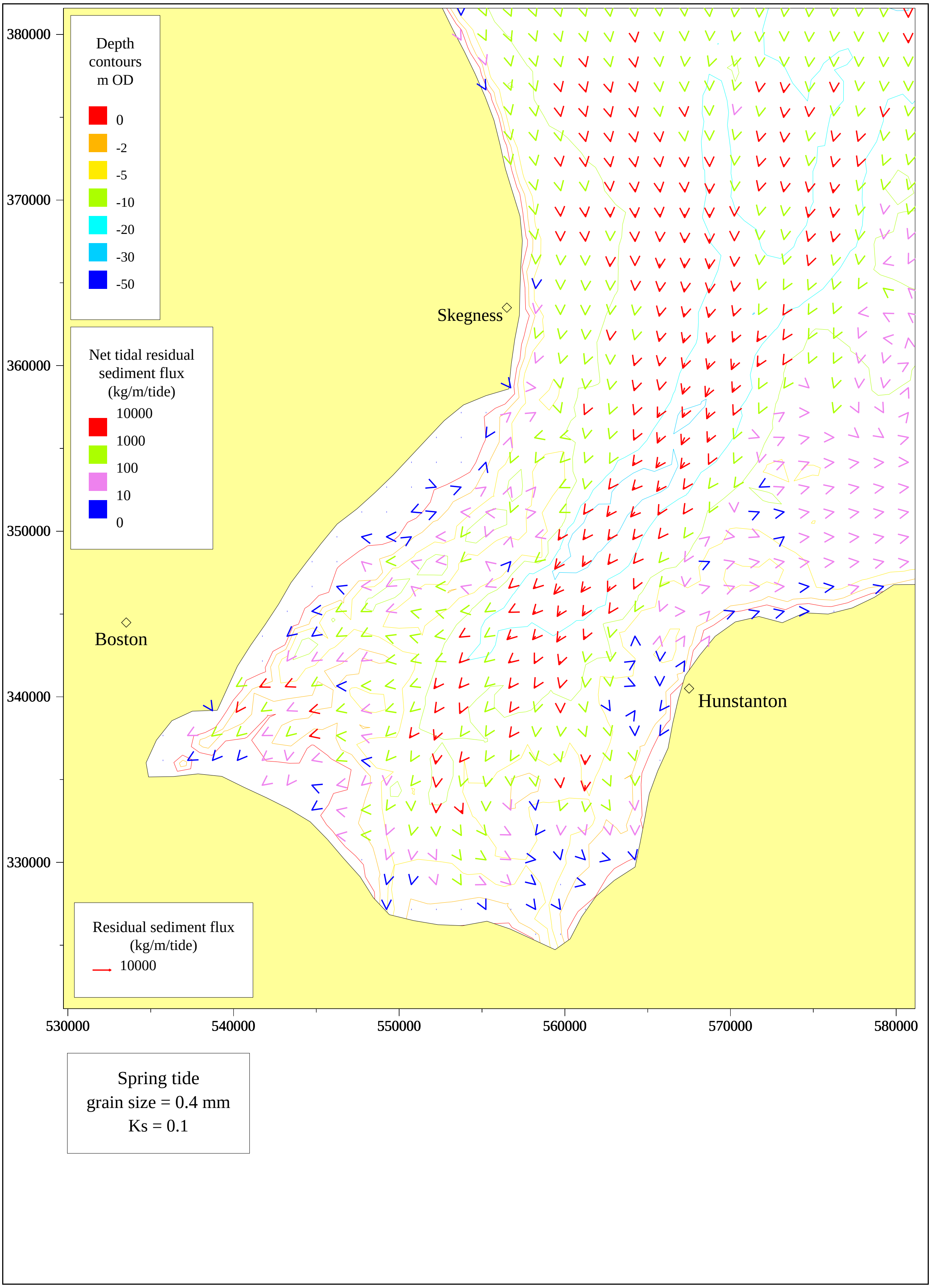

Figure 65 **Spring tide net sediment flux patterns (0.4mm sand) detail: Lincolnshire and the Wash**

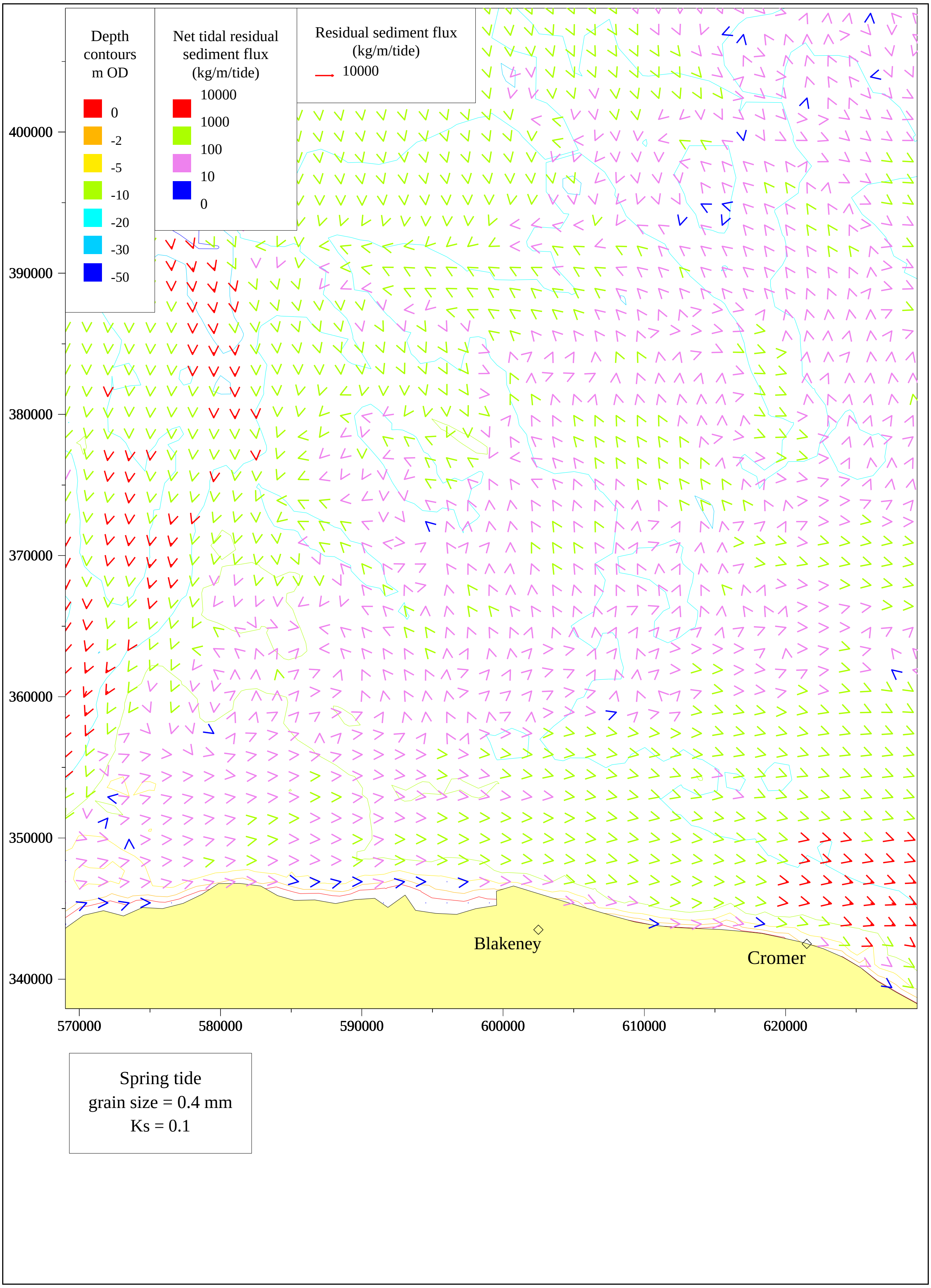

Figure 66 **Spring tide net sediment flux patterns (0.4mm sand) detail: North Norfolk**

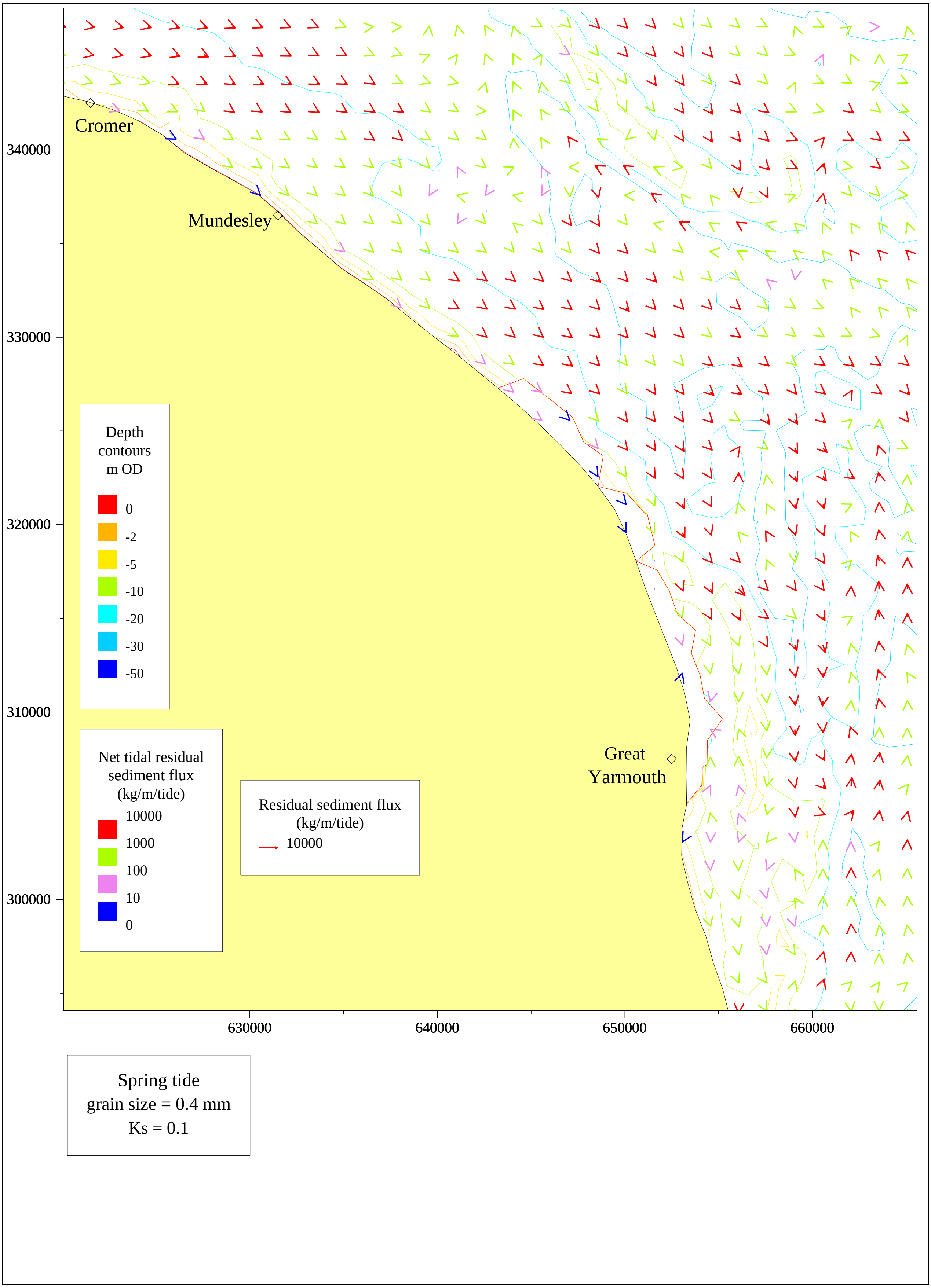

Figure 67 **Spring tide net sediment flux patterns (0.4mm sand) detail: East Norfolk**

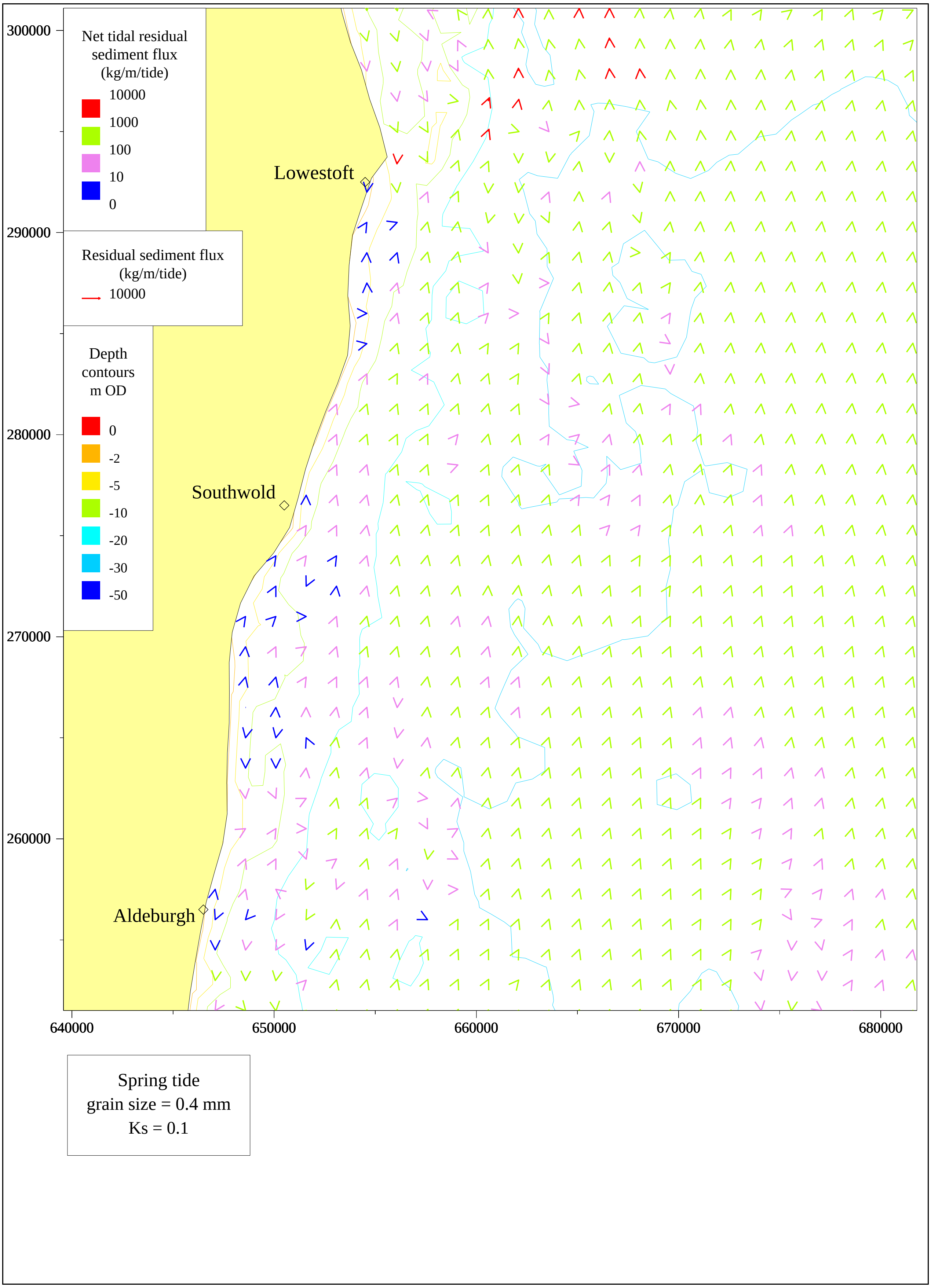

Figure 68 Spring tide net sediment flux patterns (0.4mm sand) detail: North Suffolk

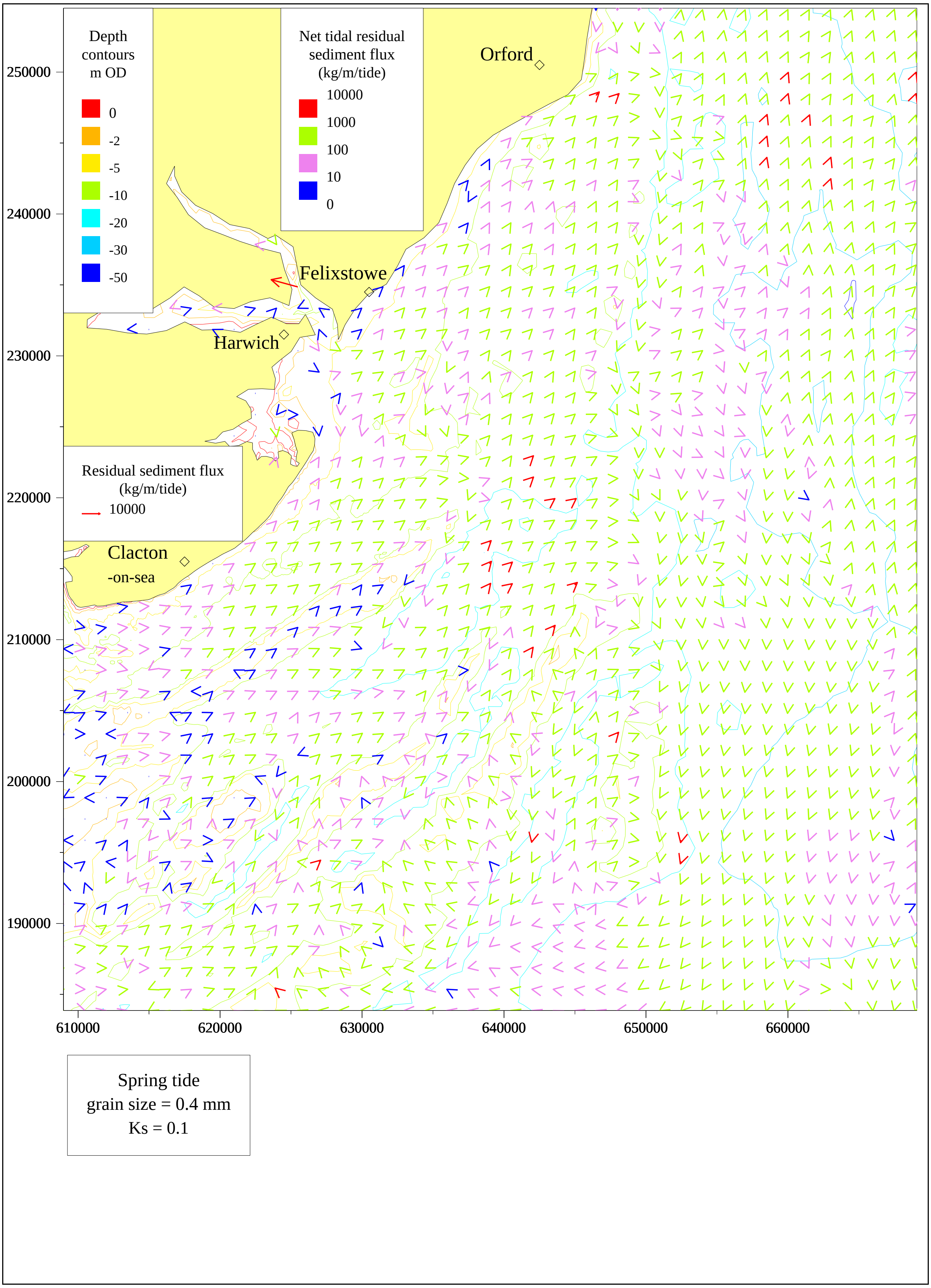

Figure 69 Spring tide net sediment flux patterns (0.4mm sand) detail: Suffolk and Essex

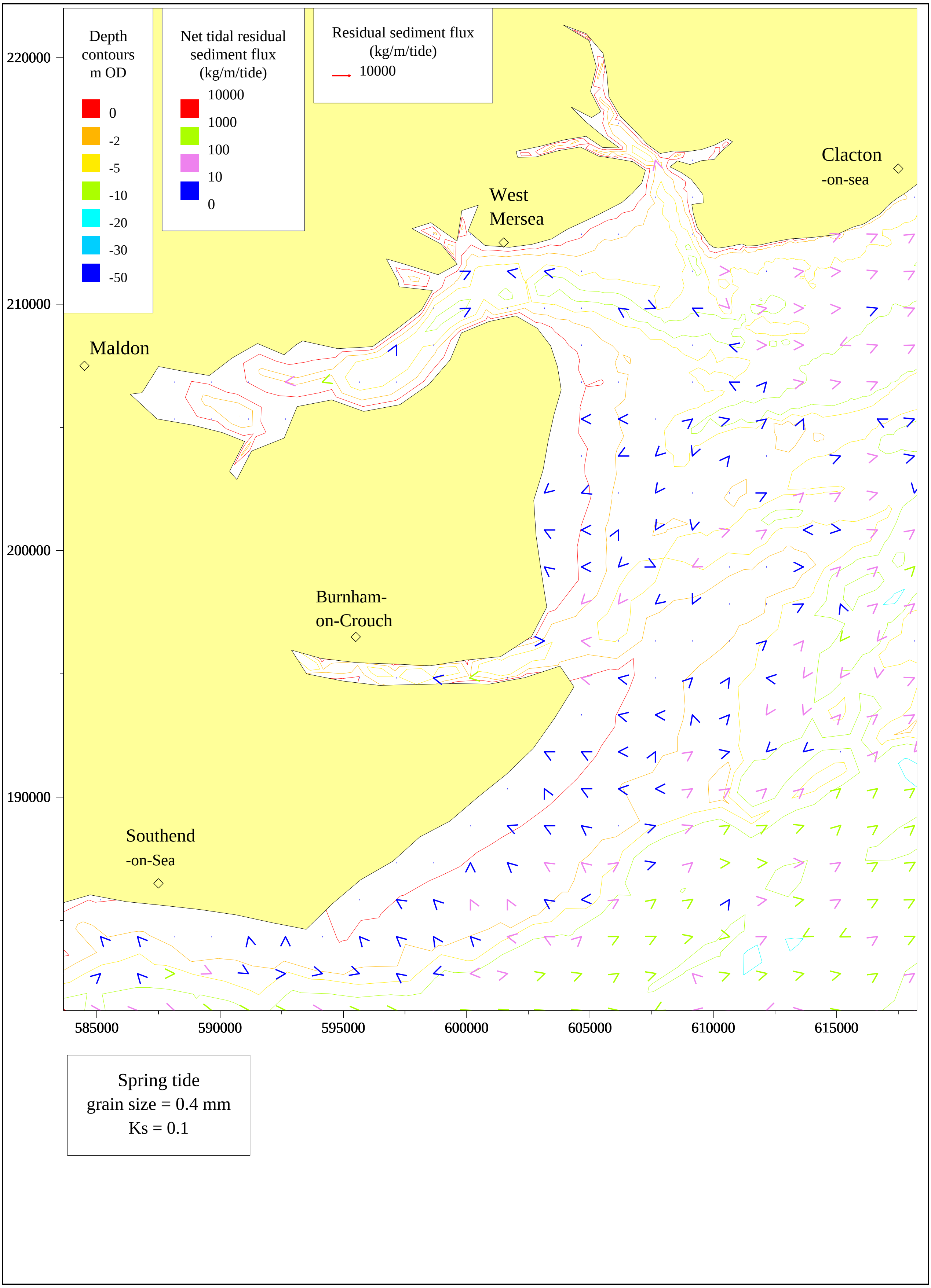

Figure 70 **Spring tide net sediment flux patterns (0.4mm sand) detail: South Essex**

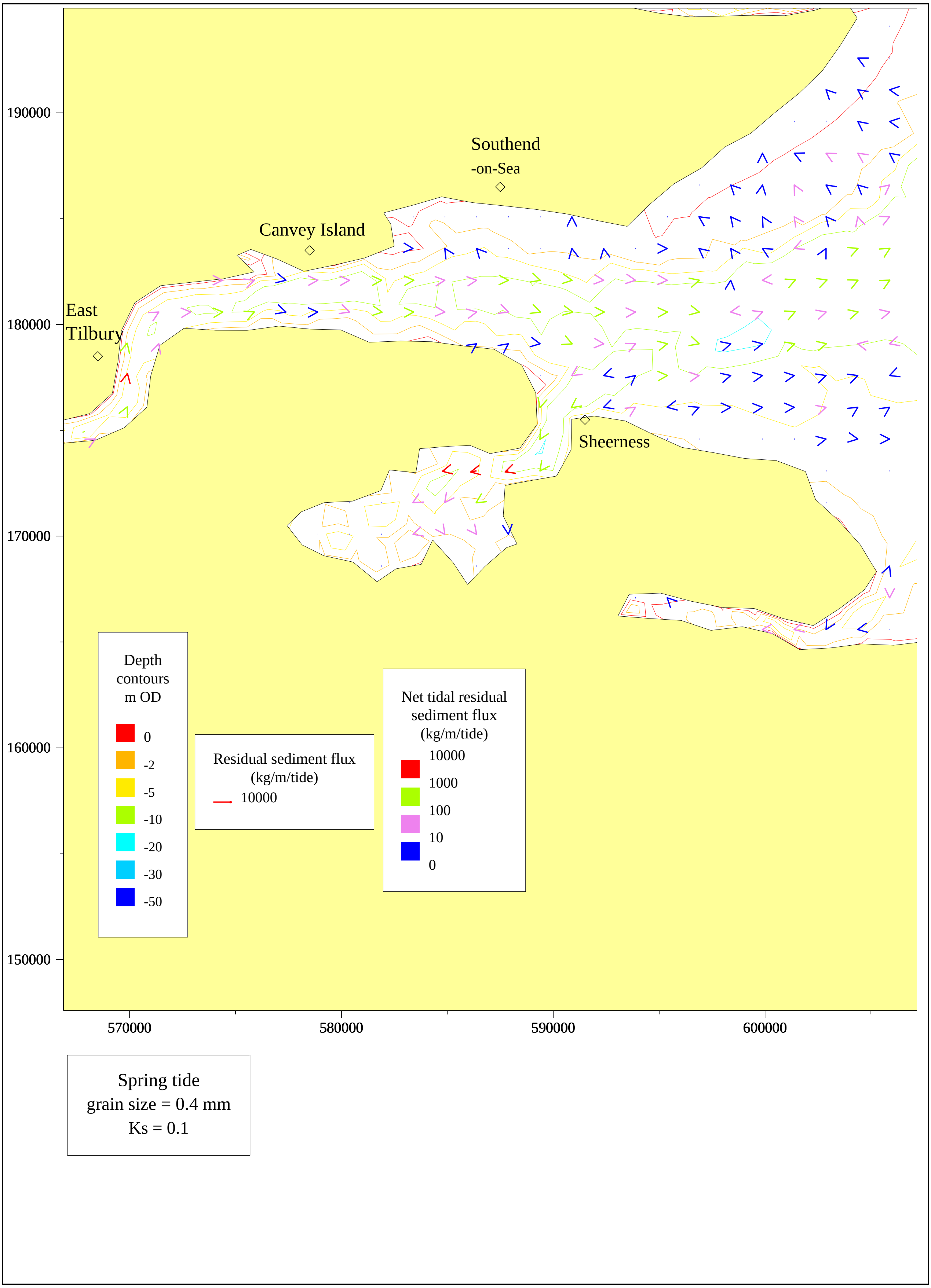

Figure 71 Spring tide net sediment flux patterns (0.4mm sand) detail: Outer Thames

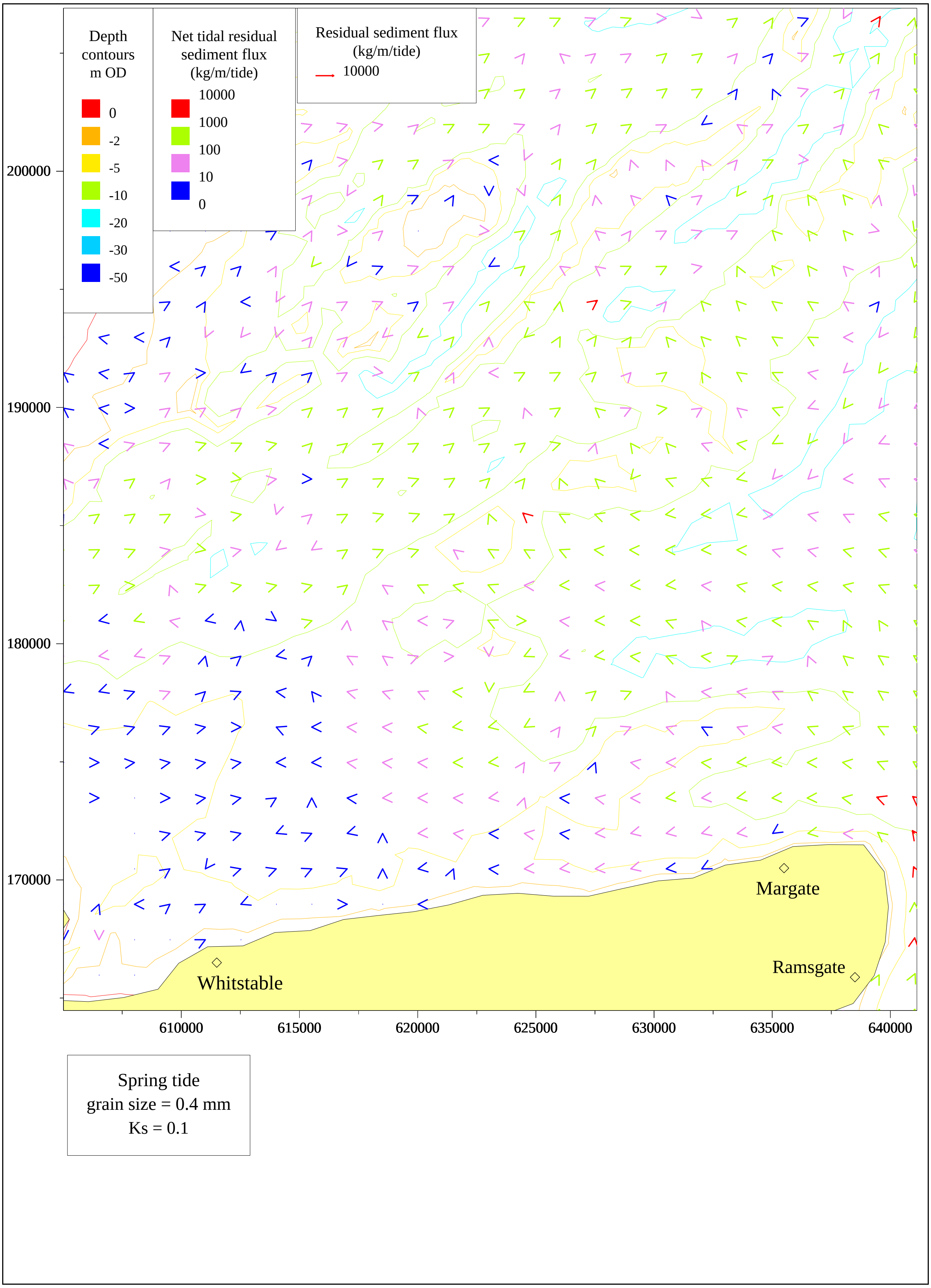

Figure 72 Spring tide net sediment flux patterns (0.4mm sand) detail: North Kent

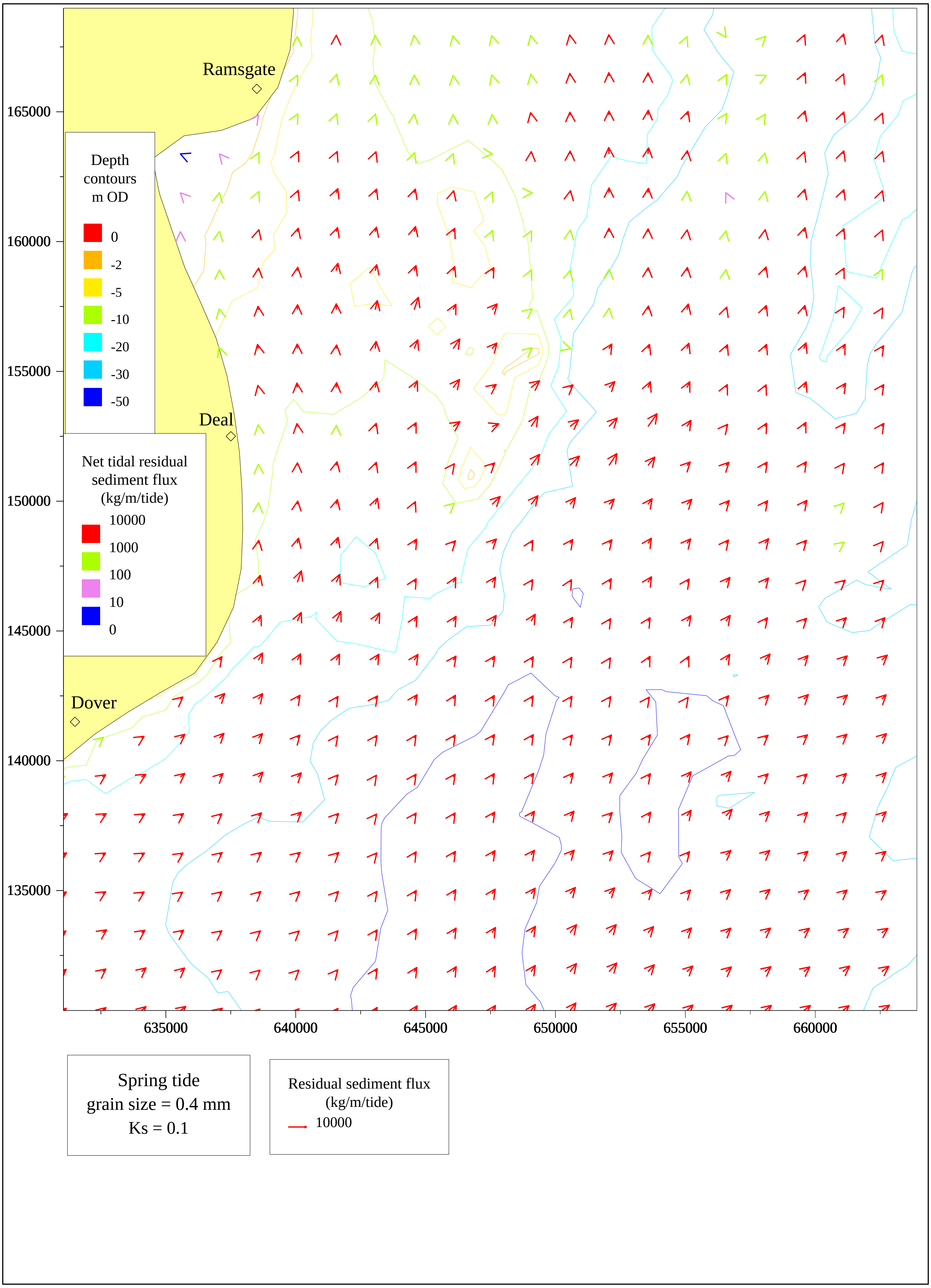

Figure 73 Spring tide net sediment flux patterns (0.4mm sand) detail: East Kent

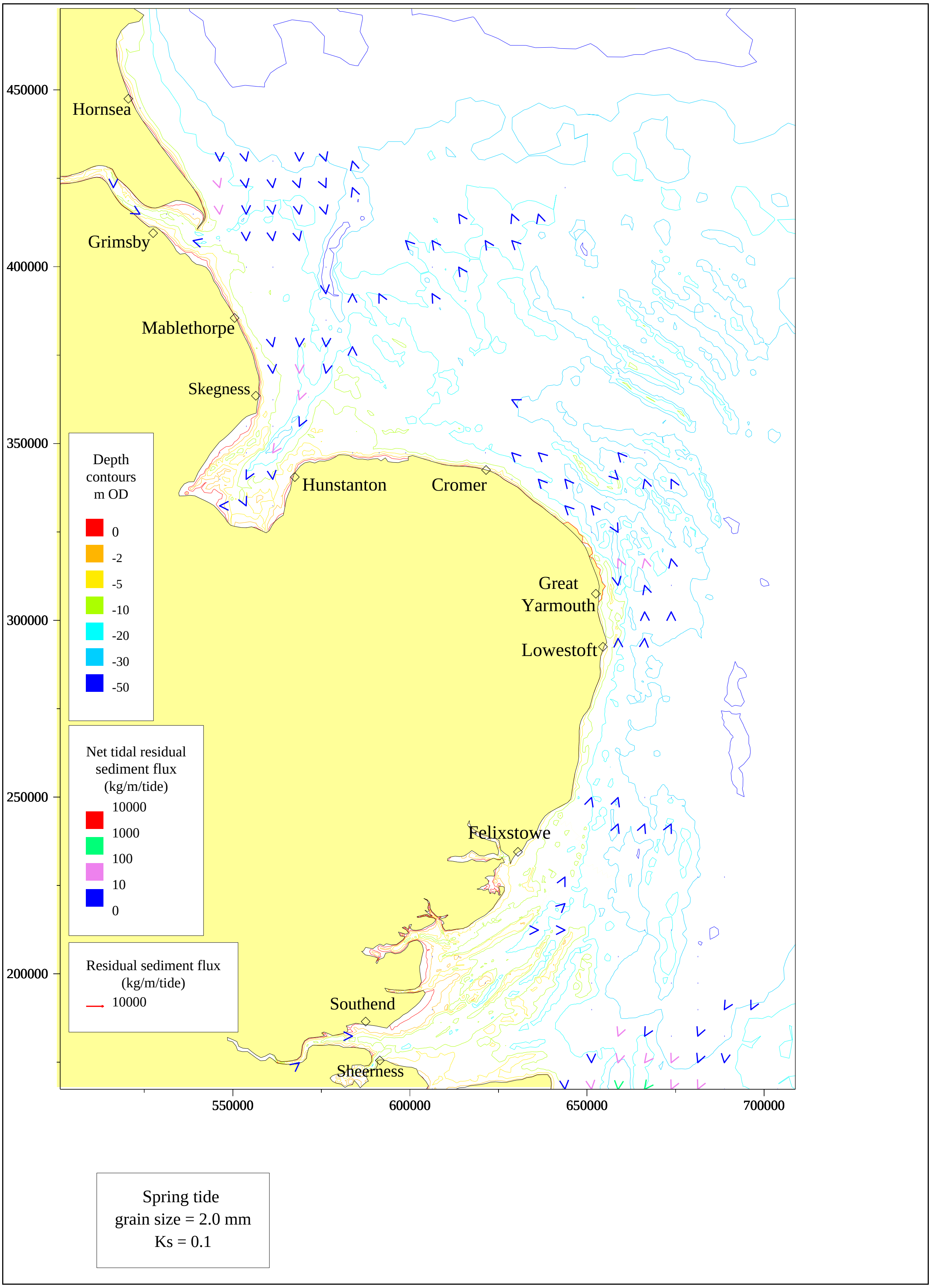

Figure 74 **Spring tide net sediment flux patterns (2mm gravel)**

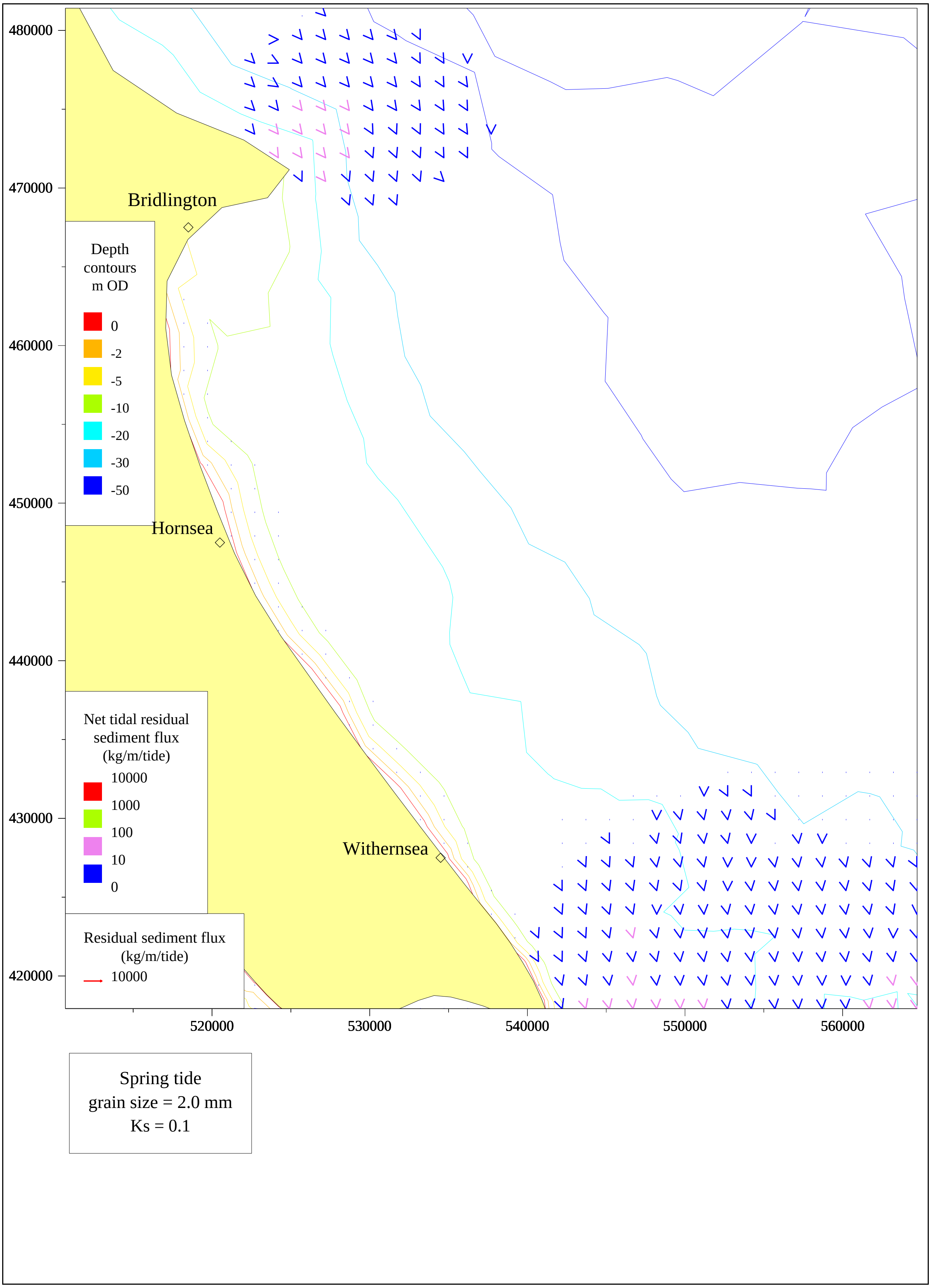

Figure 75 **Spring tide net sediment flux patterns (2mm gravel) detail: Flamborough Head to the Humber**

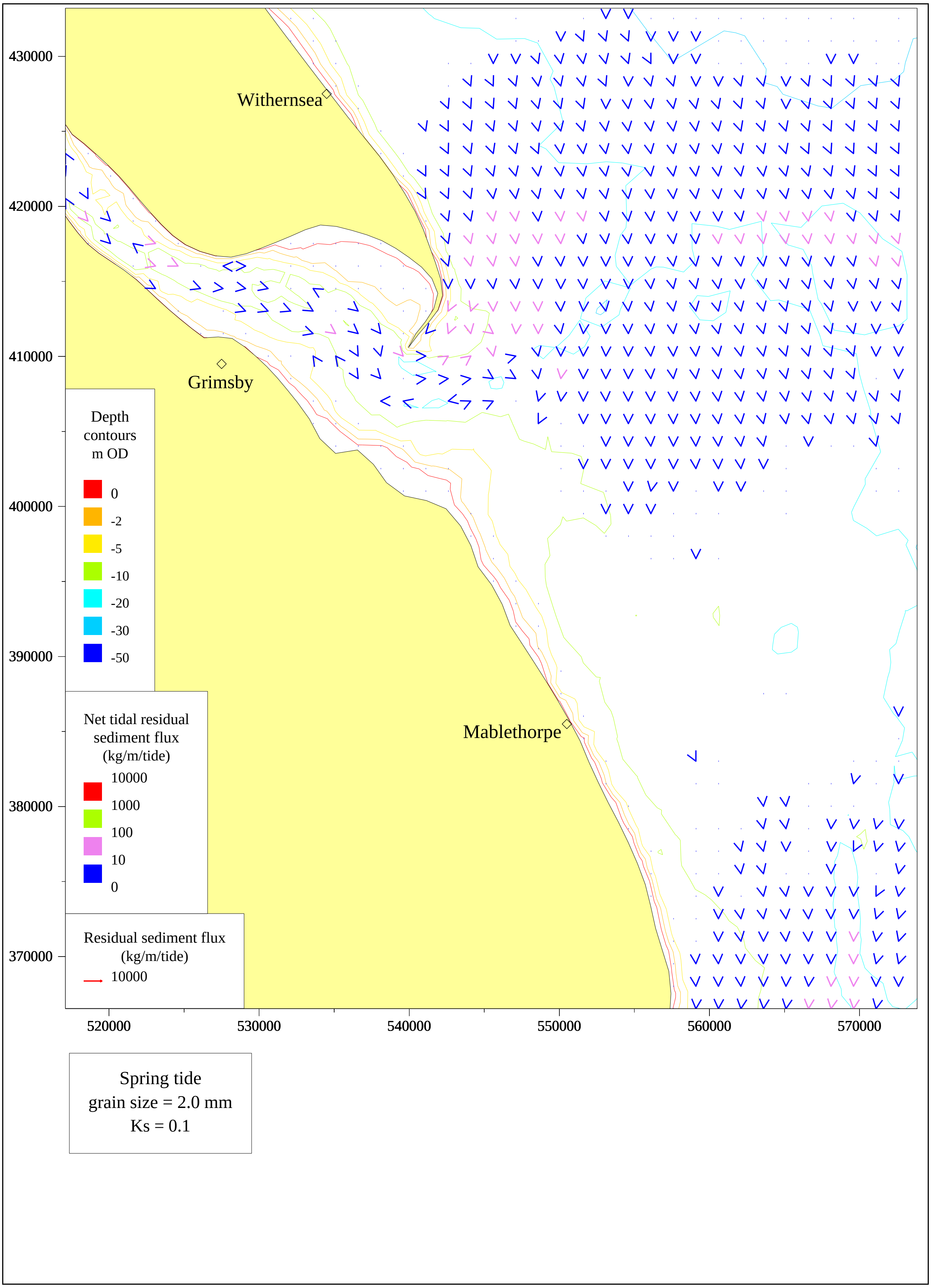

Figure 76 **Spring tide net sediment flux patterns (2mm gravel) detail: Humber Entrance and Lincolnshire**

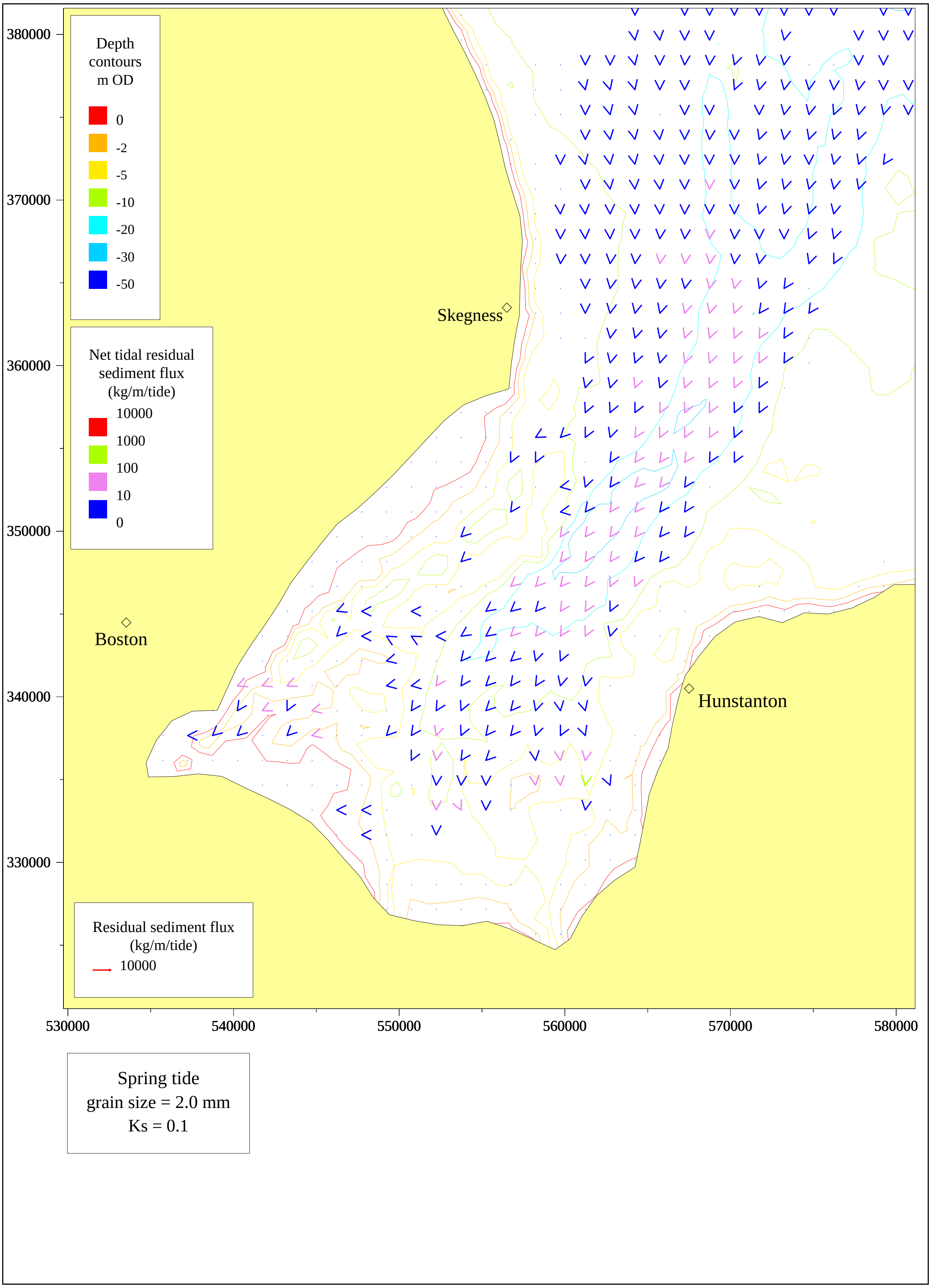

Figure 77 **Spring tide net sediment flux patterns (2mm gravel) detail: Lincolnshire and the Wash**

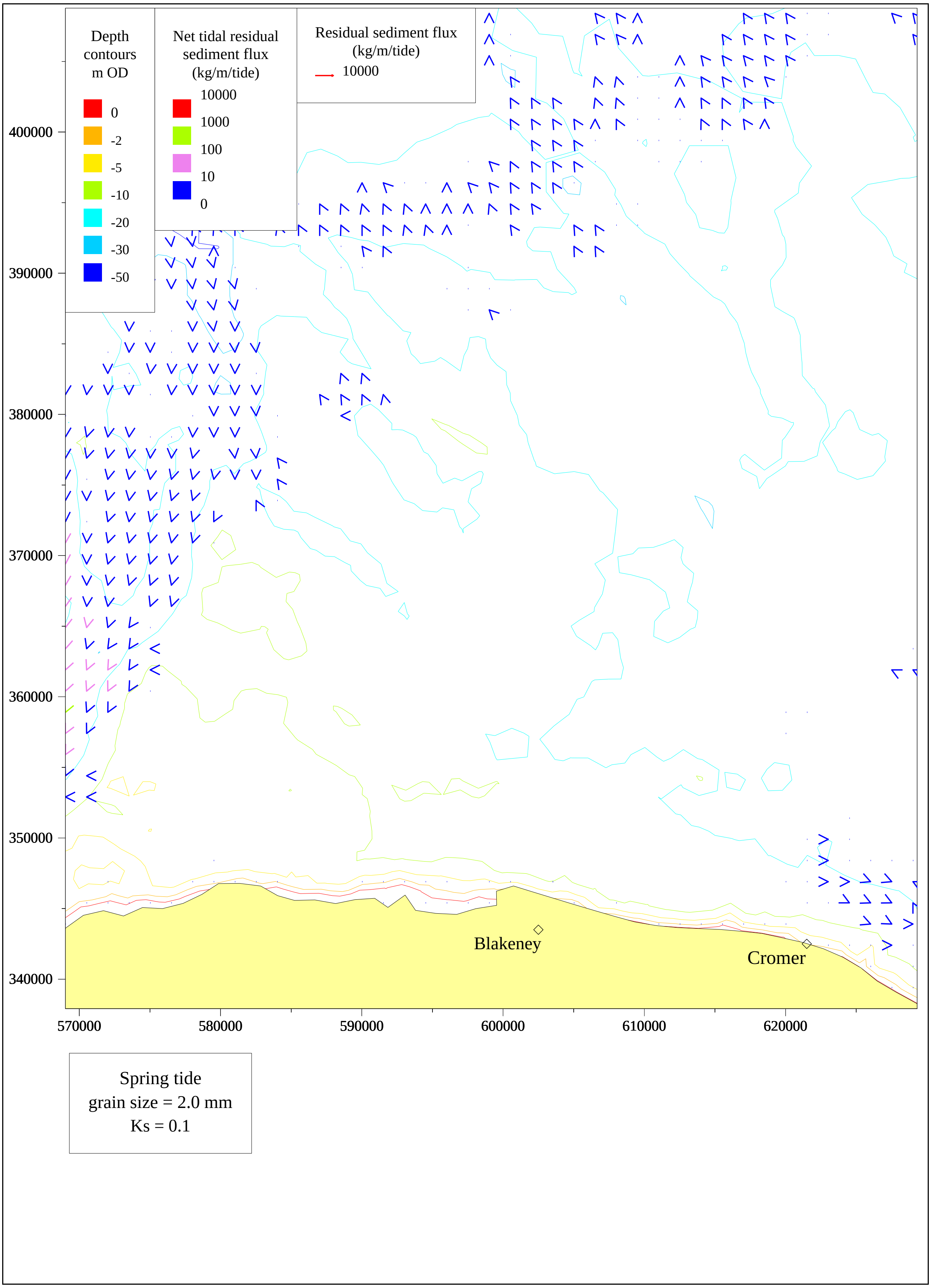

Figure 78 Spring tide net sediment flux patterns (2mm gravel) detail: North Norfolk

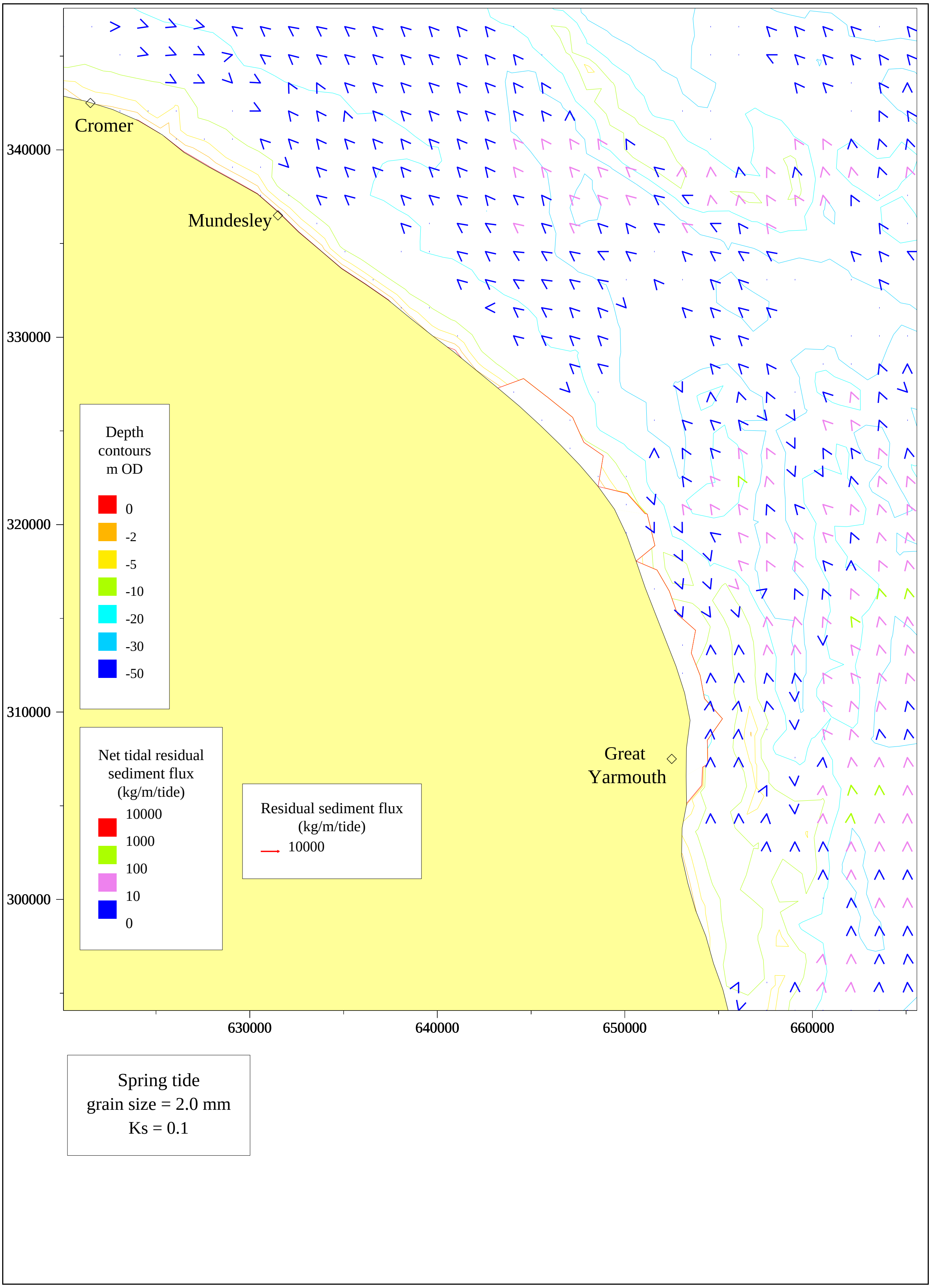

Figure 79 Spring tide net sediment flux patterns (2mm gravel) detail: East Norfolk

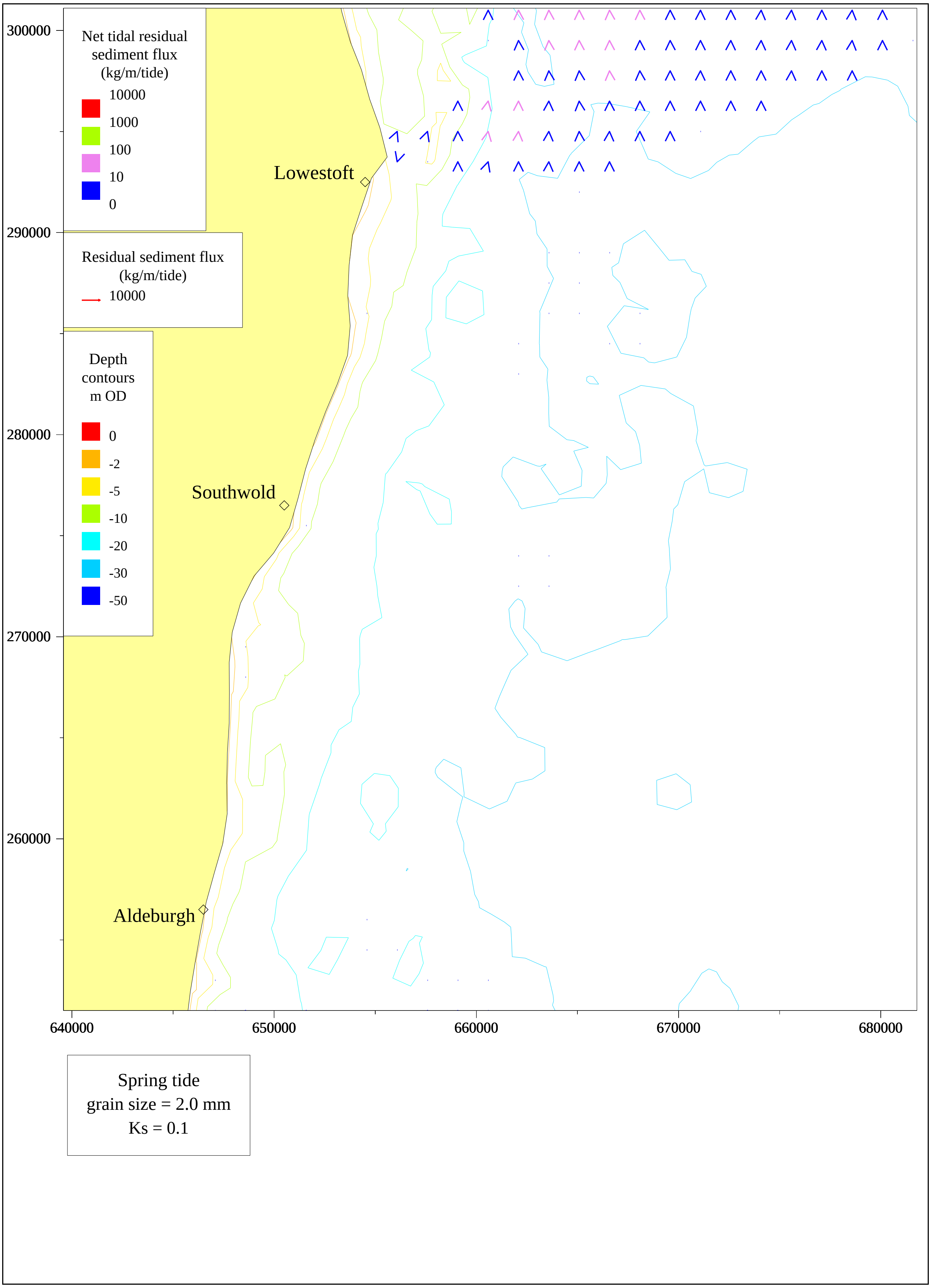

Figure 80 Spring tide net sediment flux patterns (2mm gravel) detail: North Suffolk

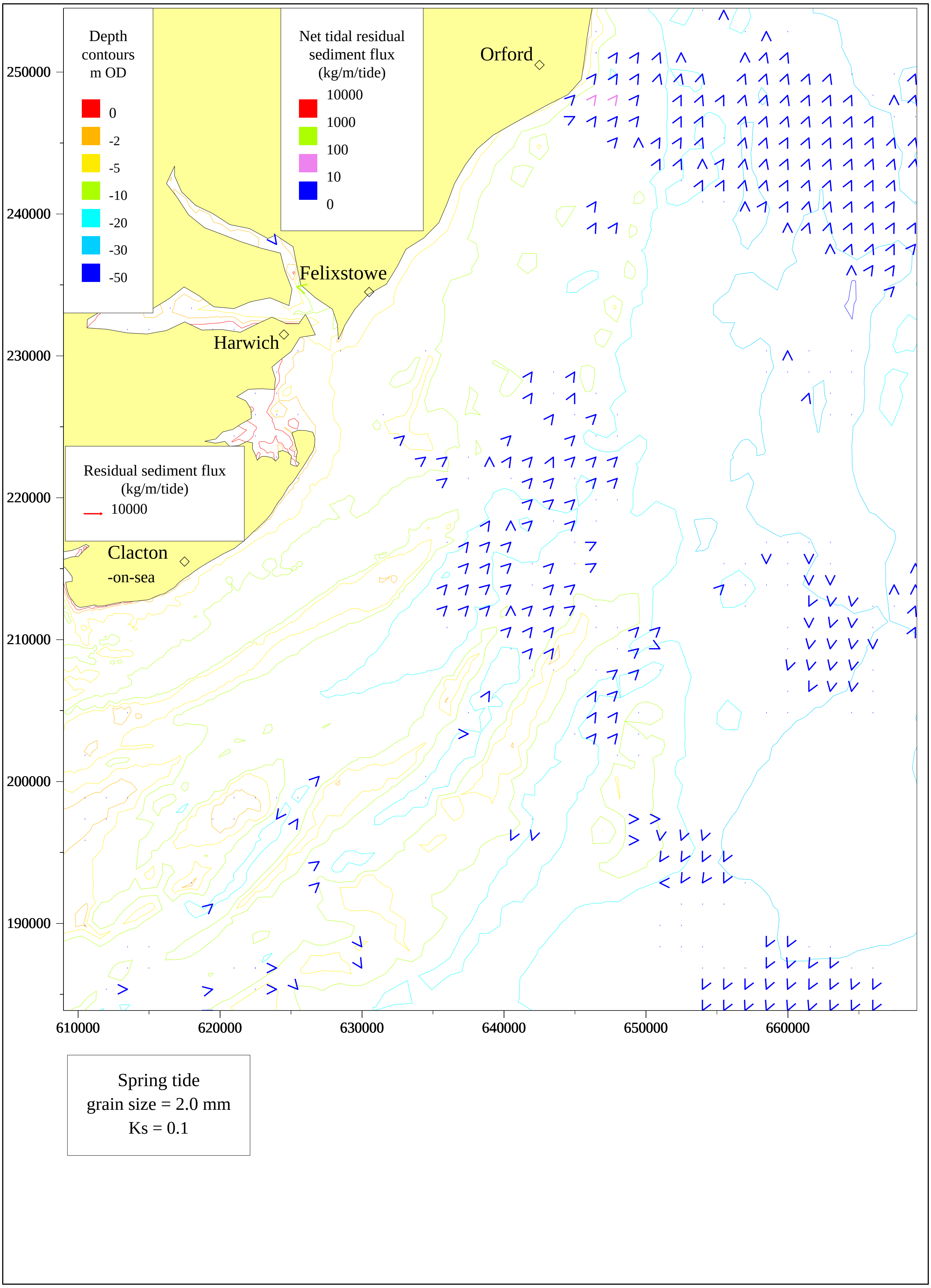

Figure 81 **Spring tide net sediment flux patterns (2mm gravel) detail: Suffolk and Essex**

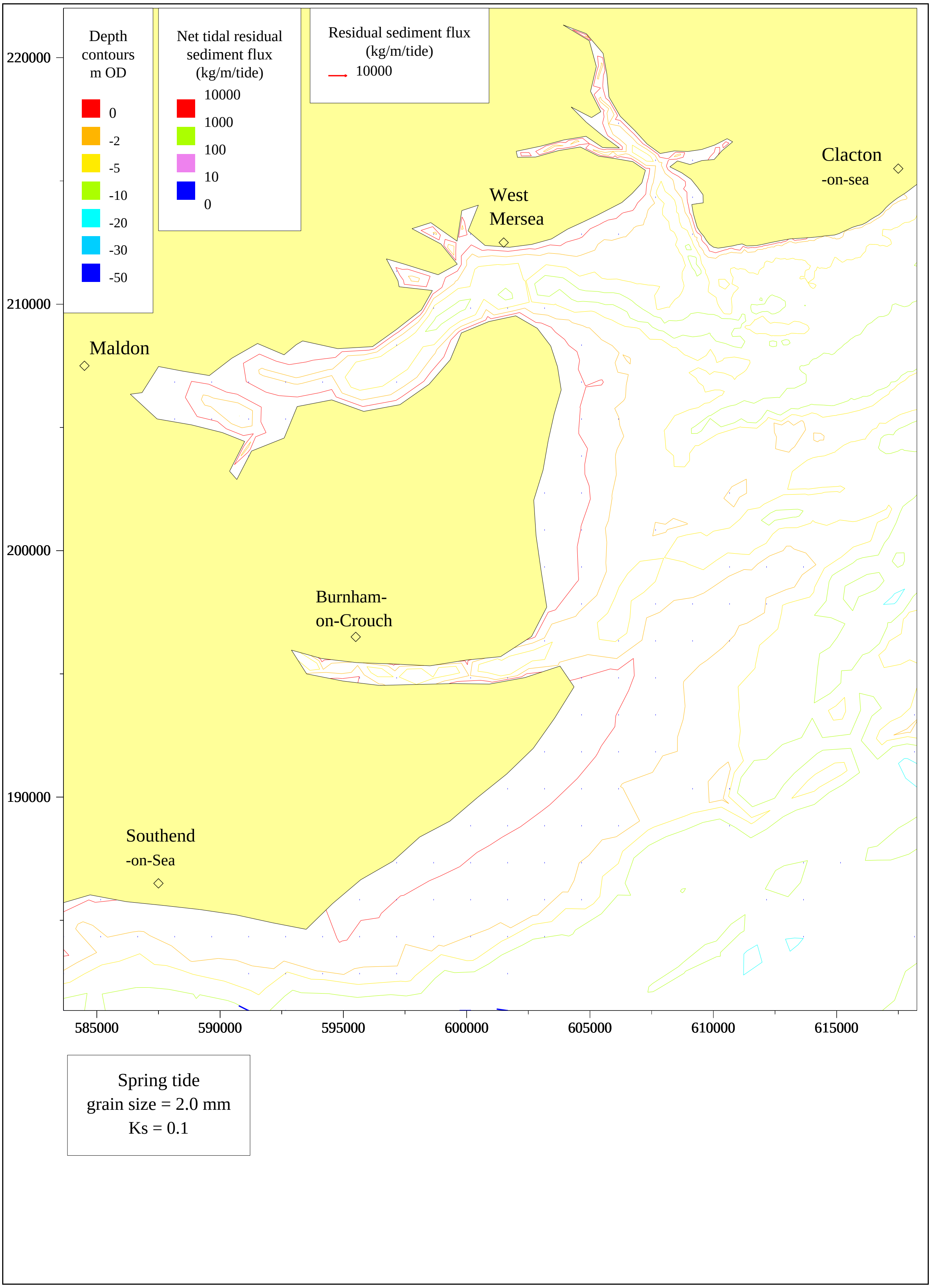

Figure 82 **Spring tide net sediment flux patterns (2mm gravel) detail: South Essex**

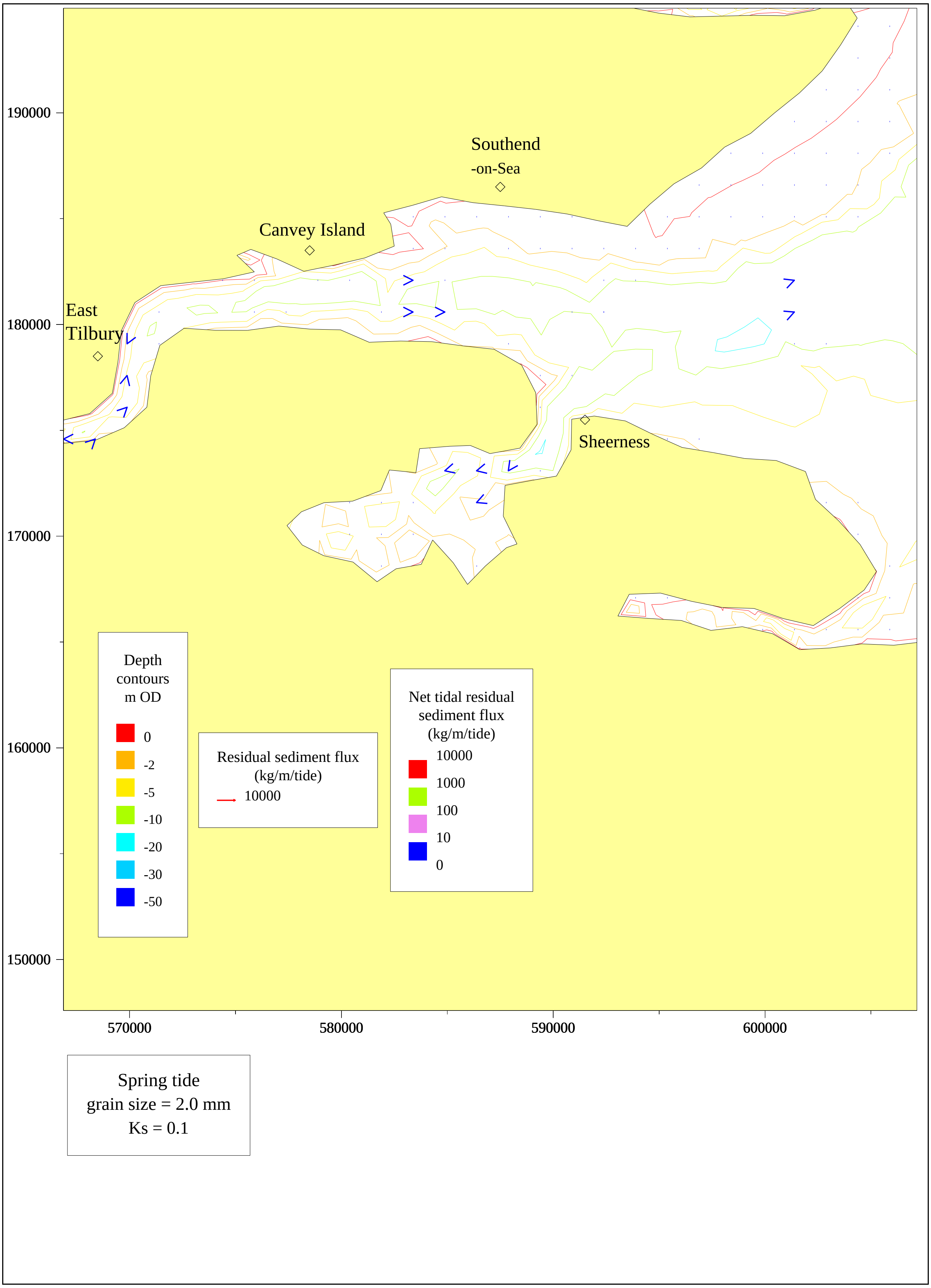

Figure 83 Spring tide net sediment flux patterns (2mm gravel) detail: Outer Thames

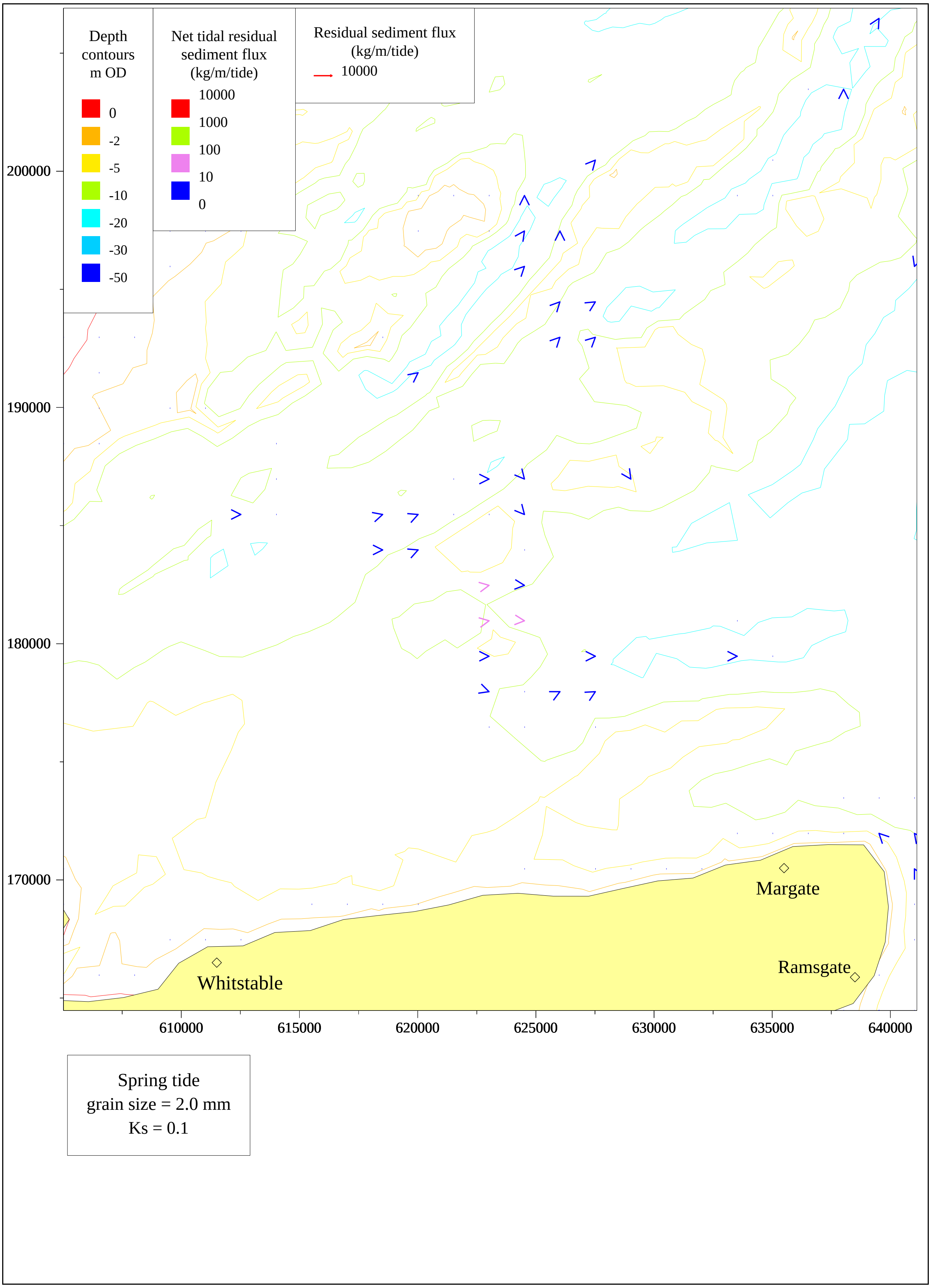

Figure 84 Spring tide net sediment flux patterns (2mm gravel) detail: North Kent

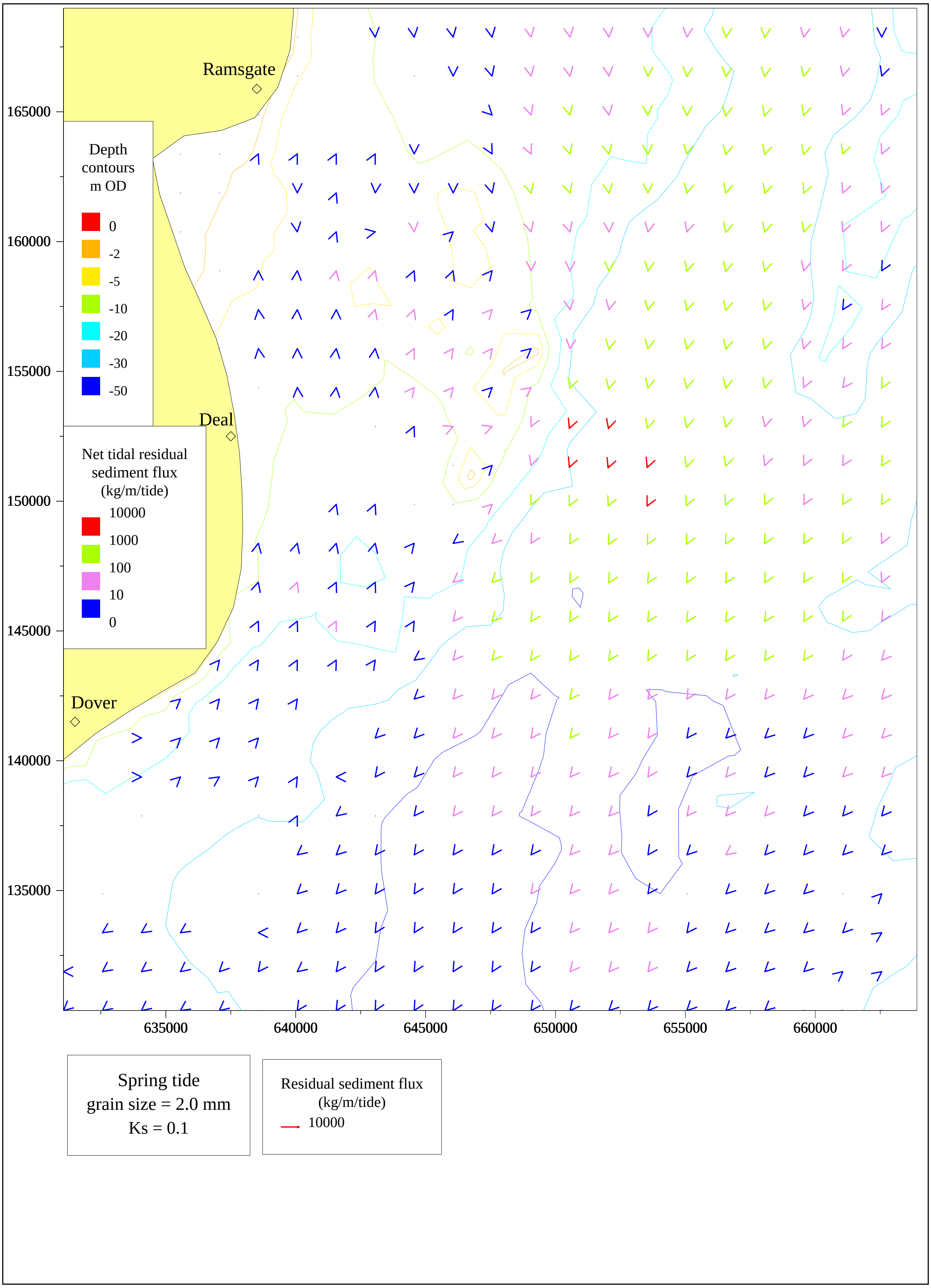

Figure 85 Spring tide net sediment flux patterns (2mm gravel) detail: East Kent

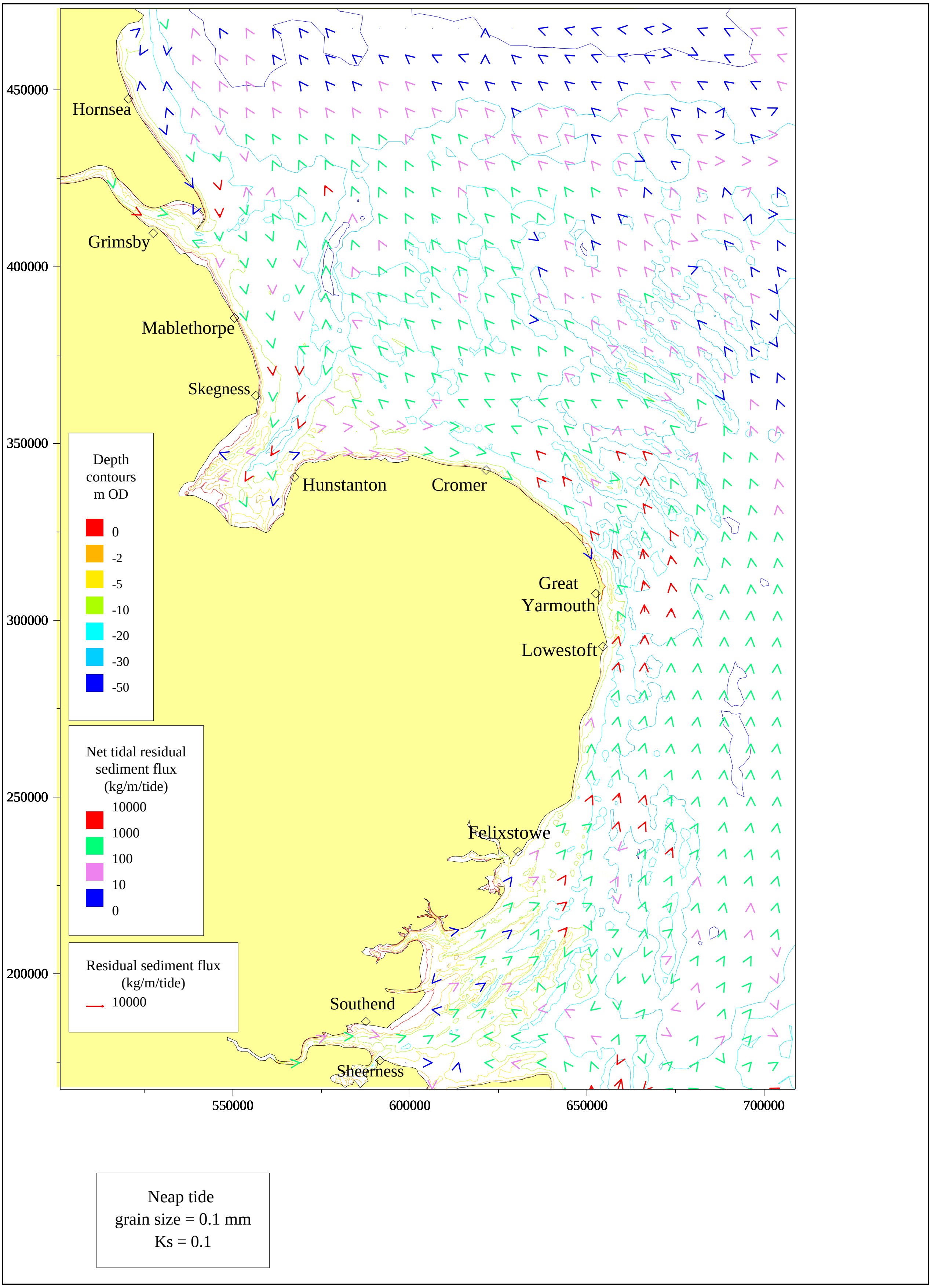

Figure 86 Neap tide net sediment flux patterns (0.1mm sand)

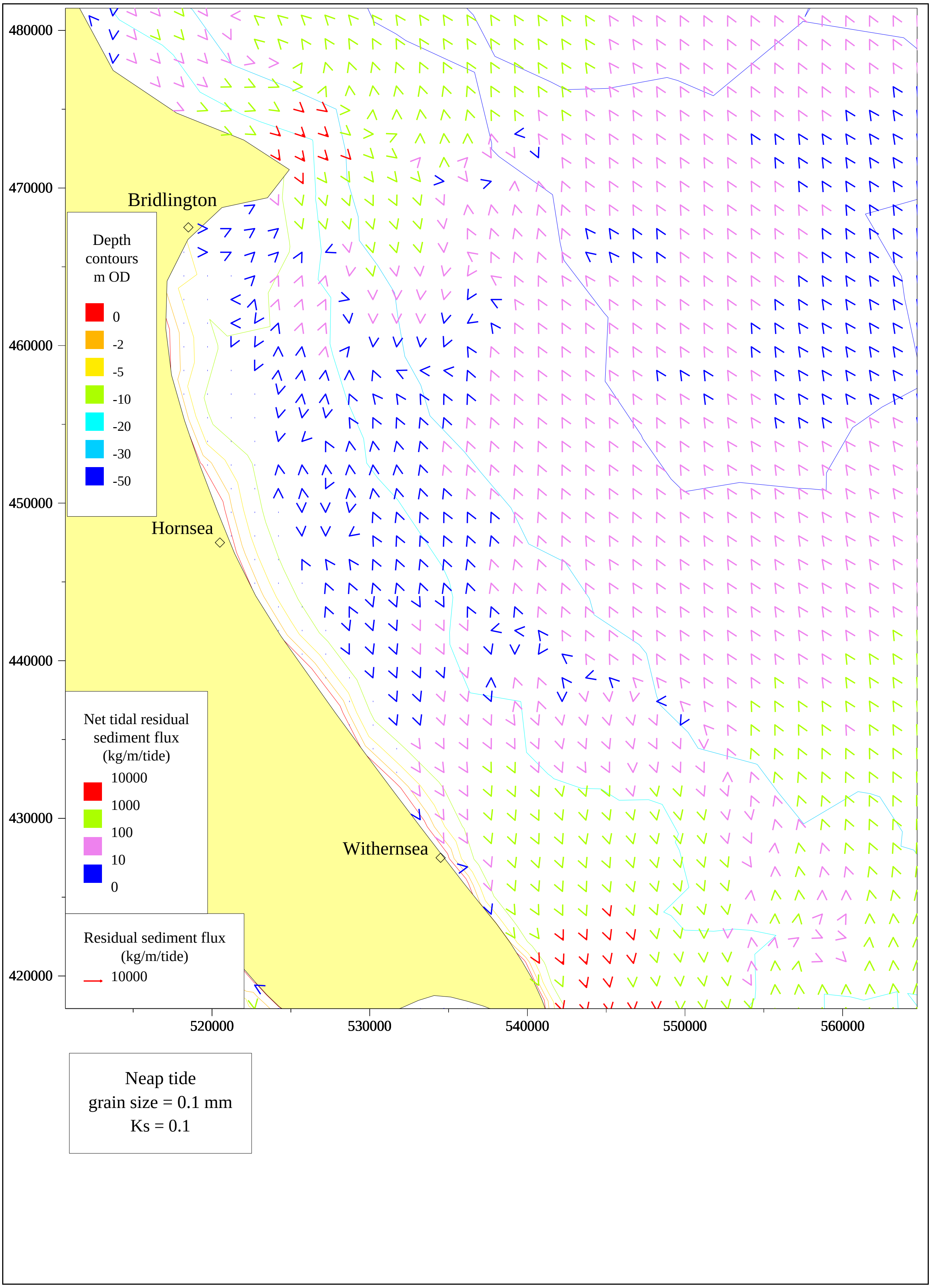

Figure 87 **Neap tide net sediment flux patterns (0.1mm sand) detail: Flamborough Head to the Humber**

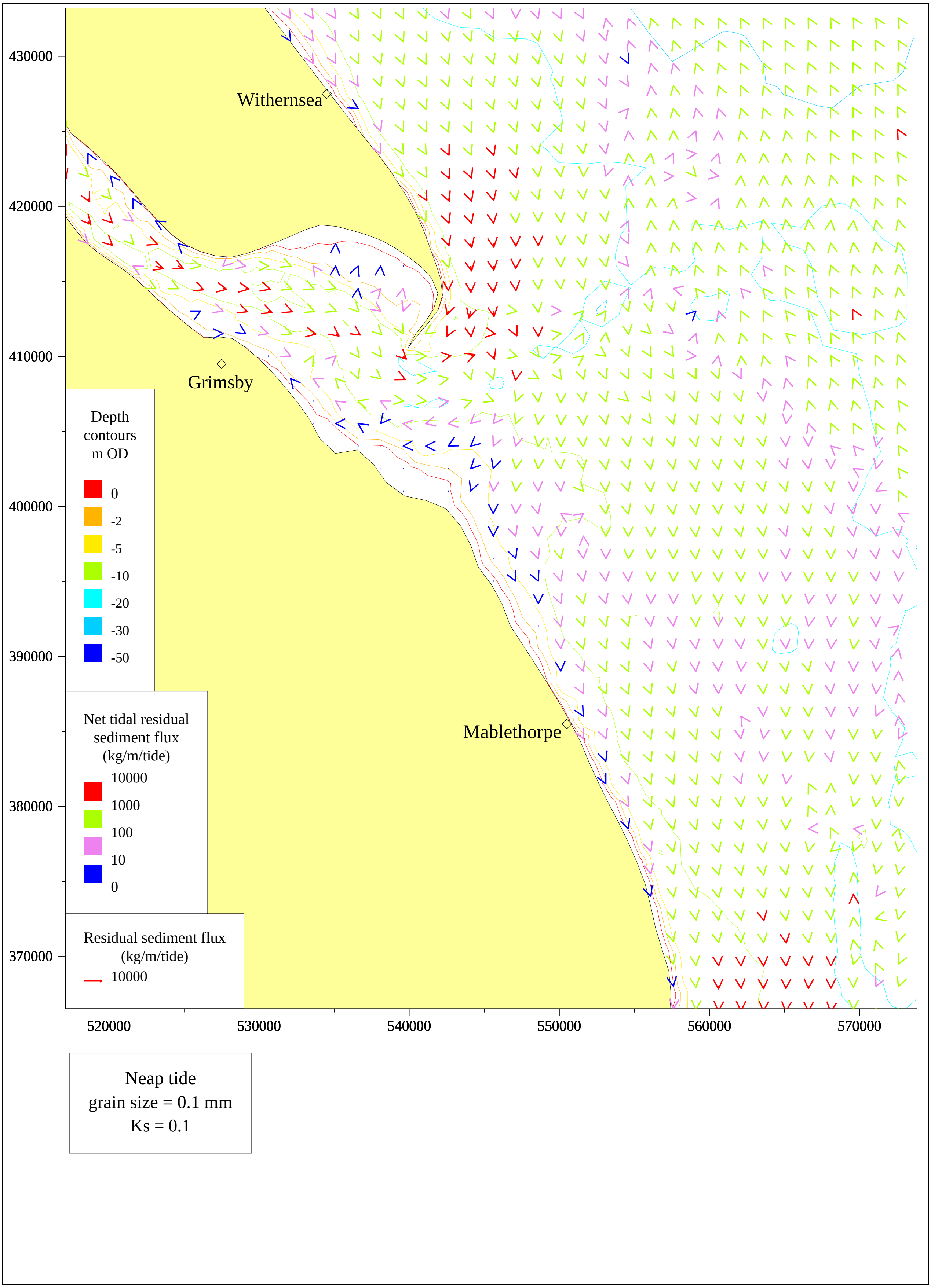

Figure 88 **Neap tide net sediment flux patterns (0.1mm sand) detail: Humber Entrance and Lincolnshire**

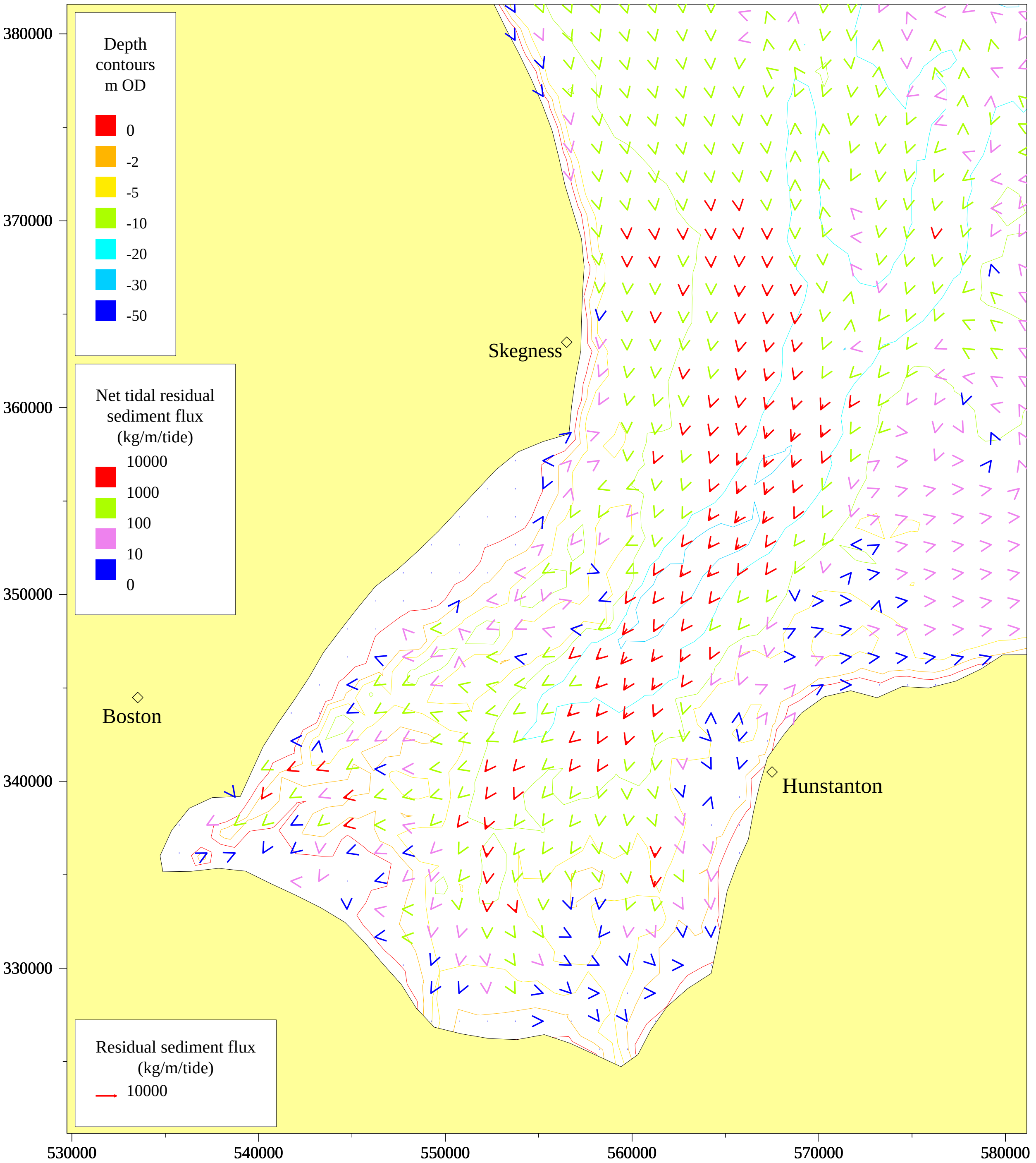

Neap tide
grain size = 0.1 mm
Ks = 0.1

Figure 89 Neap tide net sediment flux patterns (0.1mm sand) detail: Lincolnshire and the Wash

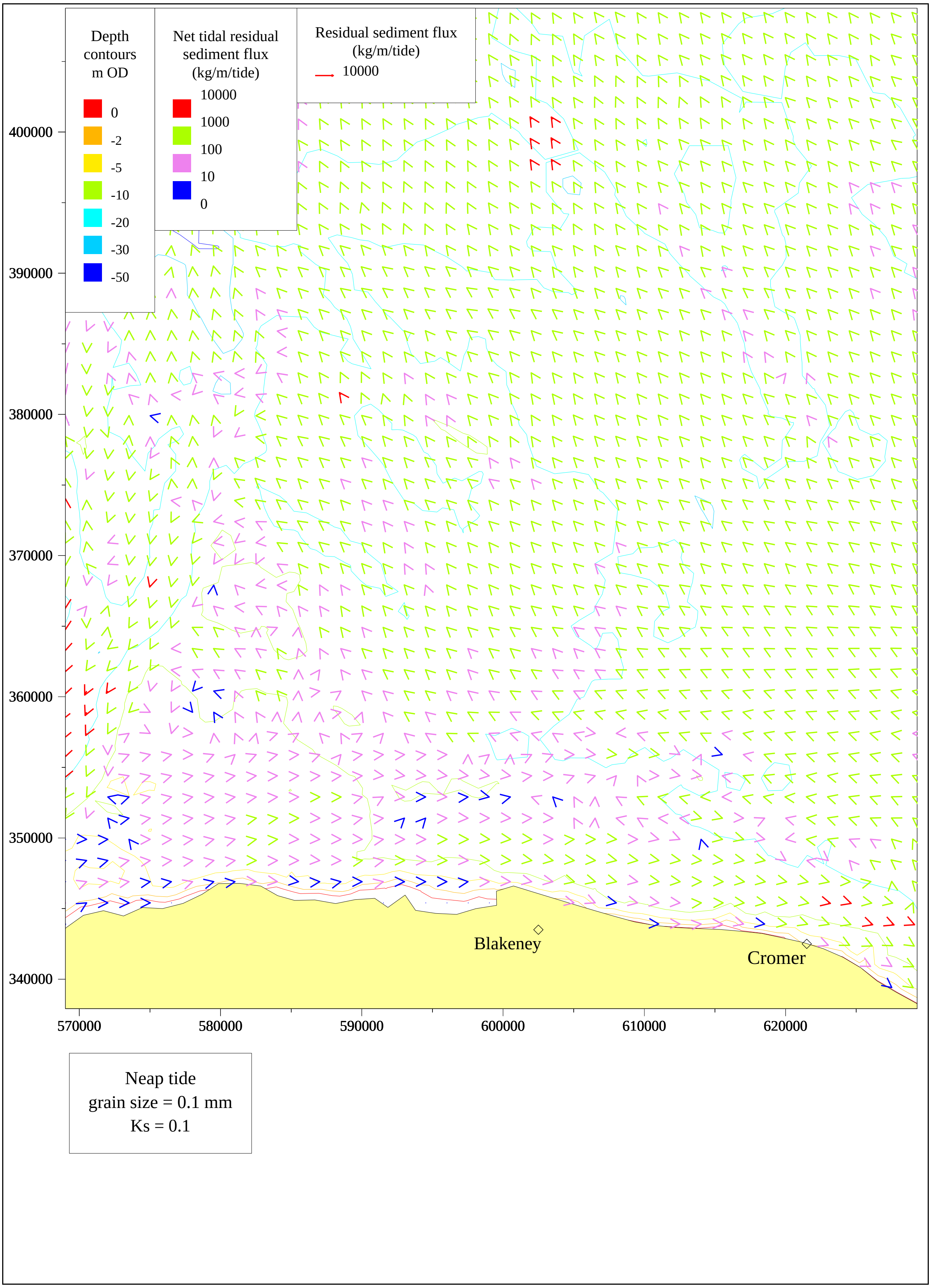

Figure 90 Neap tide net sediment flux patterns (0.1mm sand) detail: North Norfolk

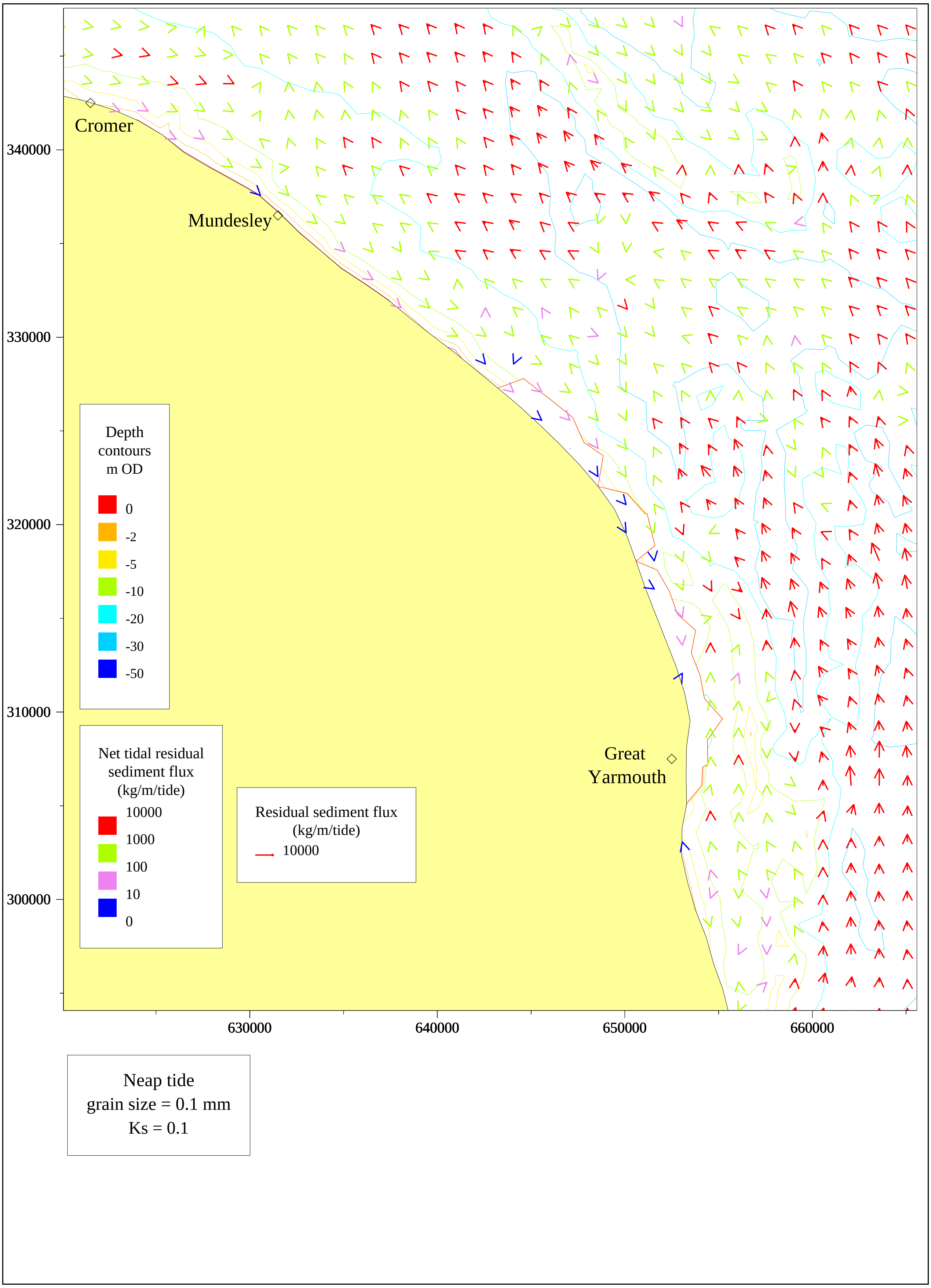

Figure 91 **Neap tide net sediment flux patterns (0.1mm sand) detail: East Norfolk**

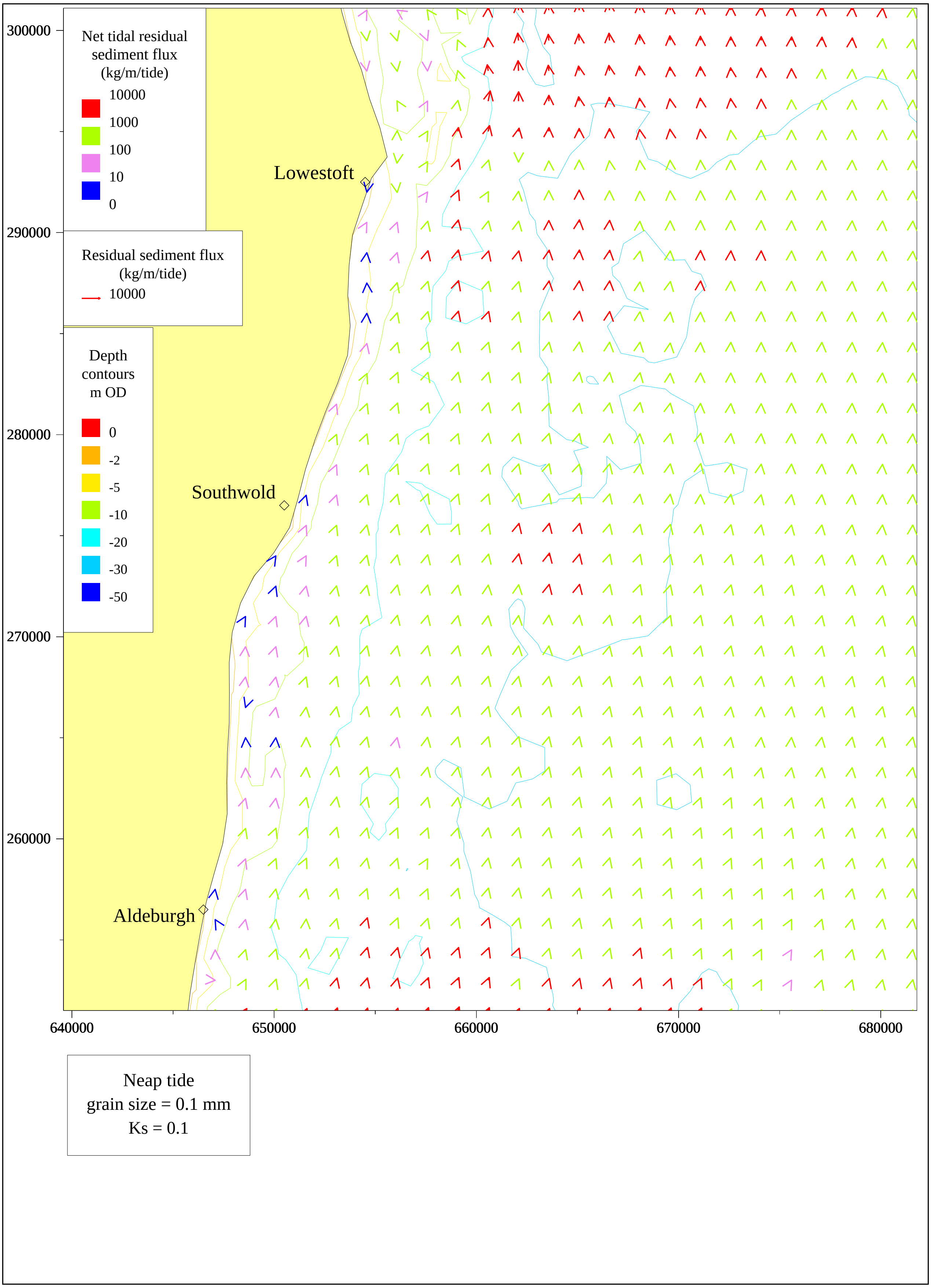

Figure 92 **Neap tide net sediment flux patterns (0.1mm sand) detail: North Suffolk**

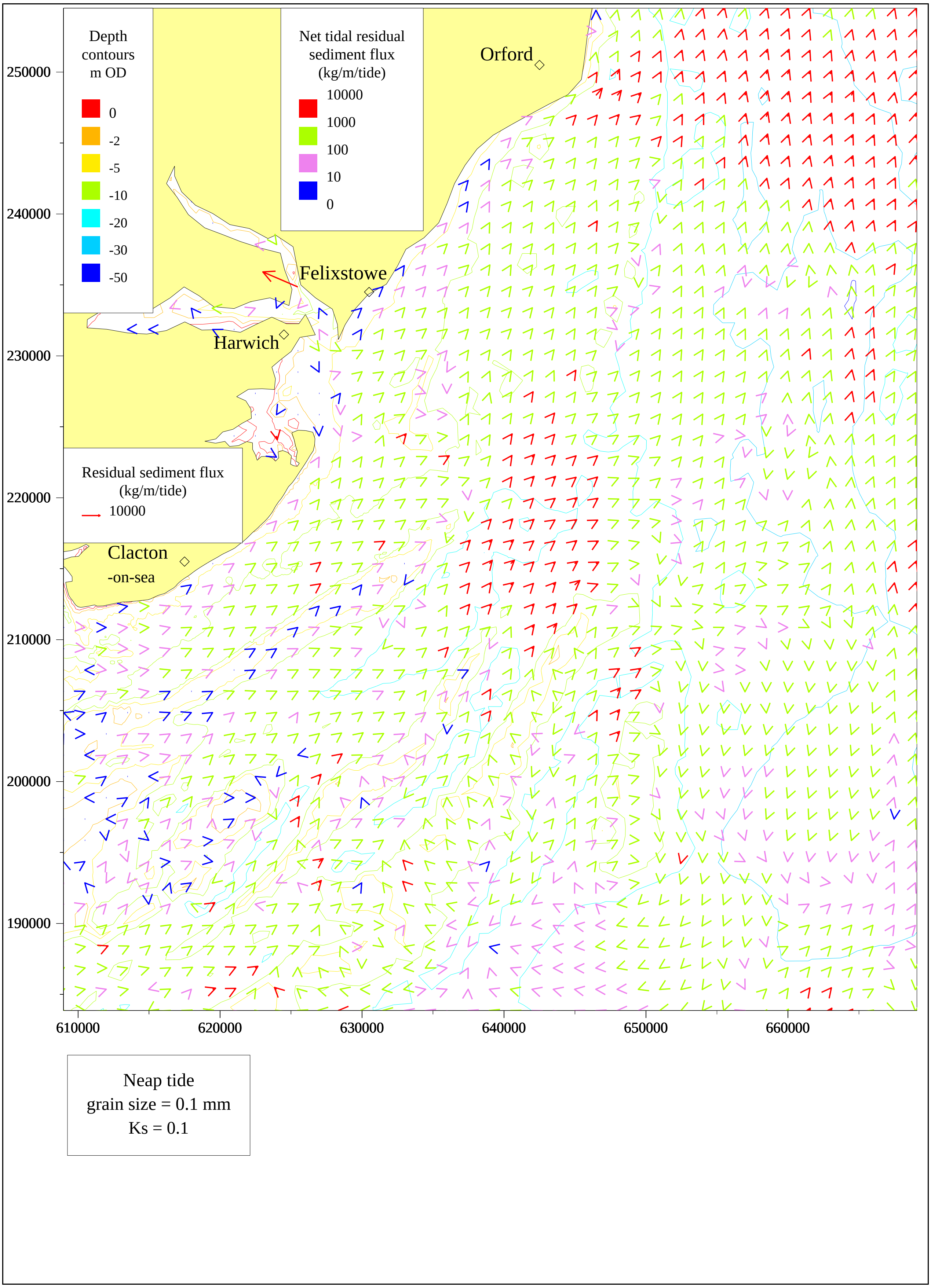

Figure 93 Neap tide net sediment flux patterns (0.1mm sand) detail: Suffolk and Essex

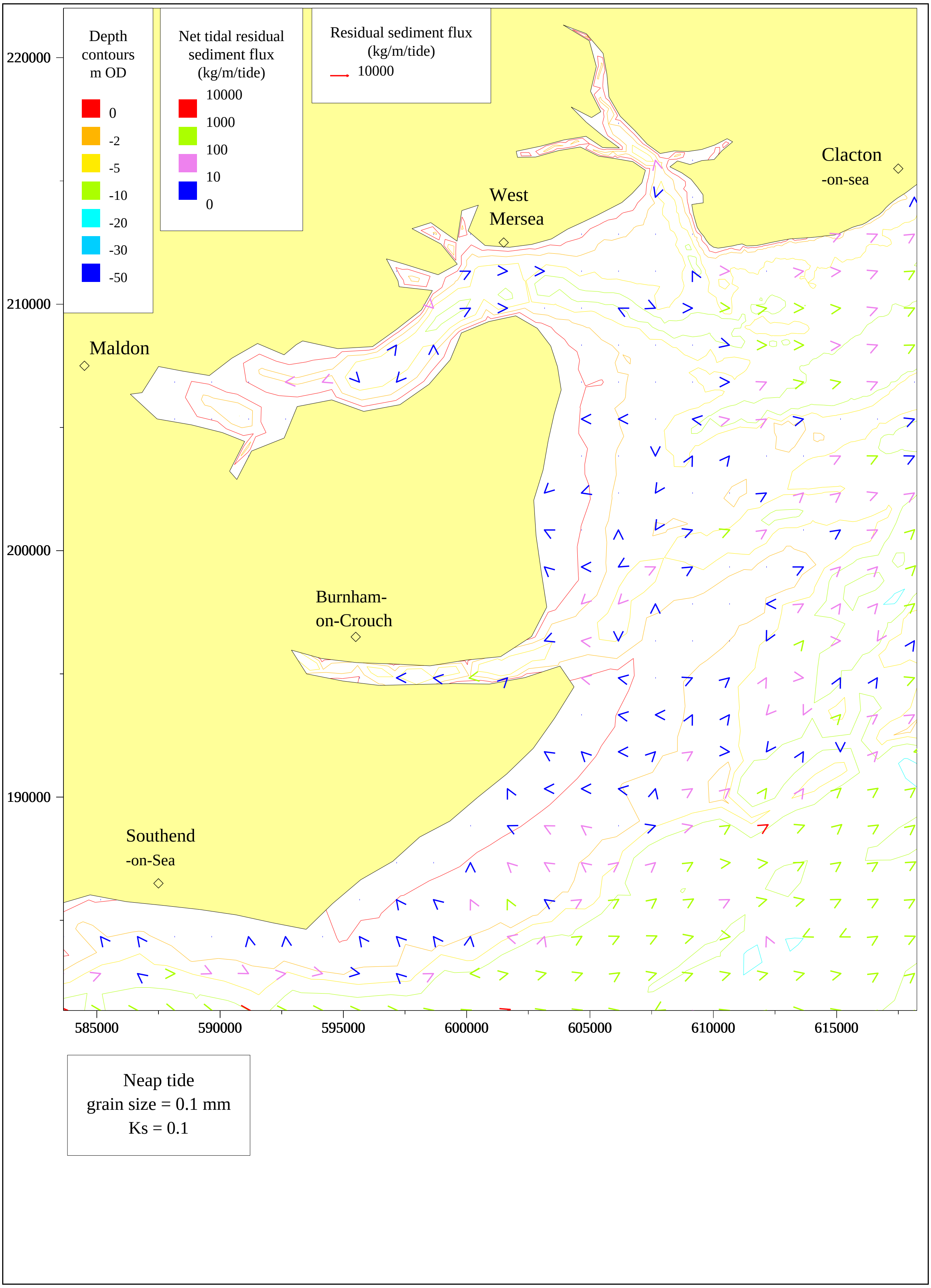

Figure 94 Neap tide net sediment flux patterns (0.1mm sand) detail: South Essex

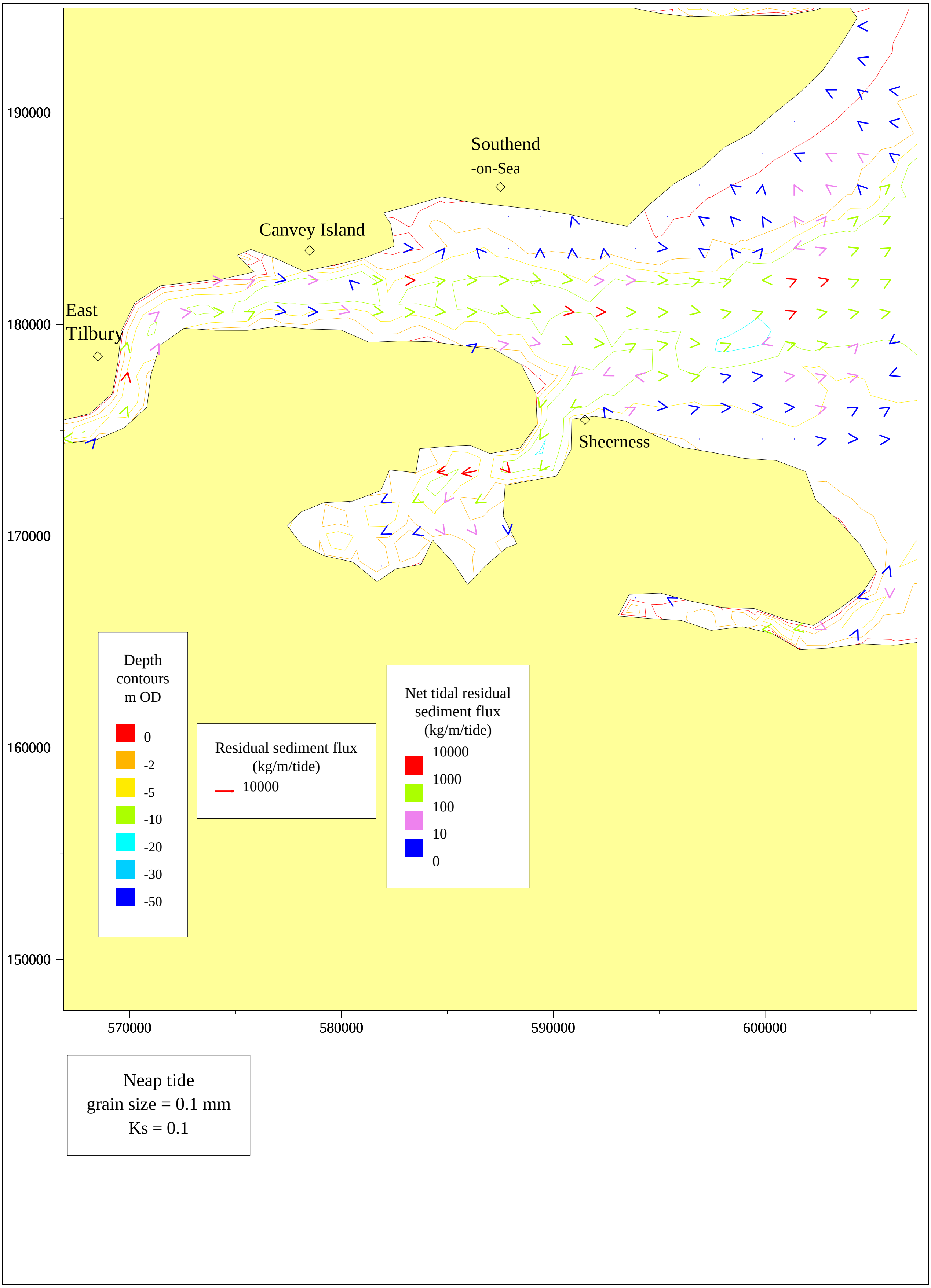

Figure 95 **Neap tide net sediment flux patterns (0.1mm sand) detail: Outer Thames**

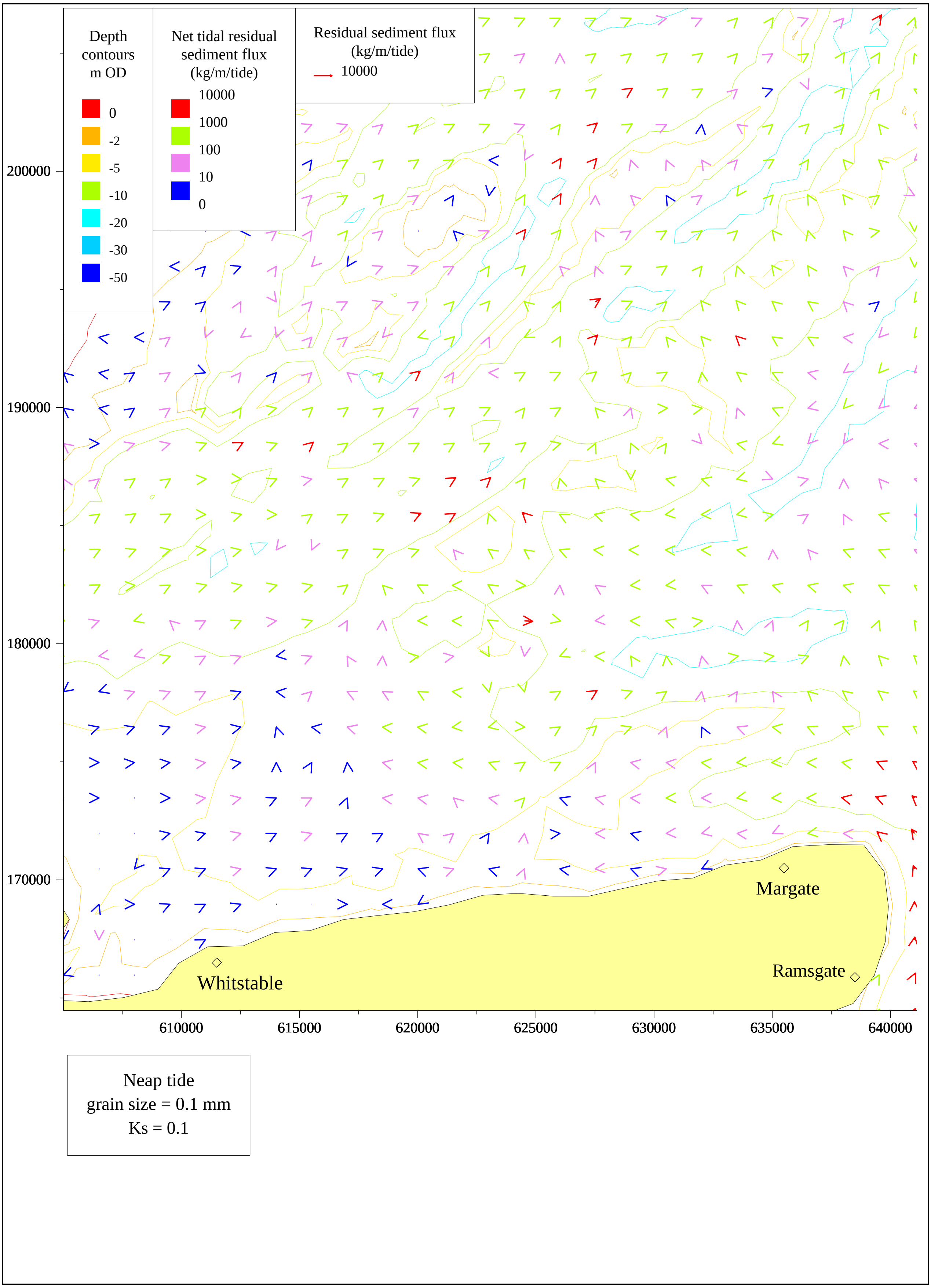

Figure 96 **Neap tide net sediment flux patterns (0.1mm sand) detail: North Kent**

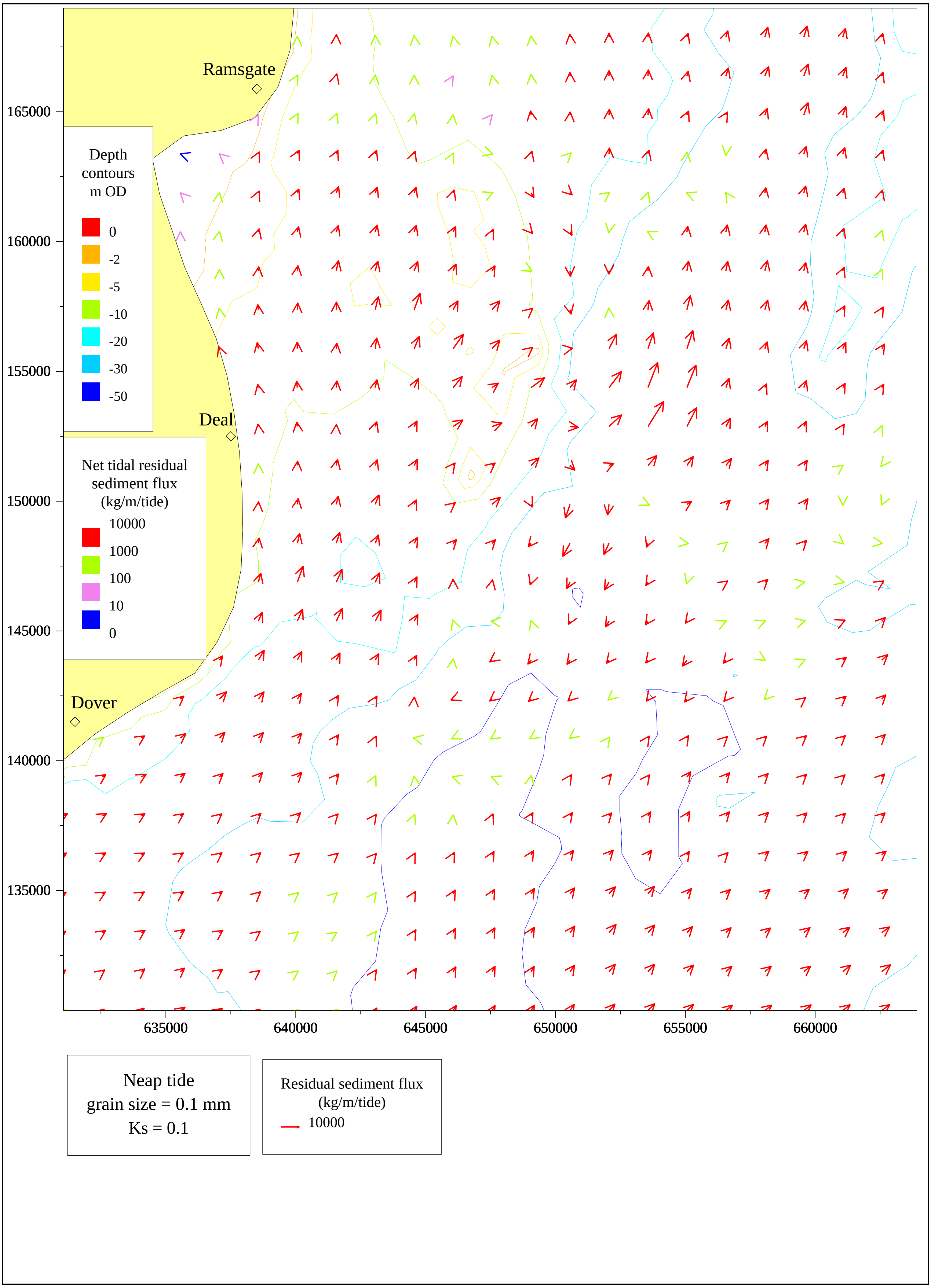

Figure 97 Neap tide net sediment flux patterns (0.1mm sand) detail: East Kent

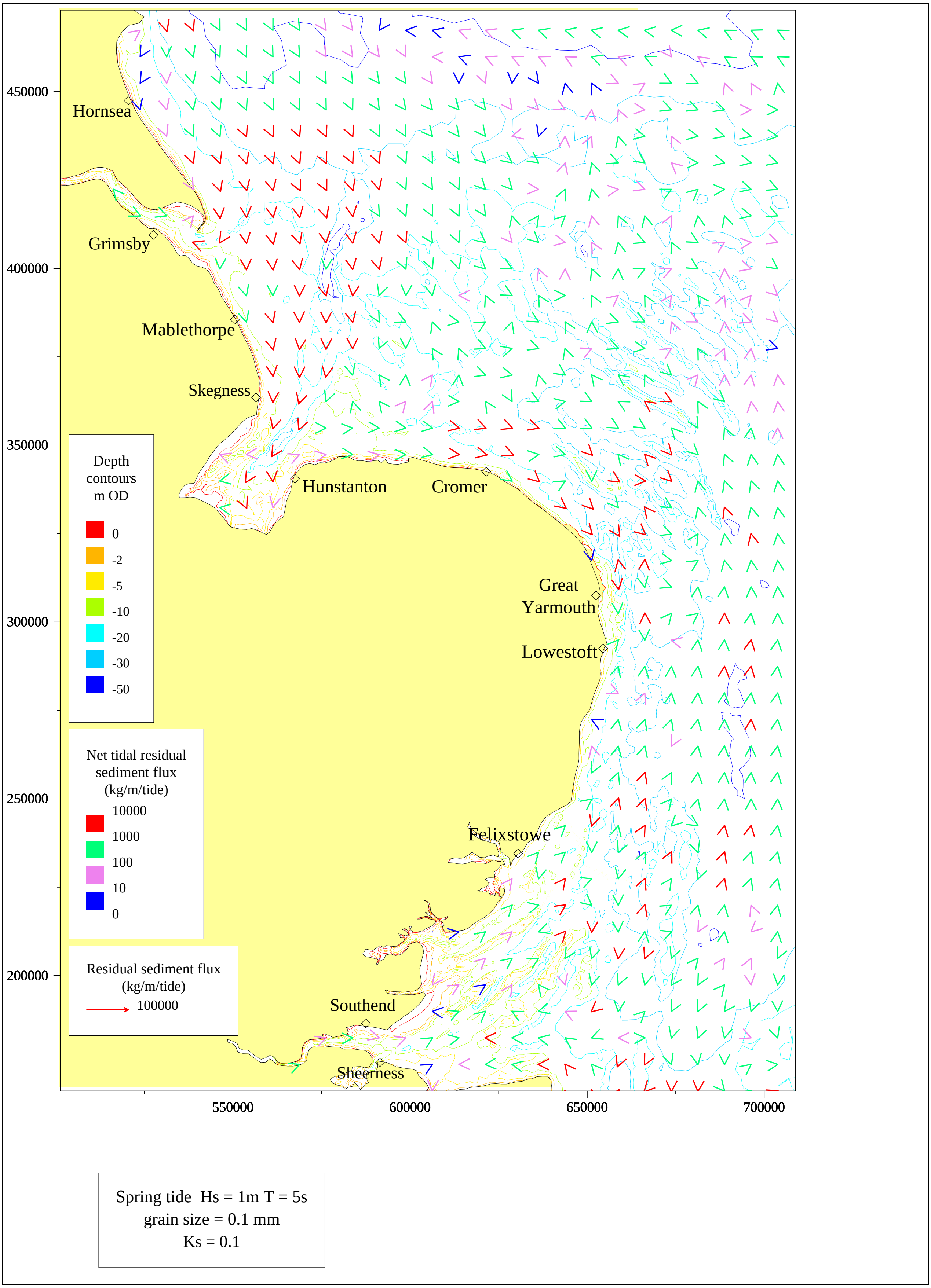

Figure 98 Spring tide with 1m 5s waves net sediment flux patterns (0.1mm sand)

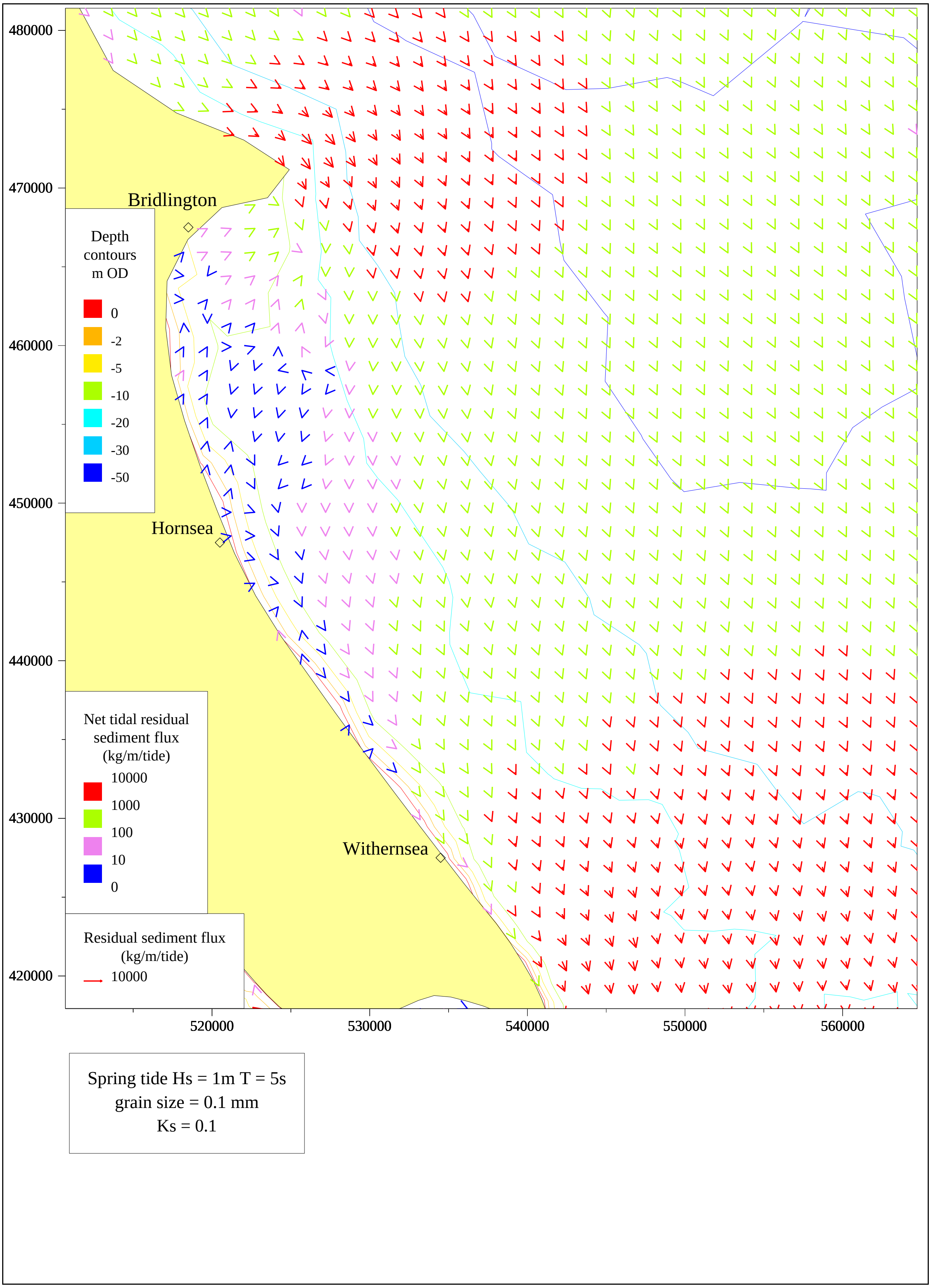

Figure 99 **Spring tide with 1m 5s waves net sediment flux patterns (0.1mm sand) detail: Flamborough Head to the Humber**

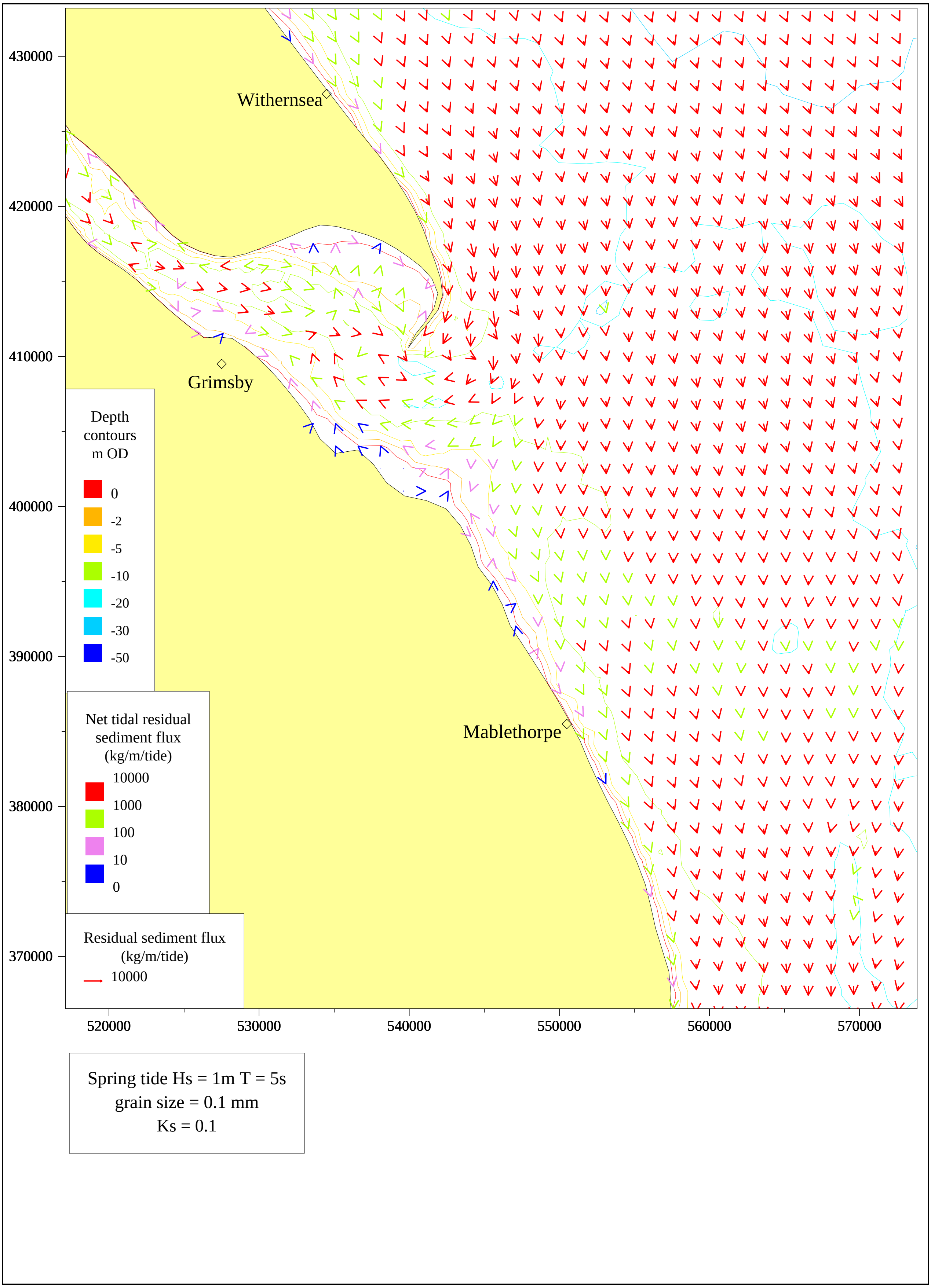

Figure 100 **Spring tide with 1m 5s waves net sediment flux patterns (0.1mm sand) detail: Humber Entrance and Lincolnshire**

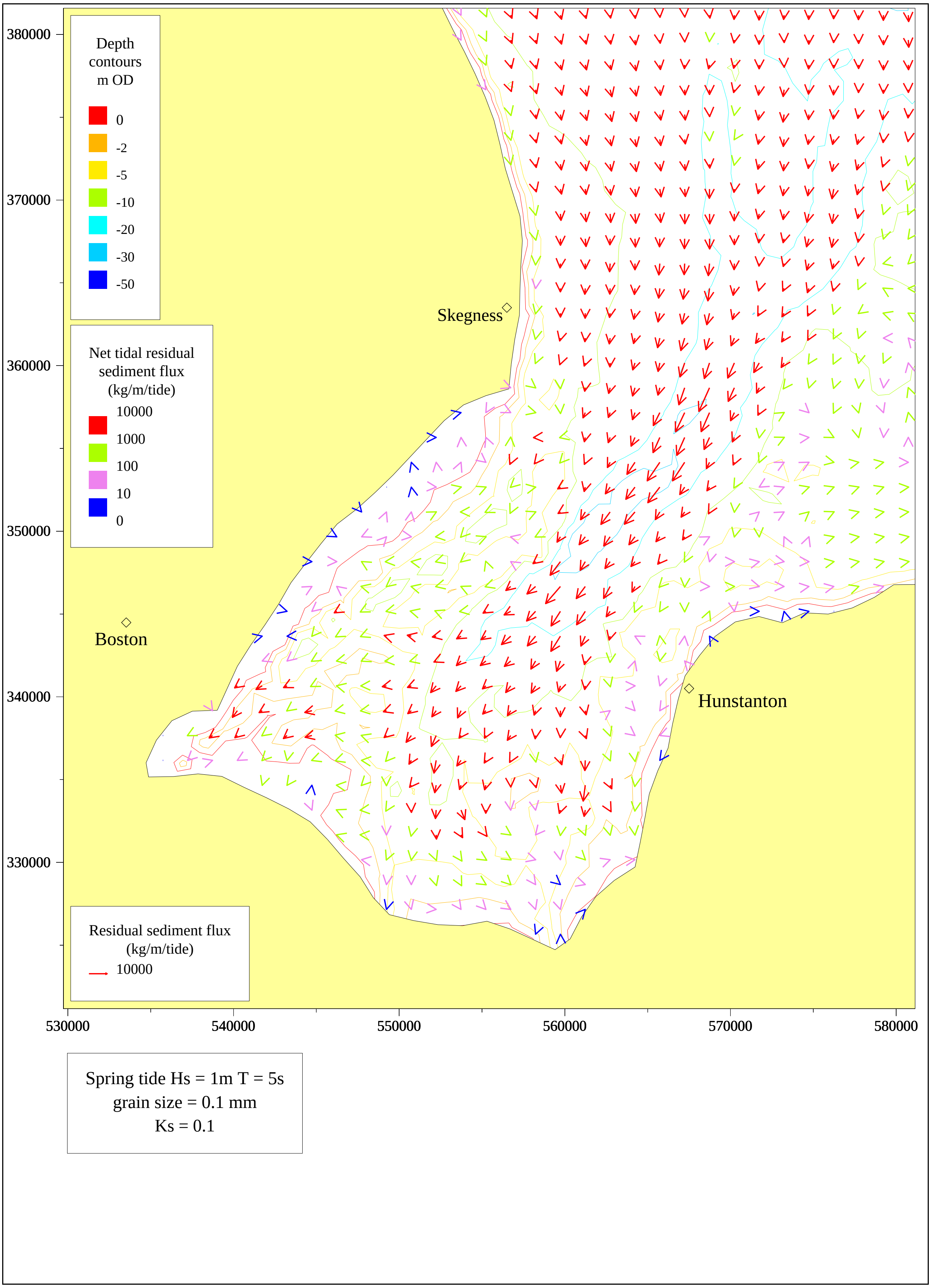

Figure 101 **Spring tide with 1m 5s waves net sediment flux patterns (0.1mm sand) detail: Lincolnshire and the Wash**

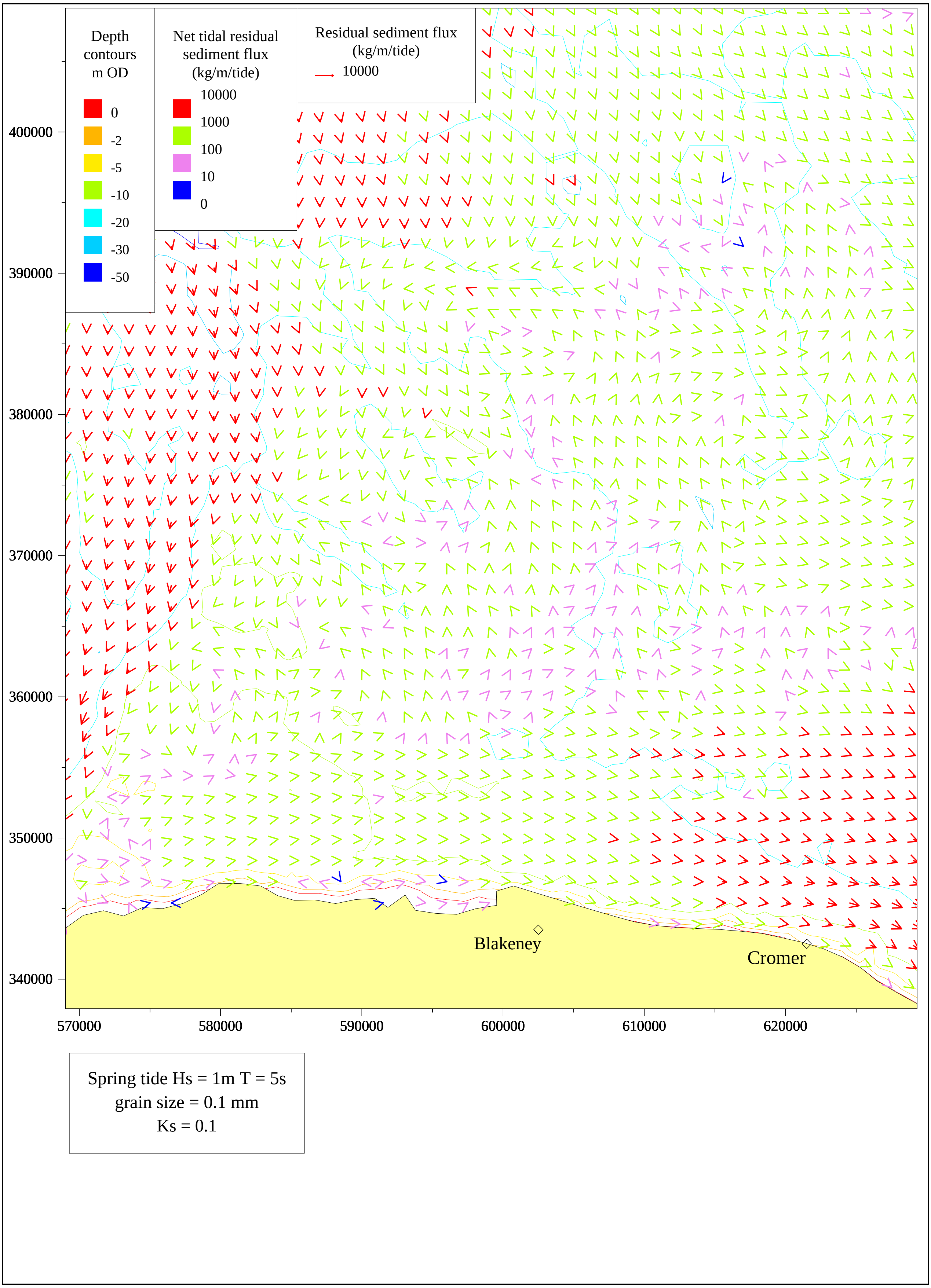

Figure 102 **Spring tide with 1m 5s waves net sediment flux patterns (0.1mm sand) detail: North Norfolk**

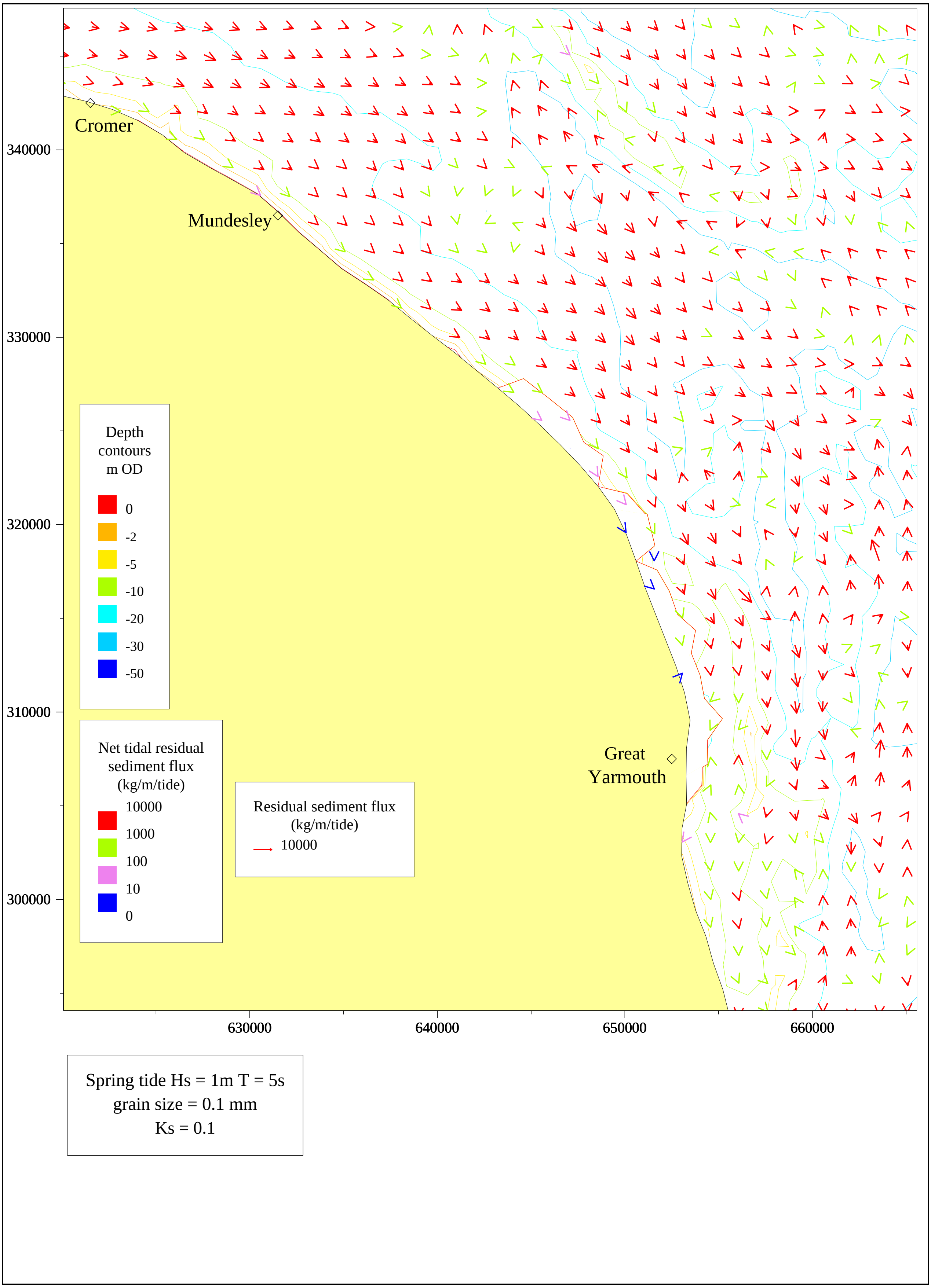

Figure 103 **Spring tide with 1m 5s waves net sediment flux patterns (0.1mm sand) detail: East Norfolk**

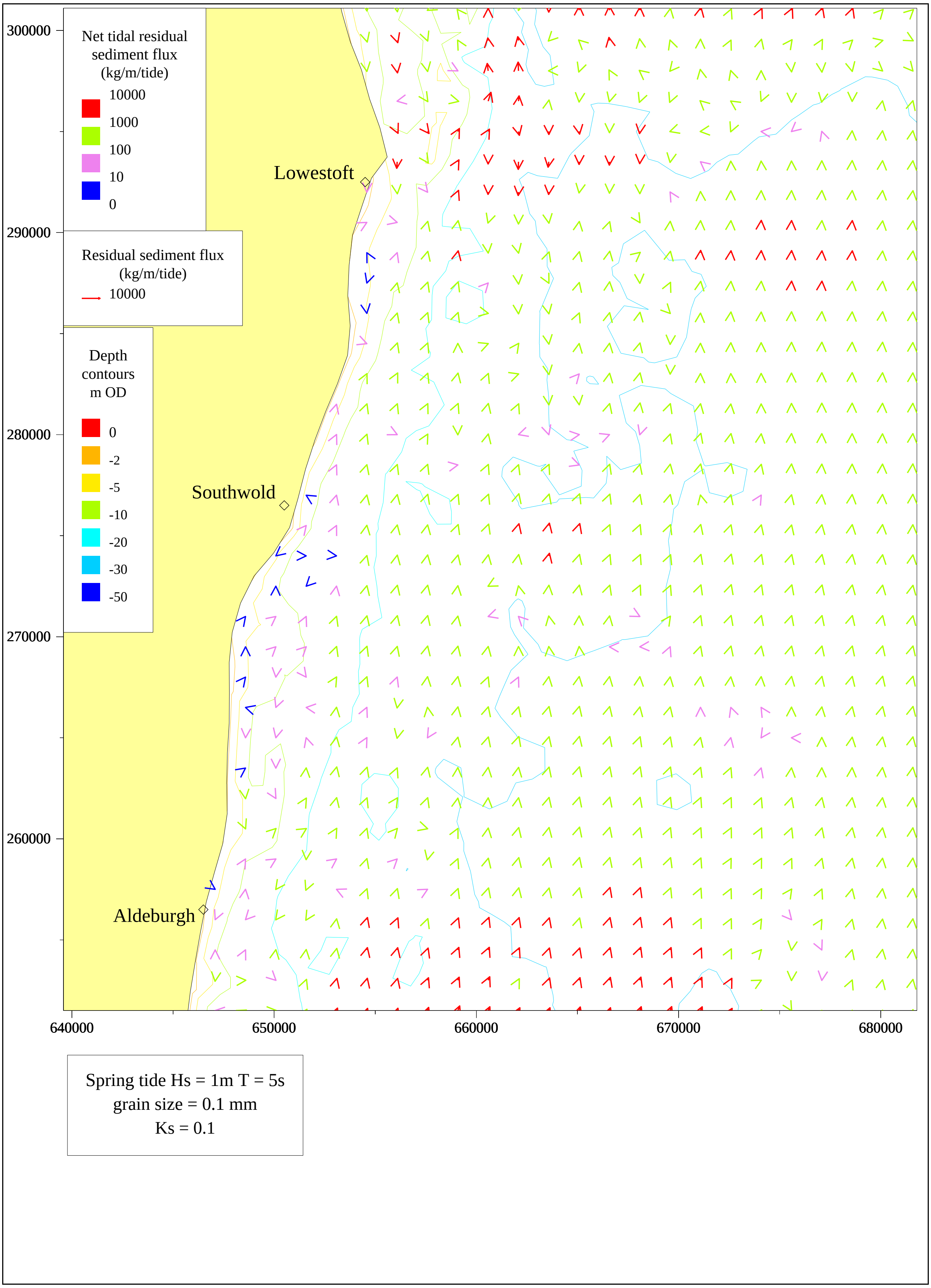

Figure 104 **Spring tide with 1m 5s waves net sediment flux patterns (0.1mm sand) detail: North Suffolk**

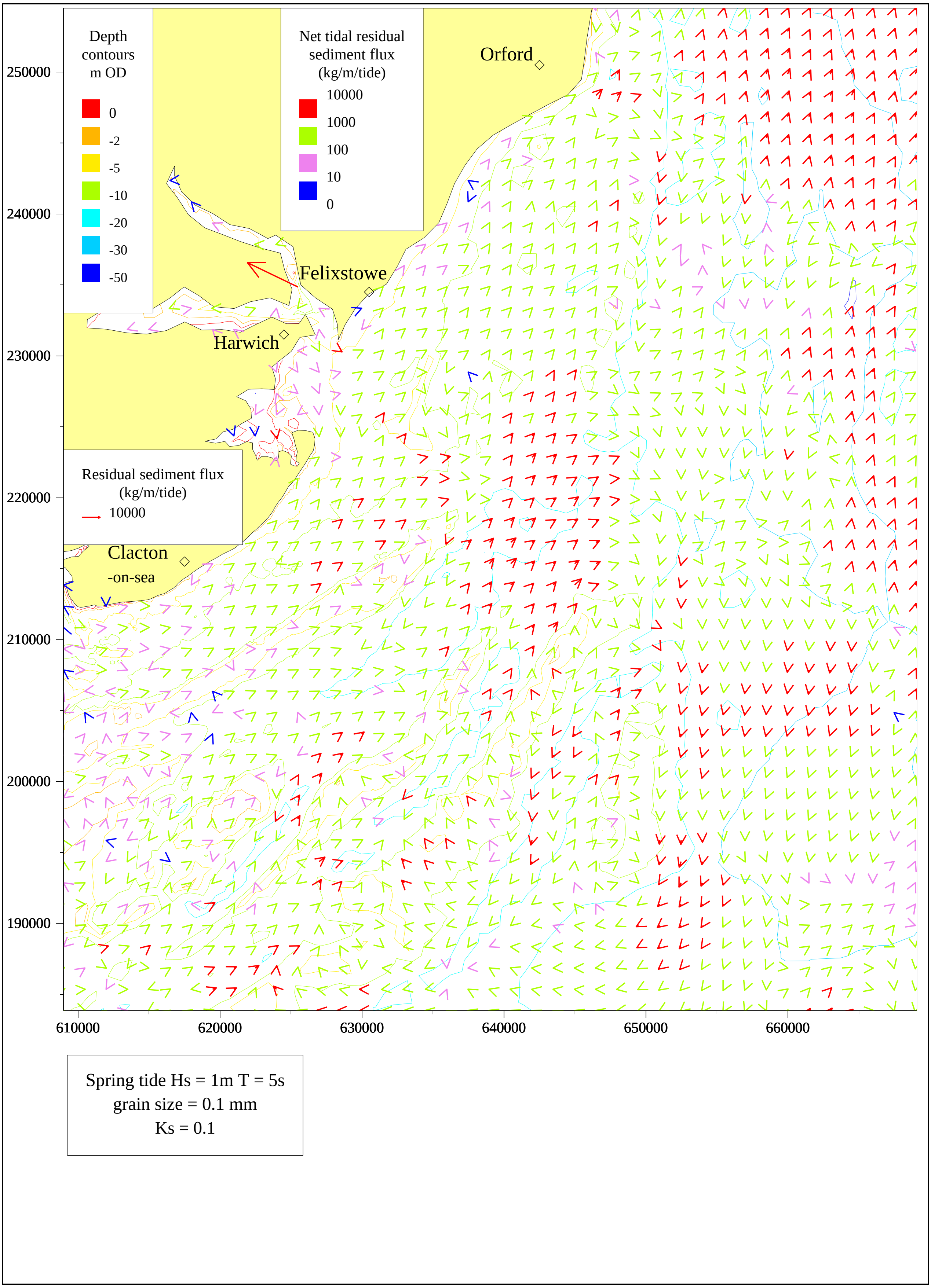

Figure 105 **Spring tide with 1m 5s waves net sediment flux patterns (0.1mm sand) detail: Suffolk and Essex**

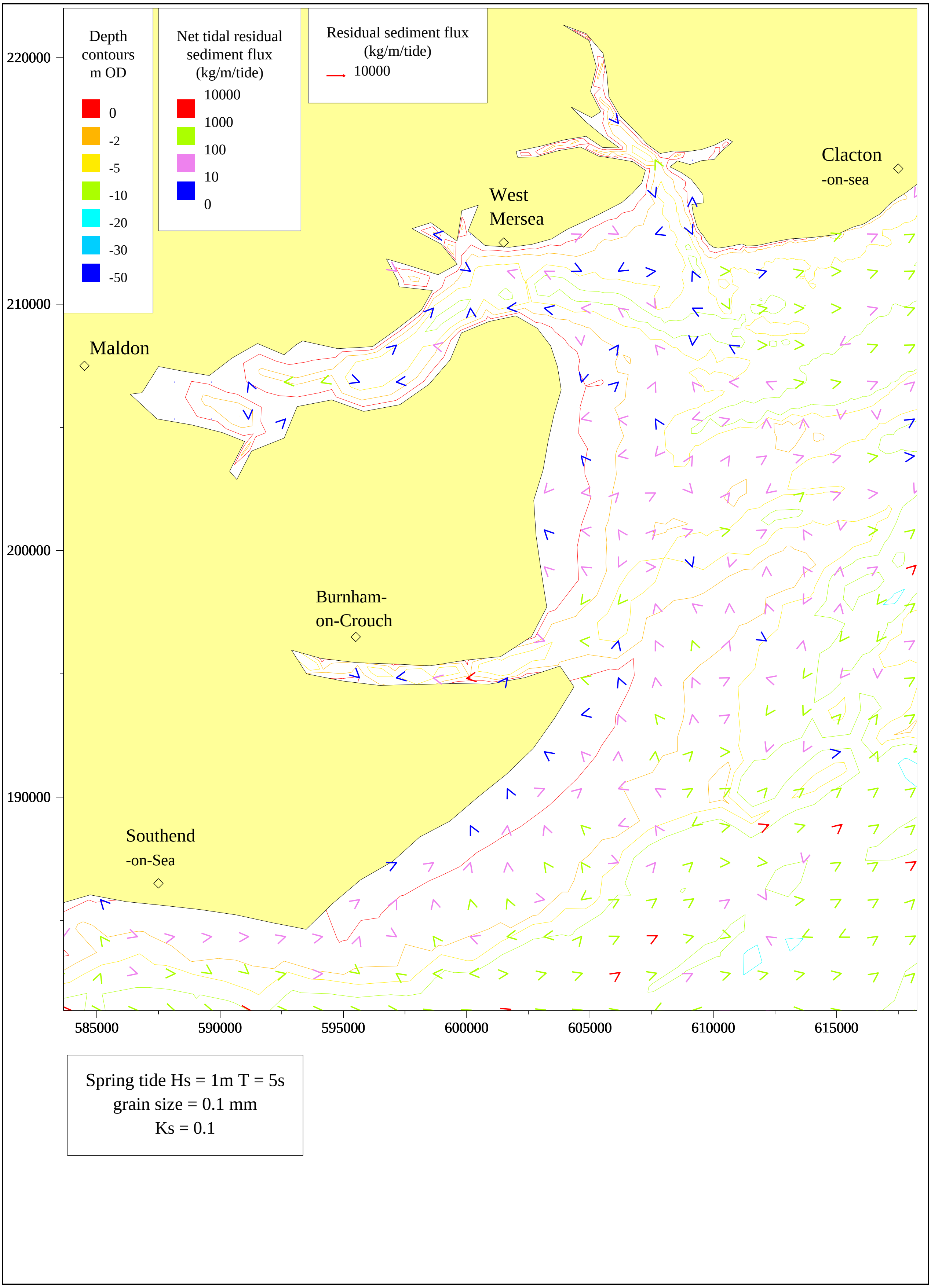

Figure 106 **Spring tide with 1m 5s waves net sediment flux patterns (0.1mm sand) detail: South Essex**

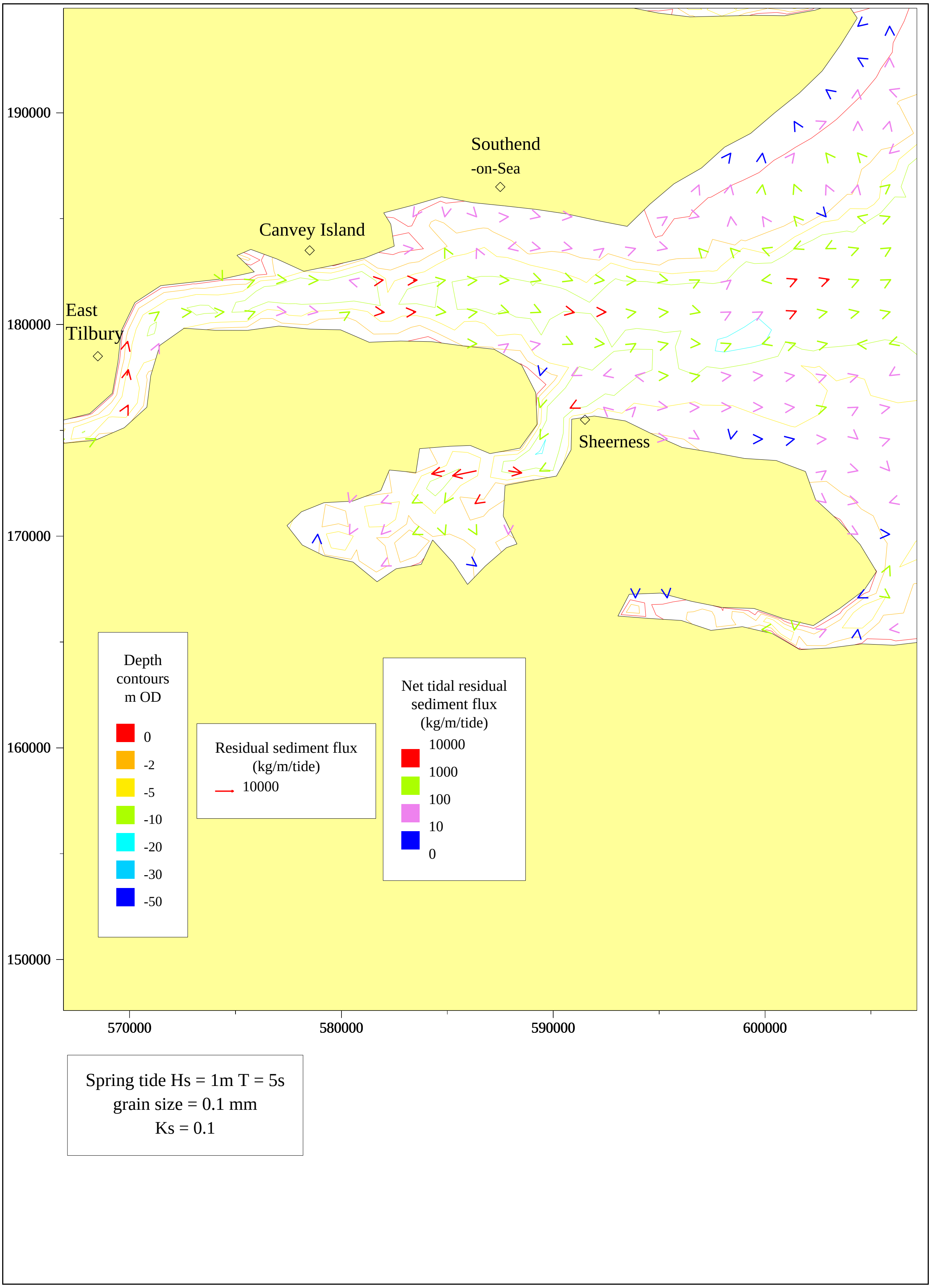

Figure 107 **Spring tide with 1m 5s waves net sediment flux patterns (0.1mm sand) detail: Outer Thames**

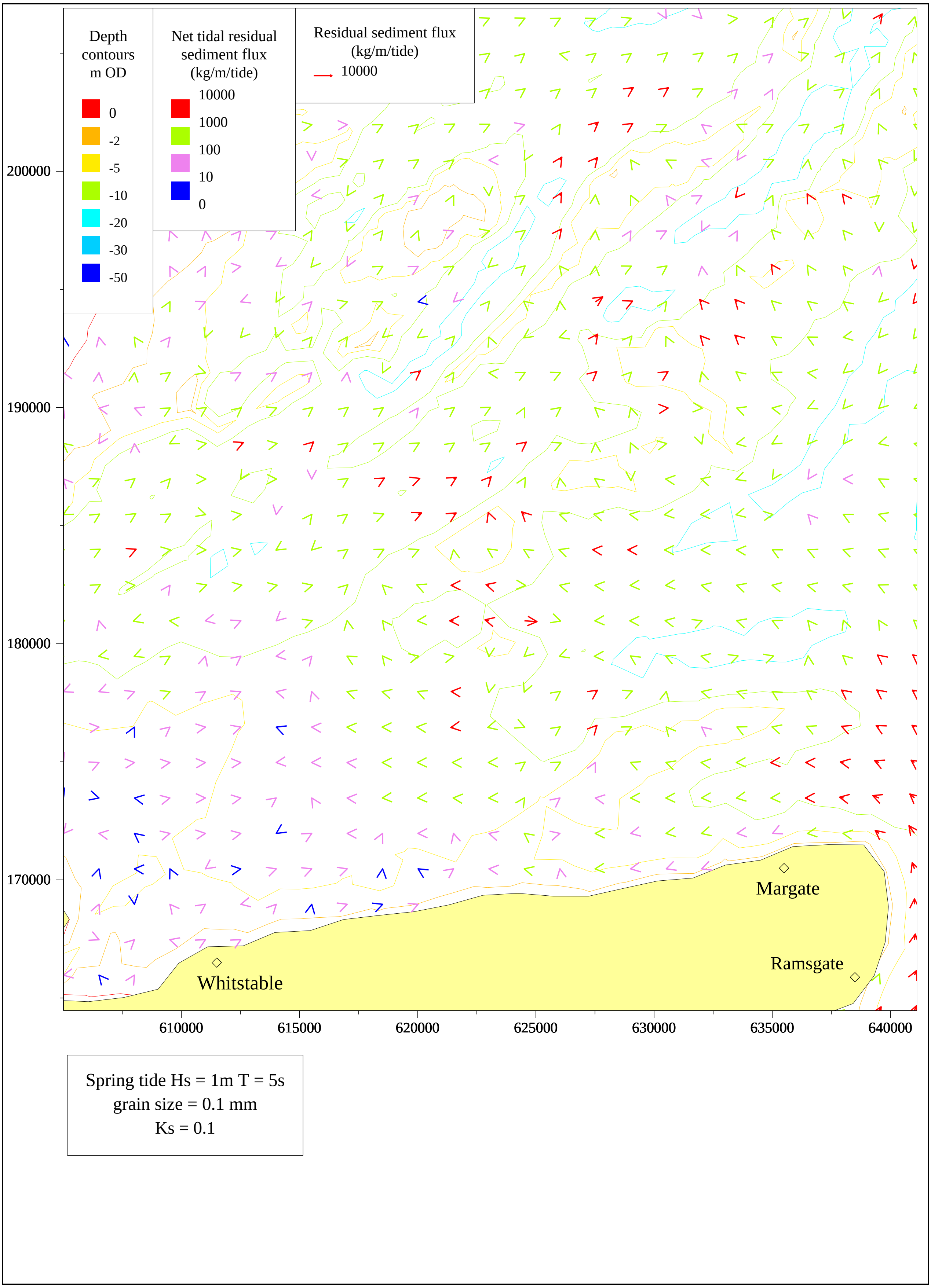

Figure 108 Spring tide with 1m 5s waves net sediment flux patterns (0.1mm sand) detail: North Kent

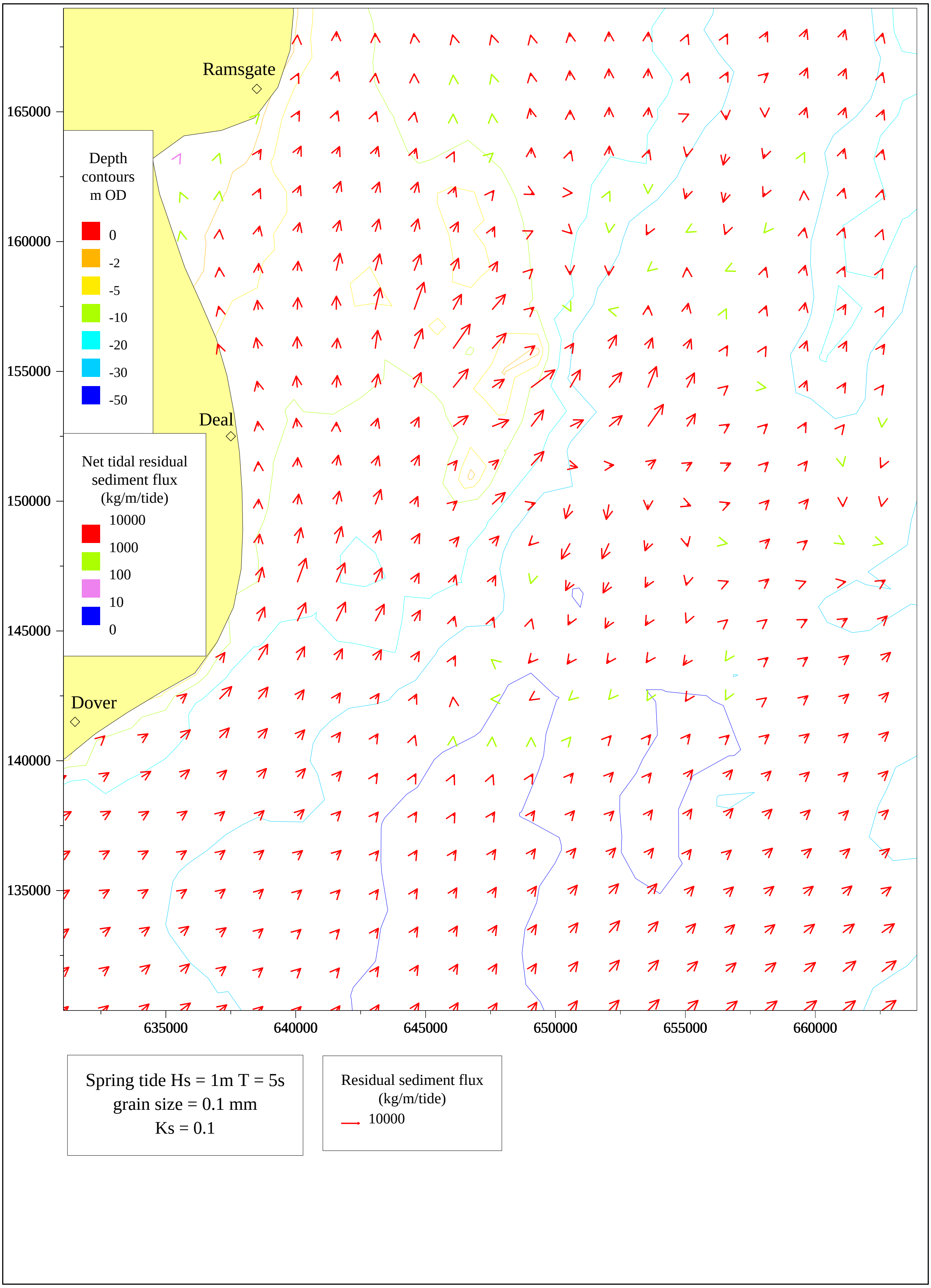

Figure 109 Spring tide with 1m 5s waves net sediment flux patterns (0.1mm sand) detail: East Kent

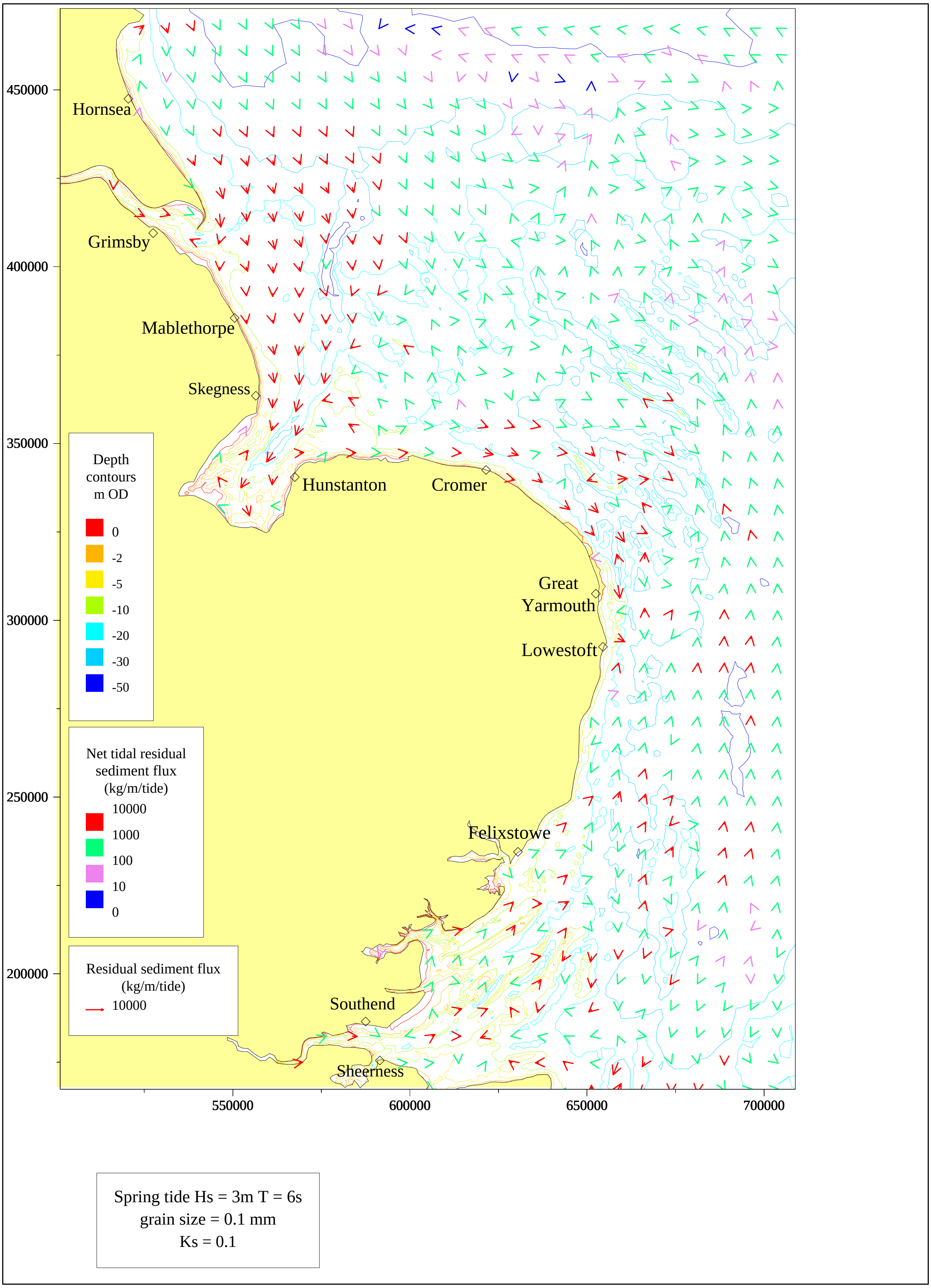

Figure 110 **Spring tide with 3m 6s storm waves net sediment flux patterns (0.1mm sand)**

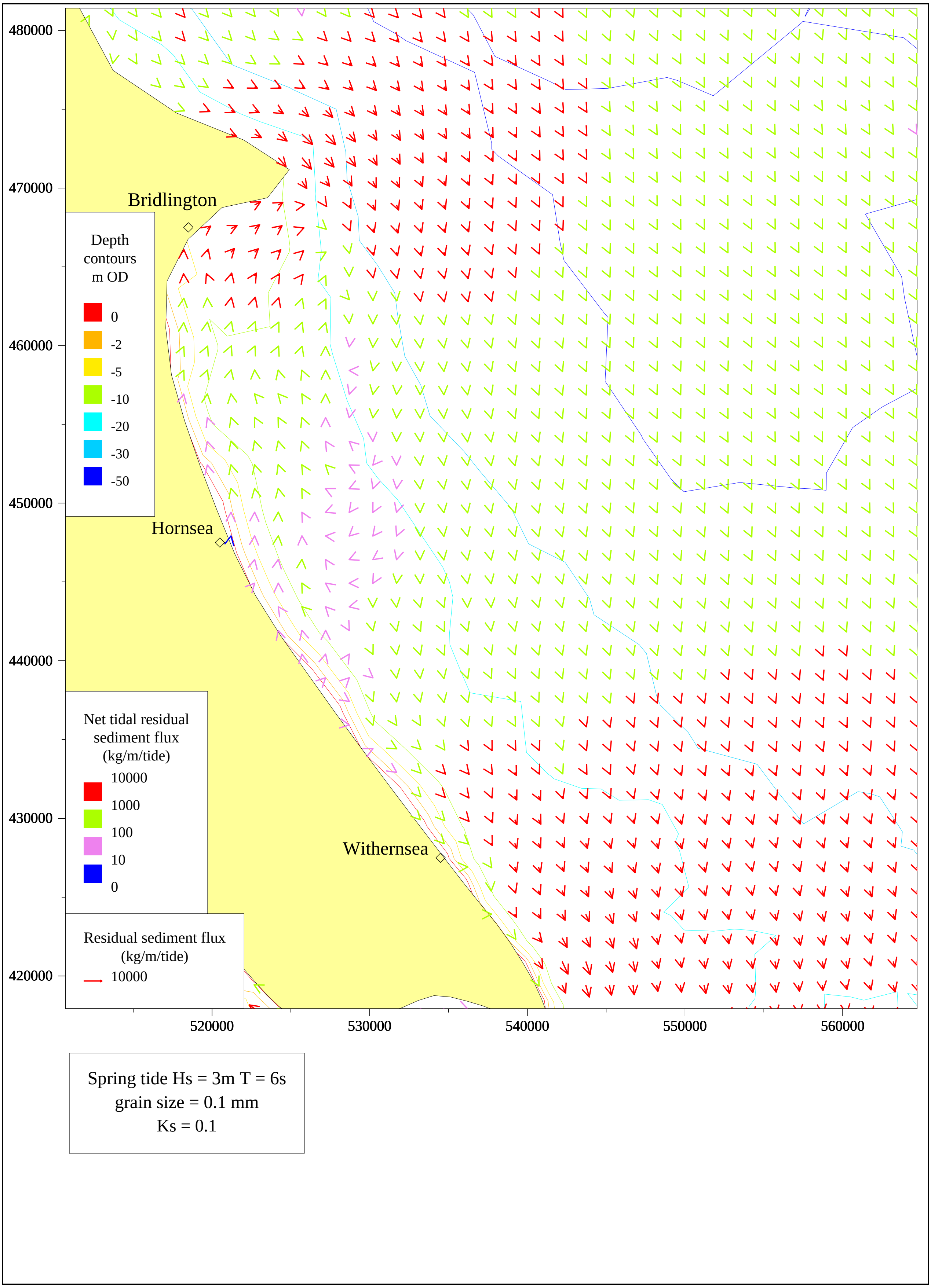

Figure 111 **Spring tide with 3m 6s storm waves net sediment flux patterns (0.1mm sand) detail: Flamborough Head to the Humber**

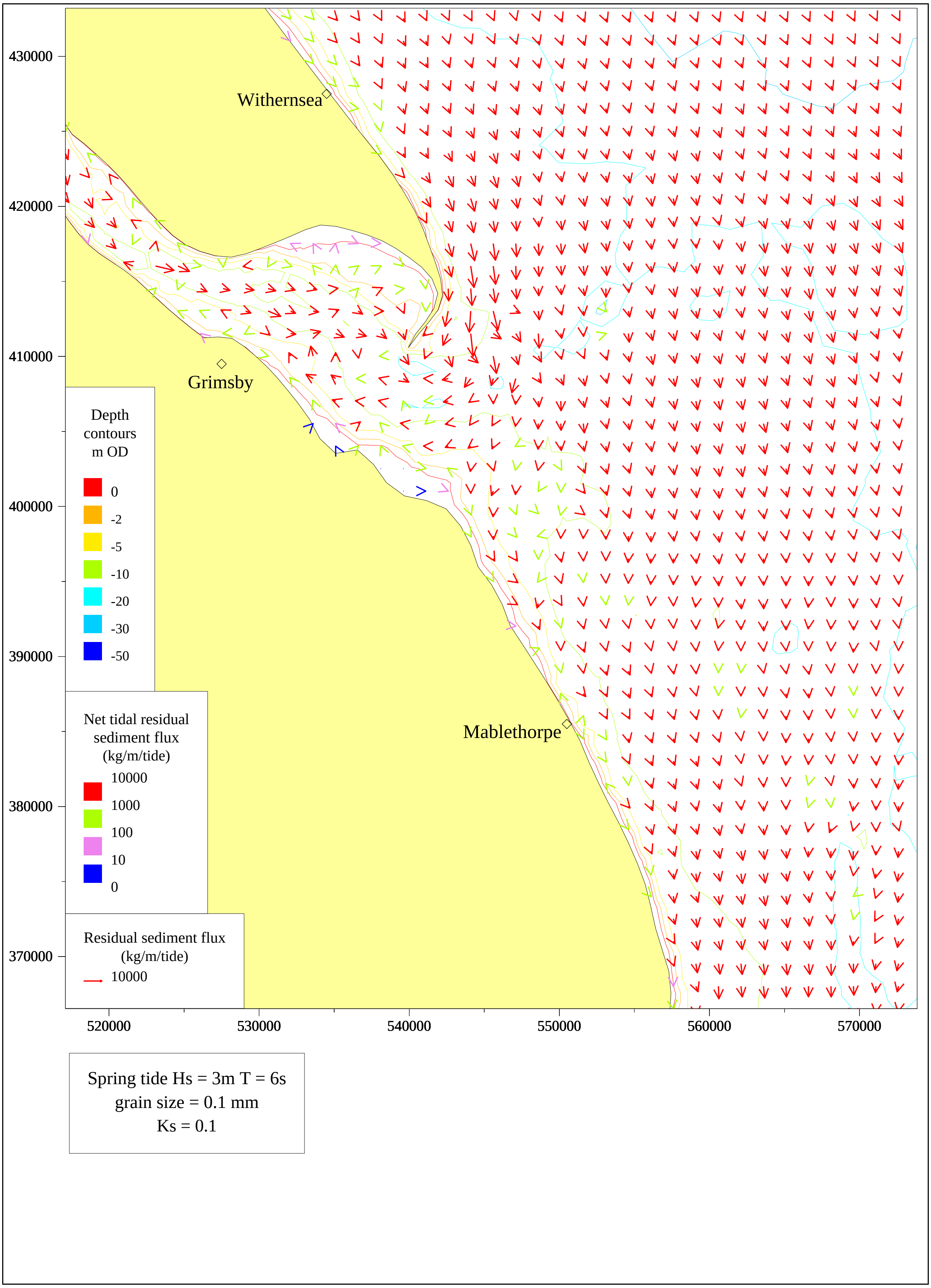

Figure 112 **Spring tide with 3m 6s storm waves net sediment flux patterns (0.1mm sand) detail: Humber Entrance and Lincolnshire**

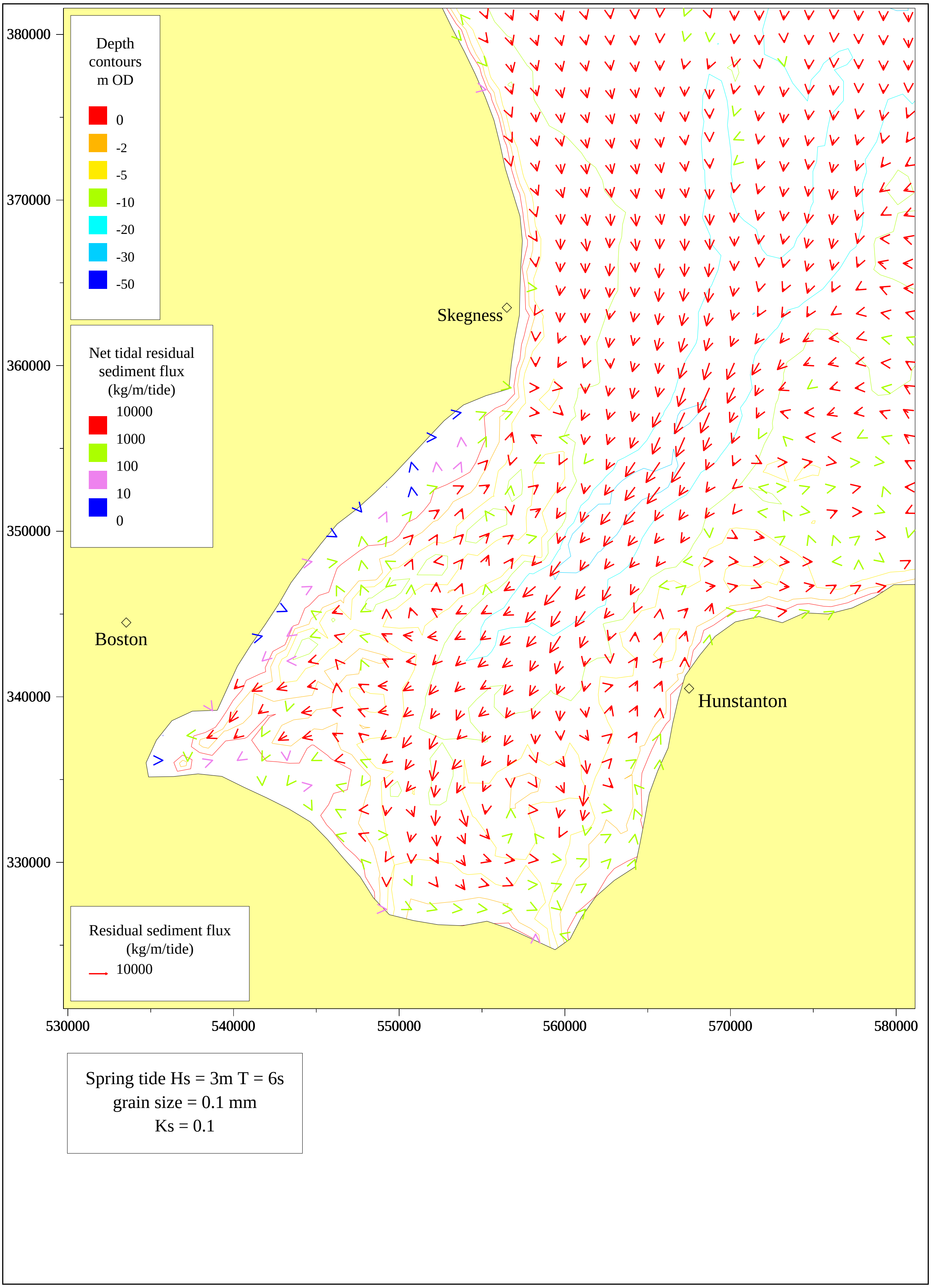

Figure 113 Spring tide with 3m 6s storm waves net sediment flux patterns (0.1mm sand) detail: Lincolnshire and the Wash

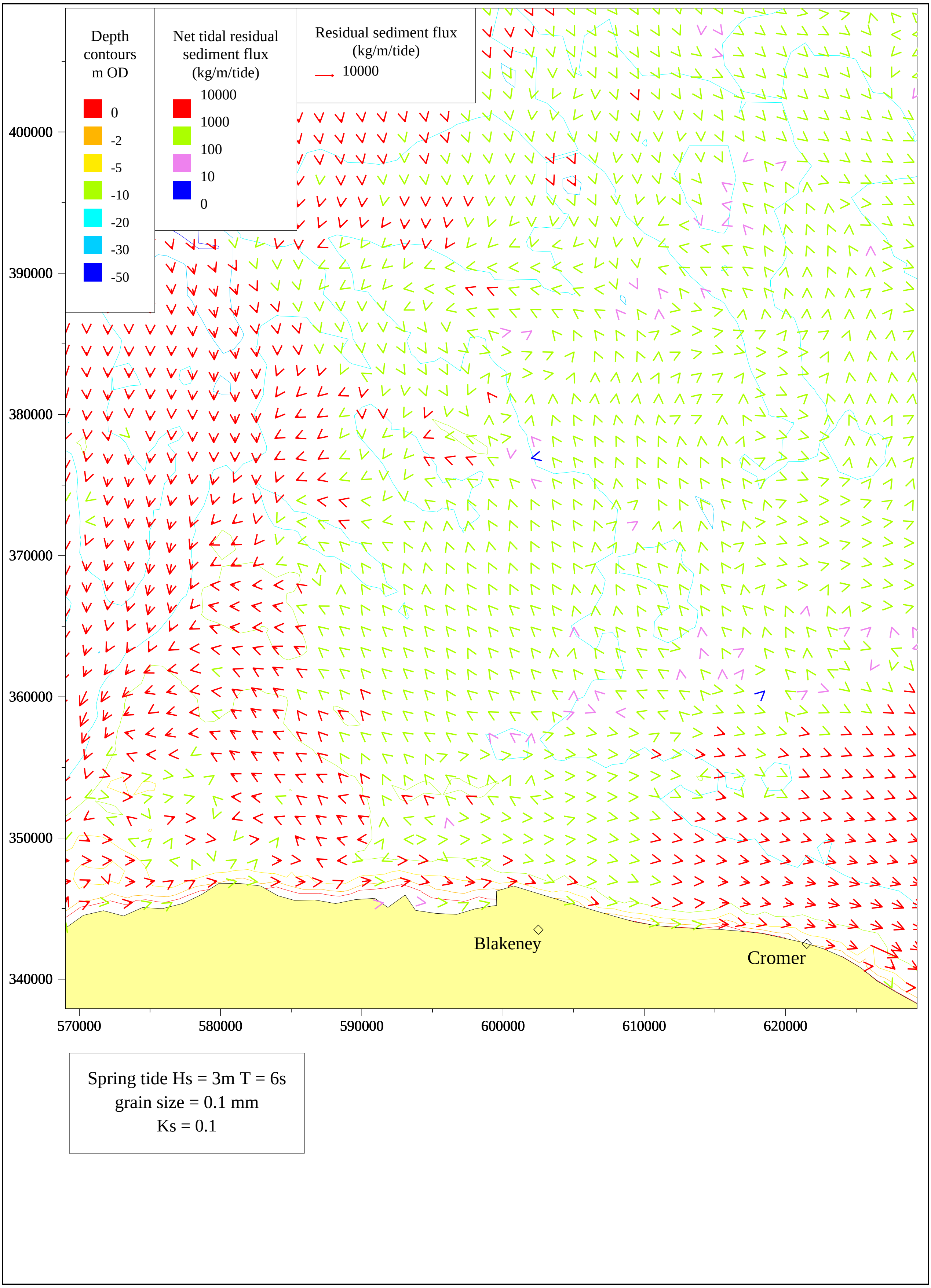

Figure 114 **Spring tide with 3m 6s storm waves net sediment flux patterns (0.1mm sand) detail: North Norfolk**

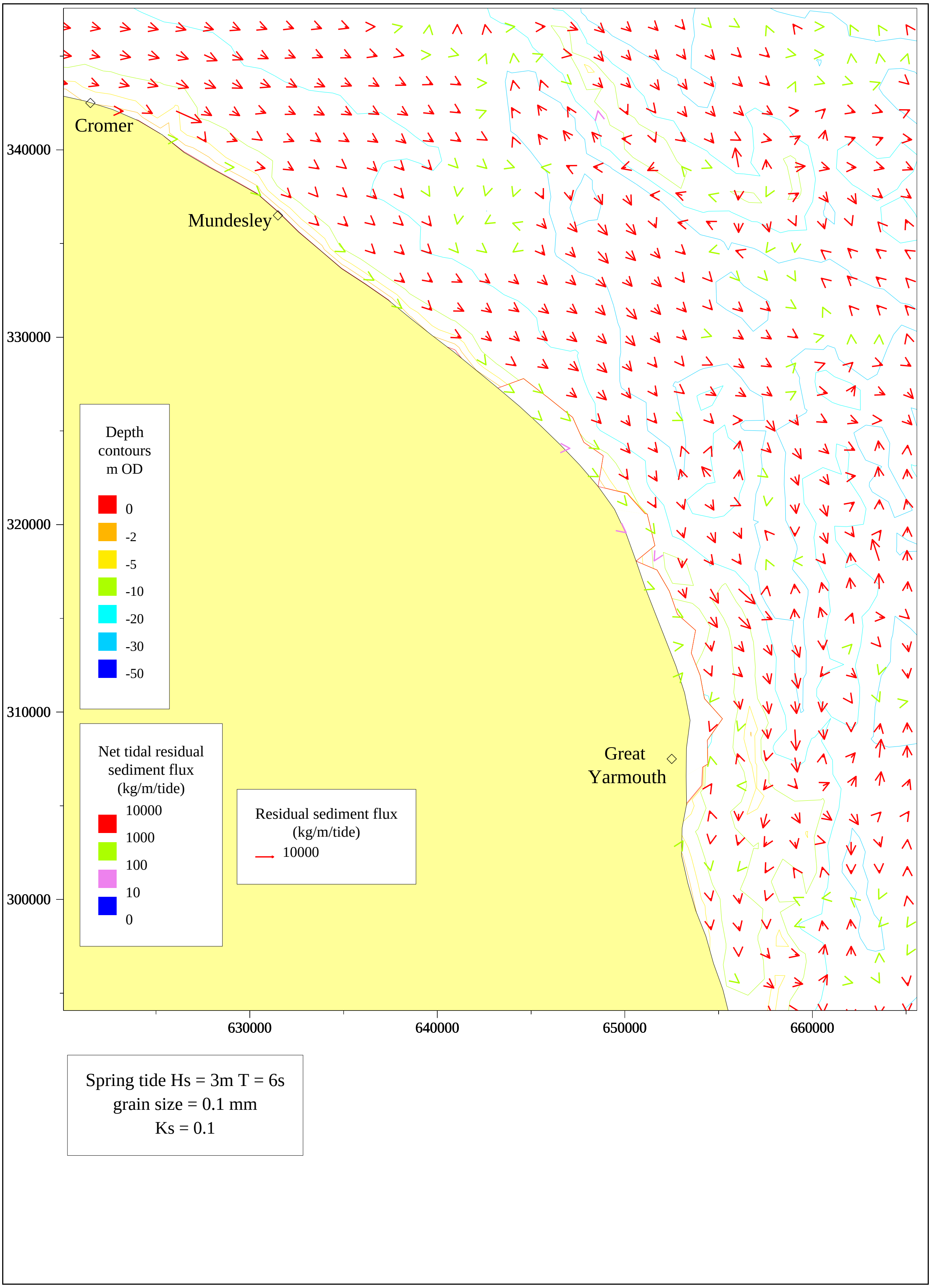

Figure 115 Spring tide with 3m 6s storm waves net sediment flux patterns (0.1mm sand) detail: East Norfolk

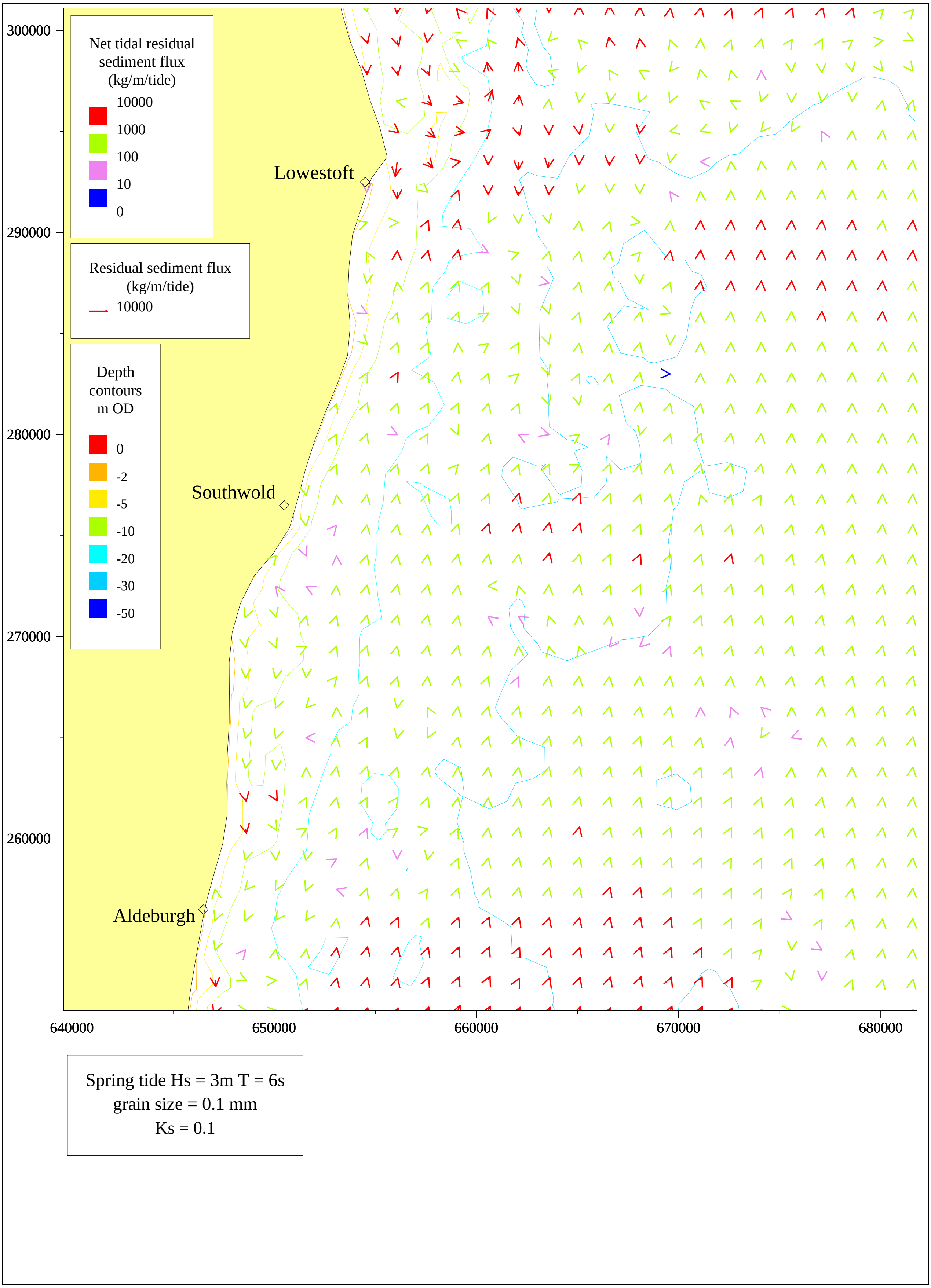

Figure 116 **Spring tide with 3m 6s storm waves net sediment flux patterns (0.1mm sand) detail: North Suffolk**

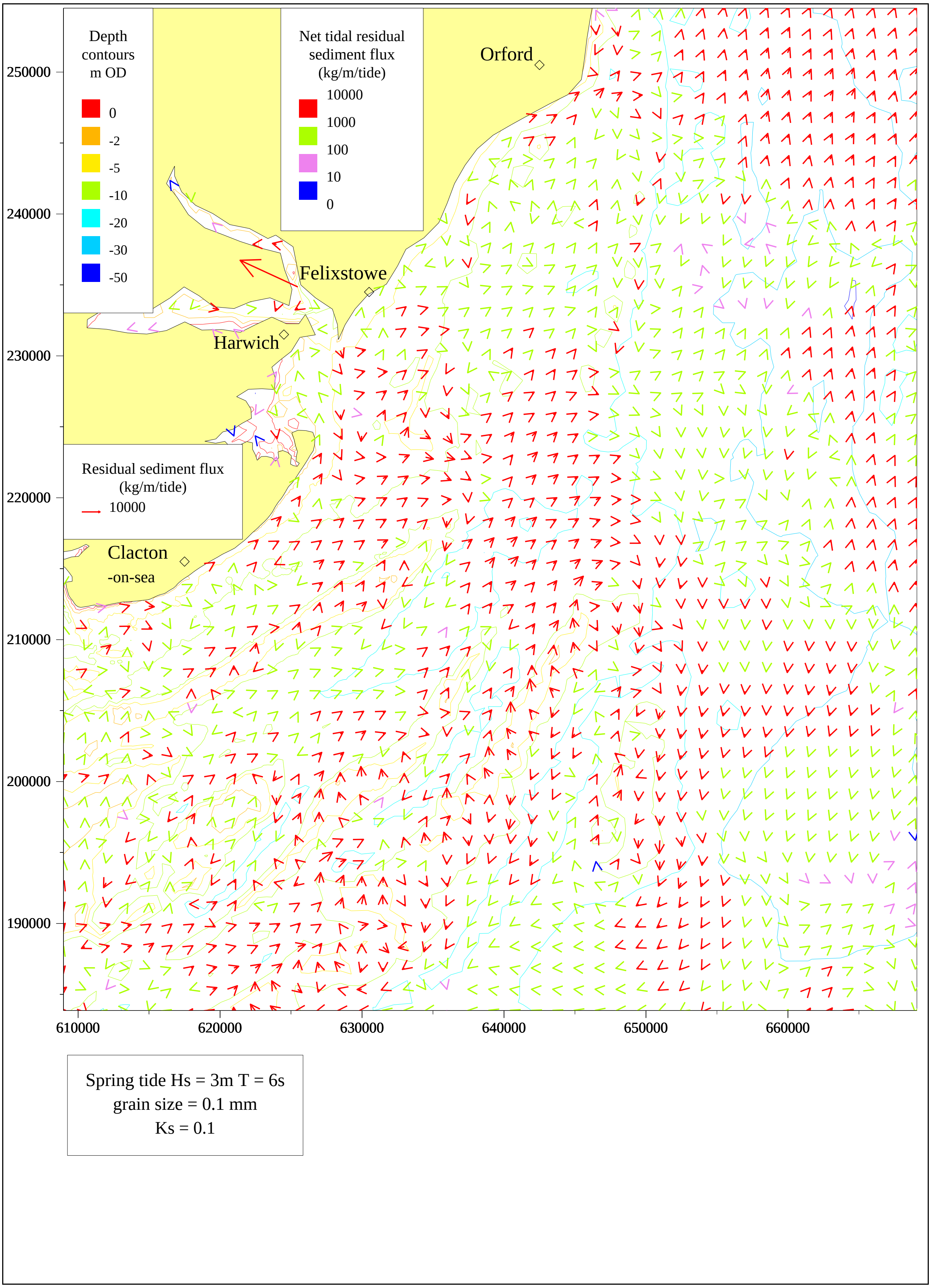

Figure 117 **Spring tide with 3m 6s storm waves net sediment flux patterns (0.1mm sand) detail: Suffolk and Essex**

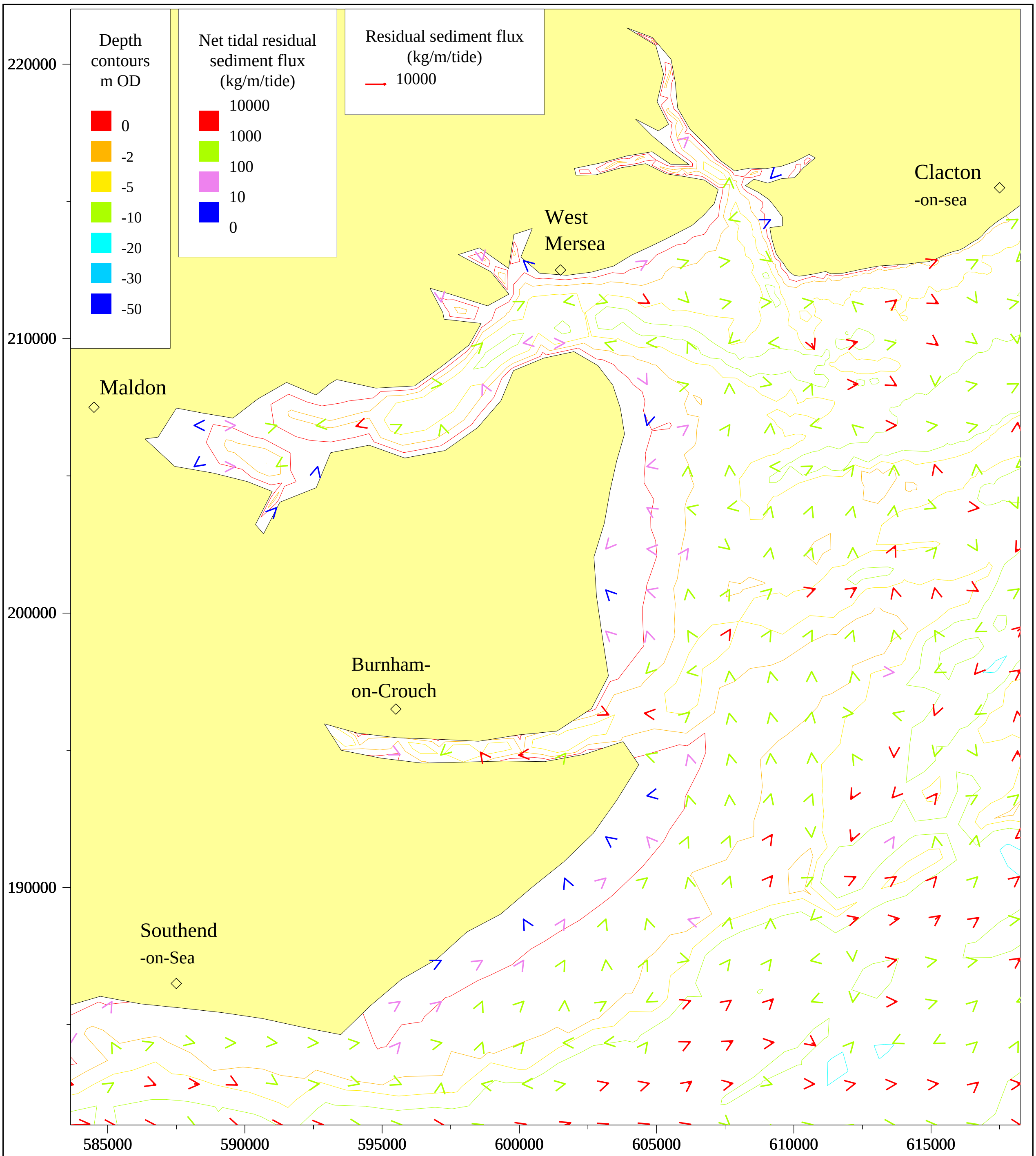

Spring tide Hs = 3m T = 6s
grain size = 0.1 mm
Ks = 0.1

Figure 118 **Spring tide with 3m 6s storm waves net sediment flux patterns (0.1mm sand) detail: South Essex**

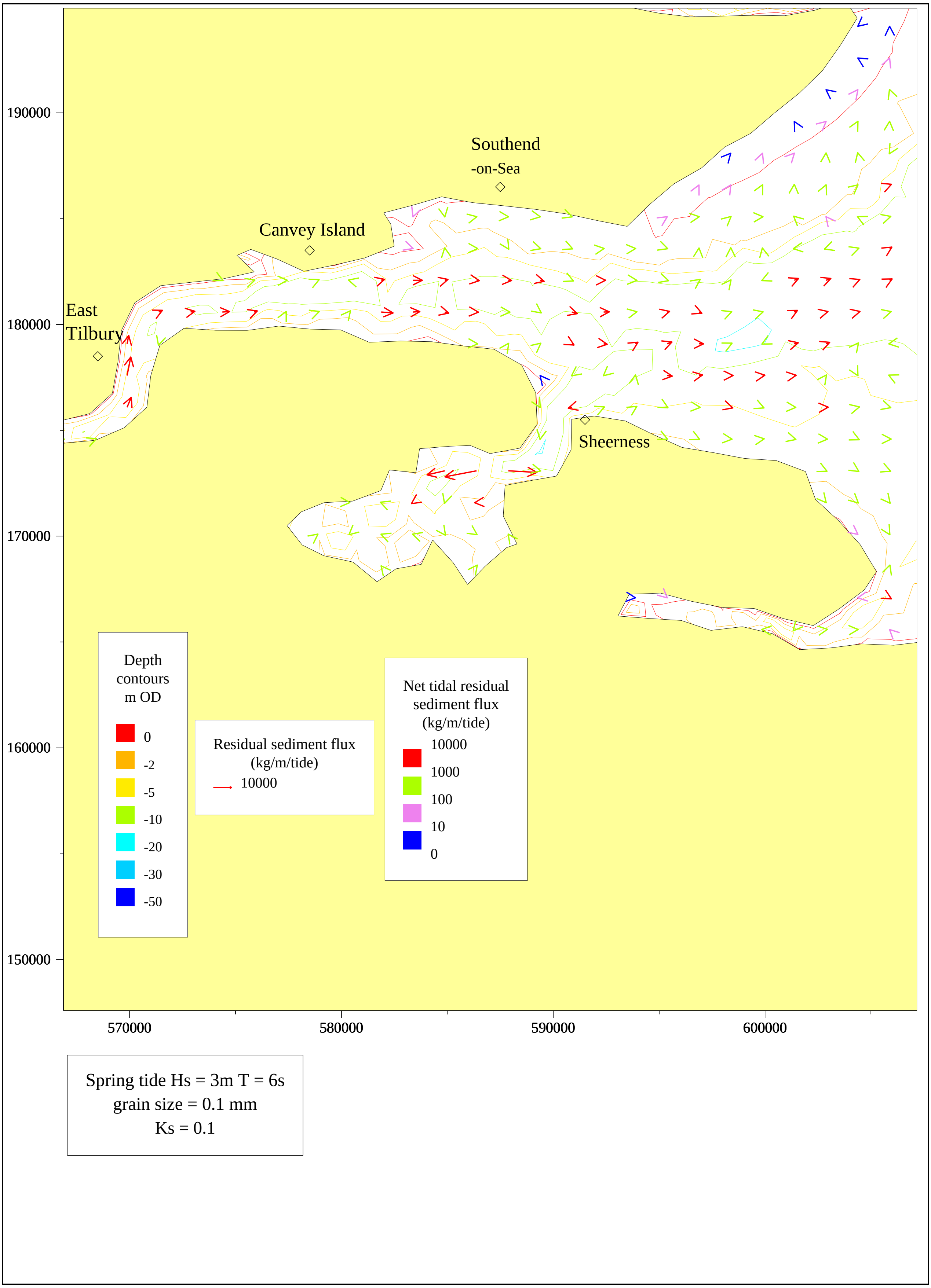

Figure 119 Spring tide with 3m 6s storm waves net sediment flux patterns (0.1mm sand) detail: Outer Thames

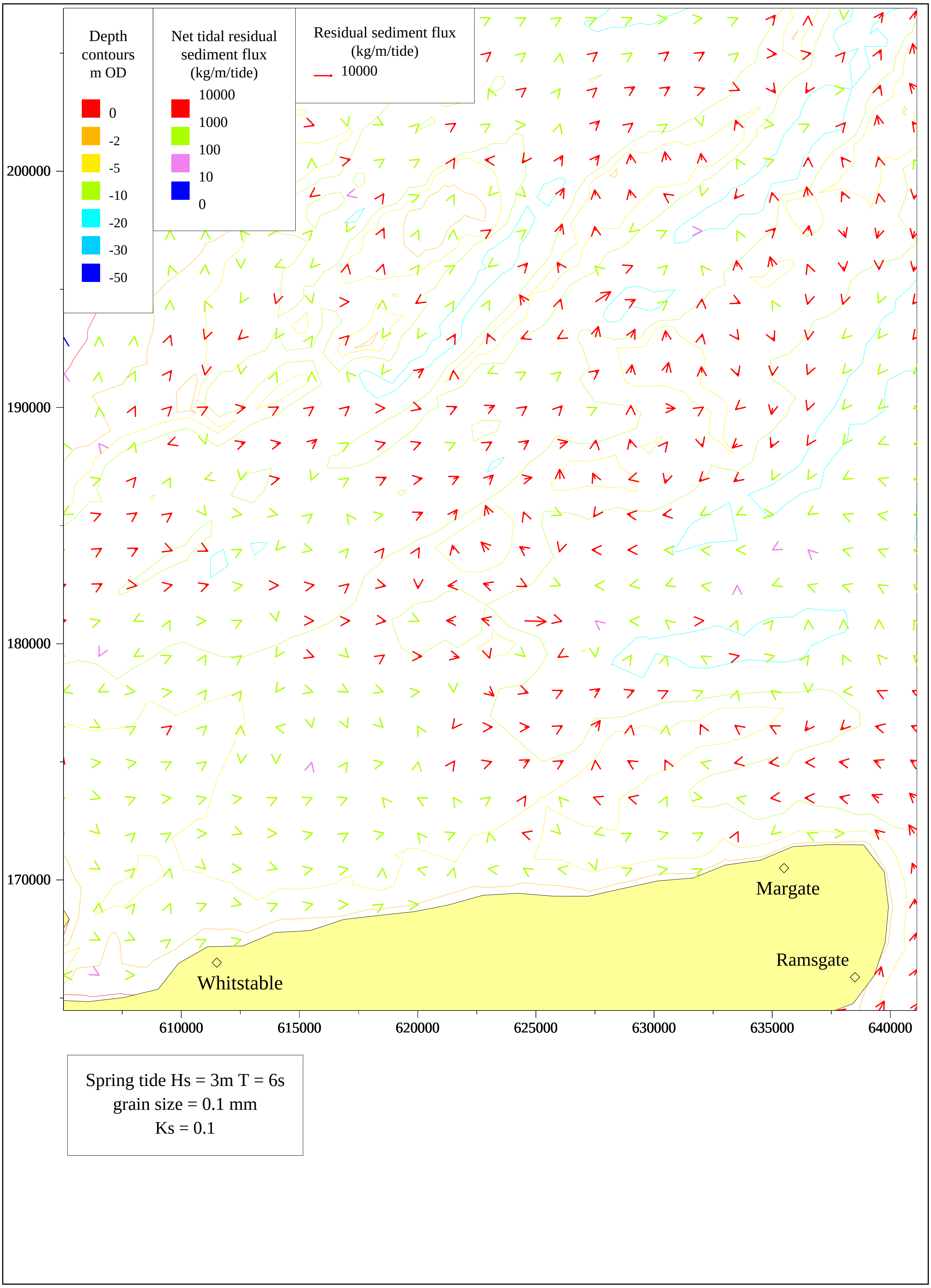

Figure 120 **Spring tide with 3m 6s storm waves net sediment flux patterns (0.1mm sand) detail: North Kent**

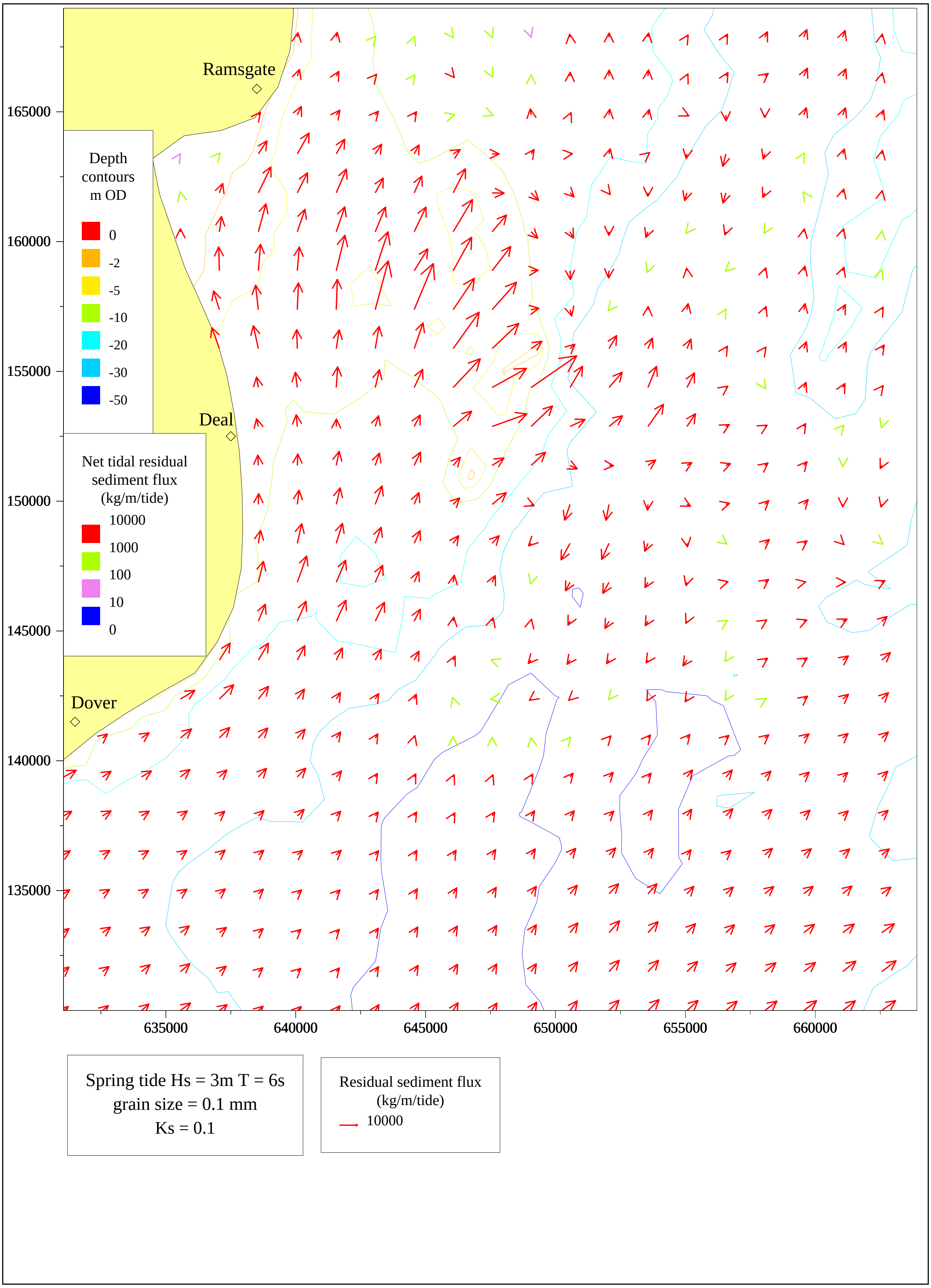

Figure 121 Spring tide with 3m 6s storm waves net sediment flux patterns (0.1mm sand) detail: East Kent

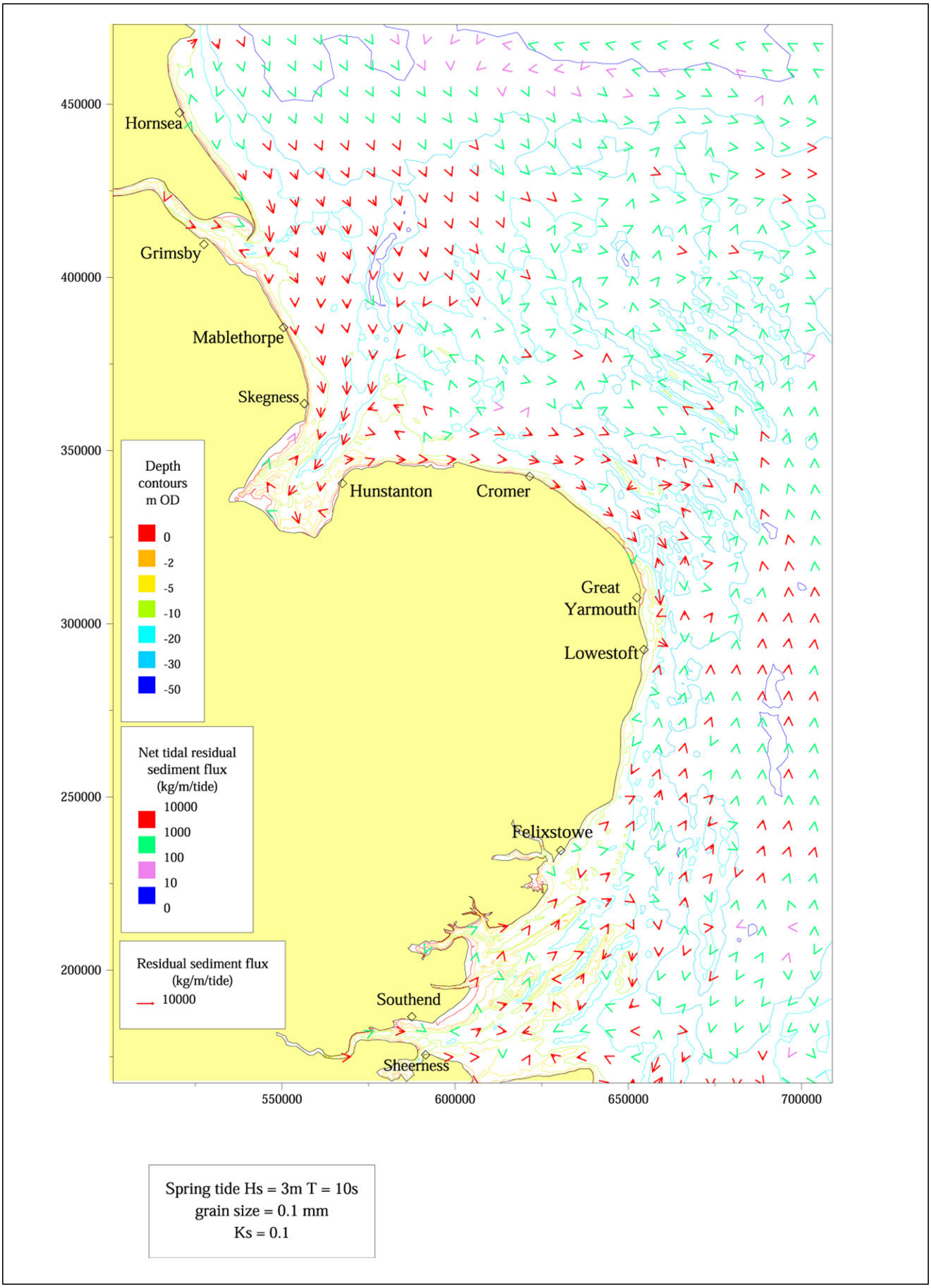

Figure 122 Spring tide with 3m 10s storm waves net sediment flux patterns (0.1mm sand)

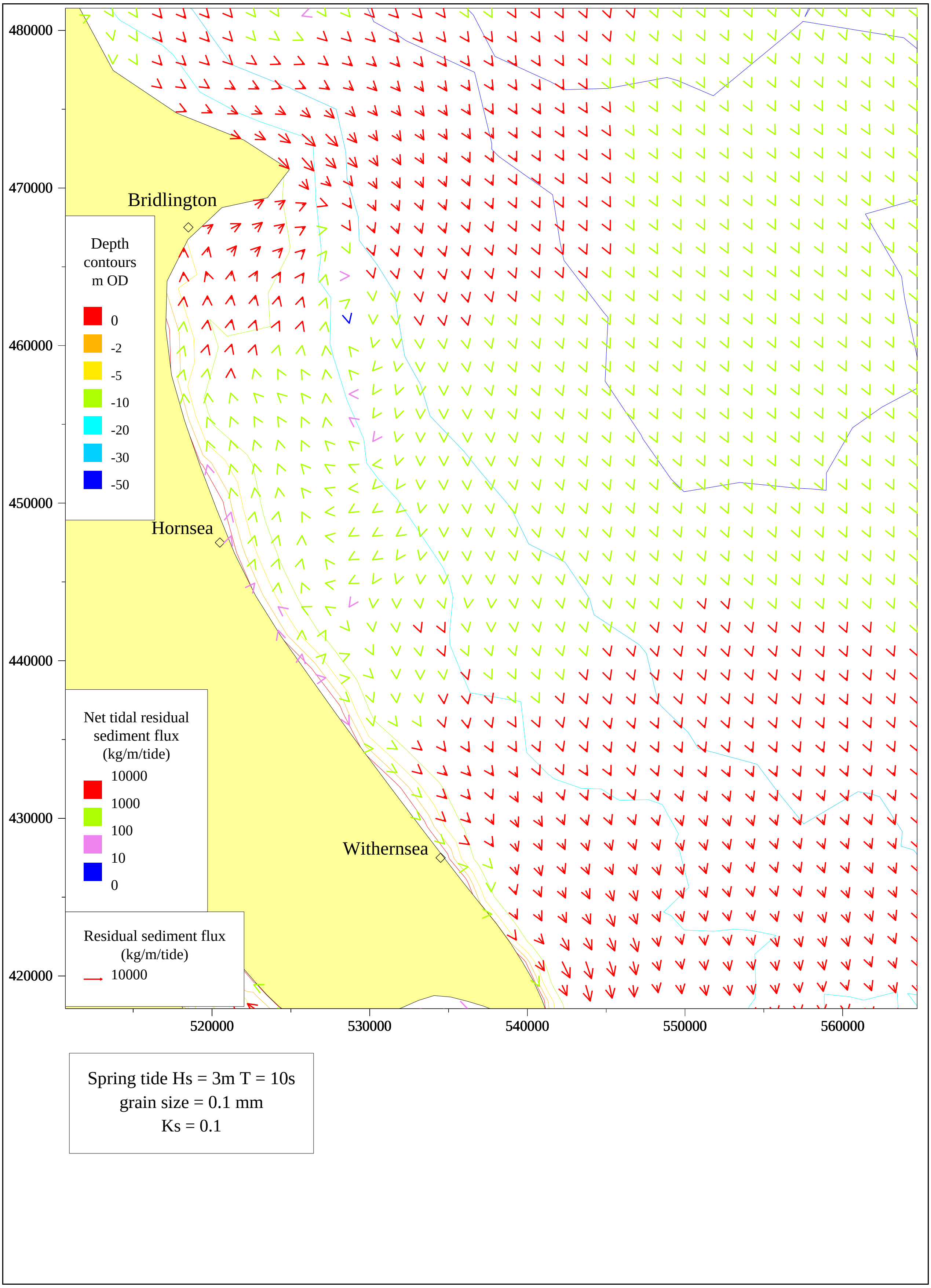

Figure 123 **Spring tide with 3m 10s storm waves net sediment flux patterns (0.1mm sand) detail: Flamborough Head to the Humber**

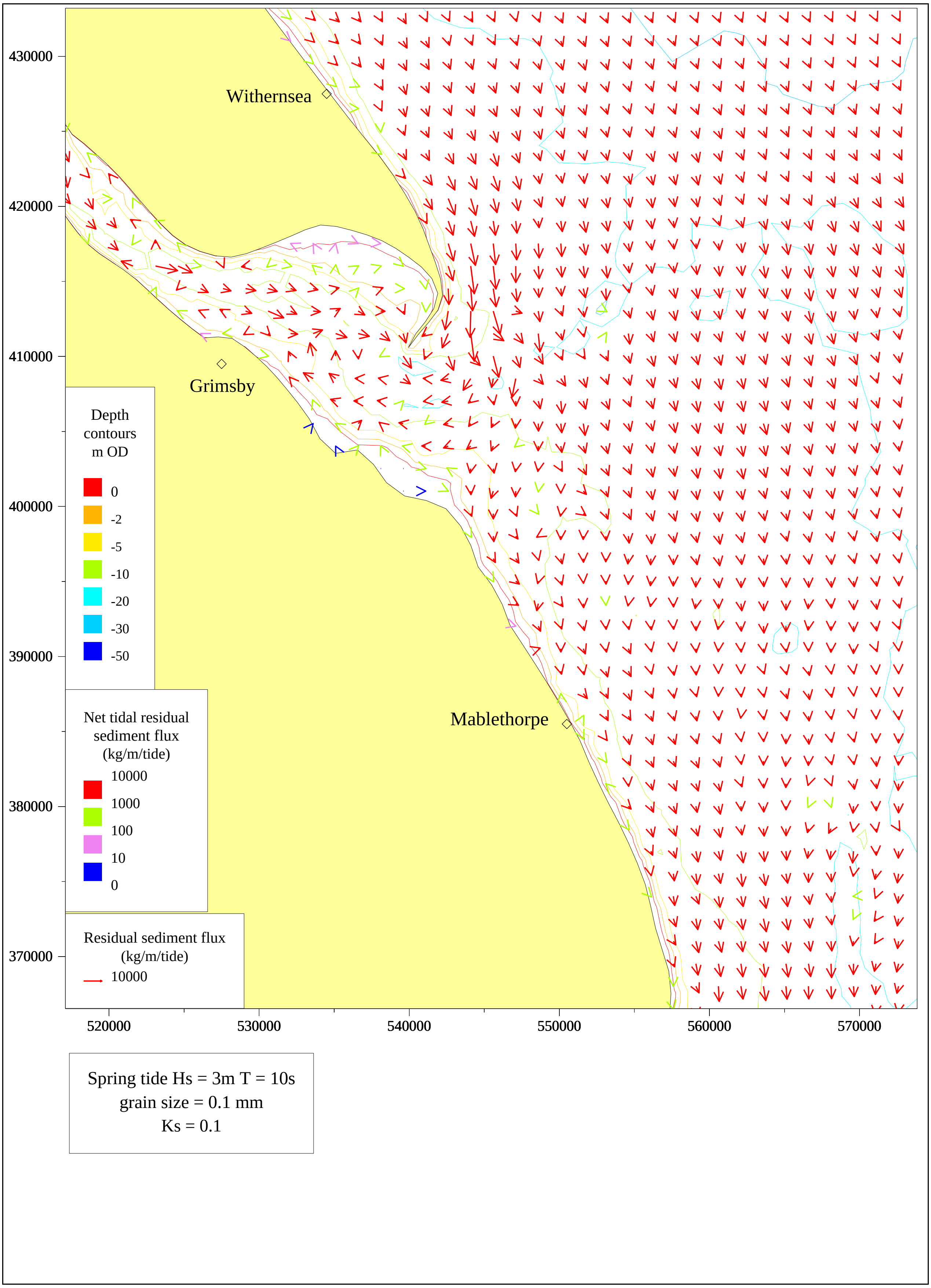

Figure 124 Spring tide with 3m 10s storm waves net sediment flux patterns (0.1mm sand) detail: Humber Entrance and Lincolnshire

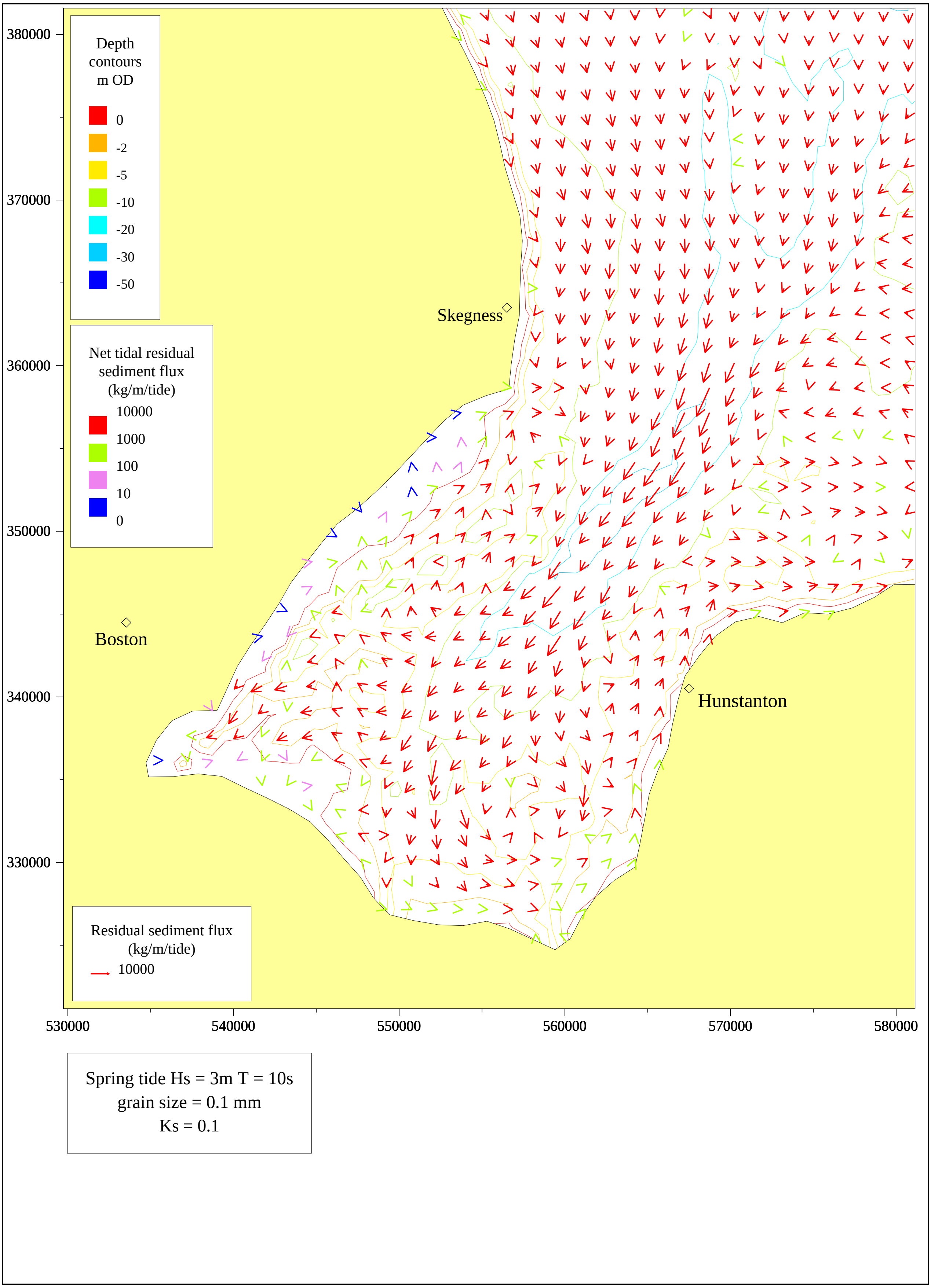

Figure 125 **Spring tide with 3m 10s storm waves net sediment flux patterns (0.1mm sand) detail Lincolnshire and the Wash**

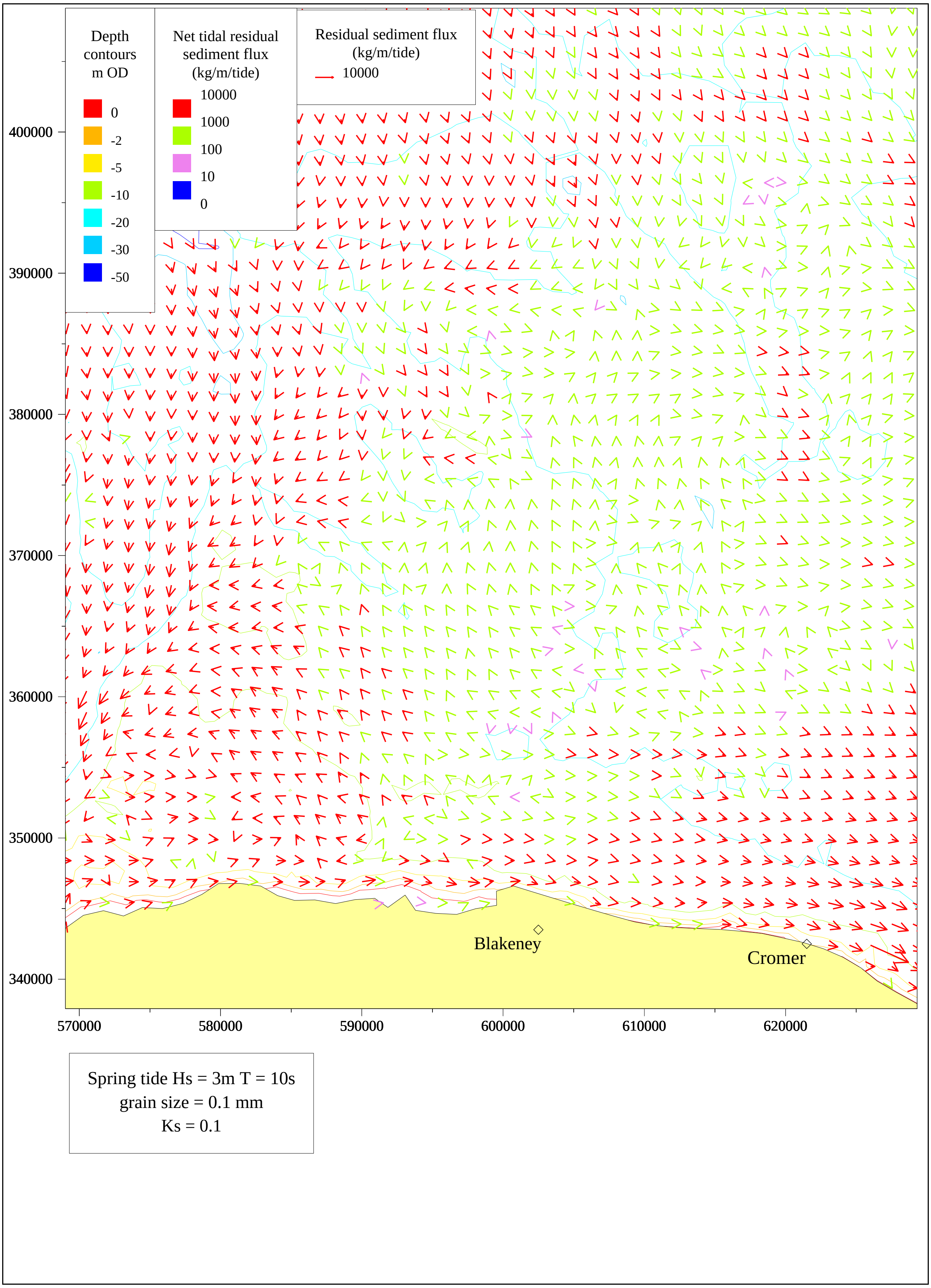

Figure 126 Spring tide with 3m 10s storm waves net sediment flux patterns (0.1mm sand) detail: North Norfolk

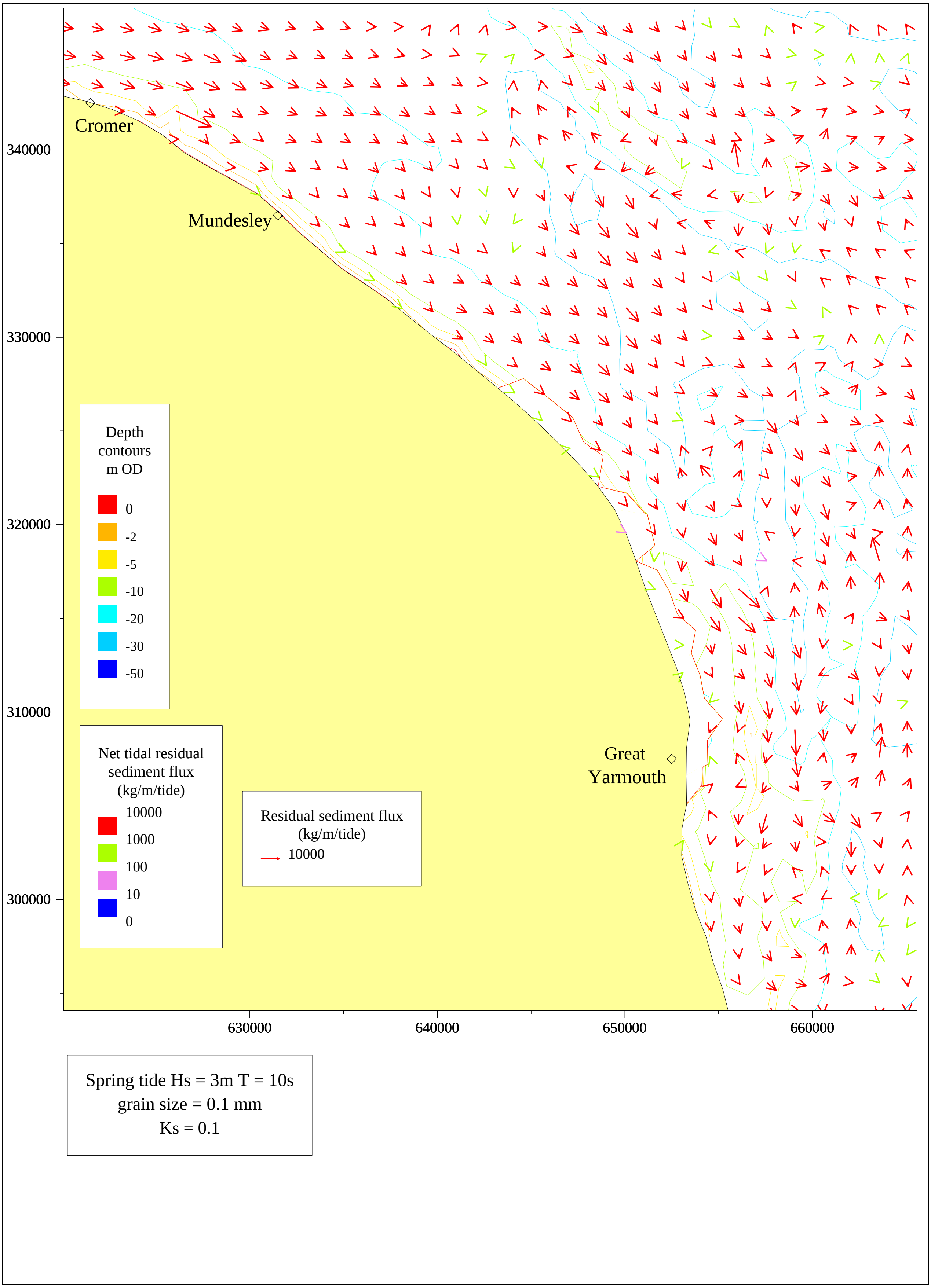

Figure 127 **Spring tide with 3m 10s storm waves net sediment flux patterns (0.1mm sand) detail: NEast Anglia**

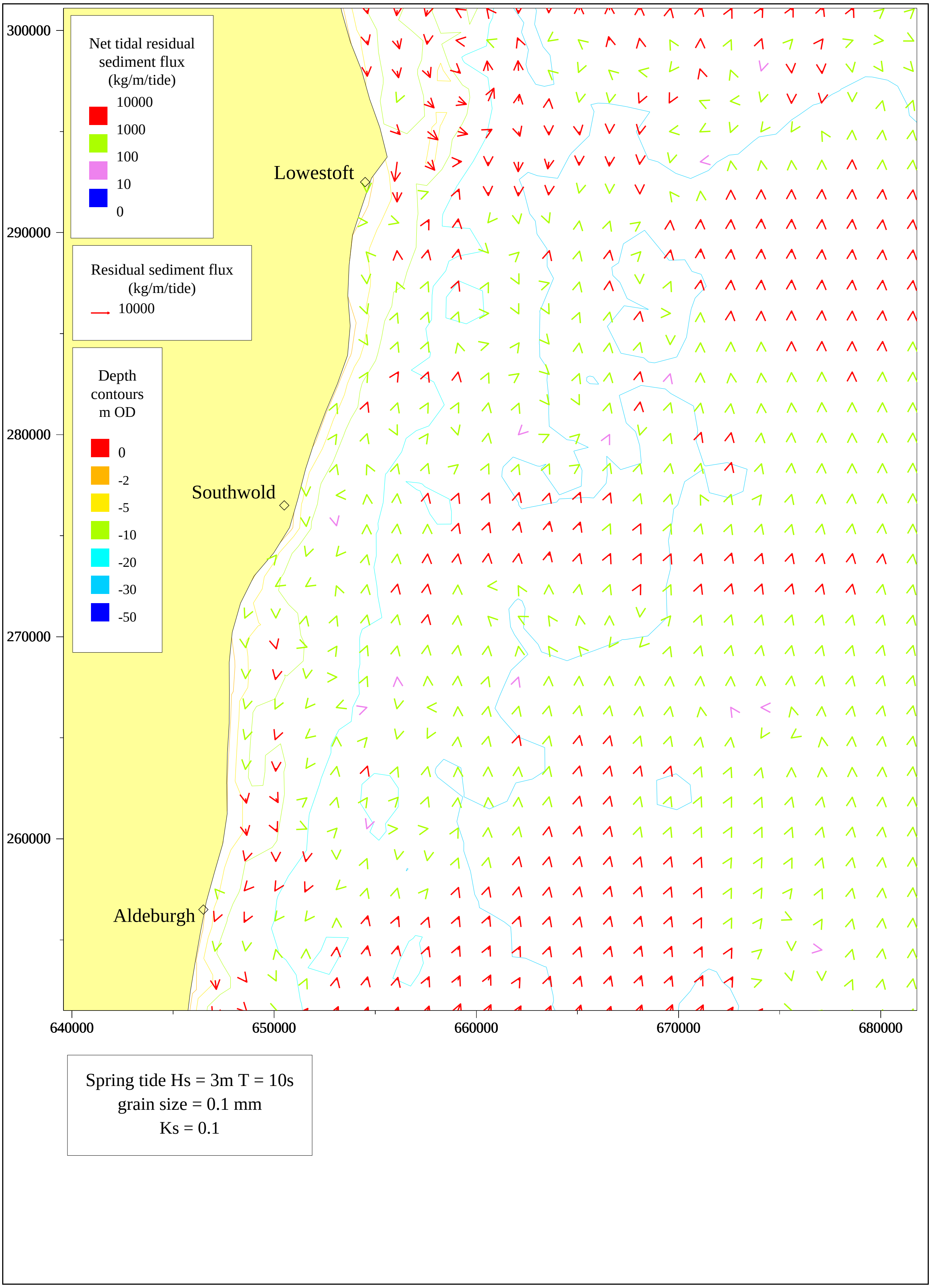

Figure 128 **Spring tide with 3m 10s storm waves net sediment flux patterns (0.1mm sand) detail: North Suffolk**

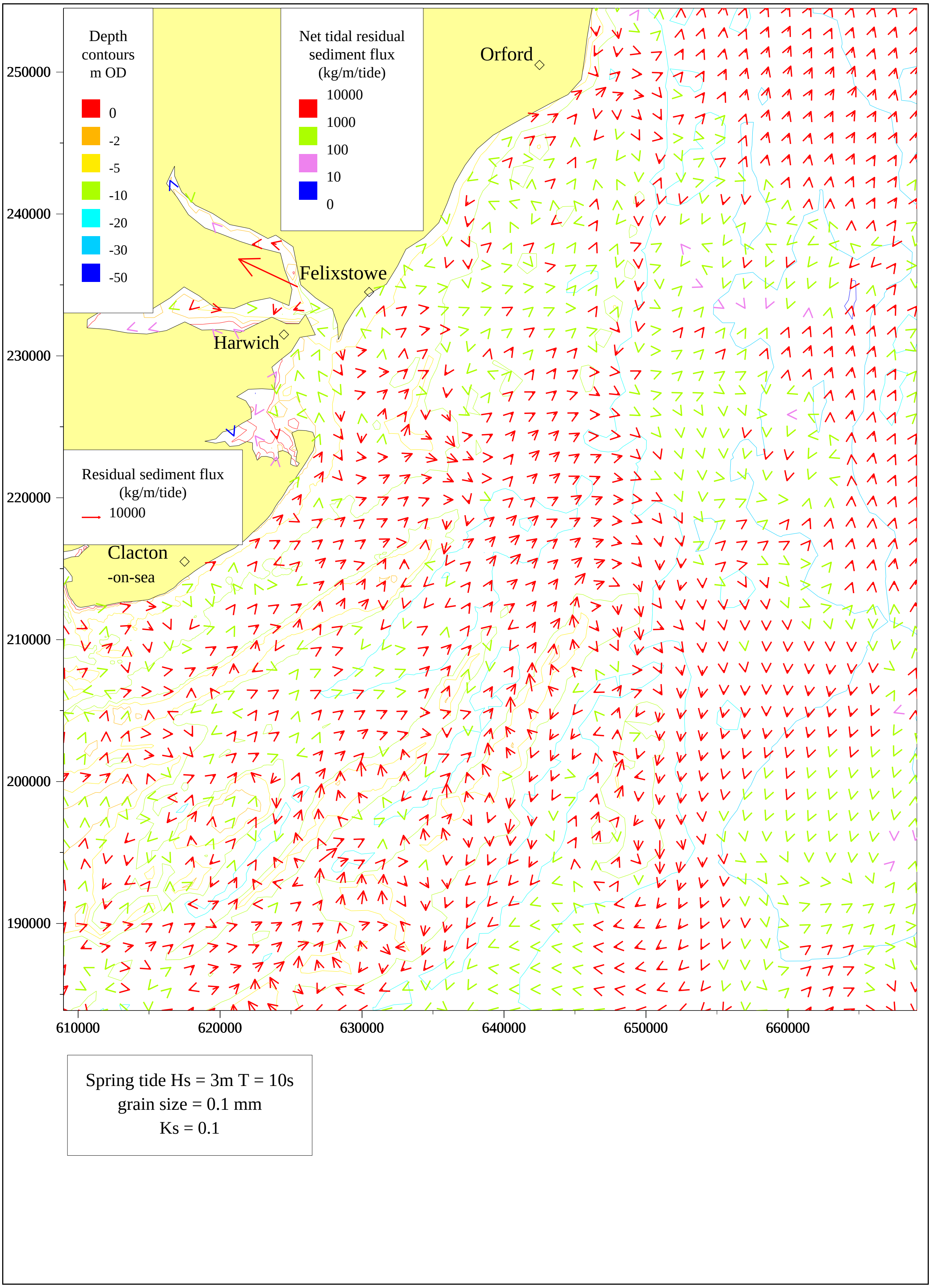

Figure 129 **Spring tide with 3m 10s storm waves net sediment flux patterns (0.1mm sand) detail: Suffolk and Essex**

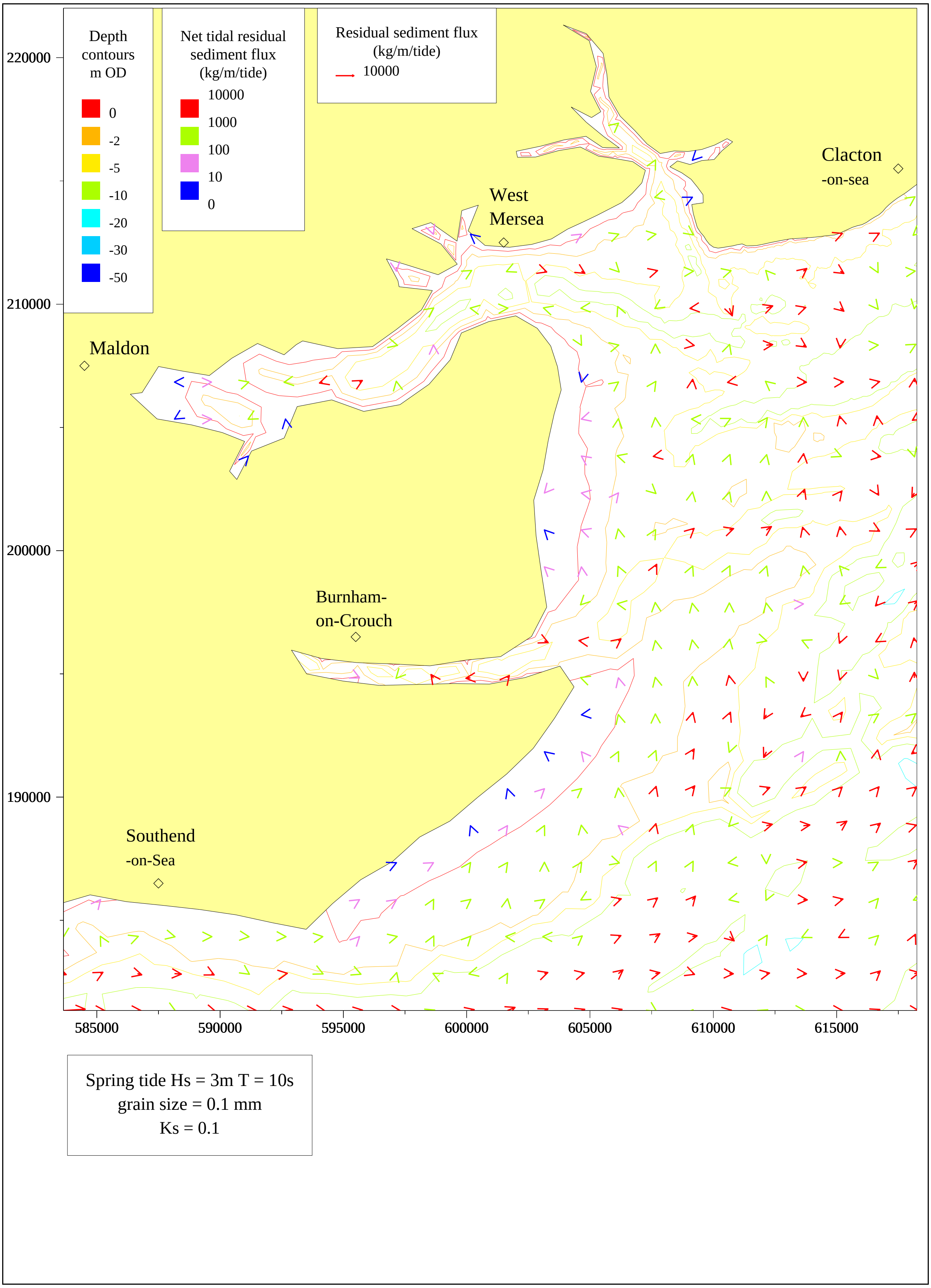

Figure 130 **Spring tide with 3m 10s storm waves net sediment flux patterns (0.1mm sand) detail: South Essex**

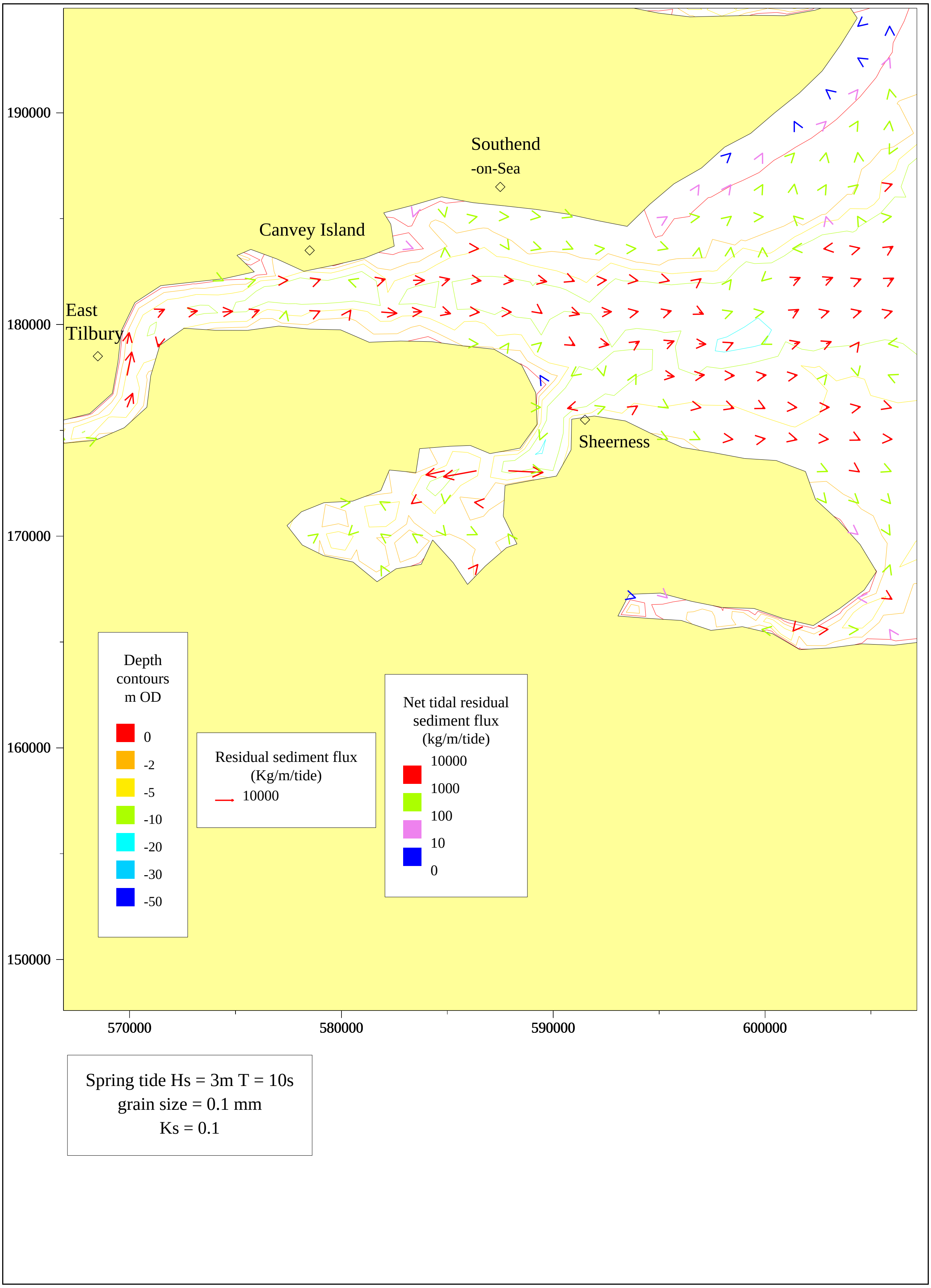

Figure 131 Spring tide with 3m 10s storm waves net sediment flux patterns (0.1mm sand) detail: Outer Thames

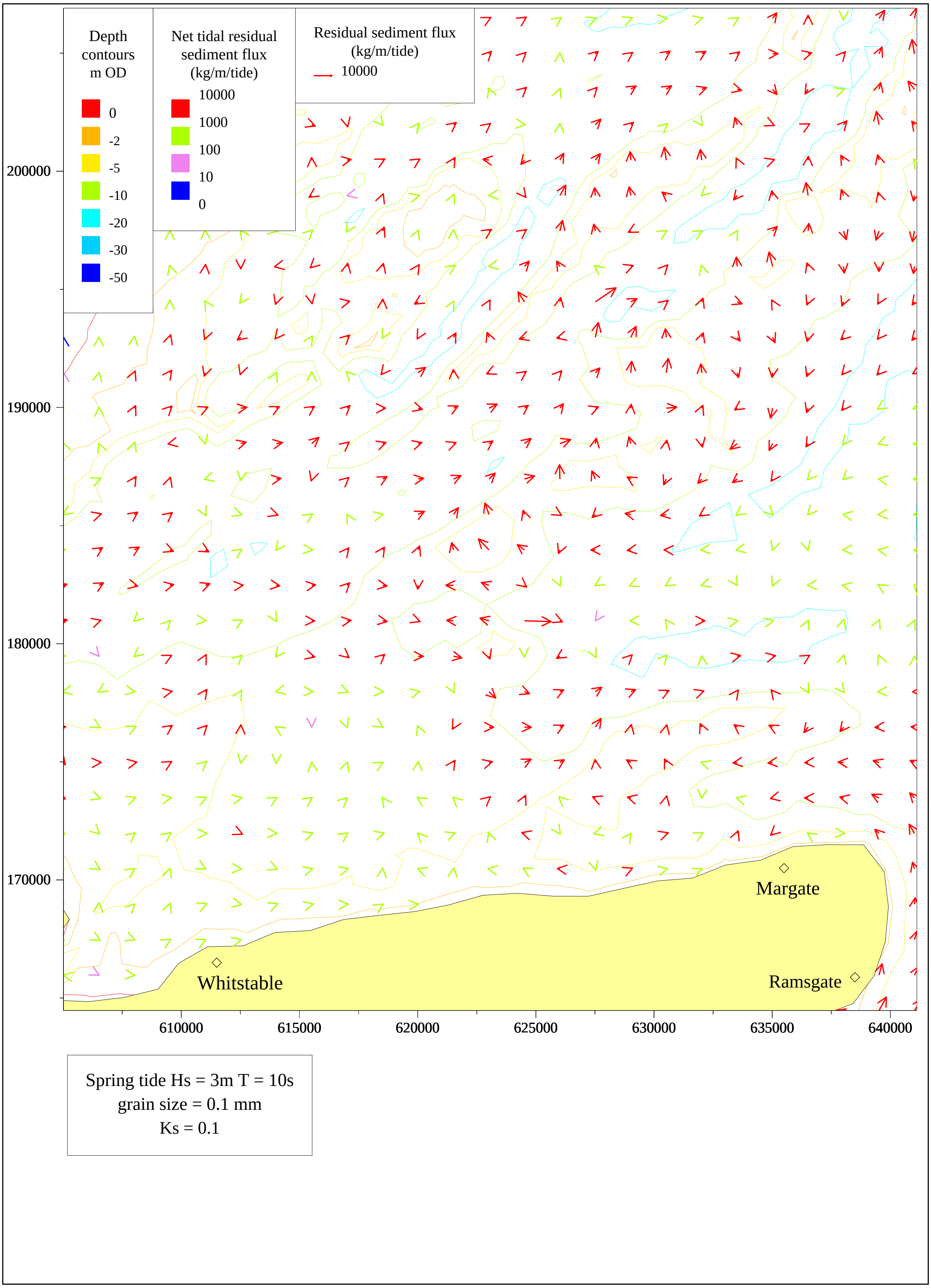

Figure 132 **Spring tide with 3m 10s storm waves net sediment flux patterns (0.1mm sand) detail: North Kent**

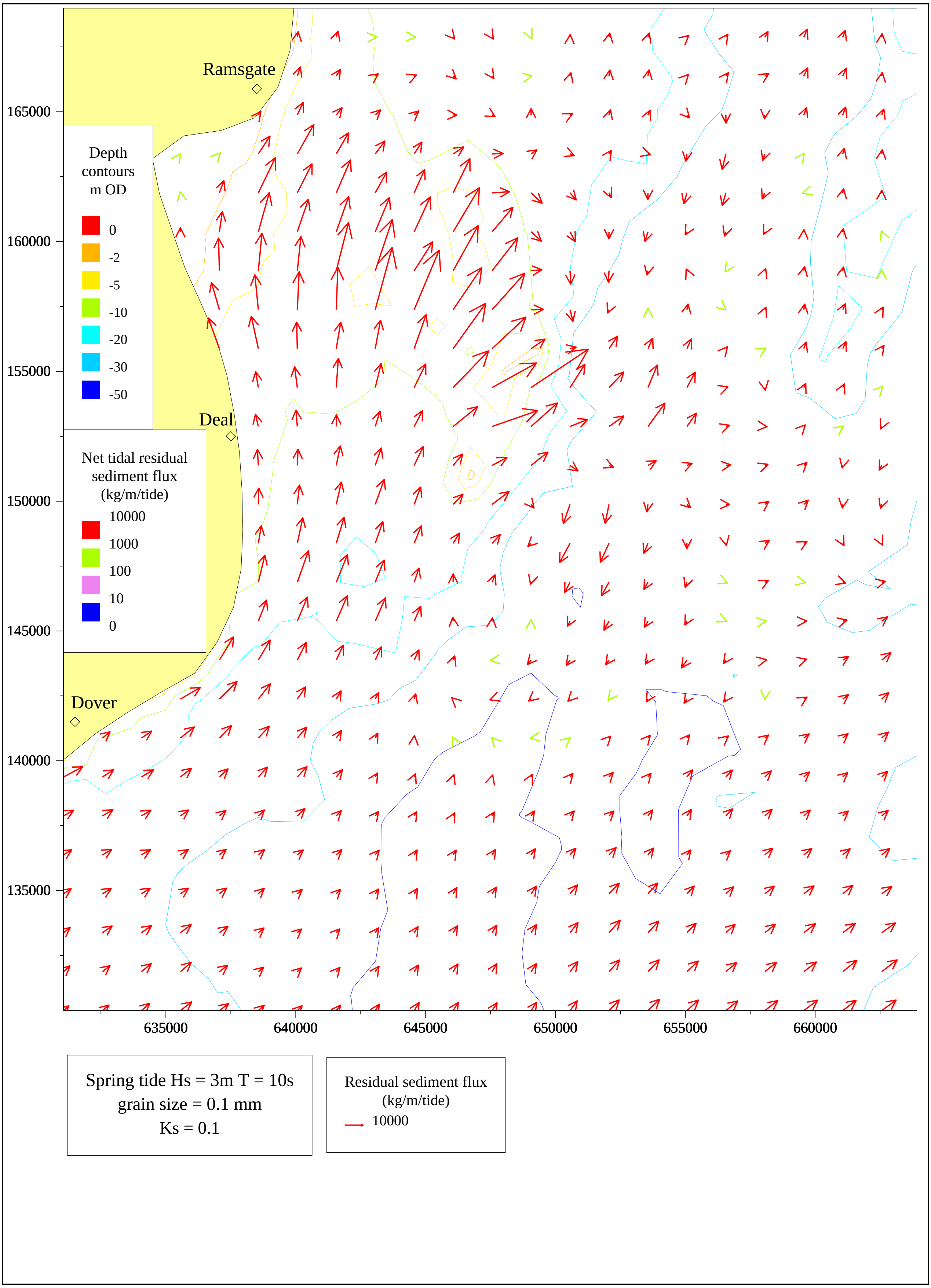

Figure 133 **Spring tide with 3m 10s storm waves net sediment flux patterns (0.1mm sand) detail: East Kent**

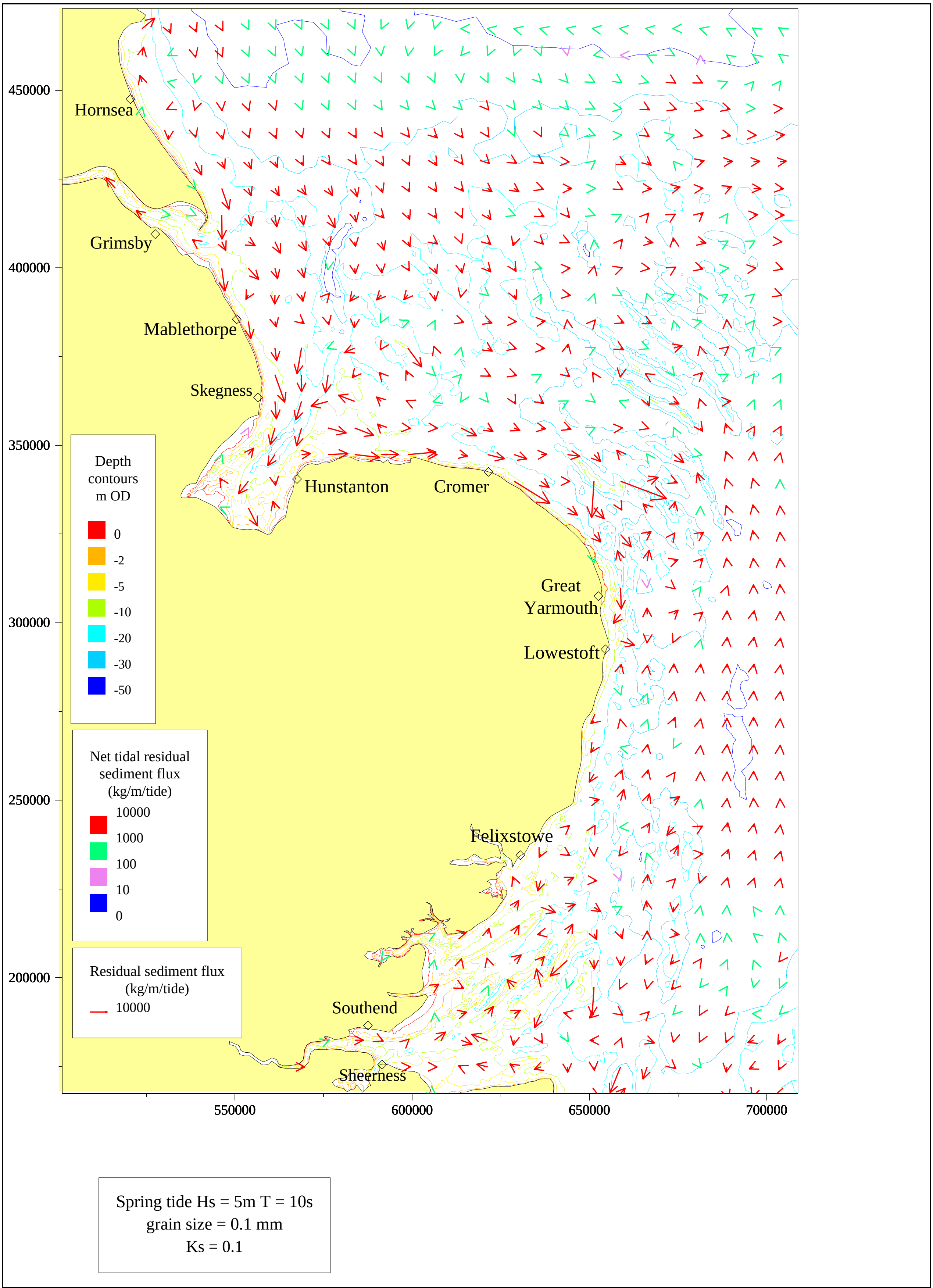

Figure 134 Spring tide with 5m 10s storm waves net sediment flux patterns (0.1mm sand)

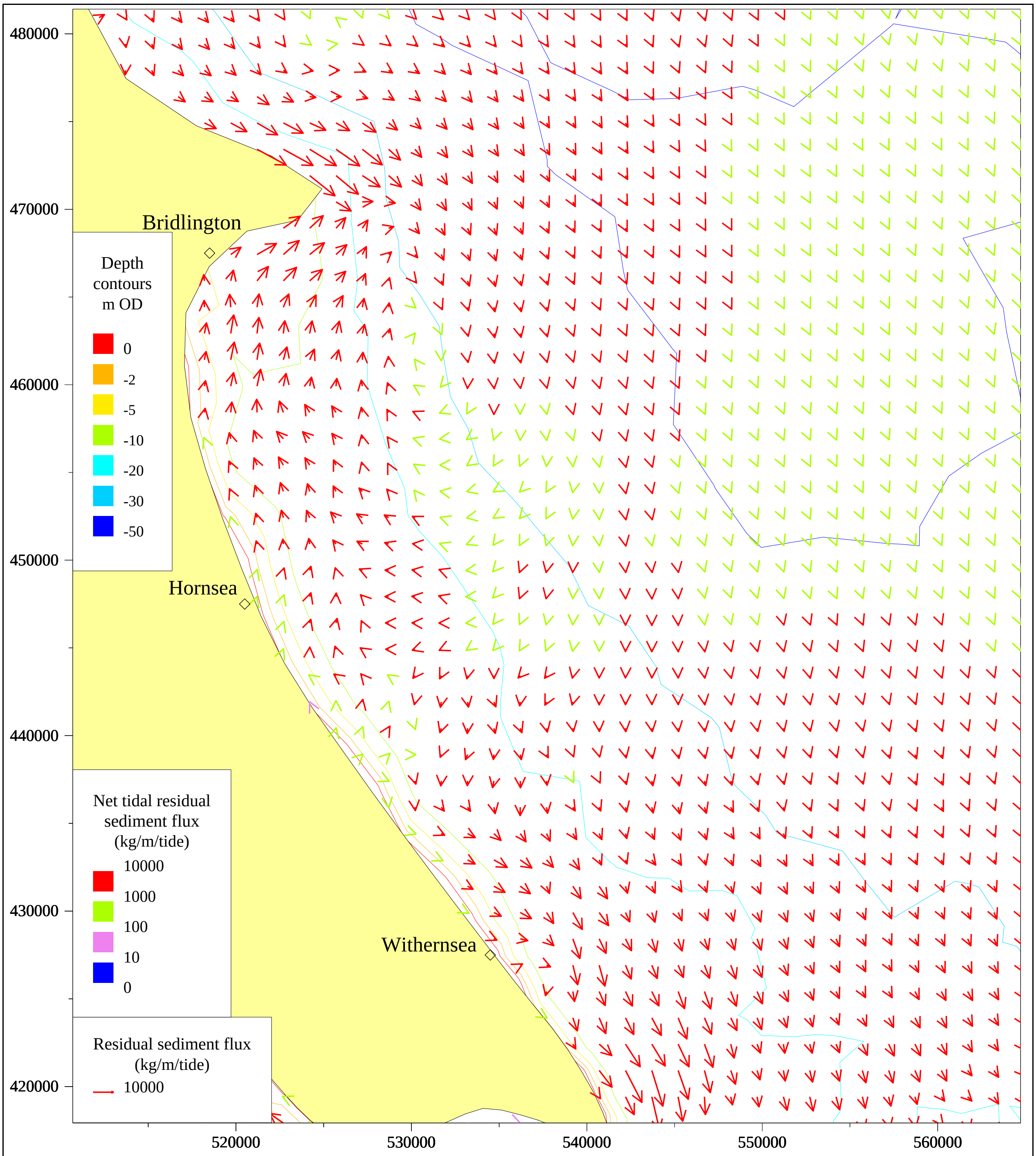

Spring tide Hs = 5m T = 10s
grain size = 0.1 mm
Ks = 0.1

Figure 135 Spring tide with 5m 10s storm waves net sediment flux patterns (0.1mm sand) detail: Flamborough Head to Humber

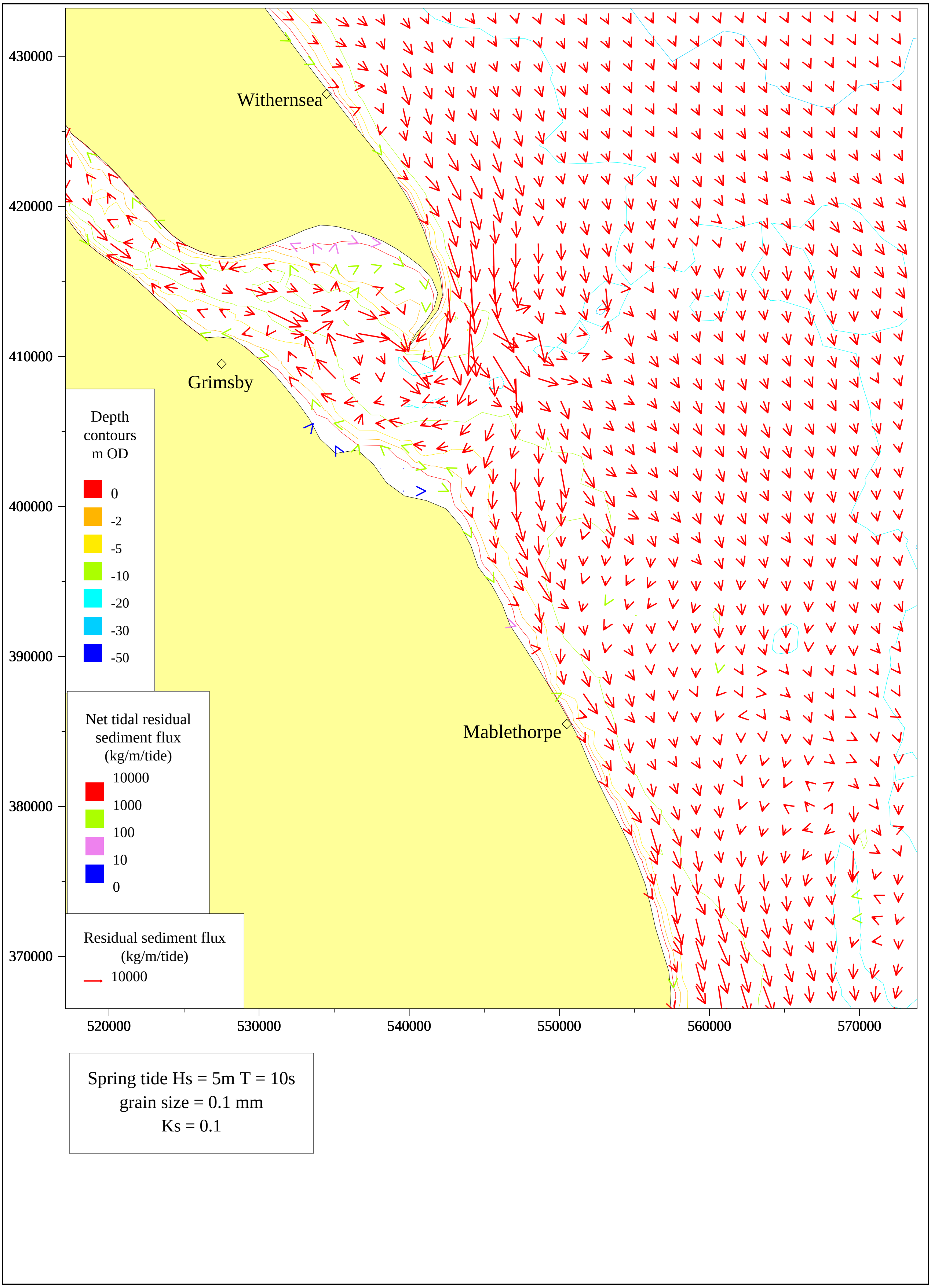

Figure 136 **Spring tide with 5m 10s storm waves net sediment flux patterns (0.1mm sand) detail: Humber Entrance and Lincolnshire**

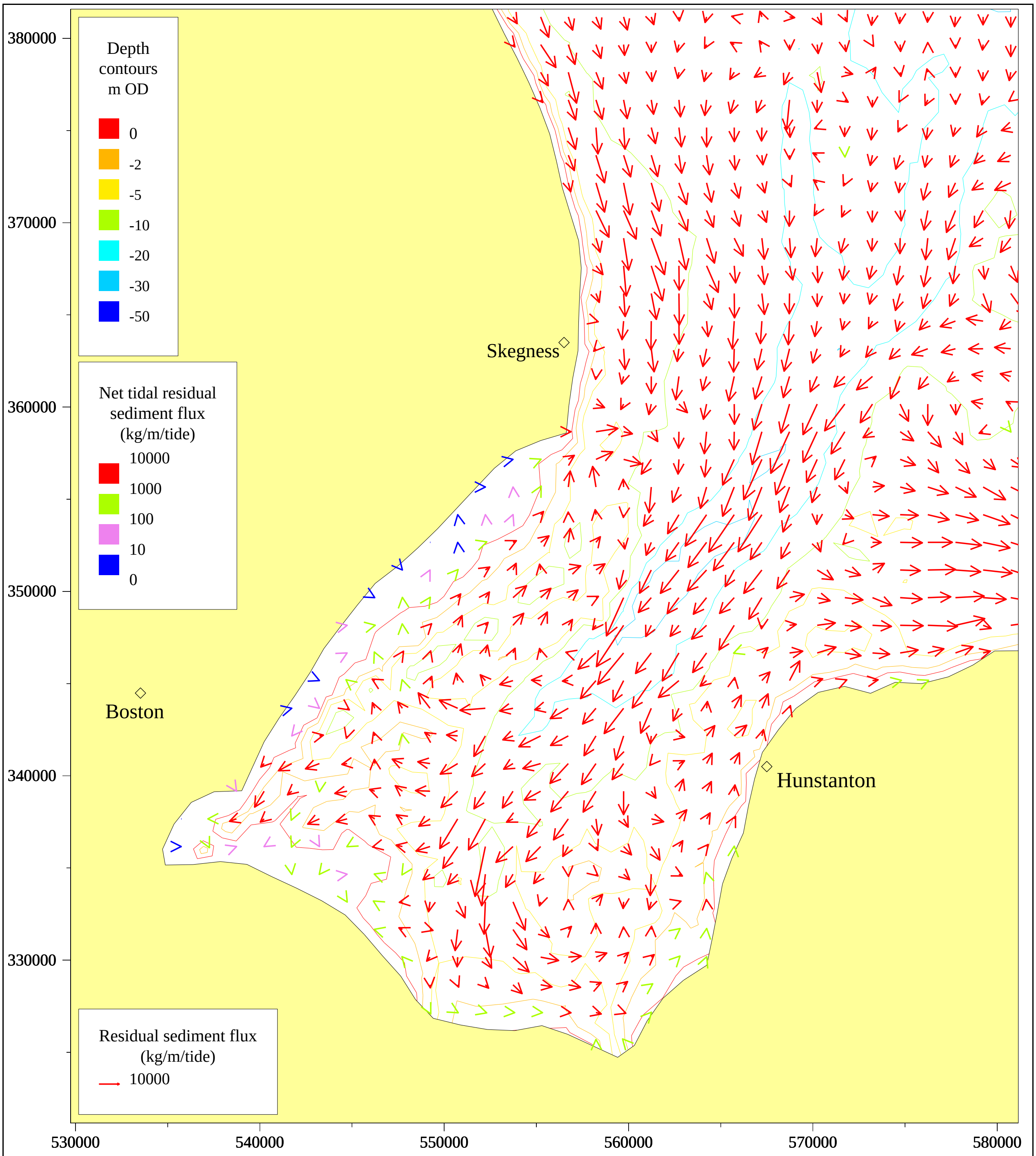

Spring tide Hs = 5m T = 10s
grain size = 0.1 mm
Ks = 0.1

Figure 137 **Spring tide with 5m 10s storm waves net sediment flux patterns (0.1mm sand) detail Lincolnshire and the Wash**

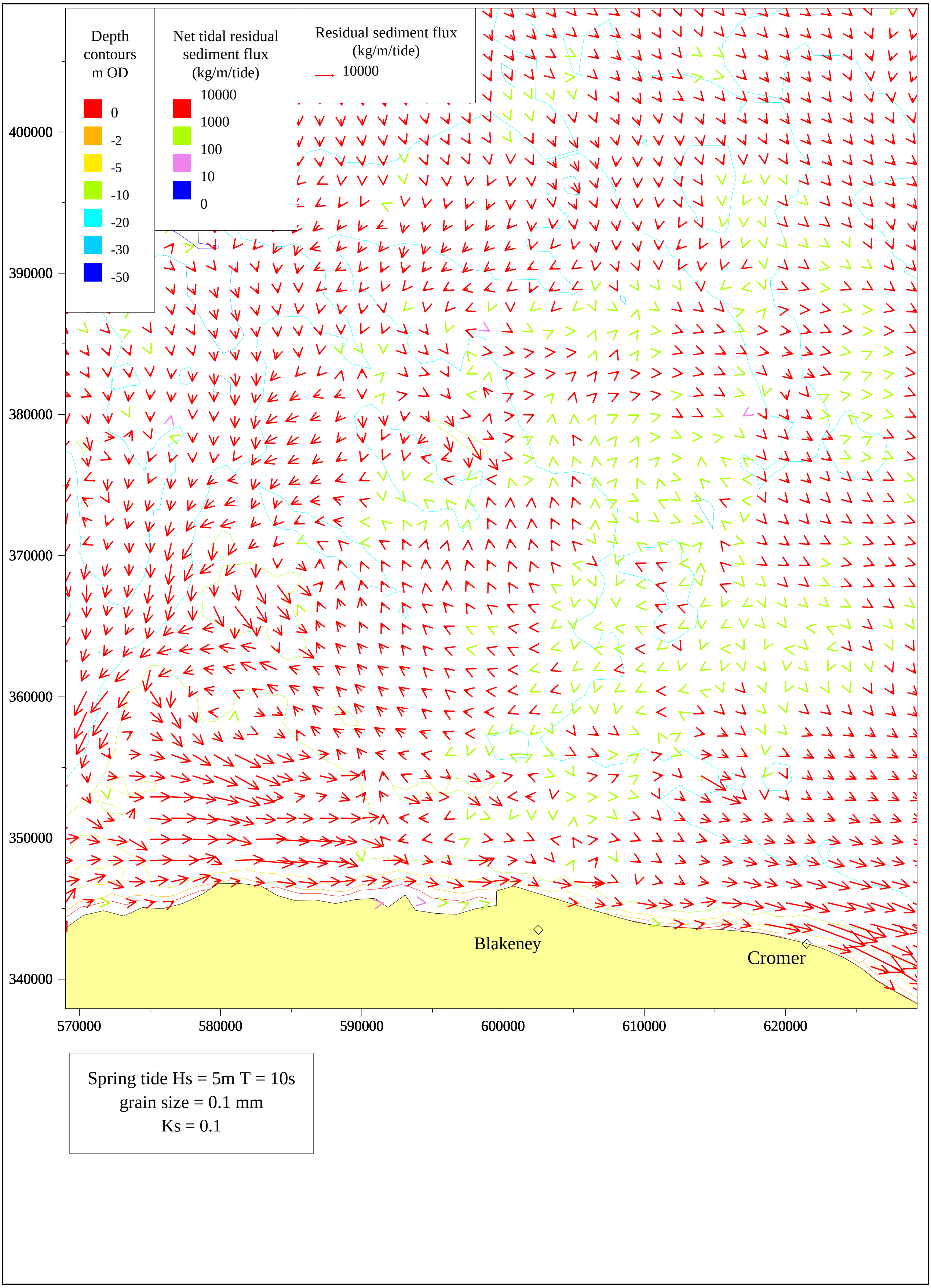

Figure 138 Spring tide with 5m 10s storm waves net sediment flux patterns (0.1mm sand) detail: North Norfolk

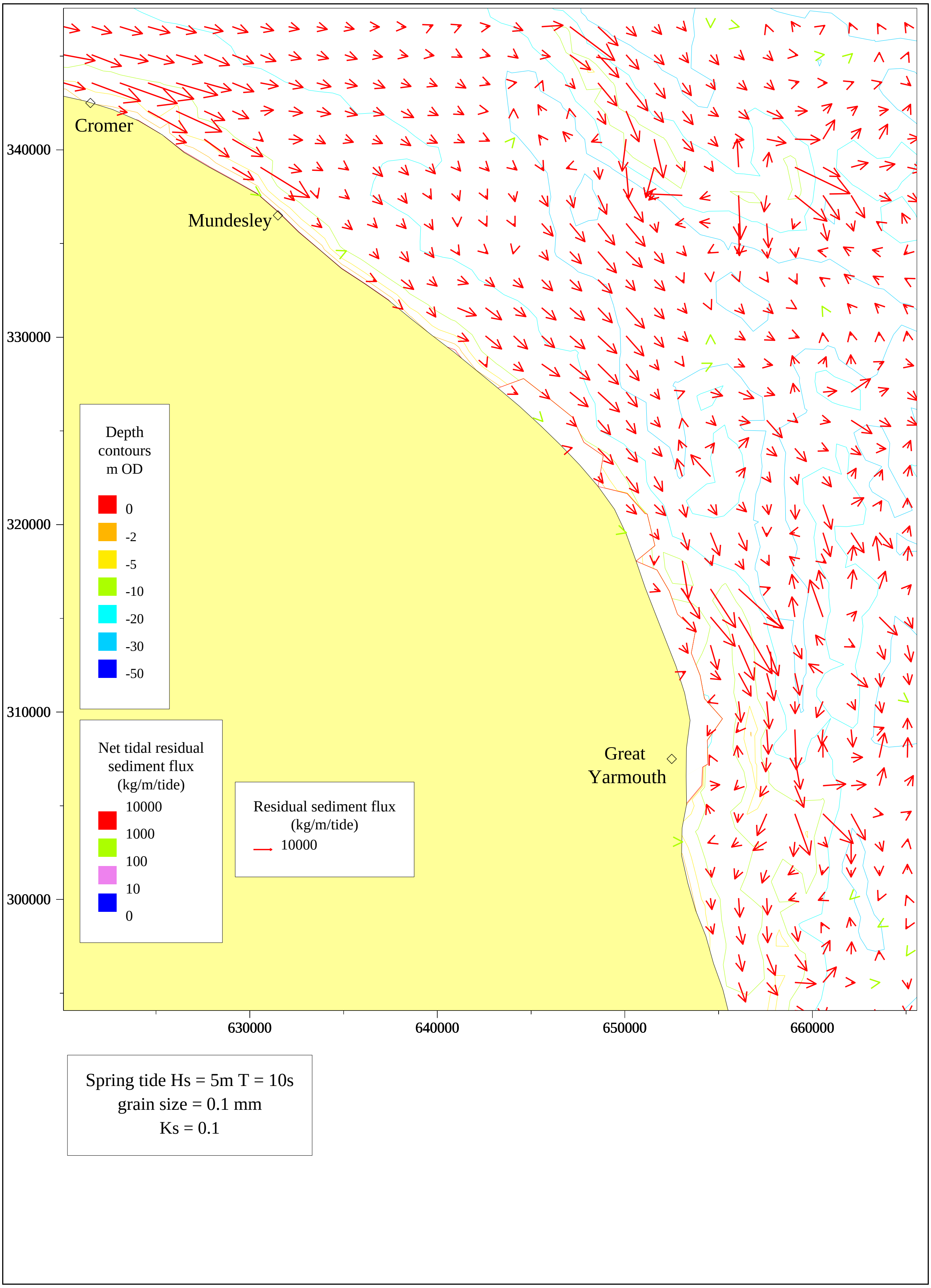

Figure 139 **Spring tide with 5m 10s storm waves net sediment flux patterns (0.1mm sand) detail: East Norfolk**

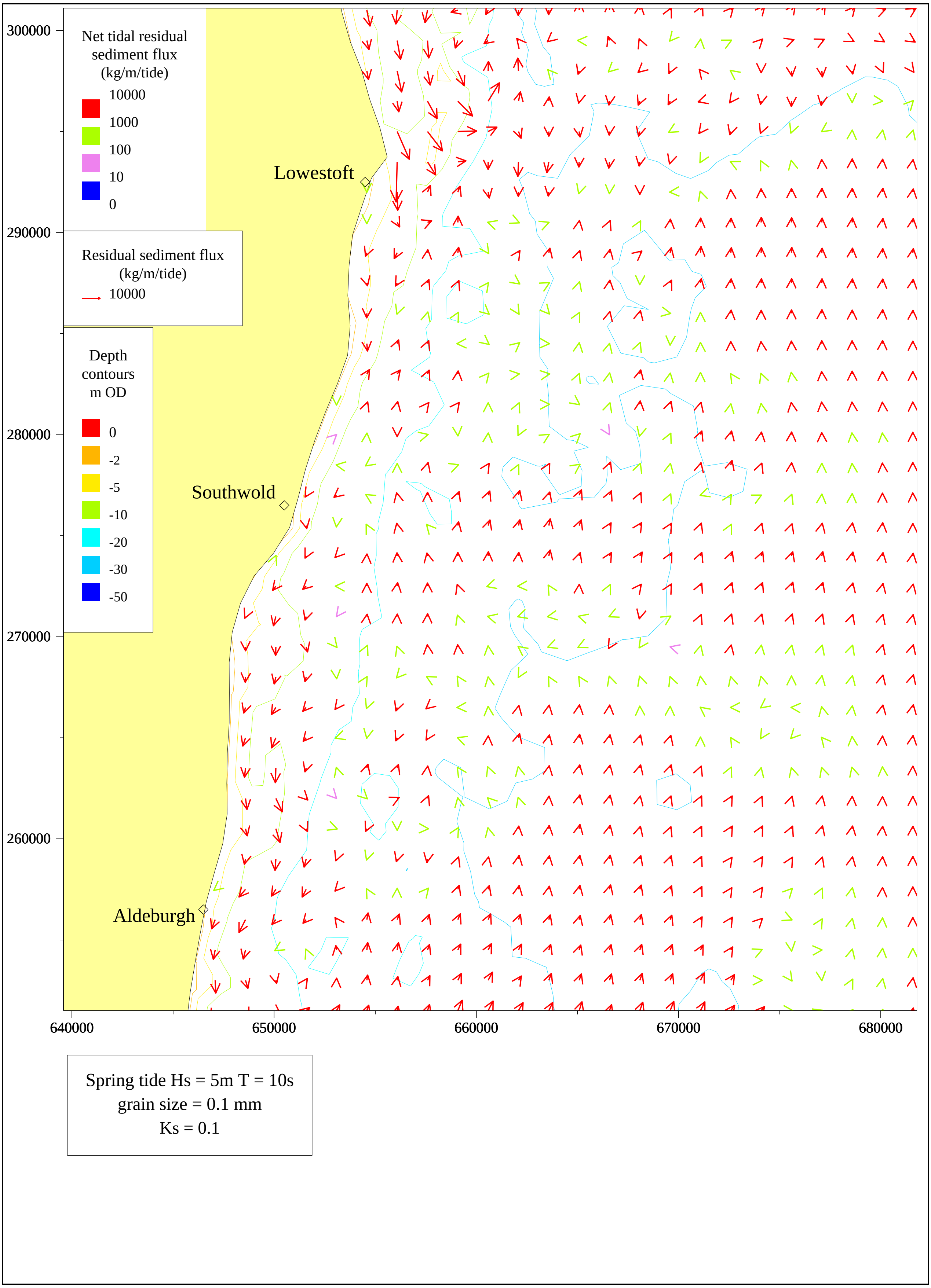

Figure 140 **Spring tide with 5m 10s storm waves net sediment flux patterns (0.1mm sand) detail: North Suffolk**

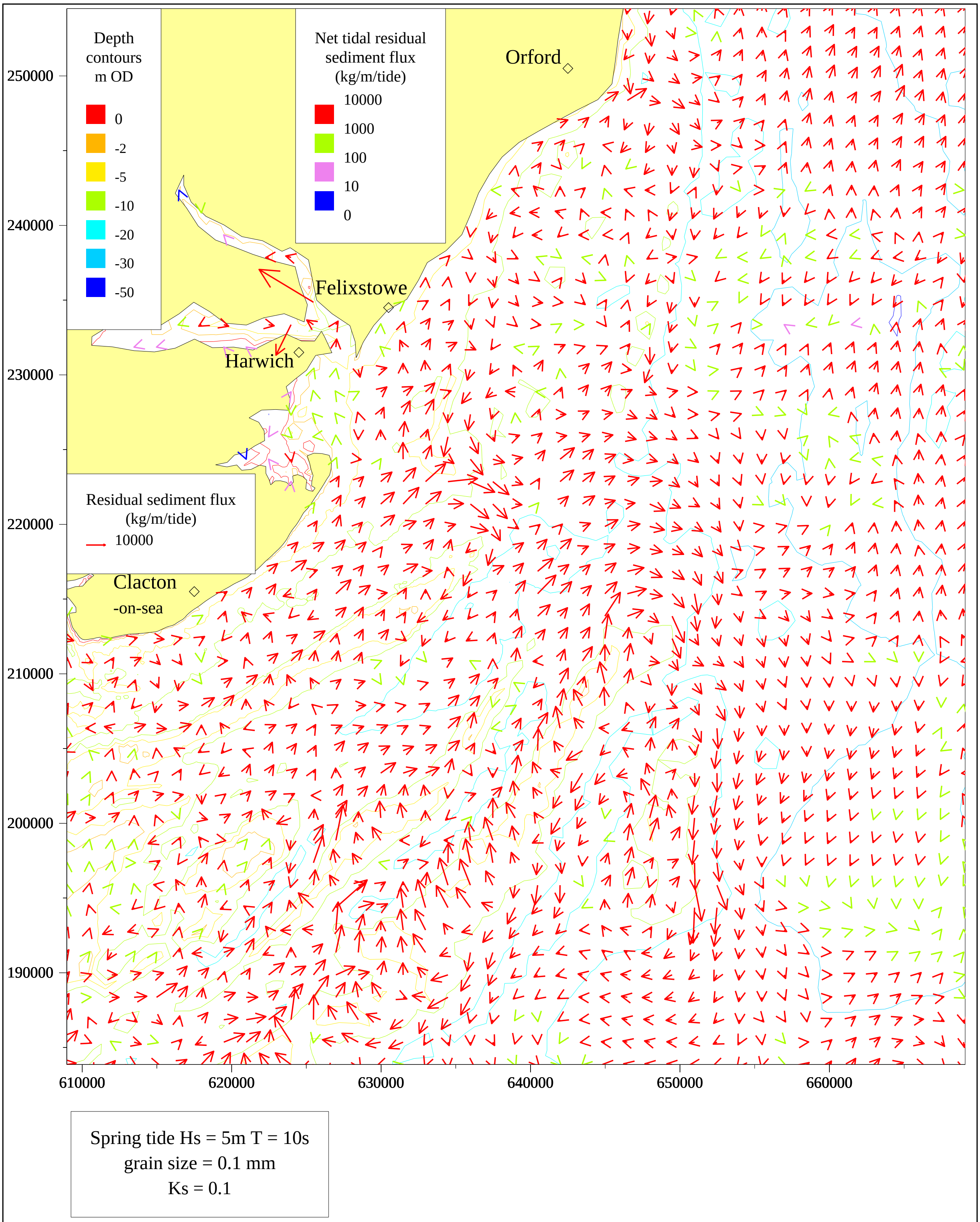

Figure 141 **Spring tide with 5m 10s storm waves net sediment flux patterns (0.1mm sand) detail: Suffolk and Essex**

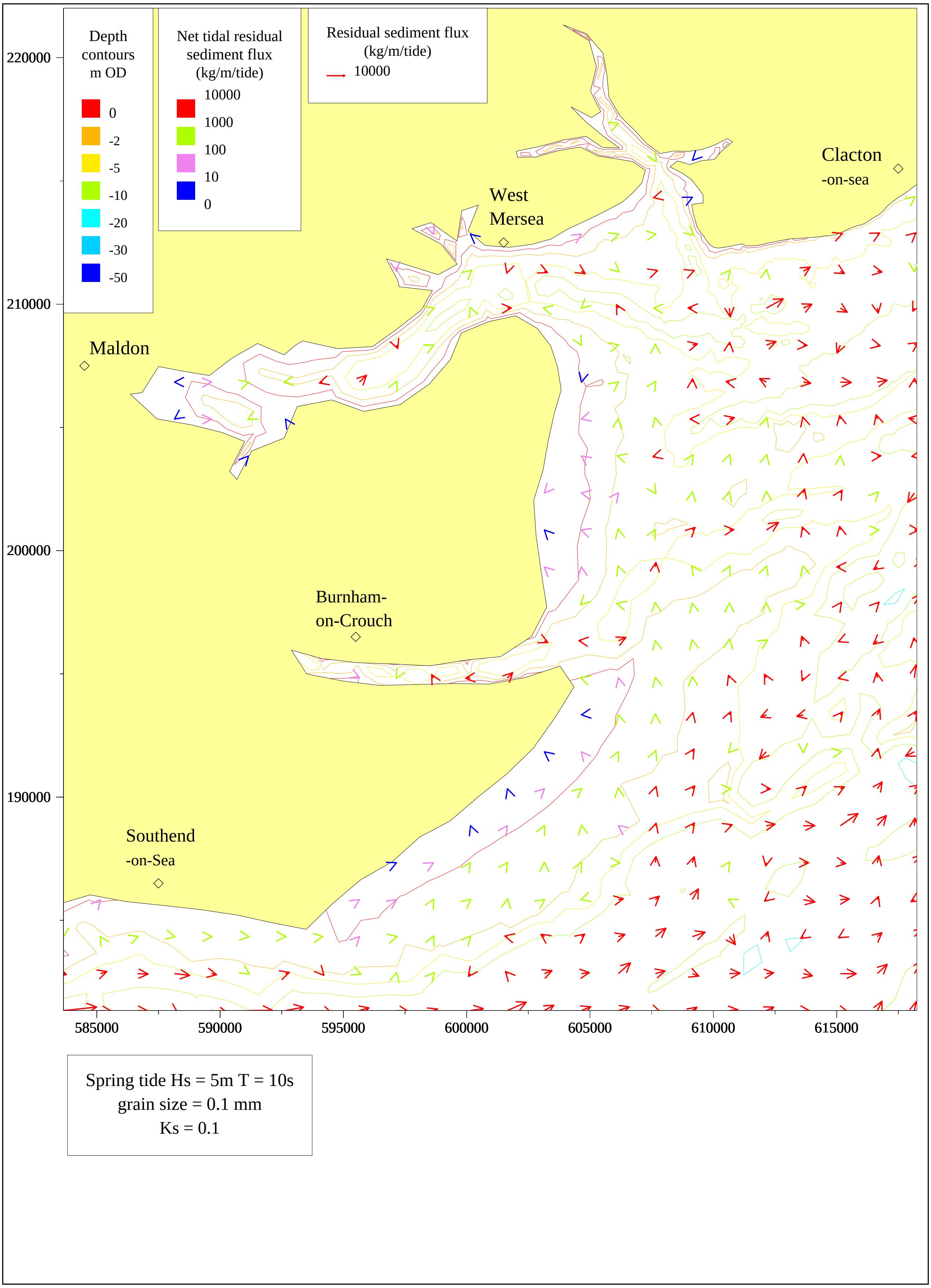

Figure 142 **Spring tide with 5m 10s storm waves net sediment flux patterns (0.1mm sand) detail: South Essex**

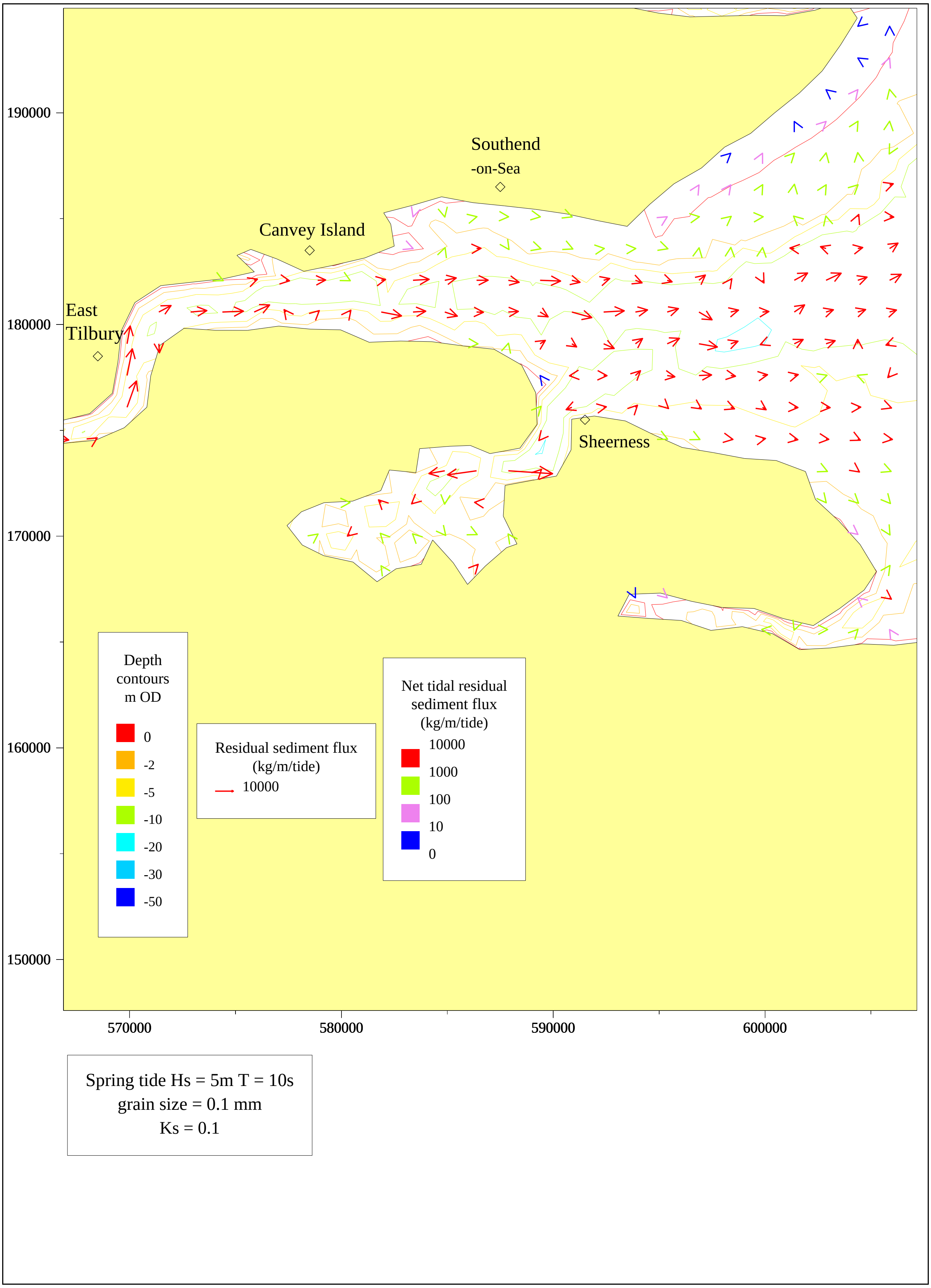

Figure 143 **Spring tide with 5m 10s storm waves net sediment flux patterns (0.1mm sand) detail: Outer Thames**

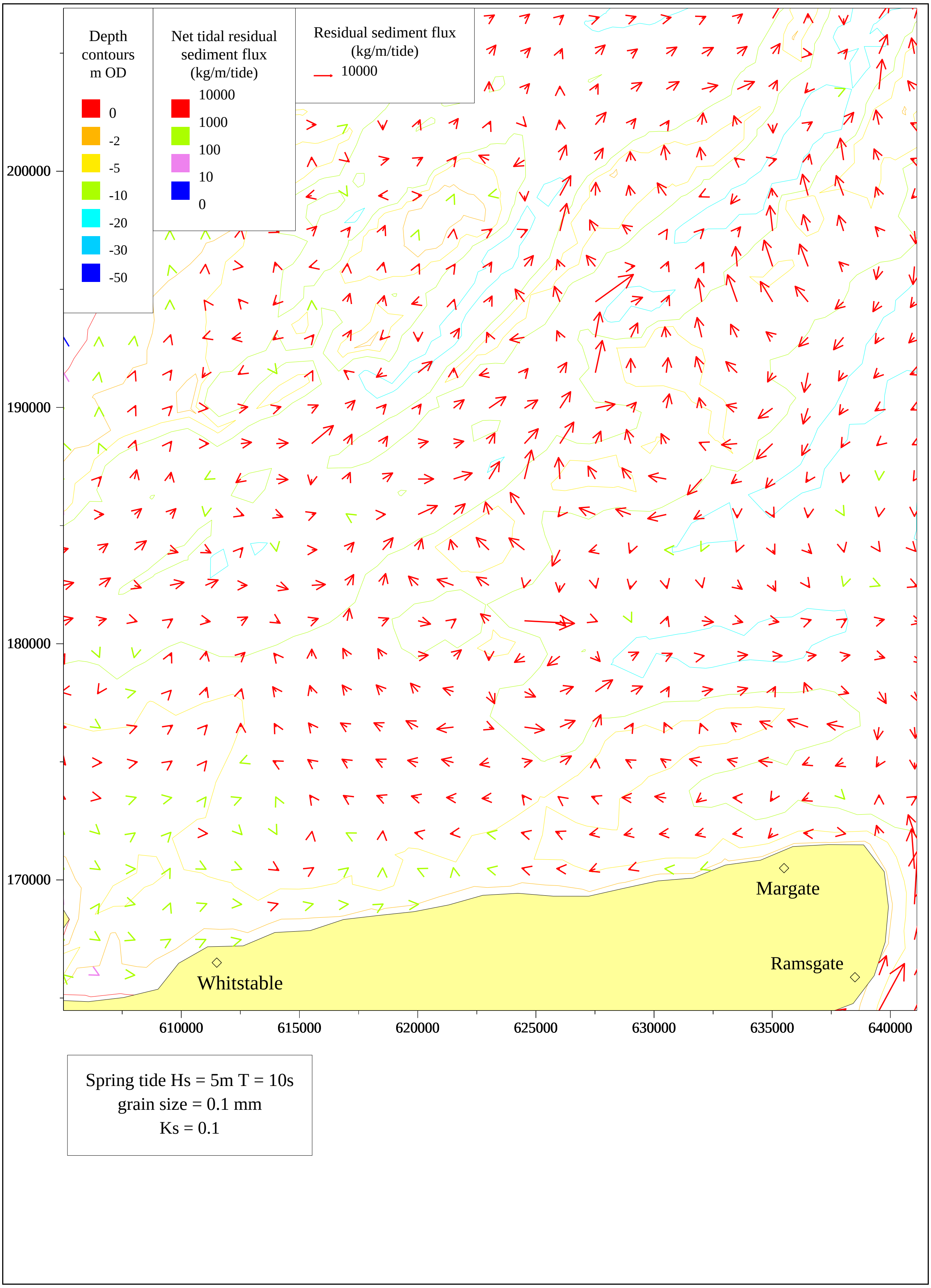

Figure 144 **Spring tide with 5m 10s storm waves net sediment flux patterns (0.1mm sand) detail: North Kent**

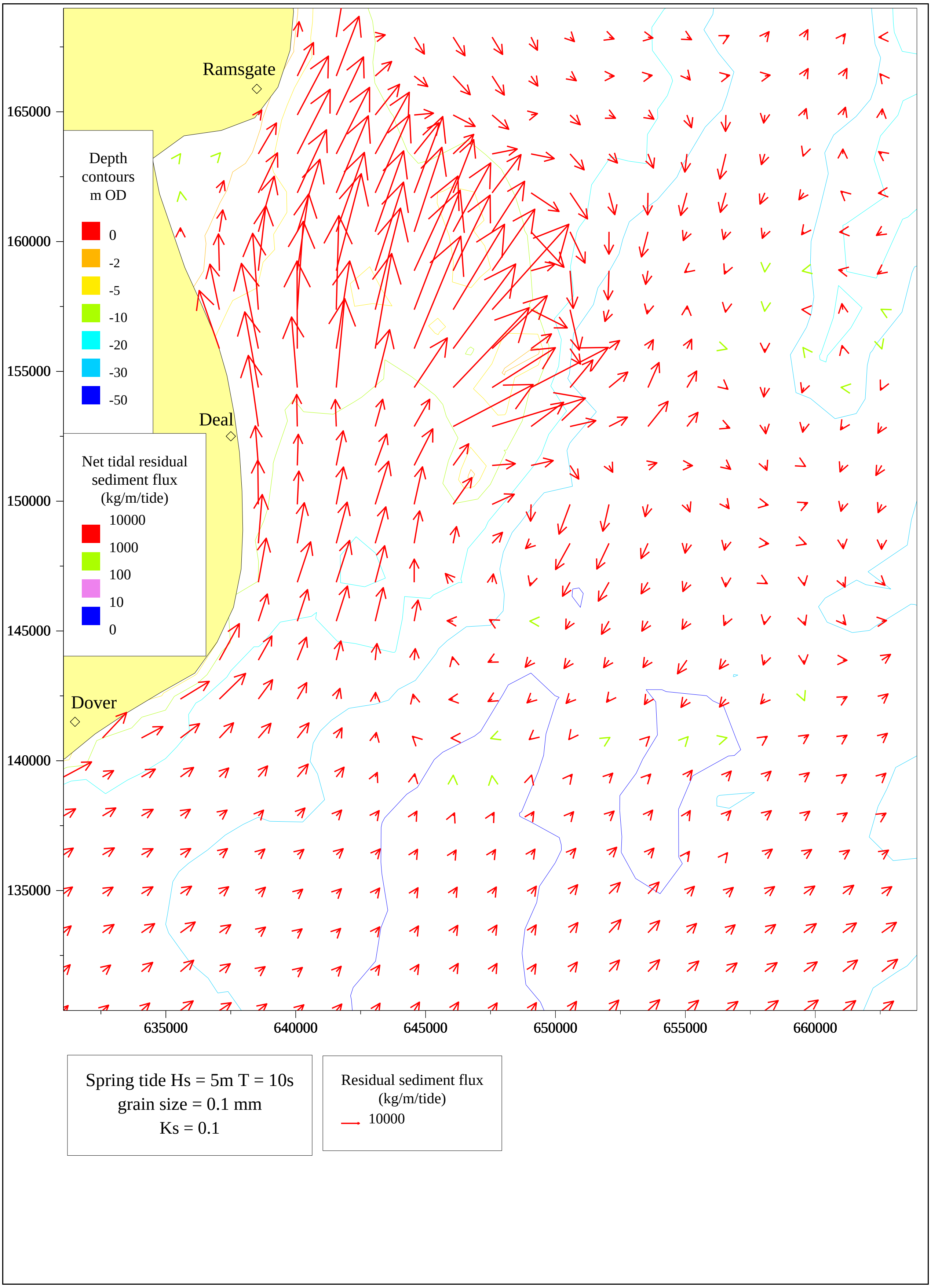

Figure 145 **Spring tide with 5m 10s storm waves net sediment flux patterns (0.1mm sand) detail: East Kent**

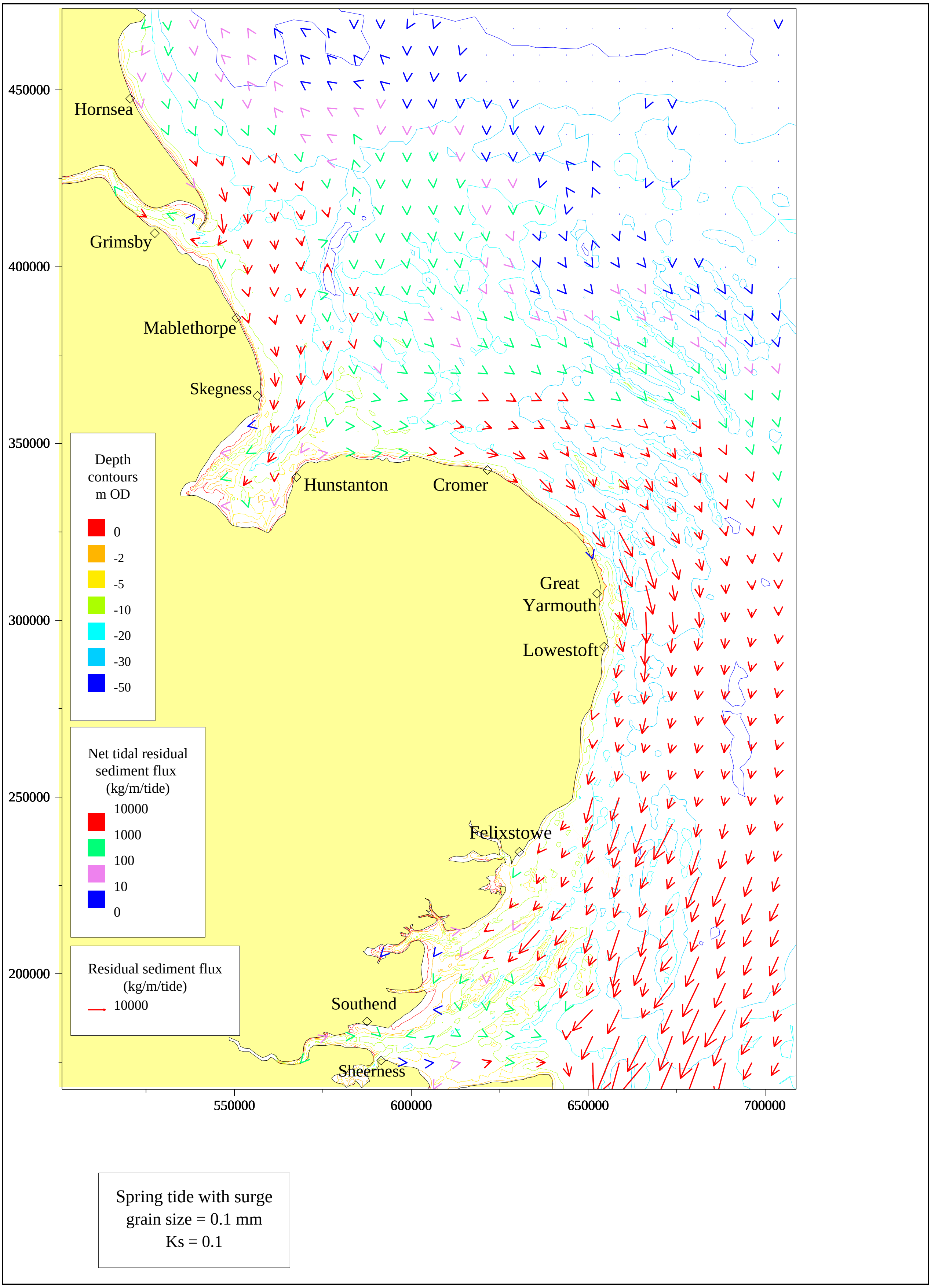

Figure 146 Spring tide with surge net sediment flux patterns (0.1mm sand)

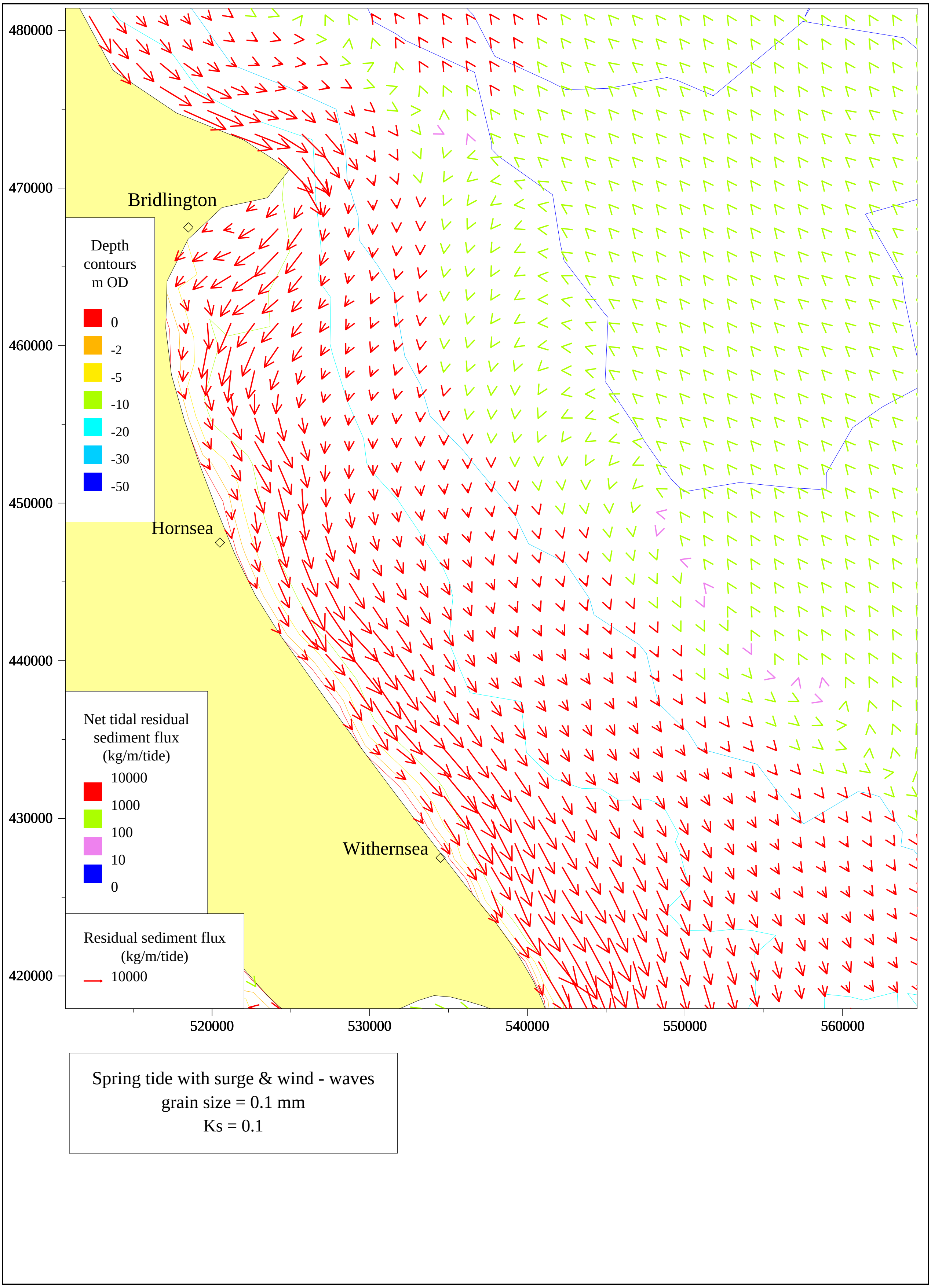

Figure 147 Spring tide with surge net sediment flux patterns (0.1mm sand) detail: Flamborough Head to Humber

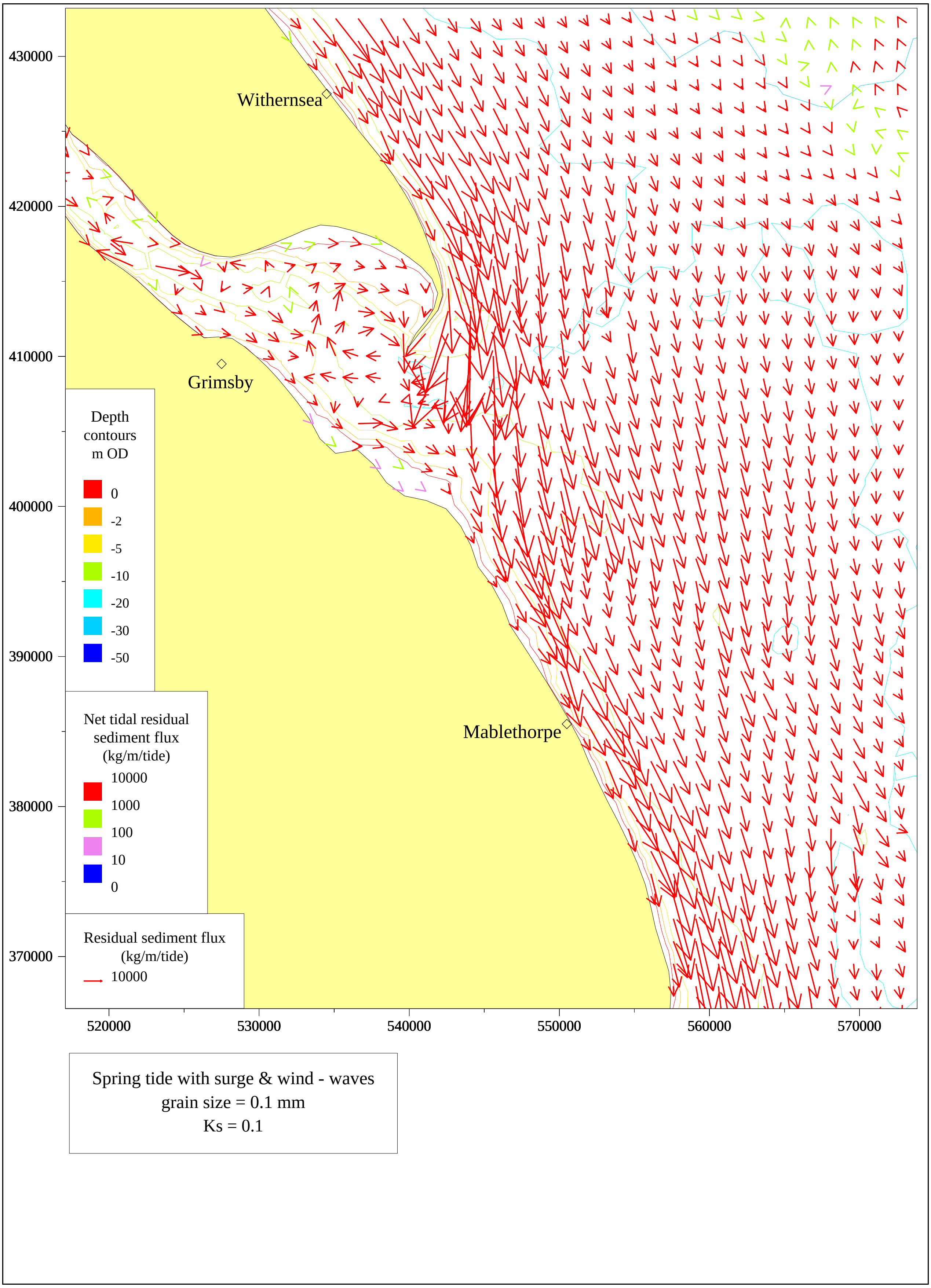

Figure 148 **Spring tide with surge net sediment flux patterns (0.1mm sand) detail: Humber Entrance and Lincolnshire**

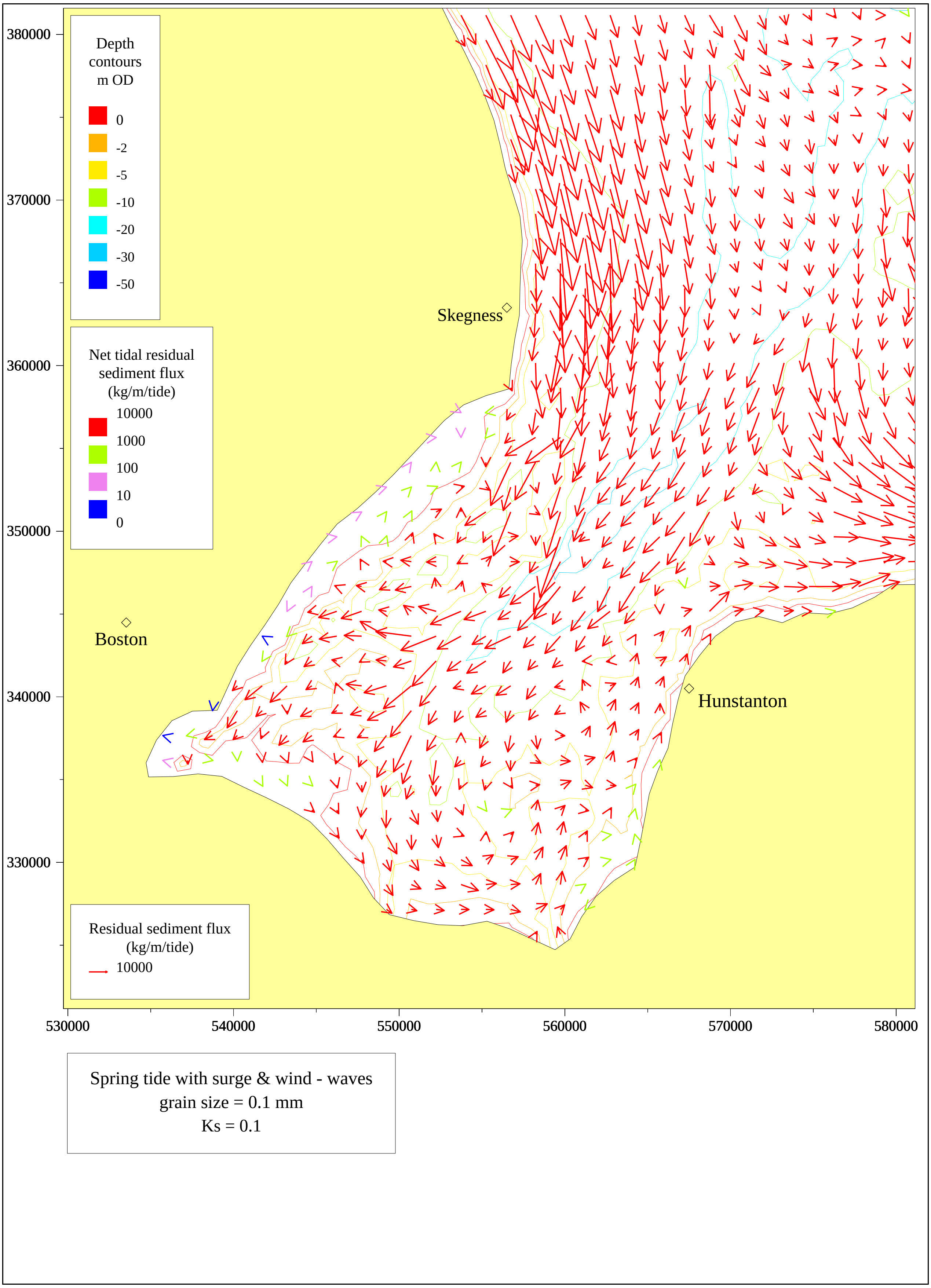

Figure 149 **Spring tide with surge net sediment flux patterns (0.1mm sand) detail Lincolnshire and the Wash**

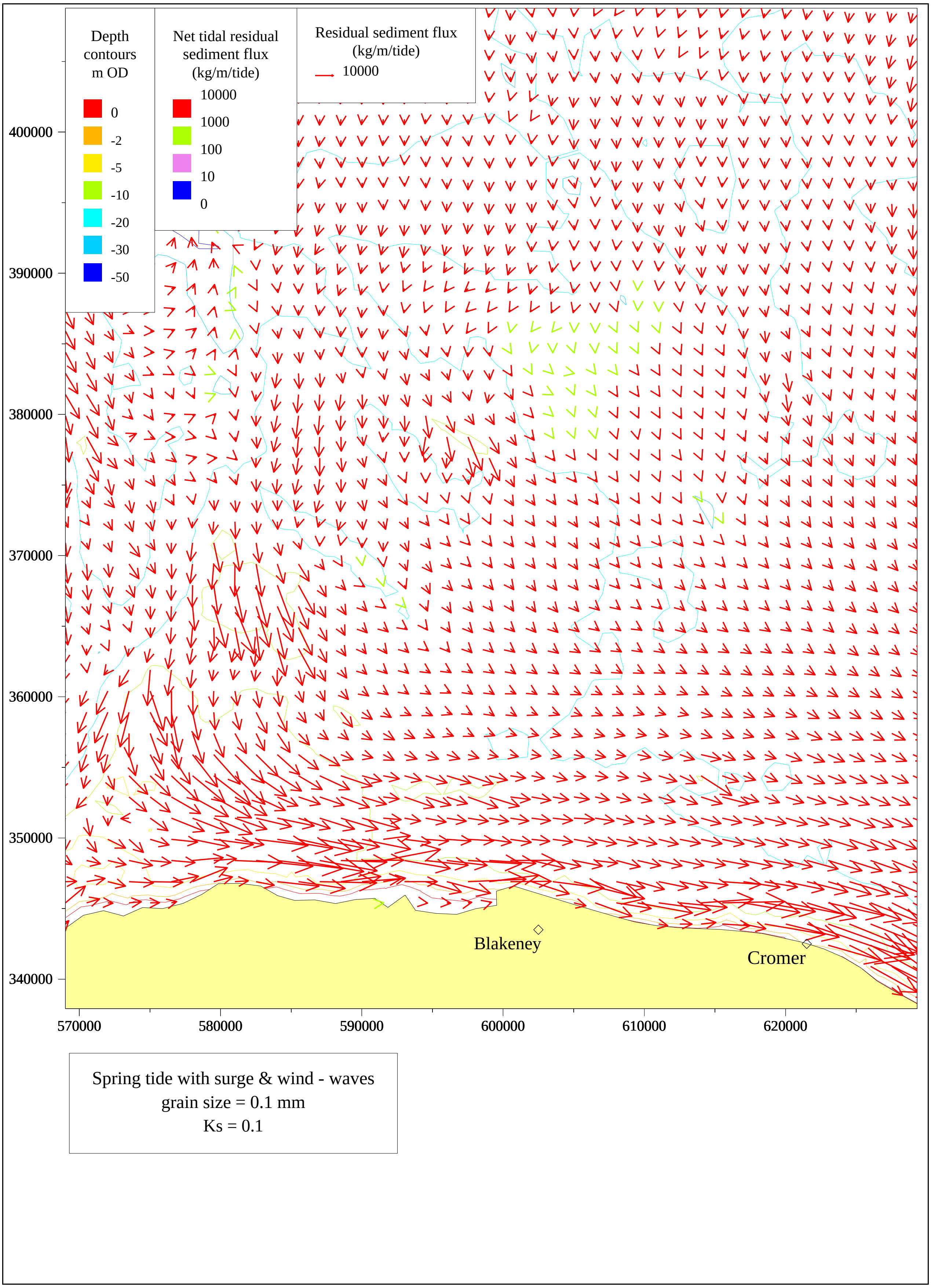

Figure 150 Spring tide with surge net sediment flux patterns (0.1mm sand) detail: North Norfolk

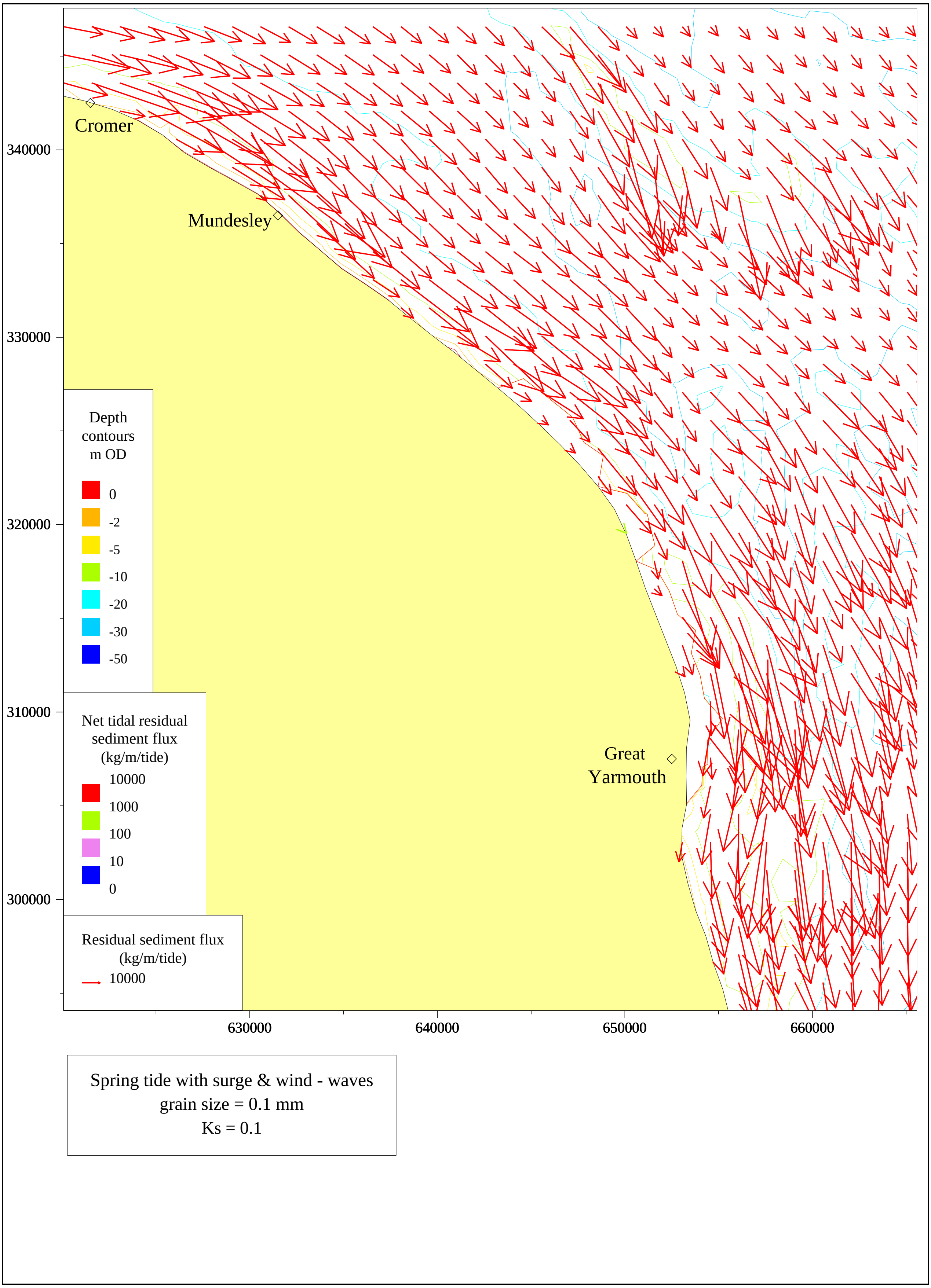

Figure 151 **Spring tide with surge net sediment flux patterns (0.1mm sand) detail: East Norfolk**

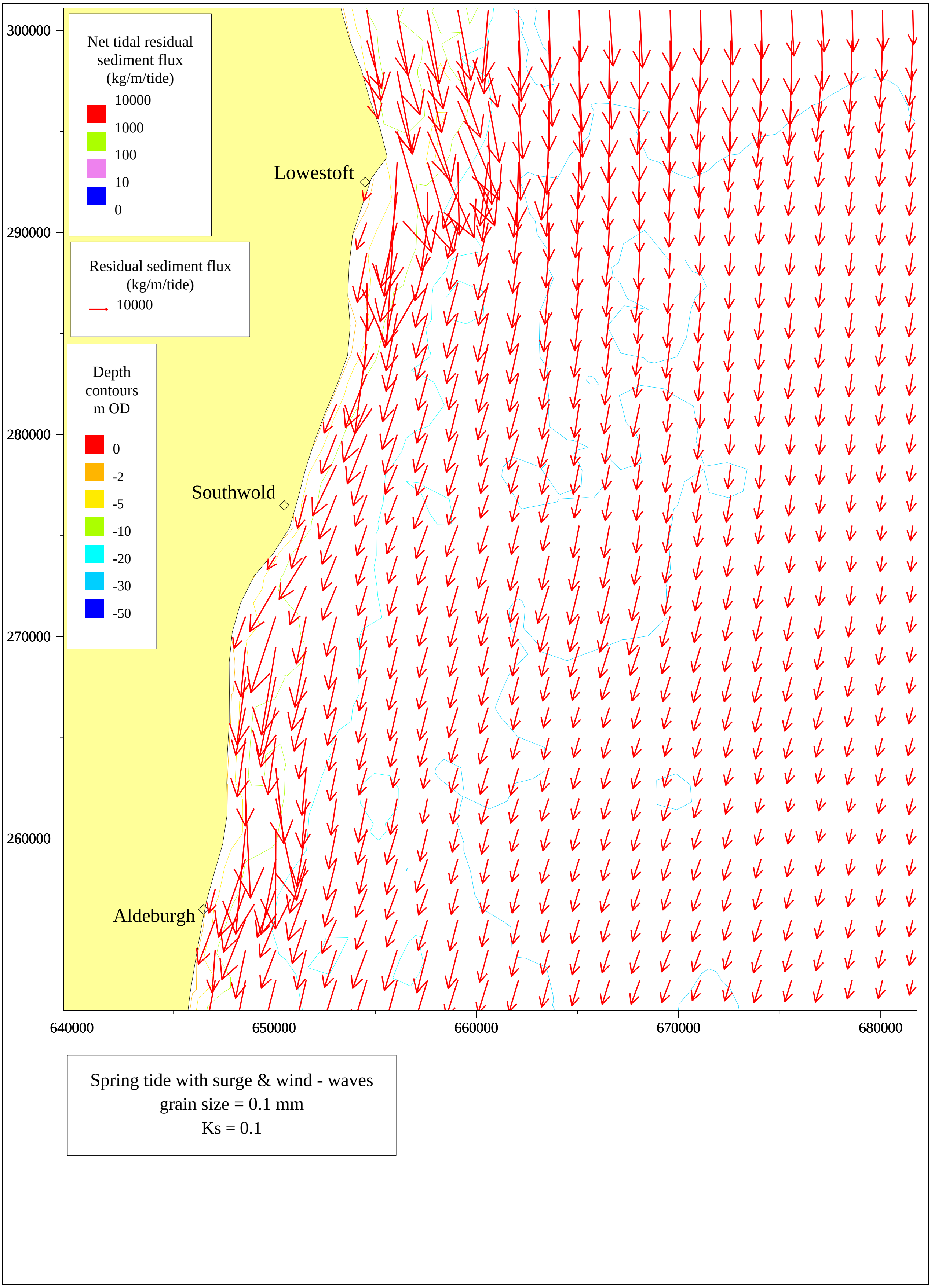

Figure 152 Spring tide with surge net sediment flux patterns (0.1mm sand) detail: North Suffolk

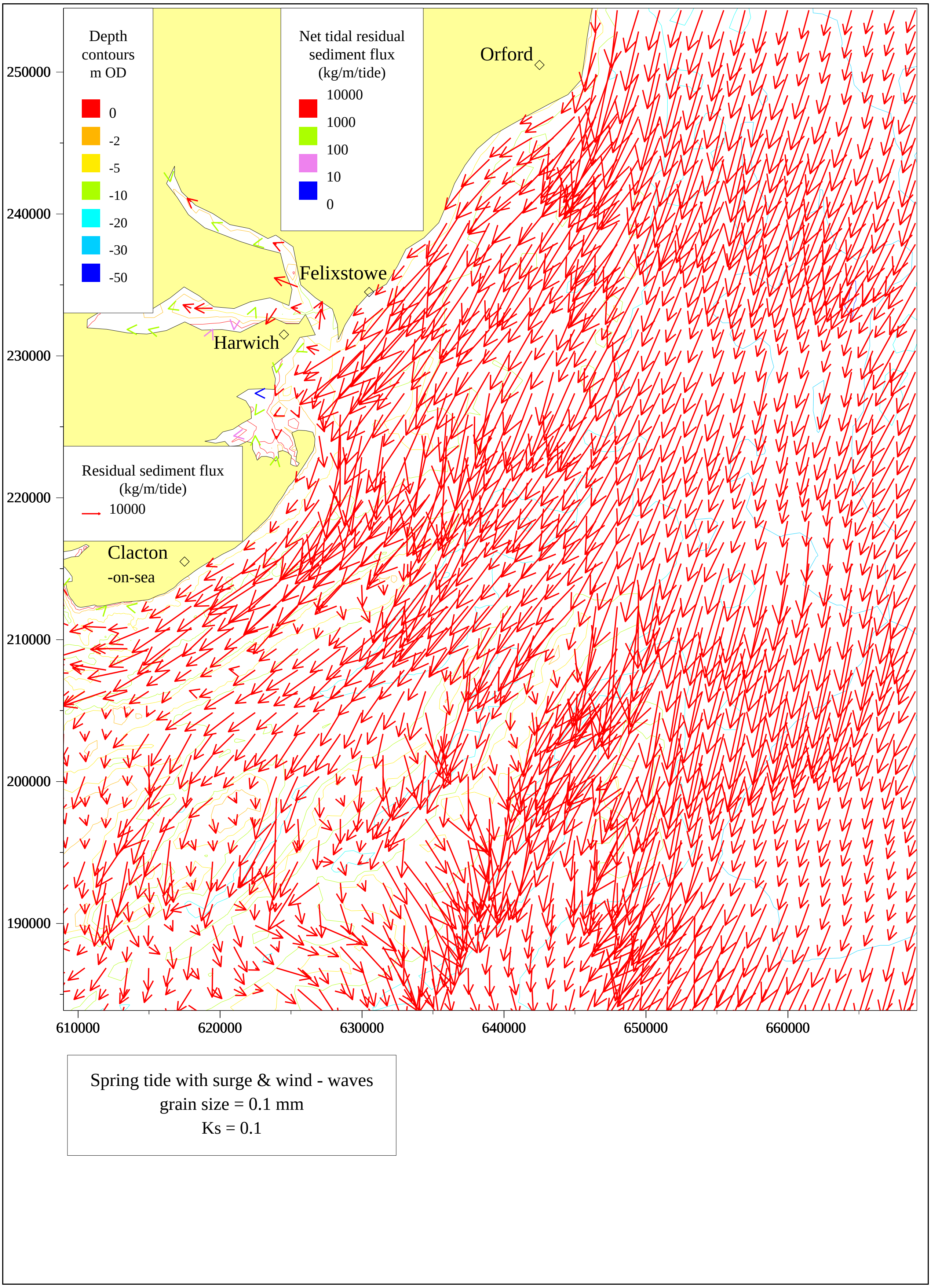

Figure 153 **Spring tide with surge net sediment flux patterns (0.1mm sand) detail: Suffolk and Essex**

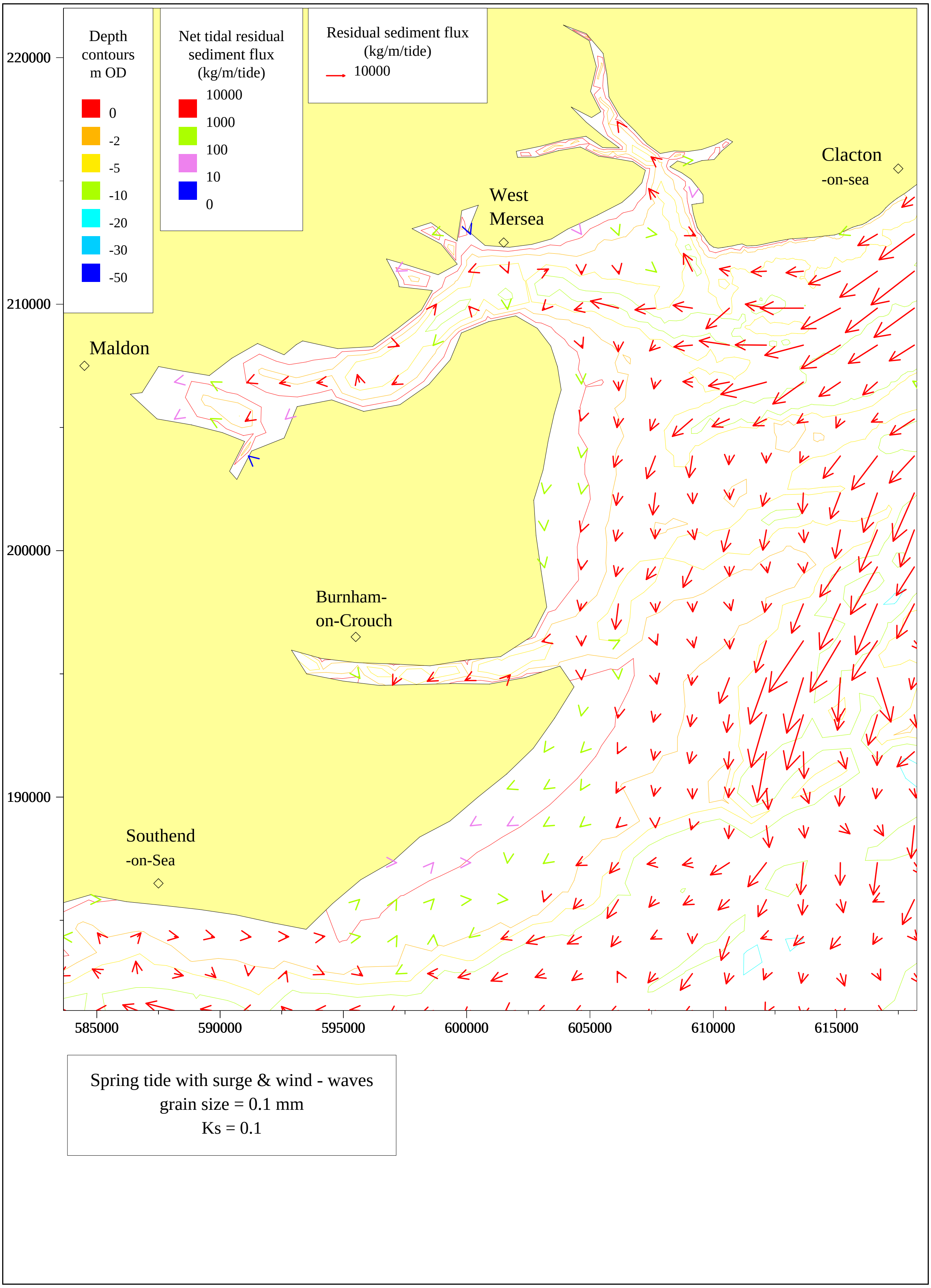

Figure 154 Spring tide with surge net sediment flux patterns (0.1mm sand) detail: South Essex

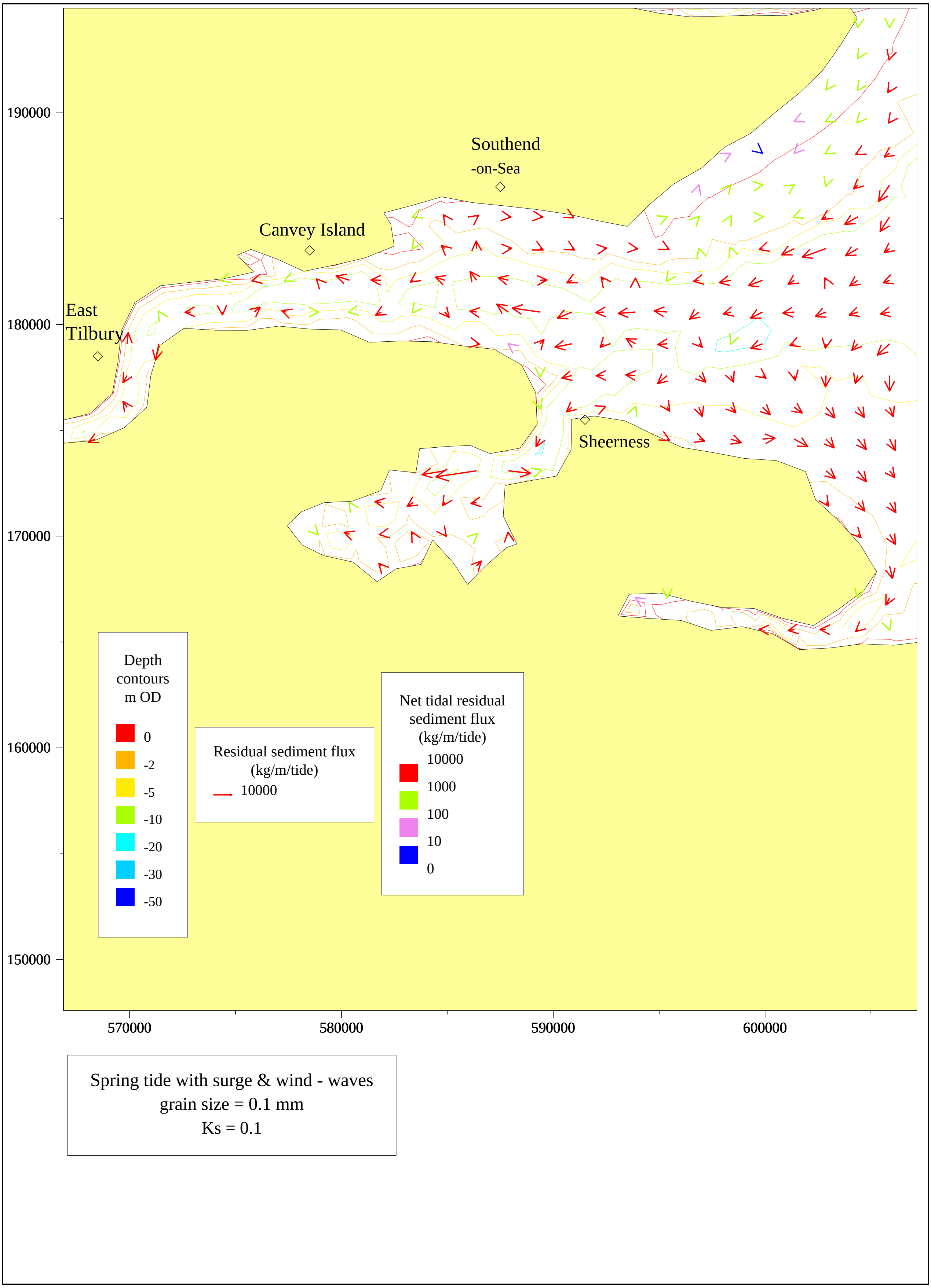

Figure 155 Spring tide with surge net sediment flux patterns (0.1mm sand) detail: Outer Thames

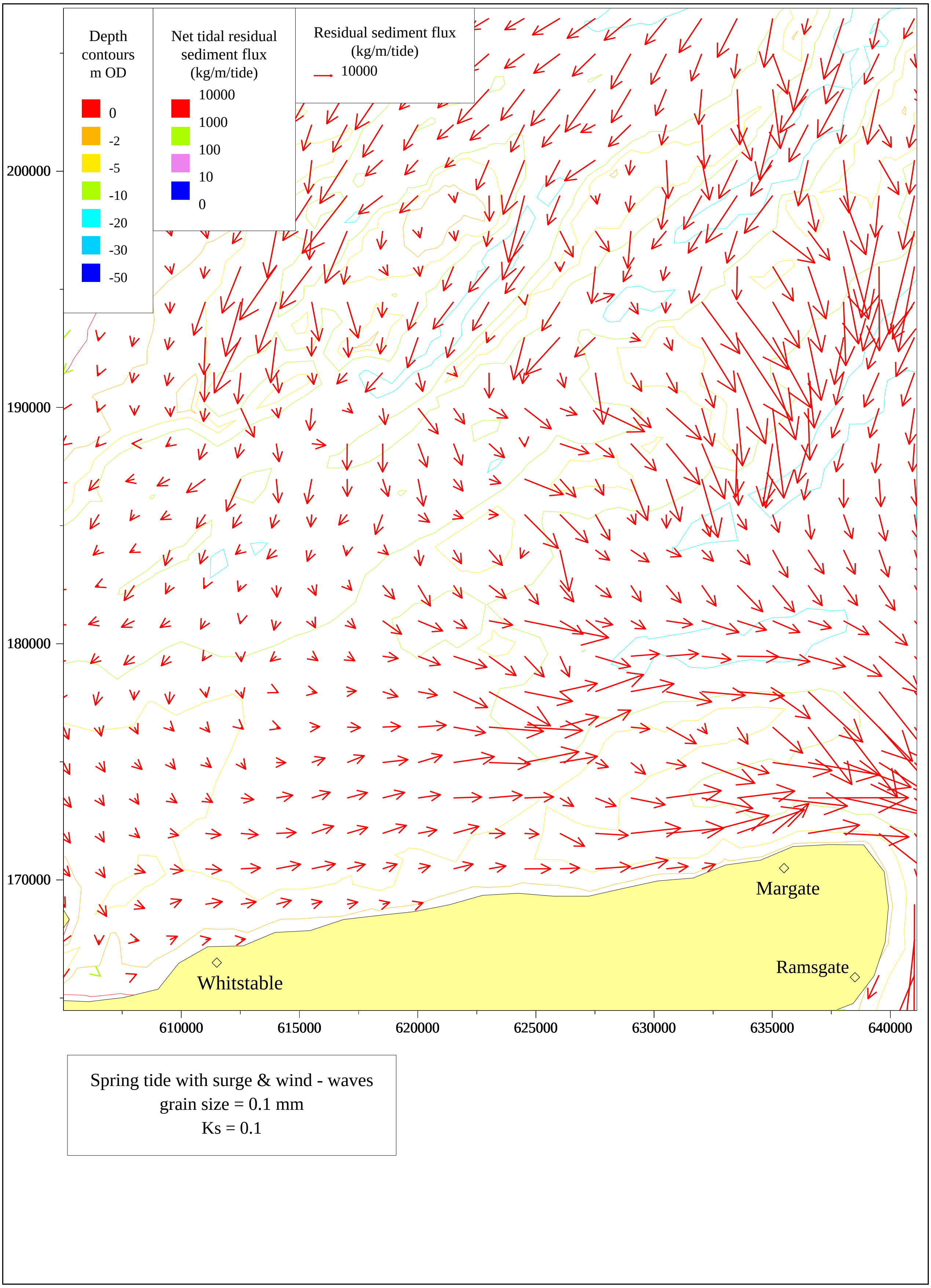

Figure 156 **Spring tide with surge net sediment flux patterns (0.1mm sand) detail: North Kent**

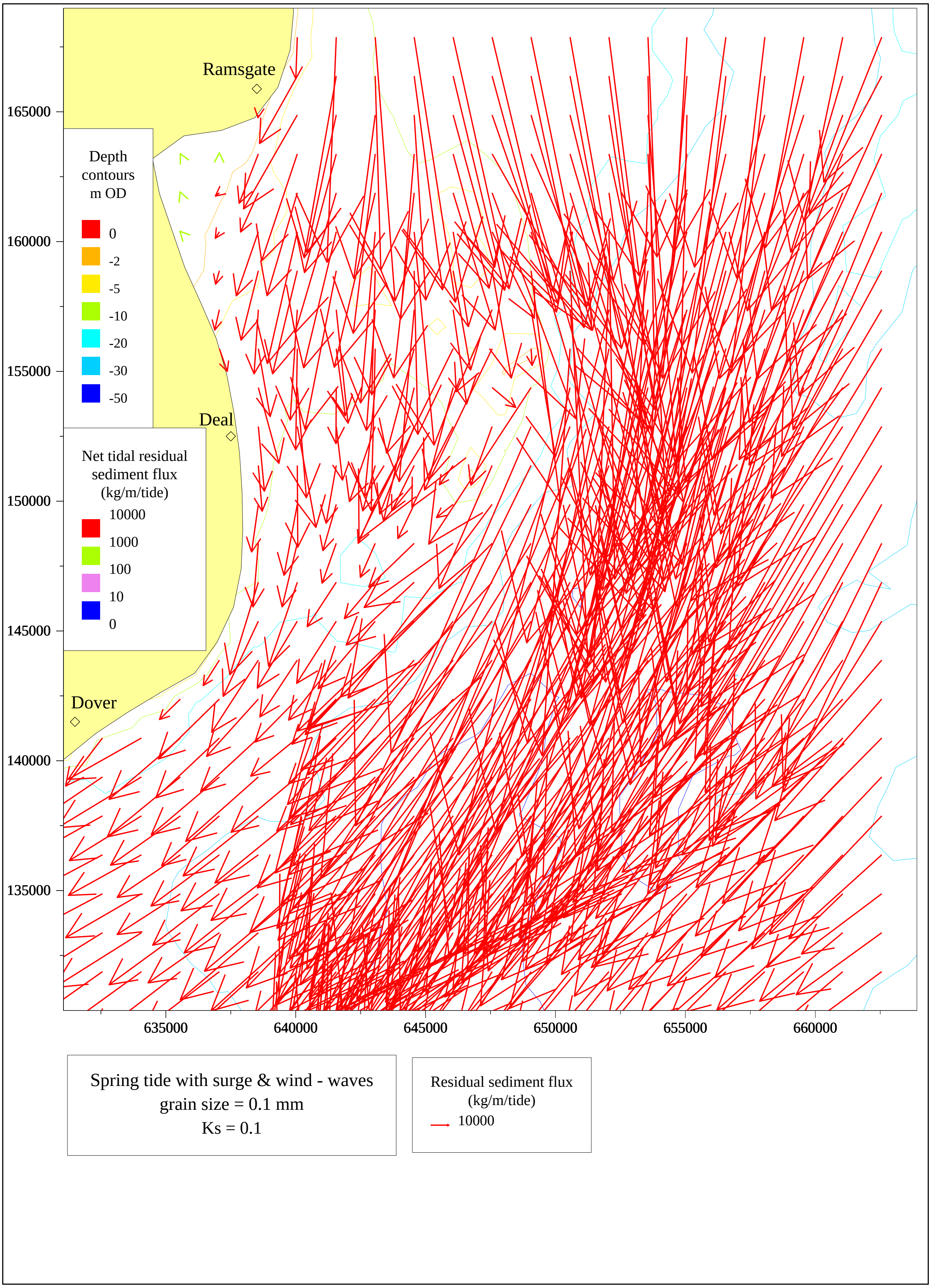

Figure 157 Spring tide with surge net sediment flux patterns (0.1mm sand) detail: East Kent

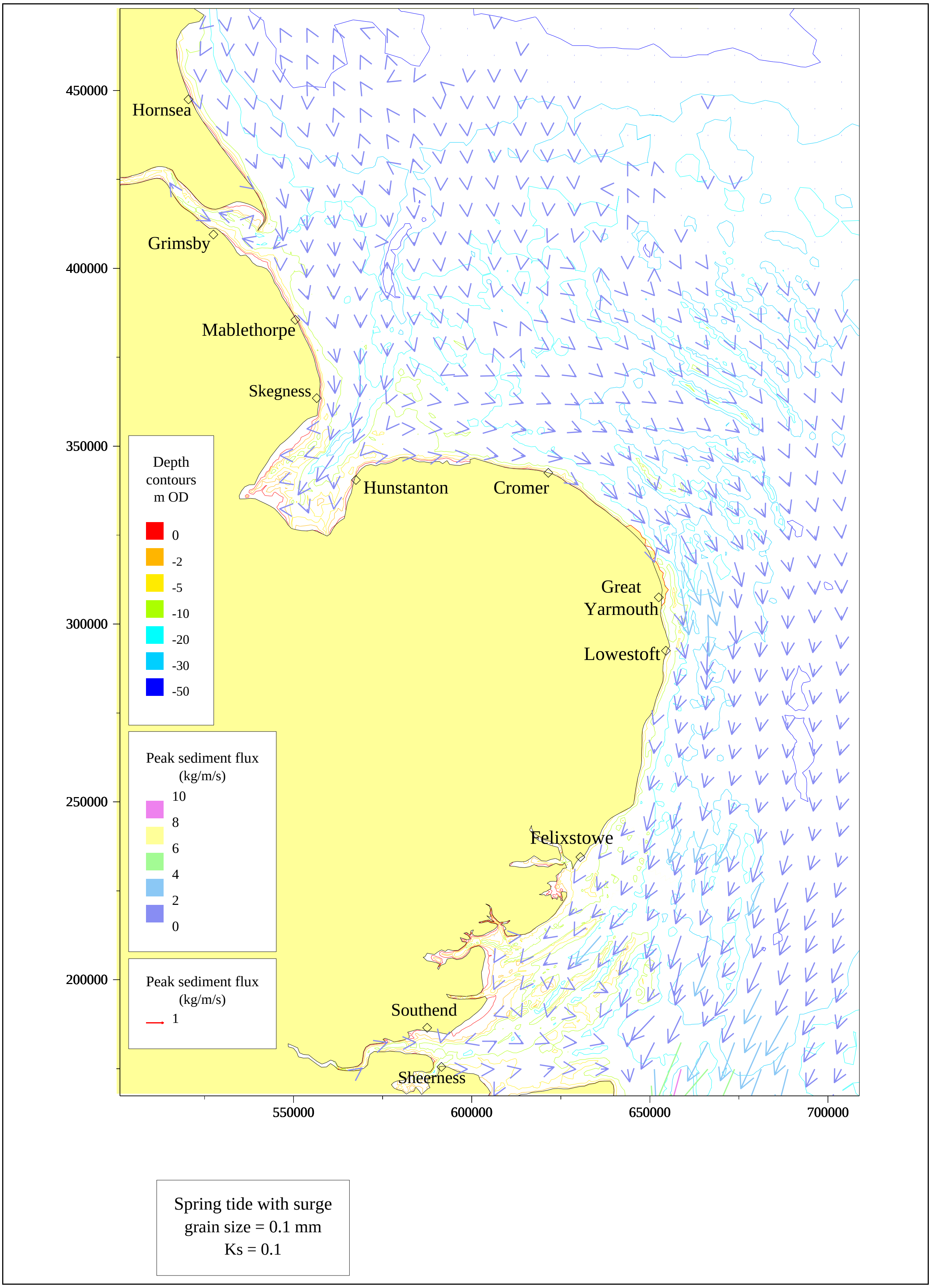

Figure 158 Peak spring tide with surge net sediment flux patterns (0.1mm sand)

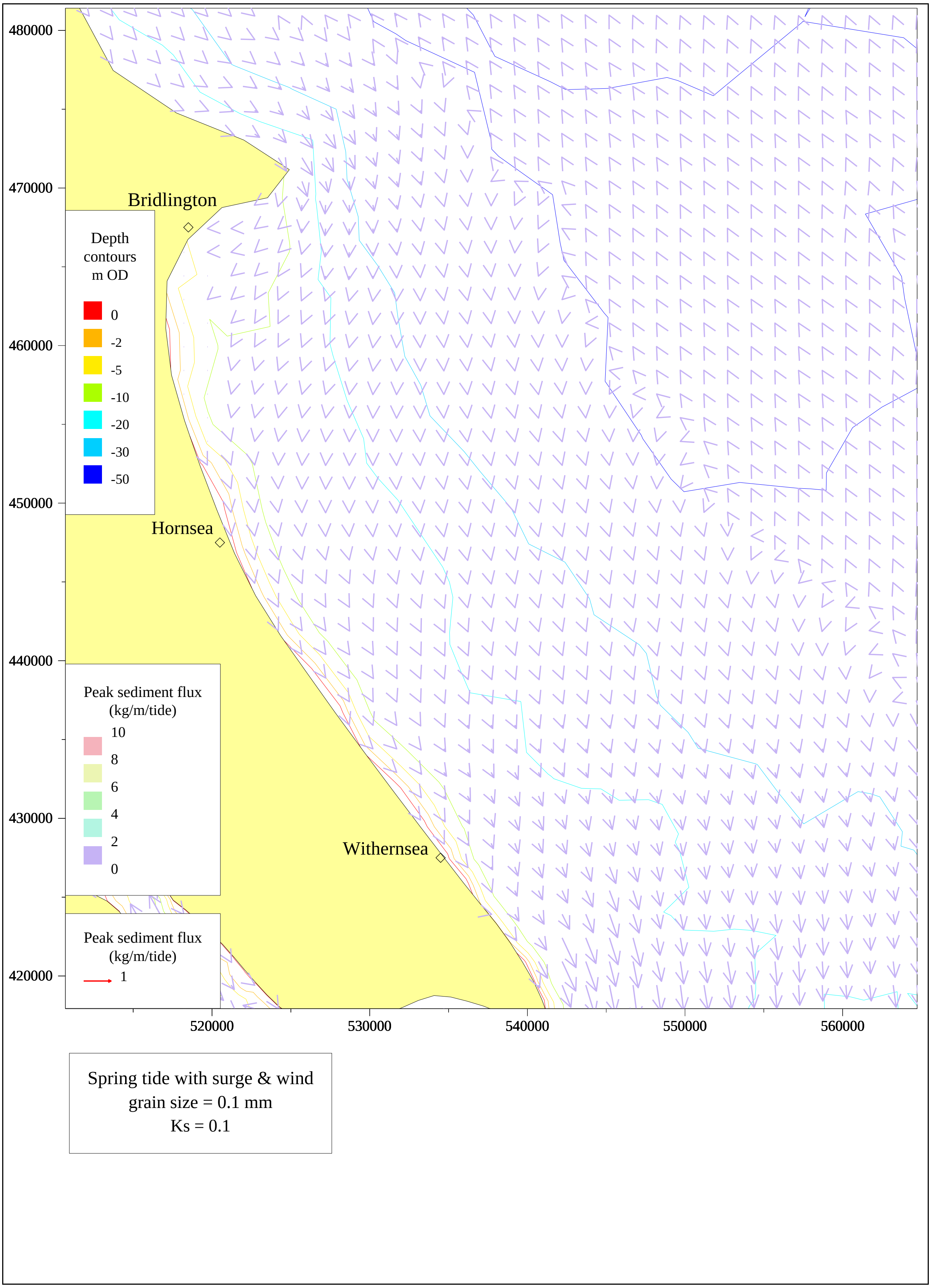

Figure 159 **Peak spring tide with surge net sediment flux patterns (0.1mm sand) detail: Flamborough Head to Humber**

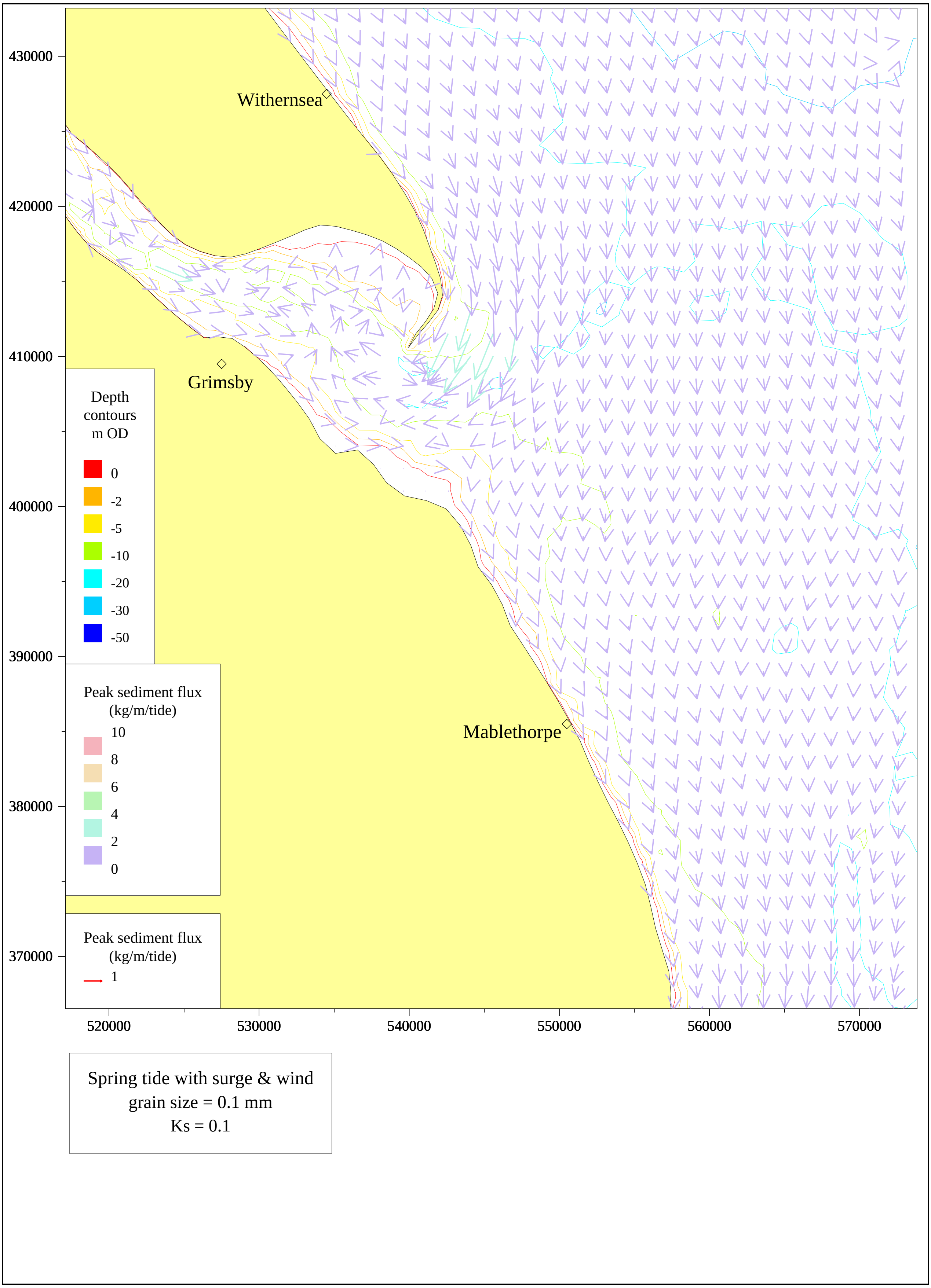

Figure 160 Peak spring tide with surge net sediment flux patterns (0.1mm sand) detail: Humber Entrance and Lincolnshire

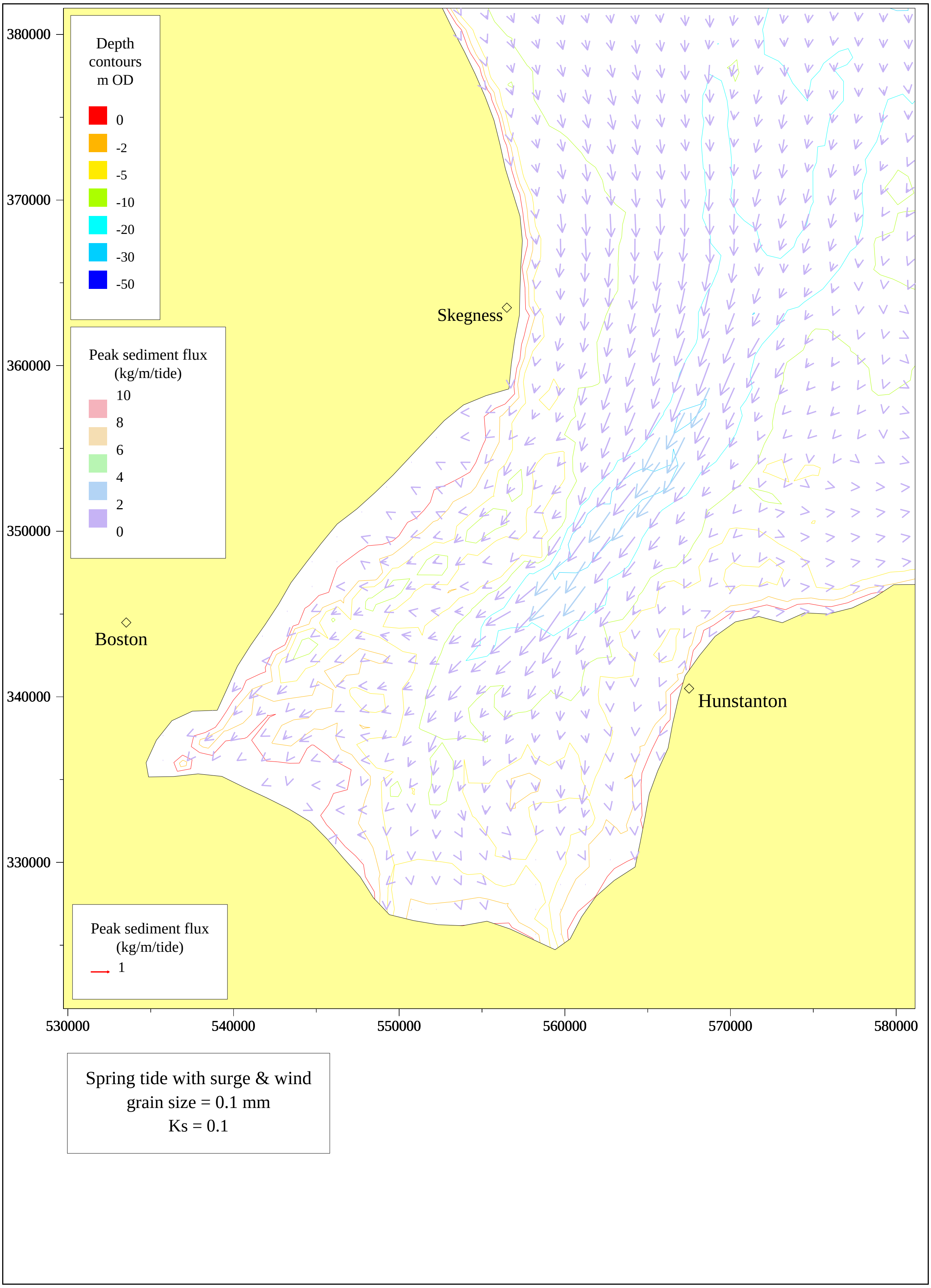

Figure 161 **Peak spring tide with surge net sediment flux patterns (0.1mm sand) detail Lincolnshire and the Wash**

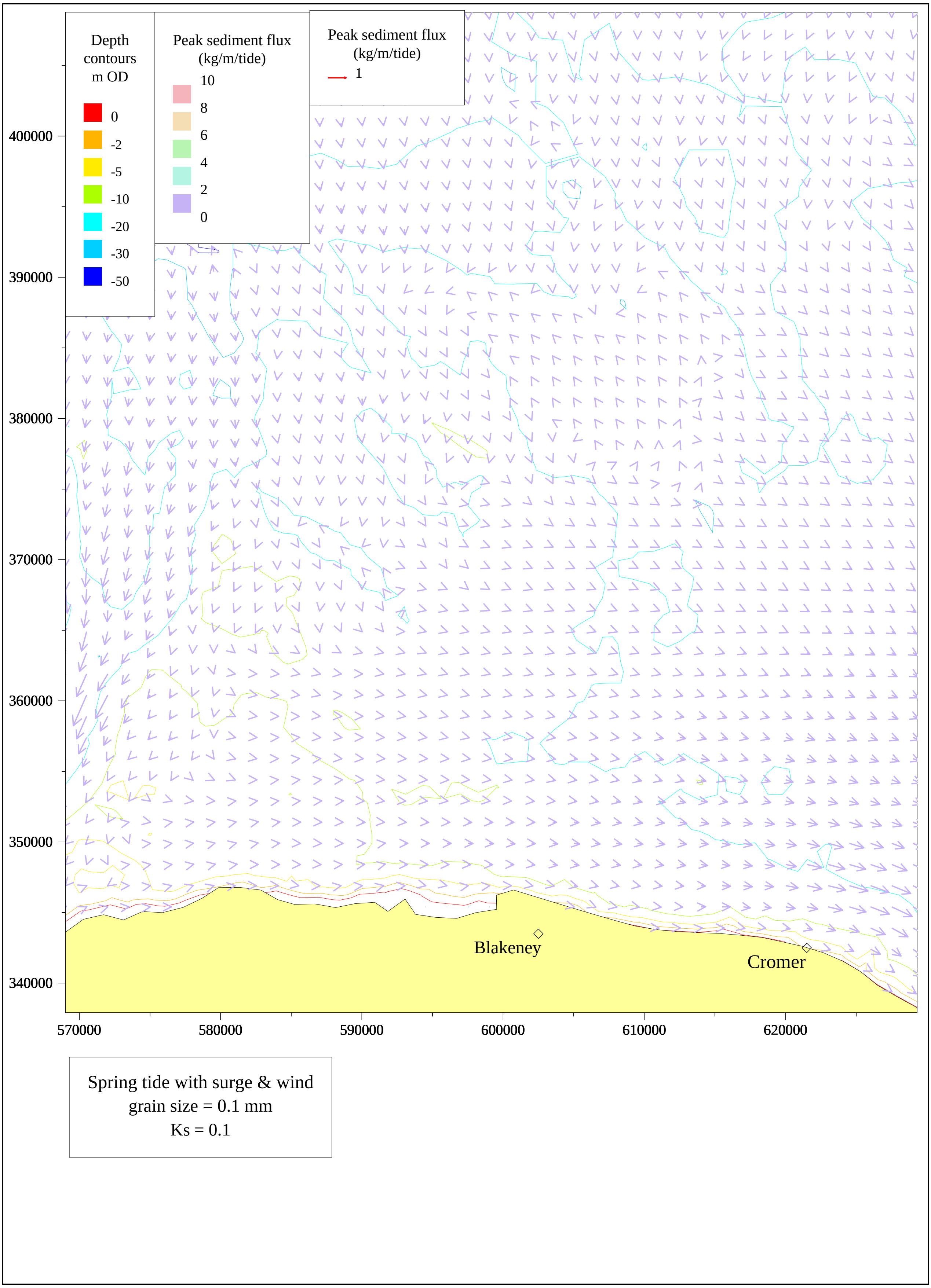

Figure 162 **Peak spring tide with surge net sediment flux patterns (0.1mm sand) detail: North Norfolk**

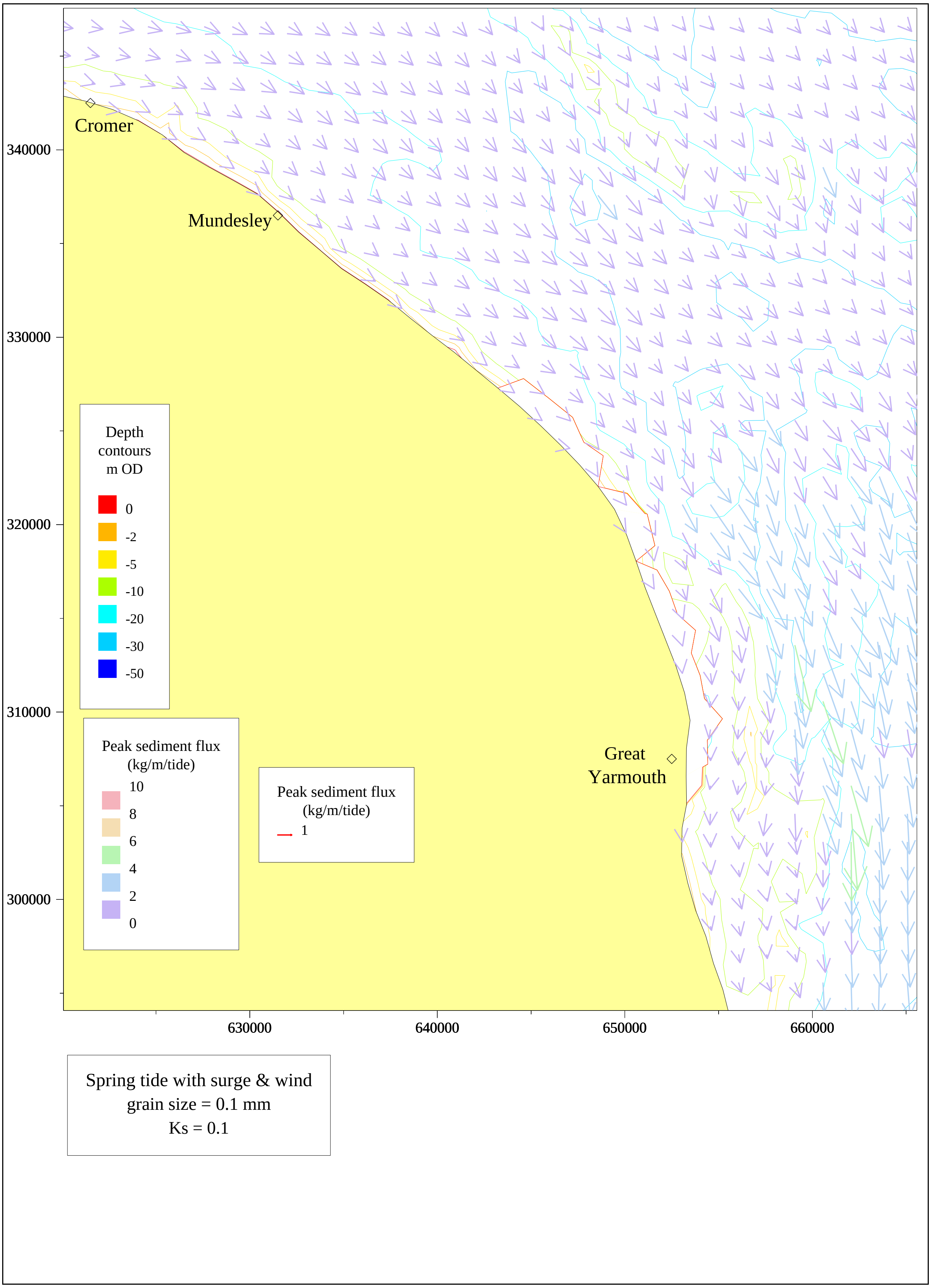

Figure 163 Peak spring tide with surge net sediment flux patterns (0.1mm sand) detail: East Norfolk

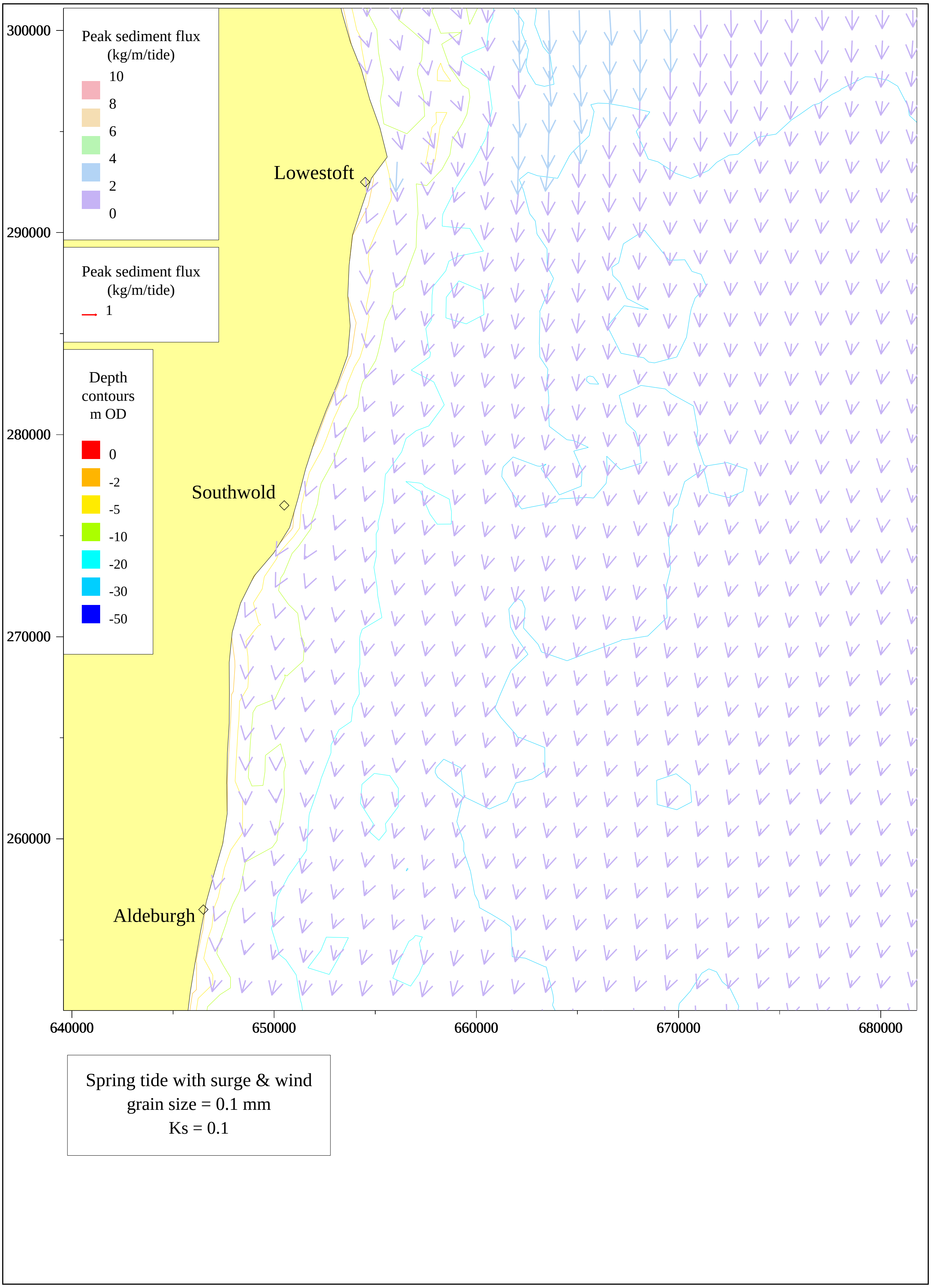

Figure 164 **Peak spring tide with surge net sediment flux patterns (0.1mm sand) detail: North Suffolk**

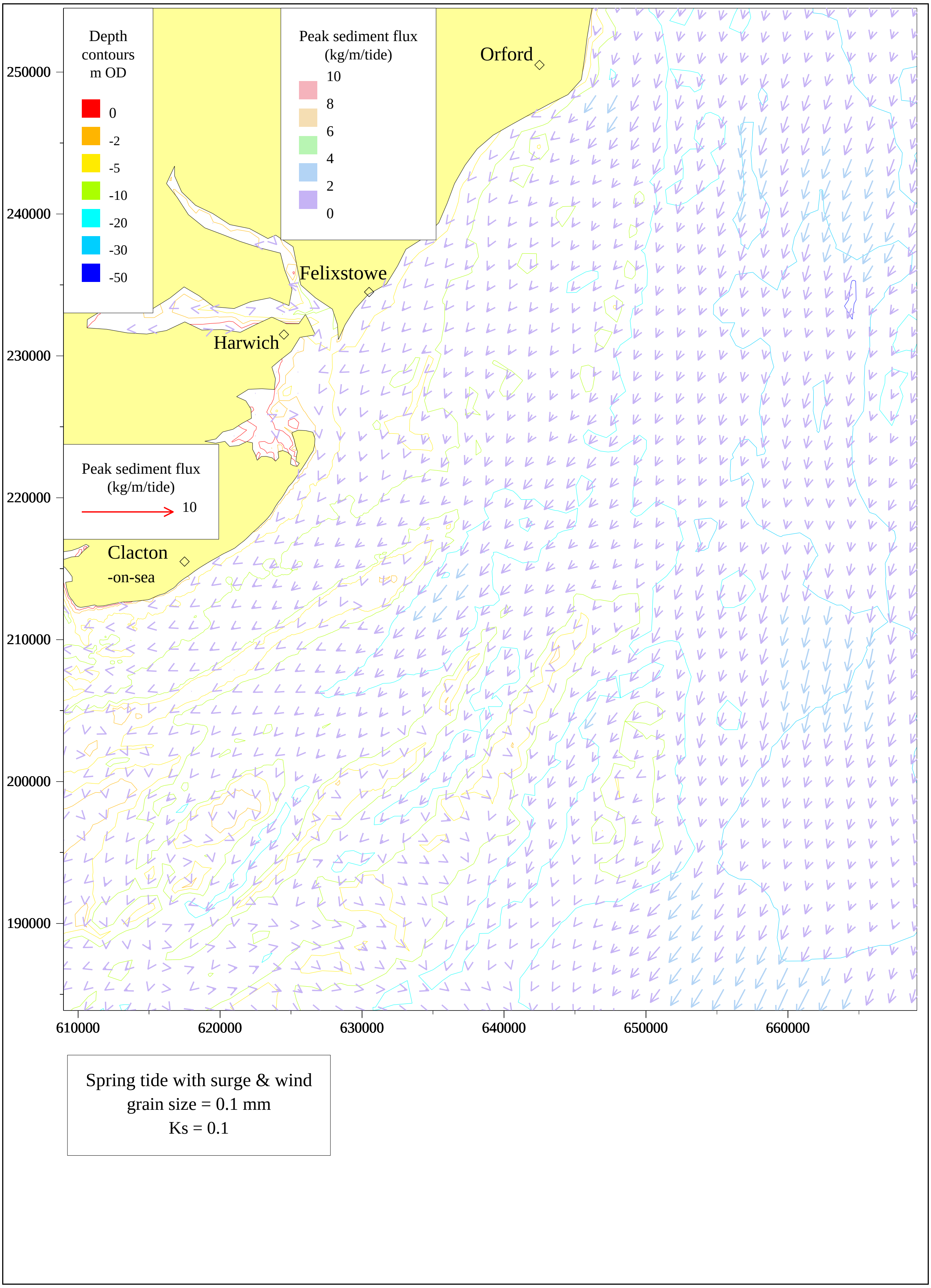

Figure 165 **Peak spring tide with surge net sediment flux patterns (0.1mm sand) detail: Suffolk and Essex**

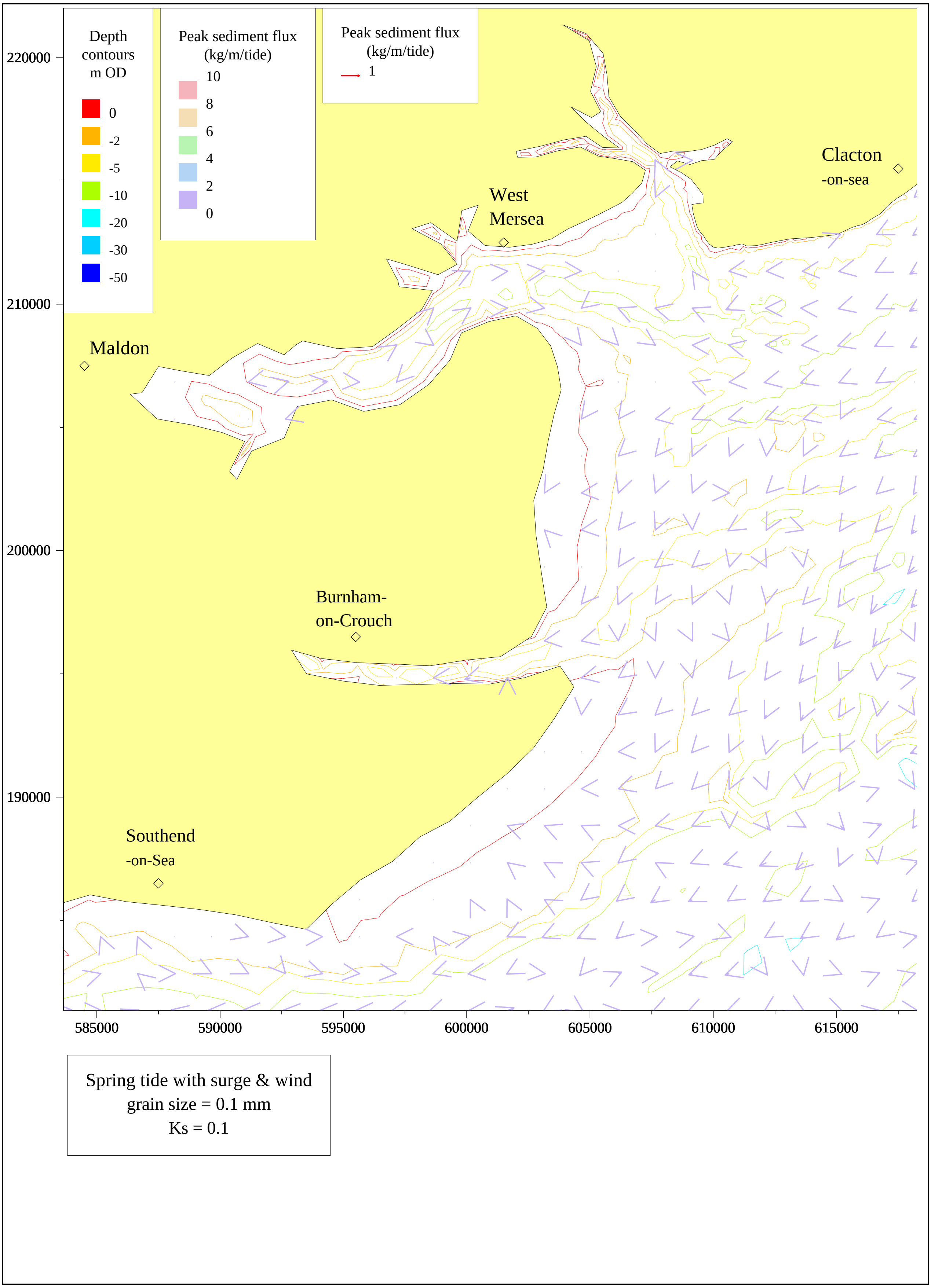

Figure 166 **Peak spring tide with surge net sediment flux patterns (0.1mm sand) detail: South Essex**

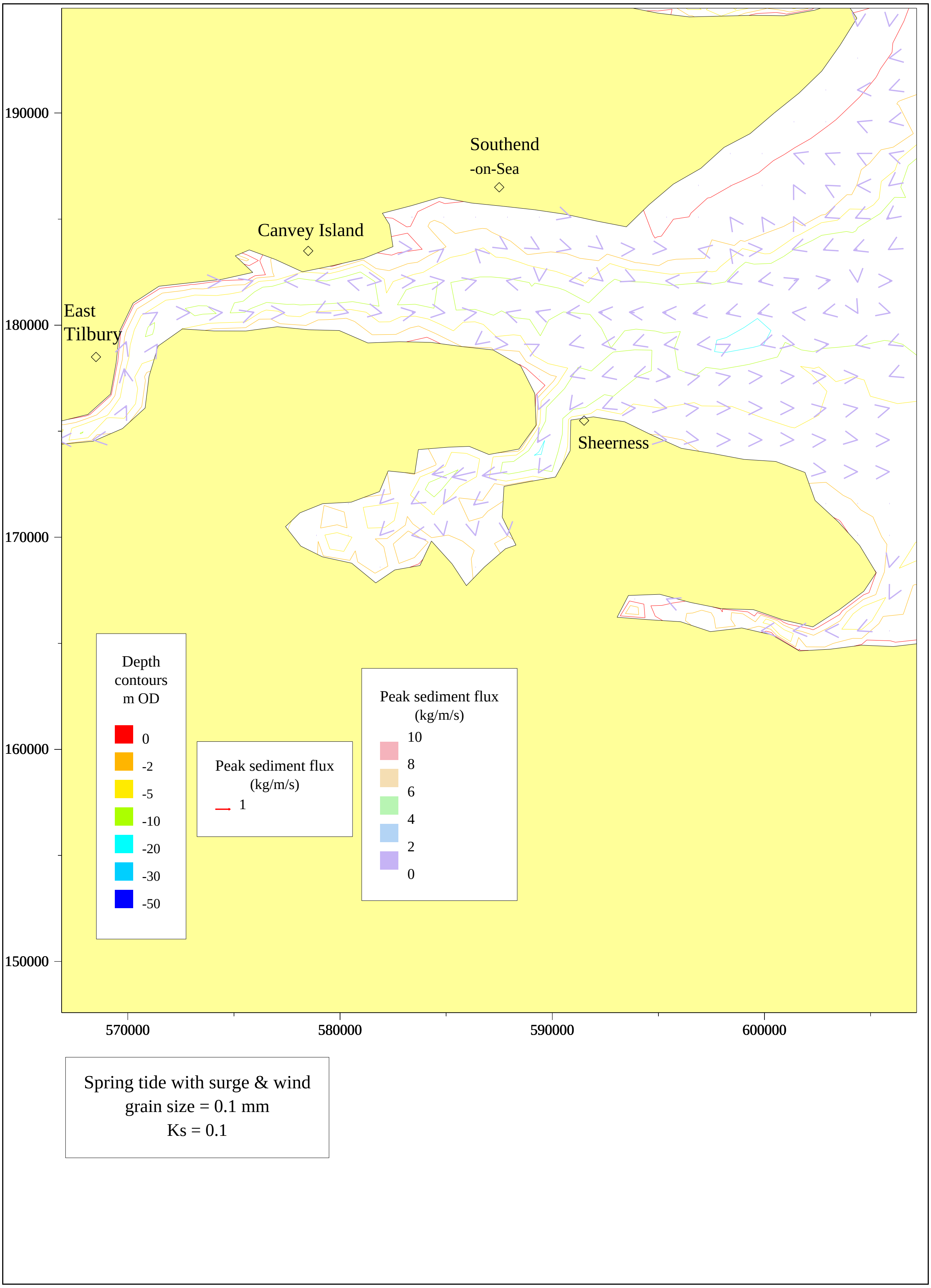

Figure 167 **Peak spring tide with surge net sediment flux patterns (0.1mm sand) detail: Outer Thames**

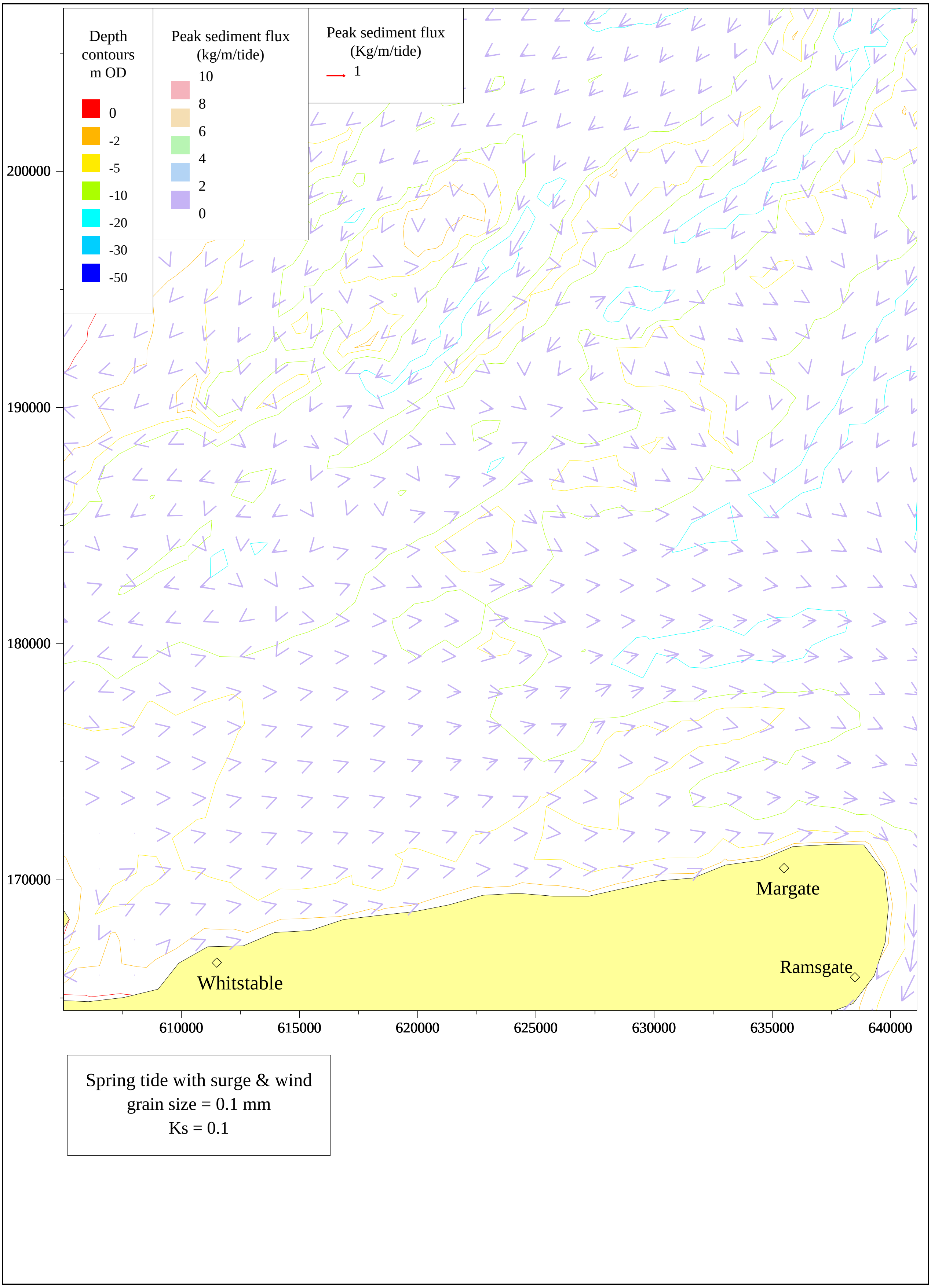

Figure 168 **Peak spring tide with surge net sediment flux patterns (0.1mm sand) detail: North Kent**

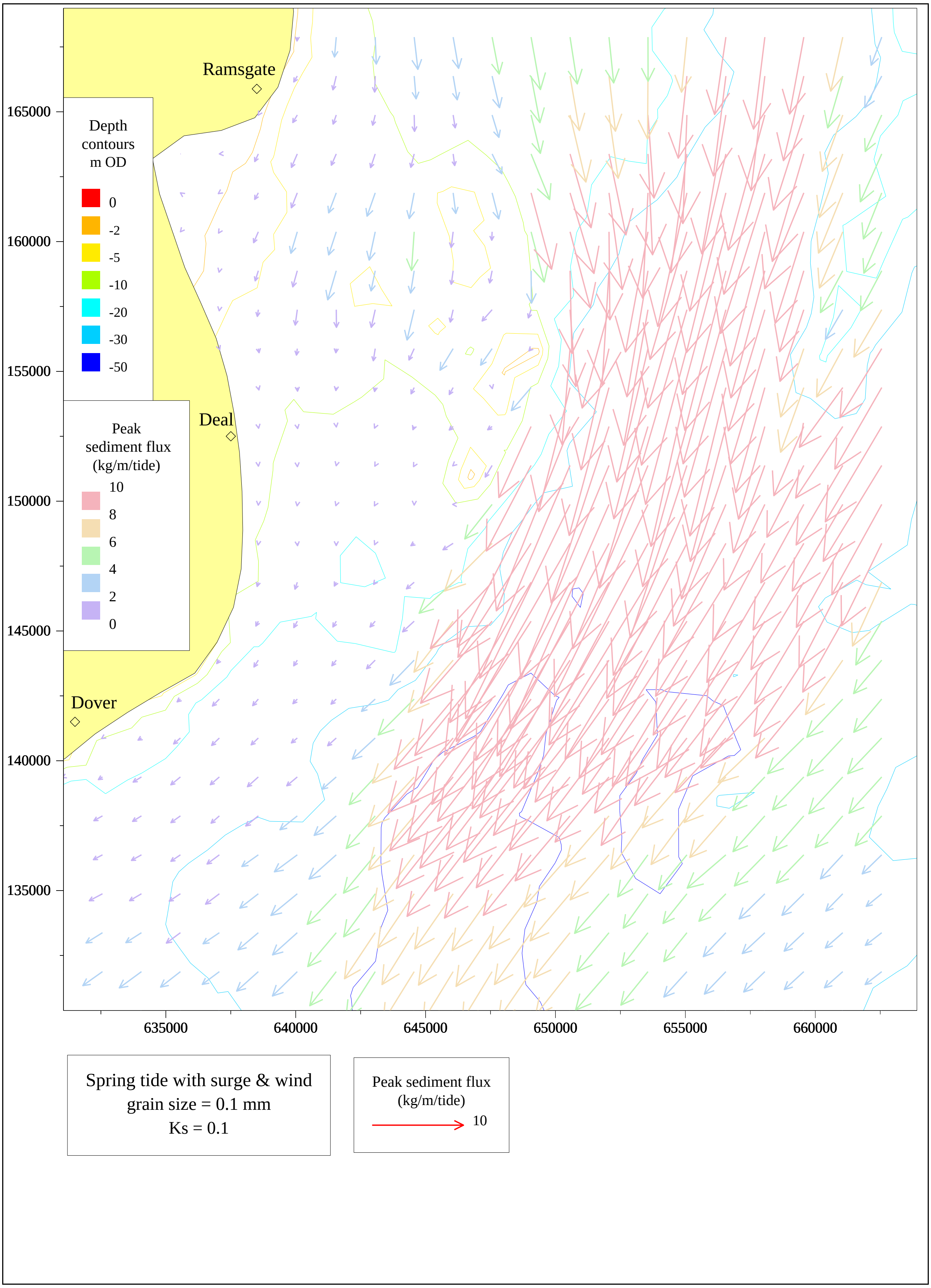

Figure 169 **Peak spring tide with surge net sediment flux patterns (0.1mm sand) detail: East Kent**

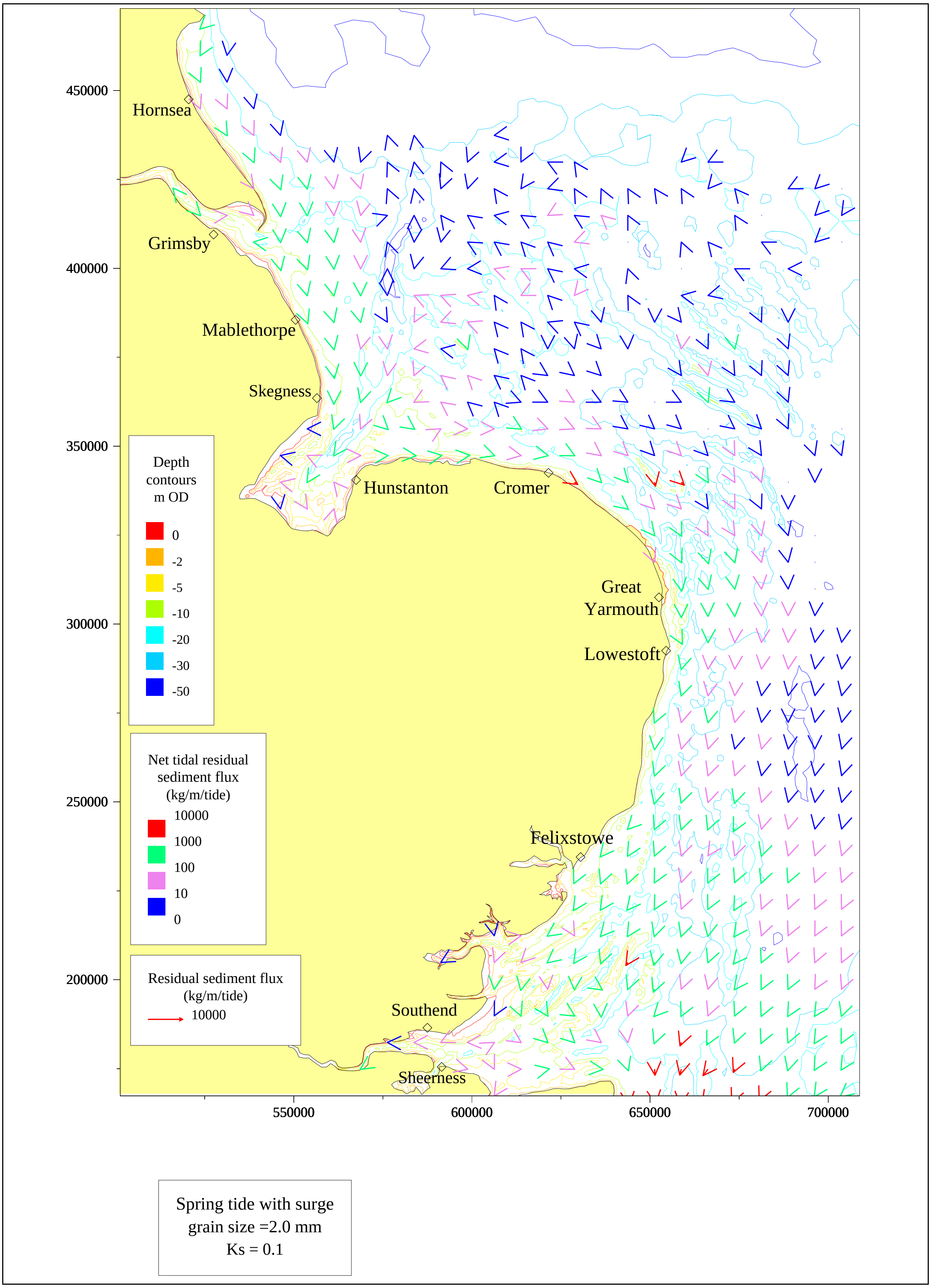

Figure 170 **Spring tide with surge net sediment flux patterns (2mm gravel)**

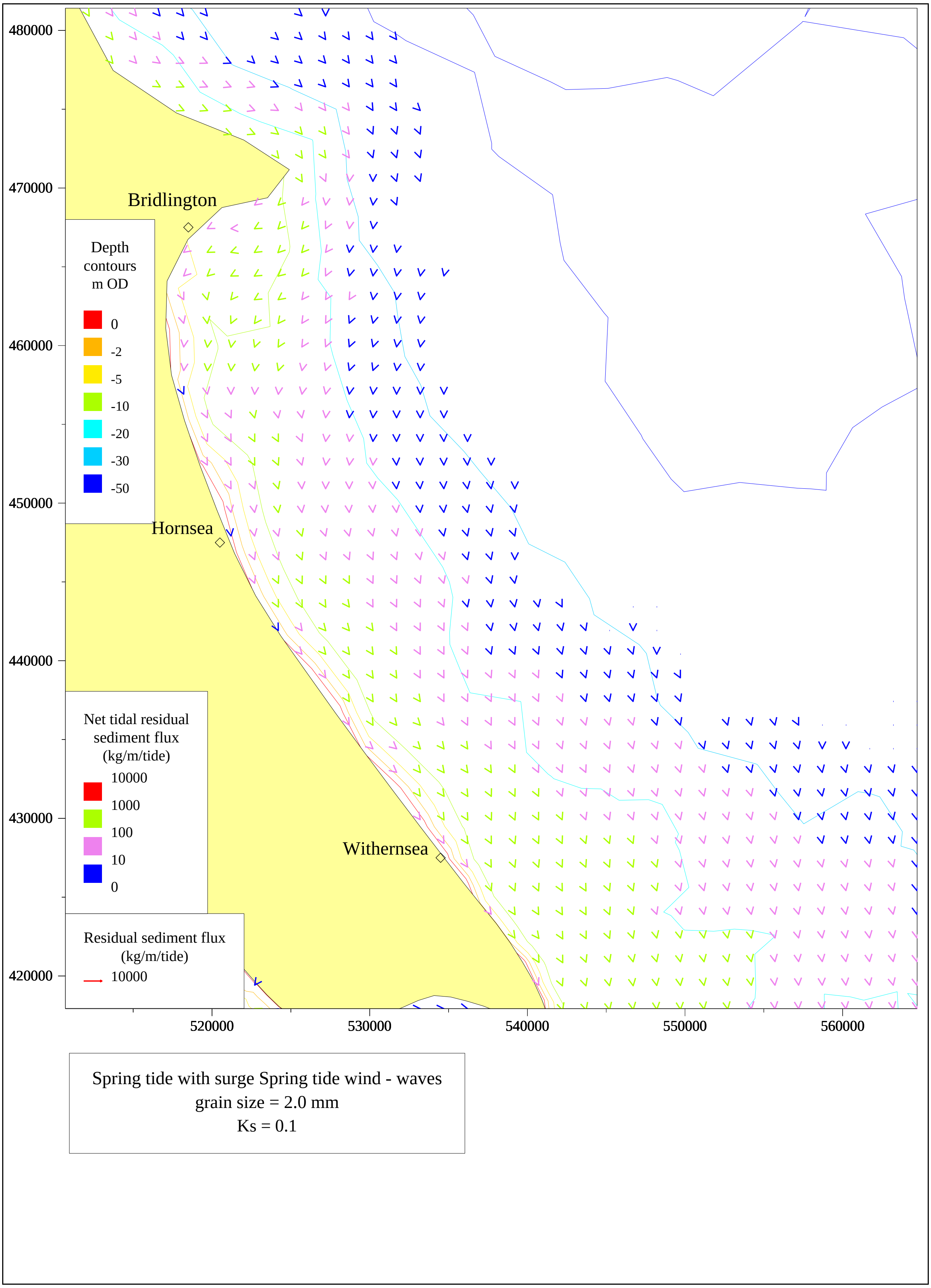

Figure 171 **Spring tide with surge net sediment flux patterns (2mm gravel) detail: Flamborough Head to Humber**

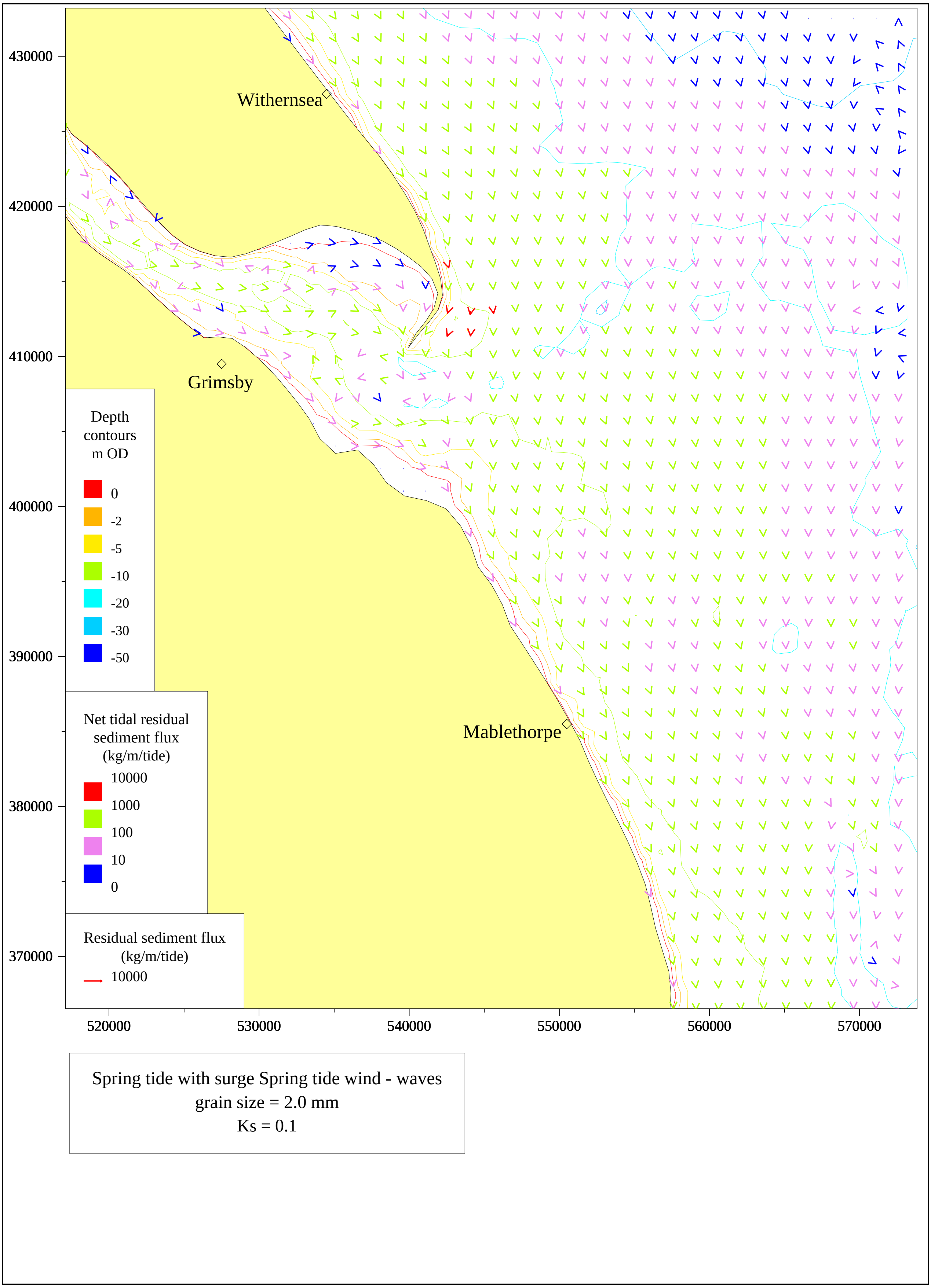

Figure 172 Spring tide with surge net sediment flux patterns (2mm gravel) detail: Humber Entrance and Lincolnshire

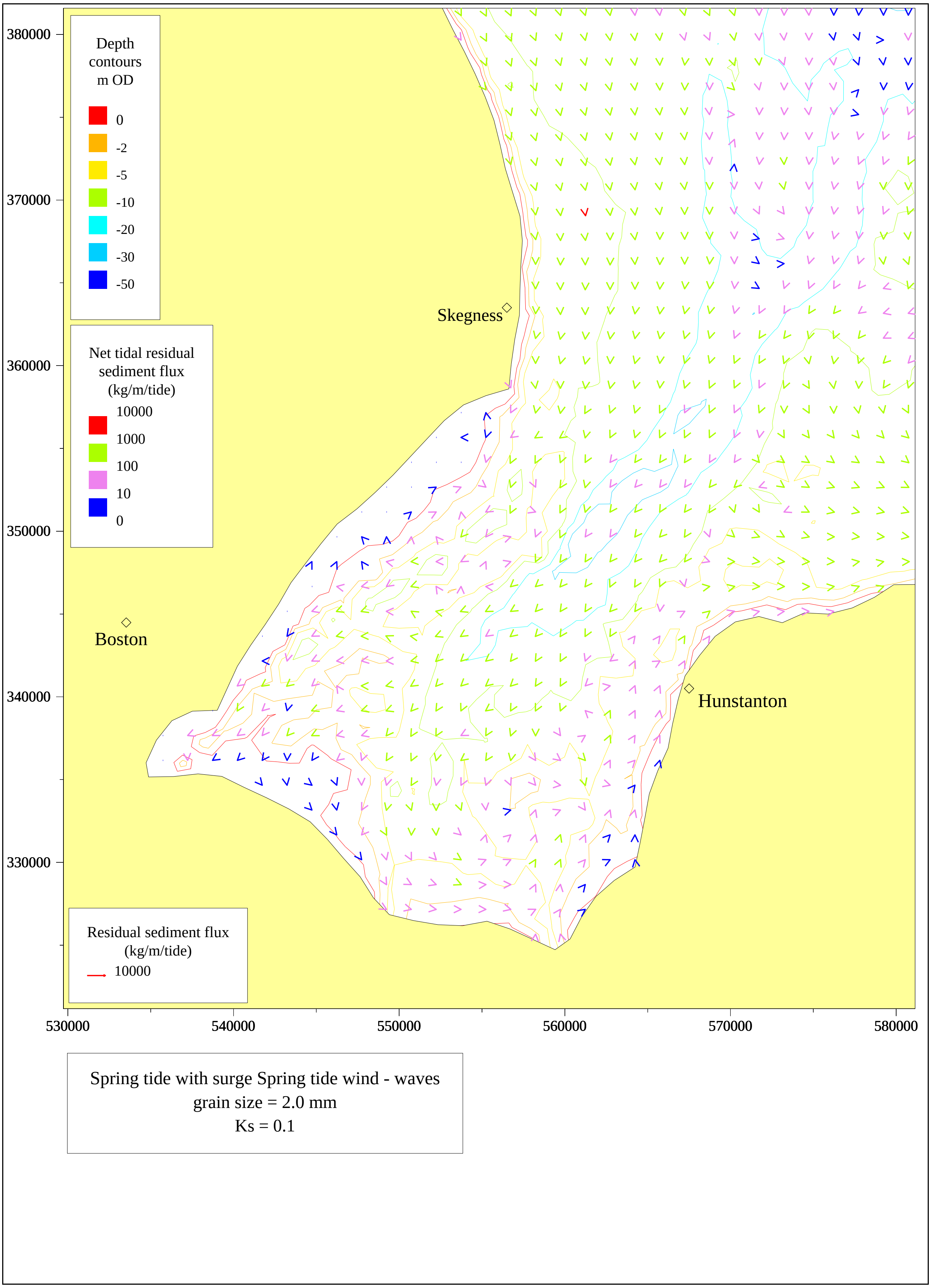

Figure 173 **Spring tide with surge net sediment flux patterns (2mm gravel) detail Lincolnshire and the Wash**

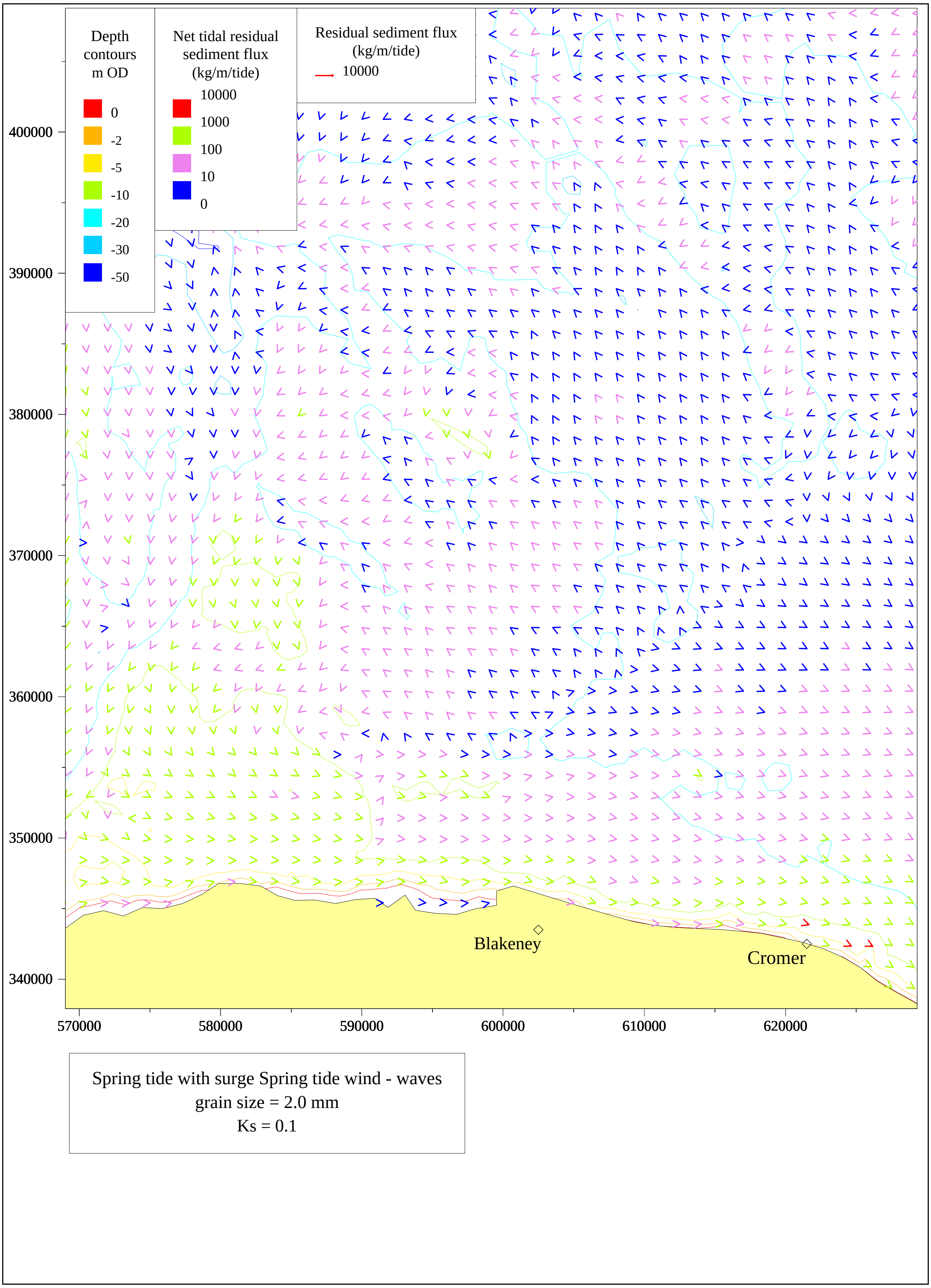

Figure 174 Spring tide with surge net sediment flux patterns (2mm gravel) detail: North Norfolk

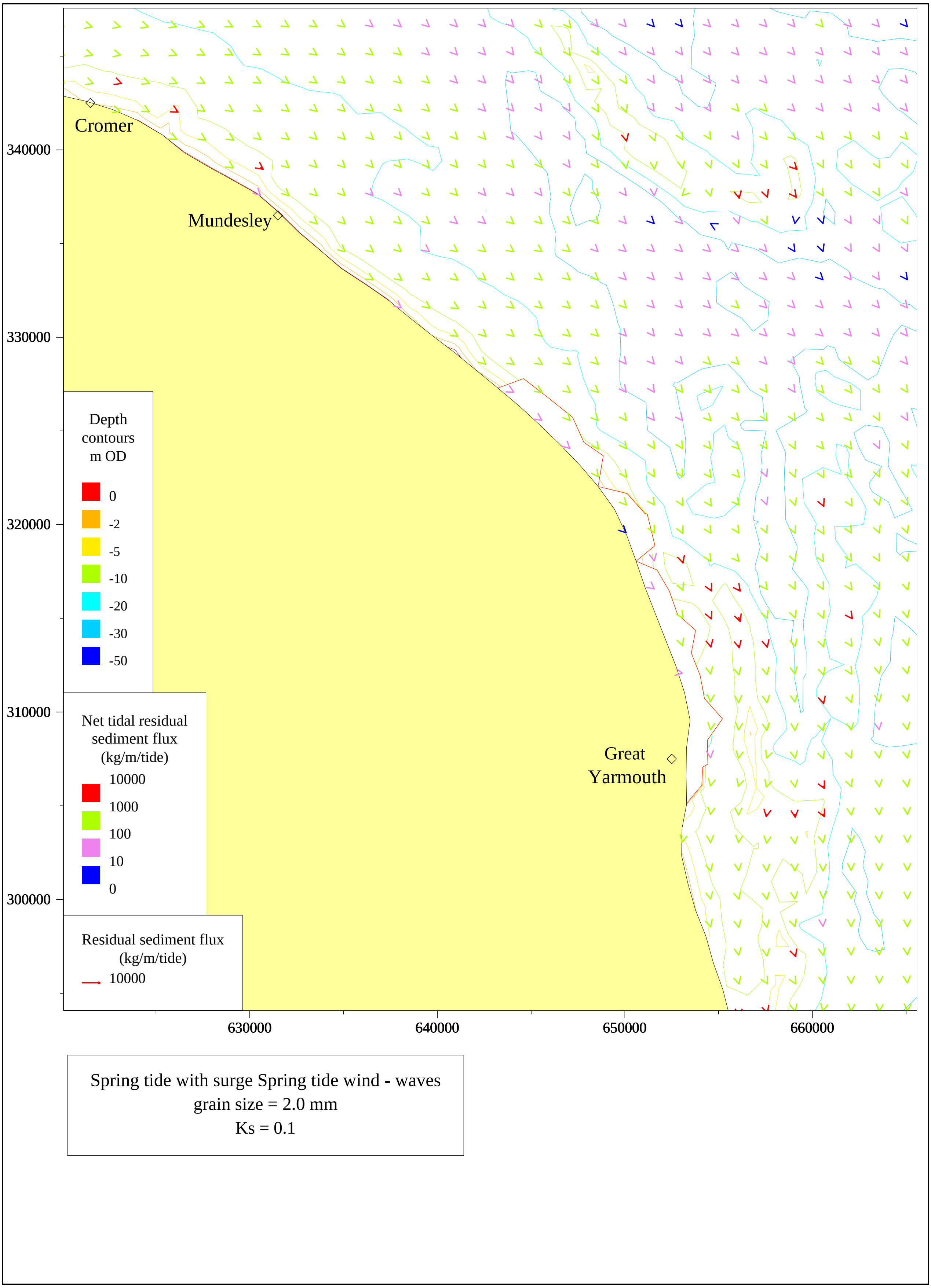

Figure 175 Spring tide with surge net sediment flux patterns (2mm gravel) detail: East Norfolk

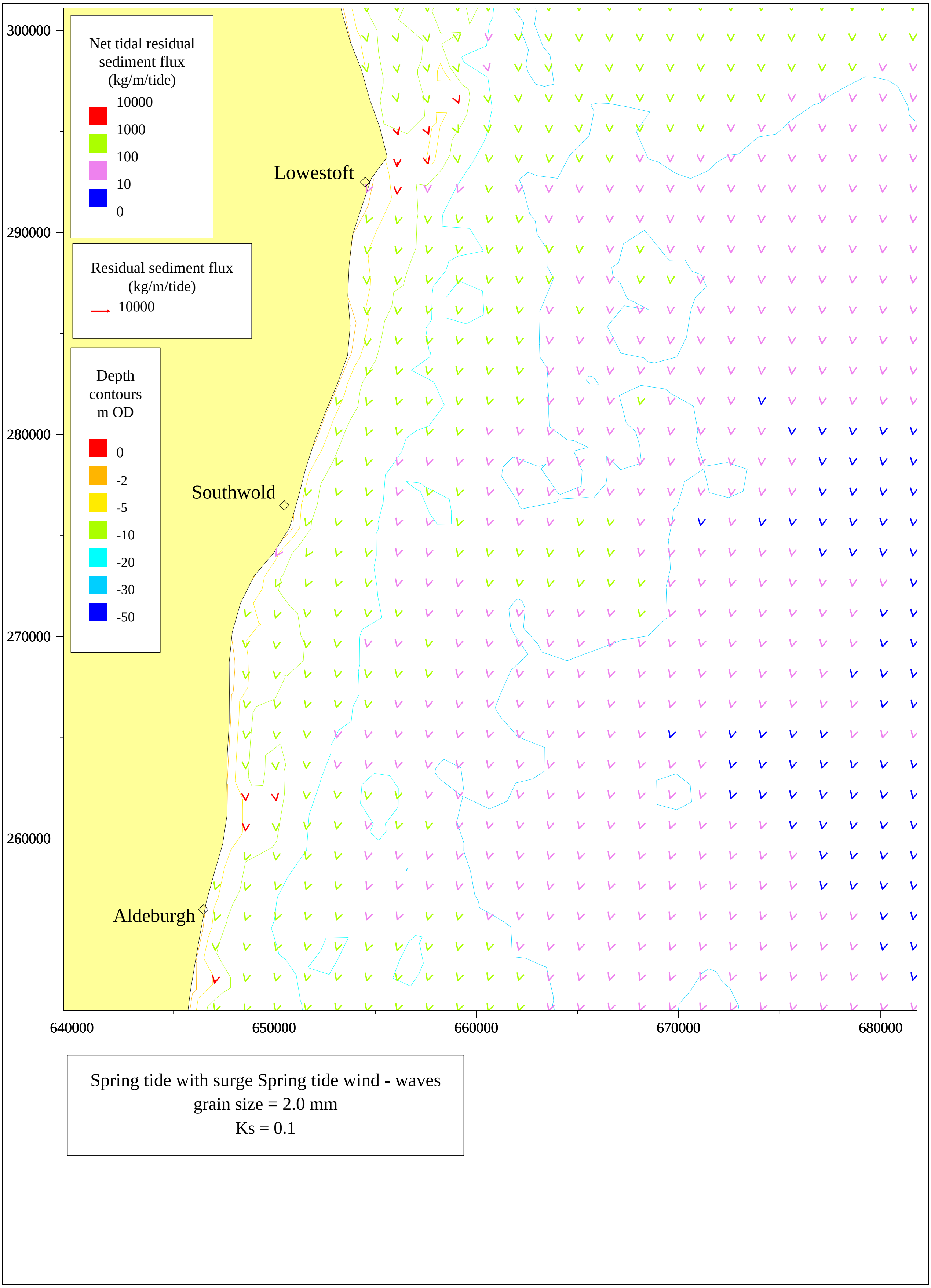

Figure 176 Spring tide with surge net sediment flux patterns (2mm gravel) detail: North Suffolk

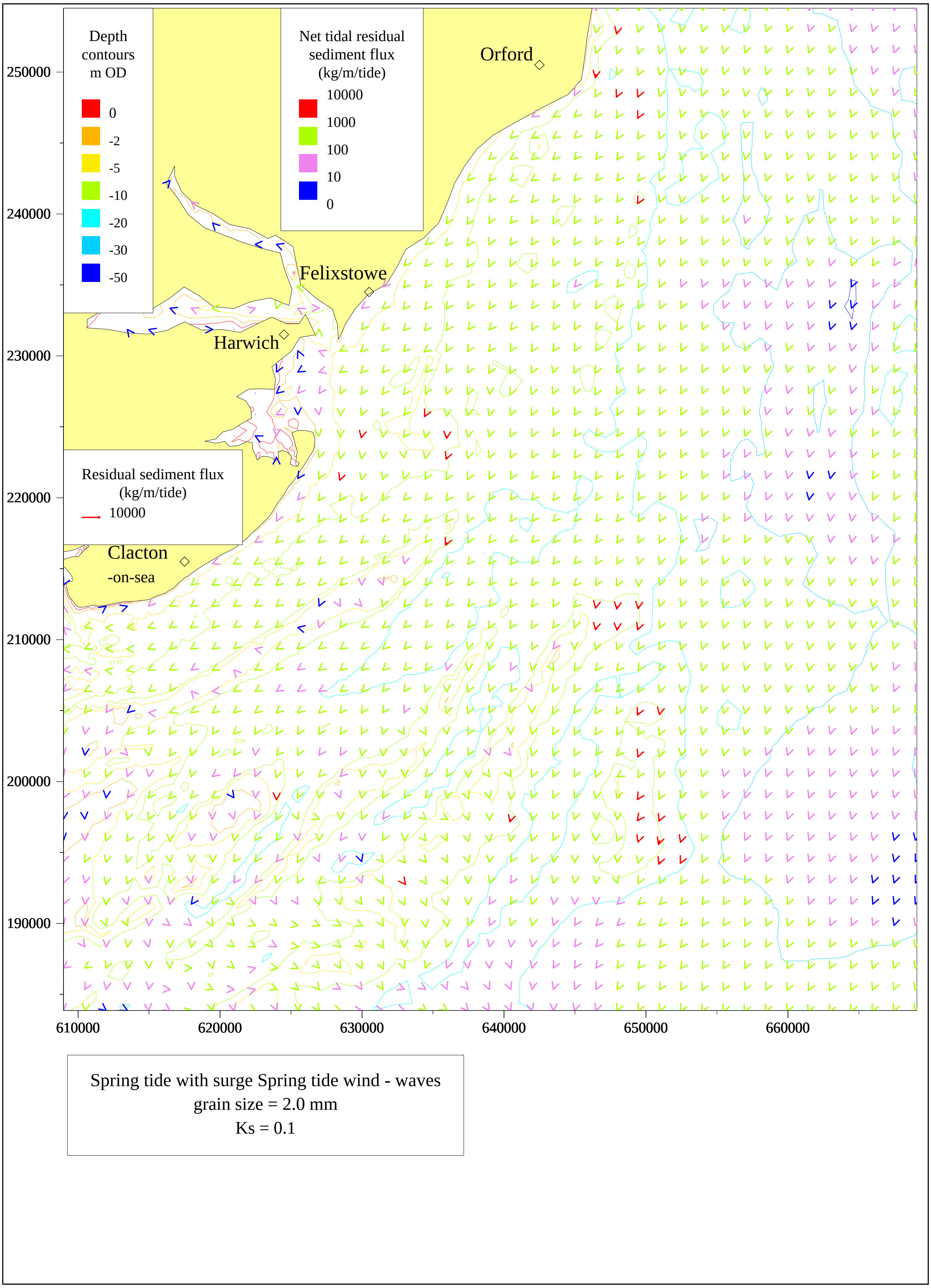

Figure 177 **Spring tide with surge net sediment flux patterns (2mm gravel) detail: Suffolk and Essex**

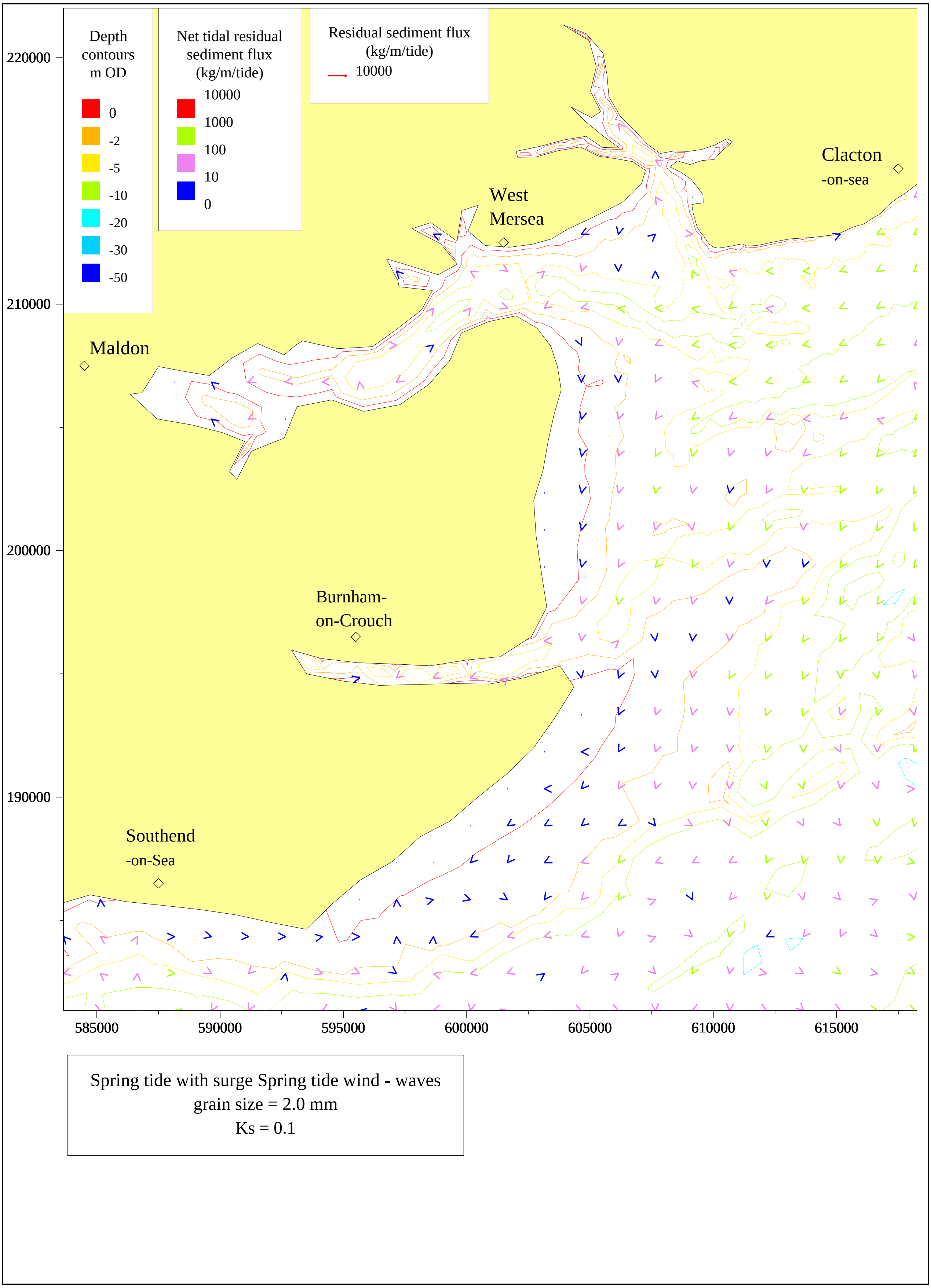

Figure 178 Spring tide with surge net sediment flux patterns (2mm gravel) detail: South Essex

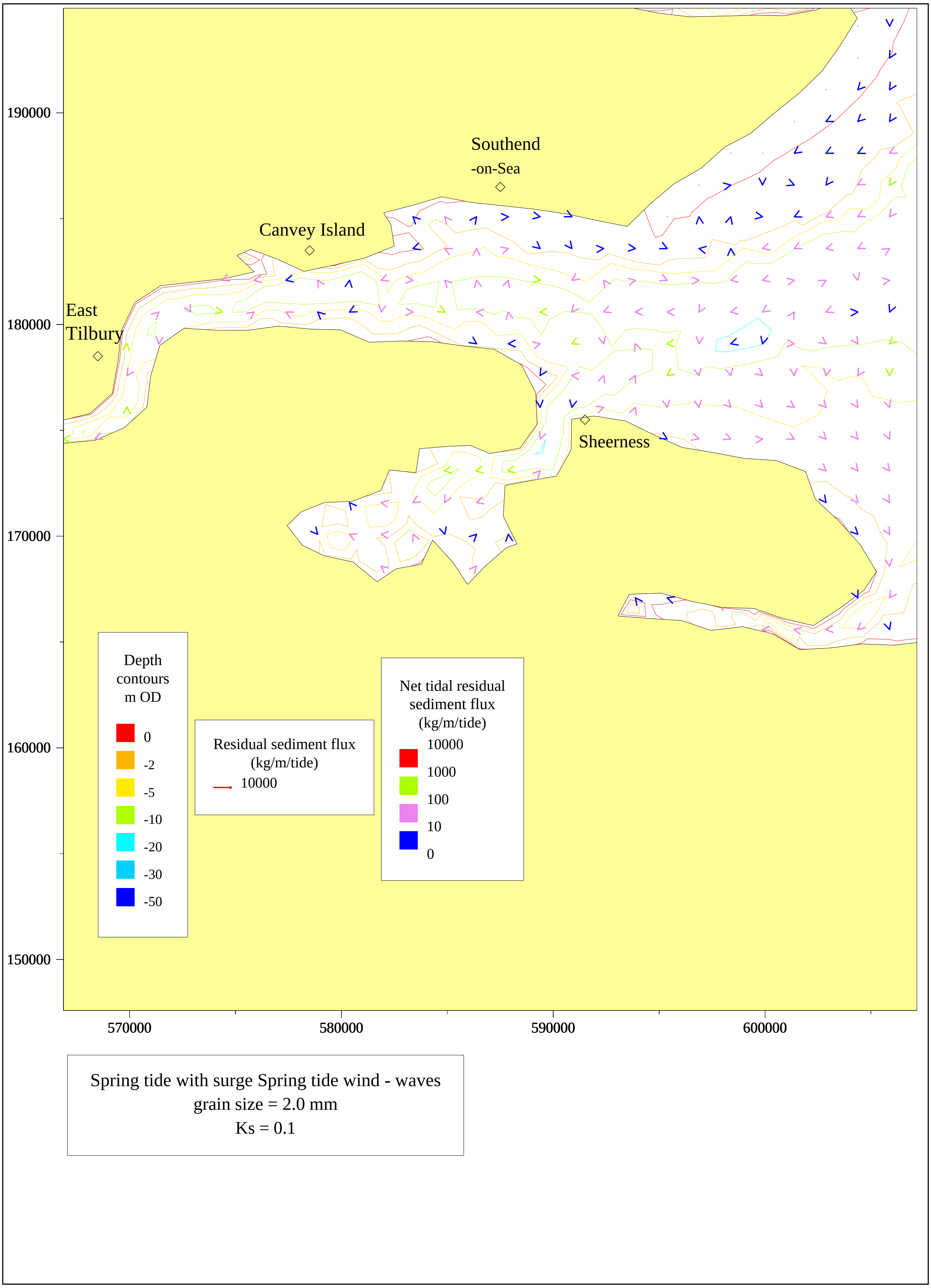

Figure 179 Spring tide with surge net sediment flux patterns (2mm gravel) detail: Outer Thames

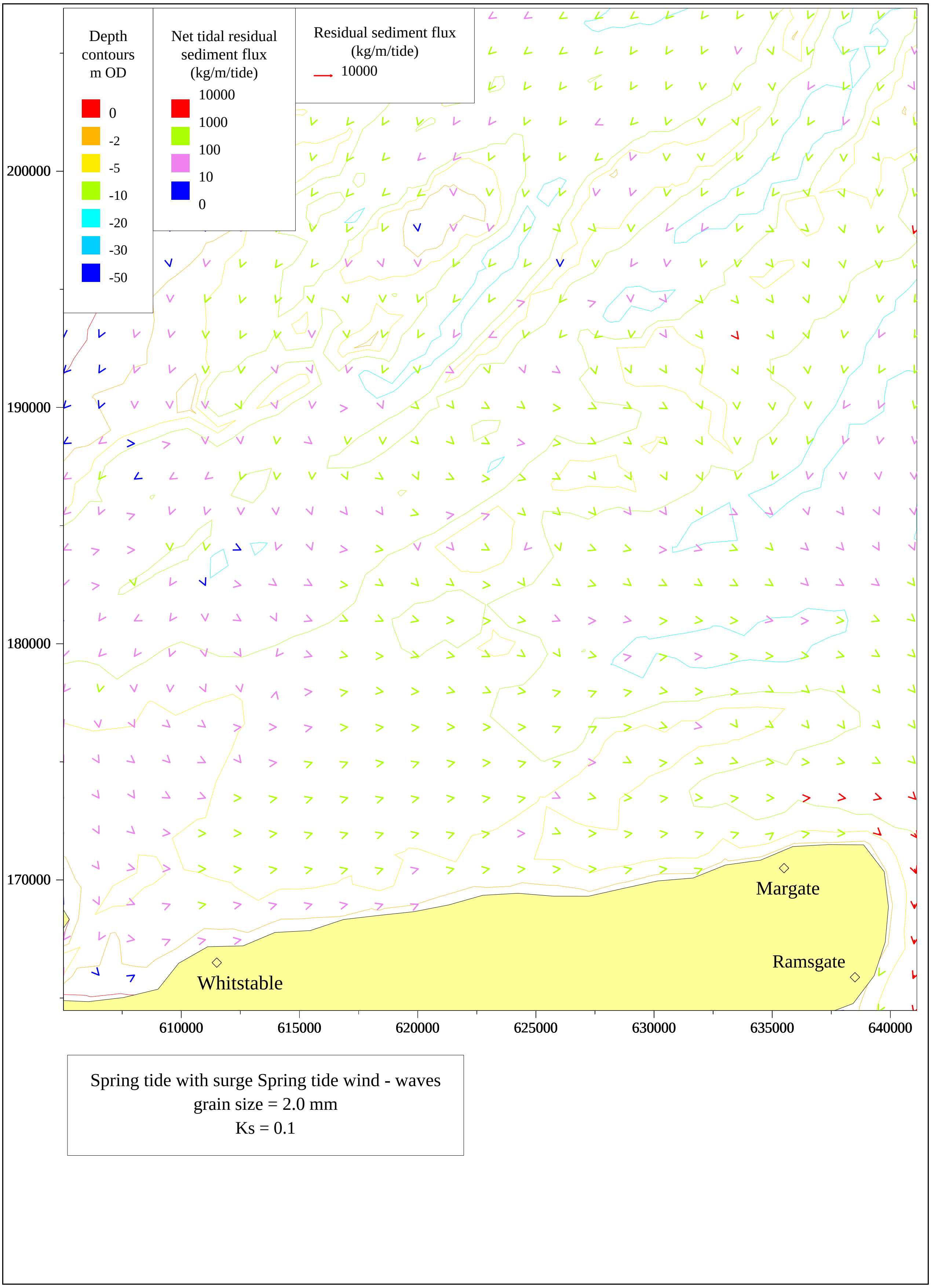

Figure 180 Spring tide with surge net sediment flux patterns (2mm gravel) detail: North Kent

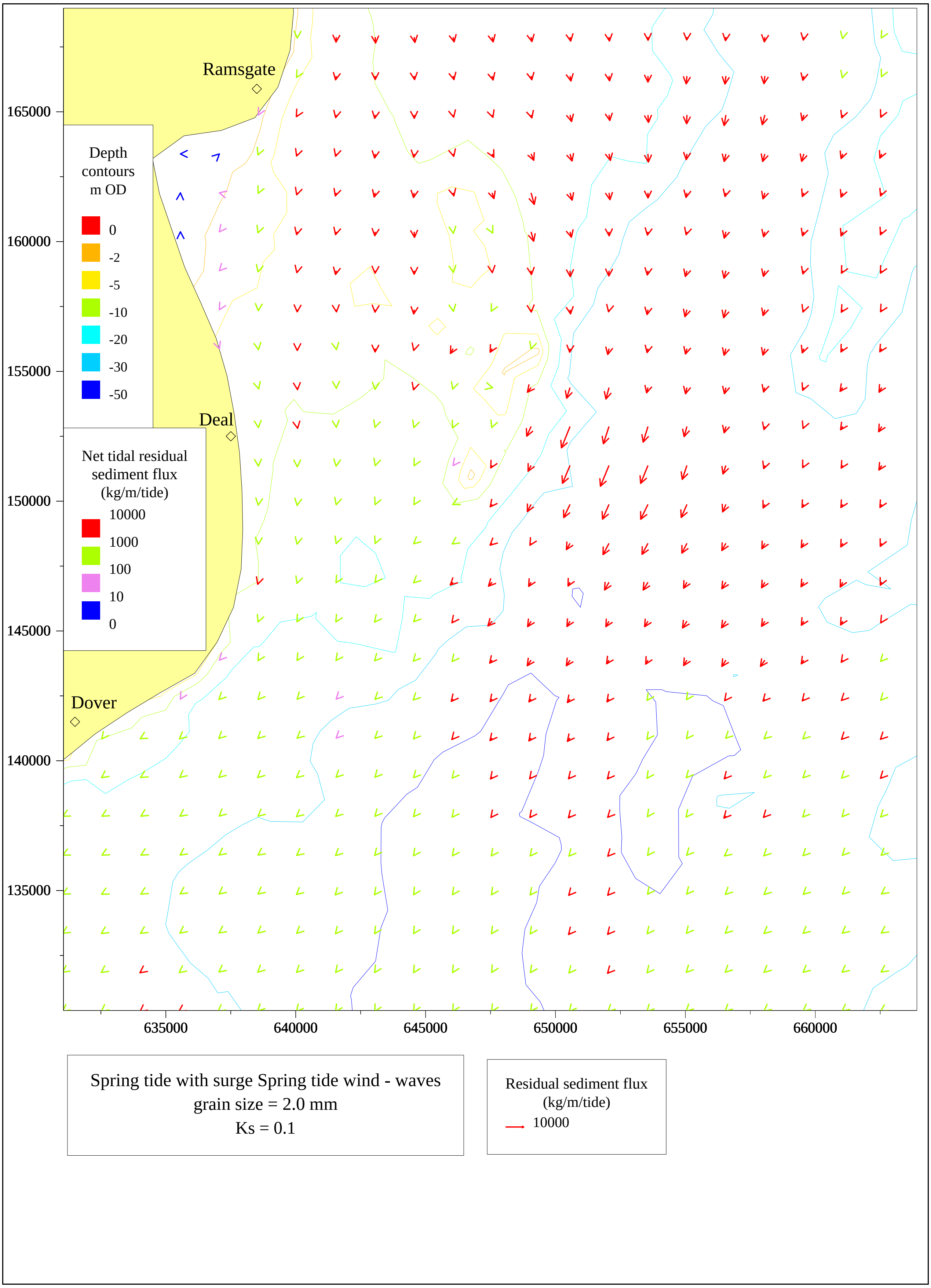

Figure 181 **Spring tide with surge net sediment flux patterns (2mm gravel) detail: East Kent**

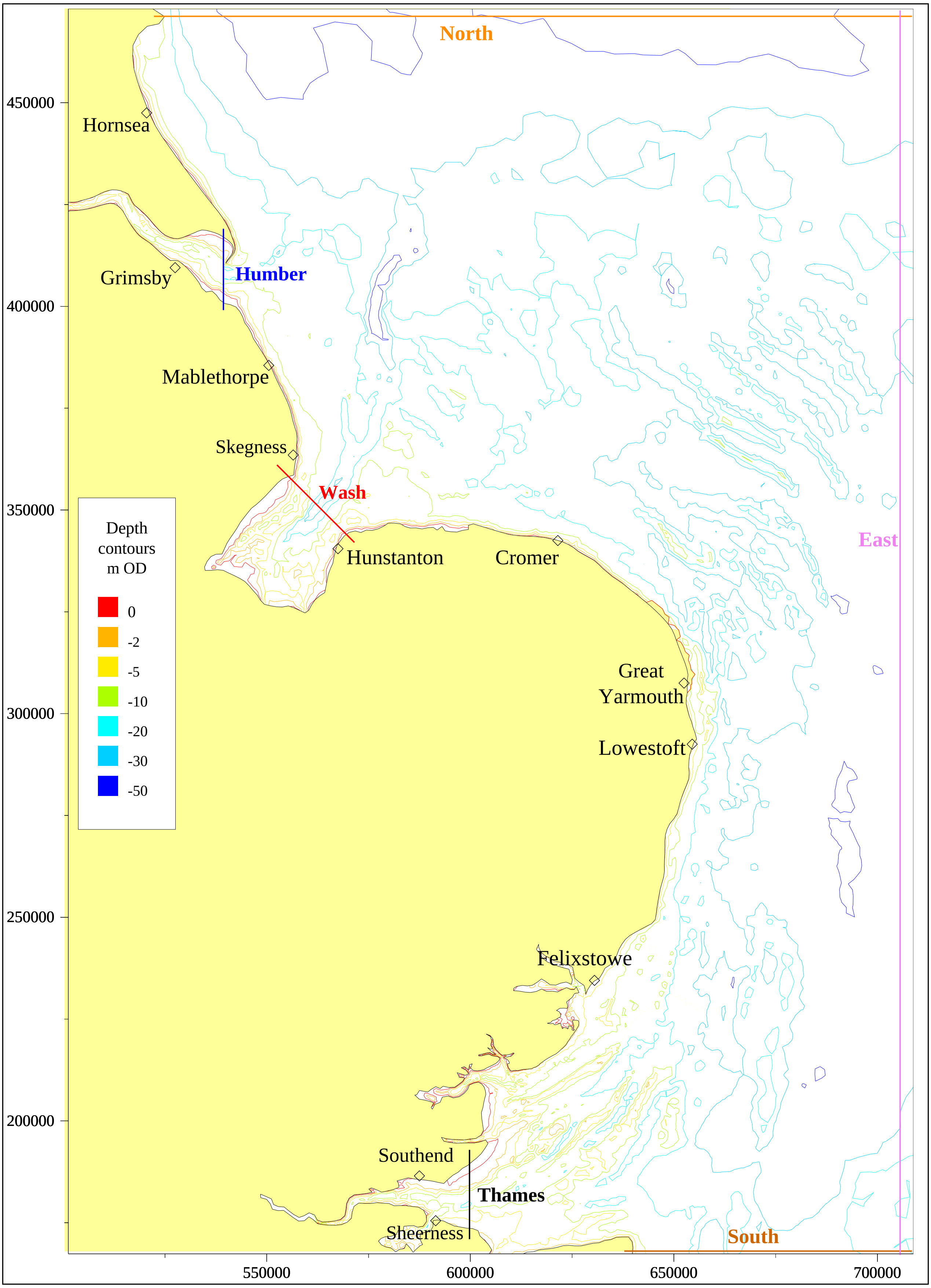

Figure 182 Model boundaries for flux integration

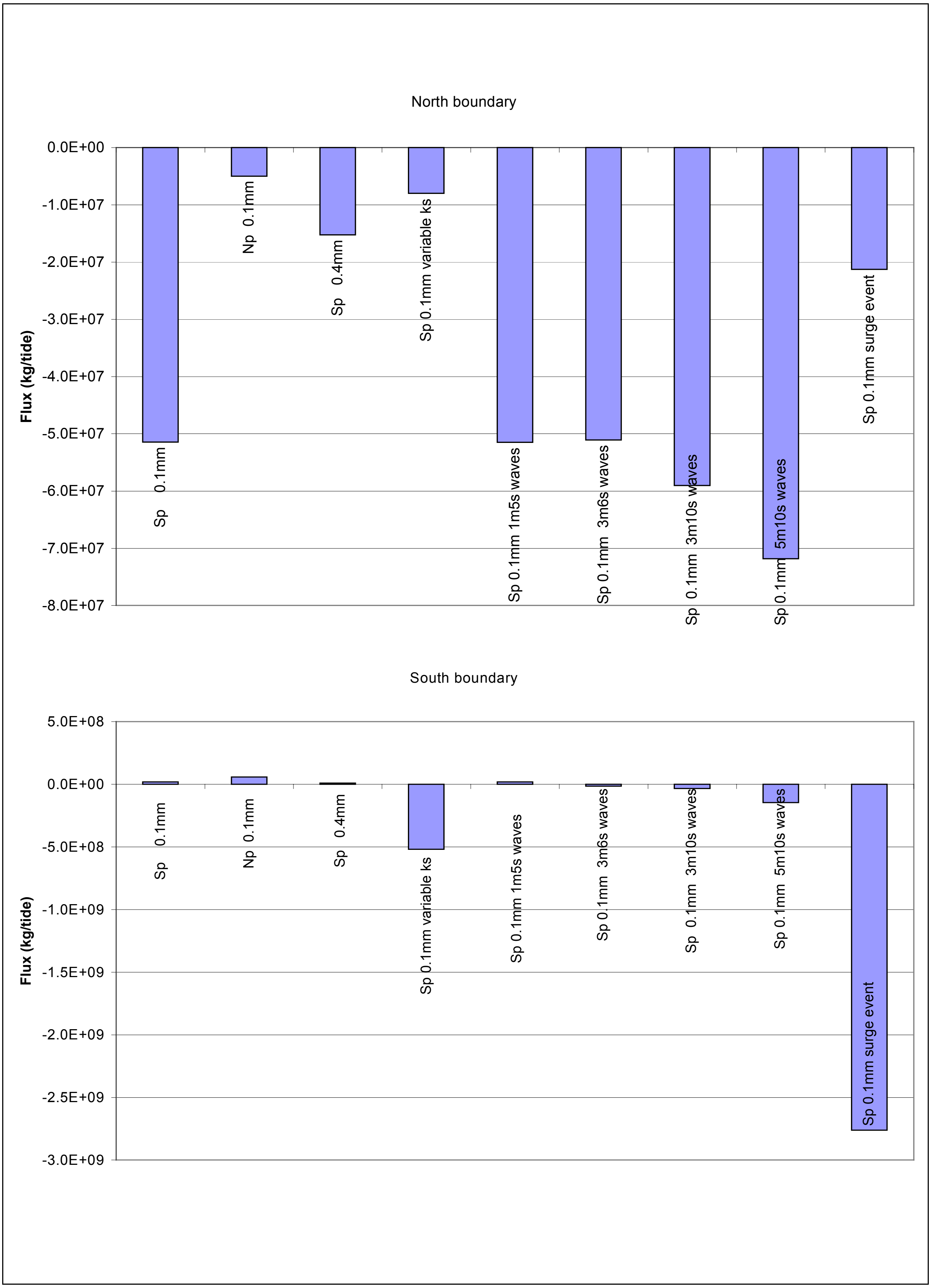

Figure 183a Integrated fluxes through model boundaries: North and south

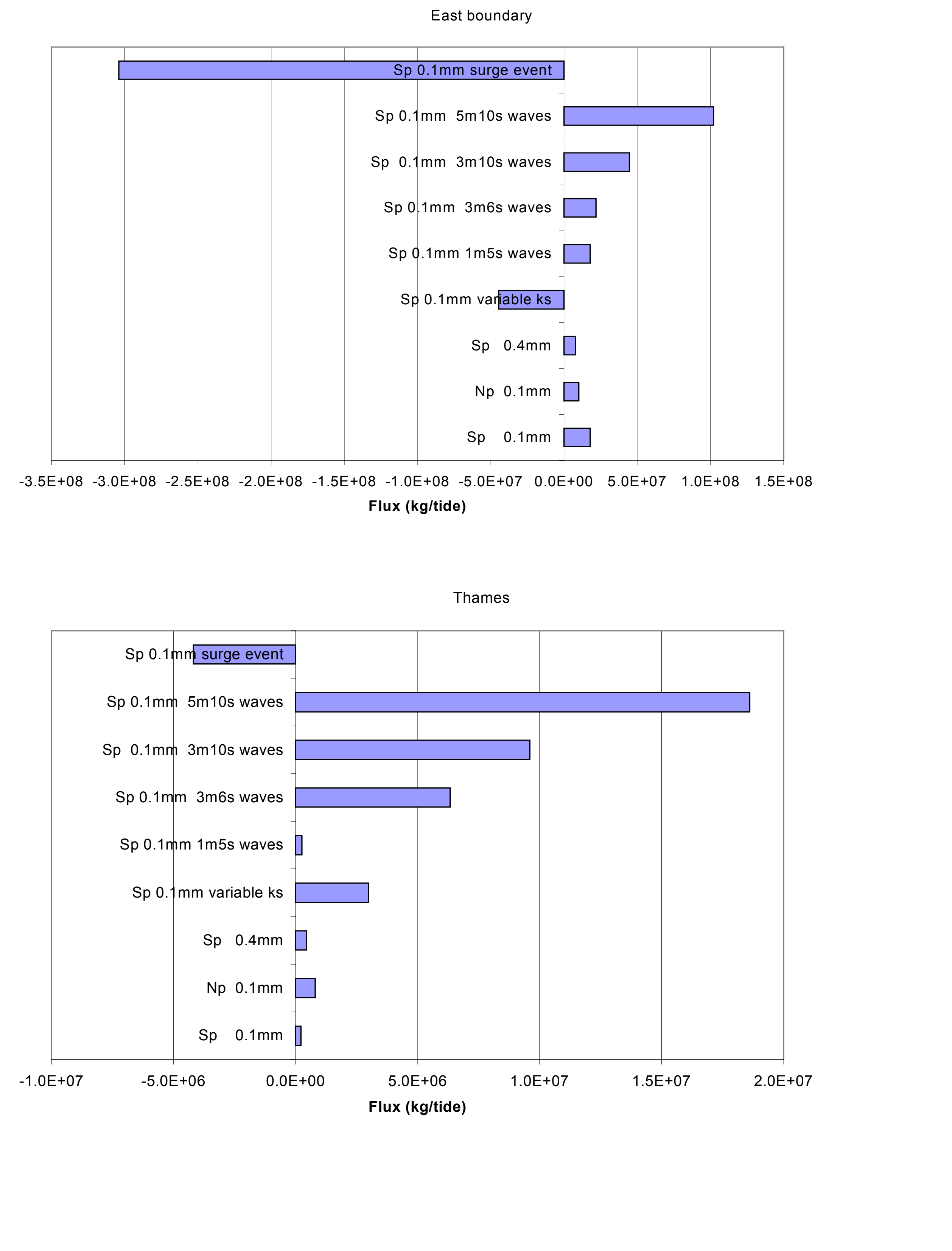

Figure 183b Integrated fluxes through model boundaries: East and Thames

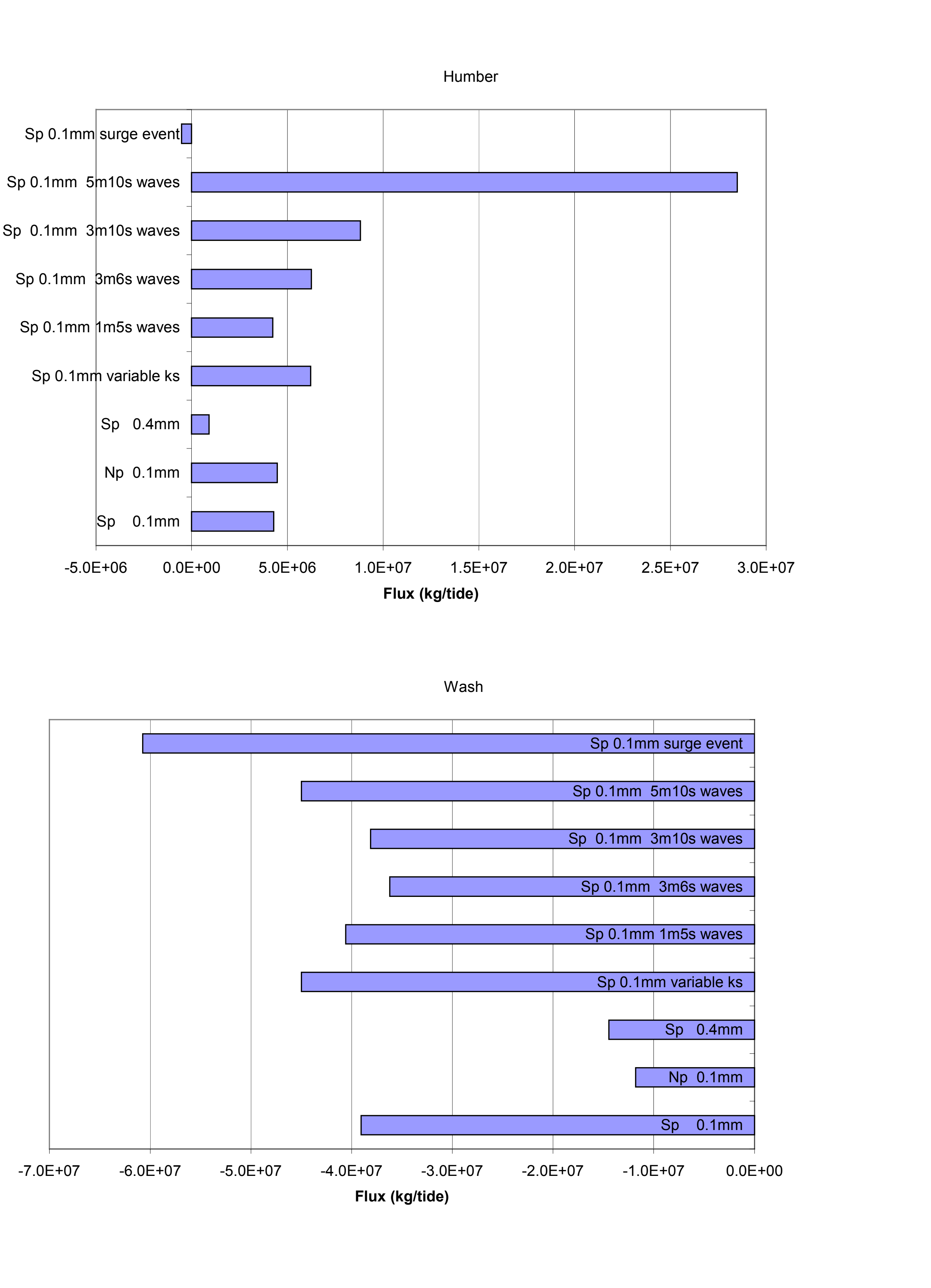

Figure 183c Integrated fluxes through model boundaries: Humber and Wash

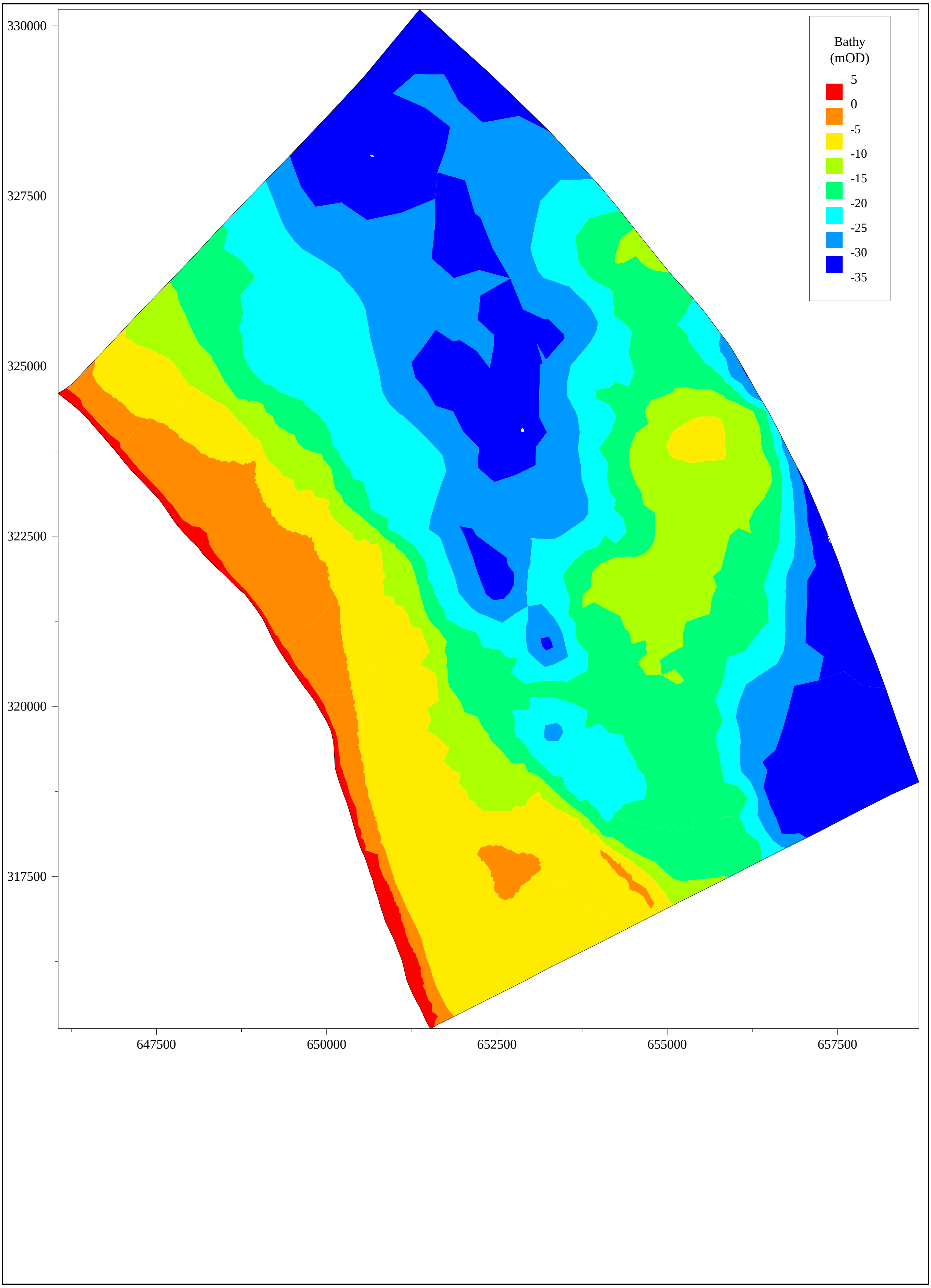

Figure 184 **Winterton Ness local area model bathymetry**

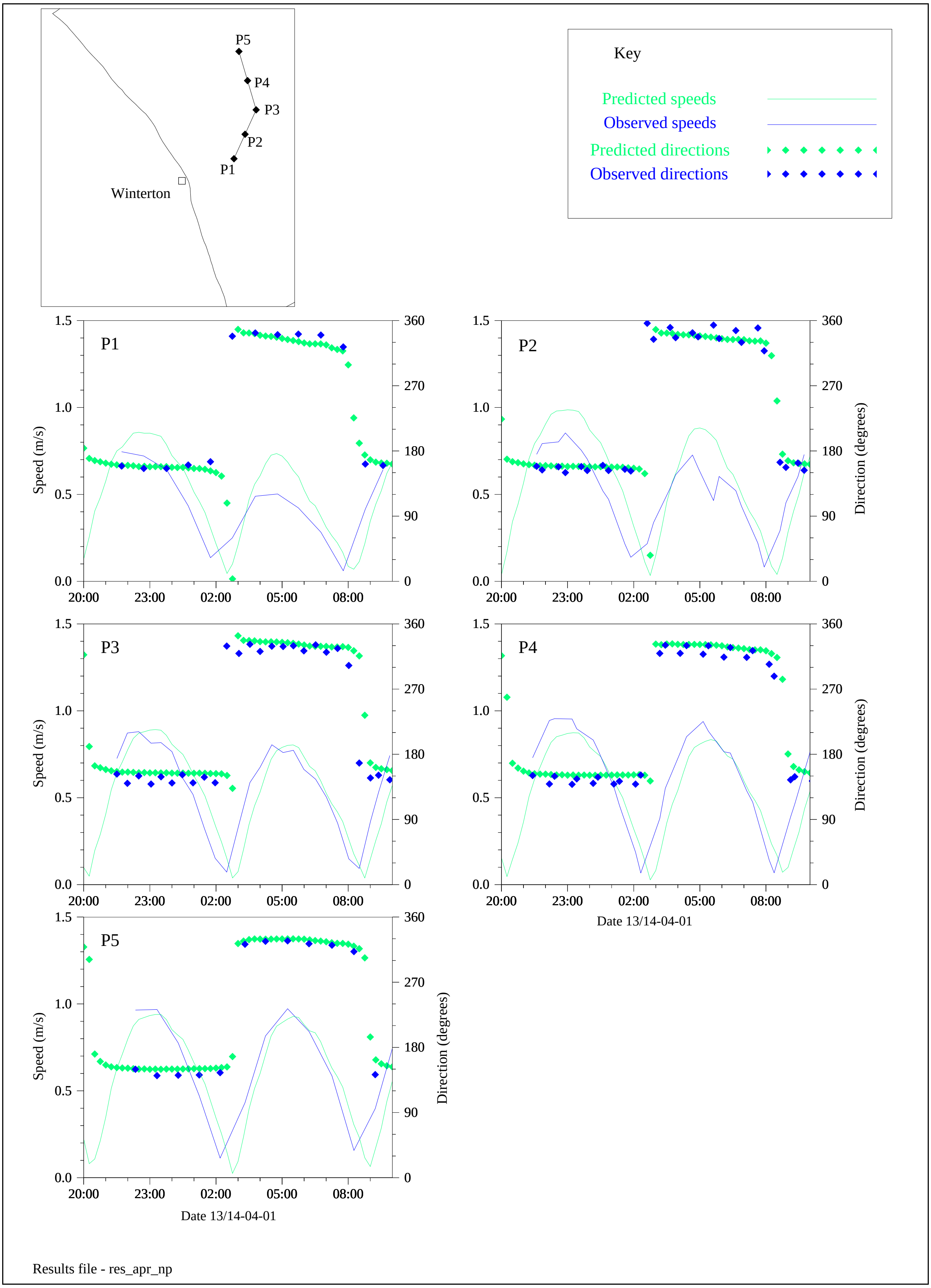

Figure 185 Comparison of model predictions with measured current speed and direction

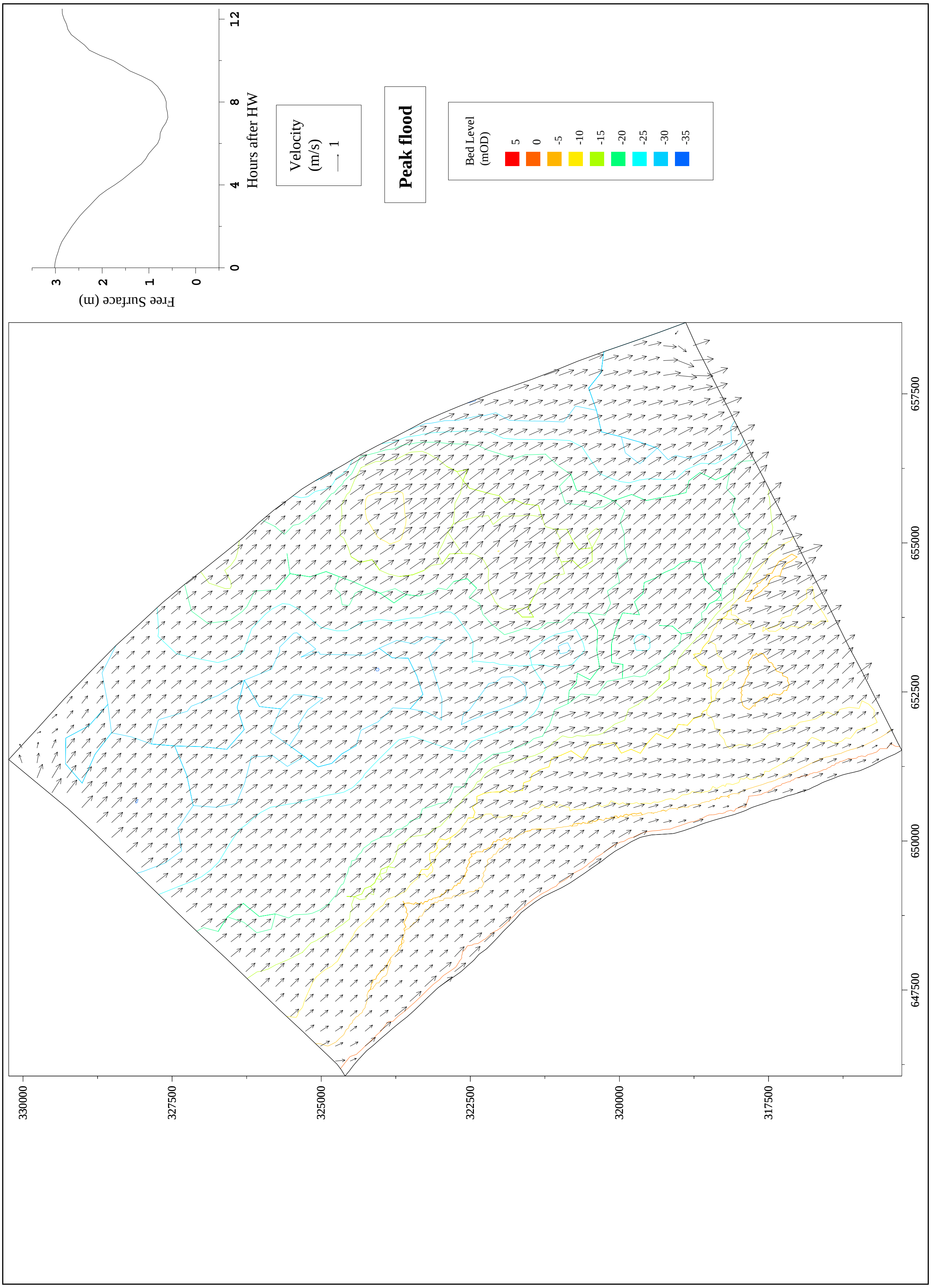

Figure 186 Peak flood current speeds on spring tide

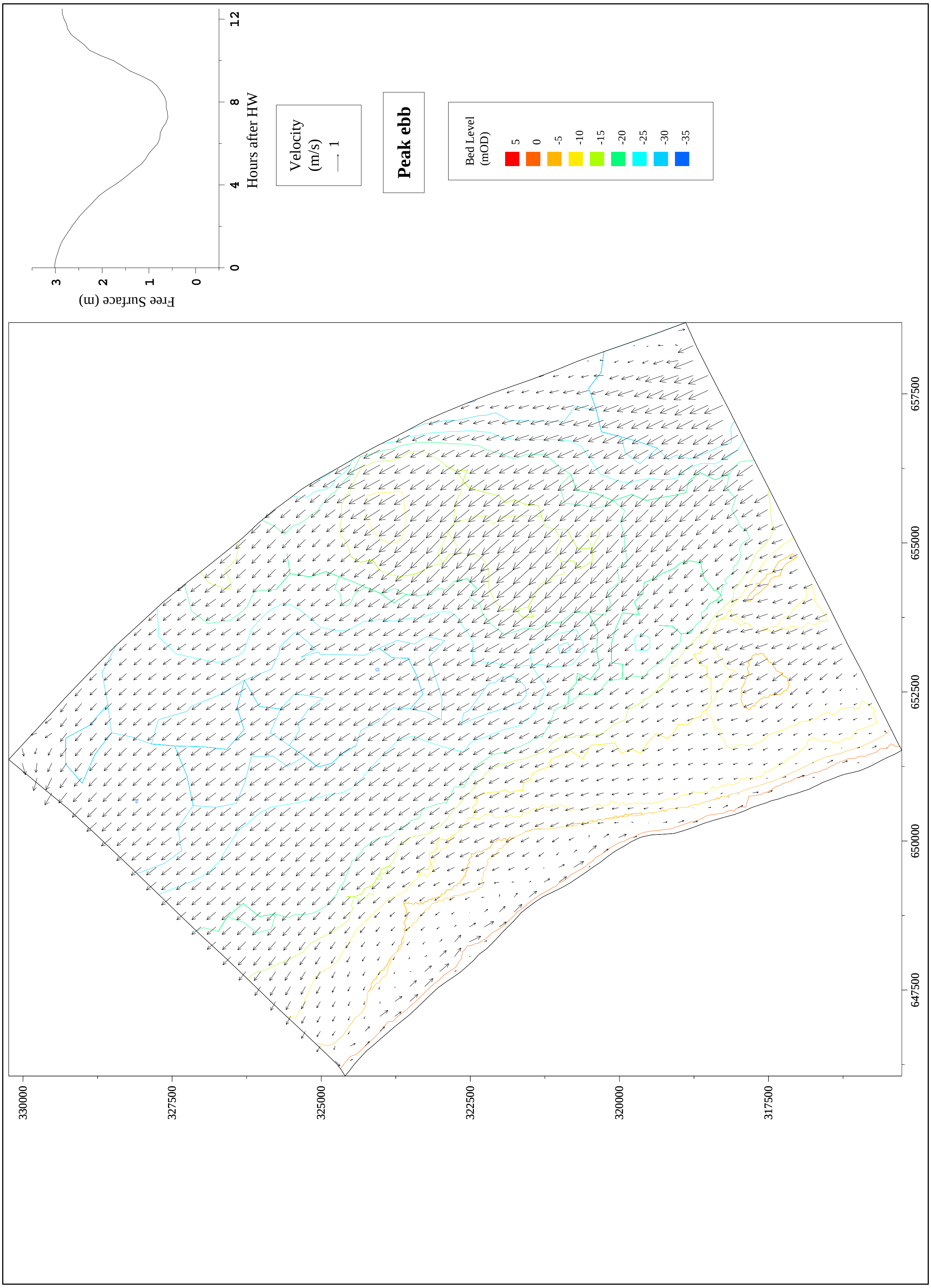

Figure 187 Peak ebb current on spring tide

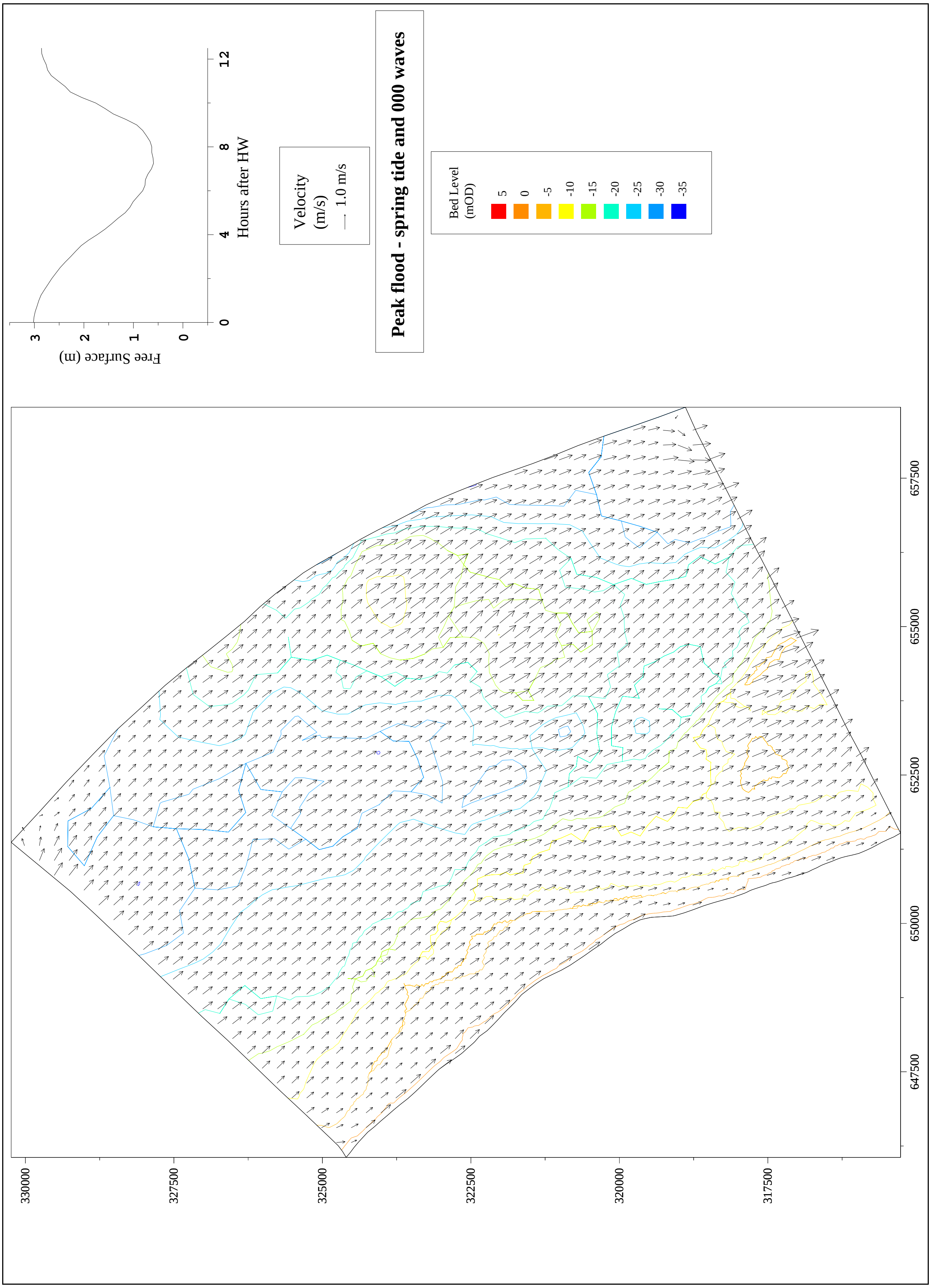

Figure 188 Peak flood current speeds on spring tide with waves from the north

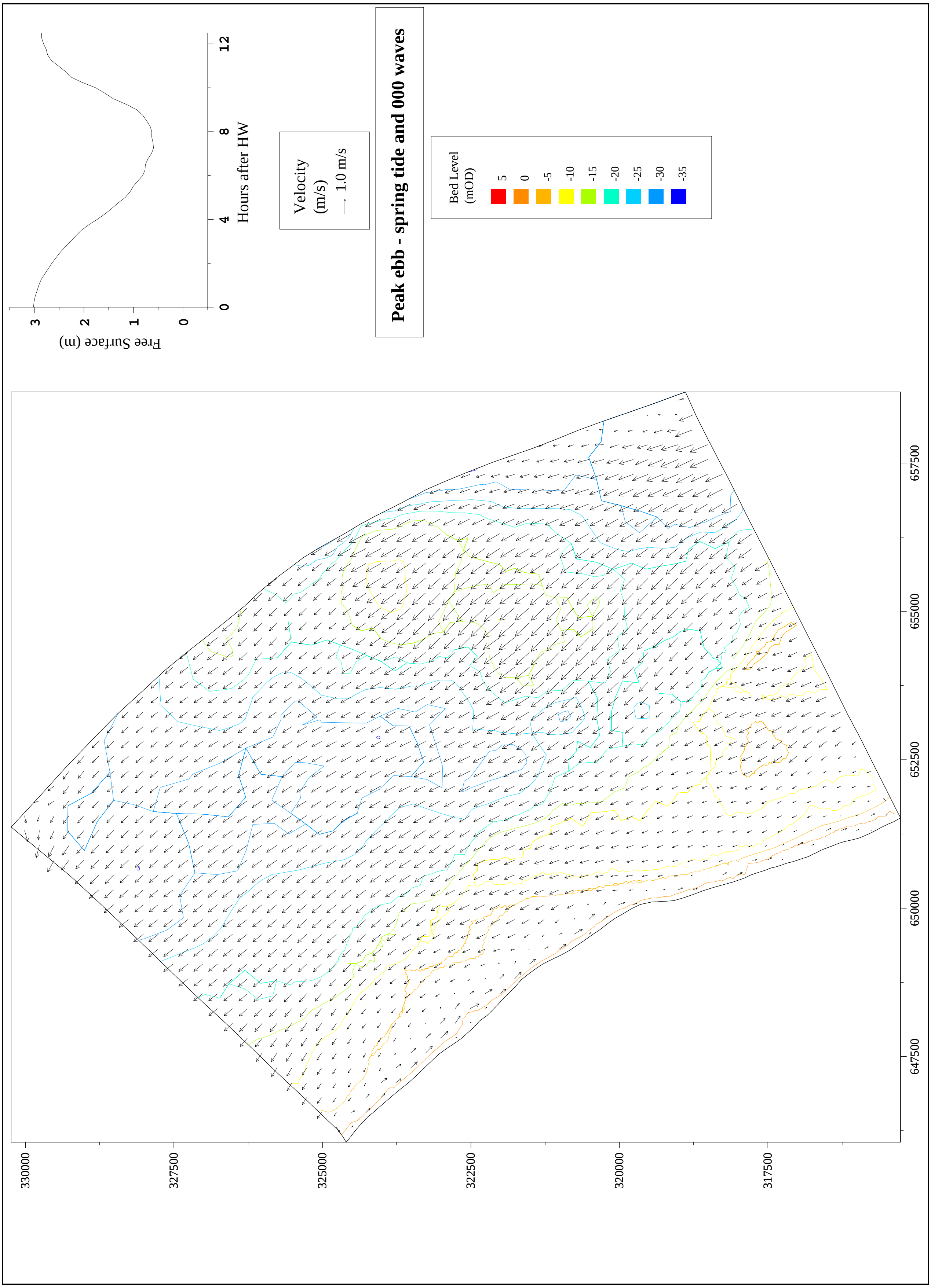

Figure 189 Peak ebb current on spring tide with waves from the north

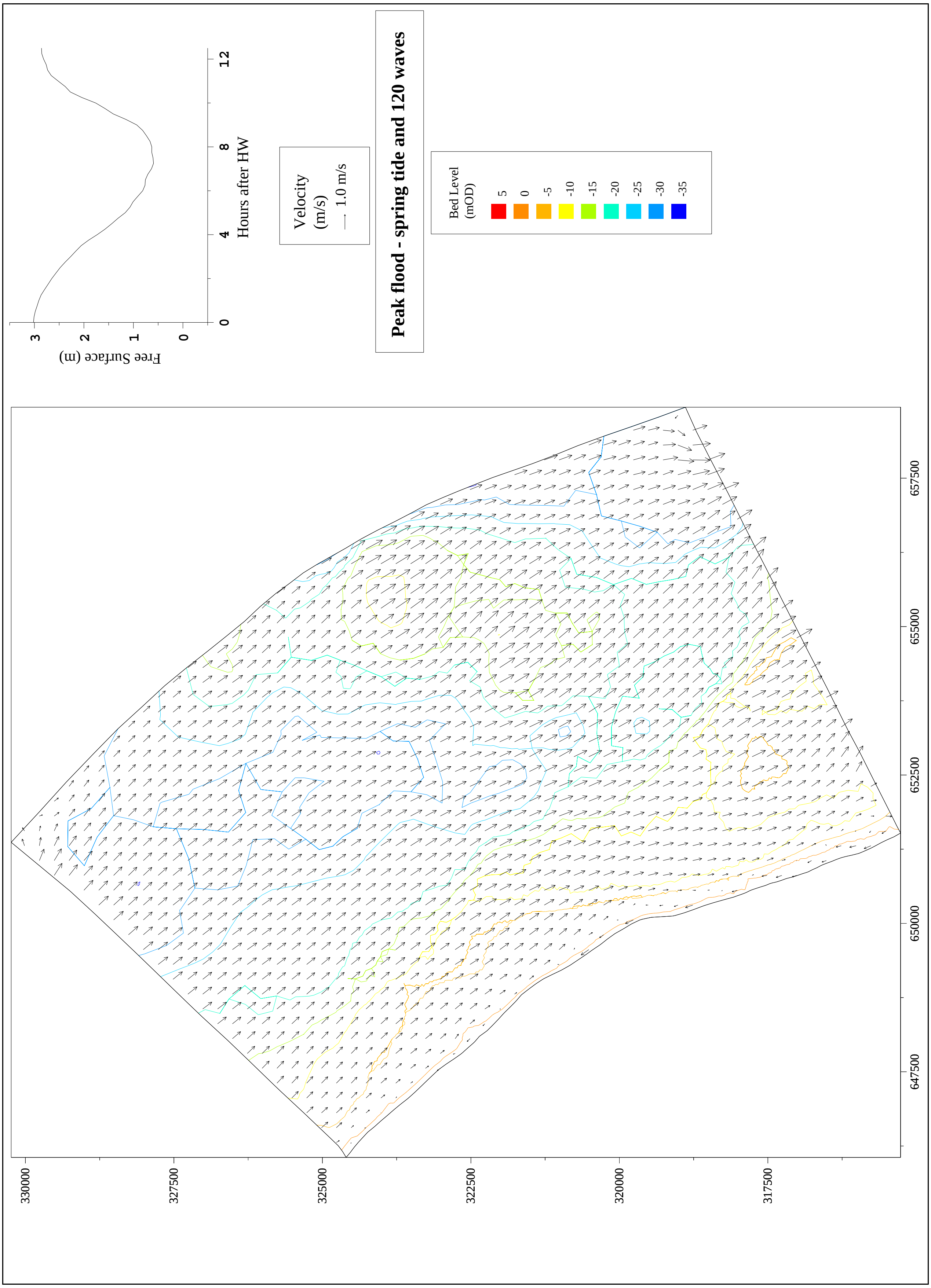

Figure 190 Peak flood current speeds with waves from the southwest quadrant (120°N)

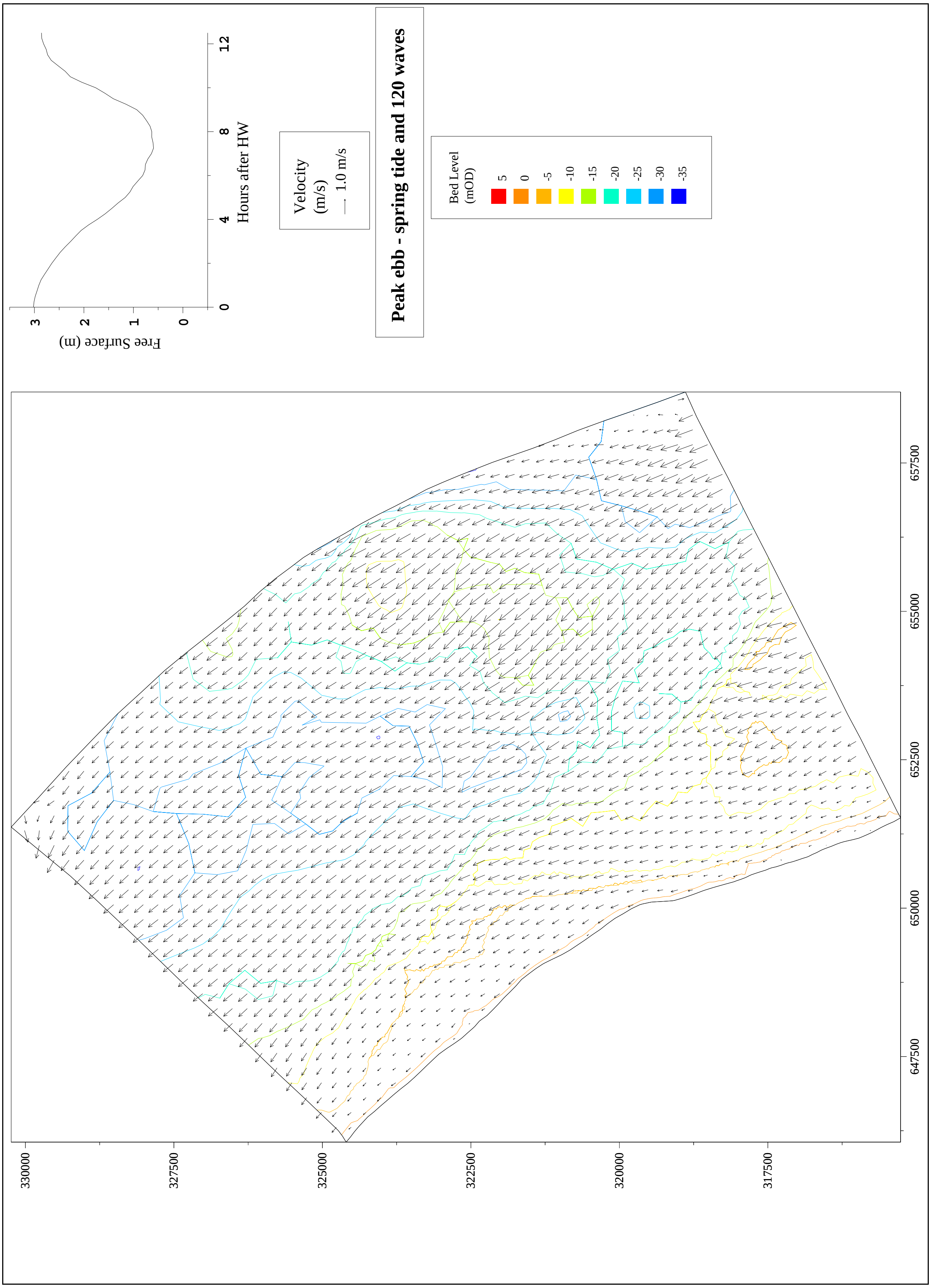

Figure 191 Peak ebb current speeds with waves from the southwest quadrant (120°N)

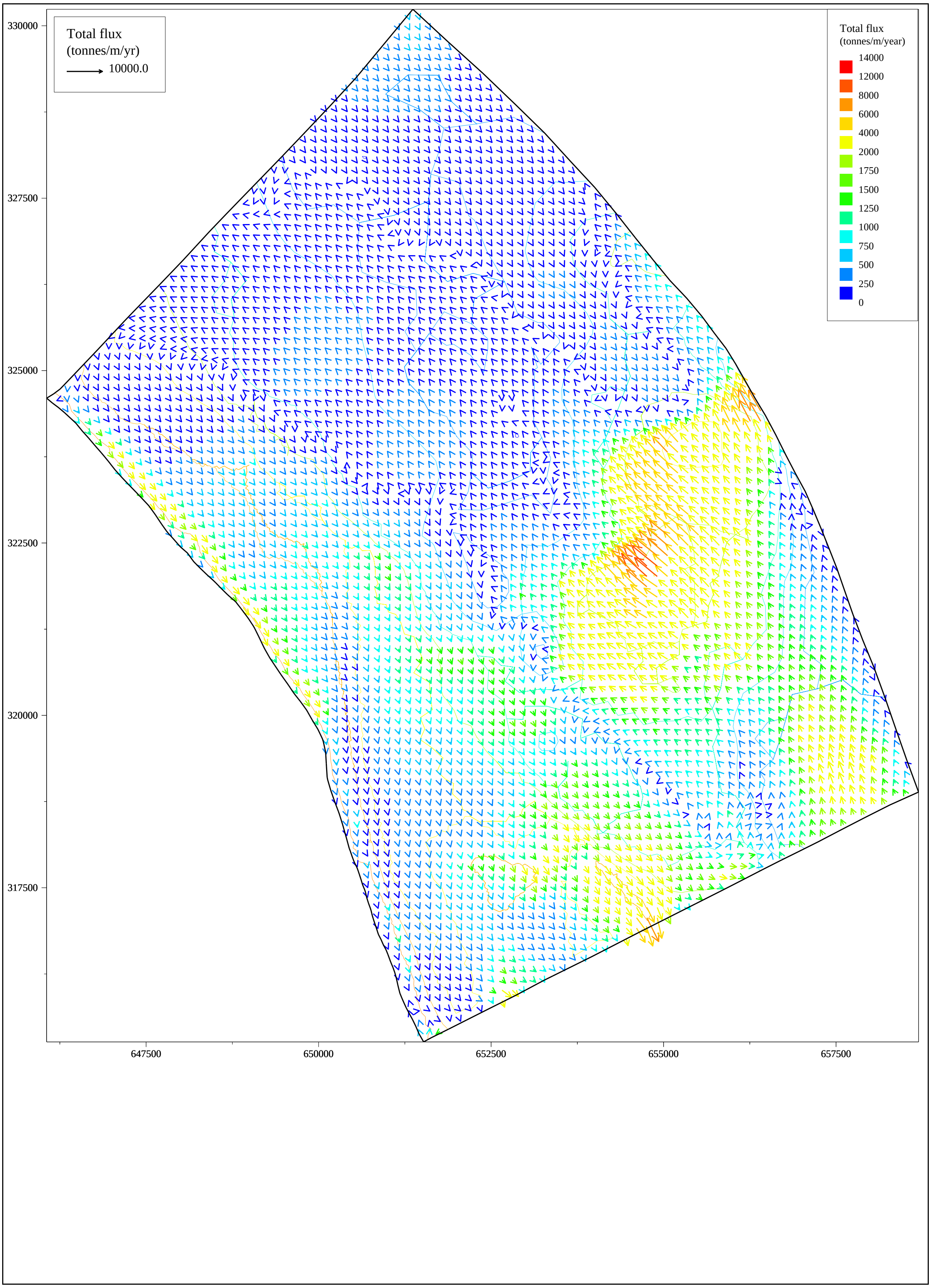

Figure 192 Net annual sediment transport flux around Winterton Ness (0.2mm sand)

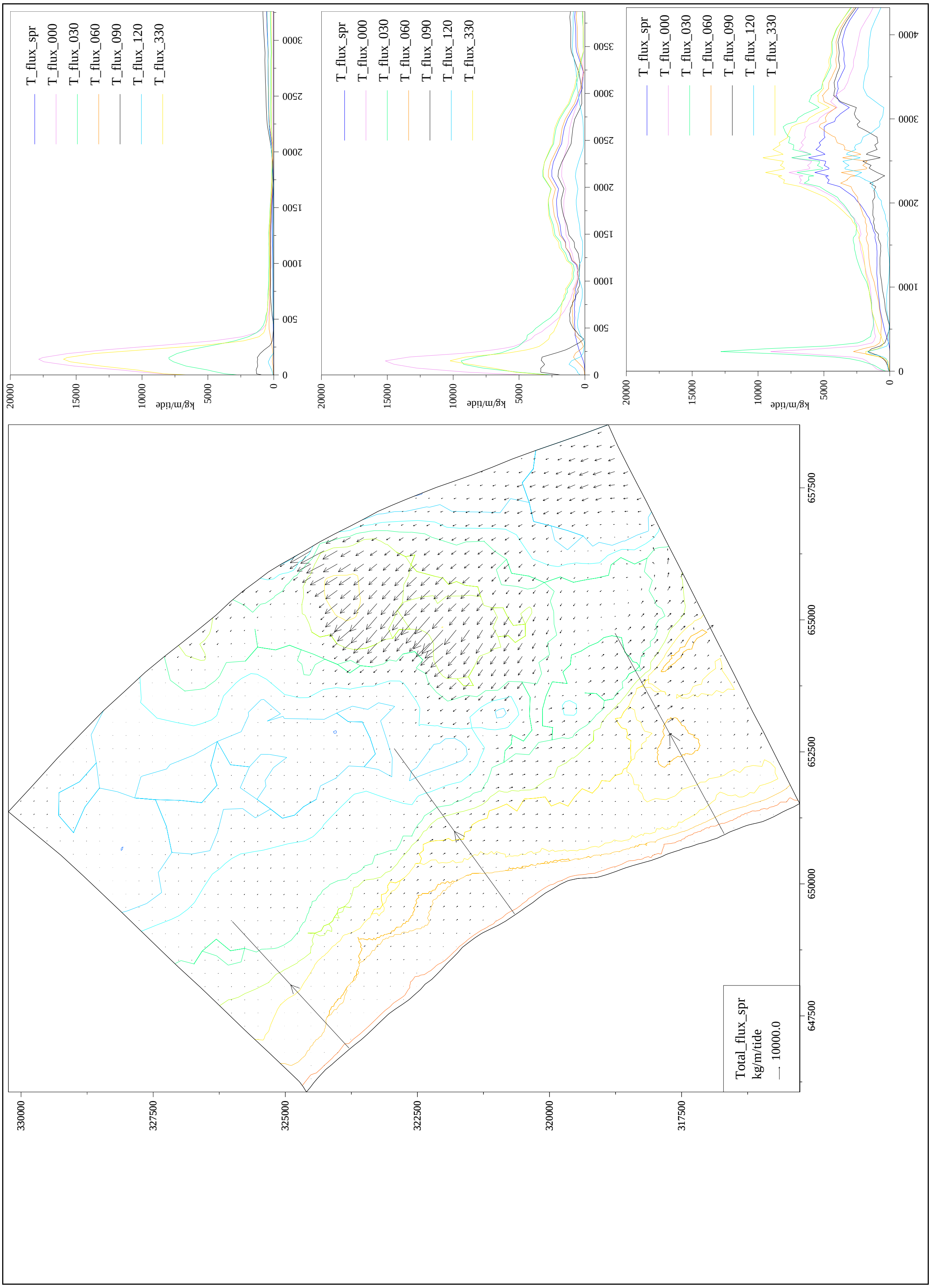

Figure 193 **Tidal net sediment flux cross shore profiles for three cross shore transects around Winterton Ness (0.2mm sand)**

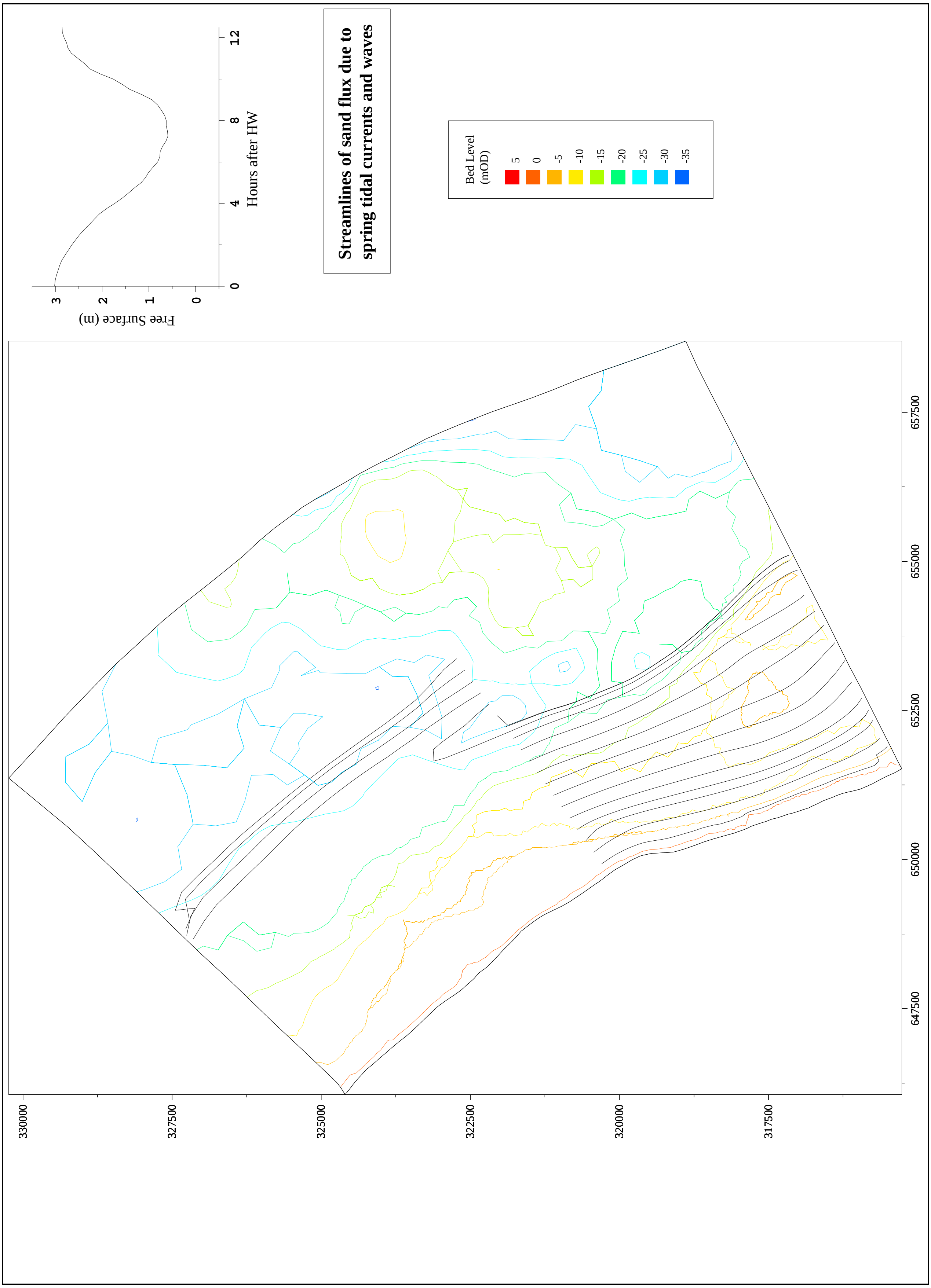

Figure 194 Streamlines of net annual sandflux around Winterton Ness (0.2mm sand)

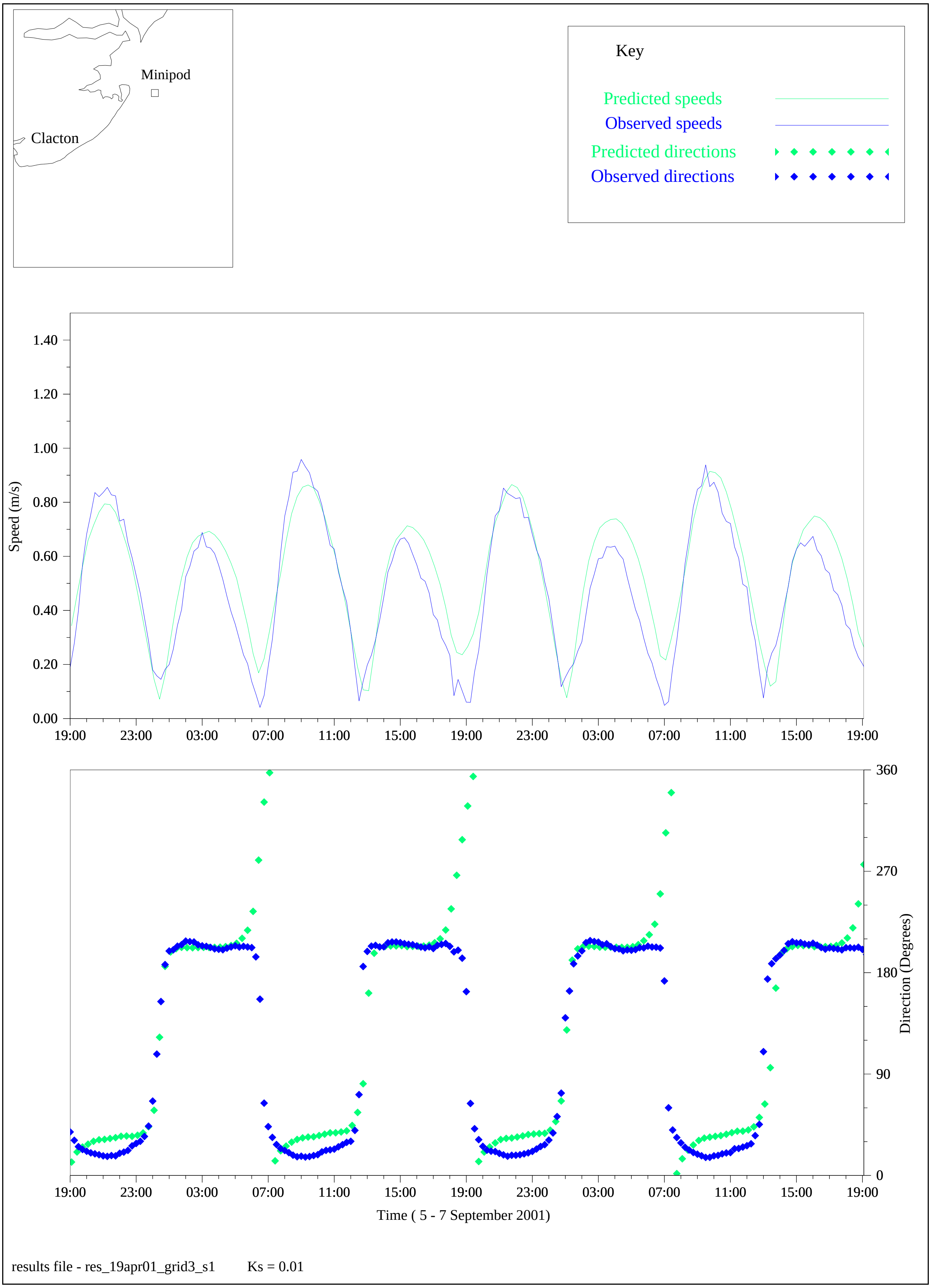

Figure 195 **Comparison of model prediction off the Naze with Minipod measured current speed and direction**

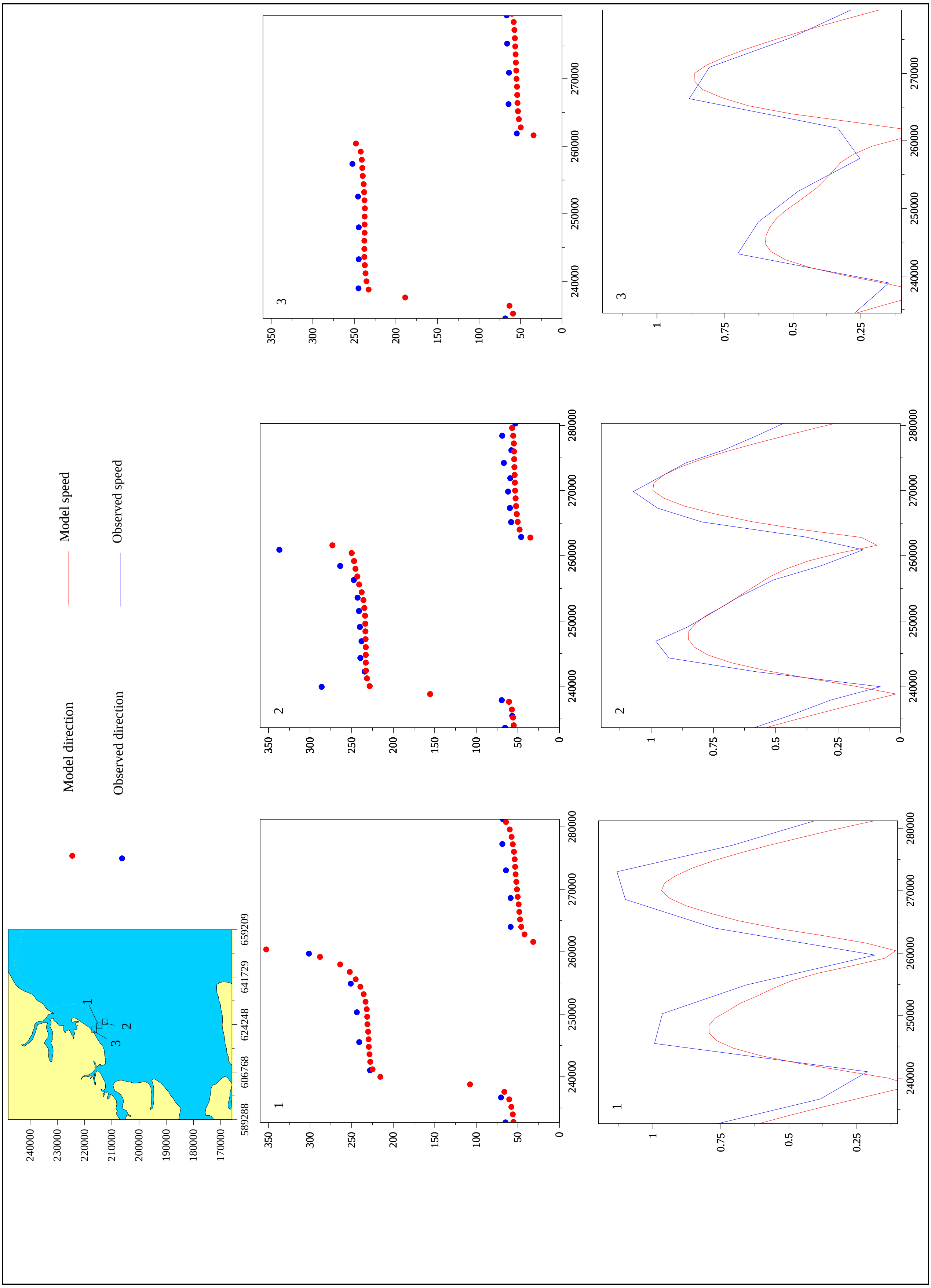

Figure 196 Comparison of model predictions between Clacton and Gunfleet Sand with ADCP measured current speed and direction

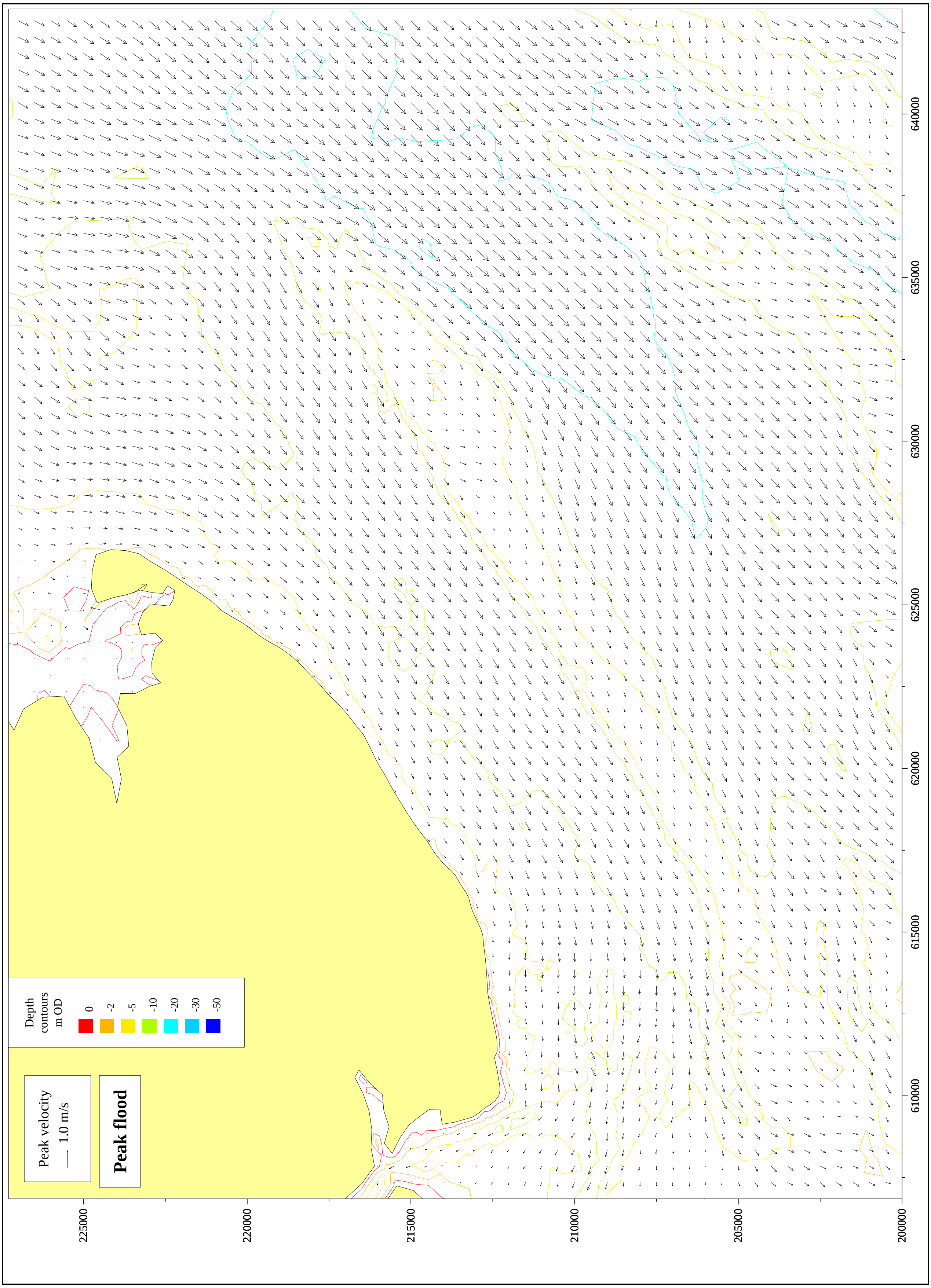

Figure 197 Model predictions of peak flood tide depth-averaged currents in the sea area around Clacton and the Gunfleet Sand bank

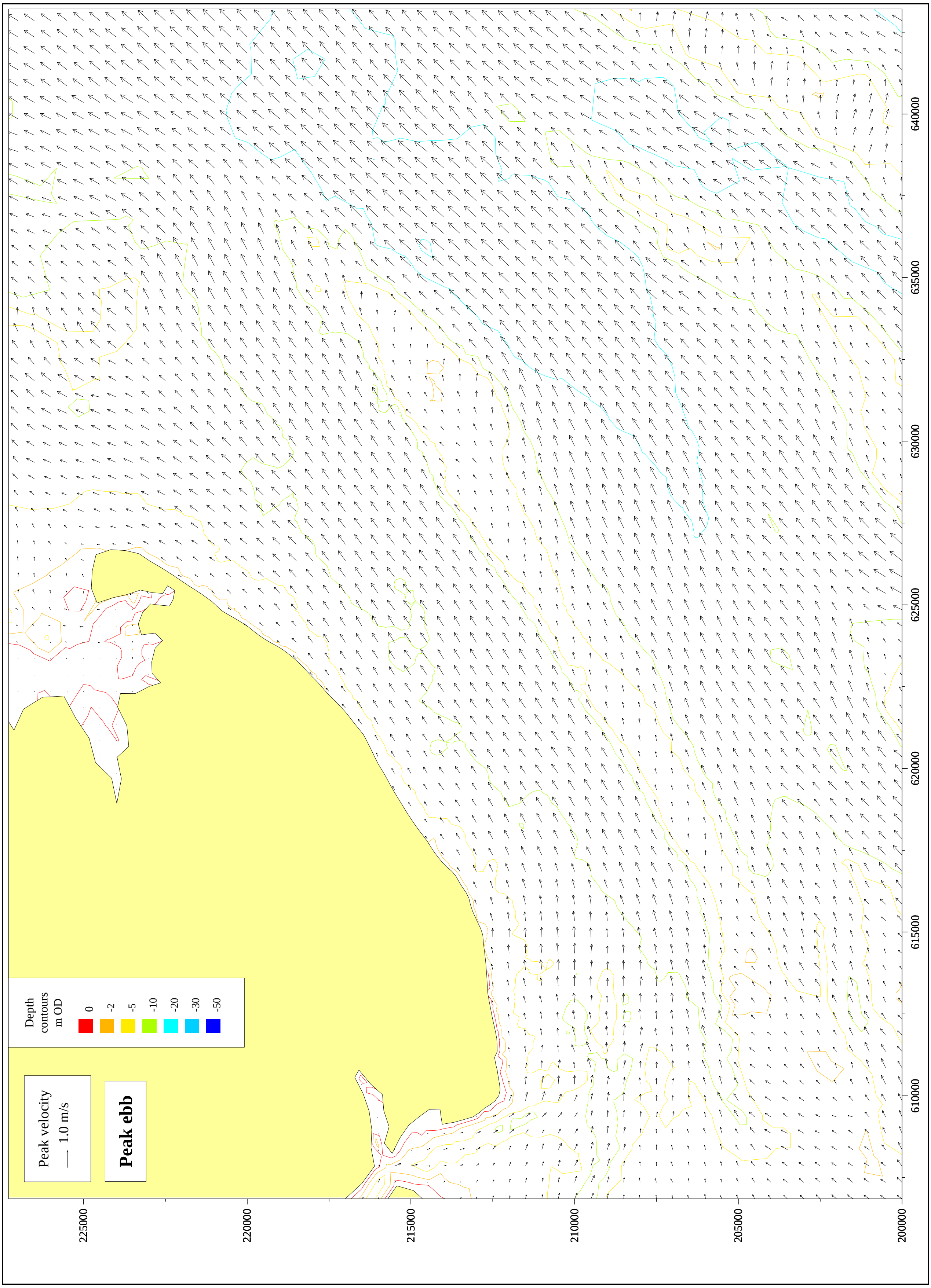

Figure 198 **Model predictions of peak ebb tide depth-averaged currents in the sea area around Clacton and the Gunfleet Sand bank**